République Algérienne Démocratique et Populaire

Ministère de l'Enseignement Supérieur et de la Recherche Scientifique

UNIVERSITE DJILLALI LIABES DE SIDI-BEL-ABBES

Faculté de Génie Electrique

Département d'Electrotechnique

Thèse présentée par :

BOUZIDI Mansour

Pour l'obtention du diplôme de :

Doctorat en Sciences

Spécialité : Electrotechnique

Option : Electronique de puissance

Intitulé de la thèse :

Nonlinear direct power control of a multilevel diode-clamped four-leg shunt active power filter

Présentée devant le jury composé de :

Mr FELLAH Mohammed Karim	Pr (U.D.L. Sidi Bel Abbés)	Président
Mr Benaissa Abdelkader	Pr (UDL Sidi Bel-Abbés)	Encadreur
Mr MAZARI Benyounes	Pr (U.S.T. Oran)	Examinateur
Mr MEROUFEL Abdelkader	Pr (U.D.L. Sidi Bel Abbés)	Examinateur
Mr ZERIKAT Mokhtar	Pr (E.N.P. Oran)	Examinateur
Mr TAHRI Ali	MCA (U.S.T. Oran)	Examinateur

Soutenue le : 27/ 02 /2017

Acknowledgement

In the name of Allah, the Most Gracious and the Most Merciful

Alhamdulillah, all praises to Allah for the strengths and His blessing in completing this thesis.

Special appreciation goes to my supervisor, Doctor Abdelkader Benaissa, Professor at Sidi-Bel-Abbes University for his constant support, his invaluable help and his constructive comments and suggestions.

Also, I would like to express my deep gratitude to Doctor Saïd Barkat, Associate Professor at the M'sila University, for his help, his advice and constant encouragement during the preparation of this work.

I thank all members of the jury who agree to judge my work and for the interest they have shown in this last.

Big thanks to all the professors who have contributed to my education without exception.

Dedication

I dedicate this work to

My mother and my father

My wife and my son Radhwane

And all my family

Contents

Chapter II : Direct power control of five-level four-leg shunt active power filter

Chapter III : Direct power control using feedback linearization technique of five-level four-leg shunt active power filter

Chapter IV : Direct power control using second order sliding mode for five-level four-leg shunt active power filter

***Chapter* V : Direct power control using fuzzy logic of five-level four-leg shunt active power filter**

List of figures

List of tables

Symbols

Symbols	*Descriptions*
S_{xi}	Inverter switching states
F_{xi}	Switching function
S_k	Sector number
θ	Angle of v^* projected in $\alpha\beta$ plane
ψ	angle of U^* projected in $\alpha\beta$ plane
M	Modulation index
PR_i	Prism number
v_{dc}	DC-link voltage
v_{dc}^*	DC-link voltage reference
v_{C_j}	DC capacitor voltage of capacitance j
v^*	Reference voltage vector
v_α^*, v_β^* and v_o^*	Reference voltage vector components
U^*	New reference voltage vector
U_α^*, U_β^* and U_o^*	New reference voltage vector components
v_1, v_2, v_3 and v_4	Adjacent switching vectors to the reference voltage vector
t_1, t_2, t_3 and t_4	On-duration time intervals of the switching vectors
v_a, v_b and v_c	Point of common coupling voltages
v_{Fa}, v_{Fb} and v_{Fc}	AC side voltages of the SAPF
v_{sa}, v_{sb} and v_{sc}	Source voltages
v_α, v_β and v_o	Voltages in $\alpha\beta$o coordinates
i_k	Inverter input currents
i_{C_j}	Current through capacitor C_j
i_{Fa}, i_{Fb}, i_{Fc} and i_{Fn}	AC side currents of the SAPF
$i_{La}, i_{Lb}, i_{Lc}$and i_{Ln}	Load currents
$i_{sa}, i_{sb}, i_{sc}$and i_{sn}	Source currents
i_α, i_β and i_o	Currents in $\alpha\beta$o coordinates
p_{dc}	Instantaneous DC power
p_L, q_L	Active and reactive power of the nonlinear load
p_s, q_s	Source active and reactive power
$q_{L\alpha}, q_{L\beta}$ and q_{Lo}	Reactive power components in $\alpha\beta$o coordinates
$\tilde{p}_L$	Oscillating active power component

p_F^*, q_F^*	Active and reactive power references of SAPF
E	Electrical energy stored in the chain of DC-link capacitors
$E_{\min}, E_{\max}$	Minimum and maximum energies stored in each capacitor
J	Cost function
C	Capacitor
C_{eq}	Equivalent capacitor
R_s, L_s	Source impedance
R_F, L_F	Filter impedance
R_l, L_l	Line impedance
R_l, L_l	Diode rectifier load
f_s	Switching frequency
f	Fundamental frequency
f_e	Sampling frequency
T_s	Switching period
T	fundamental period
T_e	Sampling period
$f(x)$ and $h(x)$	Smooth vector fields
u and y	Vectors of input and output
x	State vector
γ	Derivative number of an output
r	Relative degree
$L_f h_i$, $L_g h_i$	Lie derivatives of h_i with respect to f and g
k_p, k_i	PI coefficients
$e_{p_F}(k), e_{q_F}(k)$ and $e_{q_{F\alpha\beta}}(k)$	Actual active and reactive power tracking errors
$D(x)$	Decoupling matrix system
$\zeta(x)$	Linearization vector
v	New input vector
σ	Sliding surface
$\mu_A(x)$ s	Degree of membership
A	Fuzzy subset
X	Universe of discourse

Abbreviations

Abbreviations	*Descriptions*
THD	Total Harmonic Distorsion
IGBT	Insolated Gate Bipolar Transistor
GTO	Gate Turn off Thyristor
PWM	Pulse Width Modulation
SVM	Space Vector modulation
3DSVM	Three-Dimensional Space Vector modulation
APF	Active Power Filter
SAPF	Shunt Active Power Filter
PCC	Point of Common Coupling
PF	Power Factor
VOC	Voltage Oriented Control
DPC	Direct Power Control
DPC-SVM	Direct Power Control with Space Vector Modulation
DPC-3DSVM	Direct Power Control with Three-Dimensional Space Vector modulation
PDPC	Predictive Direct Power Control
PDPC-SVM	Predictive Direct Power Control with Space Vector Modulation
PDPC-3DSVM	Predictive Direct Power Control with Three-Dimensional Space Vector Modulation
DTC	Direct Torque Control

General introduction

In the recent years, the concept of smart distribution is taking shape. The emphasis of smart distribution system is on the efficiency enhancement by reducing distribution power losses, improving reliability, maximizing asset utilization, and better power quality free from harmonics [1]. Therefore, modern distribution systems are gaining significant attention over several power quality issues such as poor voltage regulation, high reactive power, harmonics current burden, phase unbalancing, excessive neutral line current, etc. [2]. In general, the source of these issues is secondary distribution system, which is directly connected to the customers. The secondary distribution is typically three-phase four-wire distribution system adopted to supply mixed loading, but it results in serious phase unbalance due to unequal distribution of single-phase loads [3]. Also, the presence of increasing number of non-linear loads such as adjustable speed drives, uninterruptible power supplies, etc. causes significant neutral current in the three-phase four-wire distribution system as tripled harmonics in phase currents [4]. Therefore, the total neutral line current is generated by the zero-sequence, fundamental, and harmonic components of the unbalanced load currents and thus results in the overload of neutral conductor of the three-phase four-wire distribution system [3]. The exponential growth in the nonlinear loads is responsible for further worsening of this situation. The study presented in [5] reveals that 22.6% of the distribution sites have a neutral line current in excess of 100%. The presence of phase unbalance and heavy neutral current are serious issues as they deteriorate the overall performance of distribution systems in many aspects, such as [4]:

- Increasing line losses,
- Deteriorating system voltage profiles,
- Overloading system phases,
- Malfunctioning of protective relays,
- Saturating of distribution power transformers,
- Increasing communication interference,
- Deteriorating power quality, system security and reliability of the electric supply, etc.

There are various approaches reported in the literature for compensating neutral currents and harmonics problems in three-phase four-wire systems. Passive solutions such as

passive harmonic filters [6-8], synchronous machine [9], specially designed transformers [10-14] and active solutions such as three-phase four-wire active power filter (APF) [15-23].

Among power filtering solutions, shunt active power filters (SAPF) are specially designed for neutral current compensation and harmonic elimination in line-currents [18-19]. The commercial success of these filters is due to their acceptable cost, fast response time, flexibility of control and continuous operation with virtually no maintenance. Three main topologies are available for three-phase four-wire systems: three-phase four-wire capacitor midpoint (or split-capacitor) SAPF topology, three H-bridge SAPF topology, and three-phase four-leg SAPF topology [15-23].
In the first one, the neutral wire is connected to the midpoint of the DC-link capacitors. In [15-19], this approach was studied where the inverter was operating as an active power filter. However, although it is simple in terms of topology, this approach is not suitable for SAPF application, for the following reasons [18-19]: 1) insufficient DC-link utilization, 2) high ripple on DC-link capacitors, 3) problem of DC-link capacitor voltages balance.
In the second topology, three single-phase H-bridge voltage source inverters are used to realize the four-wire SAPF. These H-bridge inverters are connected to the three-phase four-wire system by using three single-phase isolation transformers [18-20]. Since this topology requires a transformer, the four-wire SAPF size is large and the system energy efficiency is low. Slow response, increased number of switching devices, and high cost are the other disadvantages of this topology [18-19].
In the third topology the neutral wire is connected to the additional fourth leg [21-23]. This topology has been shown to be a solution for inverters operating in three-phase-four-wire systems and it offers full utilization of the DC-link voltage and lower stress on the DC-link capacitors [18-19].
Commonly, the abovementioned works are based on traditional two-level inverters. However, for medium to high power applications the multilevel inverters are the most attractive technology. Indeed, multilevel inverters have shown some significant advantages over traditional two-level inverters [24]-[27]. The main advantages of the multilevel inverters are a smaller output voltage step, lower harmonic components, a better electromagnetic compatibility and lower switching losses [24]-[27]. In the recent time, the use of multilevel inverters has been prevailing in medium-voltage active power filters without using a coupling transformer [28]-[32].
In other hand, the performance of the SAPF depends strongly on control strategies. In order to control the SAPF and achieve a proper power flow regulation in a power system, voltage-oriented control (VOC), which provides a good dynamic response by an internal current control loop, is widely used [33],[34]. As an alternative to this control method, other control strategies have been proposed in recent publications, such as predictive control and direct power control (DPC) [35]-[37].
DPC has become more widely used over the last few years due to the advantages of fast dynamic performance and simple control implementation when compared with other methods [35-37]. With DPC there are not internal current control loops and no PWM modulator bloc, because the inverter switching states are selected by a switching table based on the instantaneous errors between the commanded and estimated values of the

active / reactive powers, and voltage position vector. Therefore, the key point of the DPC implementation is the correct and fast estimation of the active and the reactive line powers. The DPC method is based on the direct torque control (DTC) which was originally proposed for controlling an induction motor in 1986 by Takahashi and Nogushi [38]. In 1995, Mannienen introduced basic principles of the DTC control method applied to the line inverter [39]. The structure of the line inverter may be exactly similar to the induction motor, the only exceptions being the connection to the grid instead of the induction motor and the introduction of the line filter. After that, the DPC was proposed by Noguchi in 1998 for PWM inverter without power source voltage sensors [40], and the same idea is developed by Malinowski in 2001 based on virtual flux estimation for three-phase PWM rectifiers system [41].
The main disadvantage of DPC with switching table is the variation of switching frequency, which generates an undesired broadband harmonic spectrum range and makes it hard to design a line filter [42]. These disadvantages can be effectively overcome by using space vector modulation (SVM) algorithm to replace the traditional switching table. The combination of SVM and traditional DPC forms the space vector modulation direct power control (SVM-DPC) [42].

Other structures of the DPC based on predictive approaches (Predictive Direct Power Control PDPC) have been recently published [43-47]. In view of switching frequency the PDPC methods can be divided into two groups: variable switching frequency and constant switching frequency. In the first group, the inverter's switching states are selected based on the minimization of a cost function value, which defines the behavior of the system. However, in such approach, switching frequency is variable and its performance depends on sampling frequency, inverter load and parameters variations [43-46]. In the second group, a predictive control algorithm, using deadbeat control principle was developed to compute the required inverter average voltage vector [47]. The computed converter average voltage vector is generated during each switching period in order to cancel out simultaneously active and reactive power tracking errors. This voltage vector is used as input to SVM in order to generate the inverter's switching states [47].

On other hand, the traditional two-dimensional SVM algorithm can be used only to control inverter connected to power system with balanced voltage/current where the hompolair component in Concordia transformation is equal to zero. In the three-phase four-wire system distribution, the case of unbalanced voltage/load is taken in consideration, therefore, the hompolair component is nonzero, and then, a three-dimensional space vector modulation (3DSVM) algorithm is needed in order to generate the desired signal.

In [48] and [49], 3DSVM schemes are analyzed for a four-leg two-level voltage source inverter. However, 3DSVM for a five-level four-leg inverter has not yet been studied in stationary reference frame. A novel algorithm of space vector modulation for a four-leg five-level inverter is proposed in this thesis.

The unbalance of the DC capacitor voltages is one of the most important drawbacks of the multilevel diode clamped inverter. Indeed, if any unbalance in the DC capacitor voltages appears, the output phase voltages/currents will be highly distorted which decreases the output signals quality [50-51].
Several approaches have been suggested to balance the DC capacitor voltages of diode clamped inverter [50-54]. In general, these schemes can be categorized into three major types. The first scheme [52] involves auxiliary balancing circuits, which incurs additional hardware costs. Second approach is applicable for the back-to-back converter topologies [53-54], where voltage balancing is achieved with the help of second converter; however it is impractical for the stand-alone diode clamped inverter applications [55]. The third approach for voltage balancing involves utilizing the redundancy in the switching patterns for the different control strategies [50-51]. This method has attained more focus these days, because no additional hardware cost is required and implementation becomes more feasible using high performance DSPs [50-51].

It is well established that conventional linear PI controllers are widely used in most industrial power electronics applications for the reasons of their simplicity and feasibility [56]. On the other hand, it is a fact that such kinds of controllers may fail to meet the high performance requirements of grid connected inverter applications due to their high vulnerability to the operation point, variations of the plant parameters and external disturbances.

Several control schemes based on linearization methods are proposed to achieve fast dynamic response to load and line disturbances [57-58]. Compared to PI controllers, they improve the general control performance of the SAPF [59-60].

Recently, fuzzy logic controllers [61-62] have received a great deal of attention in regards to their application to APFs. The advantages of fuzzy logic controllers over conventional controllers (PI) are that they do not require an accurate mathematical model, can work with imprecise inputs, can handle non-linearity, and are more robust than conventional PI controllers [61-62].

The sliding mode variable structure control (SMVSC) has been extensively studied so far owing to its robustness against parameter variations, external disturbances and model uncertainties. However; its main drawback is the chattering phenomenon, which restricts the SMVSC application [29].

With the intention of overcoming these disadvantages, Second Order Sliding Mode (SOSM) with Super-Twisting Control Law (STW) is proposed for the PWM rectifier in [64-65]. The STW is one of the most powerful second order continuous sliding mode control algorithms that handle a relative degree equal to one [65]. It generates a continuous control function that drives the sliding variable and its derivative to zero in finite time in the presence of the smooth matched disturbances with bounded gradient, when this boundary is known [64-65].

In this thesis, a three-phase five-level four-leg shunt active power filter is considered in the aim to improve power quality in four-wire systems. The use of the multilevel four-leg configuration can be justified by its ability to suppress the neutral current from the source without any drawback in the filtering performance and without using a coupling transformer. In the present work a simplified 3DSVM algorithm in $\alpha\beta o$ coordinates equipped by a balancing strategy is proposed to overcome the inherent instability of the DC capacitor voltages of four-leg multilevel inverter. Furthermore, in this thesis, new nonlinear control strategies based on the feedback linearization, super-twisting sliding mode, and fuzzy logic associated to DPC and PDPC using 3DSVM are proposed to control the five-level four-leg SAPF. The idea herein is to enhance the filtering system performance by controlling its active and reactive powers using an improved version of DPC and PDPC synthesized based on the aforementioned nonlinear control approaches.

In order to achieve these research objectives, this thesis is divided into five chapters, which are summarized as follows:

The first chapter consists of two main parts. The first part is devoted to the modeling of *m*-level four-leg diode clamped inverter and a new simplified algorithm of 3DSVM is proposed. The second part deals with the problem of unbalance of the DC capacitor voltages at the input of the five-level four-leg inverter.

In the second chapter describes a comprehensive review of neutral current compensation methods, their topologies, and their technical and economical limitations are presented also. The objective of the second section of this chapter is to present a direct power control (DPC) and predictive direct power control (PDPC) with 3DSVM based on new model of five-level four-leg SAPF.

In the third and fourth chapters, nonlinear controllers based on the feedback linearization and second order sliding mode are associated to DPC and PDPC control in order to improve the performances of the five-level four-leg SAPF.

The fifth chapter is focused on the application of the fuzzy logic controller to regulate the DC voltage and active/reactive powers in both DPC-3DSVM and PDPC-3DSVM. Also, at the end of this chapter, a comparative study of the three previous nonlinear control techniques is presented.

Finally, a main conclusion of this dissertation and some recommendations for future research topics are provided.

Chapter I

Modeling and control of four-leg multilevel diode clamped inverter

I.1. Introduction

Multilevel inverters have opened the door for advances in electric energy conversion technology. They present the features of a lower device voltage rating, lower harmonic distortion, and higher efficiency compared with conventional two-level inverters [66-67].
These inverters are typically considered for high-power applications, because they allow operating at higher DC-link voltage levels with the currently available semiconductor technology [24, 70], [50-51]. However, they can also be interesting for medium- or even low-power/voltage applications, since they allow operating with lower voltage-rated devices, with potentially better performance/economical features [68-69].
There are three basic multilevel inverter topologies: diode clamped, flying capacitor, and cascaded H-bridge with separate DC sources. Among these topologies, diode-clamped inverters are especially interesting because of their simplicity; the multiple voltage levels are generated passively through a set of series-connected capacitors (see figure (I.1)). The simplest family member, the three-level inverter, has been widely studied [24], [69-70].
In four-wire systems, unbalanced or nonlinear loads and unbalanced sources can cause a large neutral current. The extra leg in four-leg inverters provides an effective neutral connection, which allows a precise control of the neutral current. The growing interest in four-leg inverters for three-phase four-wire systems focuses in applications such as distributed power inverters, active power filters, and fault-tolerant converters. Even with voltage-limited devices, the multilevel topologies can reach high power ratings with low

harmonic distortion, reduced switching losses and good electromagnetic compatibility [66-67]. However, the implementation of multilevel four-leg diode-clamped inverters, with four or more levels, still presents some challenges. By increasing the number of levels, the difficulty to ensure the voltage balance within the DC capacitors increases as well. This voltage imbalance can be caused by many factors such as operational conditions, load power factor, modulation index, as well as the modulation technique used [50-51].
The control of the four-leg inverter switches can be achieved by several modulation techniques [22, 48, 60], [71-75]. Among these modulation techniques, the space vector modulation (SVM) stands out because it offers significant flexibility to optimize switching waveforms, improvement in DC bus utilization, and it is well suited for digital implementation. Prior art of SVM for four-leg inverters is formulated in a three-dimension space (3DSVM) [22, 48, 60], [72-75]. Based on the effective use of the redundant switching states of the inverter voltage vectors, the 3DSVM can eliminate the problem of unbalancing DC-link capacitor voltages [60].

This chapter will consist of two main parts. The first part will be devoted to the modeling of *m*-level four-leg diode clamped inverter and a new simplified algorithm of 3DSVM will be proposed. The second section will deal with the problem of unbalance of the DC capacitor voltages at the input of the five-level four-leg inverter.

I.2. Ideal *m*-level four-leg diode-clamped inverter

Figure (I.1) shows a schematic diagram of a *m*-level four-leg diode-clamped inverter in which the DC-link consists of capacitors C_1, C_2, …, C_{m-2} and C_{m-1}.

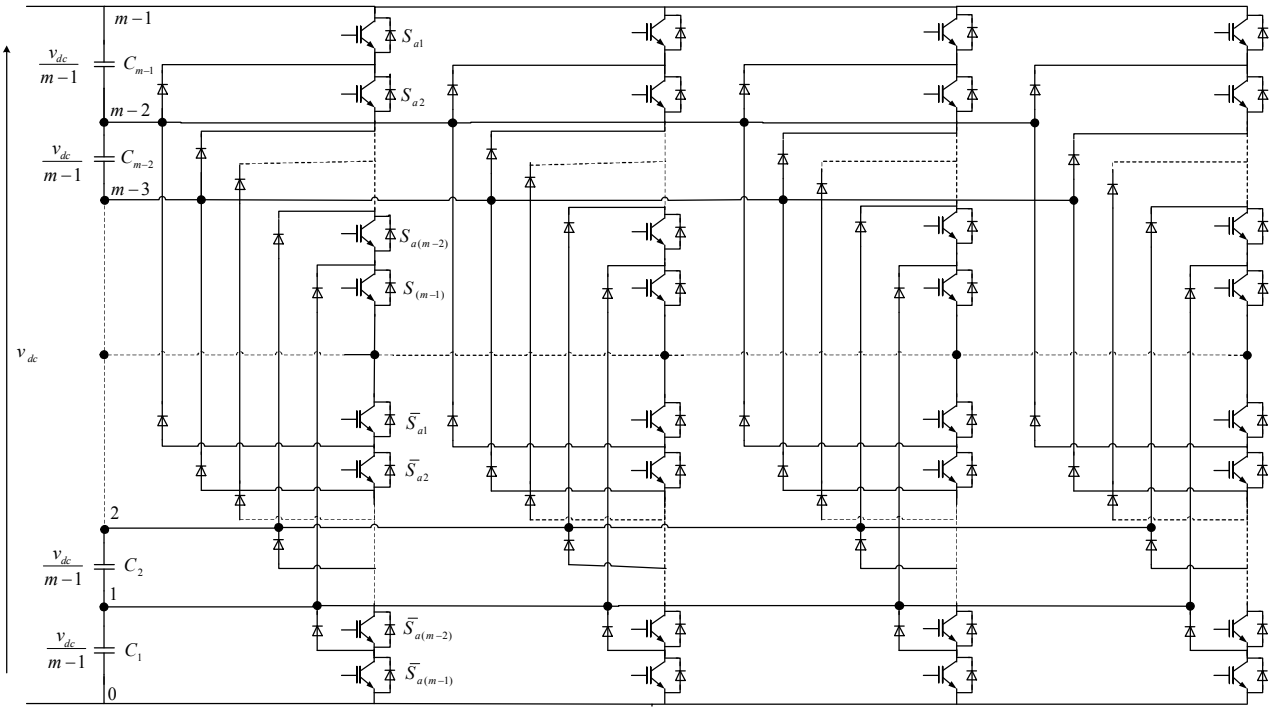

Figure (I.1): Circuit diagram of *m*-level four-leg inverter

Corresponding to the net DC-link voltage of v_{dc}, voltage across each capacitor is ideally $v_{dc}/(m\text{-}1)$. Each leg consists of $2m\text{-}2$ switches. There are m-1 complimentary switch pairs in each leg. Using first leg as an example, the complementary pairs are $\left(S_{a1}, \overline{S}_{a1}\right)$, $\left(S_{a2}, \overline{S}_{a2}\right)$,... ,$\left(S_{a(m-1)}, \overline{S}_{a(m-1)}\right)$. Gating signals $\overline{S}_{a1}, \overline{S}_{a2}$ ... $\overline{S}_{a(m-1)}$ are generated by inverting S_{a1}, S_{a2} ... $S_{a(m-1)}$ respectively.

Considering voltage of node "0" as the reference voltage, the switching combinations to synthesize different voltage levels are summarized in table (I.1).

Table (I.1): Switching states of one leg of m-level four-leg inverter (x =*a, b, c or n*)

Switching states	S_{x1}	S_{x2}	**....**	$S_{x(m-2)}$	$S_{x(m-1)}$	$\overline{S}_{x1}$	$\overline{S}_{x2}$	**....**	$\overline{S}_{x(m-2)}$	$\overline{S}_{x(m-1)}$	**Output Phase voltage** v_{x0}
***m*-1**	1	1	....	1	1	0	0	....	0	0	v_{dc}
***m*-2**	0	1	....	1	1	1	0	....	0	0	$\frac{(m-2)\,v_{dc}}{m-1}$
. . .	. . .	. . .	. . .	. . .	. . .	. . .	. . .	. . .	. . .	. . .	. . .
1	0	0	....	0	1	1	1	....	1	0	$\frac{v_{dc}}{m-1}$
0	0	0	....	0	0	1	1	....	1	1	0

The switching functions are defined as F_{ij}, where $i \in \{a,b,c,n\}$ is the phase index and $j \in \{0,1,\ldots m-1\}$ is the voltage level. As shown in figure (I.2), the switching functions F_{ij} takes value "1" if i-phase is connected to voltage level j and "0" otherwise, these switching functions can be expressed as:

$$
\begin{aligned}
F_{x(m-1)} &= S_{x(m-1)}\ S_{x(m-2)}\ S_{x(m-3)} \ldots S_{x2}\ S_{x1}\ S_{x0} \\
F_{x(m-2)} &= S_{x(m-1)}\ S_{x(m-2)}\ S_{x(m-3)} \ldots S_{x2}\ S_{x1}\ \overline{S}_{x0} \\
F_{x(m-3)} &= S_{x(m-1)}\ S_{x(m-2)}\ S_{x(m-3)} \ldots S_{x2}\ \overline{S}_{x1}\ \overline{S}_{x0} \\
&\vdots \qquad\qquad \vdots \qquad\qquad \vdots \qquad\qquad x = a,b,c \text{ or } n \\
F_{x2} &= S_{x(m-1)}\ S_{x(m-2)}\ \overline{S}_{x(m-3)} \ldots \overline{S}_{x2}\ \overline{S}_{x1}\ \overline{S}_{x0} \\
F_{x1} &= S_{x(m-1)}\ \overline{S}_{x(m-2)}\ \overline{S}_{x(m-3)} \ldots \overline{S}_{x2}\ \overline{S}_{x1}\ \overline{S}_{x0} \\
F_{x0} &= \overline{S}_{x(m-1)}\ \overline{S}_{x(m-2)}\ \overline{S}_{x(m-3)} \ldots \overline{S}_{x2}\ \overline{S}_{x1}\ \overline{S}_{x0}
\end{aligned}
\qquad \text{(I.1)}
$$

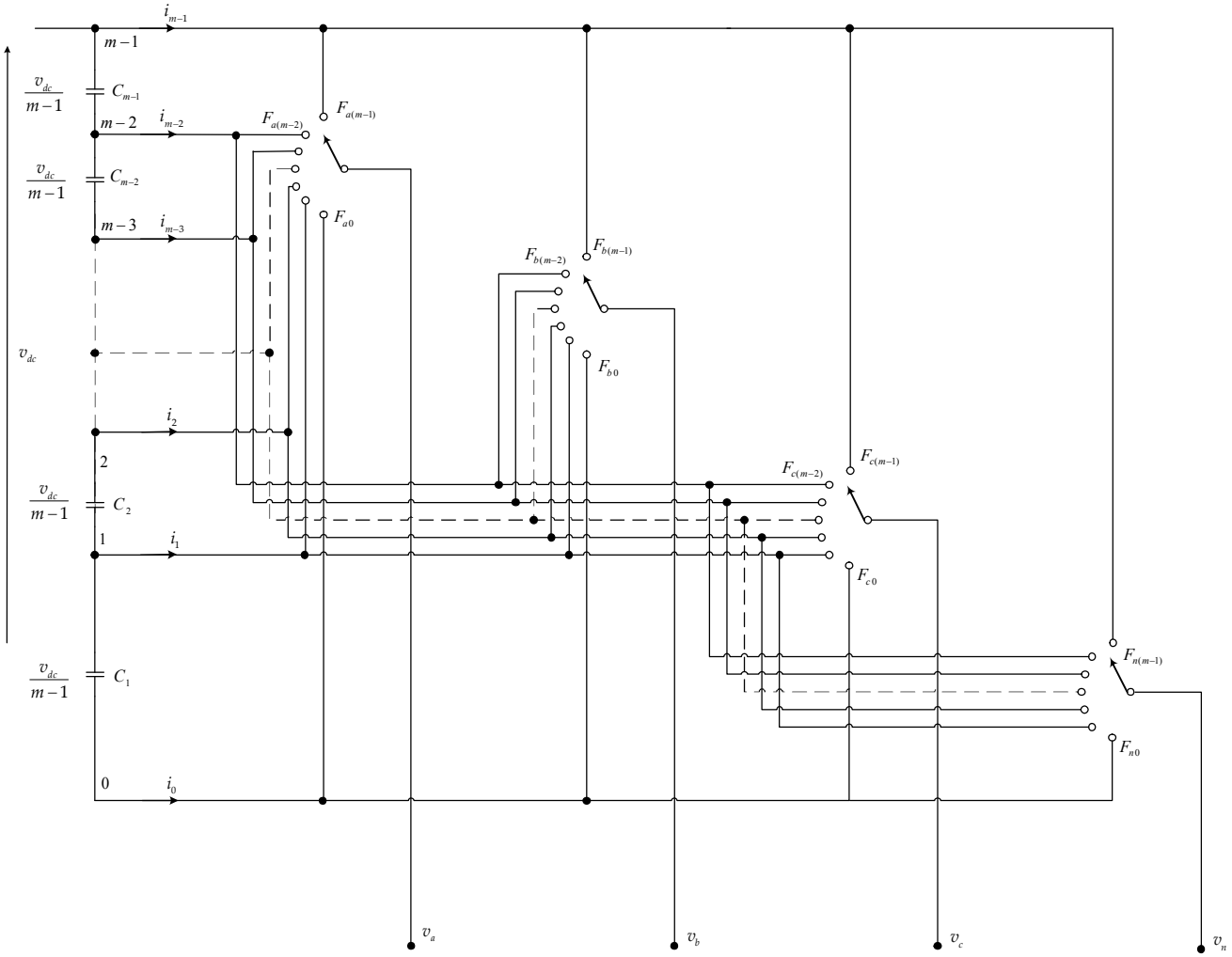

Figure (I.2): Schematic representation of the *m*-level four-leg inverter based on *m*-pole

Referring all of the voltages to the lower DC-link voltage level ("0" reference), each output voltage consists of contributions by a determinate number of consecutive capacitors:

$$v_{x0} = \sum_{j=0}^{m-1}\left(F_{xj} \sum_{i=0}^{j} v_{C_i} \right), \qquad x = a,\ b,\ c \text{ or } n \tag{I.2}$$

When balanced distribution of the DC-link voltage among the capacitors is assumed, the equation (I.2) becomes:

$$v_{x0} = \frac{v_{dc}}{m-1} \sum_{j=0}^{m-1} jF_{xj}, \qquad x = a,\ b,\ c \text{ or } n \tag{I.3}$$

The instantaneous output inverter phase to neutral voltages v_a, v_b and v_c can be expressed as:

$$\begin{bmatrix} v_a \\ v_b \\ v_c \end{bmatrix} = \begin{bmatrix} v_{a0} - v_{n0} \\ v_{b0} - v_{n0} \\ v_{c0} - v_{n0} \end{bmatrix} \tag{I.4}$$

It can be expressed in terms of switching functions and DC-link voltages capacitors as given by:

$$\begin{bmatrix} v_a \\ v_b \\ v_c \end{bmatrix} = \begin{bmatrix} F_{a(m-1)} - F_{n(m-1)} & F_{a(m-2)} - F_{n(m-2)} & \cdots & F_{a1} - F_{n1} & F_{a0} - F_{n0} \\ F_{b(m-1)} - F_{n(m-1)} & F_{b(m-2)} - F_{n(m-2)} & \cdots & F_{b1} - F_{n1} & F_{b0} - F_{n0} \\ F_{c(m-1)} - F_{n(m-1)} & F_{c(m-2)} - F_{n(m-2)} & \cdots & F_{c1} - F_{n1} & F_{c0} - F_{n0} \end{bmatrix} \begin{bmatrix} v_{dc} \\ \dfrac{(m-2)\, v_{dc}}{m-1} \\ \vdots \\ \dfrac{v_{dc}}{m-1} \\ 0 \end{bmatrix} \tag{I.5}$$

The inverter input currents i_k (k = 0, 1, ... , m-1) are expressed in terms of load currents i_a, i_b, i_c and i_n by:

$$i_k = F_{ak} i_a + F_{bk} i_b + F_{ck} i_c + F_{nk} i_n \tag{I.6}$$

In an m-level four-leg inverter, there are m^4 possible switch combinations. The switch combinations are represented by ordered sets $\left(S_a S_b S_c S_n\right)$.

Where:

$$\begin{array}{lll} S_x = m-1 & \text{if } F_{a(m-1)} = 1 & \\ S_x = m-2 & \text{if } F_{a(m-2)} = 1 & \\ \vdots & \vdots & x = a, b, c \text{ or } n \\ S_x = 1 & \text{if } F_{a1} = 1 & \\ S_x = 0 & \text{if } F_{a0} = 1 & \end{array} \tag{I.7}$$

The coordinates of each switching vector, v_α, v_β and v_o are calculated by:

$$\begin{bmatrix} v_\alpha \\ v_\beta \\ v_o \end{bmatrix} = \sqrt{\frac{2}{3}} \begin{bmatrix} 1 & -1/2 & -1/2 \\ 0 & \dfrac{\sqrt{3}}{2} & -\dfrac{\sqrt{3}}{2} \\ \dfrac{1}{\sqrt{2}} & \dfrac{1}{\sqrt{2}} & \dfrac{1}{\sqrt{2}} \end{bmatrix} \begin{bmatrix} v_a \\ v_b \\ v_c \end{bmatrix} \tag{I.8}$$

Using the different switching combinations, the vectors given by (I.8) can be described using a graphical representation in three-dimensional space as shown in figure (I.3).

There are (*m-1*) zero switching vectors, and $\left(m^4 - m\right)$ unique non-zero switching vectors.

All the m^4 switching vectors can be sorted into $\left(\left(m-1\right)6+1\right)$ layers.

The diagram of space vectors can be divided into six sectors, each sector further is divided into $\left(m-1\right)^2$ prisms and each prism is formed by tetrahedrons.

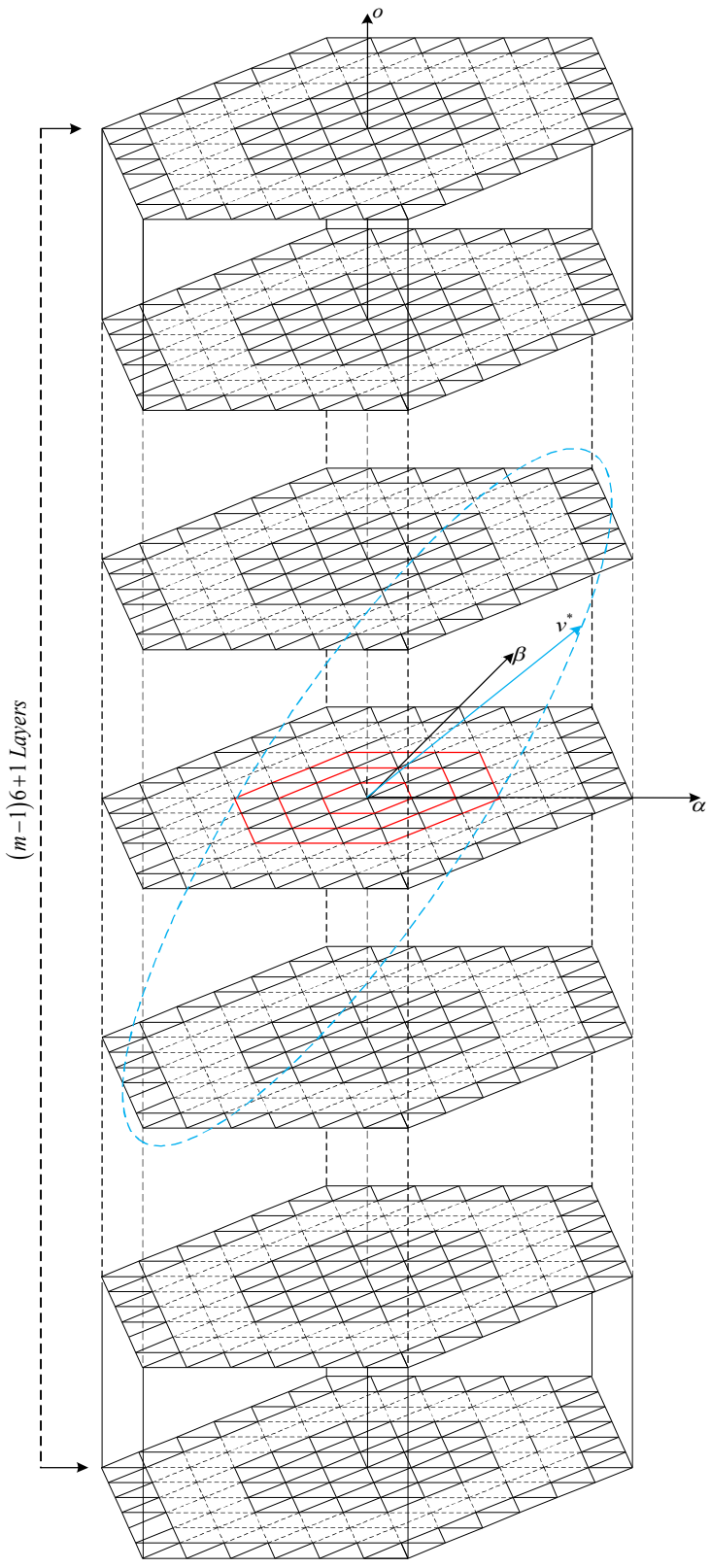

Figure (I.3): Representation of space voltage vectors of m-level four-leg inverter in three-dimensional $\alpha\beta o$ plane

Projection of three-phase reference voltages into the $\alpha\beta o$ plane is a vector called the reference voltage vector v^*, it rotates counterclockwise in space diagram with angular frequency of ω as shown in figure (I.4).

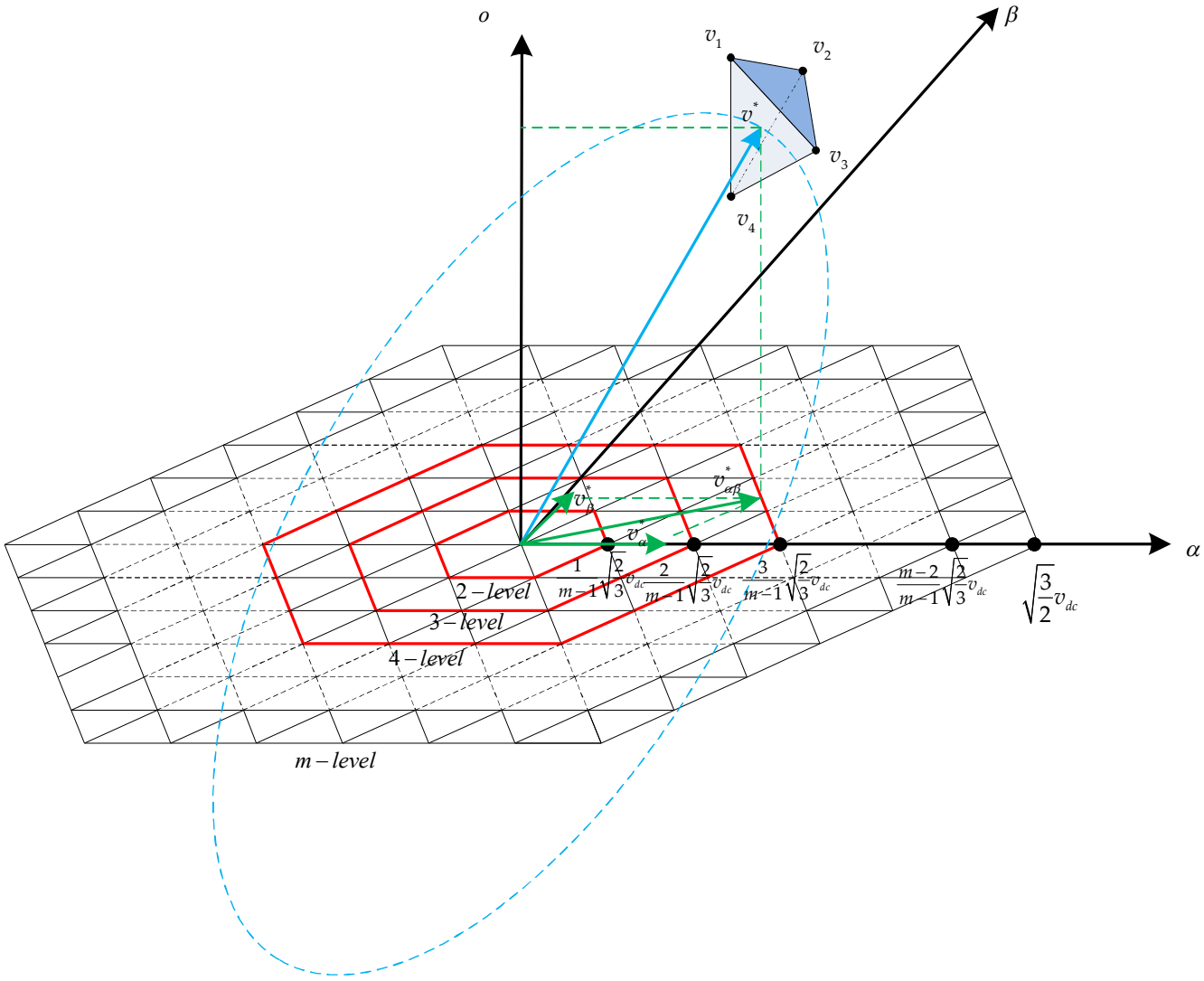

Figure (I.4): Representation of space voltage vectors of *m*-level four-leg inverter in αβo plane

I.2.1. Conventional three-dimensional space vector modulation

A 3DSVM is a discrete type of modulation technique in which a voltage reference vector v^* is synthesized by the time average of a number of appropriate switching state vectors [48]. When the reference voltage vector is located in known sector and prism at any sampling instant, the tip of the voltage vector lies in a tetrahedron formed by the four switching vectors adjacent to it, (see figure (I.4)). The adjacent vectors necessary to synthesize the reference voltage vector related by:

$$\begin{aligned} v_1 t_1 + v_2 t_2 + v_3 t_3 + v_4 t_4 &= v^* T_s \\ t_1 + t_2 + t_2 + t_4 &= T_s \end{aligned} \tag{I.9}$$

Where T_s is the switching period, v_1, v_2, v_3 and v_4 are the four switching vectors adjacent to the reference voltage vector, and t_1, t_2, t_3 and t_4 are their on-duration time intervals respectively.

The on-duration time intervals of appropriate switching vectors are calculated from the solution of (I.9).

Computational burden to synthesize a reference voltage is mostly associated with trigonometric calculations for: localization of the reference voltage vector, calculation of duration time intervals of adjacent switching vectors, and the generation of the corresponding pulses. This increases the required computational time and augments the hardware and software complexity [60].

I.3. Proposed algorithm of the three-dimensional space vector modulation

The proposed algorithm can reduce remarkably the complexity of 3DSVM by using one sector only in the conception of all modulation algorithm steps such as: determination of the space vector location, duration time calculation, and pulses generation [60].

The reference voltage vector rotates in the space $\alpha\beta o$ and crosses all the sectors (see figure (I.5)), then, it is necessary to build another vector U^* which turns only in the first sector and takes all information about v^* in the other sectors, as shown in figure (I.6).

The components of the new reference voltage vector are:

$$\begin{aligned} U_\alpha^* &= U_{\alpha\beta}^* \cos(\psi) \\ U_\beta^* &= U_{\alpha\beta}^* \sin(\psi) \\ U_o^* &= v_o^* \end{aligned} \tag{I.10}$$

Where:

$$U_{\alpha\beta}^* = \sqrt{v_\alpha^{*2} + v_\beta^{*2}} \text{ and } \psi = \mathrm{mod}(\theta,\ \frac{\pi}{3}) \in \left[0, \frac{\pi}{3}\right]$$

mod(*x*,*y*): is a function which gives the division remainder of x on y.
ψ and θ are the angles of the vectors U^* and v^* projected in $\alpha\beta$ plane respectively. The angle θ is given by:

$$\theta = \tan 2^{-1}\left(\frac{v_\beta^*}{v_\alpha^*}\right) \tag{I.11}$$

And: **tan2^{-1}**: is a function returns the four-quadrant inverse tangent.

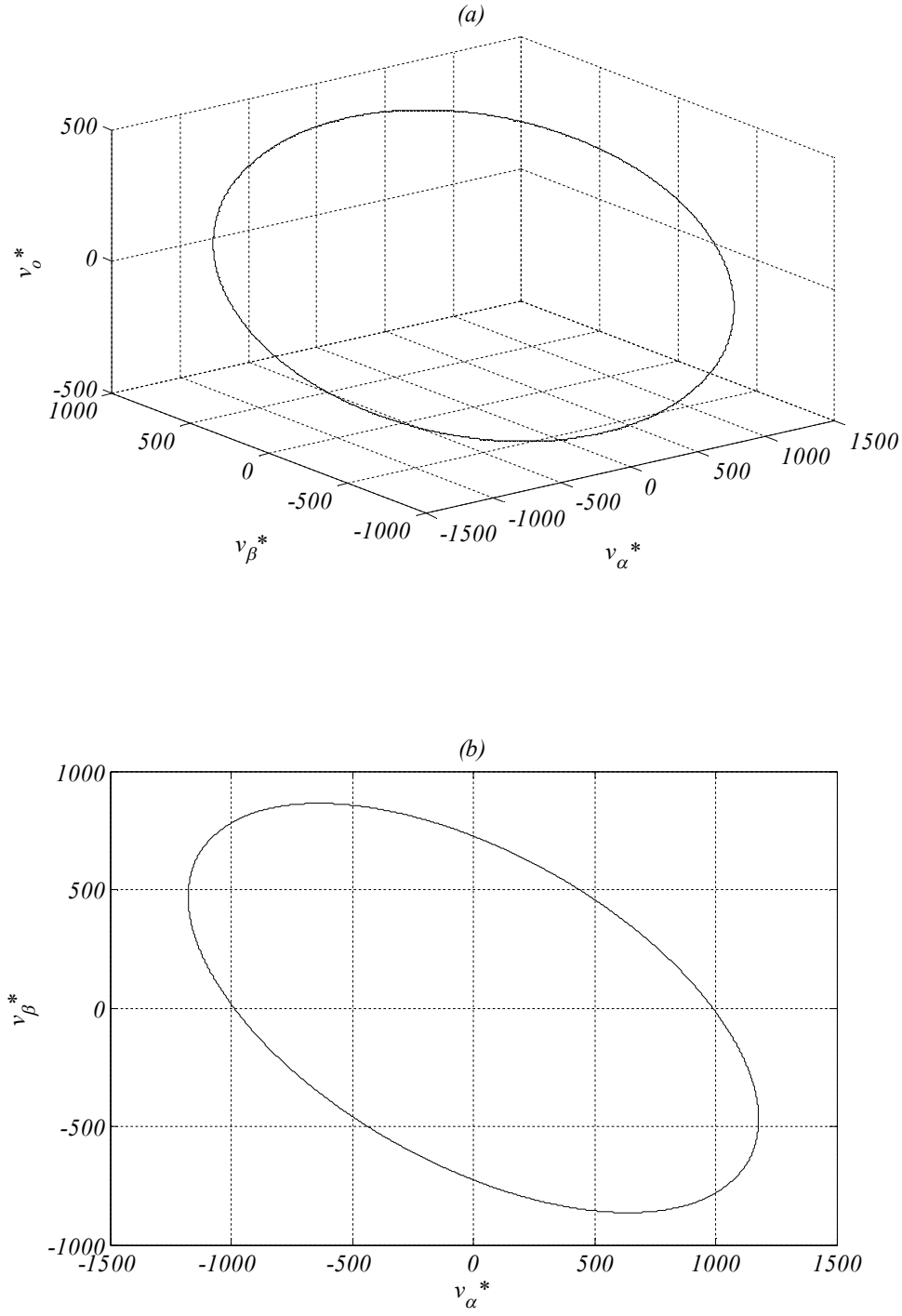

Figure (I.5): Trajectory of reference voltage vector $\vec{v}^*$ under unbalanced sinusoid condition, (a): Trajectory in three-dimensional space, (b): Projection of the trajectory on $\alpha\beta$ plane

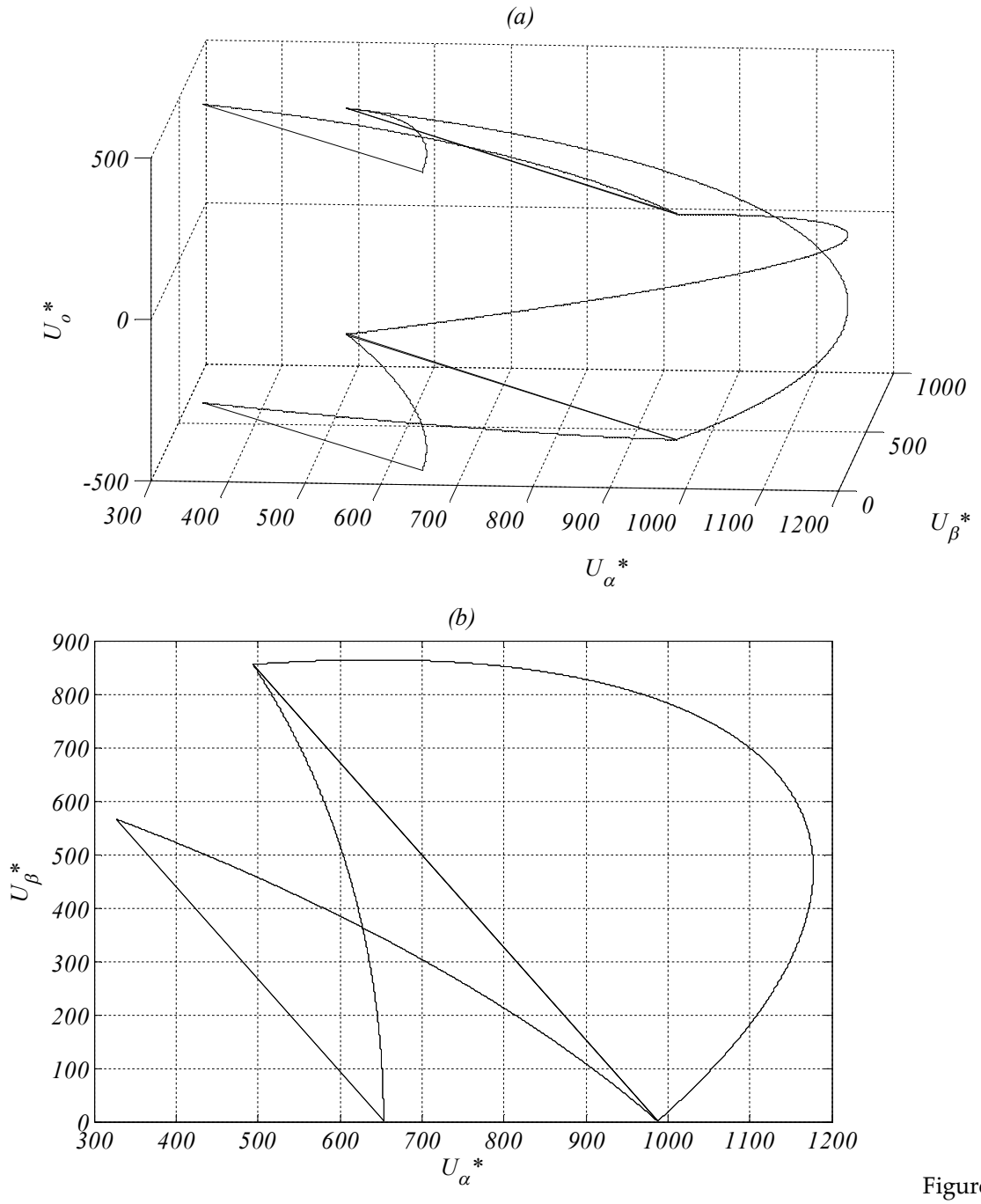

Figure (I.6): Trajectory of reference voltage vector U^* under unbalanced sinusoid condition, (a): Trajectory in three-dimensional space, (b): Projection of the trajectory on $\alpha\beta$ plane

I.3.1. Determination of the space vector location

The space vector location is determined in three steps: (1) determining the sector number of where the vector lies, (2) determining the number of prisms, and (3) determining the tetrahedron number of where the reference vector is located [60].

Step 1: Sector number computation

Sector numbers are given by:

$$S_k = \text{ceil}\left(\frac{\theta}{\pi/3}\right), k \in \{1,2,3,4,5,6\} \tag{I.12}$$

Where: **ceil** is the C-function that adjusts any real number to the nearest, but higher, integer.

Step 2: Prisms identification

Reference vector U^* is projected on the axes of 60° coordinate system as shown in figure (I.7) [30]. In the first sector, the normalized projected components are U_1^* and U_2^* given by (I.13).

$$\begin{aligned} U_1^* &= \frac{U_{\alpha\beta}^* \cos(\psi) - \frac{U_{\alpha\beta}^*}{\sqrt{3}} \sin(\psi)}{\sqrt{\frac{2}{3}} \frac{v_{dc}}{m-1}} \\ U_2^* &= \frac{\frac{2}{\sqrt{3}} U_{\alpha\beta}^* \sin(\psi)}{\sqrt{\frac{2}{3}} \frac{v_{dc}}{m-1}} \end{aligned} \tag{I.13}$$

The modulation index is given by:

$$M = \frac{U_{\alpha\beta}^*}{\sqrt{\frac{2}{3}} v_{dc}} \tag{I.14}$$

The equation (I.13) becomes:

$$\begin{aligned} U_1^* &= M(m-1)\left(U_{\alpha\beta}^* \cos(\psi) - \frac{U_{\alpha\beta}^*}{\sqrt{3}} \sin(\psi)\right) \\ U_2^* &= M(m-1)\left(\frac{2}{\sqrt{3}} U_{\alpha\beta}^* \sin(\psi)\right) \end{aligned} \tag{I.15}$$

In order to identify the prism where the required reference voltage vector is located, the following integers are used:

$$\begin{aligned} l_1 &= \text{int}\left(U_1^*\right) \\ l_2 &= \text{int}\left(U_2^*\right) \end{aligned} \tag{I.16}$$

Where the ***int*** function returns the nearest integer that is less than or equal to its argument. The following criterion determines if the reference vector is located in a prism *i* (PR_i) or prism *j* (PR_j) of the figure (I.7.a):

$$\begin{aligned} U^* &\text{ is in } PR_i \text{ if: } U_1^* + U_2^* < l_1 + l_2 + 1 \\ U^* &\text{ is in } PR_j \text{ if: } U_1^* + U_2^* \geq l_1 + l_2 + 1 \end{aligned} \tag{I.17}$$

Step 3: Tetrahedron identification

The next step is to determine the tetrahedron number according to the location of the reference voltage. As shown in figure (I.7.b), each tetrahedron is limited from the top and the bottom by two planes.

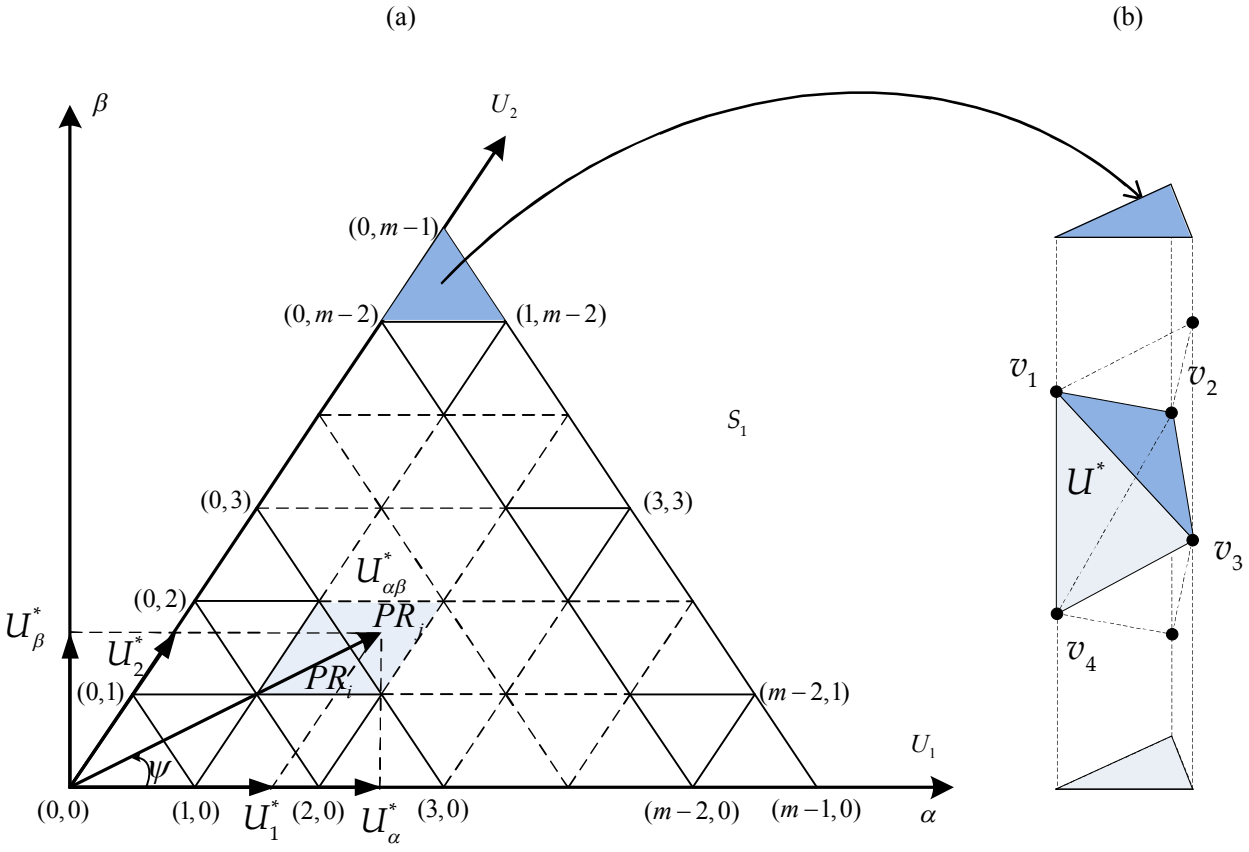

Figure (I.7): (a): Space voltage vectors for an *m*-level four-leg inverter in the first sector, (b): Example of a tetrahedron in a given prism

Each plane is created by three switching vectors. For example, the tetrahedron shown in figure (I.7.b), the top plane is formed by v_1, v_2 and v_3, and bottom plane is formed by v_2, v_3 and v_4. Equations of the top and bottom planes are written in the following form:

$$\begin{aligned} U_o^* &= a_1 U_\alpha^* + b_1 U_\beta^* + c_1 \\ U_o^* &= a_2 U_\alpha^* + b_2 U_\beta^* + c_2 \end{aligned} \tag{I.18}$$

Where: a_1, a_2, b_1, b_2, c_1, c_2 are constants, calculated by solving the equations (I.19) and (I.20):

$$\begin{bmatrix} v_{1\alpha} & v_{1\beta} & 1 \\ v_{2\alpha} & v_{2\beta} & 1 \\ v_{3\alpha} & v_{3\beta} & 1 \end{bmatrix} \begin{bmatrix} a_1 \\ b_1 \\ c_1 \end{bmatrix} = \begin{bmatrix} v_{1o} \\ v_{2o} \\ v_{3o} \end{bmatrix} \tag{I.19}$$

$$\begin{bmatrix} v_{2\alpha} & v_{2\beta} & 1 \\ v_{3\alpha} & v_{3\beta} & 1 \\ v_{4\alpha} & v_{4\beta} & 1 \end{bmatrix} \begin{bmatrix} a_2 \\ b_2 \\ c_2 \end{bmatrix} = \begin{bmatrix} v_{2o} \\ v_{3o} \\ v_{4o} \end{bmatrix} \tag{I.20}$$

Where: $v_{i\alpha}, v_{i\beta}$, and $v_{io}, i = 1,2,3$ or 4, are the components of the switching vector $v_{i\alpha}$ on $\alpha\beta$o plane.

The localization condition of this tetrahedron is given by:

$$\begin{aligned} U_o^* &< a_1 U_\alpha^* + b_1 U_\beta^* + c_1 \\ U_o^* &\geq a_2 U_\alpha^* + b_2 U_\beta^* + c_2 \end{aligned} \tag{I.21}$$

I.3.2. Duration time calculation

In order to minimize the switching losses and to reduce the current ripple, switching vectors adjacent to the reference vector should be selected [48-51]. At any sampling instant, the tip of the voltage vector lies in a tetrahedron formed by the four switching vectors. The on-duration time intervals of each vector are obtained in accordance to the average value principle, which is given by [60]:

$$\begin{aligned} v_1 t_1 + v_2 t_2 + v_3 t_3 + v_4 t_4 &= U^* T_s \\ t_1 + t_2 + t_2 + t_4 &= T_s \end{aligned} \tag{I.22}$$

Expression (I.22) can by decomposed in the $\alpha\beta o$ coordinates system as follows:

$$\begin{bmatrix} v_{1\alpha} & v_{2\alpha} & v_{3\alpha} & v_{4\alpha} \\ v_{1\beta} & v_{2\beta} & v_{3\beta} & v_{4\beta} \\ v_{1o} & v_{2o} & v_{3o} & v_{4o} \\ 1 & 1 & 1 & 1 \end{bmatrix} \begin{bmatrix} t_1 \\ t_2 \\ t_3 \\ t_4 \end{bmatrix} = \begin{bmatrix} U_\alpha^* T_s \\ U_\beta^* T_s \\ U_o^* T_s \\ T_s \end{bmatrix} \tag{I.23}$$

With the proposed algorithm, the on duration time intervals are calculated only in the first sector.

I.3.3. Pulse generation

The pulses are generated only in the first sector, the other sectors can deduced by simply interchanging the states of the output phases, each prism or switching vector in the first sector has an equivalence prism or switching vector in others sectors. This equivalence is detailed as follows:

- In odd sectors (3 and 5), we can find the equivalent vectors by rotating the first sector at an angle of $2\pi/3$ for sector 3 and $4\pi/3$ for sector 5.

- In pair sectors (2, 4 and 6), the equivalent vectors in the pair sectors can be determined by the projection of each vector of the first sector on the symmetry axis in pair sectors. The symmetry axis necessary to find the equivalence vectors in sector 2 is (Δ_1) (see figure (I.8)). The symmetry axis (Δ_2) is used for sector 4, and (Δ_3) for sector 6.

The states interchanging are given in table (I.2).

Table (I.2): Interchanging the switching states in all sectors

S_1	S_2	S_3	S_4	S_5	S_6
a	$a \to b$	$a \to b$	$a \to a$	$a \to c$	$a \to c$
b	$b \to a$	$b \to c$	$b \to c$	$b \to a$	$b \to b$
c	$c \to c$	$c \to a$	$c \to b$	$c \to b$	$c \to a$
n	$n \to n$	$n \to n$	$n \to n$	$n \to n$	$n \to n$

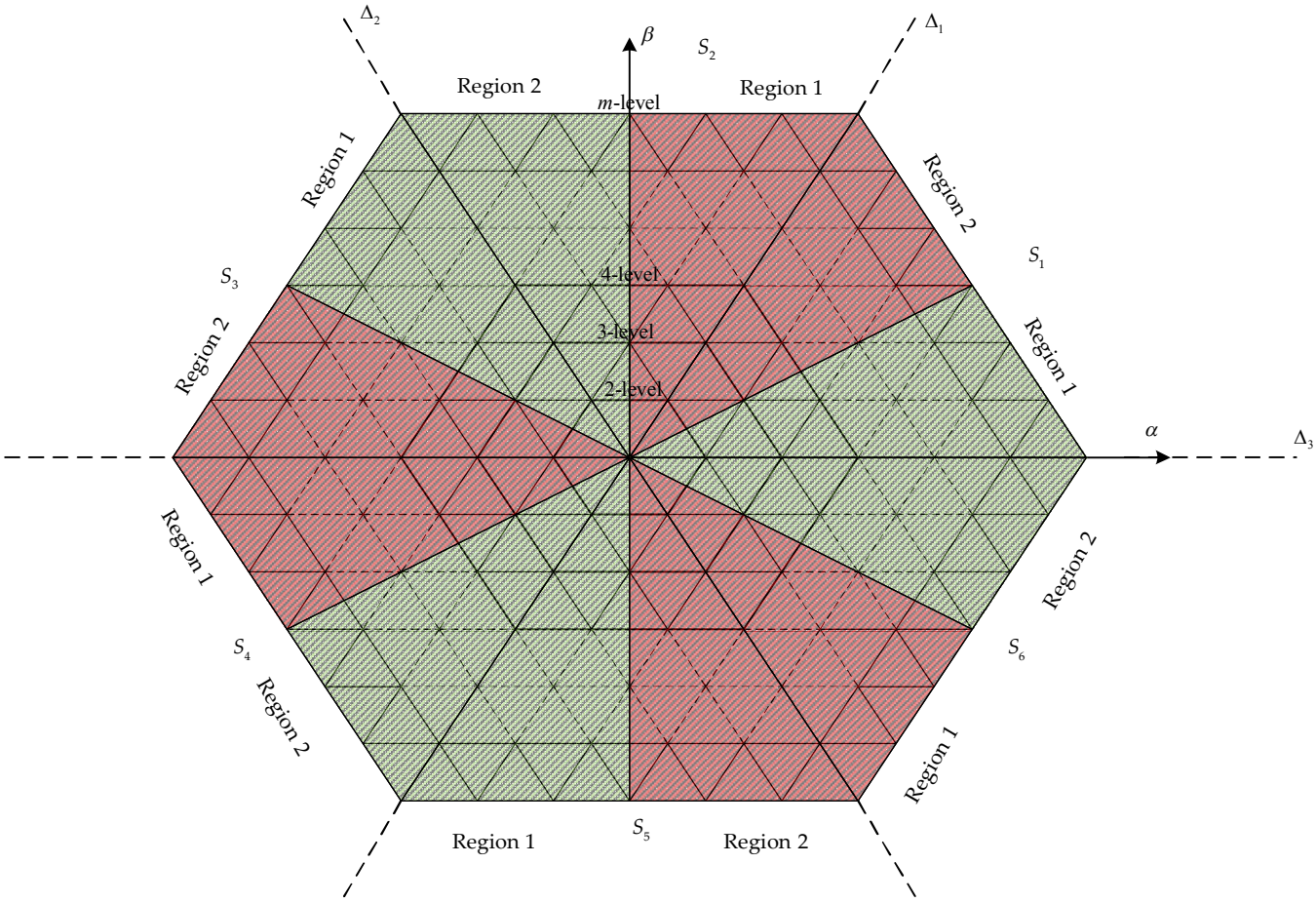

Figure (I.8): Switching vectors equivalences between the first sector and other sectors for an m-level four-leg inverter in $\alpha\beta$ plane

Finely, the implementation procedure of the proposed 3DSVM algorithm is summarized in figure (I.9).

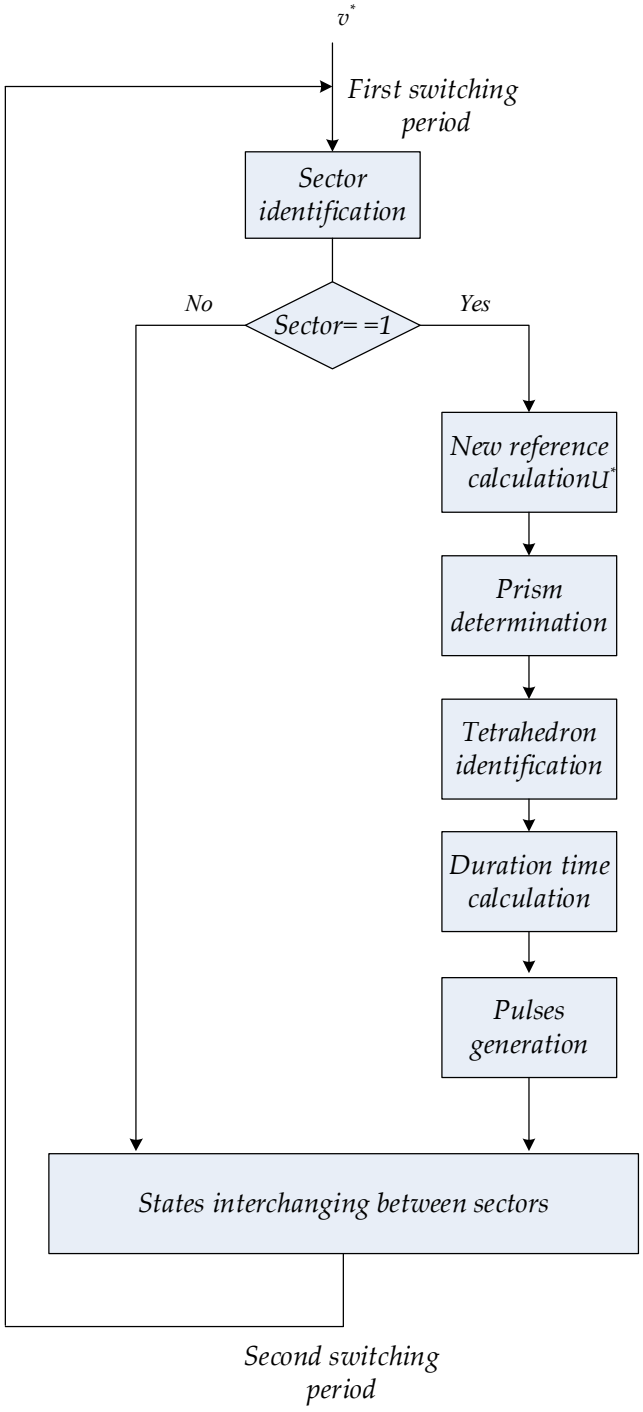

Figure (I.9): Schematic diagram of the proposed 3DSVM algorithm

I.4. Simulation Results

The validity of mathematical analysis and the feasibility of the proposed 3DSVM algorithm are verified by time-domain simulation studies for *m*-level four-leg inverter (*m* = 2, 3, 5).
The inverter's load is an inductive load (R=50Ω, L=20mH), the switching frequency is f_s =2 kHz, and the input voltage of the inverter is set to v_{dc} = 20 kV. In case of $m > 2$, the capacitors voltages are considered as ideal DC sources.

After 0.03 s, the amplitude of the reference voltage of phase (b) is reduced to 50% in order to induce an unbalanced reference voltage.

Figures (I.10), (I.12) and (I.14) show the waveforms of the output voltages and currents of *m*-level four-leg inverters (*m*= 2, 3, 5) respectively, these results are consistent with the analytical waveforms and demonstrate feasibility of the proposed algorithm for four-leg inverters with different number of levels. The improvement in the calculation overhead time is more significant as the number of levels increases.

The frequency spectrum of output voltage and current of the a-phase are presented in figure (I.11), (I.13), and (I.15) for (*m*= 2, 3, 5) respectively. Comparing the performance obtained in the case of the five-level inverter with the others levels (two and three levels), we find that under the same operating conditions (same switching frequency and the same modulation index M=0.8), the five-level four-leg inverter produces output voltage/current with less harmonics (25.07% for voltage and 1.29% for current).

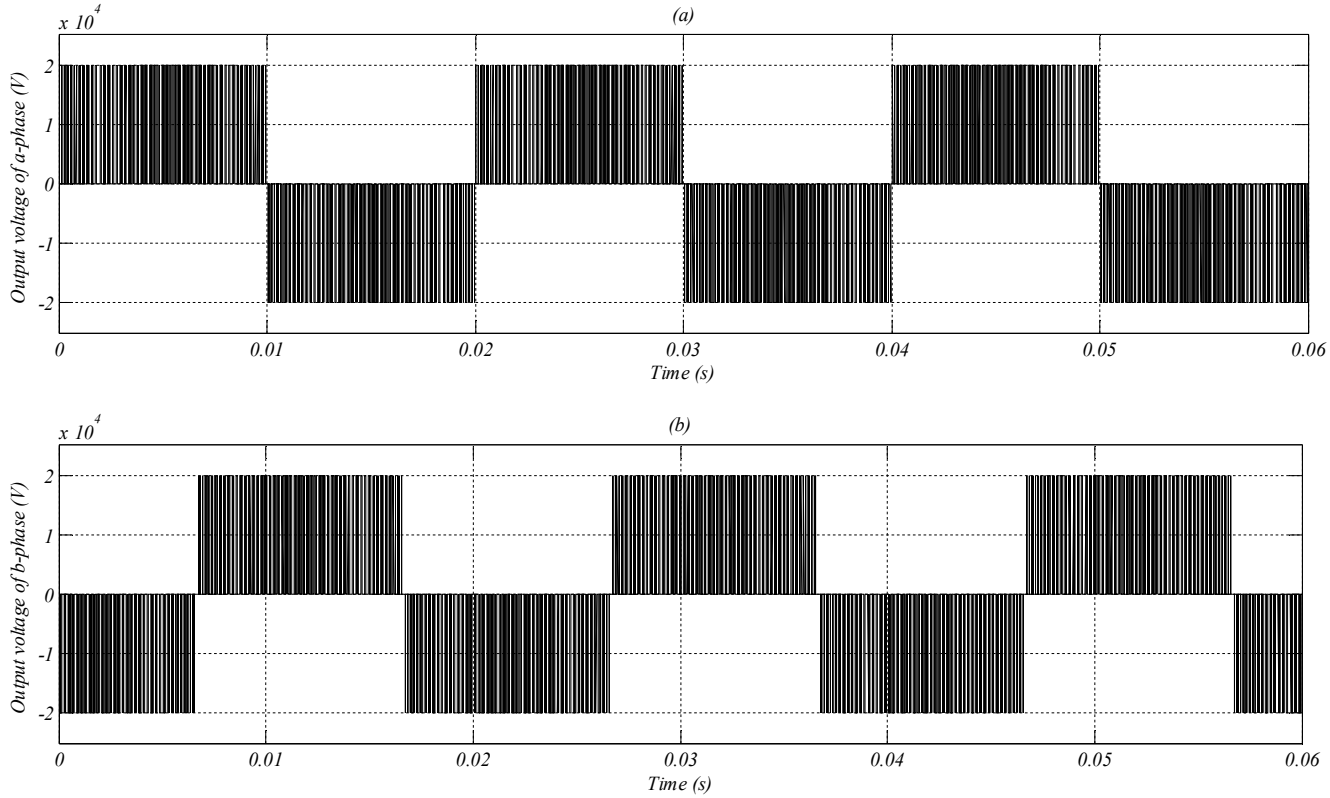

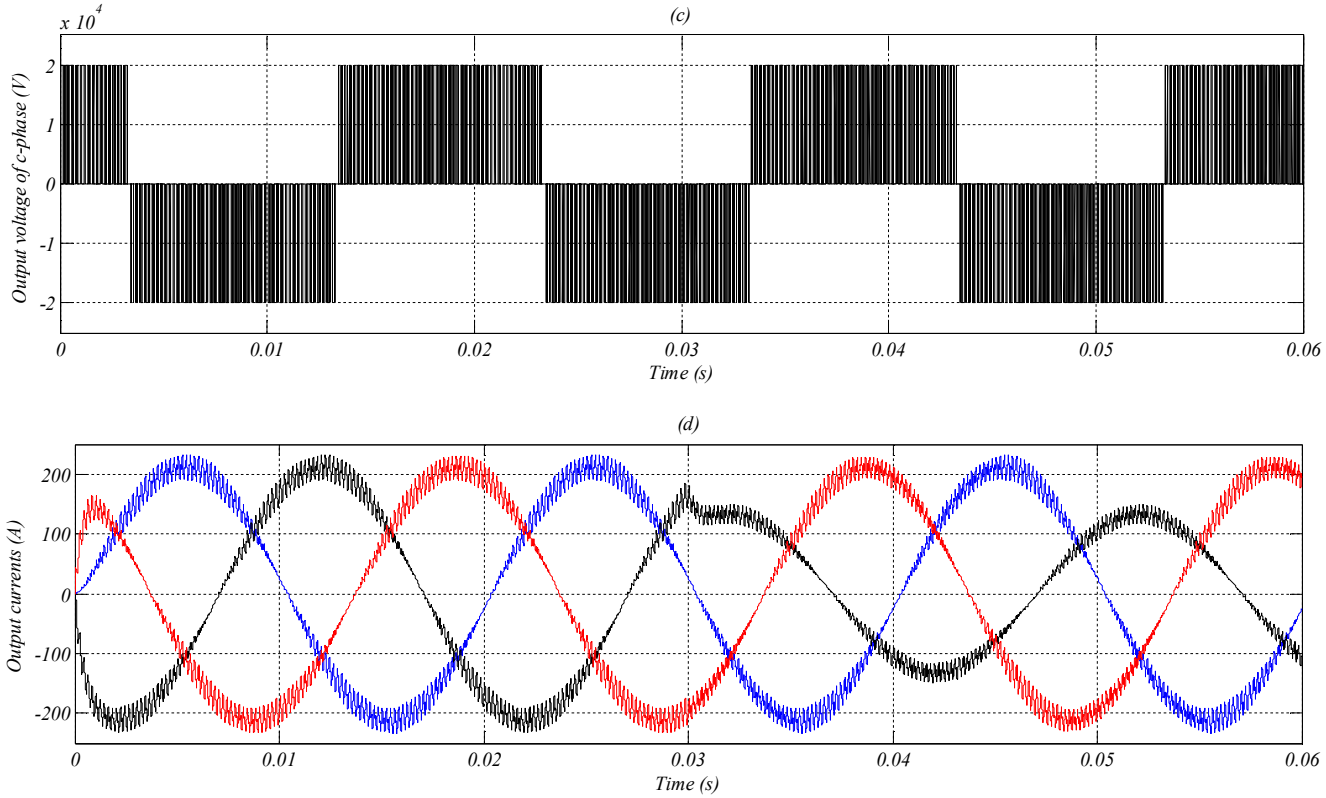

Figure (I.10): Output voltages and currents waveforms of a two-level four-leg inverter

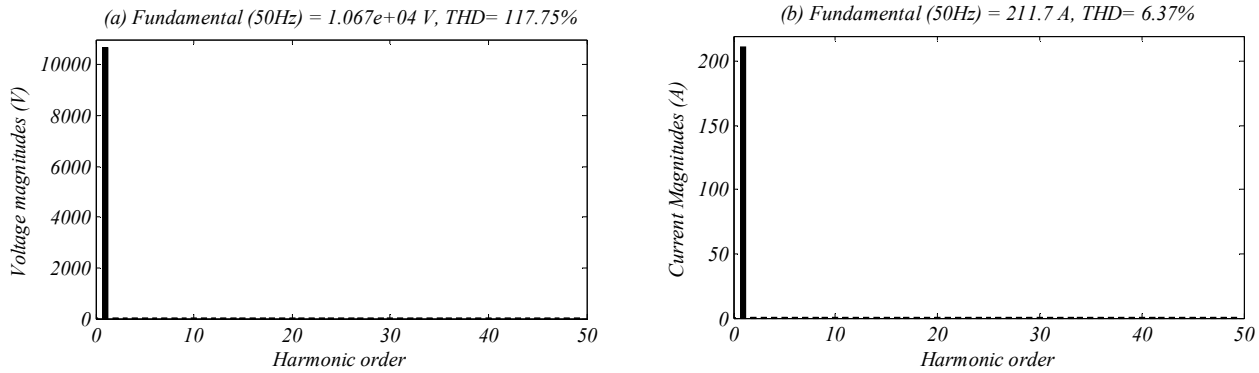

Figure (I.11): Frequency spectrum in case of two-level four-leg inverter, (a): Output voltage, (b): Output current

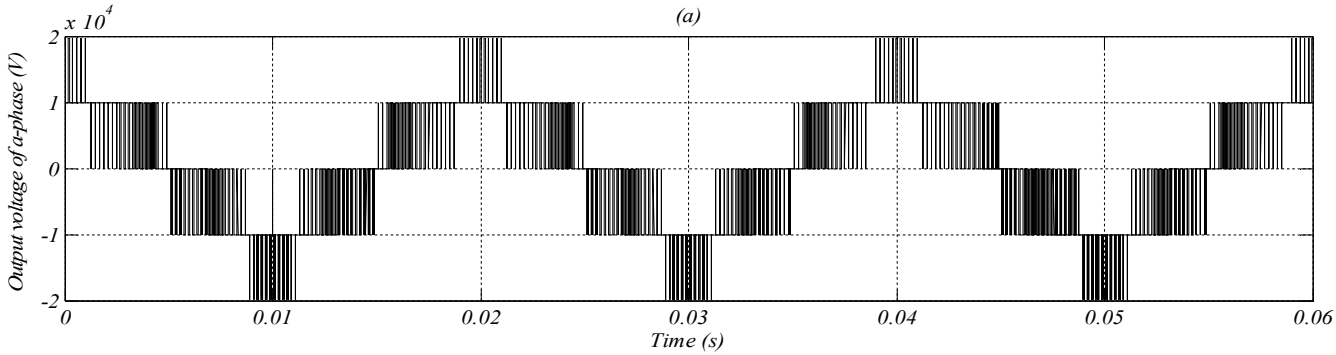

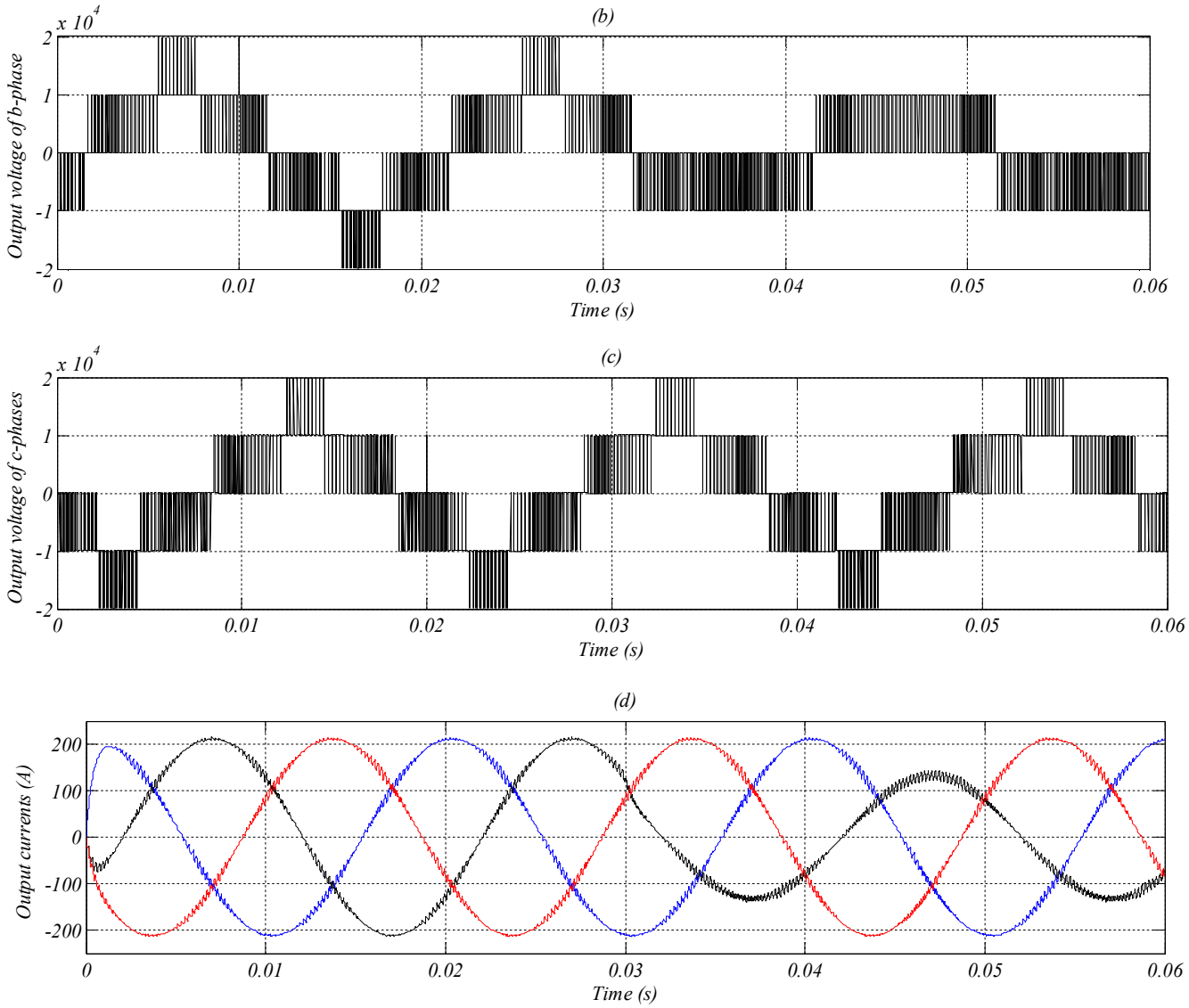

Figure (I.12): Output voltages and currents waveforms of a three-level four-leg inverter

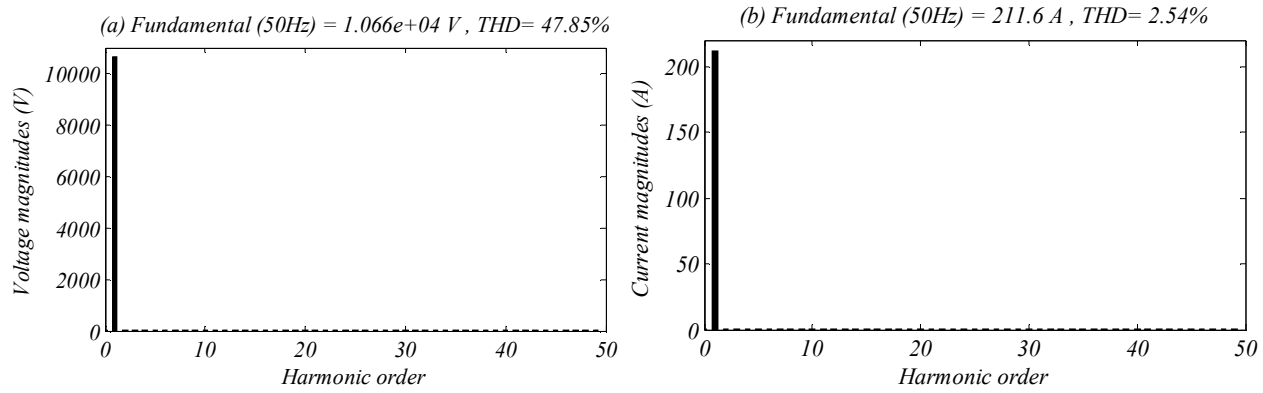

Figure (I.13): Frequency spectrum in case of three-level four-leg inverter, (a): Output voltage, (b): Output current

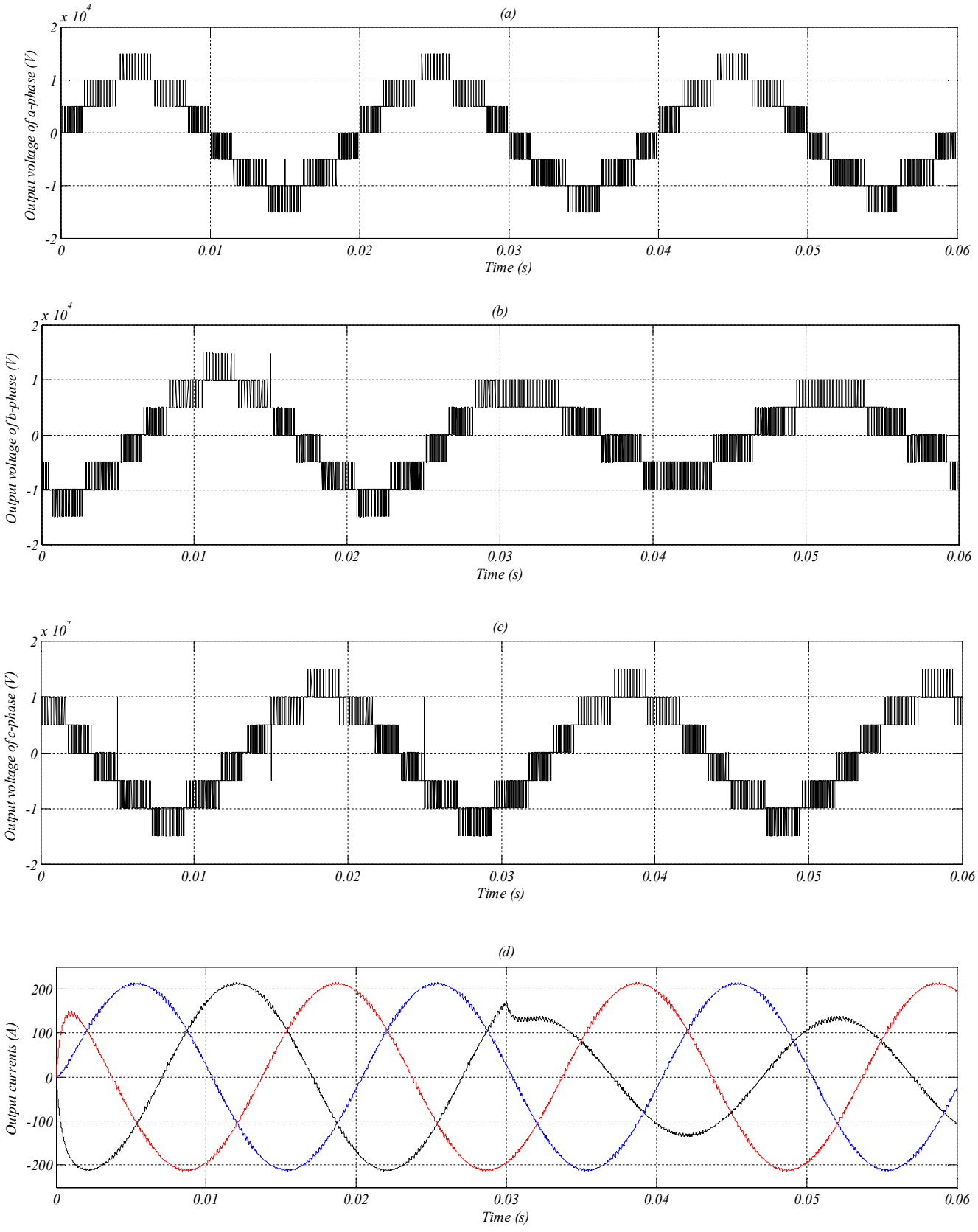

Figure (I.14): Output voltages and currents waveforms of a five-level four-leg inverter

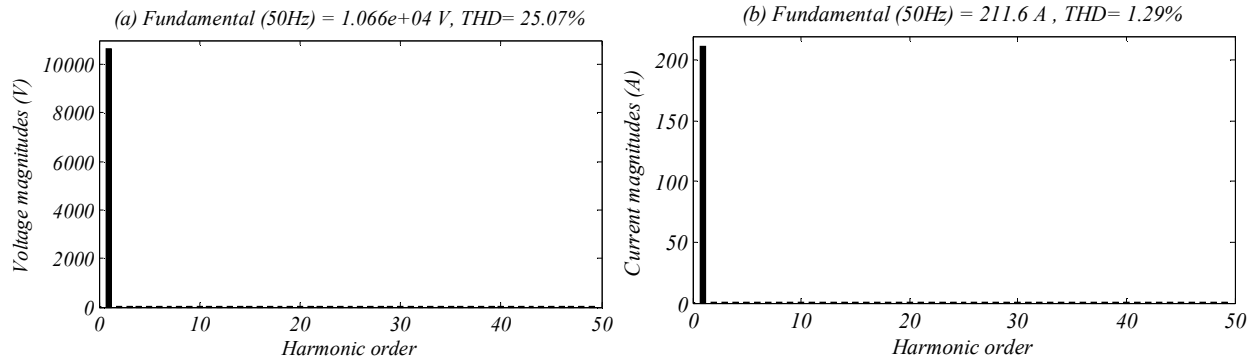

Figure (I.15): Frequency spectrum in case of five-level four-leg inverter, (a): Output voltage, (b): Output current

Figure (I.16) shows the voltage and current THD comparison between five, three and tow-level four-leg inverters at a unity power factor for different values of the modulation index. The both voltage and current THDs for five-level inverter are better than the ones of three and tow-level forms.

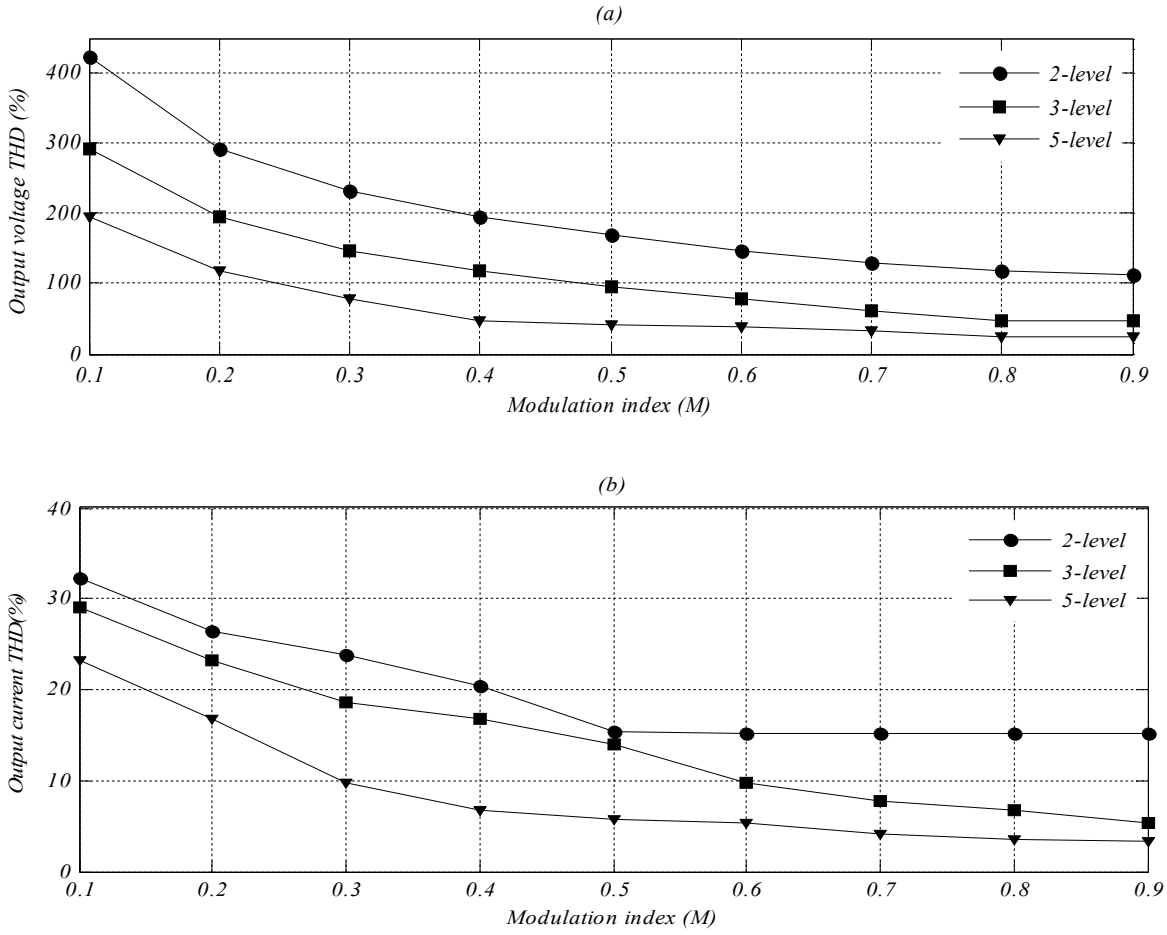

Figure (I.16) : Total harmonic distortion versus modulation index, (a) : Output voltage THD, (b) : Output current THD

Figure (I.17) illustrates the THD evolution for different values of the switching frequency at unity power factor and *M*= 0.8, one notices well that the THD decreases remarkably

with increase of the switching frequency. It can be concluded that the five-level four-leg inverter can operated with reduced switching frequency (1-2 kHz). However, to meet the internationals standards such as IEC and IEEE 519, a minimum of 2 kHz is required for five-level four-leg inverter.

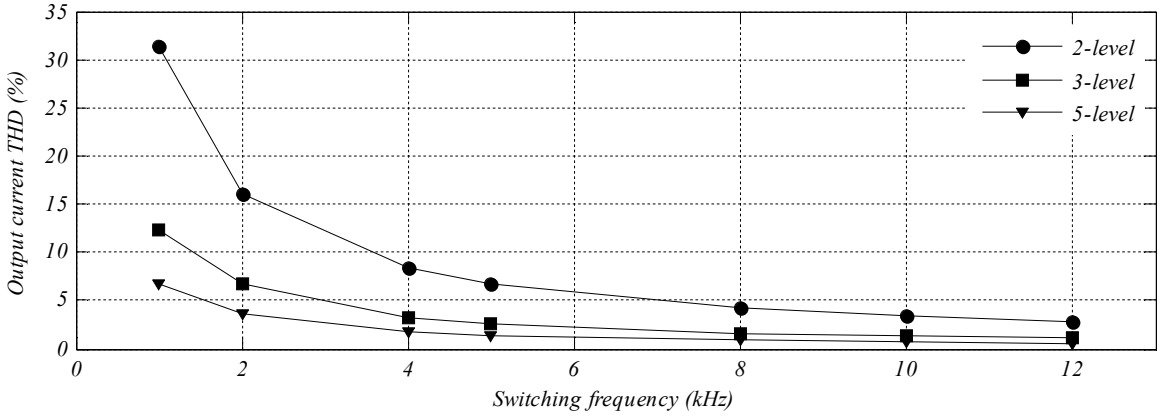

Figure (I.17): Total harmonic distortion of output current versus switching frequency

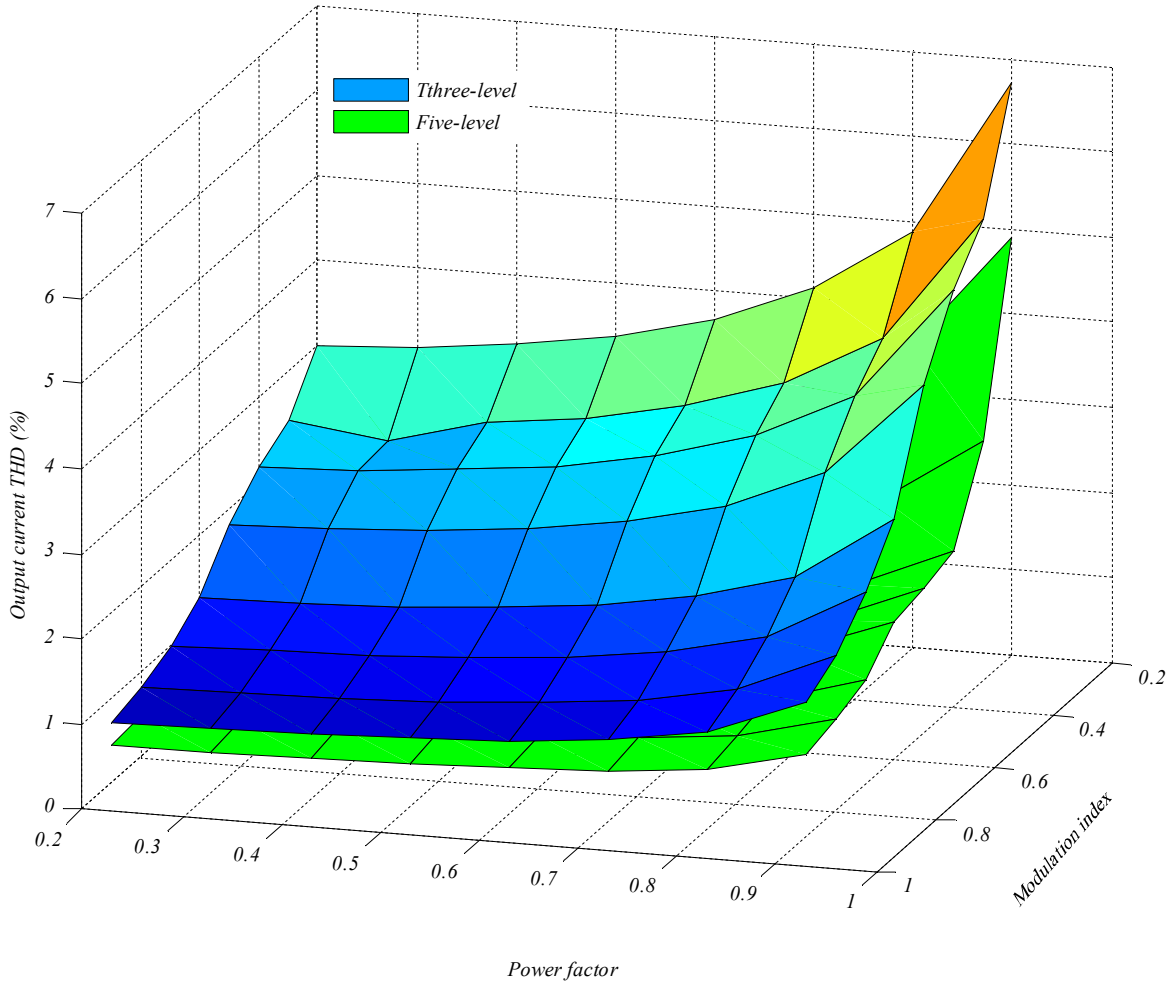

Figure (I.18): Total harmonic distortion of output current versus modulation index and load power factor

Figure (I.18) presents three-dimensional representation of current THD with two variables (modulation index and power factor). The THD decrease with increasing of the modulation index; and decreasing of the power factor. This figure confirms that the five-level inverter current harmonics are lower than three-level inverter. The THD range of five-level inverter varies between 0.44% and 4.8% whereas for the three-level inverter THD varies between 1% and 6.7%.

I.5. Capacitor voltages balancing of five-level four-leg diode clamped inverter

The balance of the DC capacitor voltages is one of the most important drawbacks of this type of inverter topologies, if any unbalance in the DC capacitor voltages appears, the output phase voltages/currents have distortion and the harmonic content of the output signals decreases their quality [50-51].
Several approaches have been suggested to balance the DC capacitor voltages of diode clamped inverter [50-54]. In general, these schemes can be categorized into three major types. The first scheme [52] involves auxiliary balancing circuits, which incurs additional hardware costs. Second approach is applicable for the back-to-back converter topologies [53-54], where voltage balancing is achieved with the help of second converter; however, it is impractical for the stand-alone diode clamped inverter applications [53-54]. The third approach for voltage balancing involves utilizing the redundancy in the switching patterns for the different control strategies [50-51]. This method has attained more focus these days, because no additional hardware cost is required and implementation becomes more feasible for the advancement of high performance DSPs [50-51, 60].
The balancing problem of the DC-link voltages can be solved using the redundant vectors due to their effect on the DC-link capacitor voltages [50-51, 60].
This section shows clearly that the balancing problem of the DC-link voltages in the five-level four-leg inverter can be solved using the redundant vectors in a similar way used in three-leg one.

Before addressing the problem of voltage unbalance, we present the modeling of five-level four-leg inverter and the detail of its 3DSVM algorithm.

I.5.1. Modeling of four-leg five-level inverter

The five-level four-leg inverter is shown in figure (I.19). The switching states and the resultant phase voltages are listed in table (I.3).

The switching functions of the five level inverter of figure (I.19) are expressed as:

$$\begin{aligned} F_{x4} &= S_{x4}\ S_{x3}\ S_{x2}\ S_{x1} \\ F_{x3} &= S_{x4}\ S_{x3}\ S_{x2}\ \overline{S}_{x1} \\ F_{x2} &= S_{x4}\ S_{x3}\ \overline{S}_{x2}\ \overline{S}_{x1} \\ F_{x1} &= S_{x4}\ \overline{S}_{x3}\ \overline{S}_{x2}\ \overline{S}_{x1} \\ F_{x0} &= \overline{S}_{x4}\ \overline{S}_{x3}\ \overline{S}_{x2}\ \overline{S}_{x1} \end{aligned} \qquad x = a,b,c \text{ or } n \qquad \text{(I.24)}$$

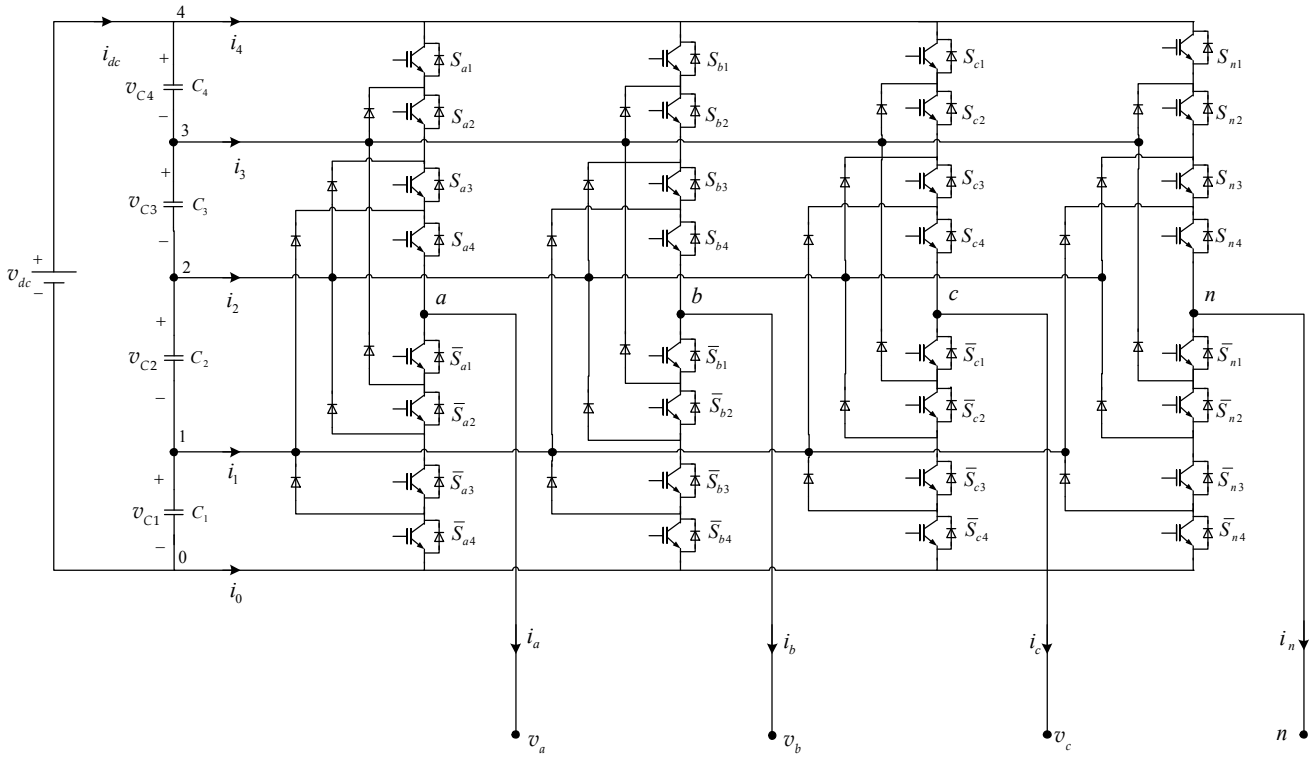

Figure (I.19): Schematic representation of five-level four-leg inverter

The output voltages are given in the following matrix form:

$$\begin{bmatrix} v_{a0} \\ v_{b0} \\ v_{c0} \\ v_{n0} \end{bmatrix} = \begin{bmatrix} F_{a4} & F_{a3} & F_{a2} & F_{a1} \\ F_{b4} & F_{b3} & F_{b2} & F_{b1} \\ F_{c4} & F_{c3} & F_{c2} & F_{c1} \\ F_{n4} & F_{n3} & F_{n2} & F_{n1} \end{bmatrix} \begin{bmatrix} v_{C4}+v_{C3}+v_{C2}+v_{C1} \\ v_{C3}+v_{C2}+v_{C1} \\ v_{C2}+v_{C1} \\ v_{C1} \end{bmatrix} \tag{I.25}$$

Where:

v_{Cj}, (j = 1, 2, 3, 4) : are capacitor voltages.

Table (I.3): Switching states of one leg of five-level four-leg inverter

Switching States	S_{x1}	S_{x2}	S_{x3}	S_{x4}	$\bar{S}_{x1}$	$\bar{S}_{x2}$	$\bar{S}_{x3}$	$\bar{S}_{x4}$	**Output phase voltage** v_{x0}
4	1	1	1	1	0	0	0	0	v_{dc}
3	0	1	1	1	1	0	0	0	$v_{C3}+v_{C2}+v_{C1}$
2	0	0	1	1	1	1	0	0	$v_{C2}+v_{C1}$
1	0	0	0	1	1	1	1	0	v_{C1}
0	0	0	0	0	1	1	1	1	0

The output phase to neutral voltages v_a, v_b and v_c can be expressed as:

$$\begin{bmatrix} v_a \\ v_b \\ v_c \end{bmatrix} = \begin{bmatrix} F_{a4}-F_{n4} & F_{a3}-F_{n3} & F_{a2}-F_{n2} & F_{a1}-F_{n1} \\ F_{b4}-F_{n4} & F_{b3}-F_{n3} & F_{b2}-F_{n2} & F_{b1}-F_{n1} \\ F_{c4}-F_{n4} & F_{c3}-F_{n3} & F_{c2}-F_{n2} & F_{c1}-F_{n1} \end{bmatrix} \begin{bmatrix} v_{C4}+v_{C3}+v_{C2}+v_{C1} \\ v_{C3}+v_{C2}+v_{C1} \\ v_{C2}+v_{C1} \\ v_{C1} \end{bmatrix} \quad \text{(I.26)}$$

The input current of the inverter is expressed as a function of the output current i_a, i_b, i_c and i_n through the switching functions by the following relationships:

$$\begin{aligned} i_4 &= F_{a4}i_a + F_{b4}i_b + F_{c4}i_c + F_{n4}i_n \\ i_3 &= F_{a3}i_a + F_{b3}i_b + F_{c3}i_c + F_{n3}i_n \\ i_2 &= F_{a2}i_a + F_{b2}i_b + F_{c2}i_c + F_{n2}i_n \\ i_1 &= F_{a1}i_a + F_{b1}i_b + F_{c1}i_c + F_{n1}i_n \\ i_0 &= F_{a0}i_a + F_{b0}i_b + F_{c0}i_c + F_{n0}i_n \end{aligned} \quad \text{(I.27)}$$

I.5.2. Three-dimensional diagram representation

As presented in figure (I.20), there are five zero switching vectors (4444 3333 2222, 1111, 0000), and (5^4-5) non-zero switching vectors. All the 5^4 switching vectors can be stored into 25 layers as shown in figure (I.21).

The diagram of space vectors can be divided into six sectors, and each sector is divided into sixteen prisms.

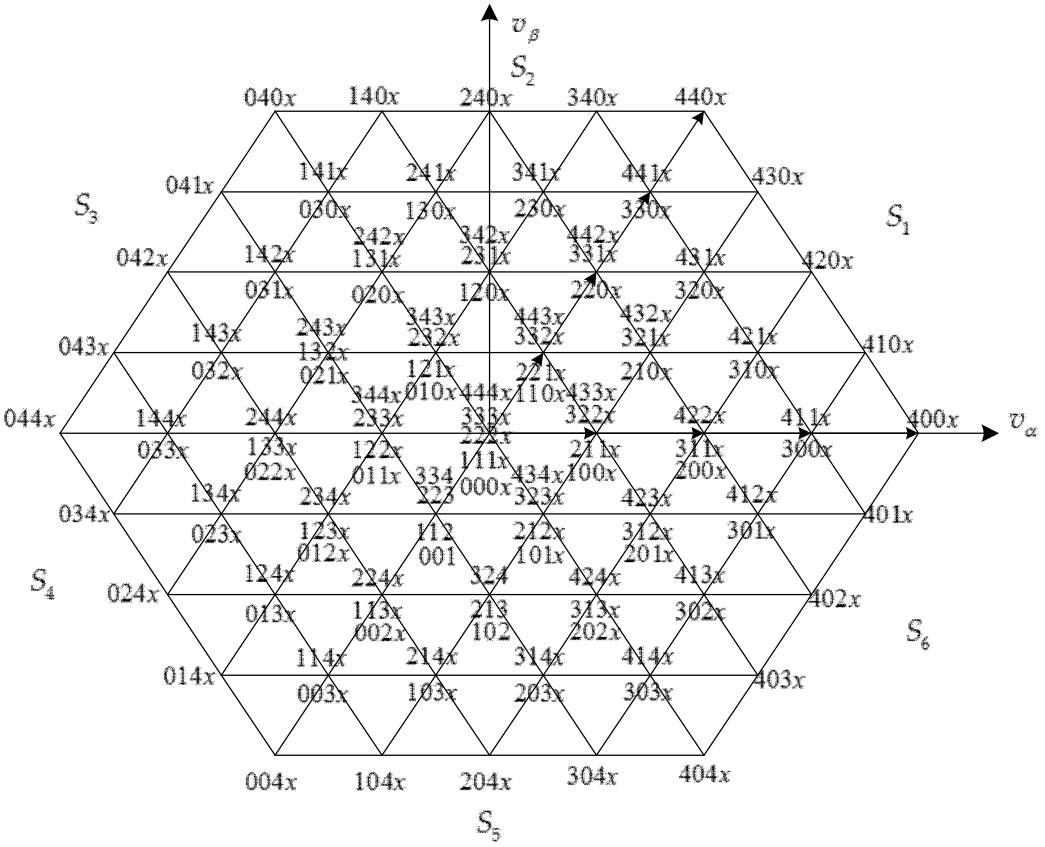

Figure (I.20): Space voltage vectors for a five-level four-leg inverter on αβ plane (x=0, 1, 2, 3, or 4)

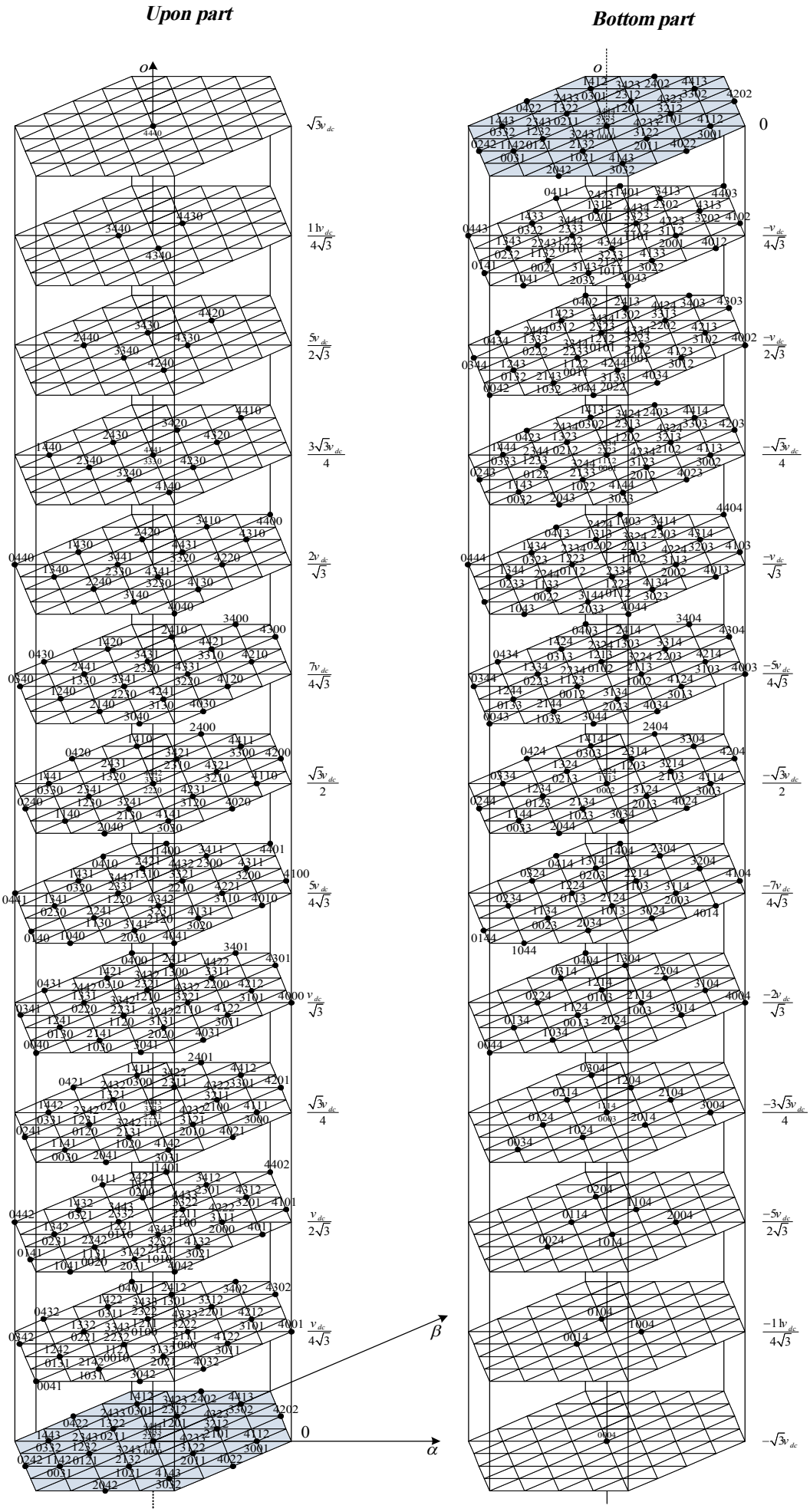

Figure (I.21): Three-dimensional representation of switching voltages vectors in αβo coordinates of five-level four-leg inverter

I.5.3. Determination of the space vector location

Step 1: Sector number computation

The sector numbers are given by equation (I.12).

Step 2: Prisms identification

The normalized projected components are U_1^* and U_2^* given by (I.15) which becomes:

$$\begin{aligned} U_1^* &= 4M\left(U_{\alpha\beta}^*\cos(\psi)-\frac{U_{\alpha\beta}^*}{\sqrt{3}}\sin(\psi)\right) \\ U_2^* &= 4M\left(\frac{2}{\sqrt{3}}U_{\alpha\beta}^*\sin(\psi)\right) \end{aligned} \tag{I.28}$$

Figure (I.22) shows the projection of U^* in the first sector.

According to the integers of equation (I.16), the first sector prisms identifications presented in figure (I.22) is summarized in table (I.4).

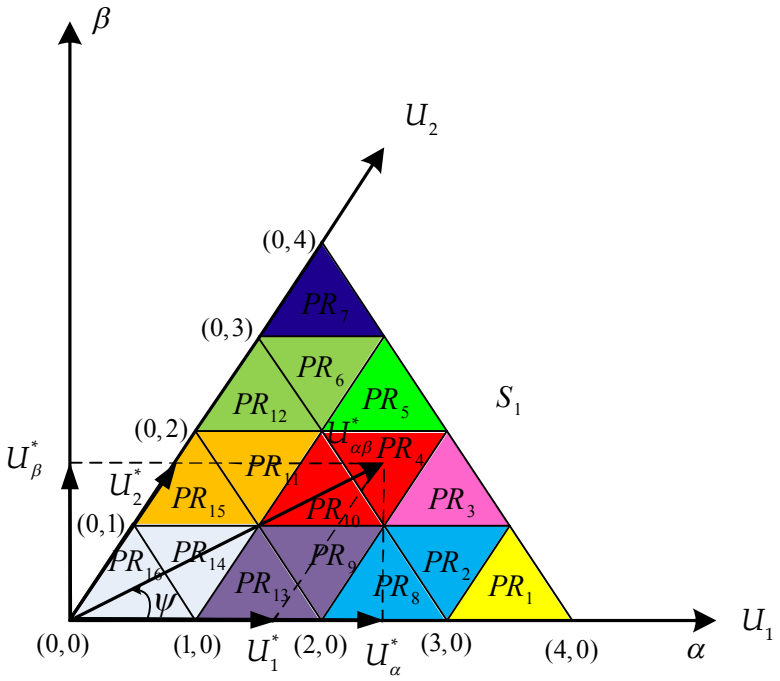

Figure (I.22): Space voltage vectors for a five-level four-leg inverter in the first sector

Table (I.4): Prism identification in the first sector

l_1	l_2	$PR_i \ (i \in \{1,..,16\})$
0	0	PR_{16} if $(U_1^* + U_2^* < 1)$
		PR_{14} if $(U_1^* + U_2^* \geq 1)$
1	0	PR_{13} if $(U_1^* + U_2^* < 2)$
		PR_9 if $(U_1^* + U_2^* \geq 2)$
2	0	PR_8 if $(U_1^* + U_2^* < 3)$
		PR_2 if $(U_1^* + U_2^* \geq 3)$
3	0	PR_1
0	1	PR_{15} if $(U_1^* + U_2^* < 2)$
		PR_{11} if $(U_1^* + U_2^* \geq 2)$
1	1	PR_{10} if $(U_1^* + U_2^* < 3)$
		PR_4 if $(U_1^* + U_2^* \geq 3)$
2	1	PR_3
0	2	PR_{12} if $(U_1^* + U_2^* < 3)$
		PR_6 if $(U_1^* + U_2^* \geq 3)$
1	2	PR_5^S
0	3	PR_7

Step 3: Tetrahedron identification

Each tetrahedron formed by four switching vectors and limited by four planes. Table (I.5) present the number of tetrahedrons in each prism of five –level four-leg inverter.

Table (I.5): Number of tetrahedrons in each prism of the first sector

Prism (PR_i)	*Number of tetrahedrons*
PR_1, PR_3, PR_5, and PR_7	13
PR_2, PR_4, and PR_6	14
PR_8, PR_{10}, and PR_{12}	16
PR_9, and PR_{11}	17
PR_{13}, and PR_{15}	19
PR_{14}	20
PR_{16}	22

As given in section I and equations (I.19), (I.20), (I.21) the localization condition of all tetrahedrons located in each prism of the first sector are summarized in table (A.1) of appendix.

I.5.4. Duration time calculation

In each tetrahedron of the first sector, we have an equation like (I.23), which must be solved. All matrixes of all tetrahedrons are given in table (A.2) of appendix .

I.5.5. Pulse generation

The generation of the pulses in all tetrahedrons of the first sector is not necessary, because it exists an equivalence between switching states of some tetrahedrons located in the same prism as clarified in table (I.6).

Table (I.6): Interchanging the switching states of each tetrahedron located in the same prism for the first sector

PR_1	TeT_1^1	TeT_2^1	TeT_3^1
	$a\ b\ c\ n$	$a \to a,\ b \to b,\ c \to n,\ n \to c$	$a \to a,\ b \to n,\ c \to b,\ n \to c$
	TeT_{12}^1		TeT_{13}^1
	$a\ b\ c\ n$		$a \to n,\ b \to b,\ c \to c,\ n \to a$
	No corresponding of $TeT_4^1, TeT_5^1, TeT_6^1, TeT_7^1, TeT_8^1, TeT_9^1, TeT_{10}^1$, and TeT_{11}^1		
PR_2	TeT_4^2		TeT_5^2
	$a\ b\ c\ n$		$a \to a,\ b \to n,\ c \to c,\ n \to b$
	TeT_{12}^2		TeT_{13}^2
	$a\ b\ c\ n$		$a \to n,\ b \to b,\ c \to c,\ n \to a$
	No corresponding of $TeT_1^2, TeT_2^2, TeT_3^2, TeT_6^2, TeT_7^2, TeT_8^2, TeT_9^2, TeT_{10}^2, TeT_{11}^2$, and TeT_{14}^2		
PR_3	TeT_1^3		TeT_2^3
	$a\ b\ c\ n$		$a \to a,\ b \to b,\ c \to n,\ n \to c$
	TeT_5^3		TeT_6^3
	$a\ b\ c\ n$		$a \to a,\ b \to n,\ c \to c,\ n \to b$
	TeT_{12}^3		TeT_{13}^3
	$a\ b\ c\ n$		$a \to n,\ b \to b,\ c \to c,\ n \to a$
	No corresponding of $TeT_3^3, TeT_4^3, TeT_7^3, TeT_8^3, TeT_9^3, TeT_{10}^3$, and TeT_{11}^3		
PR_4	TeT_2^4		TeT_3^4
	$a\ b\ c\ n$		$a \to a,\ b \to b,\ c \to n,\ n \to c$
	TeT_7^4		TeT_8^4
	$a\ b\ c\ n$		$a \to a,\ b \to n,\ c \to c,\ n \to b$
	TeT_{12}^4		TeT_{13}^4
	$a\ b\ c\ n$		$a \to n,\ b \to b,\ c \to c,\ n \to a$
	No corresponding of $TeT_1^4, TeT_4^4, TeT_5^4, TeT_6^4, TeT_9^4, TeT_{10}^4, TeT_{11}^4$, and TeT_{14}^4		
	TeT_1^5		TeT_2^5

PR_5	$a\ b\ c\ n$		$a \to a,\ b \to b,\ c \to n,\ n \to c$	
	TeT_8^5		TeT_9^5	
	$a\ b\ c\ n$		$a \to a,\ b \to n,\ c \to c,\ n \to b$	
	TeT_{12}^5		TeT_{13}^5	
	$a\ b\ c\ n$		$a \to n,\ b \to b,\ c \to c,\ n \to a$	
	No corresponding of $TeT_3^5, TeT_4^5, TeT_5^5, TeT_6^5, TeT_7^5, TeT_{10}^5$, and TeT_{11}^5			
PR_6	TeT_2^6		TeT_3^6	
	$a\ b\ c\ n$		$a \to a,\ b \to b,\ c \to n,\ n \to c$	
	TeT_{10}^6		TeT_{11}^6	
	$a\ b\ c\ n$		$a \to a,\ b \to n,\ c \to c,\ n \to b$	
	TeT_{12}^6		TeT_{13}^6	
	$a\ b\ c\ n$		$a \to n,\ b \to b,\ c \to c,\ n \to a$	
	No corresponding of $TeT_1^6, TeT_4^6, TeT_5^6, TeT_6^6, TeT_7^6, TeT_8^6, TeT_9^6$, and TeT_{14}^6			
PR_7	TeT_1^7		TeT_2^7	
	$a\ b\ c\ n$		$a \to a,\ b \to b,\ c \to n,\ n \to c$	
	TeT_{11}^7	TeT_{12}^7	TeT_{13}^7	
	$a\ b\ c\ n$	$a \to a,\ b \to n,\ c \to c,\ n \to b$	$a \to b,\ b \to n,\ c \to c,\ n \to a$	
	No corresponding of $TeT_3^7, TeT_4^7, TeT_5^7, TeT_6^7, TeT_7^7, TeT_9^7$, and TeT_{10}^7			
PR_8	TeT_4^8	TeT_5^8	TeT_6^8	
	$a\ b\ c\ n$	$a \to a,\ b \to b,\ c \to n,\ n \to c$	$a \to a,\ b \to n,\ c \to b,\ n \to c$	
	TeT_{11}^8	TeT_{12}^8	TeT_{13}^8	TeT_{11}^8
	TeT_{12}^8		TeT_{13}^8	
	$a\ b\ c\ n$		$a \to n,\ b \to b,\ c \to c,\ n \to a$	
	No corresponding of $TeT_1^8, TeT_2^8, TeT_7^8, TeT_8^8, TeT_9^8, TeT_{10}^8, TeT_{11}^8, TeT_{14}^8, TeT_{15}^8$, and TeT_{16}^8			
PR_9	TeT_5^9		TeT_6^9	
	$a\ b\ c\ n$		$a \to a,\ b \to b,\ c \to n,\ n \to c$	
	TeT_7^9		TeT_8^9	
	$a\ b\ c\ n$		$a \to a,\ b \to n,\ c \to c,\ n \to b$	
	TeT_{12}^9		TeT_{13}^9	
	$a\ b\ c\ n$		$a \to n,\ b \to b,\ c \to c,\ n \to a$	
	No corresponding of $TeT_1^9, TeT_2^9, TeT_3^9, TeT_4^9, TeT_9^9, TeT_{10}^9, TeT_{11}^9, TeT_{14}^9, TeT_{15}^9, TeT_{16}^9$, and TeT_{17}^9			
PR_{10}	TeT_4^{10}		TeT_5^{10}	
	$a\ b\ c\ n$		$a \to a,\ b \to b,\ c \to n,\ n \to c$	
	TeT_8^{10}		TeT_9^{10}	
	$a\ b\ c\ n$		$a \to a,\ b \to n,\ c \to c,\ n \to b$	
	TeT_{12}^{10}		TeT_{13}^{10}	
	$a\ b\ c\ n$		$a \to n,\ b \to b,\ c \to c,\ n \to a$	
	No corresponding of			

	$TeT_1^{10}, TeT_2^{10}, TeT_3^{10}, TeT_6^{10}, TeT_7^{10}, TeT_{10}^{10}, TeT_{11}^{10}, TeT_{14}^{10}, TeT_{15}^{10}$, and TeT_{16}^{10}		
PR_{11}	TeT_5^{11}	TeT_6^{11}	
	$a\ b\ c\ n$	$a \to a,\ b \to b,\ c \to n,\ n \to c$	
	TeT_{10}^{11}	TeT_{11}^{11}	
	$a\ b\ c\ n$	$a \to a,\ b \to n,\ c \to c,\ n \to b$	
	TeT_{12}^{11}	TeT_{13}^{11}	
	$a\ b\ c\ n$	$a \to n,\ b \to b,\ c \to c,\ n \to a$	
	No corresponding of $TeT_1^{11}, TeT_2^{11}, TeT_3^{11}, TeT_4^{11}, TeT_7^{11}, TeT_8^{11}, TeT_{11}^{11}, TeT_{14}^{11}, TeT_{15}^{11}, TeT_{16}^{11}$, and TeT_{17}^{11}		
PR_{12}	TeT_4^{12}	TeT_5^{12}	
	$a\ b\ c\ n$	$a \to a,\ b \to b,\ c \to n,\ n \to c$	
	TeT_{11}^{12}	TeT_{12}^{12}	TeT_{13}^{12}
	$a\ b\ c\ n$	$a \to a,\ b \to n,\ c \to c,\ n \to b$	$a \to b,\ b \to n,\ c \to c,\ n \to a$
	No corresponding of $TeT_1^{12}, TeT_2^{12}, TeT_3^{12}, TeT_4^{12}, TeT_7^{12}, TeT_8^{12}, TeT_{11}^{12}, TeT_{14}^{12}, TeT_{15}^{12}, TeT_{16}^{12}$, and TeT_{17}^{12}		
PR_{13}	TeT_7^{13}	TeT_8^{13}	TeT_9^{13}
	$a\ b\ c\ n$	$a \to a,\ b \to b,\ c \to n,\ n \to c$	$a \to a,\ b \to n,\ c \to b,\ n \to c$
	TeT_{12}^{13}	TeT_{13}^{13}	
	$a\ b\ c\ n$	$a \to n,\ b \to b,\ c \to c,\ n \to a$	
	No corresponding of $TeT_1^{13}, TeT_2^{13}, TeT_3^{13}, TeT_4^{13}, TeT_5^{13}, TeT_6^{13}, TeT_{10}^{13}, TeT_{11}^{13}, TeT_{14}^{13} TeT_{15}^{13}, TeT_{16}^{13}, TeT_{17}^{13}, TeT_{18}^{13}$, and TeT_{19}^{13}		
PR_{14}	TeT_8^{14}	TeT_9^{14}	
	$a\ b\ c\ n$	$a \to a,\ b \to b,\ c \to n,\ n \to c$	
	TeT_{10}^{14}	TeT_{11}^{14}	
	$a\ b\ c\ n$	$a \to a,\ b \to n,\ c \to c,\ n \to b$	
	TeT_{12}^{14}	TeT_{13}^{14}	
	$a\ b\ c\ n$	$a \to n,\ b \to b,\ c \to c,\ n \to a$	
	No corresponding of $TeT_1^{14}, TeT_2^{14}, TeT_3^{14}, TeT_4^{14}, TeT_5^{14}, TeT_6^{14}, TeT_7^{14}, TeT_{14}^{14} TeT_{15}^{14}, TeT_{16}^{14}, TeT_{17}^{14}, TeT_{18}^{14}, TeT_{19}^{14}$ and TeT_{20}^{14}		
PR_{15}	TeT_7^{15}	TeT_8^{15}	
	$a\ b\ c\ n$	$a \to a,\ b \to b,\ c \to n,\ n \to c$	
	TeT_{11}^{15}	TeT_{12}^{15}	TeT_{13}^{15}
	$a\ b\ c\ n$	$a \to a,\ b \to n,\ c \to c,\ n \to b$	$a \to n,\ b \to a,\ c \to c,\ n \to b$
	No corresponding of $TeT_1^{15}, TeT_2^{15}, TeT_3^{15}, TeT_4^{15}, TeT_5^{15}, TeT_6^{15}, TeT_9^{15}, TeT_{10}^{15}, TeT_{14}^{15}, TeT_{15}^{15}, TeT_{16}^{15}, TeT_{17}^{15}, TeT_{18}^{15}$, and TeT_{19}^{15}		
PR_{16}	TeT_{14}^{16}	TeT_9^{16}	
	$a\ b\ c\ n$	$a \to n,\ b \to a,\ c \to b,\ n \to c$	
	TeT_{10}^{16}	TeT_{11}^{16}	TeT_{12}^{16}	TeT_{13}^{16}
	$a\ b\ c\ n$	$a \to a,\ b \to b,\ c \to n,\ n \to c$	$a \to a,\ b \to n,\ c \to b,\ n \to c$	$a \to n,\ b \to a,\ c \to b,\ n \to c$
	No corresponding of $TeT_1^{16}, TeT_2^{16}, TeT_3^{16}, TeT_4^{16}, TeT_5^{16}, TeT_6^{16}, TeT_7^{16}, TeT_8^{16}, TeT_{15}^{16}, TeT_{16}^{16}, TeT_{17}^{16}, TeT_{18}^{16}, TeT_{19}^{16}, TeT_{20}^{16}, TeT_{21}^{16}$ and TeT_{22}^{16}		

I.6. DC-Capacitor voltages balancing based on minimum energy property

The electrical energy stored in the chain of DC-link capacitors is given by:

$$E = \frac{1}{2}\sum_{j=1}^{4} C v_{C_j}^2 \tag{I.29}$$

When all capacitor voltages are balanced, the total energy E reaches its minimum of $E_{\min} = C v_{dc}^{*2}/8$, with v_{dc}^{*} is the desired value of DC voltage [60]. This condition is called the minimum energy property which can be used as the basic principle for DC-capacitor voltages balancing and control [60]. The adopted control method should minimize the quadratic cost function J associated with voltage deviation of the DC-capacitors. The cost function is defined as follows:

$$J = \frac{C}{2}(\Delta v_{C1}^2 + \Delta v_{C2}^2 + \Delta v_{C3}^2 + \Delta v_{C4}^2) \tag{I.30}$$

Where:

$$\Delta v_{Cj} = v_{Cj} - v_{dc}^{*}/4, \quad j = 1,2,3,4$$

The mathematical condition to minimize J is:

$$\frac{dJ}{dt} = \Delta v_{C1} i_{C1} + \Delta v_{C2} i_{C2} + \Delta v_{C3} i_{C3} + \Delta v_{C4} i_{C4} \le 0 \tag{I.31}$$

Where i_{Cj} (j =1, 2, 3, 4) is the current through capacitor C_j. These currents are affected by the DC-side intermediate branch currents, i_1, i_2, and i_3. These currents can be calculated if the switching states used in the switching pattern are known (see equation (I.27)).
Thus, it is advantageous to express (I.31) in terms of i_1, i_2, and i_3.

From figure (I.19), we can write:

$$\begin{aligned} i_{C_4} &= i_3 + i_{C_3} \\ i_{C_3} &= i_2 + i_{C_2} \\ i_{C_2} &= i_1 + i_{C_1} \end{aligned} \tag{I.32}$$

The DC voltage v_{dc} is assumed constant, we deduce that:

$$C\sum_{j=1}^{4}\frac{dv_{C_j}}{dt} = \sum_{j=1}^{4} i_{C_j} = 0 \tag{I.33}$$

From equations (I.32) and (I.33), the capacitors currents can be expressed by:

$$\begin{aligned} i_{C_1} &= \frac{1}{4}\left(i_1 + 2i_2 + 3i_3\right) - \left(i_1 + i_2 + i_3\right) \\ i_{C_2} &= \frac{1}{4}\left(i_1 + 2i_2 + 3i_3\right) - \left(i_2 + i_3\right) \\ i_{C_3} &= \frac{1}{4}\left(i_1 + 2i_2 + 3i_3\right) - i_3 \\ i_{C_4} &= \frac{1}{4}\left(i_1 + 2i_2 + 3i_3\right) \end{aligned} \tag{I.34}$$

We can write (I.34) as follows:

$$i_{C_j} = \frac{1}{4}\sum_{x=1}^{3} x i_x - \sum_{x=j}^{3} i_x, \qquad j = 1,2,3,4. \tag{I.35}$$

By substituting the capacitors currents given by (I.35) in (I.31), the condition to achieve voltage balancing is deduced as:

$$\sum_{j=1}^{4} \Delta v_{C_j} \left(\frac{1}{4}\sum_{x=1}^{3} x i_x - \sum_{x=j}^{3} i_x \right) \leq 0 \tag{I.36}$$

When the DC link voltages v_{Cj} (j=1, 2, 3, 4) are close to their reference $v_{dc}^{*}/4$, the following condition is verified:

$$\sum_{j=1}^{4} \Delta v_{C_j} = 0 \tag{I.37}$$

Using (I.37), the equation (I.36) can be written as:

$$\sum_{j=1}^{3} \Delta v_{C_j} \left(\sum_{x=j}^{3} i_x \right) \geq 0 \tag{I.38}$$

Applying the averaging operator, over one sampling period, to (I.38) results in:

$$\frac{1}{T_s} \int_{kT_s}^{(k+1)T_s} \left[\sum_{j=1}^{3} \Delta v_{C_j} \left(\sum_{x=j}^{3} i_x \right) \right] dt \geq 0 \tag{I.39}$$

Assuming that sampling period T_s, is adequately small as compared to the time interval associated with the dynamics of capacitor voltages. These letter can be assumed to remain constant over one sampling period [60] and (I.39) is consequently simplified to:

$$\sum_{j=1}^{3} \Delta v_{C_j}(k) \left(\sum_{x=j}^{3} \bar{i}_x\ (k) \right) \geq 0 \tag{I.40}$$

Where $\Delta v_{C_j}(k)$ is the voltage drift of the capacitor C_j at sampling period kT_s, and $\overline{i_j}(k)$ is the averaged value of the i_j.

If the reference voltage vector is located in a tetrahedron formed by the four switching vectors v_1, v_2, v_3, and v_4, and t_1, t_2, t_3, and t_4 are their on-duration time intervals. The average branch currents $\overline{i_3}$, $\overline{i_2}$ et $\overline{i_1}$ are expressed as:

$$\begin{bmatrix} \overline{i_3} \\ \overline{i_2} \\ \overline{i_1} \end{bmatrix} = \frac{1}{T_s} \begin{bmatrix} i_{3_{v1}} & i_{3_{v2}} & i_{3_{v3}} & i_{3_{v4}} \\ i_{2_{v1}} & i_{2_{v2}} & i_{2_{v3}} & i_{2_{v4}} \\ i_{1_{v1}} & i_{1_{v2}} & i_{1_{v3}} & i_{1_{v4}} \end{bmatrix} \begin{bmatrix} t_1 \\ t_2 \\ t_3 \\ t_4 \end{bmatrix} \tag{I.41}$$

Where: $i_{j_{vi}}$ (j=1, 2, 3. i=1, 2, 3, 4) is the branch current obtained when the switching vector v_i is applied (see equation (I.27)).

The relationship between the branch current i_j and output currents (i_a, i_b, i_c and i_n) for different switching states of the first sector is required.

The current $\overline{i_j}$ should be computed for different combinations of adjacent redundant switching states over a sampling period and the best combination which maximizes (I.40) is selected.

The implementation procedure of the 3DSVM with proposed algorithm and voltage balancing strategy is summarized in figure (I.23).

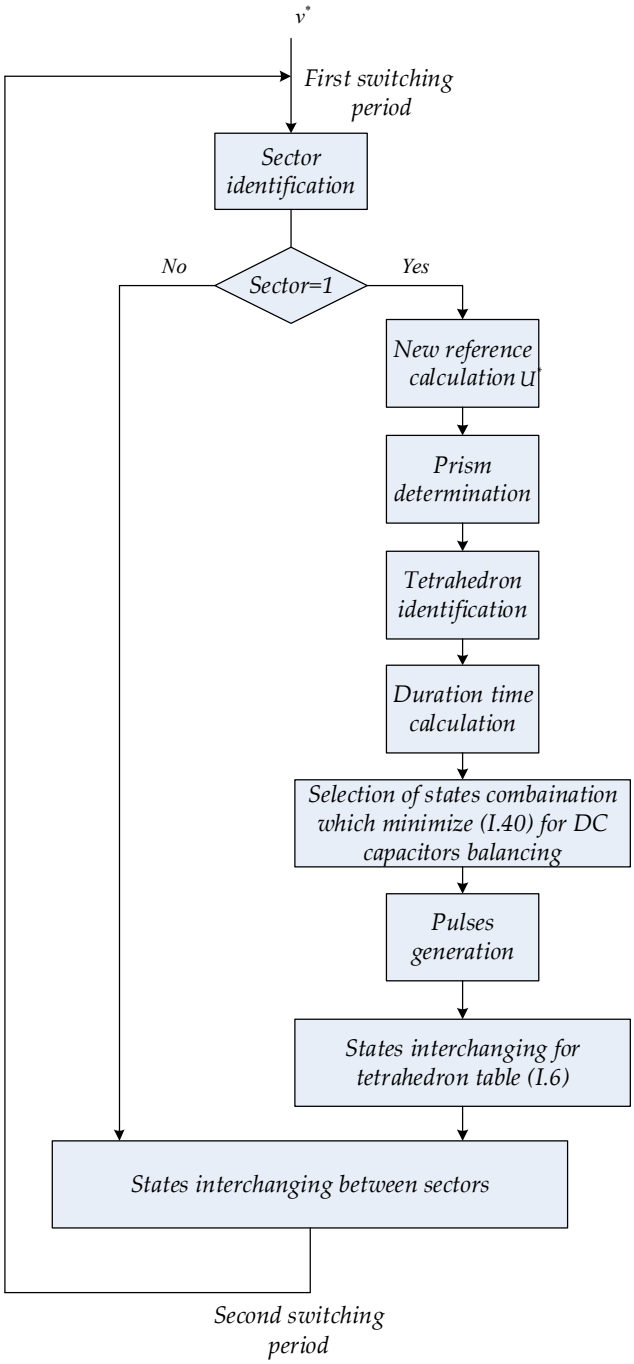

Figure (I.23): Schematic diagram of the 3DSVM with balancing strategy of 5-level 4-leg inverter

I.7. Simulation results

To verify the effectiveness of the 3DSVM with balancing capacitor voltages, the five-level four-leg inverter is simulated in different operating conditions such as:

- Balanced load condition;
- Unbalanced load condition;
- Unbalanced output voltage condition;
- Influence of the inverter parameters.

The capacitors are initially charged by unequal voltages v_{C1}=4650V, v_{C2}=5150V, v_{C3} =5350V, v_{C4}=4850V. C=5mF.

I.7.1. Balanced load condition

Figures (I.24), (I.25) and (I.26) show the output voltage of phase-a, DC capacitor voltages and output currents for the operating points A(M=0.8, PF=1), B(M=0.8, PF=0.2), and C(M=0.4, PF=1).

The DC-link capacitor voltages tend to be equal when the inverter operates in points B and C, whereas the system is unstable for operating point A, which leads to distortion in output voltage and current waveforms, as shown in figure (I.24).

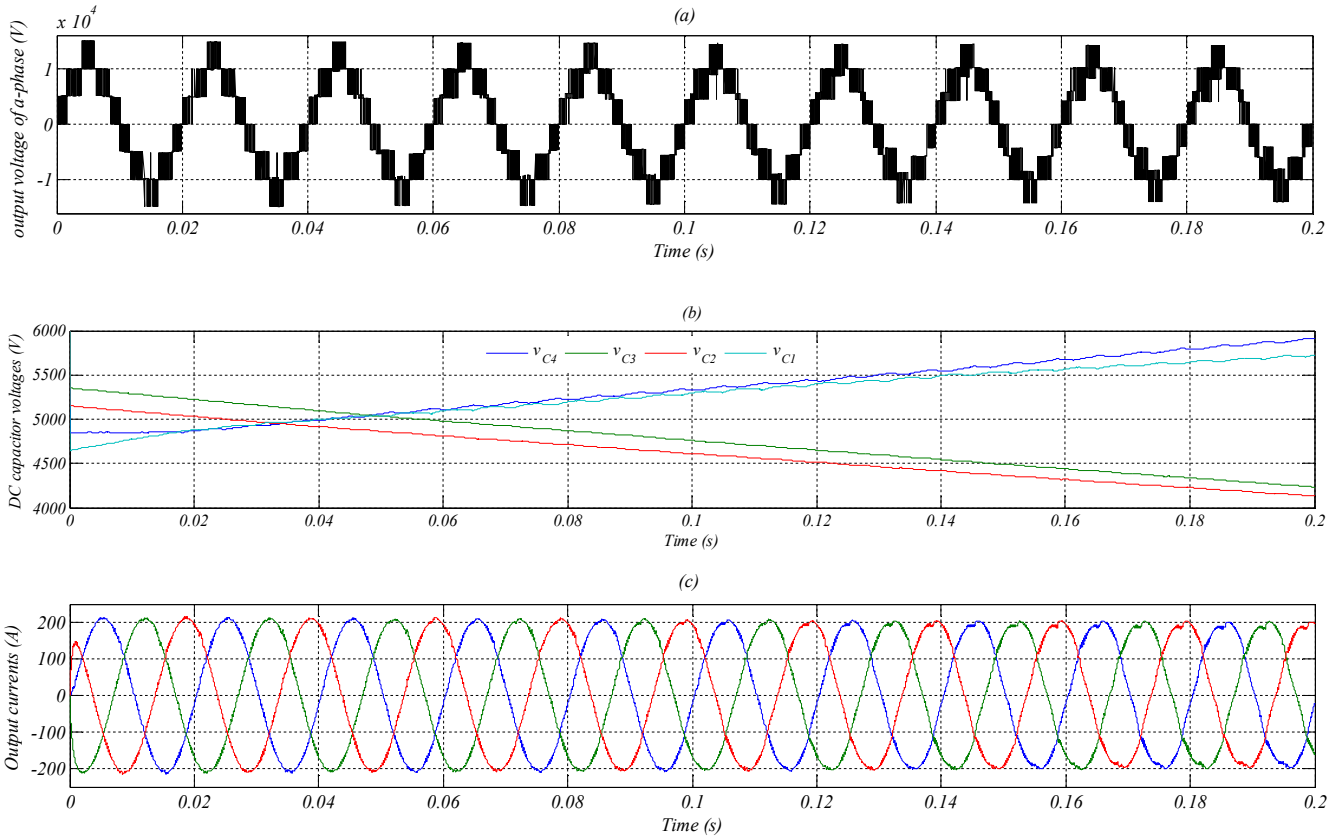

Figure (I.24): Waveforms of the inverter to the operating points (M = 0.8, PF=1), (a): Output voltage of a-phase, (b): DC capacitor voltages, (c): Output currents

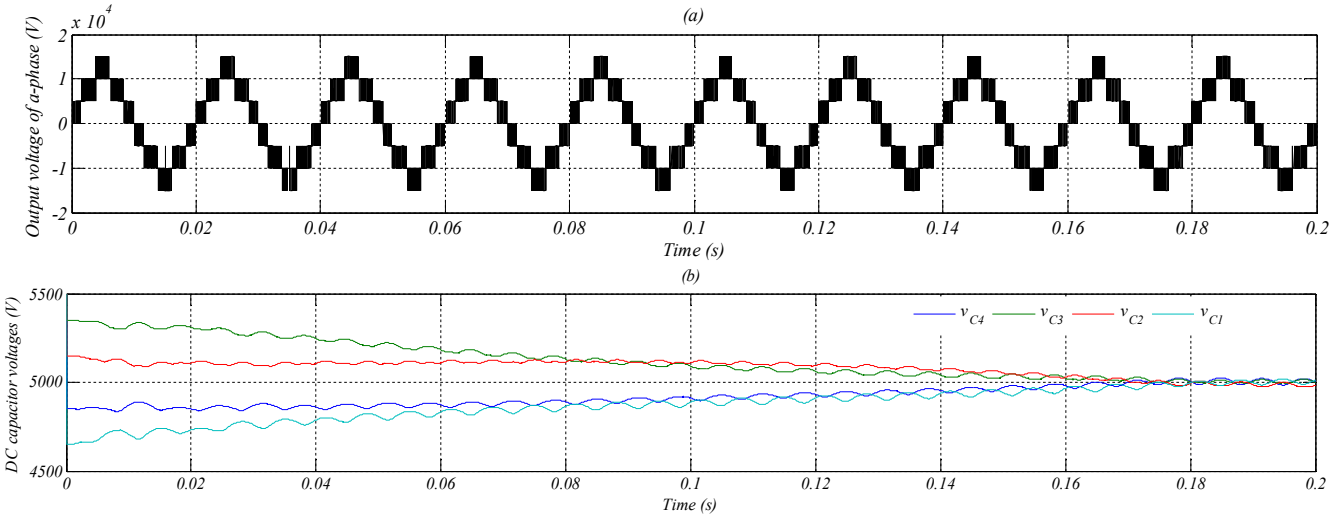

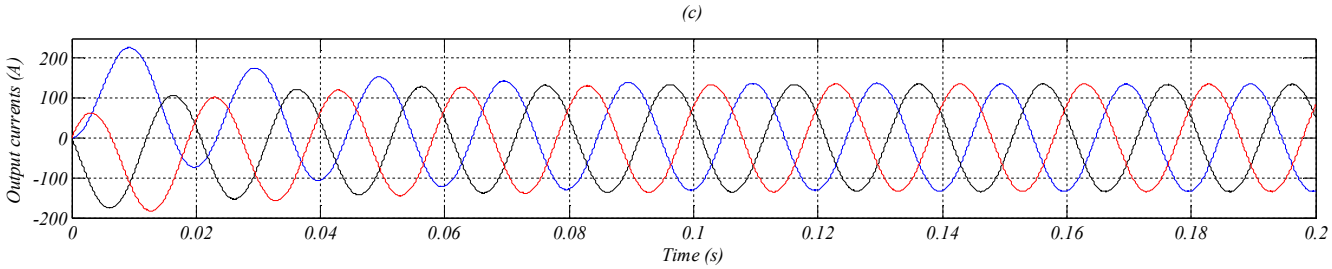

Figure (I.25): Waveforms of the inverter under the operating points (M = 0.8, PF=0.2), (a): Output voltage of a-phase, (b): DC capacitor voltages, (c): Output currents

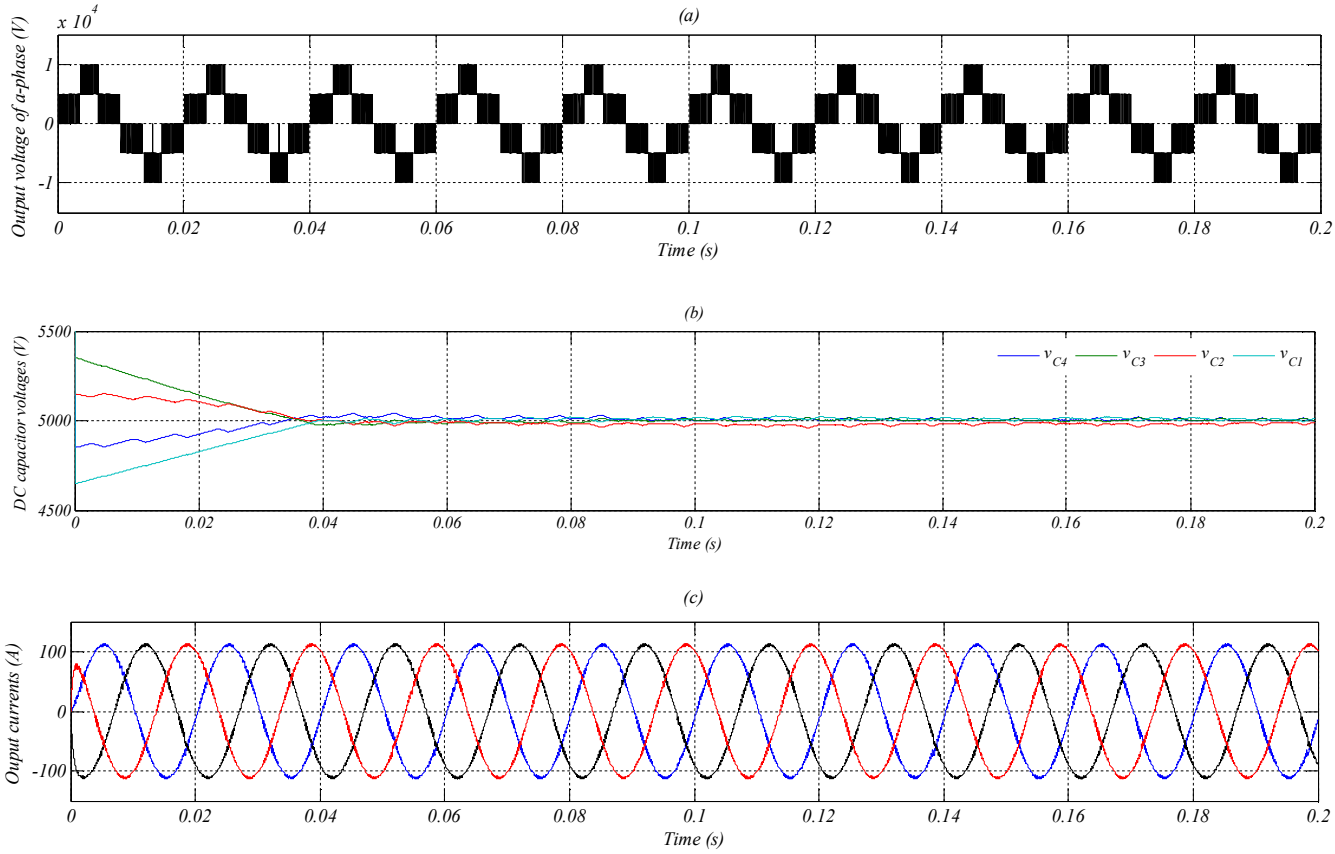

Figure (I.26): Waveforms of the inverter under the operating points (M = 0.4, PF=1), (a): Output voltage of a-phase, (b): DC capacitor voltages, (c): Output currents

I.7.2. Unbalanced load condition

This section explores effectiveness of the proposed 3DSVM with balancing strategy under unbalanced load conditions.

The same operating points B and C correspond to figures (I.27) and (I.28). The three-phase source currents are unbalanced and sinusoidal due to unbalanced load, the neutral current is also sinusoidal, because it is equal to the sum of three phase currents.

The unbalanced load causes small perturbations on the capacitor voltages without affected the balance of these voltages.

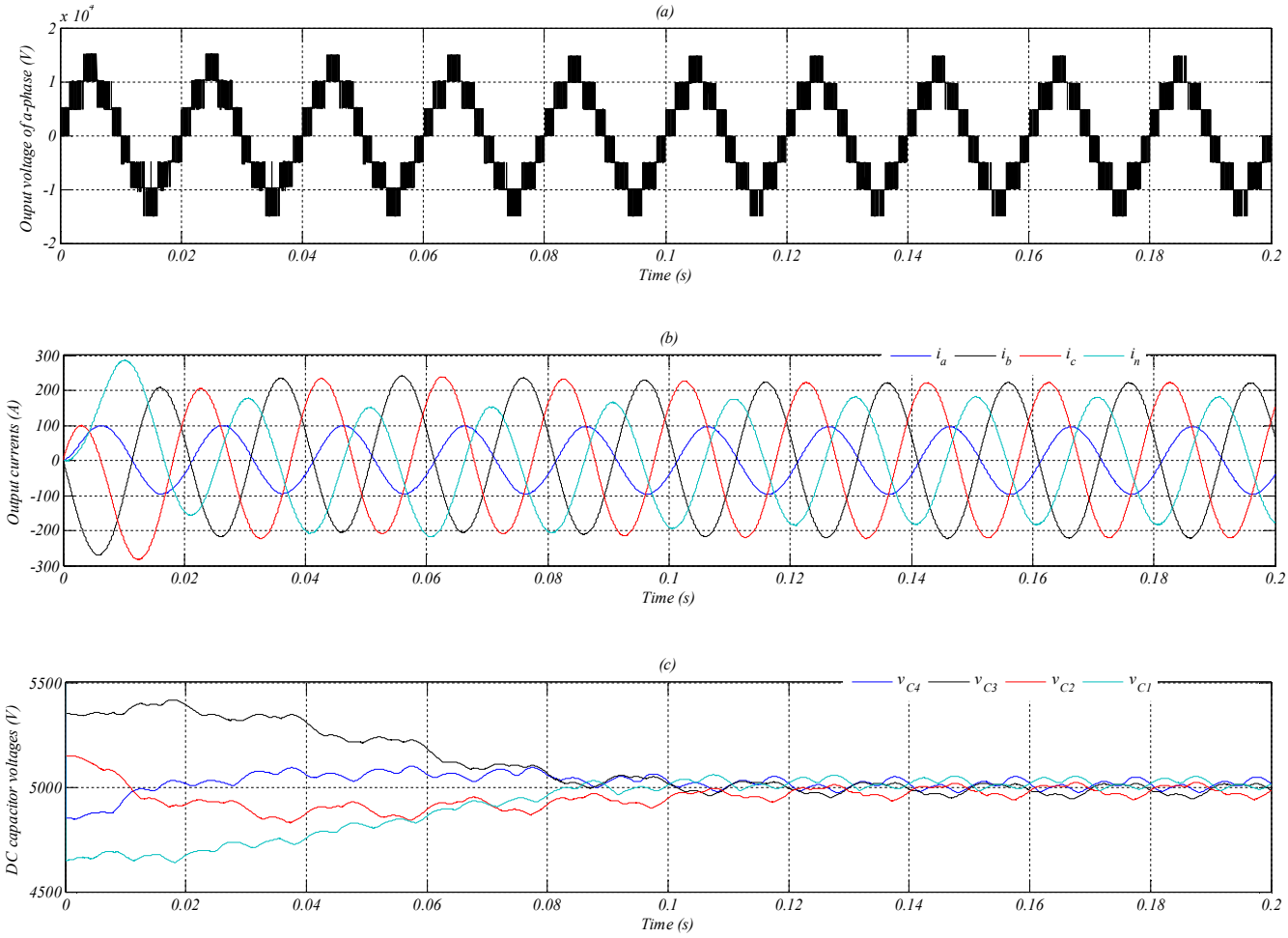

Figure (I.27): Waveforms of the inverter under the operating points (M = 0.8, PF=0.2), (a): Output voltage of a-phase, (b): Output currents (c): DC capacitor voltages

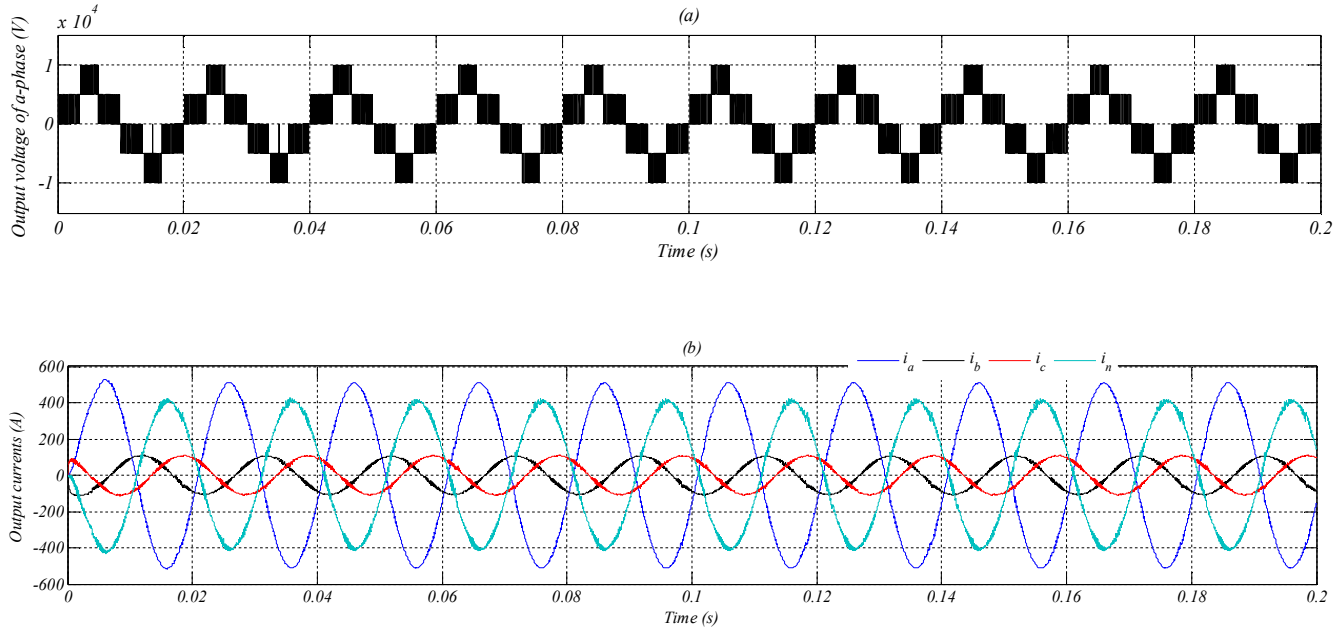

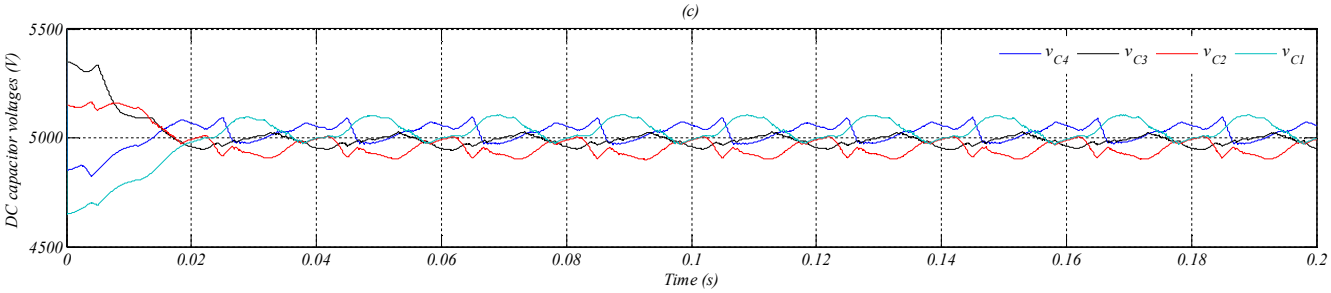

Figure (I.28): Waveforms of the inverter under the operating points (M = 0.4, PF=1), (a): Output voltage of a-phase, (b): Output currents (c): DC capacitor voltages

The five-level four-leg inverter with balanced load and source voltage have the same performance of the three-leg inverter, because the reference voltage vector is turn in $\alpha\beta$ plane, the amopolair component is equal to zero.

In literature, previous works have demonstrated that multilevel diode clamped inverter has no possibilities to balance the DC-link with a high number of levels under all the working operation conditions [30]. These limits depend on the modulation index of the reference signal and the load power factor as shown in figure (I.29).

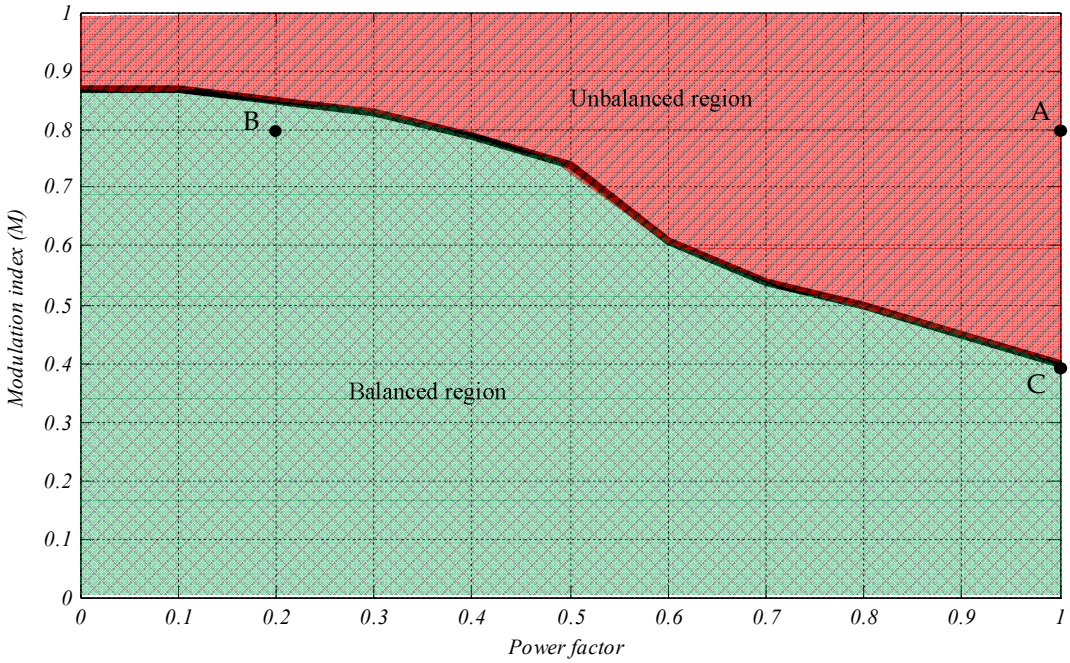

Figure (I.29): DC capacitor voltages balancing limits for five-level inverter

I.7.3. Unbalanced output voltages

In order to test the proposed technique under unbalanced output voltage, the inverter operates under different conditions of unbalanced output voltages.

If the output voltages are not balanced, the hompolair component appears, one can define the modulation index of the hompolair component $M_0 = (U_0^* / v_{dc}\sqrt{2/3})$. The ratio between

the M_0 and the modulation index M is: $M_0(\%) = \left(M_0 / M\right) * 100$. This percentage would give us the amount of output voltages unbalance.

As shown in figure (I.30), the proposed 3DSVM balancing strategy cannot achieve the DC capacitor voltages balance when the inverter works at point (M=0.8, PF= 0.5) with M_0=15%, in the other hand in figure (I.31), the DC capacitor voltages are balanced in the same operating point, just with M_0=35%.

In figure (I.32), the inverter operates at (M=0.5, PF=1) with M_0=15%, it can be seen that the DC-link capacitor voltages are not controlled and turn unstable, but with M_0=35%, according to figure (I.33), the voltages balance is achieved.

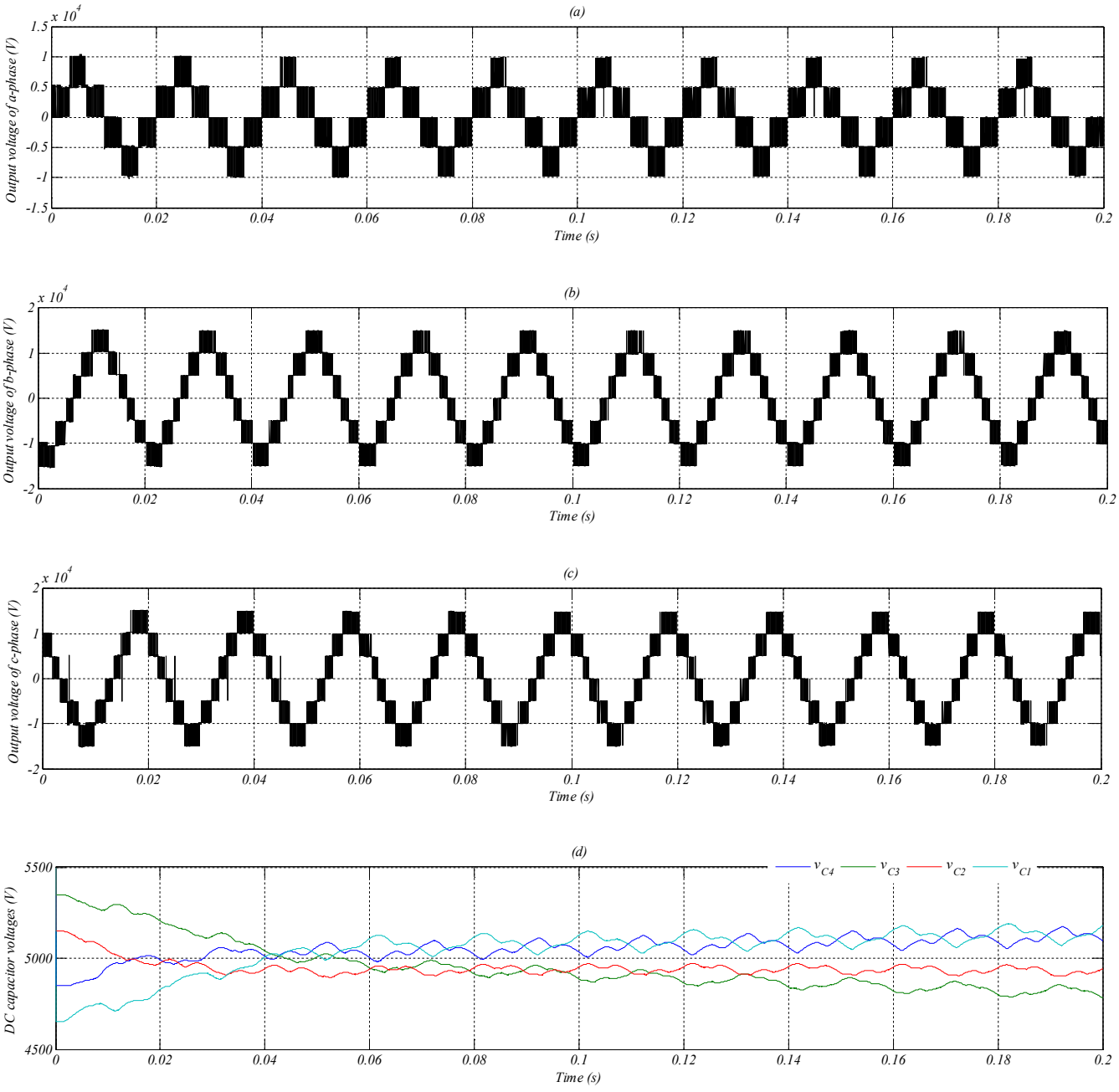

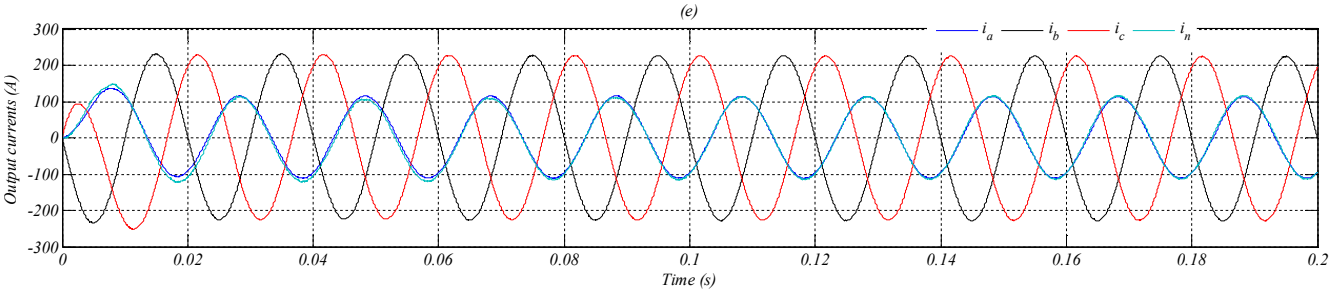

Figure (I.30): Waveforms of the inverter under the operating point (M = 0.8, PF=0.5, M_0=15%), (a, b and c): Output voltages, (d): DC capacitor voltages, (e): Output currents

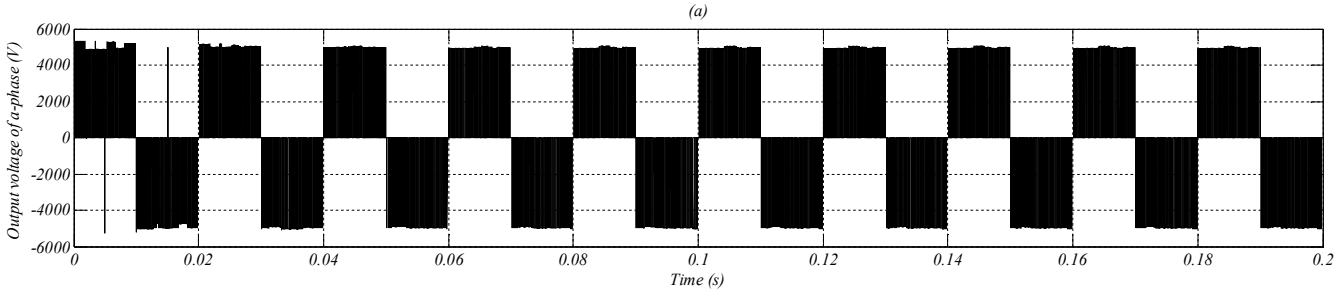

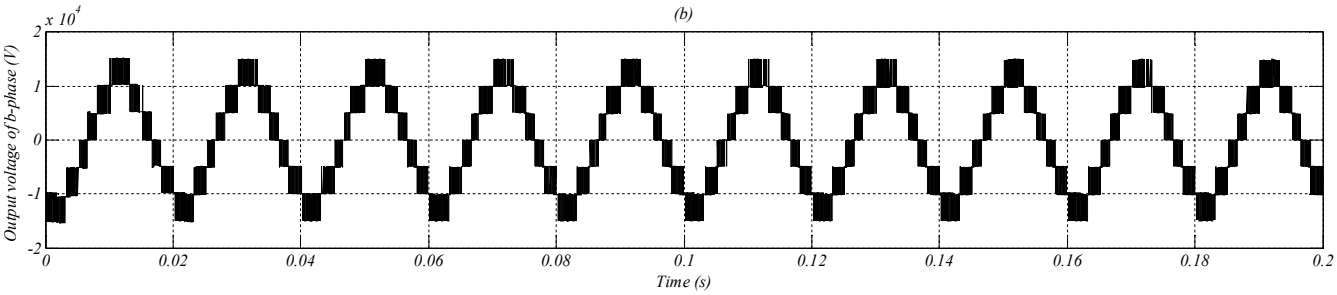

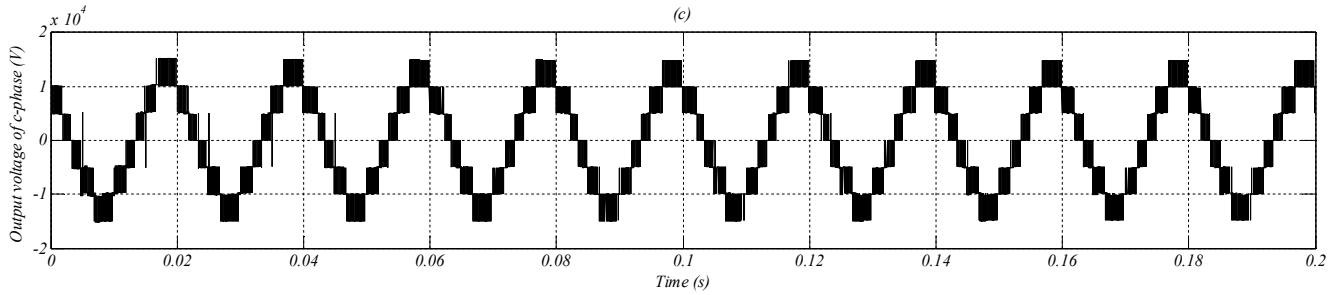

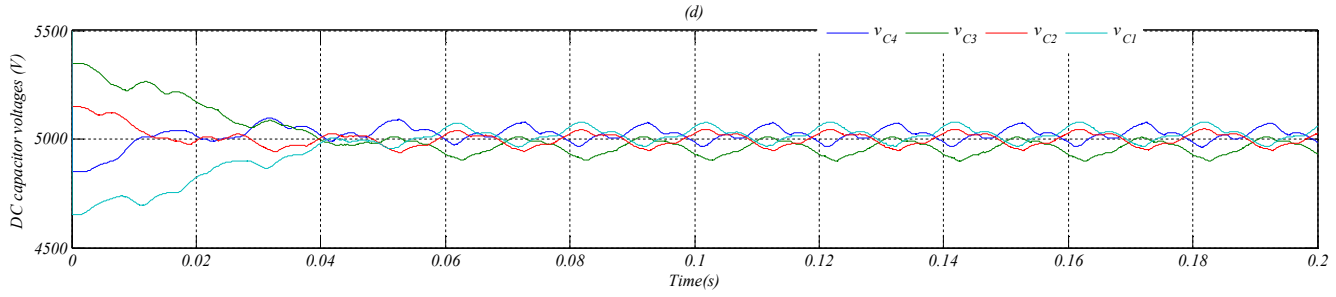

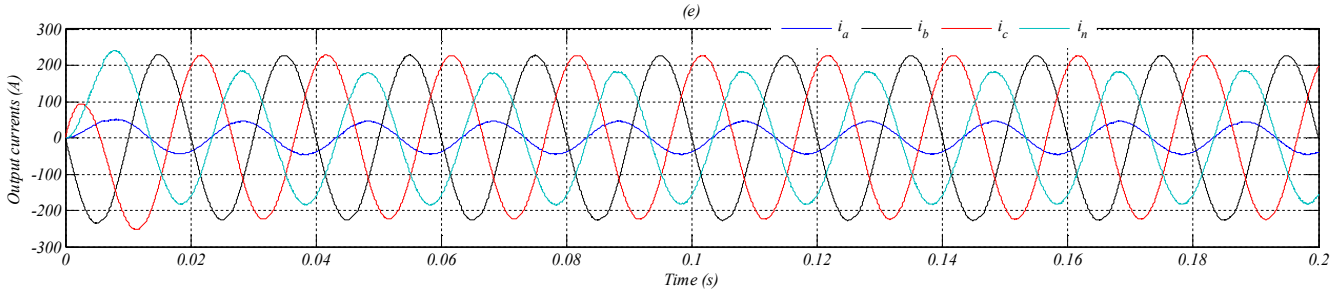

Figure (I.31): Waveforms of the inverter under the operating point (M = 0.8, PF=0.5, M_0=35%), (a, b and c): Output voltages, (d): DC capacitor voltages, (e): Output currents

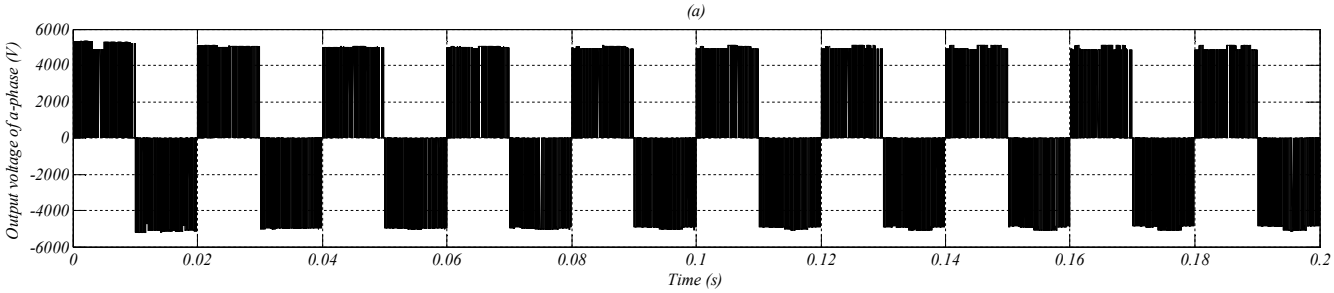

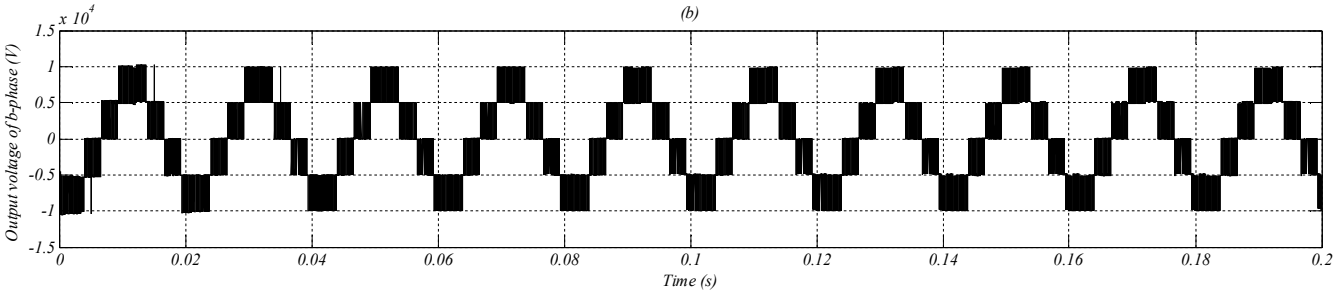

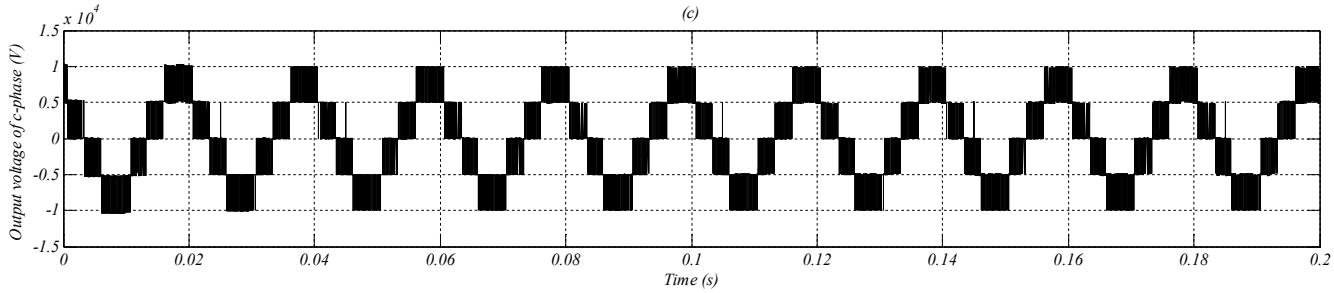

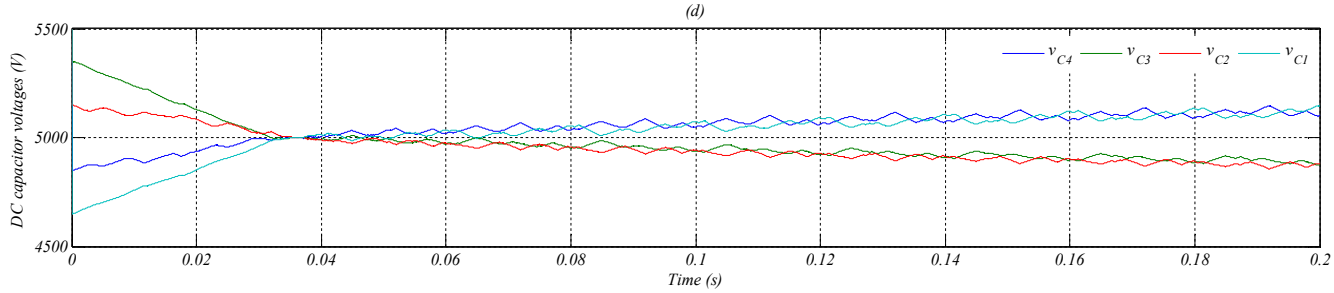

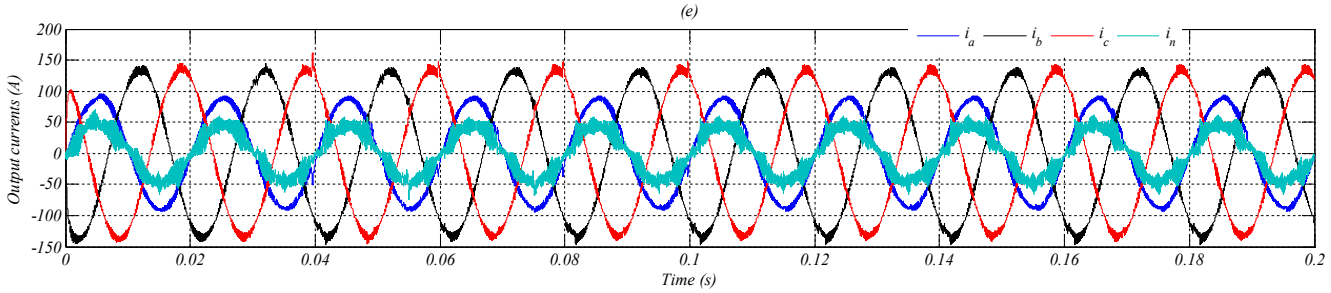

Figure (I.32): Waveforms of the inverter under the operating point (M = 0.5, PF=1, M_0=15%), (a, b and c): Output voltages, (d): DC capacitor voltages, (e): Output currents

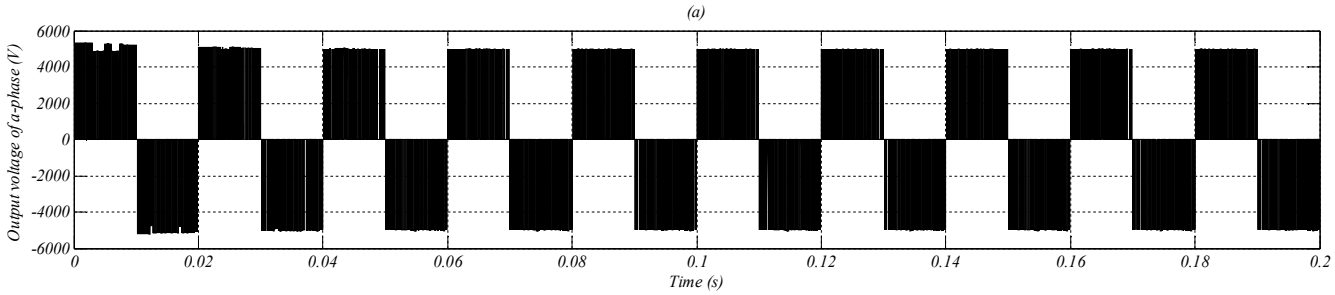

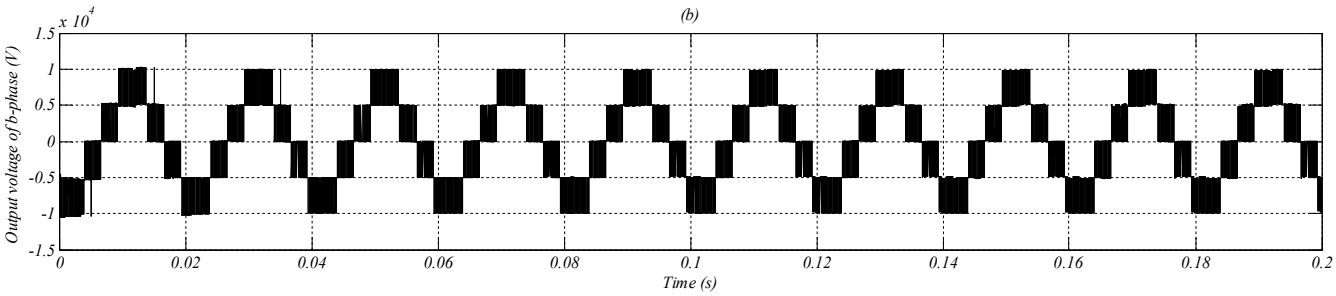

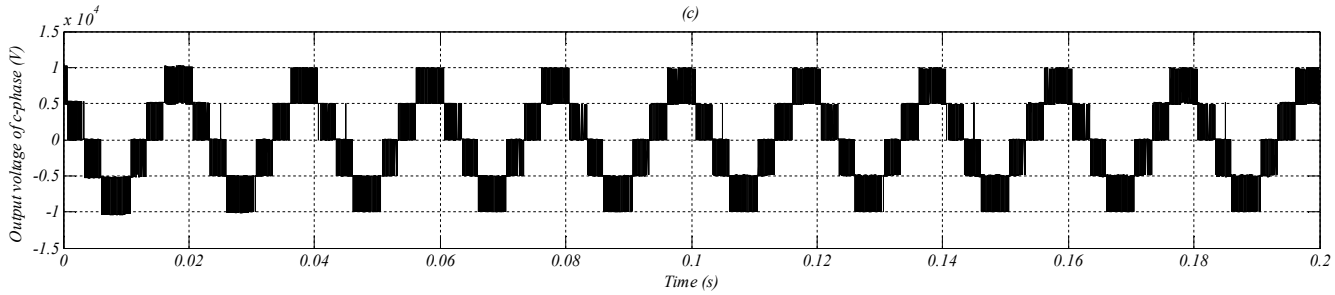

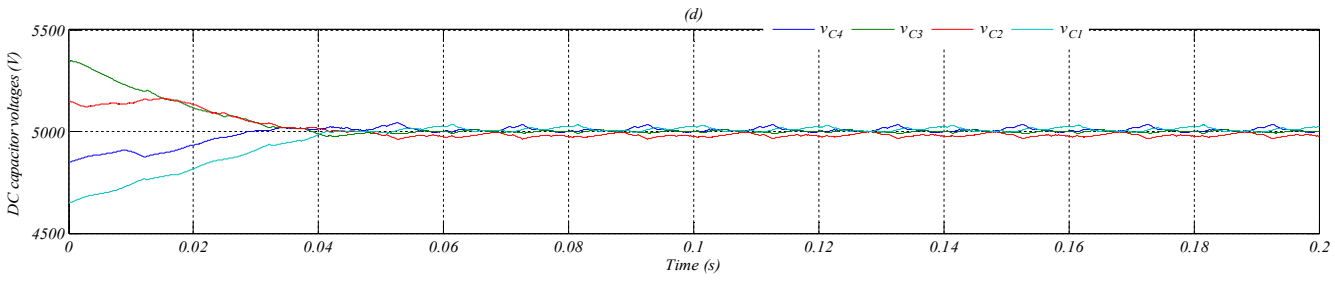

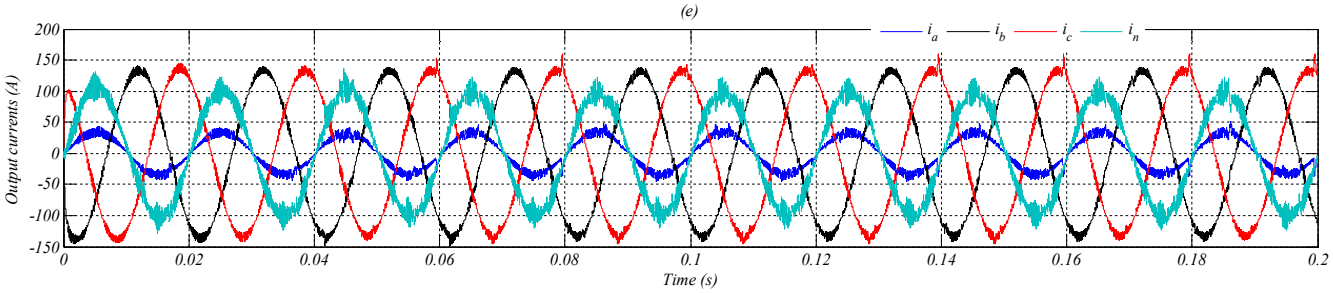

Figure (I.33): Waveforms of the inverter under the operating point (M = 0.5, PF=1, M_0=35%), (a, b and c): Output voltages, (d): DC capacitor voltages, (e): Output currents

So we can deduce that the variable M_0(%) in addition to PF and modulation index M, has an important effect on the capacitor voltages balance.

The surface in figure (I.34) shows the boundary under which the proposed 3DSVM strategy can control and achieve balanced DC-capacitor voltages. The 3DSVM can guarantee the balancing voltages under the surface shown in Figure (I.34).

This result was expected due to the fact that five-level four-leg topology presents switching redundant configurations in homopolair axes and therefore has more possibilities to use the redundant vectors in order to balance the capacitor voltages.

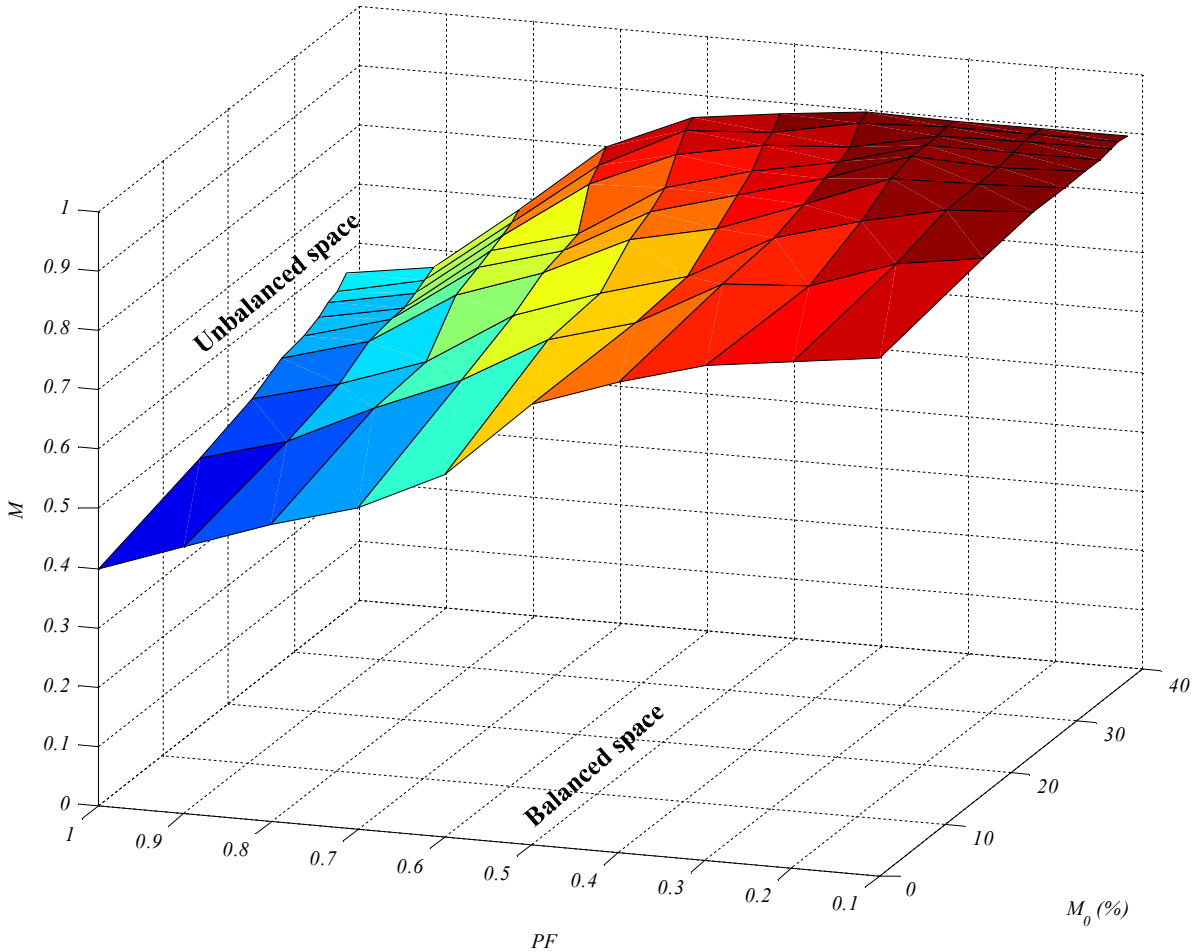

Figure (I.34): DC capacitor voltages balancing limits under unbalanced reference voltage for five-level four-leg inverter

I.7.4. Influence of the inverter parameters

The balancing algorithm performance depends on the capacitors values used at the input of the inverter and switching frequency. We will study the influence of these parameters on the balancing voltages.
Figure (I.35) illustrates the DC capacitor voltages ripple for different capacitance values for M_0= 0%, 25% and 35%. It can be observed that the DC capacitor voltages ripple increases with the increase of the M_0 and decreases with the increase of the capacitance.

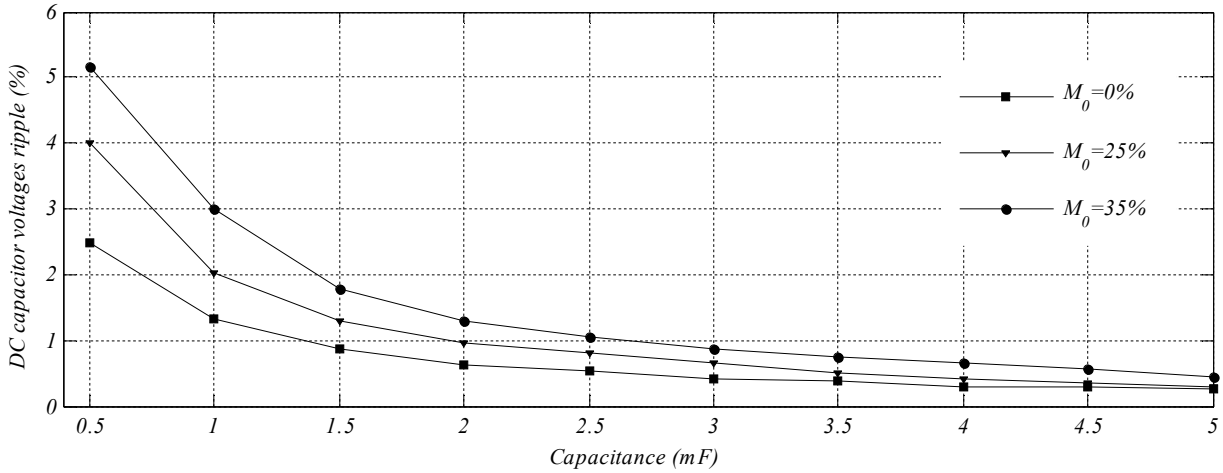

Figure (I.35): DC capacitor voltages ripple versus capacitance for (M = 0.4, PF=1) and different values of M_0

Figure (I.36) shows the capacitor voltages ripple as a function of the modulation index M with PF=0.2. One notices well that the ripple increases slowly with the increase of M, while $M \leq 0.3$. Beyond M = 0.3, the increase of the ripple becomes fast, and then returns slowly for $M \geq 0.6$.

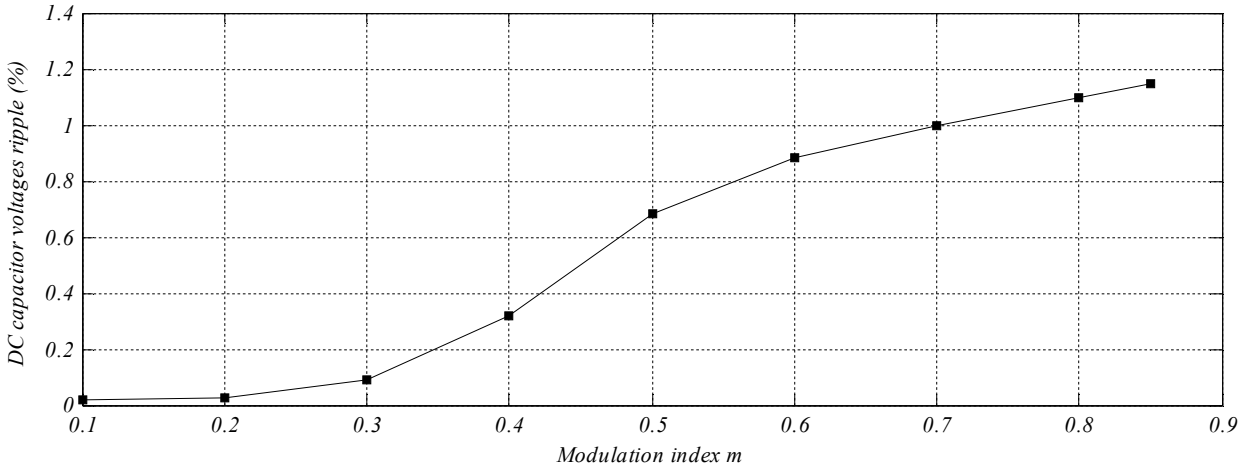

Figure (I.36): DC capacitor voltages ripple versus modulation index M

In figure (I.37), it is noted that the ripple voltages decreases remarkably with the increase of the switching frequency. However, a very high frequency cannot be supported by the electronic components used in high power applications.

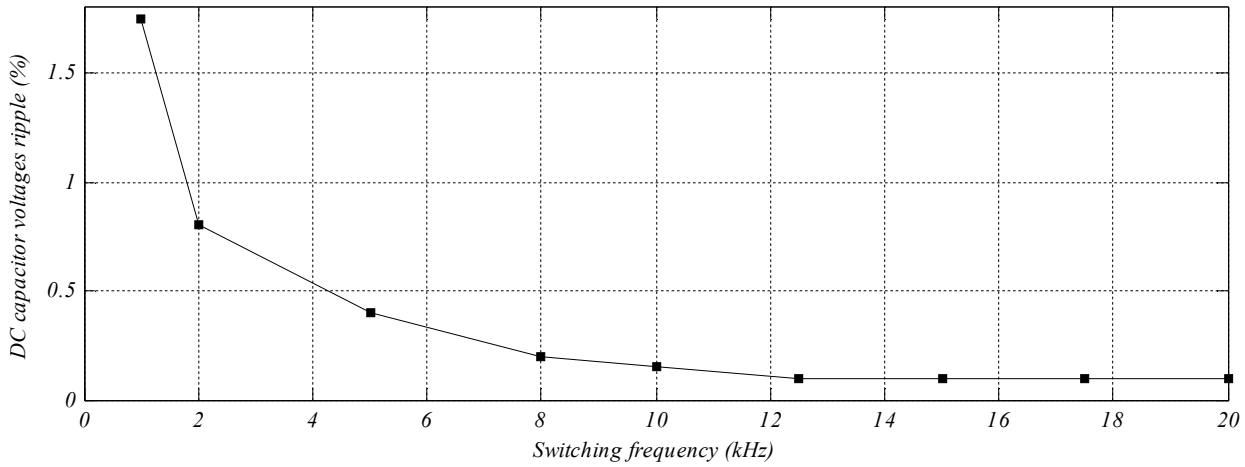

Figure (I.37): DC capacitor voltages ripple versus switching frequency (kHz) for (M=0.4, PF=1)

I.8. Conclusion

This chapter was mainly devoted to the analysis, modeling and control of multilevel four-leg diode clamped inverters; using a new multilevel 3DSVM control algorithm. Simulation results have shown that increasing the number of levels greatly improves the harmonic quality of the output voltage and current. However, with a high number of levels, the power structure is more expensive and its control is more complicated. The significant outcome of the proposed algorithm of multilevel 3DSVM is its inherent simplicity. Unlike the conventional one, that requires reference vector determination, on-duration time calculation, and pules creation in all sectors, the proposed 3DSVM algorithm is much simpler and easier for digital implementation since it reduces the hardware and software complexity and decreases the required computational time.

The second section of this chapter has been dedicated to the DC capacitor voltages balancing of the five-level four-leg diode clamped inverter. The balancing strategy is based on choosing the switching states; by taking advantage of the redundant state vectors to minimize the total energy stored in the DC capacitors.
Simulation results conclude that the proposed 3DSVM balancing control algorithm is able to carry out the voltage-balancing task under various operation conditions, with no requirement for additional power circuitry. The study results also show that the voltage balancing of the DC capacitors have three-dimensional limits depends on modulation index, load power factor and unbalancing output voltages.

In the next chapter, the five-level four-leg inverter with the proposed 3DSVM balancing control algorithm will be used to operate as a shunt active power filter.

Chapter II

Direct power control of five-level four-leg shunt active power filter

II.1. Introduction

The increasing use of power electronic devices in the distribution network, which act as nonlinear loads, has caused many power quality disturbances such as harmonics pollution, unbalanced load currents, and reactive power problems. As a result, poor power factor, weakening efficiency, overheating of motors and transformers, malfunction of sensitive devices, etc. are encountered [77-79].

Conventionally, a passive power filter is used to provide harmonic filtering as an economical and effective filtering device. However, it has some shortcomings such as fixed compensation performance, bulk in size, and resonance troubles [80-83]. Important kinds of passive power filters and their configurations are discussed in [80]. To overcome the shortcomings of passive power filters and to mitigate the power pollution in networks caused by the nonlinear loads, an active power filter (APF) was established in around

1970s [84, 24, 25]. APFs are previously not implemented in power networks, because of unavailability of high speed power switching devices. Recently the power electronic development spurred the interest in IGBTs, MOSFETs etc. Then APFs are developed incorporating power electronics technology to support the needs of industry. Shunt, series, and hybrid configuration are the three main types of three-phase, three-wire active power filters and their merits and demerits are discussed in [80].
In several areas, power is distributed through three-phase four-wire system and traditional APF is inadequate for harmonics compensation and power factor correction. To overcome this shortage, a three-phase four-wire SAPF has been introduced in the 1980s [16-23].

Among the four-wire SAPF topologies, the four-leg SAPF represents the best solution in three-phase four-wire system [22, 23, 60]. The commercial success of these filters is due to their acceptable cost, fast response time, and ability to suppress the neutral current from the source without any drawback in the filtering performance [19].

The performance of the four-leg SAPF depends strongly on control strategies. The objective of this chapter is to present a direct power control (DPC) and predictive direct power control (PDPC) with 3DSVM for five-level four-leg SAPF. However, before that, a comprehensive review of neutral current compensation methods in four-wire systems, their topologies, and their technical and economical limitations will be presented first.

II.2. Review of neutral current compensation methods in three-phase four-wire systems

In recent years, a number of schemes have been reported for solving the excess neutral currents problem in three-phase four-wire systems. These schemes can be classified as: passive, hybrid, and active solutions (see figure (II.1)). Details of these methods and their comparisons are given below [4–23].

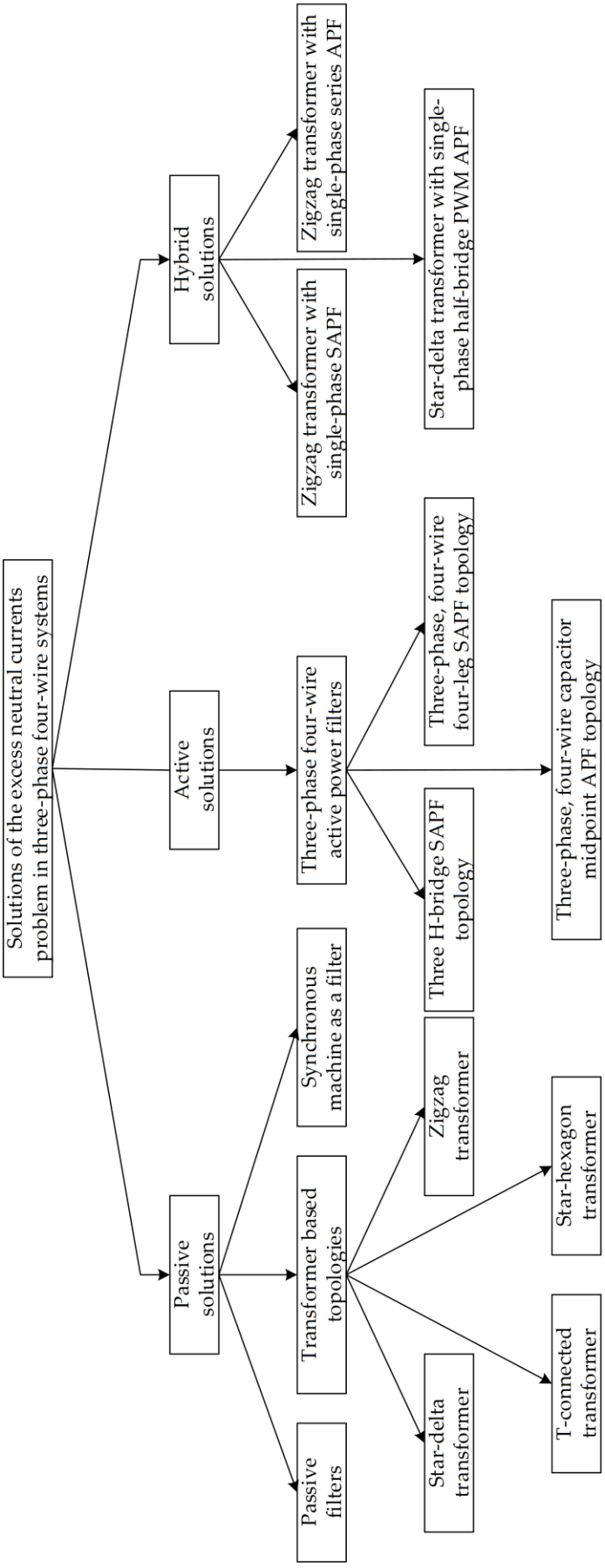

Figure (II.1): Review of neutral current compensation methods in three-phase four-wire systems

II.2.1. Passive topologies

II.2.1.1. Passive harmonic filters

The filtering of excess neutral current in three-phase four-wire systems was achieved through the use of single-phase passive filters connected between each phase conductor and the neutral wire. These passive harmonic filters comprise passive elements such as inductors, capacitors, and resistors, and tuned to a particular harmonic frequency [6]. A solution for filtering current harmonics in three-phase four-wire grids based on the usage of a four-branch star connected filter topology is depicted in figure (II.2) as presented in [6]. This topology has four individual star-connected passive branches (three phase-branches and one neutral branch). The impedance of the phase branches of the filter are identical and different from neutral branch. The phase branches are tuned to the positive/negative-sequence harmonics such as 5^{th}, 7^{th} and/or 11^{th}, 13^{th} and the neutral branch is tuned to 3^{rd} and/or 9^{th}.

Passive solutions, albeit simple, are bulky and expensive. In addition, the sensitivity of the components to temperature and ageing can result in ineffective filtering as the critical frequencies and the quality factor drift. Another bigger problem is the possibility of exciting a resonance condition with the AC system impedance, which can worsen the situation [7, 8, 19].

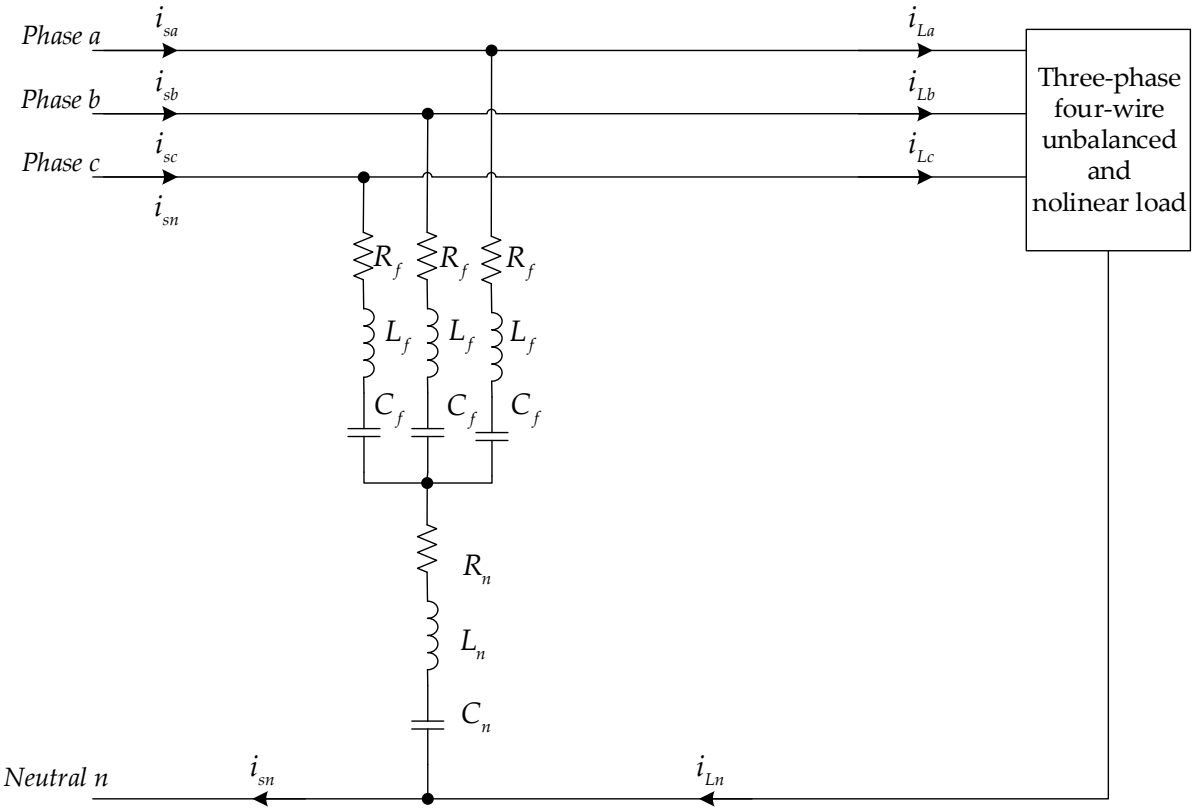

Figure (II.2): A four-branch star connected passive filter

II.2.1.2. Synchronous machine

Figure (II.3) shows the basic system in which the synchronous machine is used for absorbing the zero-sequence harmonic currents [9, 19]. In this method, the synchronous machine is connected in shunt between the grid and nonlinear load. The neutral point of the armature winding of synchronous machine is connected to the neutral line through a switch (*SW*). A buffer reactor (L_B) is installed on the grid side of the neutral line so that the harmonic compensation characteristics do not depend on the impedance of the grid side.
If the zero-sequence impedance of the synchronous machine is sufficiently smaller than that of the power source, then the synchronous machine would allow the absorption of the zero-sequence harmonic currents. This can be done by selecting the coil pitch of the armature winding as 2/3. As a result, the zero-sequence reactance of the synchronous machine reaches minimum value. The only limiting factor of zero-sequence harmonics is armature resistance of synchronous machine. Hence, it is possible to absorb all the zero-sequence harmonic currents by the synchronous machine [9, 19].
This method does not require any additional controller and the synchronous machine can be operated as a synchronous condenser to control the reactive power in distribution systems and/or operates as a motor or generator set. However, its compensation characteristics depend on zero-sequence impedance of the synchronous machine and buffer reactor. The high initial and maintenance cost of the synchronous machine limits its application.

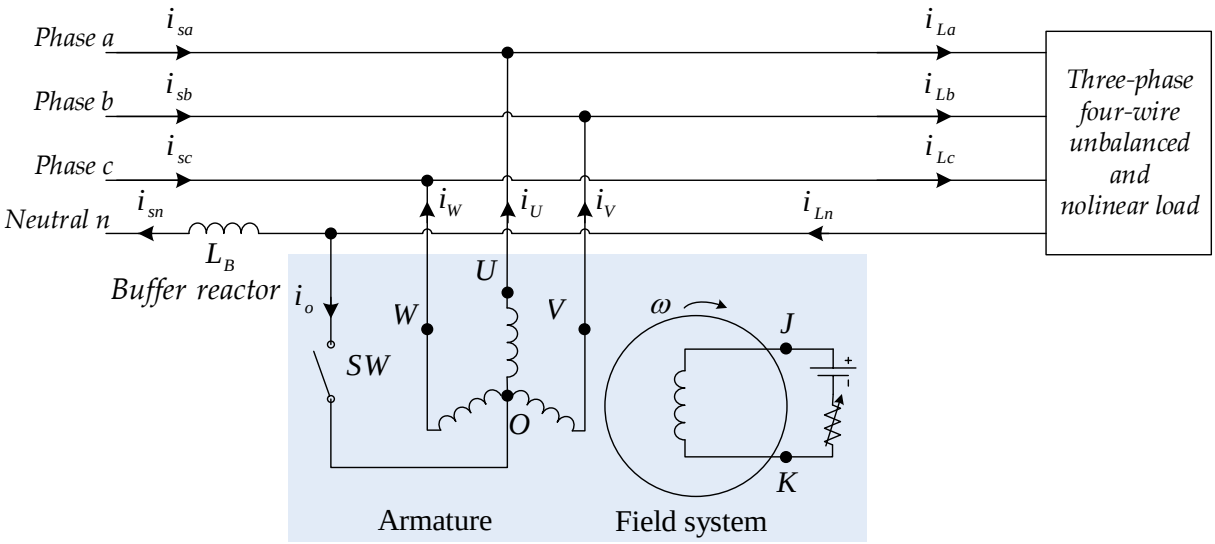

Figure (II.3): Schematic diagram for neutral current compensation with synchronous machine

II.2.1.3. Transformer based topologies

II.2.1.3.1. Zigzag transformer

As shown in figure (II.4), the zigzag transformer is connected as close as possible in parallel to the load. In this case, the turn rats of the zigzag transformer is 1:1. Therefore, the three-phase currents flowing into the primary and secondary windings must be equal.

Hence, ideally the zigzag transformer can be regarded as open-circuit for the positive-sequence and the negative-sequence currents [10]. Then, the current flowing through the zigzag transformer is only the zero-sequence component. But in practice the impedance offered for the zero-sequence currents is a function of the zero-sequence impedances of the grid system, zigzag transformer and the neutral conductor [10]. However, the impedance of the grid system, the zigzag transformer, and the neutral conductor are very small in most practical cases [10]. So a large value of the zero-sequence currents will circulate between zigzag transformer and load.

The rating of the zigzag transformer depends on the amount of load imbalance and harmonic content. To reduce the neutral current of utility side furthermore it is advised to insert an inductor (Z_n) in the neutral conductor of the utility side in order to split the current into two paths, one to the distribution transformer and the other to the zigzag transformer [10].

The main disadvantage of this topology is that its compensation characteristics depend on the impedance of the transformer, and its location [10]. However, this method can reduce only the neural current to a large extent but it will not completely compensated.

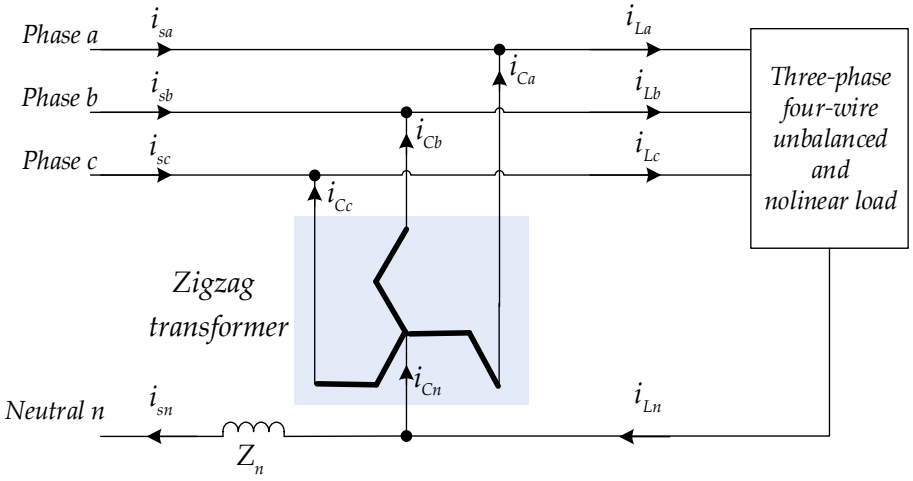

Figure (II.4): A zigzag transformer for reducing the neutral current in three-phase four-wire systems

II.2.1.3.2. Star-delta transformer

The power circuit of the star-delta transformer for neutral current reduction in three-phase four-wire system is shown in figure (II.5) [19]. Normally a limb core construction is used in the star winding of the transformer, because the zero sequence flux in the three legs does not add to zero as in the positive sequence case. Instead, the sum of these fluxes must seek a path through the air or through the transformer tank, either of which presents a large reluctance. The result is a low zero sequence excitation impedance. Hence, the star connected primary winding of the transformer offers a low impedance path for the zero sequence currents. The delta connected secondary winding provides a path for the induced zero sequence currents to circulate [19]. The use of this transformer has the same disadvantages of the zigzag transformer.

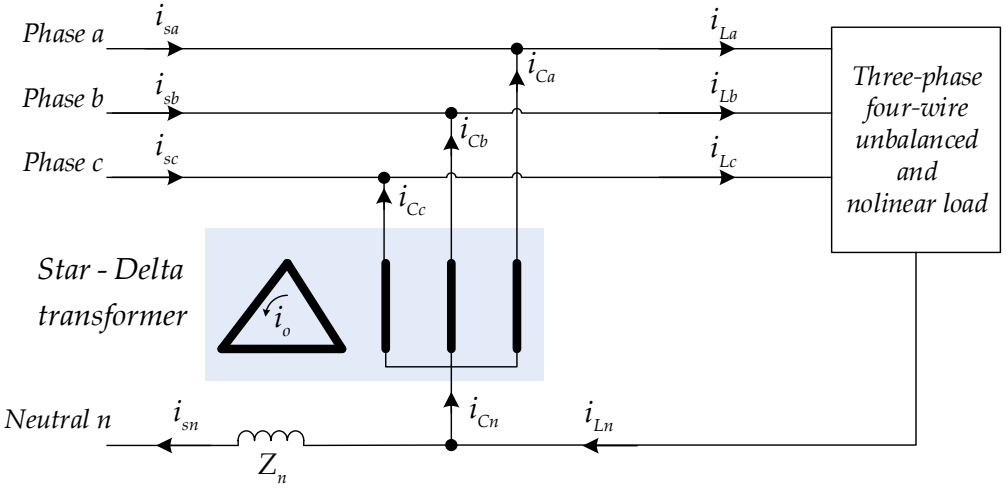

Figure (II.5): A star-delta transformer for reducing the neutral current in three-phase four-wire systems.

II.2.1.3.3. T-connected transformer

As presented in figure (II.6), the T-connected transformer is connected in parallel and as close as possible to the load. It consists of two single-phase transformers (one two-winding and one three-winding) arranged in a T-connection [11]. This arrangement has the advantage of using standard two single-phase transformers; consequently, the cores are economical to build and easy to assemble. Accordingly, the transformer is small in floor space, low in height, and with a lower weight than any of the other types of transformers available [12].

The compensation principal of the T-connected is similar to the zigzag transformer. its compensation characteristics depend on the impedance of the transformer, and its location [19].

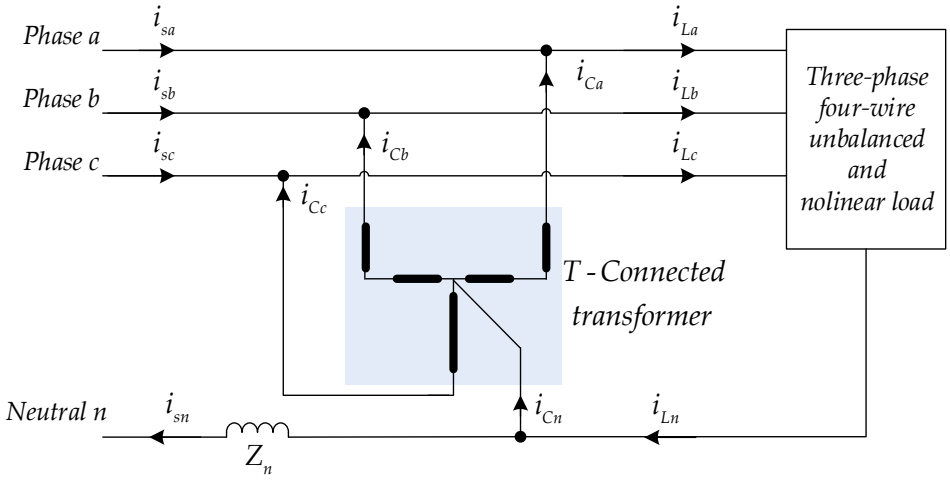

Figure (II.6): A T-connected transformer for reducing the neutral current in three-phase four-wire systems.

II.2.1.3.4. Star-hexagon transformer

A star-hexagon transformer can also be used for neutral current reduction in three-phase four-wire systems [14]. Figure (II.7) shows the schematic diagram of star-hexagon

transformer configuration for neutral current compensation in three-phase four-wire system. A star-hexagon transformer is constructed from three single-phase three-winding transformers. In this method, the star connected primary provides a low impedance path for the zero-sequence harmonic currents. The hexagon connected secondary winding provides a path for the induced zero sequence currents to circulate [14]. Similar to the zigzag transformer, its compensation characteristic has the same disadvantages of the zigzag transformer [19].

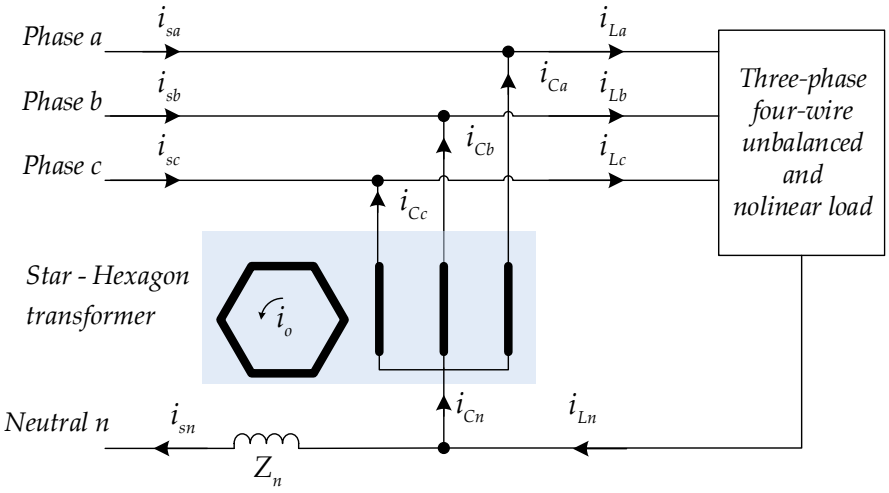

Figure (II.7): A star-hexagon transformer for reducing the neutral current in three-phase four-wire systems

The comparison of the neutral current compensation methods in three-phase four-wire systems with different transformer configurations are summarized in table (II.1) [19]. The kVA rating of the transformer is primarily decided by the amount of the neutral current. The kVA rating of the transformer is calculated by considering the product of the *RMS* values of the voltage and current associated with each of its windings. It is observed from table (II.1) that, zigzag transformer approach requires least kVA rating but it may require three single-phase transformers with turn's ratio of 1:1. The T-connected transformer requires only two single-phase transformers and also its rating is nearly equal to the zigzag transformer and far less than star/delta transformer. However, the transformer based methods can reduce the neural current to a large extent but it will not completely compensated [19].

Table (II.1): Comparison of neutral current compensation methods in three-phase, four-wire system with different transformer configurations [19]

Transformer type	*Zigzag*	*Star-delta*	*T-connected*	*Star-hexagon*
Number of transformers required to build	3 (single-phase two-winding)	1 (three-phase two-winding)	2 (single-phase three-winding and single-phase two-winding)	3 (single-phase three-winding)
Winding voltages (v_l = line-to-line voltage)	$\frac{v_l}{3}:\frac{v_l}{3}$	$\frac{v_l}{\sqrt{3}}:\frac{v_l}{\sqrt{3}}$	$\frac{v_l}{\sqrt{3}}:\frac{v_l}{2\sqrt{3}}:\frac{v_l}{2\sqrt{3}}$ and $\frac{v_l}{2}:\frac{v_l}{2}$	$\frac{v_l}{\sqrt{3}}:\frac{v_l}{\sqrt{3}}:\frac{v_l}{\sqrt{3}}$
Primary winding current (I_n = neutral current)	$\frac{I_n}{3}$	$\frac{I_n}{3}$	$\frac{I_n}{3}$	$\frac{I_n}{3}$
Transformer rating	$\frac{v_l I_n}{3} = 0.333 v_l I_n$	$\frac{v_l I_n}{\sqrt{3}} = 0.577 v_l I_n$	$\left(\frac{1}{3\sqrt{3}}+\frac{1}{6}\right)v_l I_n = 0.359 v_l I_n$	$\frac{v_l I_n}{\sqrt{3}} = 0.577 v_l I_n$
Is it a standard transformer?	No	Yes	No	No
Space requirement	Low	High	Lowest	Highest
Induce circulating currents in the secondary winding	No	Yes	No	Yes
***Effectiveness of neutral current compensation (based on simulation study under ideal grid voltage from* [19])**	Better than star-delta and star-hexagon	Good	Better than star-delta and star-hexagon	Good
Cost of the compensator	Low	High	Lowest	Highest

II.2.2. Hybrid approaches

II.2.2.1. Zigzag transformer with single-phase SAPF

As shown in figure (II.8), a single phase SAPF is connected between the neutral conductor of the grid and the neutral point of the zigzag transformer [19].
When switch (*S*) is closed, the single-phase SAPF is bypassed as the same case when the zigzag transformer is used alone.
When switch (*S*) is open, the SAPF comes into operation and produces the desired current for compensating source neutral current and forcibly injects the current through the neutral of the zigzag transformer. This current splits equally and flows through each of the zigzag windings. As the SAPF forcibly circulates the neutral current to the load via the zigzag transformer, its effectiveness does not depend on the zero-sequence impedance of the zigzag transformer and its location. Hence, the special design of the zigzag transformer for low zero-sequence impedance is not necessary [19].

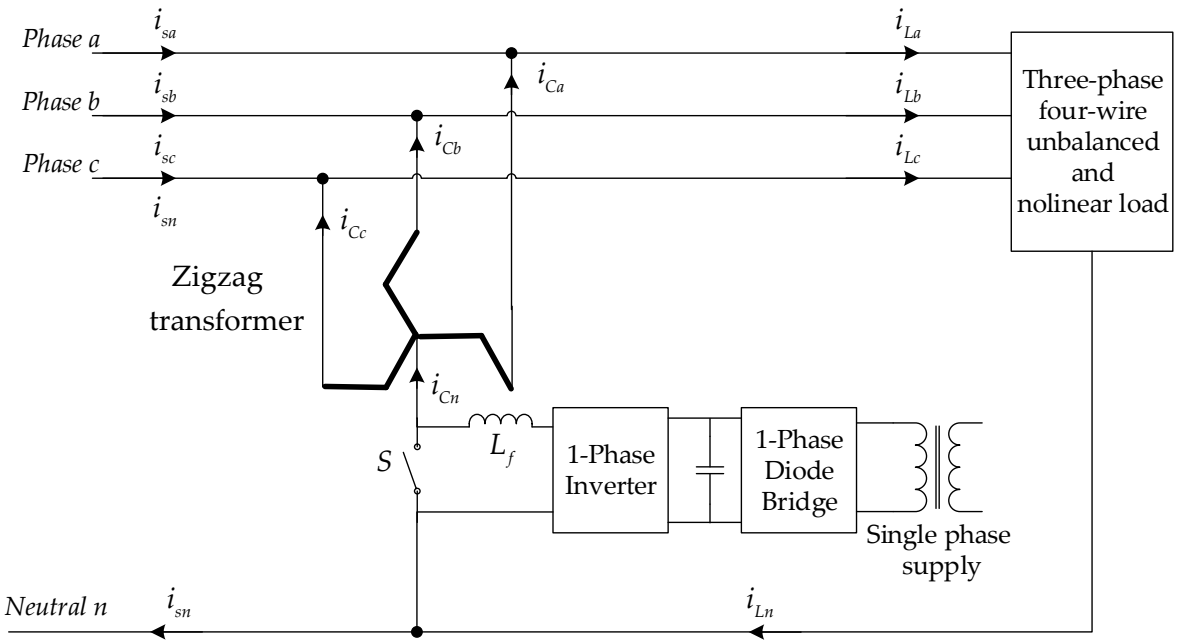

Figure (II.8): A hybrid approach for compensation of neutral current: a zigzag transformer with single-phase SAPF

II.2.2.2. Zigzag transformer with single-phase series APF

Figure (II.9) shows a filter scheme for compensation of neutral current in three-phase four-wire system [4, 19]. In this type of hybrid filter topology, the zigzag transformer is connected in parallel with the load and a single-phase PWM APF is connected in series with the neutral conductor. Proper operation of PWM APF increases the effectiveness of circulation of the neutral current of the load via the zigzag transformer. The DC capacitor of the PWM APF is recovered by drawing real power from the utility or from an external supply [4, 19]. This series connection of the PWM APF results in significant reduction in kVA rating of the inverter [4, 19]. This is because, only the currents other than zero-sequence (the zero-sequence will flow through the zigzag transformer) could only flow through the inverter [4, 19]. A bypass switch (S) is placed in parallel with the active power filter and will be operated in case of inverter failure or under abnormal utility conditions [4, 19].

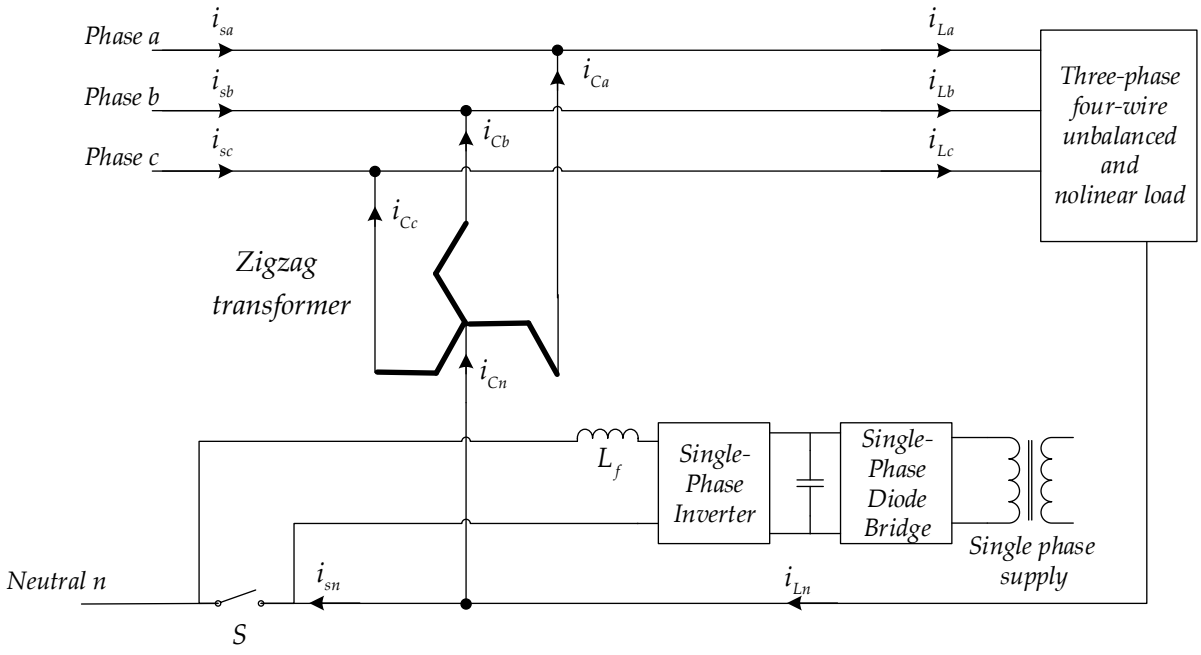

Figure (II.9): A hybrid approach for compensation of neutral current: a zigzag transformer with single-phase series APF

II.2.2.3. Star-delta transformer with single-phase half-bridge APF

Figure (II.10) shows a hybrid topology with star-delta transformer [19]. In this method a single-phase half-bridge PWM APF is connected to the neutral of the transformer primary and neutral conductor. A three-phase diode bridge rectifier is connected to the delta winding to provide the necessary real power to maintain the DC voltage across the capacitors of the single-phase half-bridge PWM APF. Proper switching signals are used to control the PWM APF in such a way that it produces the desired current to compensate the neutral current. This harmonic current is injected through the neutral of the transformer.

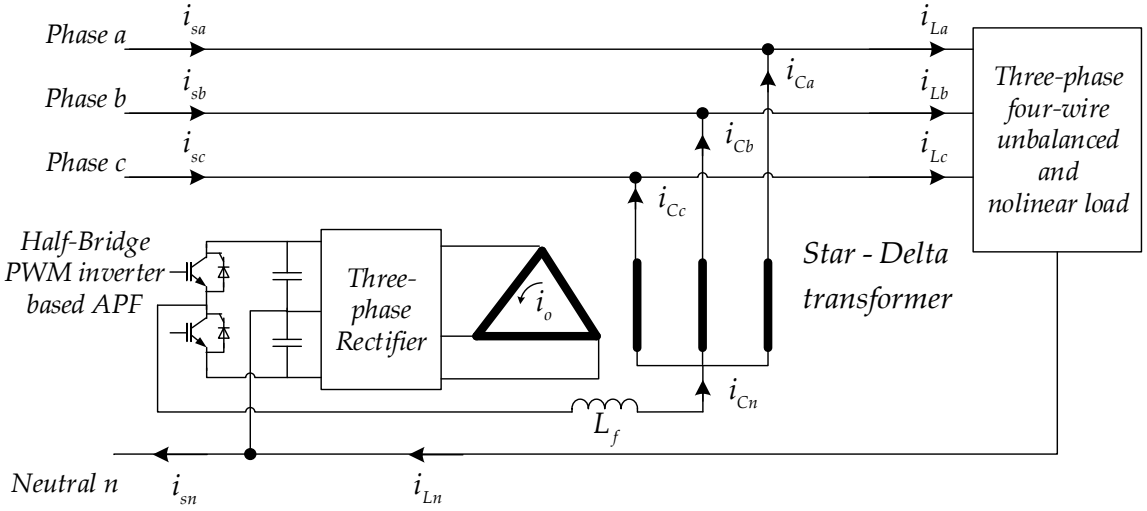

Figure (II.10): A hybrid approach for compensation of neutral current: a star-delta transformer with single-phase APF

II.2.3. Active topologies

SAPFs are specially designed to three-phase four-wire systems; it can compensate not only the neutral current, but also compensate harmonics from the positive- and negative-sequence components of the load current. Three different kinds are available for three-phase four-wire systems and are given below:

- Three H-bridge SAPF topology.
- Three-phase four-wire capacitor midpoint (or split-capacitor) SAPF topology.
- Three-phase four-leg SAPF topology.

II.2.3.1. Three H-bridge SAPF topology

Figure (II.11) shows the three H-bridge SAPF topology. It consists of three single-phase full bridge (H-bridge) inverters with a common self-supporting DC bus [18-20]. Here all 12 switching devices are used to realize the three-phase four-wire SAPF system. These H-bridge inverters are connected to the three-phase four-wire system by using three single-phase isolation transformers.
Considering the structural advantage of this topology, the control can be done either as a three-phase unit or three separate single-phase units. An independent phase control approach based on single-phase instantaneous reactive power theory is presented in [18-20].
In this topology the maximum voltage that appears across each H-bridge is the single-phase voltage and not the three-phase voltage, as in the case of split-capacitor or four-leg topology [18-20]. This result into a reduction of DC bus voltage by a factor of $\sqrt{3}$ Thus the reference DC bus voltage needed for proper operation of SAPF also reduces by a maximum factor of $\sqrt{3}$, which reduces in its turn the inverter rating. However, the main disadvantages of this topology are the increased number of switching devices and the use of transformers.

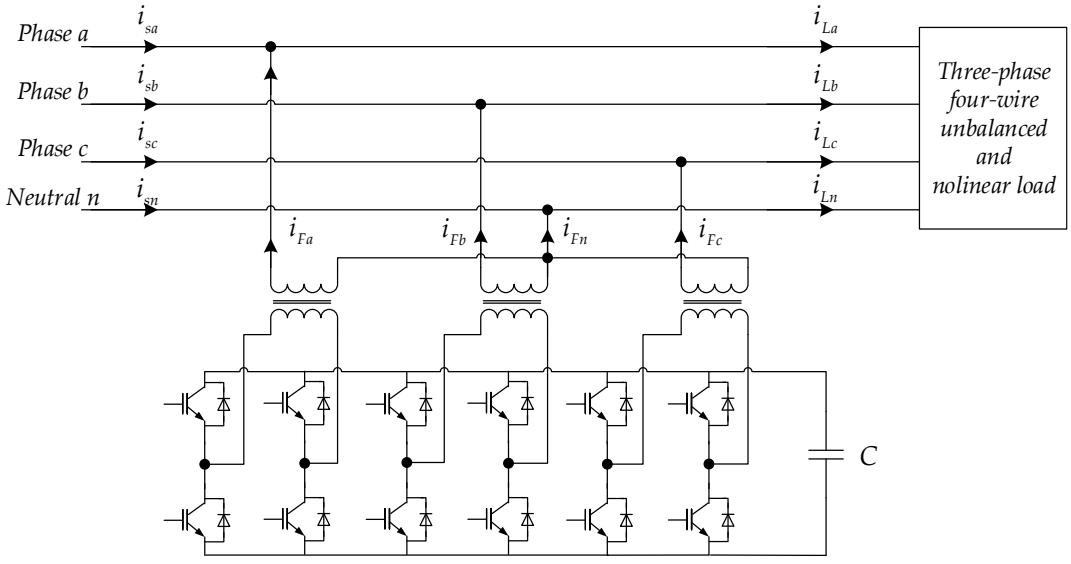

Figure (II.11): Three H-bridge based three-phase four-wire SAPF topology

II.2.3.2. Three-phase four-wire capacitor midpoint APF topology

As shown in figure (II.12), the capacitor midpoint SAPF topology utilizes the standard three-phase conventional inverter where the DC capacitor is split and the neutral wire is directly connected to the electrical midpoint of the capacitors [15-17]. The split capacitors allow load neutral current to flow through one of the DC capacitors, and return to the AC neural wire.

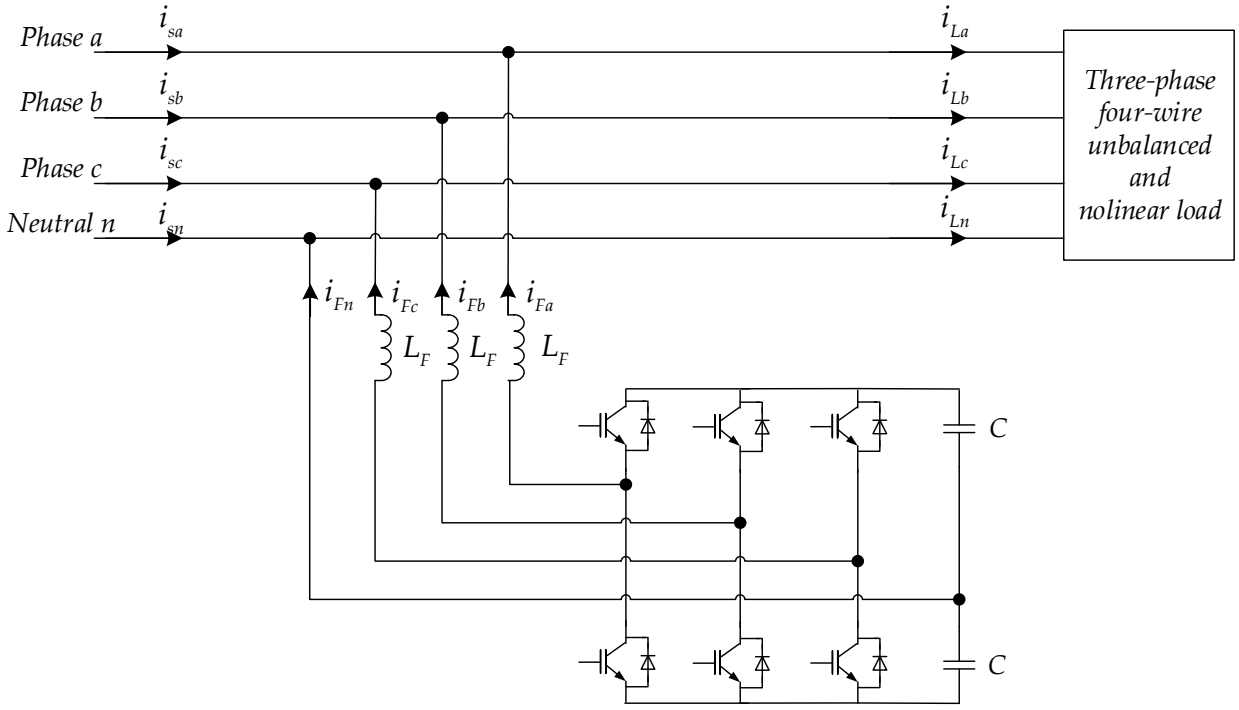

Figure (II.12): Three-phase midpoint based three-phase four-wire SAPF topology

One of the serious problems with this topology is voltage unbalance between the capacitors [19]. This is due to the direct flow of the neutral current through one of the capacitors, causing voltage variations among them. There are two possible ways to balance the capacitors:

- By adjusting the switching of the inverter (such as dynamic hysteresis controller) [85]. This approach requires additional control circuitry.
- By using additional power electronic switching circuitry (such as choppers) [86]. This approach increases the cost when compared with the former one.

II.2.3.3. Three-phase four-leg SAPF topology

Figure (II.13) shows the four-leg SAPF topology used in three-phase four-wire systems [21-23]. In this topology three of the switch legs are connected to the three phase conductors through series inductances while the fourth switch leg is connected directly to the neutral conductor. This topology is most suitable for compensation of high neutral currents [19, 60]. Despite having, higher number of switching devices this topology outweighed the split-capacitor topology by number of factors [19, 60].

- Better controllability: In this topology only one DC-bus voltage needs to be regulated, as opposed to two in the capacitor midpoint topology. This significantly simplifies the control circuitry with better controllability.
- Lower DC voltage and current requirement.
- High order harmonics in DC side current: The DC side current in three H-bridge and capacitor midpoint topology must handle the low order harmonics, which contribute to significant ripple on the DC-bus voltage. However, in four-leg topology, the DC side current has only higher order harmonics.

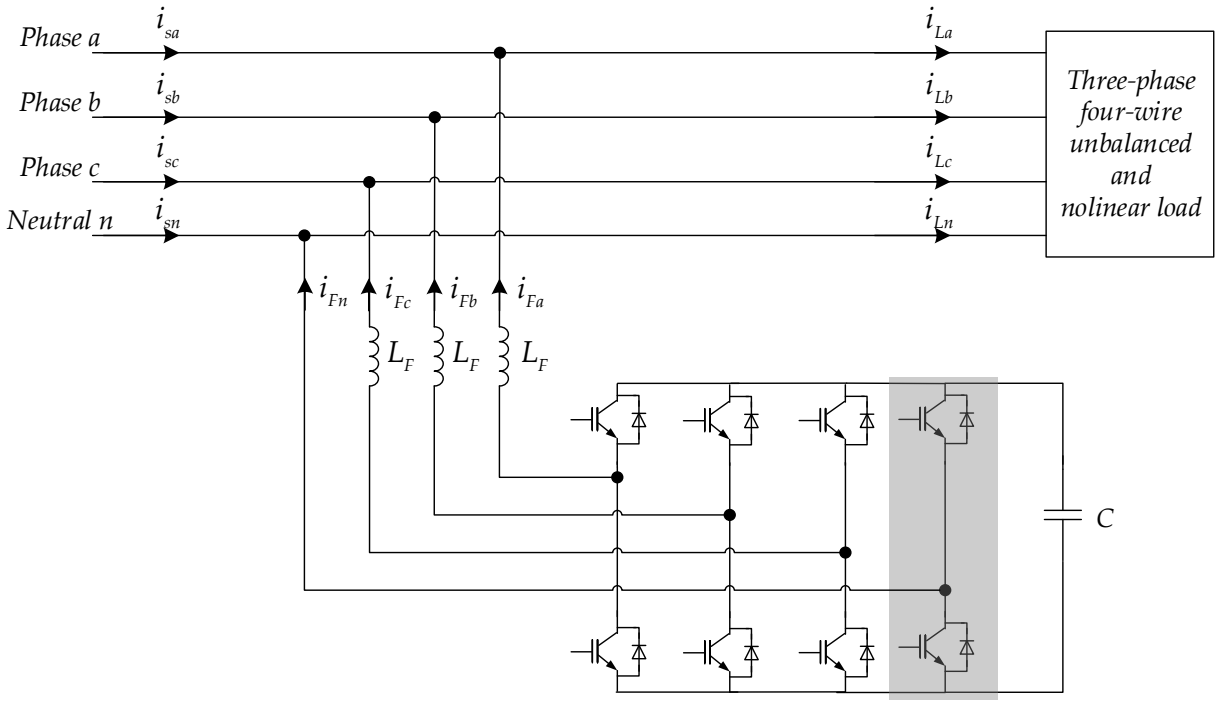

Figure (II.13): **T**hree-phase four-leg SAPF topology

The comparison of three-phase four-wire SAPFs are given in table (II. 2) [19]. The significant factor that may decide the selection of these topologies is the overall cost involved to realize the three-phase four-wire SAPF. Owing to the topological advantage of three H-bridge topology, the required reference DC bus voltage for SAPF is reduced maximum by a factor of $\sqrt{3}$. The high cost of three H-bridge topology owing to an increased number of semiconductor devices can be counter balanced by reduction in voltage rating of the devices, and thus making this topology suitable for high-voltage and high power application. For low-to-medium power applications, the low cost of capacitor midpoint topology can be selected. For better performance at moderate cost, the four-leg topology could be a best option for low-to-medium-power applications [19].

Table (II.2): Comparison between three-phase four-wire SAPF topologies [19]

SAPF topologies	*Three H-bridge*	*Capacitor midpoint*	*Four-leg*
Number of switching devices (2-level inverter)	12	6	8
Number of capacitors	1	2	1
Additional sensor requirement	None	One extra DC bus voltage sensor (total two)	One extra current sensor
DC-Side Voltage (v_l=line-to-line voltage)	$\geq \frac{\sqrt{2}}{3} v_l$	$\geq \frac{\sqrt{2}}{0.87} v_l$	$\geq \sqrt{2} v_l$
DC-side current harmonics	Lower order harmonics	Lower order harmonics	Higher order harmonics only
Need of coupling transformer	Necessary	Not necessary	Not necessary
Control over neutral current	Indirect	Indirect	Direct (using 4th leg)
Effectiveness of neutral current compensation	Better performance than capacitor midpoint	May degrade with high neutral currents	Better performance than capacitor midpoint and three H-bridge
Overall cost	High	Low	Moderate
Main advantage	Reduced DC voltage requirement	Least number of switching devices	Better controllability
Main disadvantage	More number of switching devices and the use of coupling transformer	Capacitor unbalance problem due to voltage difference across two capacitors	More number of switching devices
Application and topology selection	Suitable for high voltage, medium to high power applications. Suitable for compensating high neutral currents	Suitable for low to medium power applications	Suitable for low to medium power applications. Suitable for compensating high neutral currents

Finally from the three main topologies above motioned (passive, active and hybrid solutions), we can conclude these points:

- Passive harmonic filters for neutral current compensation are bulky and may cause resonance with system impedance. The transformer based methods can reduce the neutral current to a large extent, but it will not completely compensated and also its compensation characteristics depend on zero-sequence impedance of the transformer and the grid voltage conditions.
- In the hybrid approach, the application of transformers for reduction of neutral current has an advantage due to passive compensation, ruggedness, and less complexity compared with active compensation techniques. But many problems such as size, cost, and slow response remain to be solved.
- The three-phase four-wire SAPFs are specially designed for neutral current compensation and harmonic elimination in line-currents. The commercial success of these filters is due to their acceptable cost, fast response time, flexibility of control and continuous operation with virtually no maintenance. However, the large rating of the

inverter is the main drawback of these topologies. This disadvantage can be solved using multilevel inverters.

II.3. Five-level four-leg shunt active power filter

II.3.1. System description and modeling

The basic structure of the five-level four-leg SAPF is shown in figure (II.14). The main task of the five-level four-leg SAPF is to reduce harmonic currents and to ensure reactive power compensation. Ideally, the five-level four-leg SAPF needs to generate just enough reactive and harmonic current to compensate the nonlinear load harmonic in the line. The resulting total current drawn from the AC main is sinusoidal and balanced. The compensated neutral current is provided through a fourth leg allowing a better controllability. The main advantage of the four-leg configuration is the ability to suppress the neutral current from the source without any drawback in the filtering performance.

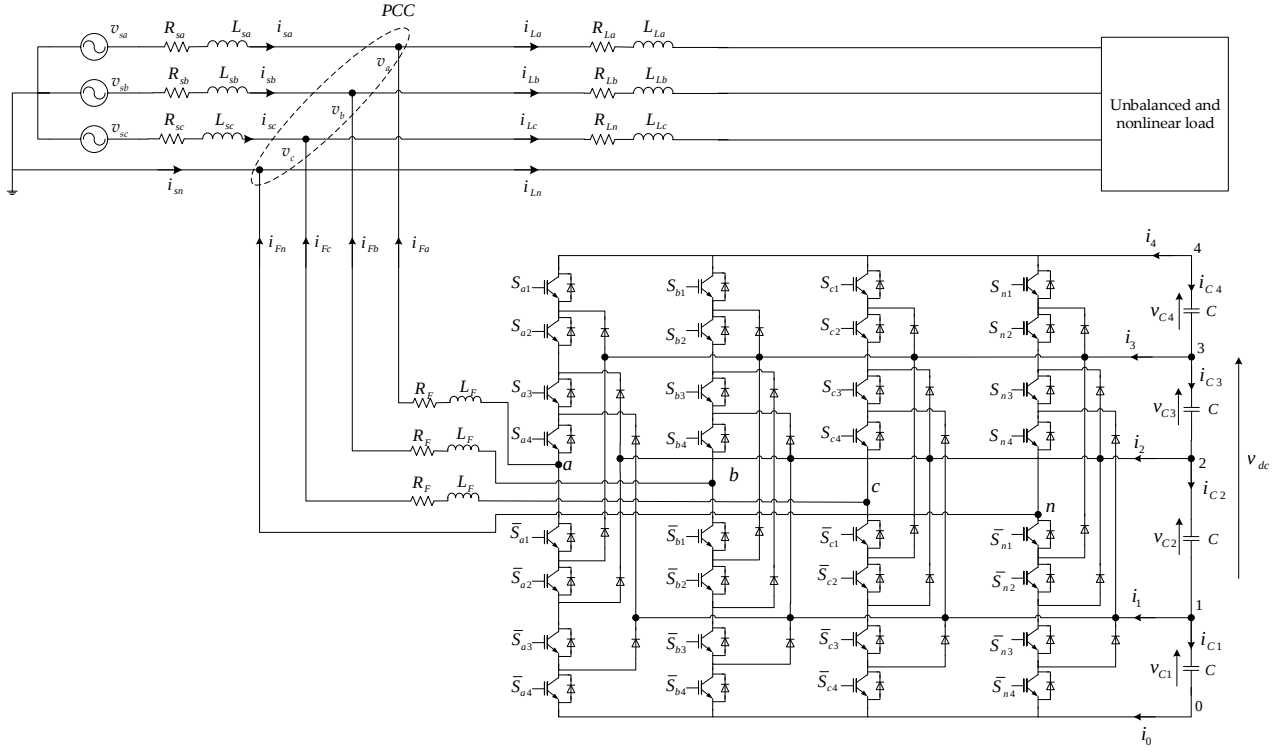

Figure (II. 14): Five-level four-leg SAPF configuration

The structure of the five-level inverter operating in SAPF is represented by the figure (II.14), where expressions of SAPF currents are defined by:

$$\begin{aligned}
\frac{di_{Fa}}{dt} &= \frac{1}{L_F}(v_{Fa} - v_a - R_F i_{Fa}) \\
\frac{di_{Fb}}{dt} &= \frac{1}{L_F}(v_{Fb} - v_b - R_F i_{Fb}) \\
\frac{di_{Fc}}{dt} &= \frac{1}{L_F}(v_{Fc} - v_c - R_F i_{Fc})
\end{aligned} \tag{II.1}$$

Where, v_a, v_b and v_c are the point of common coupling (PCC) voltages, i_{Fa}, i_{Fb} and i_{Fc}, v_{Fa}, v_{Fb} and v_{Fc} represent AC side currents and voltages of the SAPF, respectively.
On the other hand, we have:

$$\frac{dv_{dc}}{dt} = \frac{d}{dt}\left(v_{C1} + v_{C2} + v_{C3} + v_{C4}\right) \tag{II.2}$$

Equation (II.2) can also be written in the form:

$$\frac{dv_{dc}}{dt} = \frac{1}{C}\left(i_{C1} + i_{C2} + i_{C3} + i_{C4}\right) \tag{II.3}$$

Multiplying (II.3) by v_{dc} gives:

$$\frac{1}{2}\frac{dv_{dc}^2}{dt} = \frac{4}{C}\left(\frac{v_{dc}}{4}i_{C1} + \frac{v_{dc}}{4}i_{C2} + \frac{v_{dc}}{4}i_{C3} + \frac{v_{dc}}{4}i_{C4}\right) \tag{II.4}$$

By assuming that the capacitor voltages are balanced ($v_{Ci} = v_{dc}/4,\ (i = 1,2,3,4)$), equation (II.4) becomes:

$$\frac{dv_{dc}^2}{dt} = \frac{2p_{dc}}{C_{eq}} \tag{II.5}$$

Where: p_{dc} is the instantaneous DC power, and $C_{eq} = C/4$ is the equivalent capacitor.

The mathematical equations which govern the behaviour of the SAPF in *abc* reference frame are:

$$\begin{aligned}
\frac{di_{Fa}}{dt} &= \frac{-R_F}{L_F}i_{Fa} - \frac{v_a}{L_F} + \frac{v_{Fa}}{L_F}\\
\frac{di_{Fb}}{dt} &= \frac{-R_F}{L_F}i_{Fb} - \frac{v_b}{L_F} + \frac{v_{Fb}}{L_F}\\
\frac{di_{Fc}}{dt} &= \frac{-R_F}{L_F}i_{Fc} - \frac{v_c}{L_F} + \frac{v_{Fc}}{L_F}\\
\frac{dv_{dc}^2}{dt} &= \frac{2p_{dc}}{C_{eq}}
\end{aligned} \tag{II.6}$$

Based on the Concordia coordinates transformation, the differential equations describing the dynamic model of the four-leg SAPF in $\alpha\beta o$ reference frame are given by (II.7):

$$\begin{aligned}
\frac{di_{F\alpha}}{dt} &= \frac{1}{L_F}(v_{F\alpha} - v_\alpha - R_F i_{F\alpha})\\
\frac{di_{F\beta}}{dt} &= \frac{1}{L_F}(v_{F\beta} - v_\beta - R_F i_{F\beta})\\
\frac{di_{Fo}}{dt} &= \frac{1}{L_F}(v_{Fo} - v_o - R_F i_{Fo})\\
\frac{dv_{dc}^2}{dt} &= \frac{2p_{dc}}{C_{eq}}
\end{aligned} \tag{II.7}$$

II.3.2. Direct power control strategies of five-level four-leg SAPF

II.3.2.1. DPC-3DSVM of five-level four-leg SAPF

The basic operation of the proposed control method is shown in figure (II.15). The nonlinear loads are constructed from three uncontrolled single-phase rectifiers. The DC voltage is compared with its reference value v_{dc}^{*}, in order to maintain the energy stored in the capacitors constant. The PI controller is used to regulate the error between the capacitor voltage and its reference. The output of PI voltage controller presents the reference of DC active power p_{dc}^{*}. The compensating powers are computed using the modified p-q theory. The alternate value of active power is extracted using high-pass filter (HPF). The output signals from power controllers are used for switching signals generation by the 3DSVM.

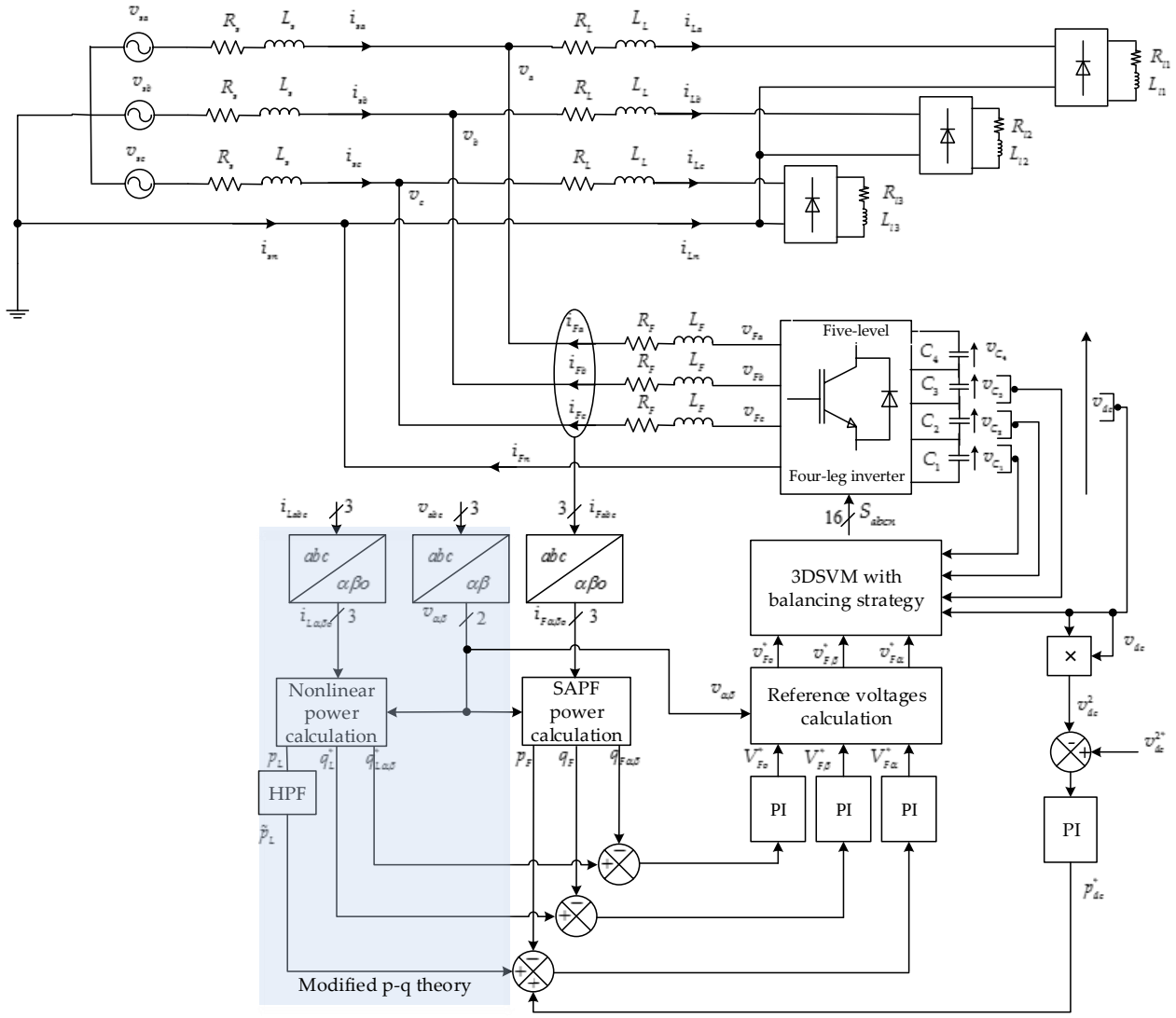

Figure (II.15): DPC-3DSVM of five-level four-leg SAPF

II.3.2.1.1. Modified p-q power theory (cross vector)

Harmonic extraction is the process in which reference current is generated by using the distorted waveform. Many theories have been developed such as p-q theory (instantaneous reactive power theory), d-q theory (synchronous reference frame), PLL with fuzzy logic controller [87], neural network [88] etc. Out of these theories, the p-q theory is the most widely used power theory to formulate the control of SAPF [89]. To compensate the zero sequence current and zero sequence power that exist in three-phase four-wire system under unbalance-load condition, the modified p-q theory [89] is adapted to calculate the compensating powers. The modified p-q theory is the power theory developed on the basic of p-q theory, which takes into account the zero sequence components that occurs in a three-phase four-wire system under unbalanced load conditions. The modified p-q power theory is very suitable for direct power control, because just active and reactive powers are used for this extraction technique.

The instantaneous active power of the nonlinear load, p_L is defined as the dot product of the PCC voltage vector $v = \begin{bmatrix} v_\alpha & v_\beta & v_o \end{bmatrix}$ and load current vector, $i_L = \begin{bmatrix} i_{L\alpha} & i_{L\beta} & i_{Lo} \end{bmatrix}$, which can be further decomposed into its average and oscillating components, $\bar{p}_L$ and $\tilde{p}_L$. On the other hand, the cross product of i_L and v gives the instantaneous reactive power as a vector $\vec{q}_L$, which can be further decomposed into $\alpha\beta$o components as $q_{L\alpha}$, $q_{L\beta}$, and q_{Lo}. The magnitude of the instantaneous imaginary power is the norm of the vector, $\vec{q}_L$. The powers p_L and $\vec{q}_L$ are given by:

$$p_L = v_\alpha i_{L\alpha} + v_\beta i_{L\beta} + v_o i_{Lo}$$

$$\vec{q}_L = \begin{bmatrix} q_{L\alpha} \\ q_{L\beta} \\ q_{Lo} \end{bmatrix} = \begin{bmatrix} 0 & -v_o & v_\beta \\ v_o & 0 & -v_\alpha \\ -v_\beta & v_\alpha & 0 \end{bmatrix} \begin{bmatrix} i_{L\alpha} \\ i_{L\beta} \\ i_{Lo} \end{bmatrix} \tag{II.8}$$

Note that the new reactive power q_{Lo} is the same as the original reactive power q_L in [89]. The other two reactive powers $q_{L\alpha}$ and $q_{L\beta}$ relate α and β components with zero sequences voltage and current, which are not considered in the original *p-q* theory [89]. The norm of the instantaneous reactive power vector expresses the total instantaneous reactive power q_L as follows:

$$q_L = \sqrt{q_{L\alpha}^2 + q_{L\beta}^2 + q_{Lo}^2} \tag{II.9}$$

The instantaneous powers defined in (II.8) are combined in a matrix expression as follows:

$$\begin{bmatrix} p_L \\ q_L \\ q_{L\alpha\beta} \end{bmatrix} = \begin{bmatrix} v_\alpha & v_\beta & v_o \\ -v_\beta & v_\alpha & 0 \\ v_o & -v_o & v_\beta - v_\alpha \end{bmatrix} \begin{bmatrix} i_{L\alpha} \\ i_{L\beta} \\ i_{Lo} \end{bmatrix} \quad \text{(II.10)}$$

Where:

$q_{L\alpha\beta} = q_{L\alpha} + q_{L\beta}$: is the sum of α and β reactive power components.

For harmonic, reactive power compensation and balancing three-phase source currents, all of the reactive powers q_L, $q_{L\alpha\beta}$ and oscillating active power components $\tilde{p}_L$ are selected to calculate SAPF references powers as follows:

$$\begin{bmatrix} p_F^* \\ q_F^* \\ q_{F\alpha\beta}^* \end{bmatrix} = \begin{bmatrix} \tilde{p}_L - p_{dc}^* \\ q_L \\ q_{L\alpha\beta} \end{bmatrix} \quad \text{(II.11)}$$

Where: p_{dc}^* is the instantaneous DC power that causes and additional flow of energy to/from the DC capacitors in order to keep the DC voltage around a fixed reference value, this power is obtained from the output of the DC voltage controller.

II.3.2.1.2. New model of four-leg SAPF based on active and reactive powers

In general, the source voltages are balanced, and after the balancing of line currents, the PCC voltage are also become balanced, then, the hompolair voltage v_o can be neglected. The powers at the output of the SAPF are given as:

$$\begin{bmatrix} p_F \\ q_F \\ q_{F\alpha\beta} \end{bmatrix} = \begin{bmatrix} v_\alpha & v_\beta & 0 \\ -v_\beta & v_\alpha & 0 \\ 0 & 0 & v_\beta - v_\alpha \end{bmatrix} \begin{bmatrix} i_{F\alpha} \\ i_{F\beta} \\ i_{Fo} \end{bmatrix} \quad \text{(II.12)}$$

In order to calculate the powers derivatives, the lie derivative method is used; the active and reactive powers must be chosen as outputs. The three first equations of the system (II.7) can be written as follow:

$$\begin{aligned} \dot{x} &= f(x) + g(x)u \\ y &= h(x) \end{aligned} \quad \text{(II.13)}$$

Where:

$$x=\begin{bmatrix} i_{F\alpha} \\ i_{F\beta} \\ i_{Fo} \end{bmatrix},\ f(x)=\begin{bmatrix} f_1 \\ f_2 \\ f_3 \end{bmatrix}=\frac{1}{L_F}\begin{bmatrix} -R_F i_{F\alpha}-v_\alpha \\ -R_F i_{F\beta}-v_\beta \\ -R_F i_{Fo}-v_o \end{bmatrix}$$

$$g(x)=\frac{1}{L_F}\begin{bmatrix} 1 & 0 & 0 \\ 0 & 1 & 0 \\ 0 & 0 & 1 \end{bmatrix},\ u=\begin{bmatrix} v_{F\alpha} \\ v_{F\beta} \\ v_{Fo} \end{bmatrix},\ y=\begin{bmatrix} h_1 \\ h_2 \\ h_3 \end{bmatrix}=\begin{bmatrix} p_F \\ q_F \\ q_{F\alpha\beta} \end{bmatrix}$$

$f(x)$ and $h(x)$ are 3rd order smooth vector fields, $g(x)$ is an 3×3 matrix of smooth vector field columns g_i, u and y are 3×1 vectors of input and output respectively.

The derivative of each output can be expressed as follows [90]:

$$y_i^{(\gamma)}=L_f^{\gamma}h_i+\sum_{j=1}^{3}L_{g_j}L_f^{\gamma-1}h_i u_j \tag{II.14}$$

Where: γ is the number of derivative of output y_i, in this case $\gamma=1$.
Than the derivative of output y_i is:

$$\dot{y}_i=L_f h_i+L_g h_i u \tag{II.15}$$

Where $L_f h_i$, $L_g h_i$ are the Lie derivatives of h_i with respect to f and g, respectively.
The derivative of powers are given as:

$$\begin{aligned} \frac{dp_F}{dt}&=v_\alpha f_1+v_\beta f_2+\frac{v_\alpha}{L_F}v_{F\alpha}+\frac{v_\beta}{L_F}v_{F\beta} \\ \frac{dq_F}{dt}&=-v_\beta f_1+v_\alpha f_2-\frac{v_\beta}{L_F}v_{F\alpha}+\frac{v_\alpha}{L_F}v_{F\beta} \\ \frac{dq_{F\alpha\beta}}{dt}&=\left(v_\beta-v_\alpha\right)f_3+\frac{\left(v_\beta-v_\alpha\right)}{L_F}v_{Fo} \end{aligned} \tag{II.16}$$

After more simplification, the final new model of the four-leg SAPF is given as follows:

$$\begin{aligned} \frac{dp_F}{dt}&=\frac{1}{L_F}(-R_F p_F+V_{F\alpha}) \\ \frac{dq_F}{dt}&=\frac{1}{L_F}(-R_F q_F+V_{F\beta}) \\ \frac{dq_{F\alpha\beta}}{dt}&=\frac{1}{L_F}(-R_F q_{F\alpha\beta}+V_{Fo}) \\ \frac{dv_{dc}^2}{dt}&=\frac{2p_{dc}}{C_{eq}} \end{aligned} \tag{II.17}$$

Where:

$$V_{F\alpha} = v_\alpha v_{F\alpha} + v_\beta v_{F\beta} - \left(v_\alpha^2 + v_\beta^2\right)$$
$$V_{F\beta} = -v_\beta v_{F\alpha} + v_\alpha v_{F\beta}$$
$$V_{Fo} = \left(v_\beta - v_\alpha\right) v_{Fo}$$

II.3.2.1.3. Controllers synthesis

II.3.2.1.3.1. DC voltage controller synthesis

The role of the DC voltage control loop is to maintain DC voltage at a constant reference value by controlling the active power flow between the PCC and the DC bus. The DC voltage controller has as inputs the reference voltage v_{dc}^{*2} and the measured voltage v_{dc}^2.

From the fourth equation of the system (II.17), we deduce the following transfer function:

$$\frac{v_{dc}^2(s)}{p_{dc}(s)} = \frac{2}{C_{eq}s} \tag{II.18}$$

Where: s is the Laplace operator.

The diagram presented in figure (II.16) shows the DC voltage regulation with a PI controller.

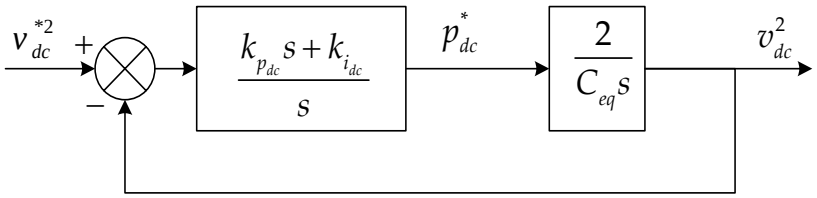

Figure (II.16): Regulation of DC voltage with a PI controller

The closed loop transfer function is given by:

$$H(s) = \frac{2\left(\frac{k_{p_{dc}}}{C_{eq}}s + \frac{k_{i_{dc}}}{C_{eq}}\right)}{s^2 + \frac{2k_{p_{dc}}}{C_{eq}}s + \frac{2k_{i_{dc}}}{C_{eq}}} \tag{II.19}$$

To control the closed loop system, it is necessary to choose the PI coefficients $k_{p_{dc}}$ and $k_{i_{dc}}$.
By comparing (II.19) with a desired transfer function of a second order system given by:

$$F(s)=\frac{2\xi_{dc}\omega_{n_{dc}}s+\omega_{n_{dc}}^2}{s^2+2\xi_{dc}\omega_n s+\omega_{n_{dc}}^2} \tag{II.20}$$

By identification between expressions (II.19) and (II.20), the PI coefficients are calculated as:

$$\begin{aligned} k_{p_{dc}} &= C_{eq}\xi_{dc}\omega_{n_{dc}}/2 \\ k_{i_{dc}} &= C_{eq}\omega_{n_{dc}}^2/2 \end{aligned} \tag{II.21}$$

II.3.2.1.3.2. Powers controllers synthesis

To ensure full compensation for harmonic phase currents, reactive power, and neutral current, the SAPF must deliver active and reactive powers as close as possible to their reference powers p_F^*, q_F^* and $q_{F\alpha\beta}^*$ to the PCC. So three PI regulators must be used to cancel the errors among the filter powers p_F, q_F and $q_{F\alpha\beta}$ and their reference values. The compensated output of these regulators are reference voltages ($V_{F\alpha}, V_{F\beta}$ and V_{Fo}) in the $\alpha\beta o$ coordinate system.

From first three equations of system (II.17), the transfer functions of p_F, q_F and $q_{F\alpha\beta}$ are given as:

$$\begin{aligned} \frac{p_F}{V_{F\alpha}} &= \frac{1}{L_F s+R_F} \\ \frac{q_F}{V_{F\beta}} &= \frac{1}{L_F s+R_F} \\ \frac{q_{F\alpha\beta}}{V_{Fo}} &= \frac{1}{L_F s+R_F} \end{aligned} \tag{II.22}$$

By introducing the power PI controllers the following diagrams are obtained:

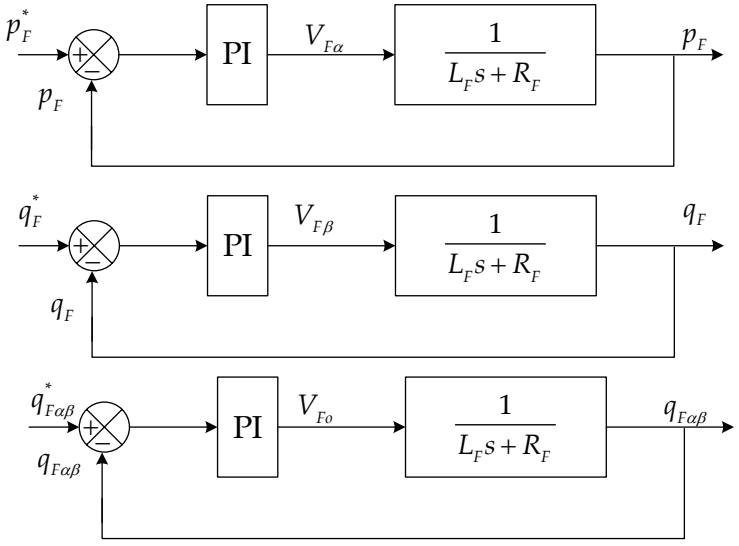

Figure (II.17): SAPF powers regulation by three PI controllers

The closed loop transfer function of each one is given by:

$$H(s) = \frac{k_p s + k_i}{L_F s^2 + (k_p + R_F)s + k_i} \tag{II.23}$$

Than the PI constants are obtained on (II.24):

$$\begin{aligned} k_p &= 2L_F \xi \omega_n - R_F \\ k_i &= L_F \omega_n{}^2 \end{aligned} \tag{II.24}$$

Note that equation (II.24) is valid for three regulators.
Once the output $V_{F\alpha}, V_{F\beta}$ and V_{Fo} are determined, the output voltages $v_{F\alpha}, v_{F\beta}$ and v_{Fo} can be deduced from (II.17).

II.3.2.2. PDPC-3DSVM of five-level four-leg SAPF

The proposed predictive PDPC scheme is based on the computation of the SAPF average voltage vector $V_{F\alpha\beta o}$ using a predictive control algorithm, which makes instantaneous active and reactive powers equal to their reference values at each sampling period. For this reason, instantaneous active and reactive power measures and commands are used as input data variables of predictive control algorithm block as shown in figure (II.18). At the beginning of each sampling period T_e, the SAPF average voltage vector $V_{F\alpha\beta o}$, which allows cancellation of instantaneous active and reactive power tracking errors at the end of the sampling period, is computed. Then, 3DSVM technique is used to generate a sequence of switching states to achieve the control objective with constant switching frequency.
The PDPC uses the same DC voltage PI controller developed in the previous control strategy to produce the reference DC power component p_{dc}^{*}.

PDPC requires a predictive model of the instantaneous power behavior, which is described in the following steps.

If the sampling period T_e is infinitely small compared with the fundamental period. The discretization of the three first equations of (II.17) yields:

$$\begin{aligned} p_F(k+1) - p_F(k) &= \frac{T_e}{L_F}(-R_F p_F(k) + V_{F\alpha}(k)) \\ q_F(k+1) - q_F(k) &= \frac{T_e}{L_F}(-R_F q_F(k) + V_{F\beta}(k)) \\ q_{F\alpha\beta}(k+1) - q_{F\alpha\beta}(k) &= \frac{T_e}{L_F}(-R_F q_{F\alpha\beta}(k) + V_{Fo}(k)) \end{aligned} \tag{II.25}$$

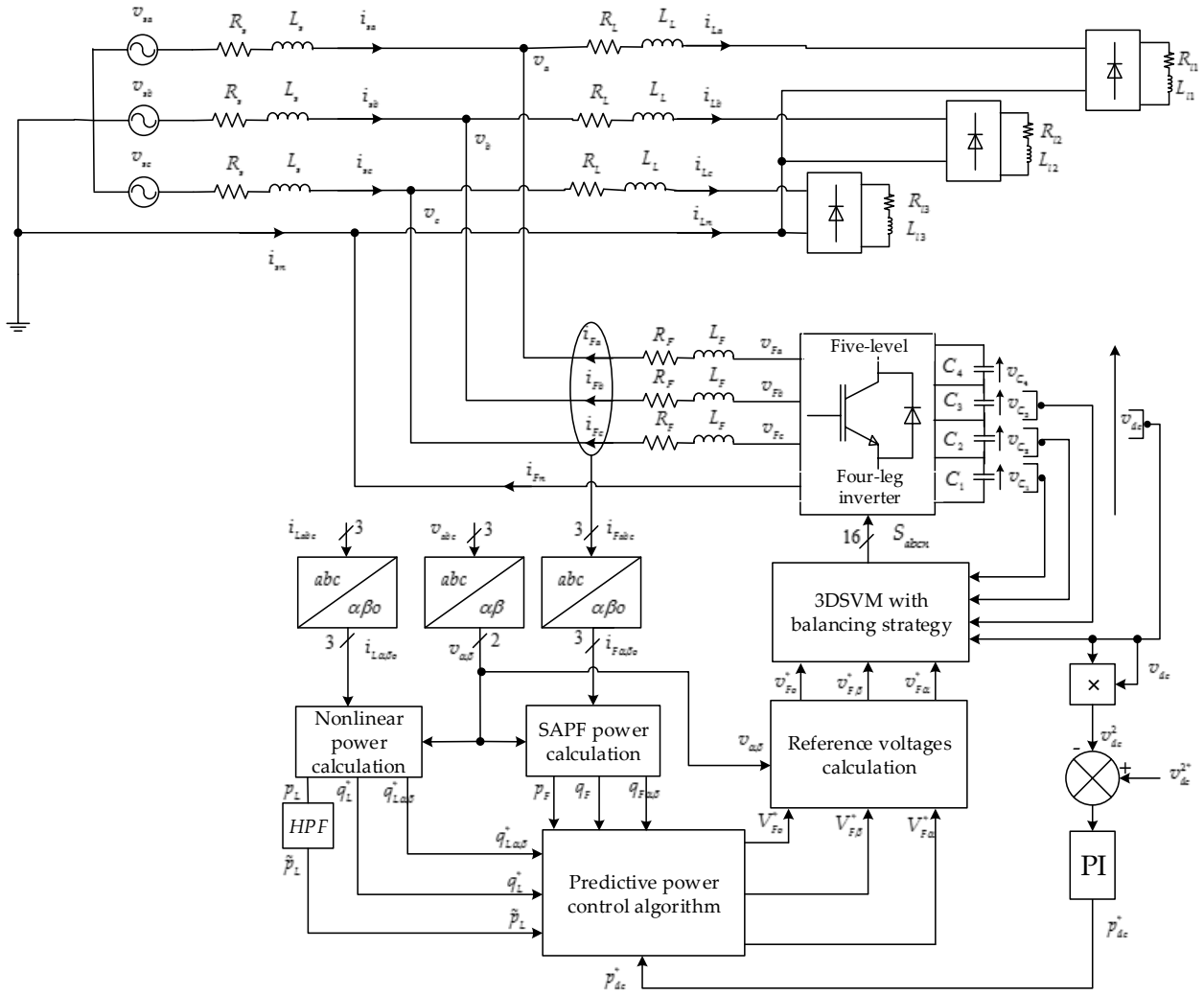

Figure (II.18): PDPC-3DSVM of five-level four-leg SAPF

Since the control objective is to force active and reactive powers to be equal to their reference values at the next sampling period, equation (II.25) can be rewritten as follows:

$$\begin{aligned} p_F^*(k+1) &= p_F(k+1) = \frac{T_e}{L_F}(-R_F p_F(k) + V_{F\alpha}(k)) \\ q_F^*(k+1) &= q_F(k+1) = \frac{T_e}{L_F}(-R_F q_F(k) + V_{F\beta}(k)) \\ q_{F\alpha\beta}^*(k+1) &= q_{F\alpha\beta}(k+1) = \frac{T_e}{L_F}(-R_F q_{F\alpha\beta}(k) + V_{Fo}(k)) \end{aligned} \tag{II.26}$$

Using (II.26), the required SAPF average voltage vector is expressed as follows:

$$\begin{bmatrix} V_{F\alpha}(k) \\ V_{F\beta}(k) \\ V_{Fo}(k) \end{bmatrix} = R_F \begin{bmatrix} p_F(k) \\ q_F(k) \\ q_{F\alpha\beta}(k) \end{bmatrix} + \frac{L_F}{T_e} \begin{bmatrix} p_F^*(k+1) - p_F(k) \\ q_F^*(k+1) - q_F(k) \\ q_{F\alpha\beta}^*(k+1) - q_{F\alpha\beta}(k) \end{bmatrix} \tag{II.27}$$

The instantaneous power references at the next sampling period (k+1) can be estimated using a linear extrapolation as shown in figure (II.19).

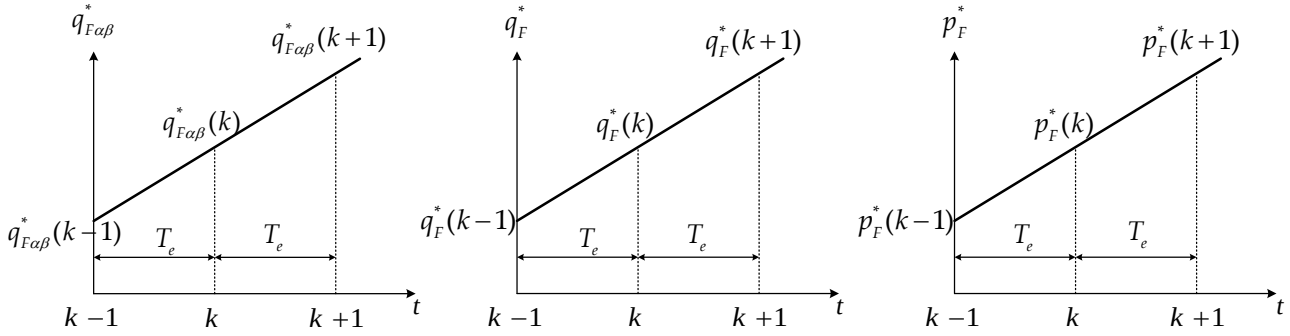

Figure (II.19): Predictive value estimation of reference powers

The estimated power references are given by:

$$\begin{aligned} p^*_F(k+1) &= 2p^*_F(k) - p^*_F(k-1) \\ q^*_F(k+1) &= 2q^*_F(k) - q^*_F(k-1) \\ q^*_{F\alpha\beta}(k+1) &= 2q^*_{F\alpha\beta}(k) - q^*_{F\alpha\beta}(k-1) \end{aligned} \tag{II.28}$$

The digital PDPC control law which provides the required SAPF average voltage vector to be applied during each sampling period is given by the following equation:

$$\begin{bmatrix} V_{F\alpha}(k) \\ V_{F\beta}(k) \\ V_{Fo}(k) \end{bmatrix} = R_F \begin{bmatrix} p_F(k) \\ q_F(k) \\ q_{F\alpha\beta}(k) \end{bmatrix} + \frac{L_F}{T_e} \begin{bmatrix} \Delta p^*_F(k) + e_{p_F}(k) \\ \Delta q^*_F(k) + e_{q_F}(k) \\ \Delta q^*_{F\alpha\beta}(k) + e_{q_{F\alpha\beta}}(k) \end{bmatrix} \tag{II.29}$$

Where: $e_{p_F}(k), e_{q_F}(k)$ and $e_{q_{F\alpha\beta}}(k)$ are the actual active and reactive power tracking errors defined as:

$$\begin{bmatrix} e_{p_F}(k) \\ e_{q_F}(k) \\ e_{q_{F\alpha\beta}}(k) \end{bmatrix} = \begin{bmatrix} p^*_F(k) - p_F(k) \\ q^*_F(k) - q_F(k) \\ q^*_{F\alpha\beta}(k) - q_{F\alpha\beta}(k) \end{bmatrix} \tag{II.30}$$

$\Delta p^*_F(k)$, $\Delta q^*_F(k)$ and $\Delta q^*_{F\alpha\beta}(k)$ are the actual change in active and reactive power references given by:

$$\begin{bmatrix} \Delta p^*_F(k) \\ \Delta q^*_F(k) \\ \Delta q^*_{F\alpha\beta}(k) \end{bmatrix} = \begin{bmatrix} p^*_F(k) - p^*_F(k-1) \\ q^*_F(k) - q^*_F(k-1) \\ q^*_{F\alpha\beta}(k) - q^*_{F\alpha\beta}(k-1) \end{bmatrix} \tag{II.31}$$

II.3.3. Passive components sizing

The passive components values have a strong effect on the size, efficiency, and cost of the filtering system. This is the reason why they represent an interesting topic for designers and manufacturers. In literature there are many studies that discuss different methods of design [91-97]. However, the selection of the coupling inductance (L_F), DC link capacitor (C), and the reference DC voltage v_{dc}^{*} values are subject to several constraints, namely the harmonic distortion, the current ripple, and the power compensation.

II.3.3.1. Selecting the reference DC voltage value

The reference DC voltage value is selected by considering the capability of reactive power compensation [91-92].

The single-phase phasor diagram for representing the reactive power flow and capacity of the SAPF is shown in figure (II.20). The SAPF adjusts its current $\overline{i}_{F1}$ (1 means fundamental) to compensate the reactive power of the load. If the SAPF has compensated all of the reactive power, the source current $\overline{i}_{s1}$, should be in phase with the source voltage $\overline{v}_s$ and the SAPF current $\overline{i}_{F1}$ should be orthogonal to $\overline{v}_s$.
Based on the circuit theory, we can write:

$$\overline{v}_{F1} = \overline{v}_s + j\omega L_F \overline{i}_{F1} \tag{II.32}$$

Where: the $\overline{v}_{F1}$ is the fundamental of output voltage inverter, and ω: is the angular pulsation.

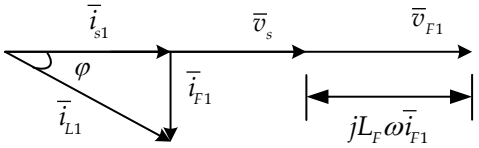

Figure (II.20): Single-phase phasor diagram of the SAPF

According to the figure (II.20), the relationship between $\overline{v}_{F1}, \overline{v}_s$ and $\overline{i}_{F1}$ become linear, and the fundamental of the SAPF current can be deduced as:

$$i_{F1} = \frac{v_{F1} - v_s}{\omega L_F} = \frac{v_{F1}}{\omega L_F}\left(1 - \frac{v_s}{v_{F1}}\right) \tag{II.33}$$

The reactive power delivered from the SAPF to the system also can be calculated as:

$$q_F = 3v_s i_{F1} = \frac{3v_s v_{F1}}{\omega L_F}\left(1 - \frac{v_s}{v_{F1}}\right) \tag{II.34}$$

The equation (II.34) indicates that the SAPF can compensate the lagging reactive power only when $v_{F1} \geq v_s$. By solving $dq_F / dv_s = 0$, one also can find that the maximum capacity of the SAPF occurs at $v_{F1} = 2v_s$ and the maximum capacity is [91-92]:

$$q_{F\max} = \frac{3v_s^2}{\omega L_F} \tag{II.35}$$

The exact range of v_{F1} must be set according to the capacity requirement of the filtering system [91-92]. However, based on the above analysis, the allowable v_{F1} should locate in the range:

$$v_s \leq v_{F1} \leq 2v_s \tag{II.36}$$

In the other hand, v_{F1} can be expressed in term of DC voltage v_{dc} when the modulation index *M*=1, as follows:

$$v_{F1} = \frac{v_{dc}}{\sqrt{6}} \tag{II.37}$$

Once v_{F1} is determined, the required v_{dc} can be found using (II.37).

For instance, for $v_s = 5.5\ kV$, and if v_{F1} is selected as $v_{F1} = 1.5v_s$, it results: $v_{dc} = 20.2\ kV$.
In the present study, the value chosen for v_{dc} is 20 kV.

II.3.3.2. Coupling inductance selection (L_F)

As is well-known, the coupling inductance reduces the current harmonics ripples injected to the PCC. The design of this device can be carried out in different ways; considering the voltage drop in the inductor, analyzing the current ripple in high frequencies, identifying the harmonic spectrum generated by the inverter and, others [91-97].

In this case an approach based on high frequency analyses has been developed. Thus, high frequency analysis will define the minimum inductor value (L_{Fmin}) taking into account the current ripple values [97].

The inductor voltage v_{L_F} is given by:

$$v_{L_F} = v_F - v_s \tag{II.38}$$

Where: v_F is the output voltage inverter.

At high switching frequencies, we can consider that over a switching period, the source voltage is constant [97], it is noted by $v_s = v_{smoy}$.

The current ripple is related to the instantaneous output voltage inverter. Equation (II.39) gives the maximum instantaneous output voltage step that can be deliver by the five-level four-leg inverter.

$$\Delta v_F = \frac{v_{dc}}{4} \tag{II.39}$$

From the figure (II.21), the average value of the voltage v_F is given by:

$$v_{Fmoy} = \frac{\alpha v_{dc}}{4} \tag{II.40}$$

Where : $\alpha \in [0 \;\; 1]$ is the duty cycle.

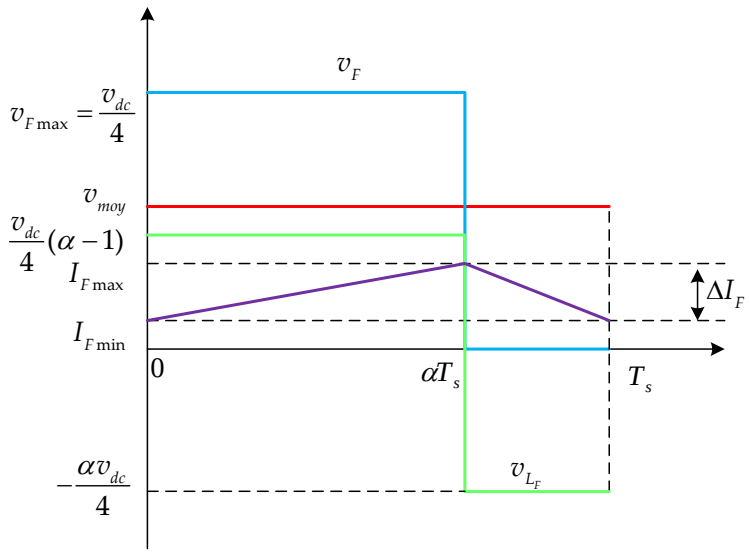

Figure (II.21): Current ripple during a switching period

The current ripple is calculated by the following expression:

$$\Delta I_F = \frac{v_{dc}(1-\alpha)\alpha T_s}{4L_F} \tag{II.41}$$

It will be maximum for α = 1/2. In this case, the inductance value is given by:

$$L_F \geq L_{F\min} = \frac{v_{dc} T_s}{16 \Delta I_{F\max}} \tag{II.42}$$

For proposed filtering system, we have:

$f_s = 2kHz, T_s = 0.5ms, v_{dc} = 20\text{kV}$, and $\Delta I_{F\max} = 10\%$, which gives $L_{F\min} = 0.8mH$.

The inductor value used in this work is L_F=1mH.

II.3.3.3. DC-link capacitors sizing

The DC-link capacitors have an important influence on the filtering quality because they store the energy that is necessary for the proper functioning of the filtering system. Indeed the ripples in capacitors voltages are mainly caused by the exchange of energy between DC and AC side of SAPF [96].

The RMS value of the fundamental load current I_{L1}, is given by [96]:

$$I_{L1} = \frac{\sqrt{6}}{\pi} I_l \tag{II.43}$$

Where: I_l is the rectifier load current.

The load harmonic current I_{Lhar} represents the difference between the load current I_L and its fundamental. The load harmonic current is given by [96]:

$$I_{Lhar} = \sqrt{I_L^2 - I_{L1}^2} = \left(\sqrt{\frac{2}{3} - \frac{6}{\pi^2}} \right) I_l = 0.2423 I_l \tag{II.44}$$

The SAPF must provide the corresponding power to the harmonics generated by the load. The ratio between the SAPF power S_F and the nonlinear load power S_L is [96]:

$$\frac{S_F}{S_L} = \frac{S_{Lhar}}{S_L} = \frac{3 I_{Lhar} v_s}{3 I_L v_s} = \frac{I_{Lhar}}{I_L} = \frac{0.2423 I_l}{\sqrt{\frac{2}{3}} I_l} = 0.2968 \tag{II.45}$$

Hence, one can express the SAPF power according to the pollutant load power by:

$$S_F = 0.2968 S_L \tag{II.46}$$

The load power S_L is made of active power p_L, reactive power q_L and distorting power D_L. It is given by the following equation:

$$S_L = \sqrt{p_L^2 + q_L^2 + D_L^2} \tag{II.47}$$

In the case of simultaneous compensation of harmonics and reactive power, the SAPF power is given by [96]:

$$S_F = \sqrt{q_L^2 + D_L^2} \tag{II.48}$$

From (II.46), (II.47) and (II.48), we have:

$$\frac{S_F}{S_L} = \frac{\sqrt{q_L^2 + D_L^2}}{\sqrt{p_L^2 + q_L^2 + D_L^2}} = 0.2968 \tag{II.49}$$

From equation (II.49), the SAPF power can be expressed in terms of the load active power by:

$$S_F = 0.3036 p_L \tag{II.50}$$

In the case of a five-level inverter, each capacitor must be sized for a voltage equal to v_{dc} / 4. The capacitors of the SAPF must produce a power variation which must be equal or greater than the equivalent energy of $0.3036 p_L$. The minimum and maximum energies stored in each capacitor are given by:

$$\begin{aligned} E_{\min} &= \frac{1}{2} C \frac{v_{dc.\min}^2}{16} \\ E_{\max} &= \frac{1}{2} C \frac{v_{dc.\max}^2}{16} \end{aligned} \tag{II.51}$$

The change in the capacitor energy during a ripple period of the DC voltage (ΔT) must be greater or equal to than the energy that must be produced by the SAPF [96].

$$4\left(E_{\max} - E_{\min}\right) = \frac{1}{32} C v_{dc.\max}^2 - \frac{1}{32} C v_{dc.\min}^2 \geq 0.3036 p_L \Delta T \tag{II.52}$$

The ripple period of the capacitor voltage is chosen six times lower than the fundamental period, we can find.

$$C \geq \frac{8 * 0.3036 p_L}{6 f \left(v_{dc.\max}^2 - v_{dc.\min}^2\right)} \tag{II.53}$$

If the DC voltage ripple is fixed at Δv_{dc} =2%, the following expression can be written:

$$v_{dc\max(\min)} = v_{dc} \pm \frac{\Delta v_{dc}}{2} \tag{II.54}$$

For the system under study, we have:

f = 50Hz, p_L = 5 MW, and v_{dc} = 20 kV. It results that $C \geq 4mF$, the adapted capacitance is $C=5mF$.

II.4. Simulation results

The effectiveness of five-level four-leg SAPF controlled by DPC-3DSVM and PDPC-3DSVMin terms of harmonic current filtering, reactive power compensation, load current balancing, and neutral current elimination performance have been examined under balanced/unbalanced nonlinear load and distorted source voltage conditions. The parameters used in simulation are gathered in table (II.3).

Table (II.3): System parameters

RMS value of phase voltage	5.5 kV
DC-link capacitor C	5 mF
Source impedance R_s, L_s	0.1 mΩ, 1 mH
Filter impedance R_F, L_F	0.1 mΩ, 1 mH
Line impedance R_l, L_l	0.1 mΩ, 1 mH
DC-link voltage reference $v_{dc\ ref}$	20 kV
Diode rectifier load R_l, L_l	10 Ω, 50 mH
Switching frequency f_s	2 kHz

II.4.1. Steady state operation

The source current of the first phase and its harmonic spectrum before and after compensation are illustrated in figures (II.22), (II.23) and (II.24). It results that the SAPF decreases the total harmonic distortion (THD) in the source currents from 33.40% to 2.07% with DPC-3DSVM technique. However, with PDPC-3DSVM, the THD is reduced to 0.66% which proves the effectiveness of the PDPC-3DSVM over DPC-3DSVM for this operation condition.

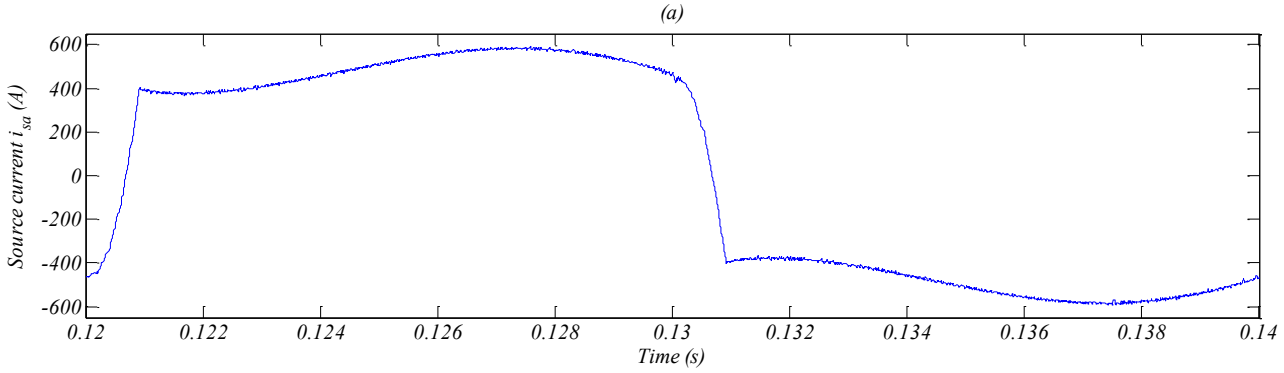

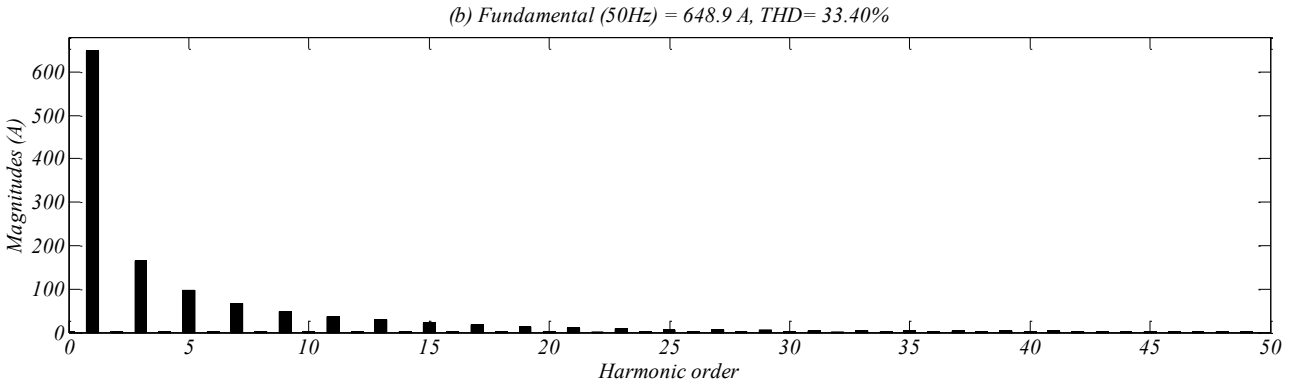

Figure (II.22): (a): Source current before harmonics compensation, (b): Its harmonic spectrum

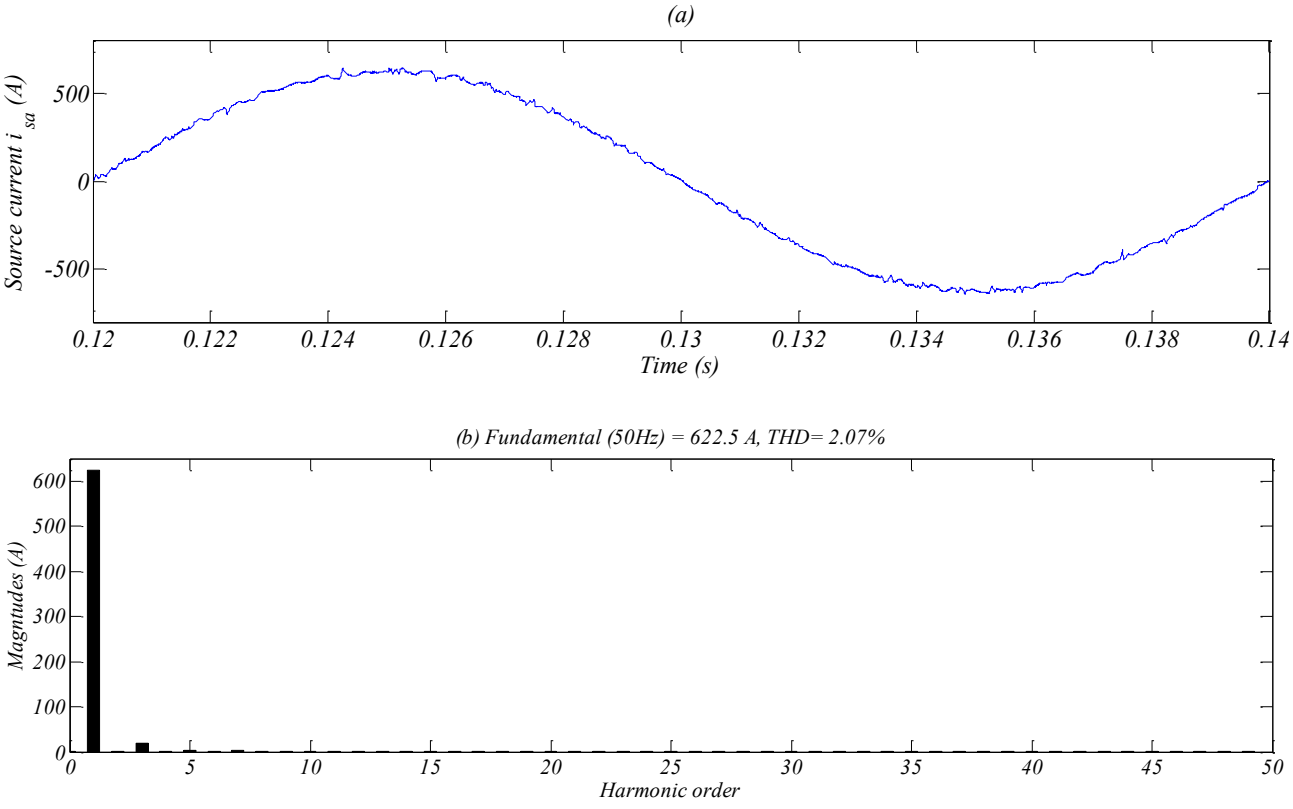

Figure (II.23): (a): Source current after harmonics compensation using DPC-3DSVM, (b) Its harmonic spectrum

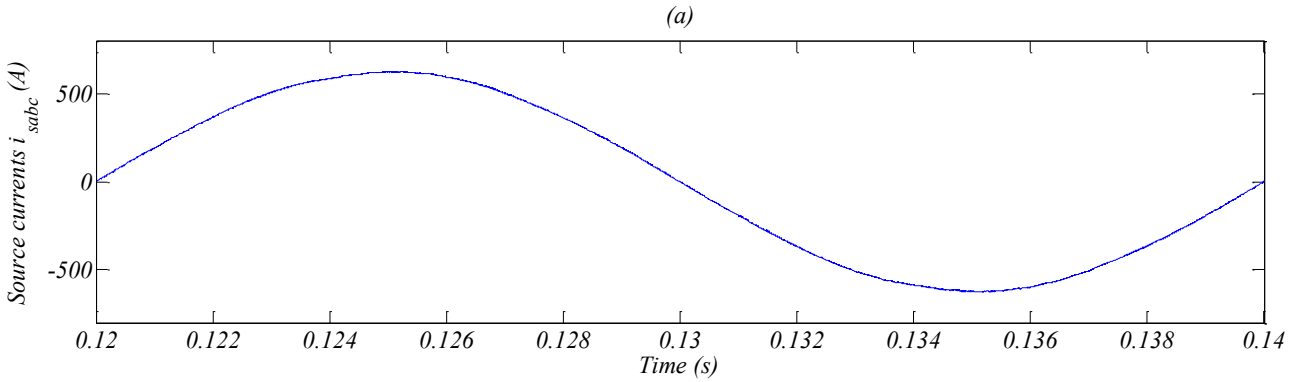

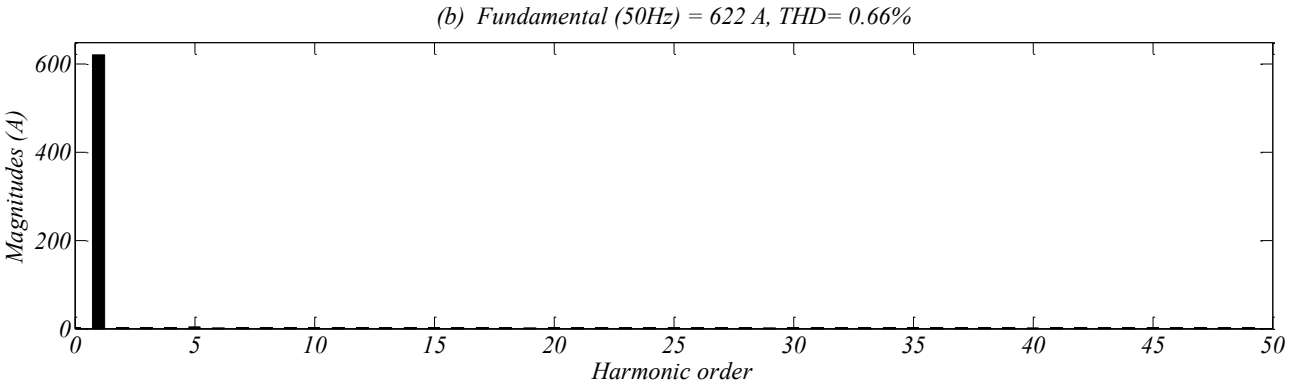

Figure (II.24): (a): Source current after harmonics compensation using PDPC-3DSVM, (b) Its harmonic spectrum

II.4.2. Balanced and unbalanced load condition

Figures (II.25) and (II.26) present the dynamic behavior of the system for DPC and PDPC strategies respectively. After 0.15s, an additional load is added in single-phase diode bridge rectifier in phase (b) in order to induce an unbalanced load.

It can be observed that the three-phase source currents are balanced and sinusoidal after compensation with both control methods. As shown in figures (II.25.c) and (II.26.c), the neutral current is almost canceled with a low ripple in case where the PDPC-3DSVM control is applied (1.61% for the PDPC-3DSVM and 9.67% for the DPC-3DSVM). Neutral currents are illustrated also in figures (II.25.d) and (II.25.e), where the load neutral current is almost equal to the SAPF neutral current, which results a null source neutral current.

In figures (II.25.f) and (II.26.f), one can see that the source active power joins its nominal value while the source reactive power is remaining to its null value. For clarity, a phase-a of source current and its corresponding phase voltage are shown for illustration in figures (II.25.g) and (II.26.g). It can be observed that the unity power factor operation is successfully achieved.

The DC bus voltage variation due to the load change is about 100V, and the recovery time of DC voltage is about 0.01s (see figures (II.25.h) and (II.26.h)). We can see also that the DC capacitors voltages are balancing at their reference values with small ripple around the balance point (2%); which confirms the effectiveness of the 3DSVM equipped with balancing strategy.

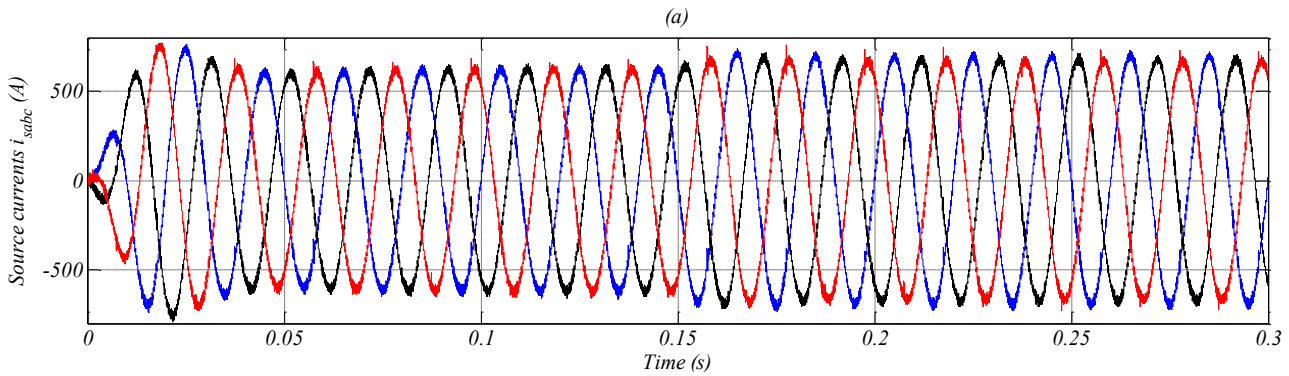

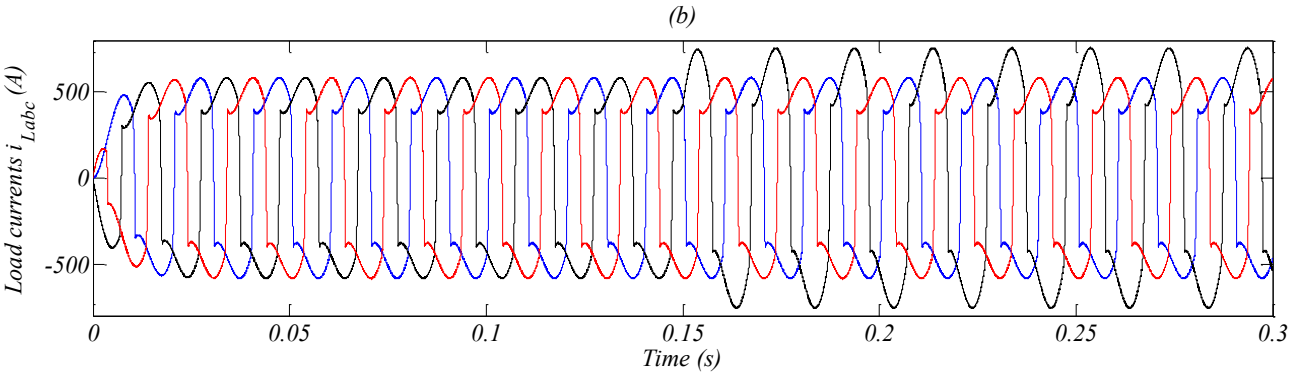
(b)
Load currents i_{Labc} (A)
500
0
-500
0
0.05
0.1
0.15
0.2
0.25
0.3
Time (s)

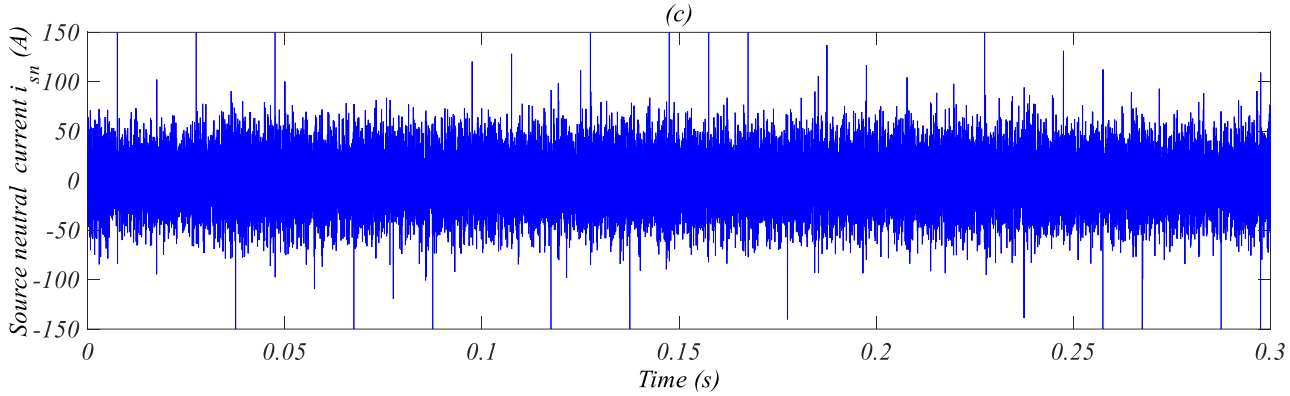
(c)
Source neutral current i_{sn} (A)
150
100
50
0
-50
-100
-150
0
0.05
0.1
0.15
0.2
0.25
0.3
Time (s)

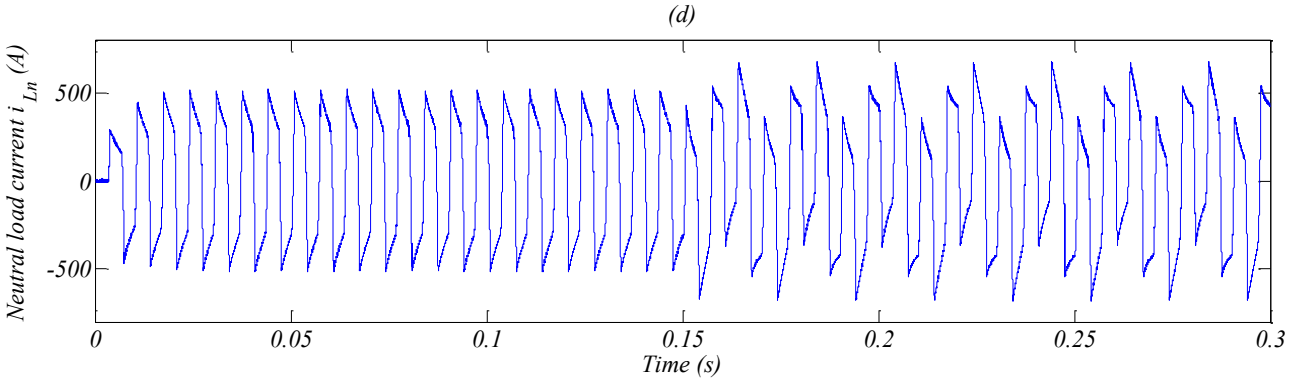
(d)
Neutral load current i_{Ln} (A)
500
0
-500
0
0.05
0.1
0.15
0.2
0.25
0.3
Time (s)

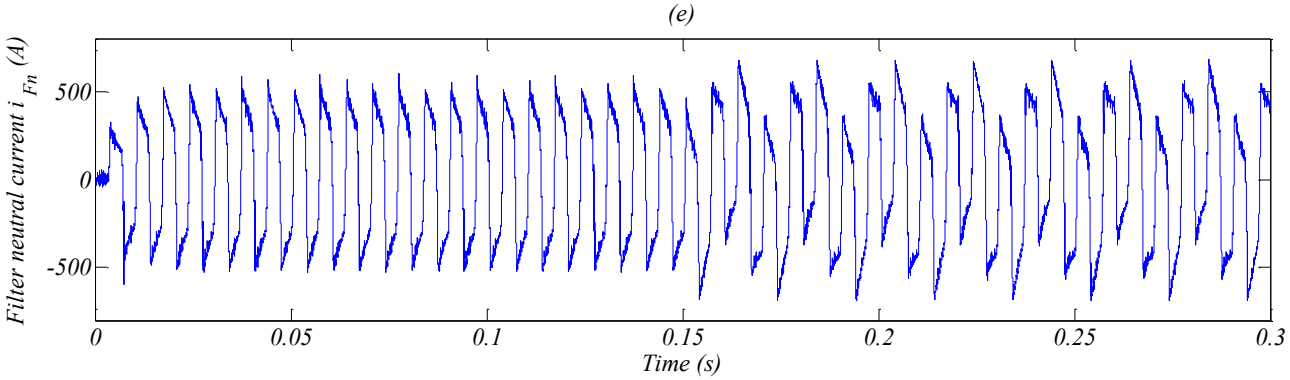
(e)
Filter neutral current i_{Fn} (A)
500
0
-500
0
0.05
0.1
0.15
0.2
0.25
0.3
Time (s)

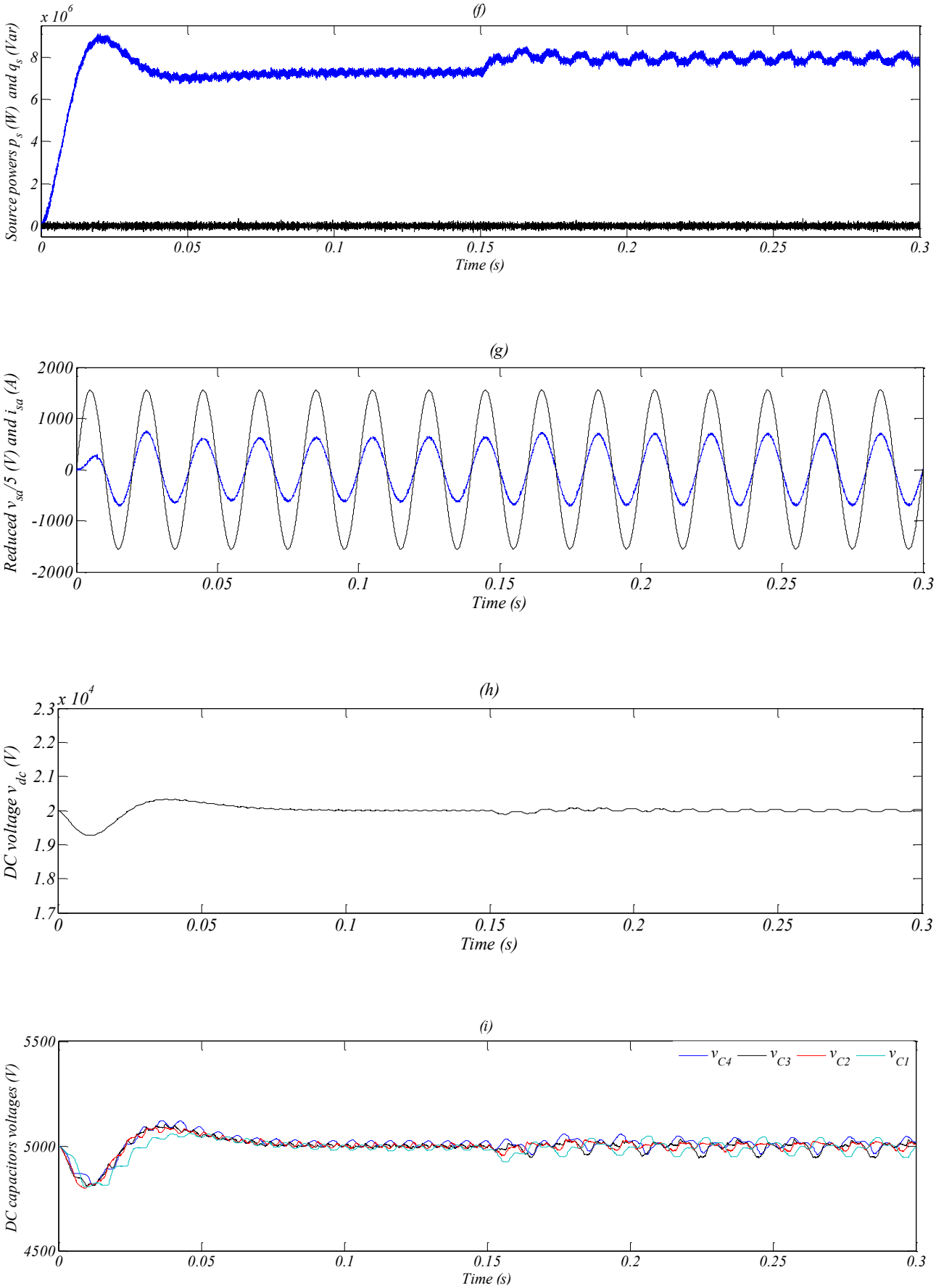

Figure (II.25): Simulation results of the five-level four-leg SAPF controlled by DPC-3DSVM under unbalanced load condition

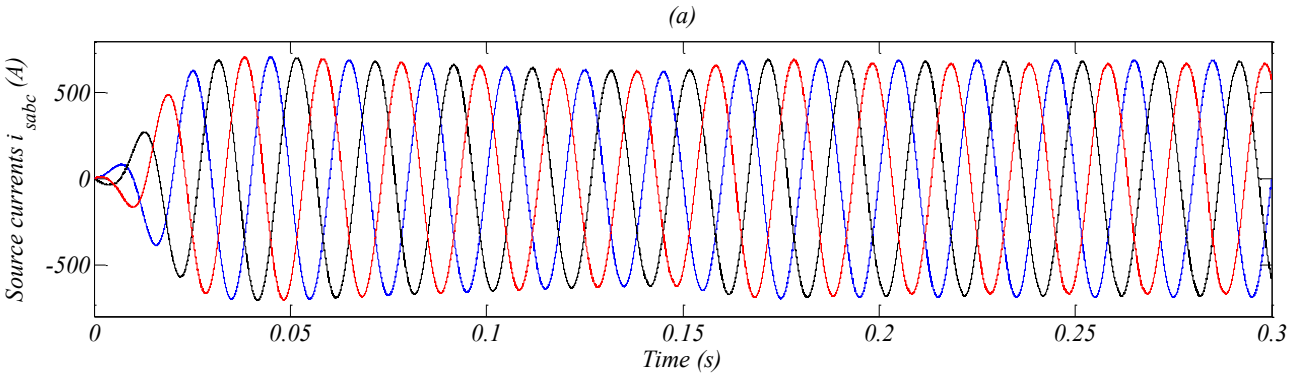
(a)
Source currents i_{sabc} (A)
500
0
-500
0
0.05
0.1
0.15
0.2
0.25
0.3
Time (s)

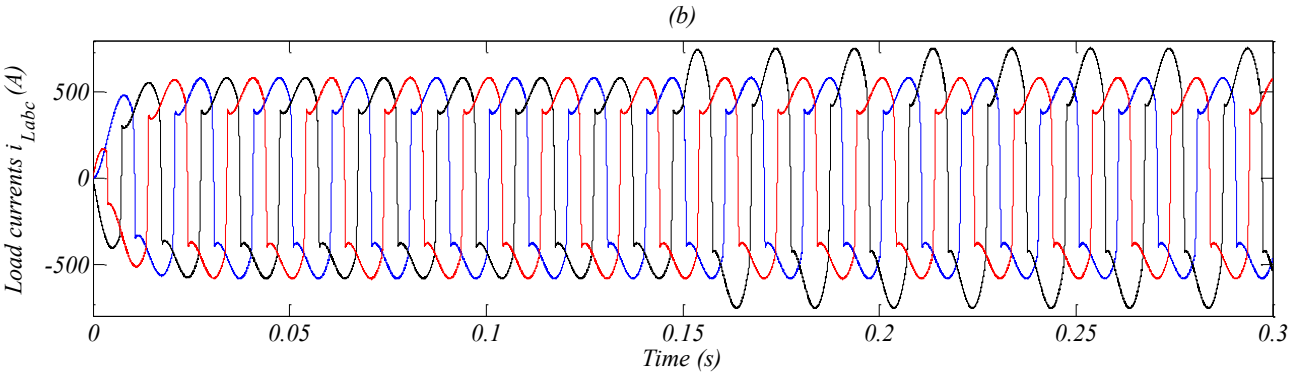
(b)
Load currents i_{Labc} (A)
500
0
-500
0
0.05
0.1
0.15
0.2
0.25
0.3
Time (s)

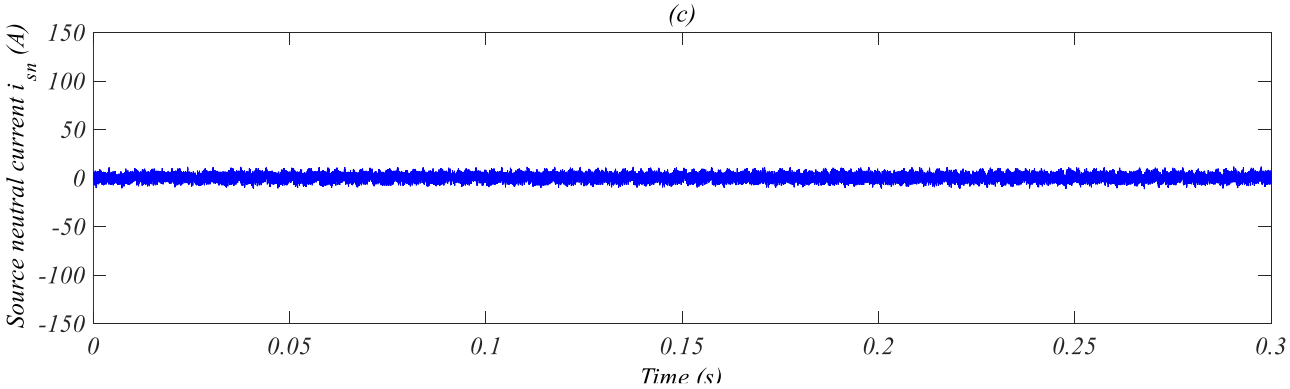
(c)
Source neutral current i_{sn} (A)
150
100
50
0
-50
-100
-150
0
0.05
0.1
0.15
0.2
0.25
0.3
Time (s)

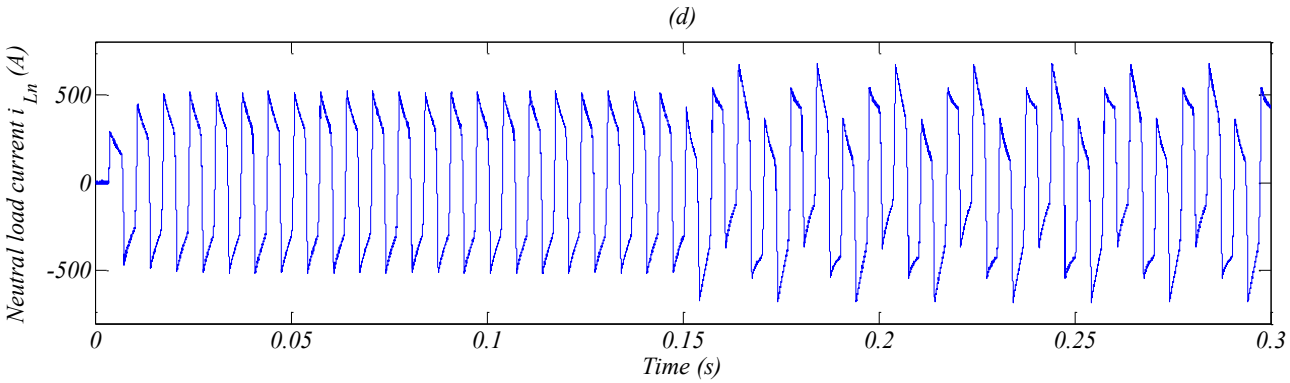
(d)
Neutral load current i_{Ln} (A)
500
0
-500
0
0.05
0.1
0.15
0.2
0.25
0.3
Time (s)

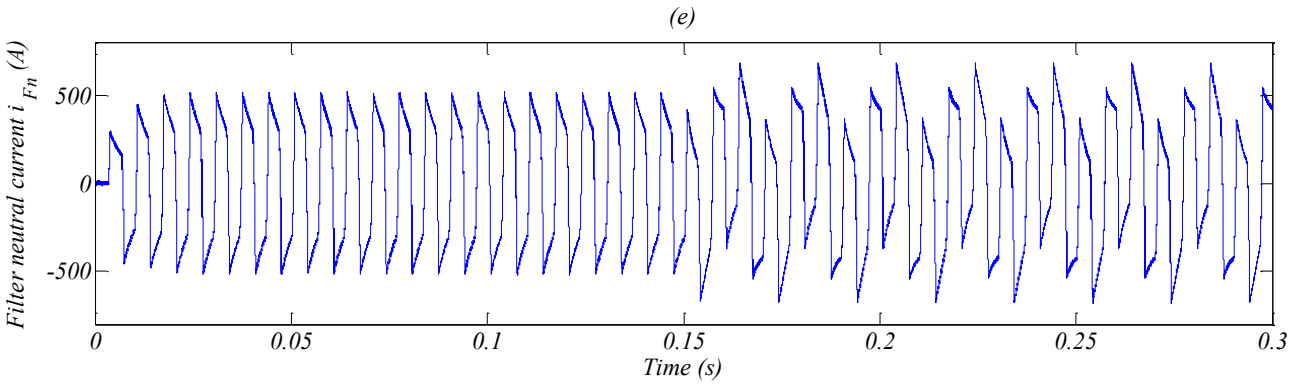
(e)
Filter neutral current i_{Fn} (A)
500
0
-500
0
0.05
0.1
0.15
0.2
0.25
0.3
Time (s)

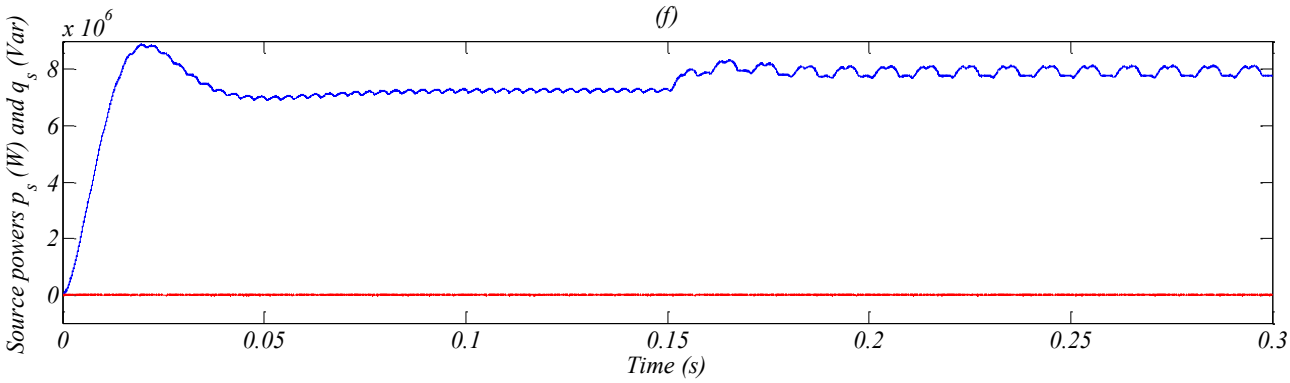
(f)
x 10^6
Source powers p_s (W) and q_s (Var)
8
6
4
2
0
0
0.05
0.1
0.15
0.2
0.25
0.3
Time (s)

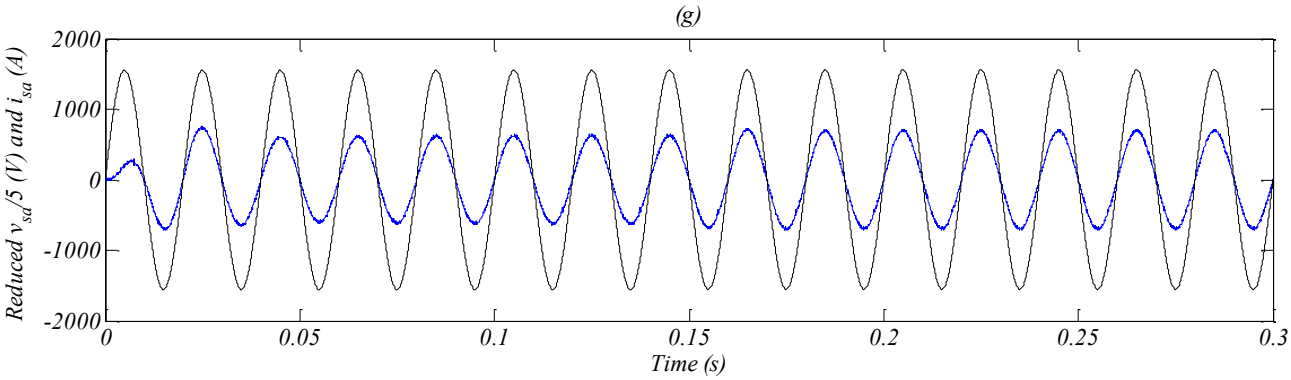
(g)
Reduced v_{sa}/5 (V) and i_{sa} (A)
2000
1000
0
-1000
-2000
0
0.05
0.1
0.15
0.2
0.25
0.3
Time (s)

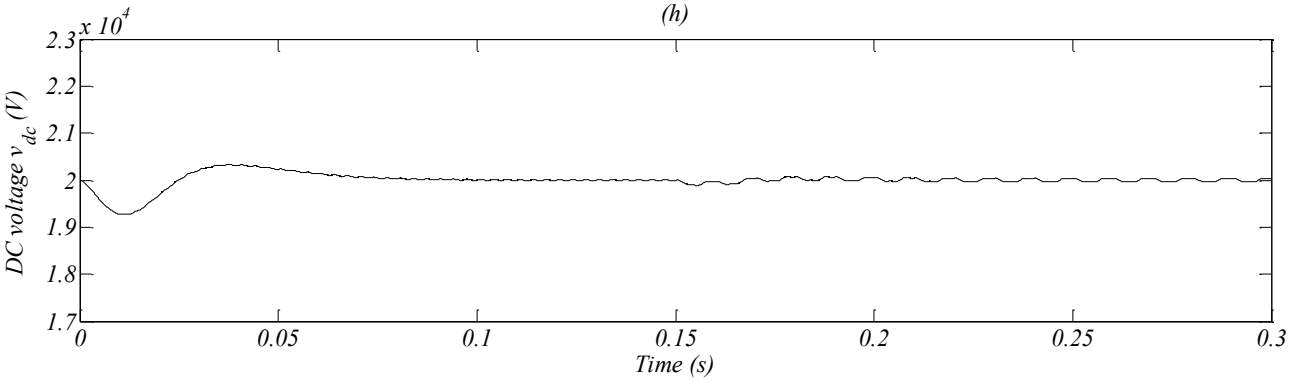
(h)
x 10^4
DC voltage v_{dc} (V)
2.3
2.2
2.1
2
1.9
1.8
1.7
0
0.05
0.1
0.15
0.2
0.25
0.3
Time (s)

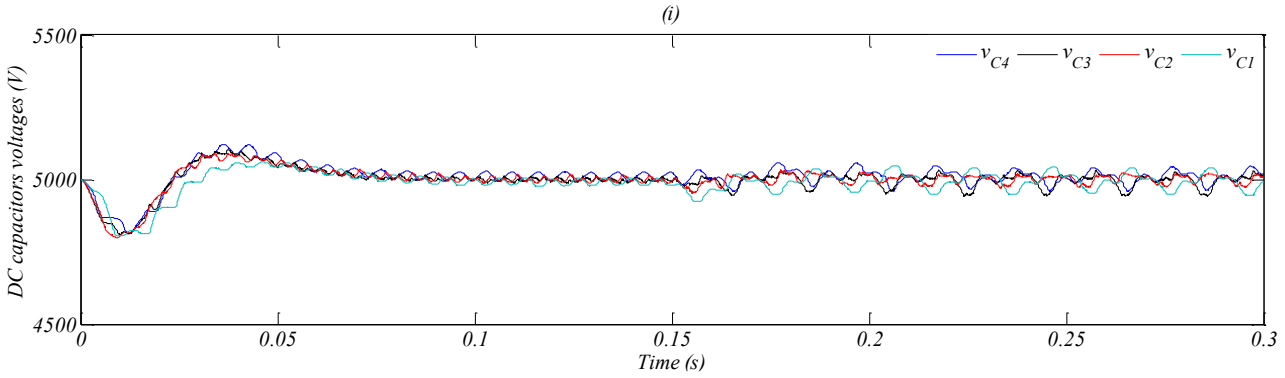

Figure (II.26): Simulation results of the five-level four-leg SAPF controlled by PDPC-3DSVM under unbalanced load condition

II.4.3. Distorted source voltage condition

In an ideal situation, the source usually consists of a balanced three-phase power system with sinusoidal voltage-waves. However, the source voltage is frequently distorted and the systems which are connected to the PCC should be able to tolerate this situation. One of the main disturbances is the presence of line voltage harmonics of order 5, 7 and 11.

Figures (II.27) and (II.28) show the waveforms in which a fifth harmonic voltage component of 5% is intentionally superimposed on the fundamental source voltage for DPC-3DSVM and PDPC-3DSVM respectively.
It can be observed that the source currents are balanced, the unity power factor operation is successfully achieved, and the neutral current is eliminated under distorted source voltages condition.

The source neutral current is eliminated and reactive power compensation is successfully achieved with both control strategies. However, the neutral current and the powers ripples are smaller using PDPC-3DSVM. As shown in figure (II.29) the total harmonic distortion of source current is 5.35% with DPC-3DSVM and 4.99% with PDPC-3DSVM. Therefore, the distortion in source current with PDPC-3DSVM under distorted source voltage is also less than in case of DPC-3DSVM.

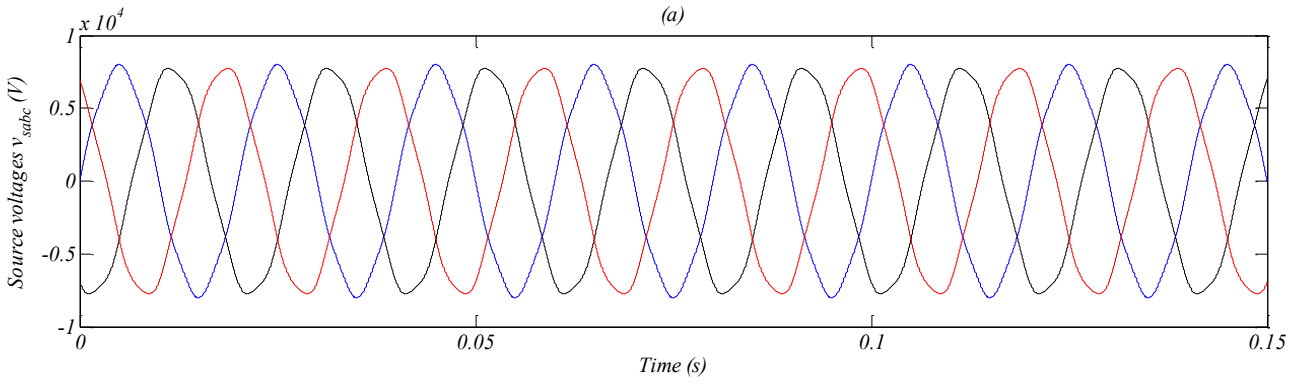

(b)

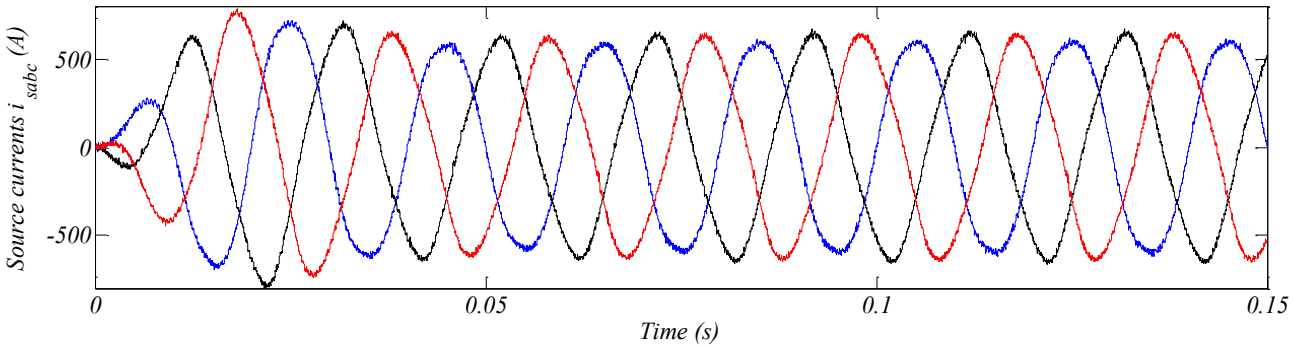
Source currents i_{sabc} (A)
500
0
-500
0
0.05
0.1
0.15
Time (s)

(c)

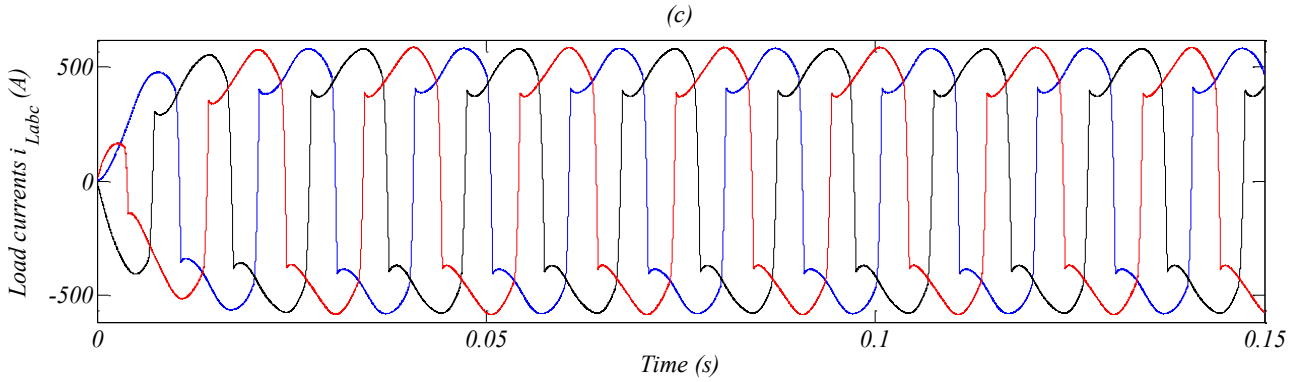
Load currents i_{Labc} (A)
500
0
-500
0
0.05
0.1
0.15
Time (s)

(d)

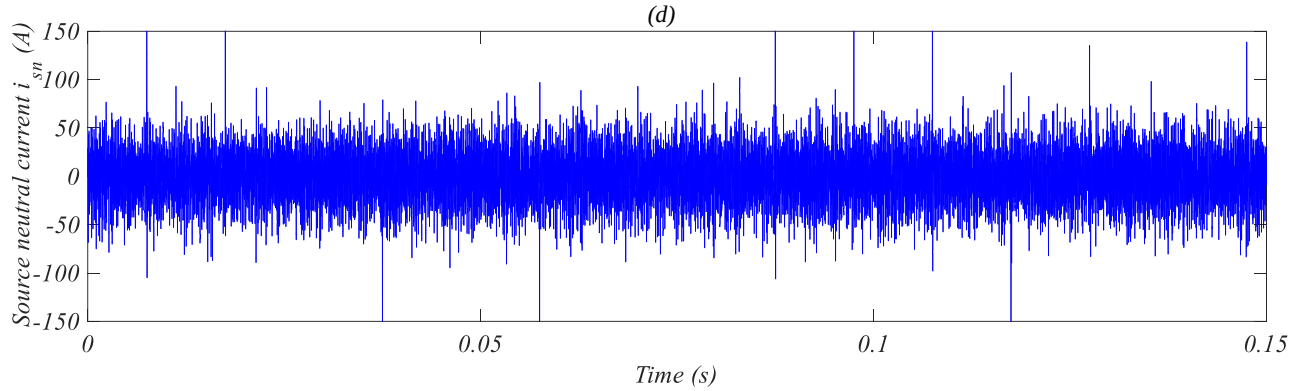
Source neutral current i_{sn} (A)
150
100
50
0
-50
-100
-150
0
0.05
0.1
0.15
Time (s)

(e)

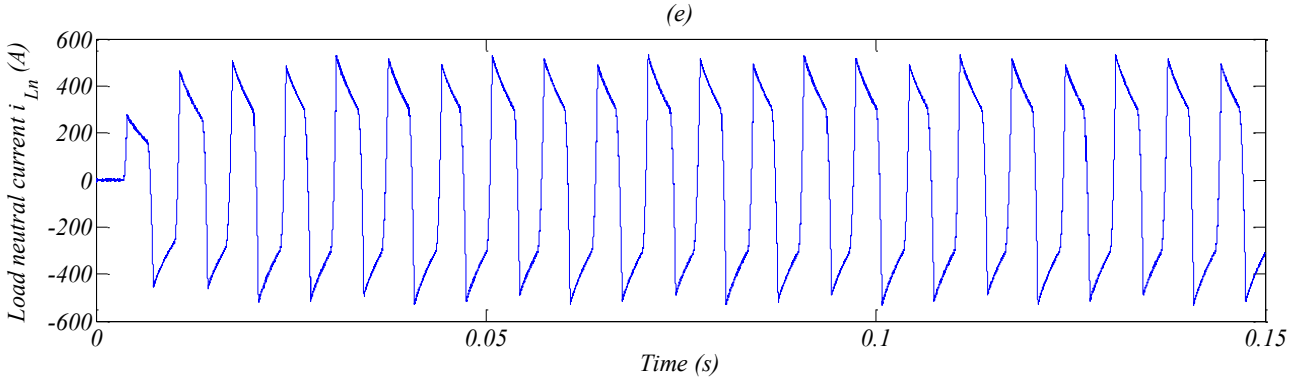
Load neutral current i_{Ln} (A)
600
400
200
0
-200
-400
-600
0
0.05
0.1
0.15
Time (s)

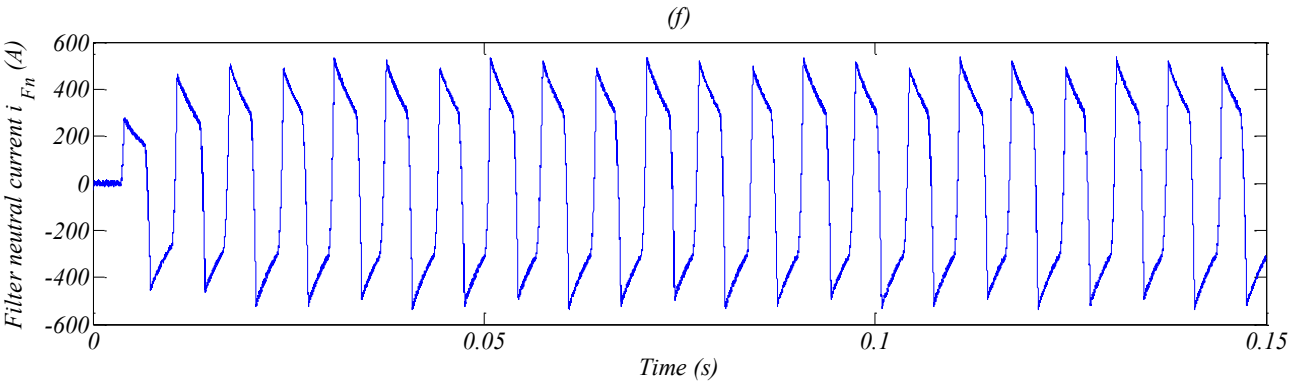
(f)
Filter neutral current i_{Fn} (A)
600
400
200
0
-200
-400
-600
0
0.05
0.1
0.15
Time (s)

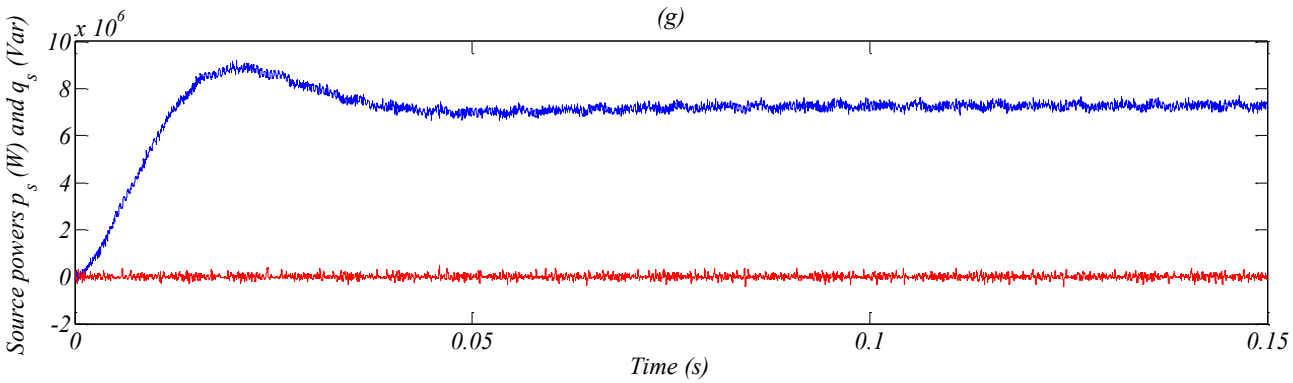
(g)
x 10^6
Source powers p_s (W) and q_s (Var)
10
8
6
4
2
0
-2
0
0.05
0.1
0.15
Time (s)

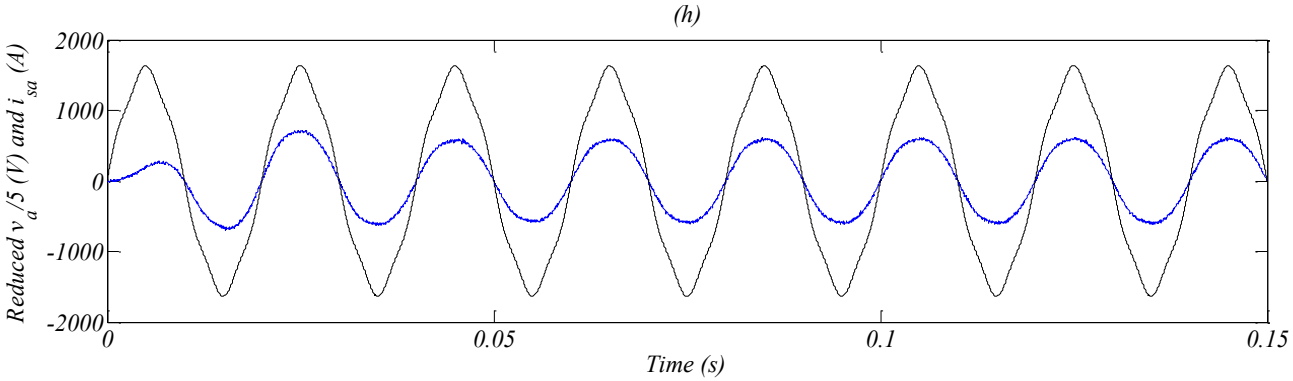
(h)
Reduced v_a /5 (V) and i_{sa} (A)
2000
1000
0
-1000
-2000
0
0.05
0.1
0.15
Time (s)

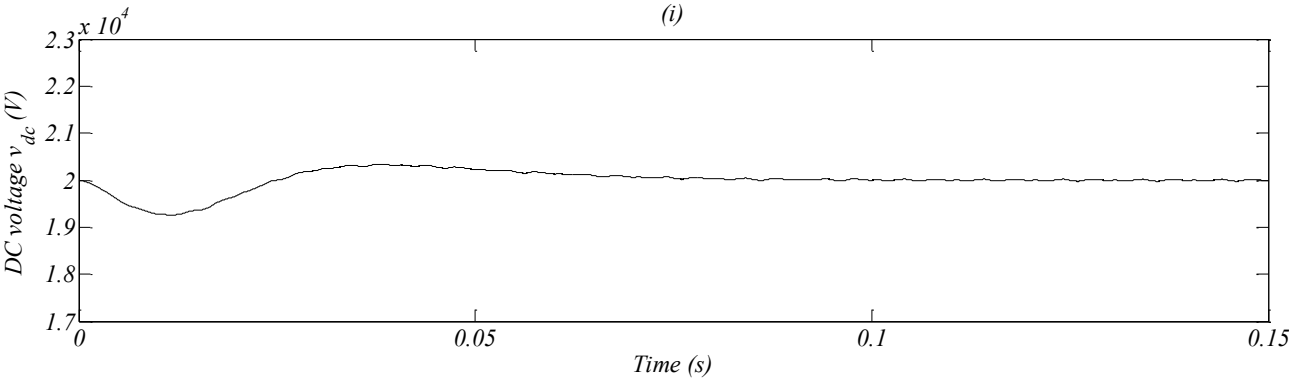
(i)
x 10^4
DC voltage v_{dc} (V)
2.3
2.2
2.1
2
1.9
1.8
1.7
0
0.05
0.1
0.15
Time (s)

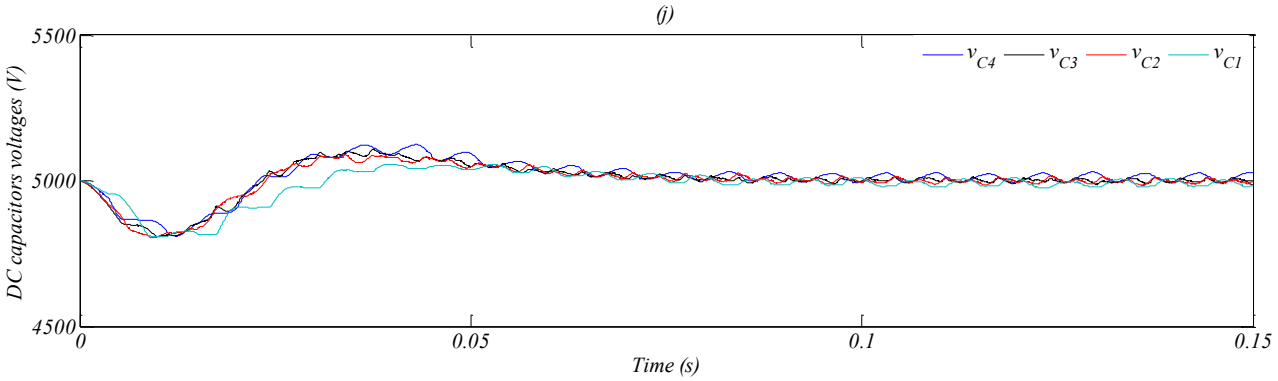

Figure (II.27): Simulation results of the five-level four-leg SAPF controlled by DPC-3DSVM under distorted source voltage

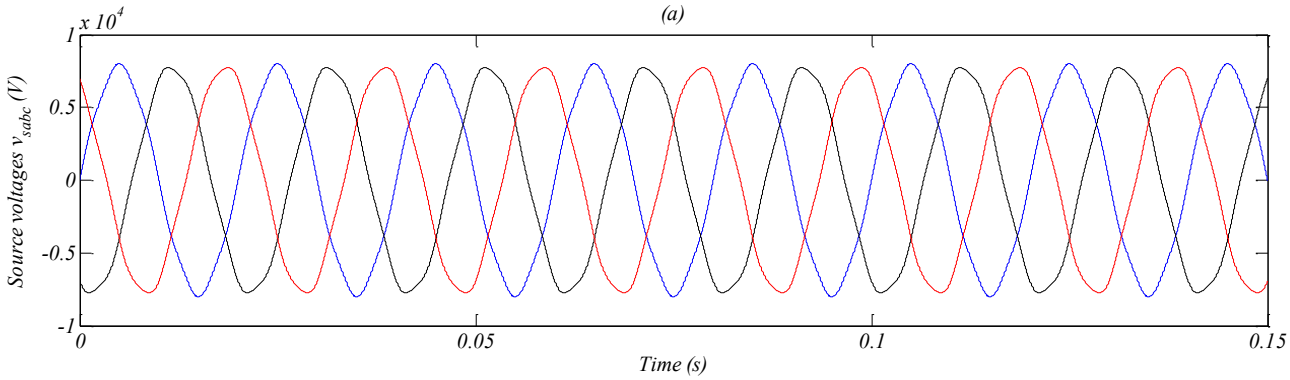

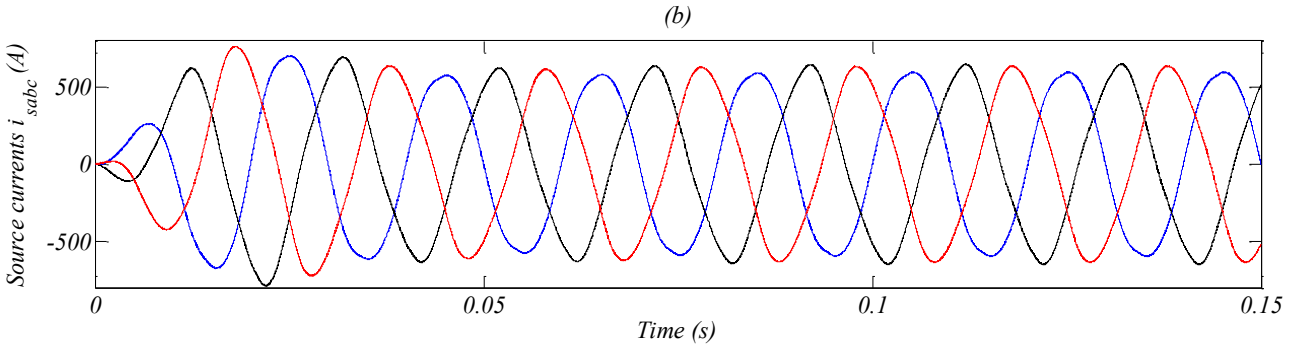

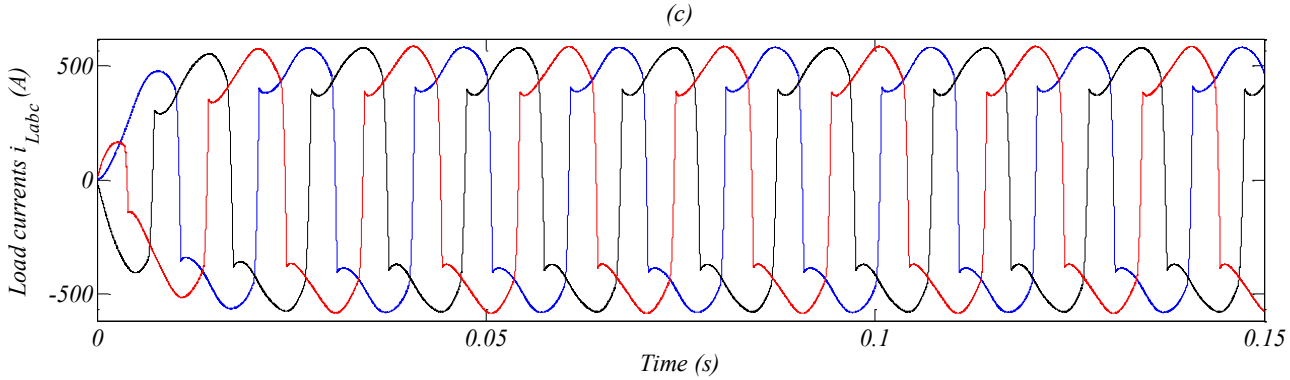

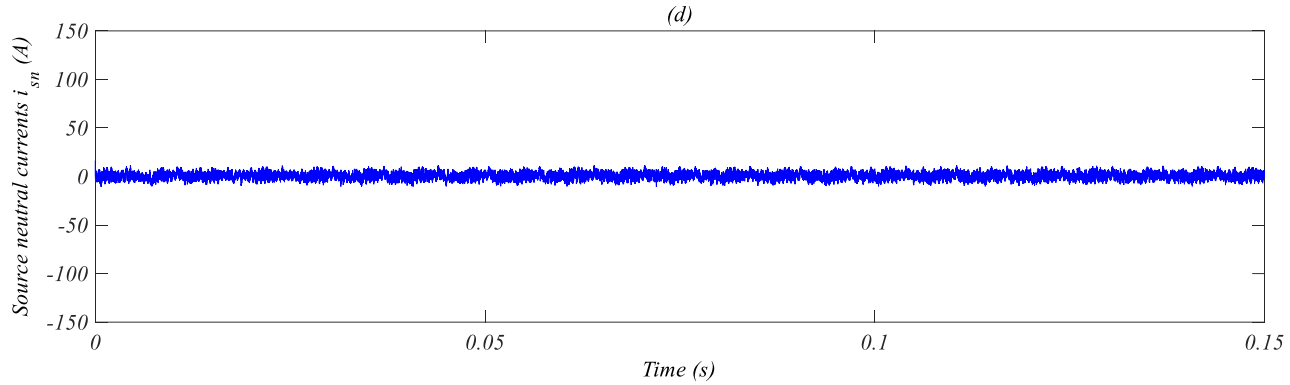
(d)
Source neutral currents i_{sn} (A)
150
100
50
0
-50
-100
-150
0
0.05
0.1
0.15
Time (s)

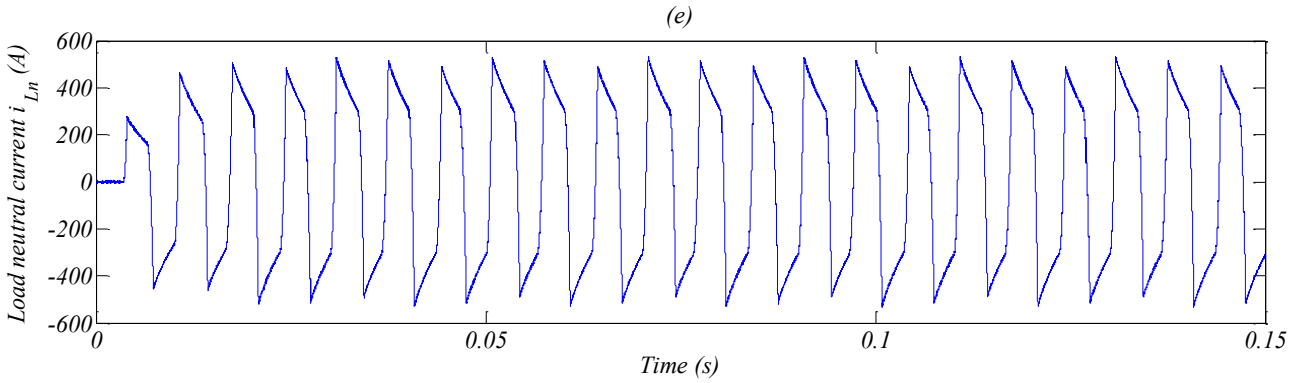
(e)
Load neutral current i_{Ln} (A)
600
400
200
0
-200
-400
-600
0
0.05
0.1
0.15
Time (s)

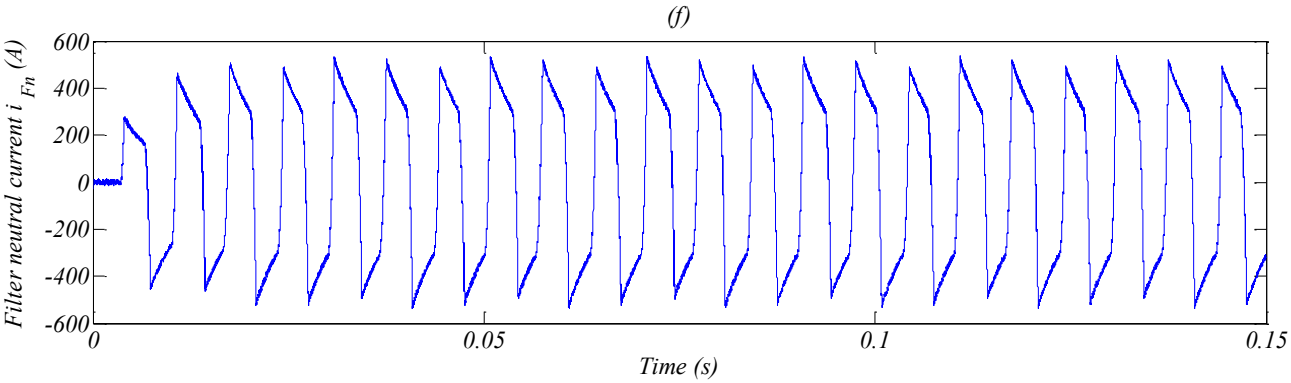
(f)
Filter neutral current i_{Fn} (A)
600
400
200
0
-200
-400
-600
0
0.05
0.1
0.15
Time (s)

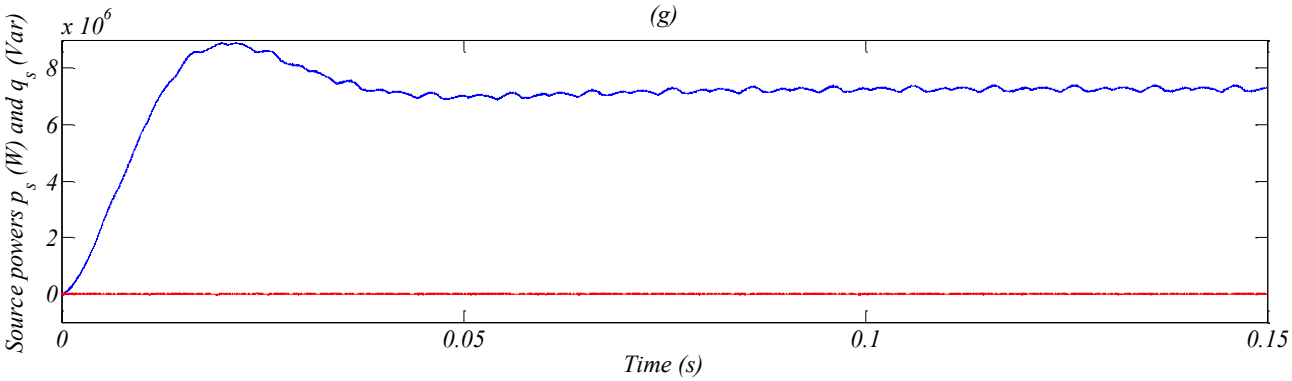
(g)
x 10^6
Source powers p_s (W) and q_s (Var)
8
6
4
2
0
0
0.05
0.1
0.15
Time (s)

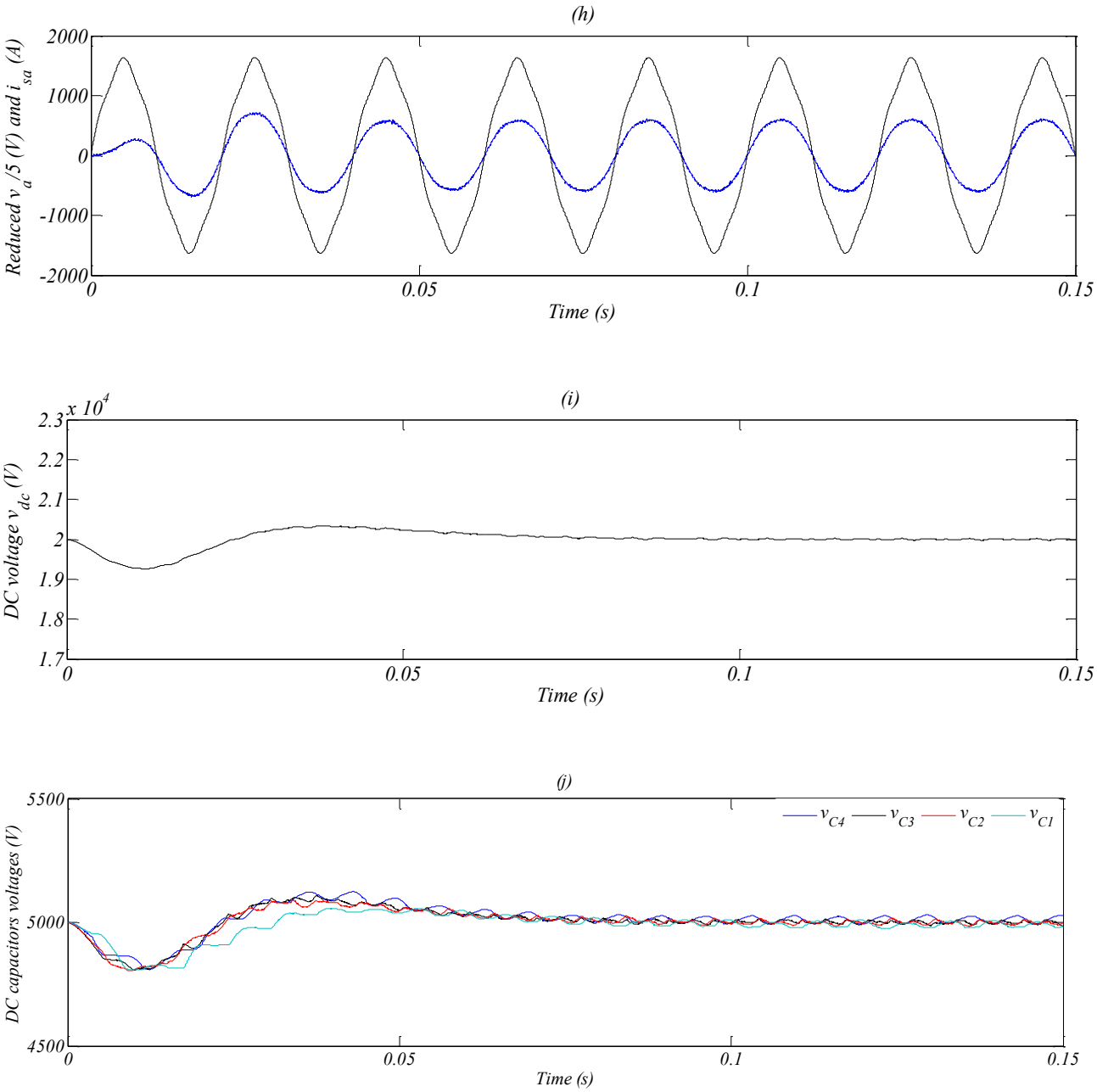

Figure (II.28): Simulation results of the five-level four-leg SAPF controlled by PDPC-3DSVM under distorted source voltage

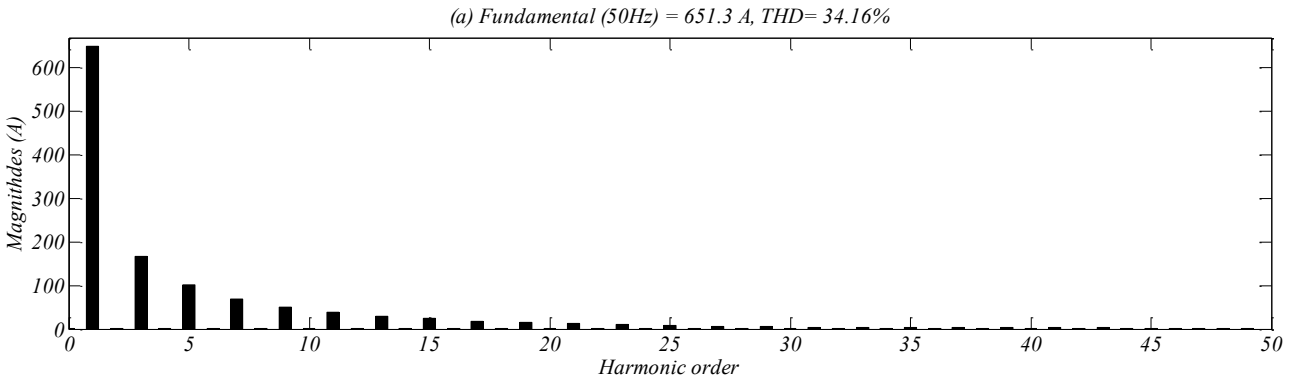

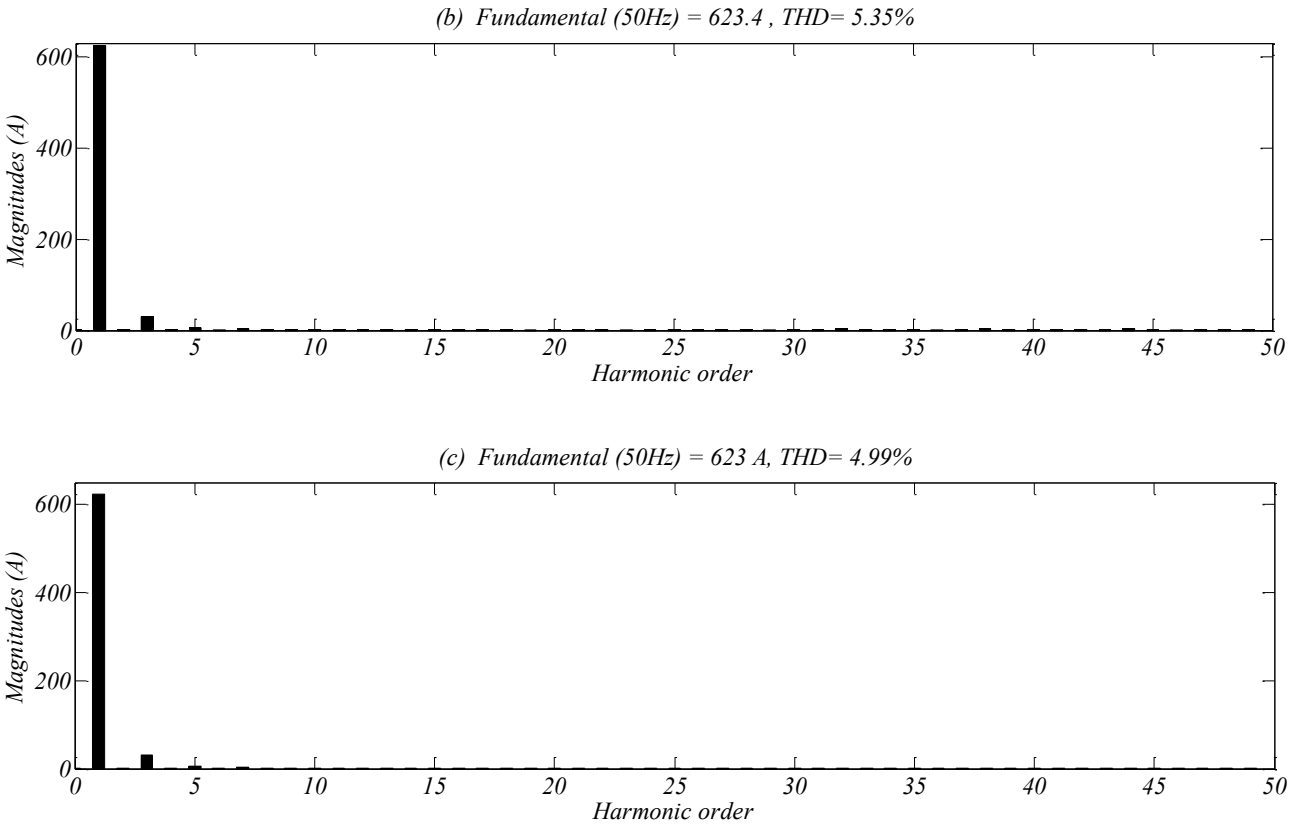

Figure (II.29): Harmonic spectrum of source current under distorted source voltage: (a) Before compensation, (b) After compensation using DPC-3DSVM, (c) After compensation using PDPC-3DSVM

Figure (II.30) shows several current THD values, in presence of different magnitudes of fifth source voltage harmonic. This figure describes a global trend of source current THD according to the magnitude of fifth line voltage harmonic. As shown, both control methods have the same sensitivity to this disturbance for high fifth harmonic magnitude.

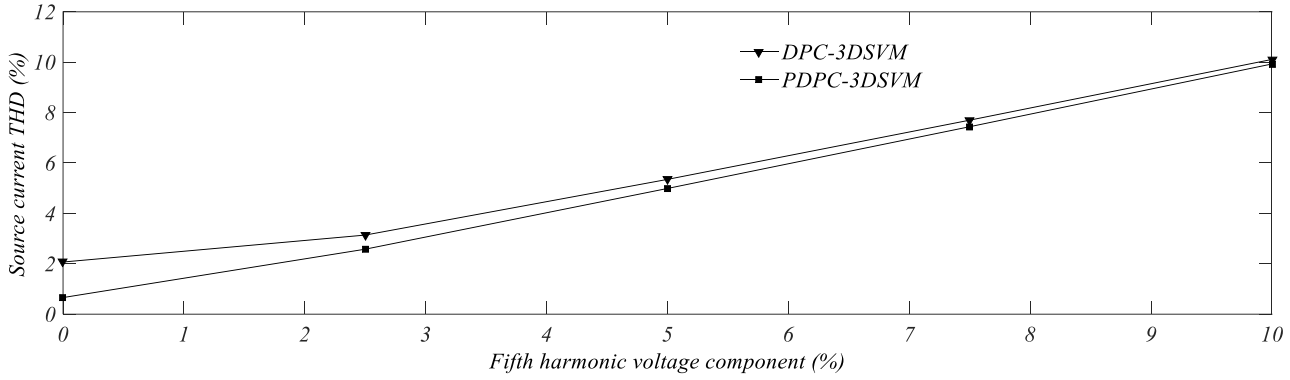

Figure (II.30): Source current THD versus fifth harmonic voltage magnitude component

II.4.4. Coupling filter variations

In this test, coupling inductance L_F and resistance R_F values variation effect will be investigated for DPC-3DSVM and PDPC-3DSVM control methods. As presented in figure (II.31.a), the inductance variations have a small effect in case of DPC technique. However, the PDPC-3DSVM is totally insensitive to these variations.

It can be seen in figure (II.31.b) that the R_F variations do not have influence on control performance in both control techniques. The voltage drop on coupling resistance is much less than voltage drop on coupling inductance. Therefore, for further investigations R_F changes will not be performed.

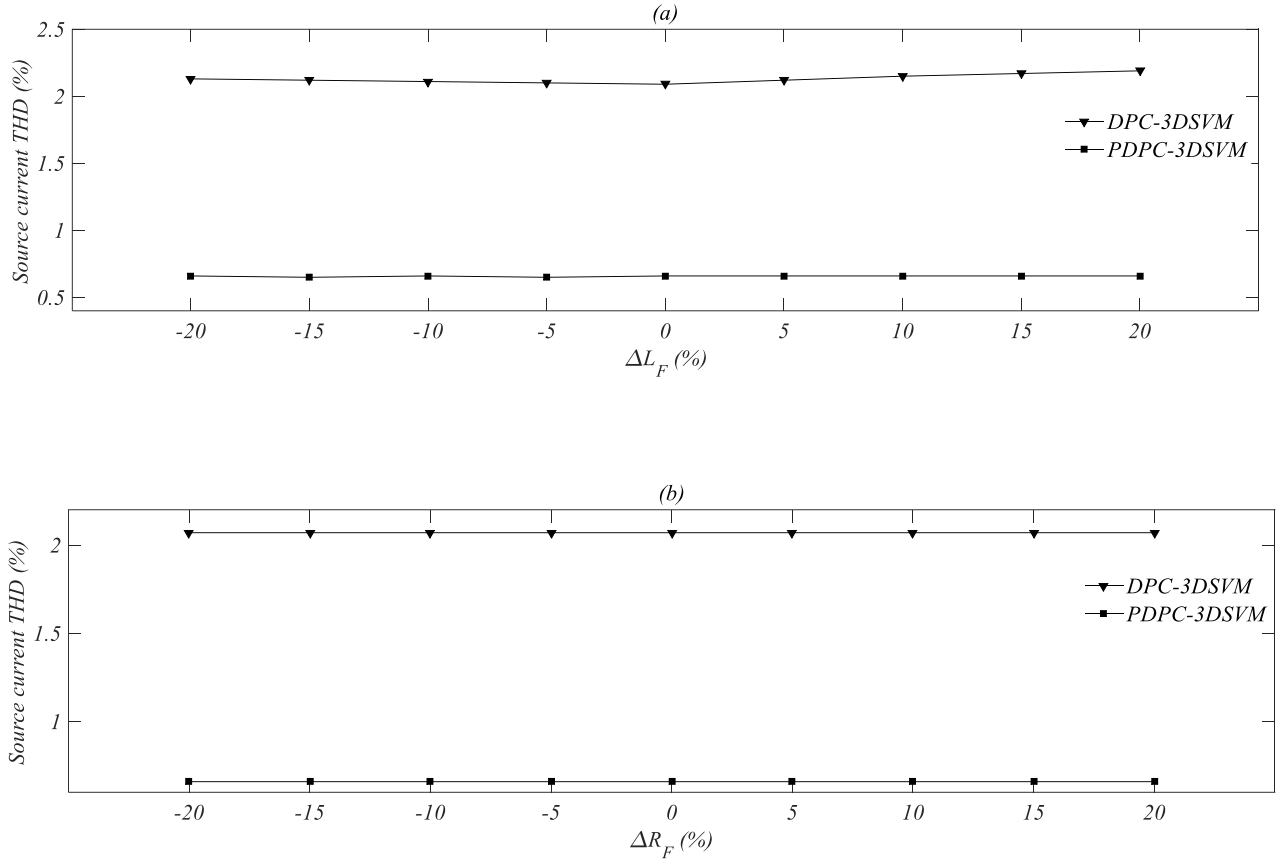

Figure (II.31): Source current THD versus, (a): coupling inductance variations ΔL_F (%), (b): coupling resistance variations ΔR_F (%)

II.5. Conclusion

The purpose of this chapter was to present a theoretical study with simulation of direct power control and predictive direct power control for a five-level four-leg shunt active power filter.

In the first part, causes, problems, and mitigation techniques of excess neutral current have been investigated for three-phase four-wire distribution system. Three main topologies have been presented, passive, hybrid, and active technique, the active one presents the best solution due to its acceptable cost, fast response time, flexibility of control, and continuous operation with virtually no maintenance.

In the second part of this chapter, a description of the operating principle of the five-level four-leg SFAP, followed by a new mathematical model based on the active and reactive powers derivatives was undertaken, where the DPC and PDPC are synthesized based on this new model. One can see that the control algorithm of both control methods is simple, coordinate transformation and decoupling between active and reactive current are not required, there is constant switching frequency by 3DSVM application, and there is no current regulation loops. We find that the PDPC-3DSVM control gives high performance of the five-level four-leg SAPF compared with DPC-3DSVM under both dynamic and steady state operations in terms of the current harmonics filtering, reactive power compensation, source current balancing, and neutral current elimination.

To improve the performances of the proposed filtering structures, the use of nonlinear regulators seems a promising solution. The following chapters will aim to explore this issue.

Chapter III

Direct power control using feedback linearization technique of five-level four-leg shunt active power filter

III.1. Introduction

In the previous chapter, both direct power control and predictive direct power control strategies for five-level four-leg SAPF are based on traditional PI control. Obviously, linear controllers designed for such system cannot always give robust solutions and optimum performance. In order to improve the performance of five-level four-leg SAPF, various nonlinear control strategies have been reported in the literature [29, 98-102].
In this chapter, a nonlinear control based on the feedback linearization associated to DPC and PDPC control is applied to five-level four-leg SAPF in order to improve its performance.

III.2. Input-output feedback linearization technique

The basic idea of feedback linearization method is first to transform a nonlinear system into a fully or partially linear system, and then to use the well-known and powerful linear design techniques to complete the control design. It is completely different from

conventional linearization. In feedback linearization, instead of linear approximations of the dynamics, the process is carried out by exact state transformation and feedback. Besides, it is thought that the original system is transformed into an equivalent simpler form. Furthermore, there are two feedback linearization methods that are input-state and input-output feedback linearization, [90, 104-106].

The input-output feedback linearization technique can be summarized by the following three steps:

- Derivating the output until input appears,
- Choosing a new control variable which provides to reduce the tracking error and to eliminate the nonlinearity,
- Studying stability of the internal dynamics which are the part of system dynamics cannot be observed in input-output linearization [111].

A large class of nonlinear control systems can be made to have linear input-output behavior through a choice of nonlinear state feedback control law. For a MIMO nonlinear system having *n* states and *p* inputs/outputs the following representation is used:

$$\begin{aligned} \dot{x} &= f(x) + \sum_{i=1}^{p} g_i(x) u_i \qquad i = 1,2,...,p \\ y_i &= h_i(x) \end{aligned} \tag{III.1}$$

Where $x \in \Re^n$ is the state vector, $u \in \Re^p$ is the control input vector, and $y \in \Re^p$ is the output vector.

The problem of finding the vector relative degree of the system (III.1) implies differentiation of each output signal until one of the input signals appear explicitly in the differentiation. For each output signal, we define r_j as the smallest integer such that at least one of the inputs appears in $y_j^{(r_j)}$ [90]:

$$y_j^{(r_j)} = L_f{}^{r_j} h(x) + \sum_{i=1}^{p} L_{g_i} (L_f{}^{r_j - 1} h_j(x)) u_i \qquad j = 1,2,...,p \tag{III.2}$$

Where: $L_f h(x) : \Re^n \to \Re$ and $L_g h(x) : \Re^n \to \Re$ stand for *Lie derivatives* of *h* with respect to *f* and *g*, respectively.

The global relative degree (*r*) is defined as the sum of all the relative degrees obtained using (III.2). It must be less than or equal to the order of the system: $r = \sum_{j=1}^{p} r_j \le n$.

One says that the system (III.1) has relative degree r_j if it satisfies:

$$L_{gi}L_f{}^{k}h_j = 0 \qquad 0 < k < r_j - 1 \qquad 1 < j < p \qquad 1 < i < p \tag{III.3}$$

and

$$L_{gi}L_f{}^{k}h_j \neq 0 \qquad k = r_j - 1 \tag{III.4}$$

To find the expression of linearizing law u that allows making linear the relationship between inputs and outputs, the expression (III.2) can be written in its matrix form:

$$\left[y_1^{(r_j)} \quad \dots \quad \dots \quad y_p^{(r_p)} \right]^T = \zeta(x) + D(x)u \tag{III.5}$$

Where :

$$\zeta(x) = \begin{bmatrix} L_f{}^{r_1}h_1(x) \\ L_f{}^{r_2}h_2(x) \\ \vdots \\ L_f{}^{r_p}h_p(x) \end{bmatrix} \tag{III.6}$$

and

$$D(x) = \begin{bmatrix} L_{g_1}L_f{}^{r_1-1}h_1(x) & L_{g_2}L_f{}^{r_1-1}h_1(x) & \dots & L_{g_p}L_f{}^{r_1-1}h_1(x) \\ L_{g_1}L_f{}^{r_2-1}h_2(x) & L_{g_2}L_f{}^{r_2-1}h_2(x) & \dots & L_{g_p}L_f{}^{r_2-1}h_2(x) \\ \dots & \dots & \dots & \dots \\ L_{g_1}L_f{}^{r_p-1}h_p(x) & L_{g_2}L_f{}^{r_p-1}h_p(x) & \dots & L_{g_p}L_f{}^{r_p-1}h_p(x) \end{bmatrix} \tag{III.7}$$

$D(x)$ is called the decoupling matrix system.

Assuming that $D(x)$ is not singular, the linearizing control law has the following form [9]:

$$u = D(x)^{-1}(-\zeta(x) + v) \tag{III.8}$$

Notice that linearization would be possible only if the decoupling matrix $D(x)$ is reversible. The block diagram of the linearized system is given in figure (III.1).

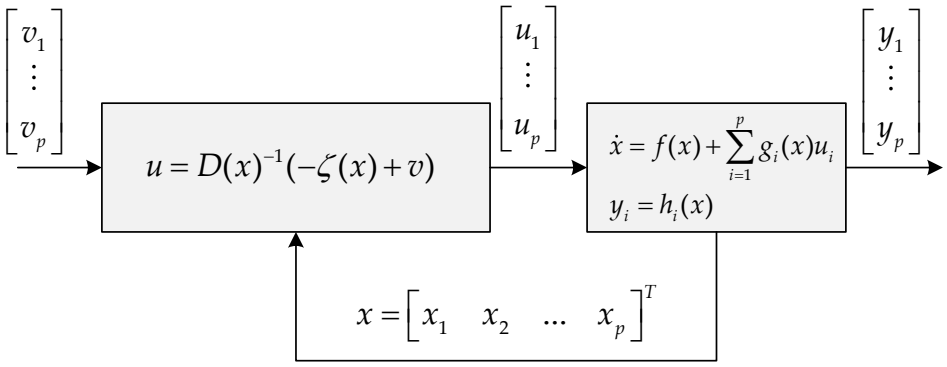

Figure (III.1): Block diagram of linearized MIMO system

Replacing (III.8) in (III.1), the equivalent system becomes linear and completely decoupled of the form [104]:

$$\begin{bmatrix} y_1^{r_1} & y_2^{r_2} & \dots & y_p^{r_p} \end{bmatrix}^T = \begin{bmatrix} v_1 & v_2 & \dots & v_p \end{bmatrix}^T \tag{III.9}$$

Note that the expression (III.9) represents p cascaded integrator as shown in figure (III.2).

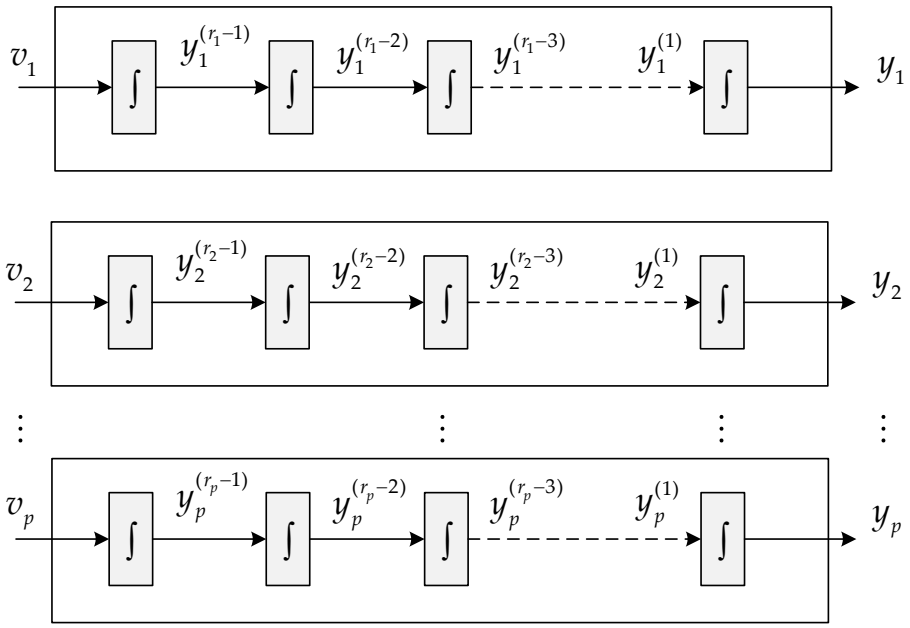

Figure (III.2): Dynamics of the linearized MIMO System

In case of a MIMO system, the new input is a vector of dimension (p×1) given by:

$$v = \begin{bmatrix} v_1 \\ v_2 \\ \vdots \\ v_p \end{bmatrix} = \begin{bmatrix} y_1^{*(r_1)} + k_{r_1-1}(y_1^{*(r_1-1)} - y_1^{(r_1-1)}) + \dots + k_1(y_1^* - y_1) \\ y_2^{*(r_2)} + k_{r_2-1}(y_2^{*(r_2-1)} - y_2^{(r_2-1)}) + \dots + k_1(y_2^* - y_2) \\ \vdots \\ y_p^{*(r_p)} + k_{r_p-1}(y_p^{*(r_p-1)} - y_p^{(r_p-1)}) + \dots + k_1(y_p^* - y_p) \end{bmatrix} \tag{III.10}$$

Where the vectors $\left\{ y_j^*,\ y_j^{*(1)},\ \dots.,\ y_j^{*(r_j-2)},\ y_j^{*(r_j-1)} \right\}$, $j = 1,\dots p$ define the reference trajectories imposed for the different outputs. If k_i (i =1, 2, …, j-1) are chosen so that the polynomial $S^{r_j} + k_{r_j-1}S^{r_j-1} + \dots + k_2 S + k_1 = 0$ is a Hurwitz polynomial [104], then it can be shown that the errors $e_j(t) = y_j^*(t) - y_j(t)$ satisfies:

$$\lim_{t\to\infty} e_j(t) = 0 \tag{III.11}$$

The linearized closed loop system is presented in figure (III.3).

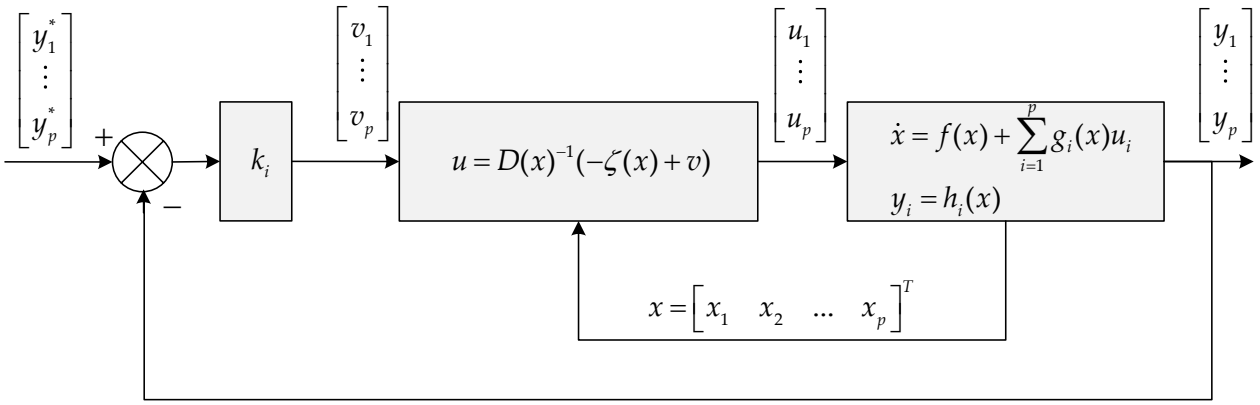

Figure (III.3): Block diagram of closed loop of linearized MIMO system

III.2.1. Application of feedback linearization to DPC-3DSVM for five-level four-leg SAPF

The block diagram of the DPC-3DSVM combined with feedback linearization for the five-level four-leg SAPF is represented in the figure (III.4). In this section, DC voltage and powers controllers will be synthesized.

III.2.1.1. Model subdivision

There are four outputs to control. It is about DC capacitor voltage v_{dc}, active power p_F, reactive powers q_F and $q_{F\alpha\beta}$, each one of them must follow its corresponding reference v_{dc}^*, p_F^*, q_F^* and $q_{F\alpha\beta}^*$ respectively. To carry out this objective, it is necessary to subdivide the new model of SAPF in two subsystems.
Remember that the new model of SAPF was written as follows:

$$\begin{aligned} \frac{dp_F}{dt} &= \frac{1}{L_F}(-R_F p_F + V_{F\alpha}) \\ \frac{dq_F}{dt} &= \frac{1}{L_F}(-R_F q_F + V_{F\beta}) \\ \frac{dq_{F\alpha\beta}}{dt} &= \frac{1}{L_F}(-R_F q_{F\alpha\beta} + V_{Fo}) \\ \frac{dv_{dc}^2}{dt} &= \frac{2p_{dc}}{C_{eq}} \end{aligned} \qquad \text{(III.12)}$$

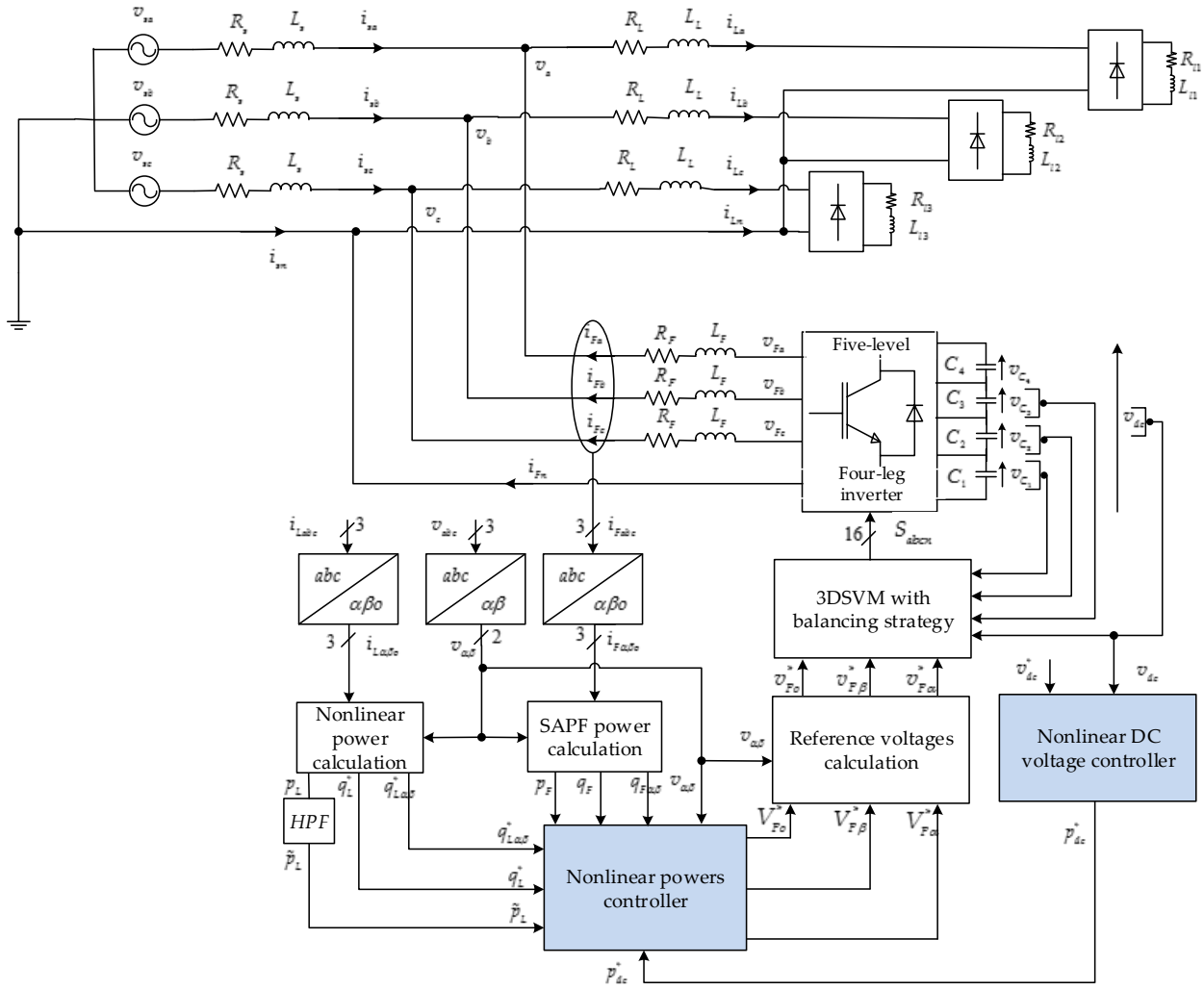

Figure (III.4): Feedback linearization of DPC-3DSVM for five-level four-leg SAPF

***Subsystem* 1:**

The first subsystem is described by the following equation:

$$\begin{aligned}\frac{dp_F}{dt} &= \frac{1}{L_F}(-R_F p_F + V_{F\alpha}) \\ \frac{dq_F}{dt} &= \frac{1}{L_F}(-R_F q_F + V_{F\beta}) \\ \frac{dq_{F\alpha\beta}}{dt} &= \frac{1}{L_F}(-R_F q_{F\alpha\beta} + V_{Fo})\end{aligned} \tag{III.13}$$

When the first subsystem is expressed in the form of (III.14):

$$\begin{aligned}\dot{x} &= f(x) + g(x)u \\ y &= h(x)\end{aligned} \tag{III.14}$$

It results:

$$f(x)=\begin{bmatrix} f_1 \\ f_2 \\ f_2 \end{bmatrix}=\begin{bmatrix} -\frac{R_F}{L_F}x_1 \\ -\frac{R_F}{L_F}x_2 \\ -\frac{R_F}{L_F}x_3 \end{bmatrix},\quad g(x)=\begin{bmatrix} \frac{1}{L_F} & 0 & 0 \\ 0 & \frac{1}{L_F} & 0 \\ 0 & 0 & \frac{1}{L_F} \end{bmatrix},\quad x=\begin{bmatrix} x_1 \\ x_2 \\ x_3 \end{bmatrix}=\begin{bmatrix} p_F \\ q_F \\ q_{F\alpha\beta} \end{bmatrix}$$

$$u=\begin{bmatrix} u_1 \\ u_2 \\ u_3 \end{bmatrix}=\begin{bmatrix} V_{F\alpha} \\ V_{F\beta} \\ V_{Fo} \end{bmatrix},\quad y=\begin{bmatrix} y_1 \\ y_2 \\ y_3 \end{bmatrix}=\begin{bmatrix} h_1 \\ h_2 \\ h_3 \end{bmatrix}$$

***Subsystem* 2:**

The second subsystem is defined by the fourth equation of the system (III.12).

$$\frac{dv_{dc}^2}{dt}=\frac{2p_{dc}}{C_{eq}} \tag{III.15}$$

It has only one state $x=v_{dc}^2$ and only one control input $u=p_{dc}$. So, the second subsystem can be also written in the form (III.14).

Where:

$$f(x)=0\ ,\quad g(x)=\frac{2}{C_{eq}}$$

III.2.1.2. DC voltage controller synthesis

The synthesis of the DC voltage controller is based on the second subsystem.
The derivative of the output $y=h=v_{dc}^2$ is given by:

$$\dot{y}=L_f h(x)+L_g h(x)u\ \ =\frac{2}{C_{eq}}p_{dc} \tag{III.16}$$

The control input p_{dc} appear in (III.16), so the relative degree is r=1. The relative degree of this output is equal to the order of subsystem 2, which corresponds clearly to an exact linearization [104].
Then the control law is obtained by:

$$p_{dc}^{*}=2C_{eq}v \tag{III.17}$$

Where:

$$\dot{y} = v \tag{III.18}$$

For a problem of trajectory tracking defined by $v_{dc}^{*}(t)$, the term v is expressed by:

$$v = k(v_{dc}^{*2} - v_{dc}^{2}) + \frac{dv_{dc}^{*2}}{dt} \tag{III.19}$$

Where, k is a positive constant.

III.2.1.3. Power controllers synthesis

Each output derivative is given by:

$$\dot{y}_j = L_f\, h(x) + \sum_{i=1}^{3} L_{g_i} h_j(x) u_i \qquad j = 1,2,3 \tag{III.20}$$

Then (III.20) can be written in matrix form as:

$$\begin{bmatrix} \dot{y}_1 \\ \dot{y}_2 \\ \dot{y}_3 \end{bmatrix} = \begin{bmatrix} -\frac{R_F}{L_F} x_1 \\ -\frac{R_F}{L_F} x_2 \\ -\frac{R_F}{L_F} x_3 \end{bmatrix} + \begin{bmatrix} \frac{1}{L_F} & 0 & 0 \\ 0 & \frac{1}{L_F} & 0 \\ 0 & 0 & \frac{1}{L_F} \end{bmatrix} \begin{bmatrix} u_1 \\ u_2 \\ u_3 \end{bmatrix} \tag{III.21}$$

The control inputs appear in (III.21). In this case, the relative degree of the subsystem 1 is $r = r_1 + r_2 + r_3 = 3$. The relative degree of the chosen outputs is equal to the order of subsystem 1, than it is about of an exact linearization [104].
The decoupling matrix determinant is different to zero, and then the control law is given as:

$$u = \begin{bmatrix} u_1 \\ u_2 \\ u_3 \end{bmatrix} = D(x)^{-1} \left[-\zeta(x) + \begin{bmatrix} v_1 \\ v_2 \\ v_3 \end{bmatrix} \right] \tag{III.22}$$

The application of the linearization law on the first subsystem leads to the following decoupled linear system:

$$\begin{bmatrix} \dot{y}_1 \\ \dot{y}_2 \\ \dot{y}_3 \end{bmatrix} = \begin{bmatrix} v_1 \\ v_2 \\ v_3 \end{bmatrix} \tag{III.23}$$

The control law used for tracking is:

$$\begin{aligned} v_1 &= k_1(p_F^* - p_F) + \frac{dp_F^*}{dt} \\ v_2 &= k_2(q_F^* - q_F) + \frac{dq_F^*}{dt} \\ v_3 &= k_3(q_{F\alpha\beta}^* - q_{F\alpha\beta}) + \frac{dq_{F\alpha\beta}^*}{dt} \end{aligned} \tag{III.24}$$

Where k_1, k_2 and k_3 are positive constants.

III.2.2. Feedback linearization of PDPC-3DSVM of five-level four-leg SAPF

The schematic diagram of the feedback linearization of PDPC-3DSVM control for five-level four-leg SAPF is presented in figure (III.5). This control strategy uses the same non-linear controller of the DC voltage developed in the previous section. The PDPC scheme is based on the computation of the SAPF average voltage vector $v_{F\alpha\beta o}^*$ using a predictive control algorithm, which makes instantaneous active and reactive powers equal to their reference values at each sampling period.

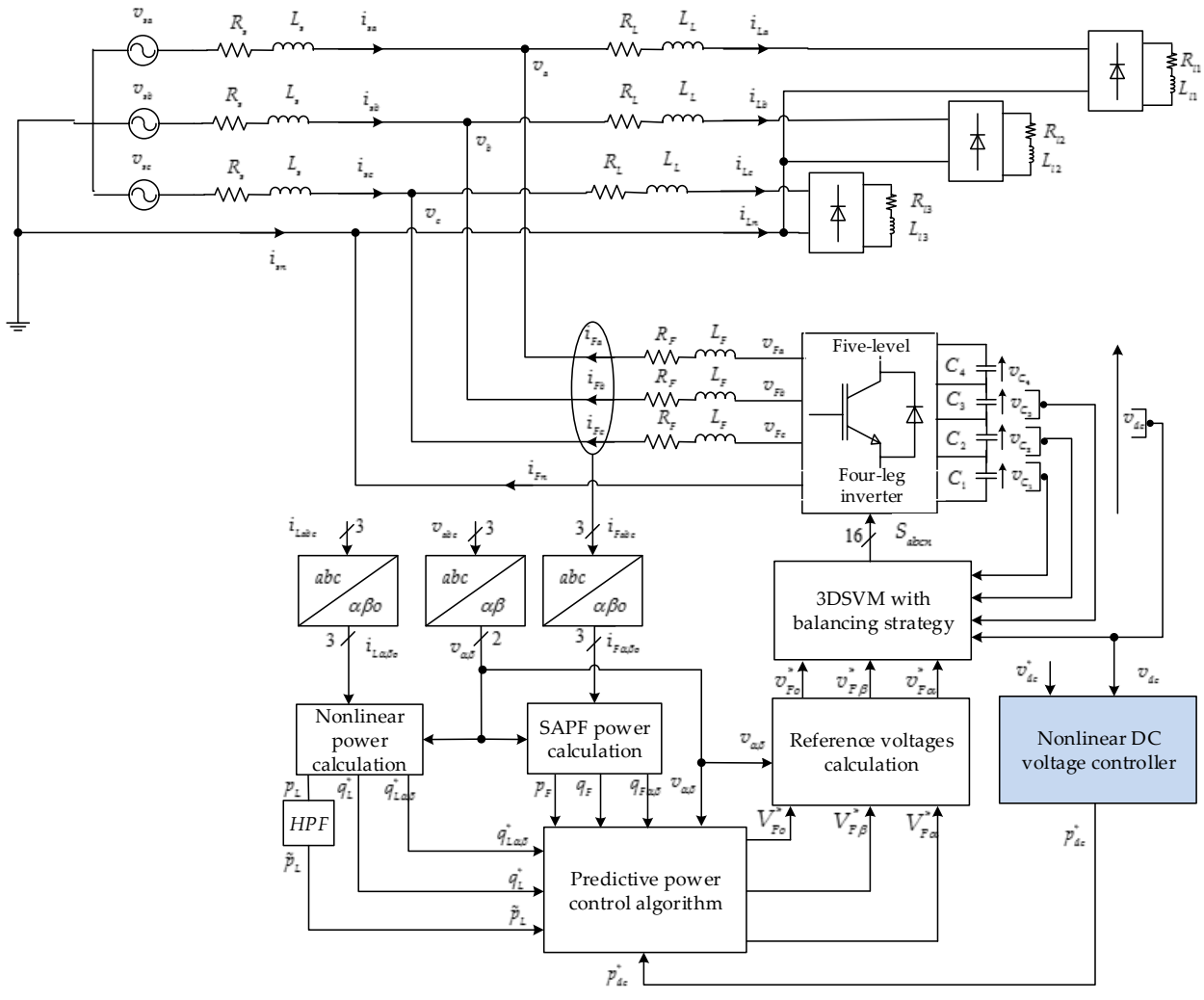

Figure (III.5): Feedback linearization of PDPC-3DSVM for five-level four-leg SAPF

III.3. Simulation results

The simulation parameters used in this section are the same used previous chapter, with: $k = 100$, $k_1 = k_2 = 10^5$, and $k_3 = 10^6$.

III.3.1. Steady state operation

From the figures (III.7) and (III.8), the source current is almost sinusoidal with both control strategies with THD = 1.21% for DPC-3DSVM and 0.43% for PDPC-3DSVM.

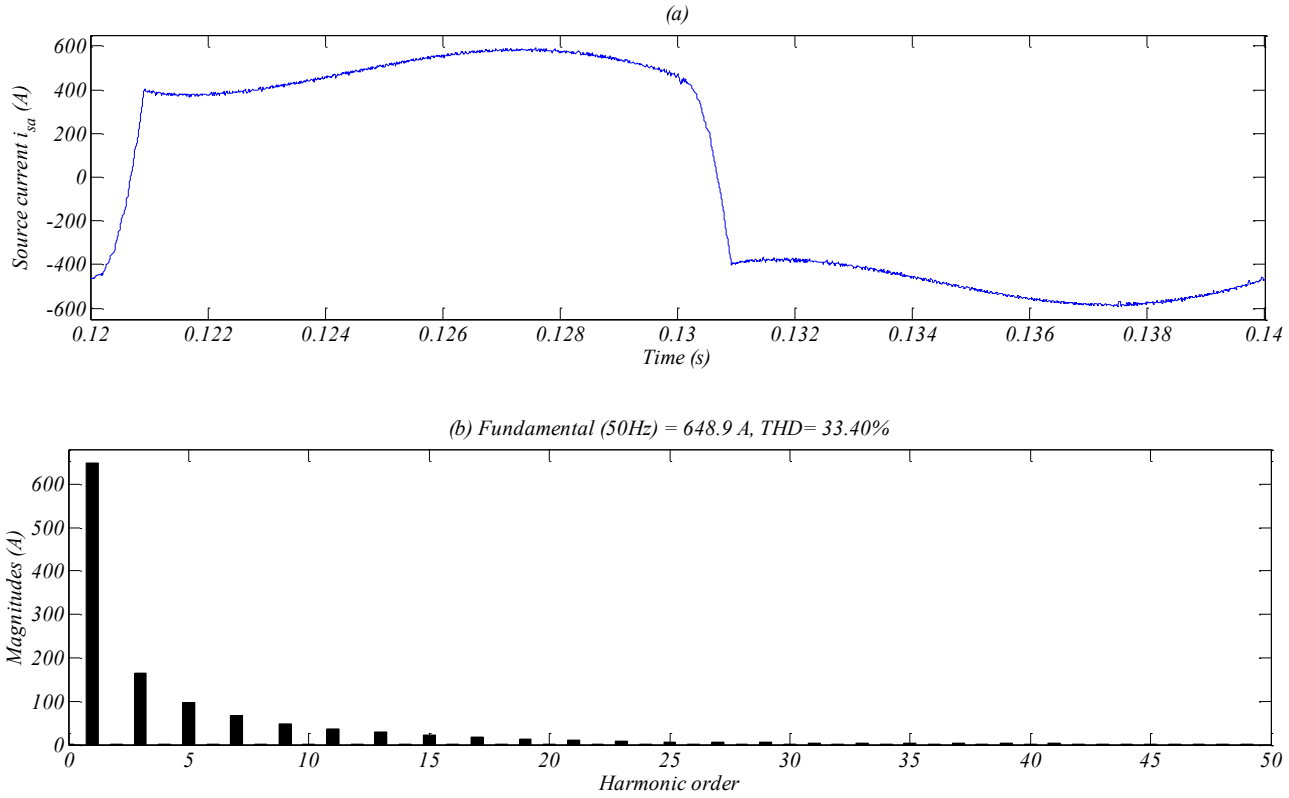

Figure (III.6): (a): Source current before harmonics compensation, (b): Its harmonic spectrum

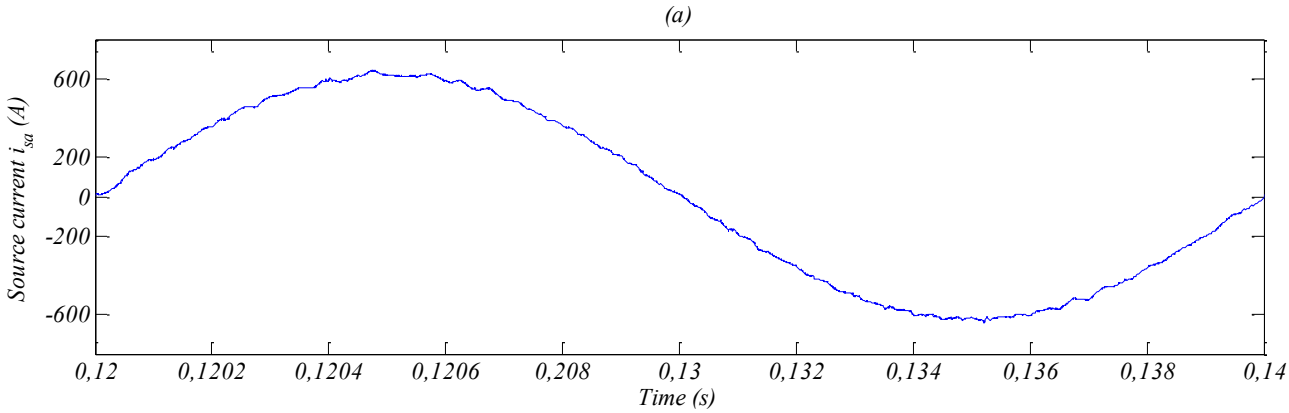

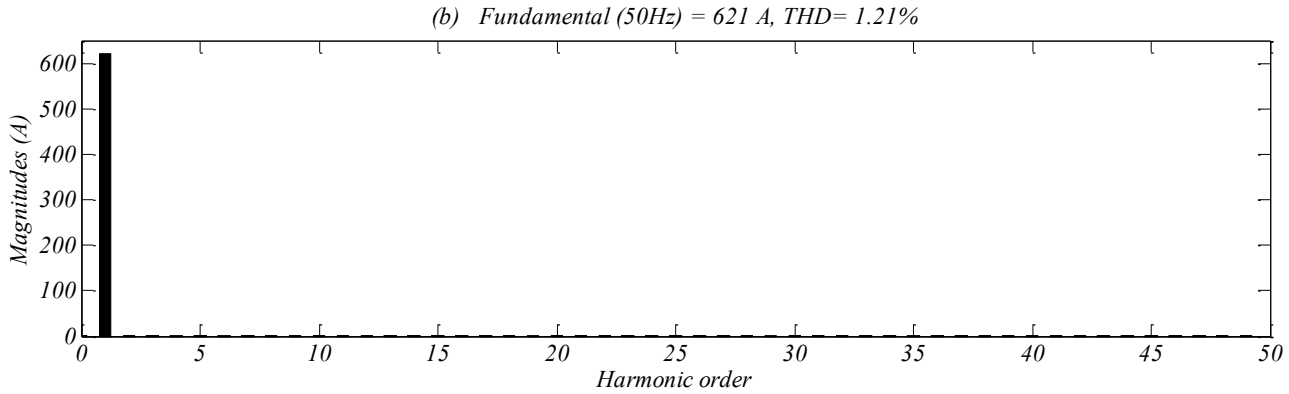

Figure (III.7): (a): Source current after harmonics compensation using feedback linearization-DPC-3DSVM, (b) Its harmonic spectrum

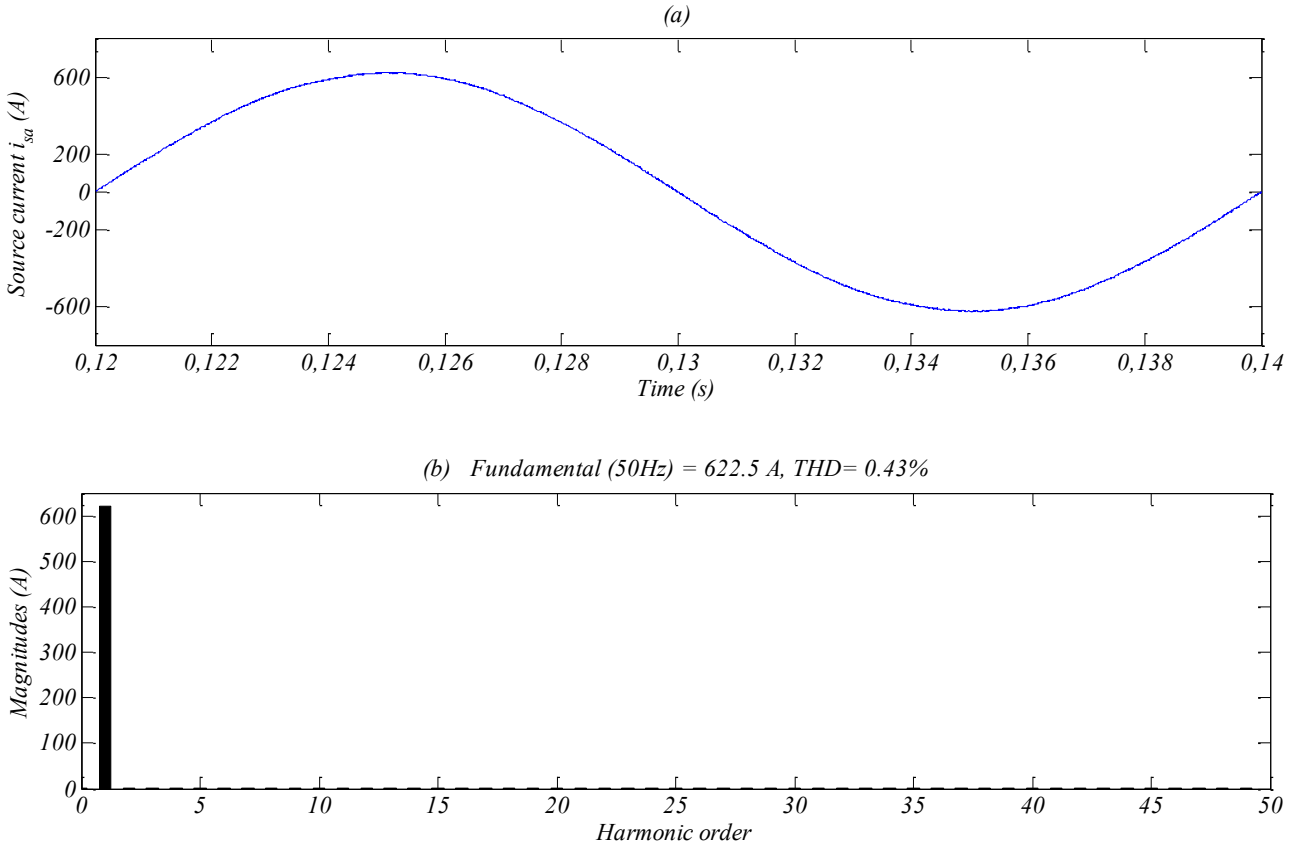

Figure (III.8): (a): Source current after harmonics compensation using Feedback linearization-PDPC-3DSVM, (b) Its harmonic spectrum

III.3.2. Balanced and unbalanced load condition

The dynamic behavior under a step change of the nonlinear load in phase *b* at $t = 0.15$s of DPC-3DSVM and PDPC-3DSVM with nonlinear controllers are presented respectively in figures (III.9) and (III.10).

From this figures, it can be seen that both control strategies have roughly the same performance in balanced and unbalanced load conditions.

It can be observed that the source current become sinusoidal and balanced, the unity power factor operation is successfully achieved, even in unbalanced load condition. The neutral current is almost canceled with a low ripple of 1.6% in both control methods.

Notice also that, after a short transient, the DC voltage is maintained close to its reference value without overshot. One can see also that the source active power joins its nominal value while the source reactive power is remaining to its null value with small ripples.

The absence of an overshoot in DC voltage response during load change, low response time and low source current THD, demonstrates the effectiveness of the nonlinear controllers in both control strategies.

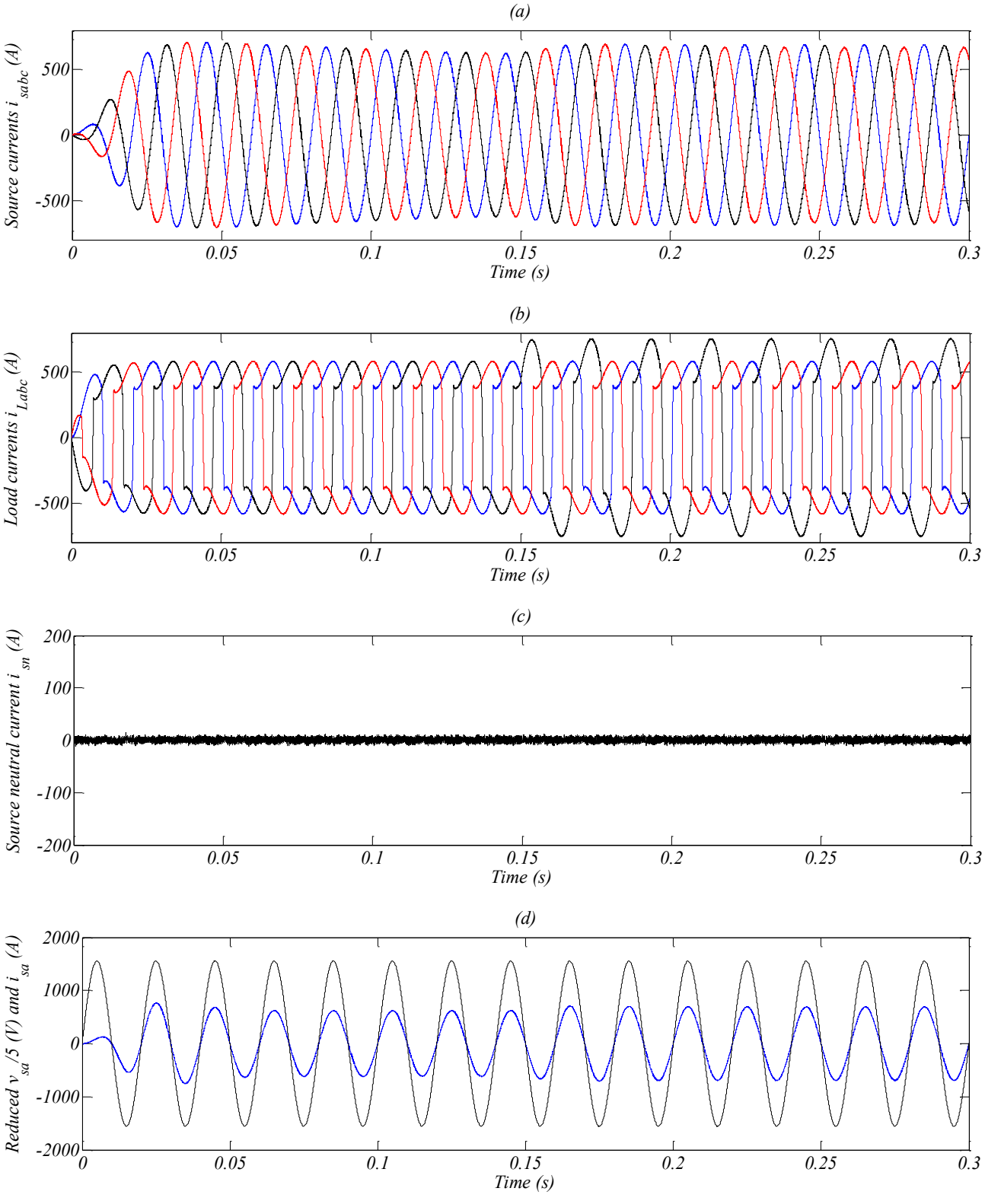

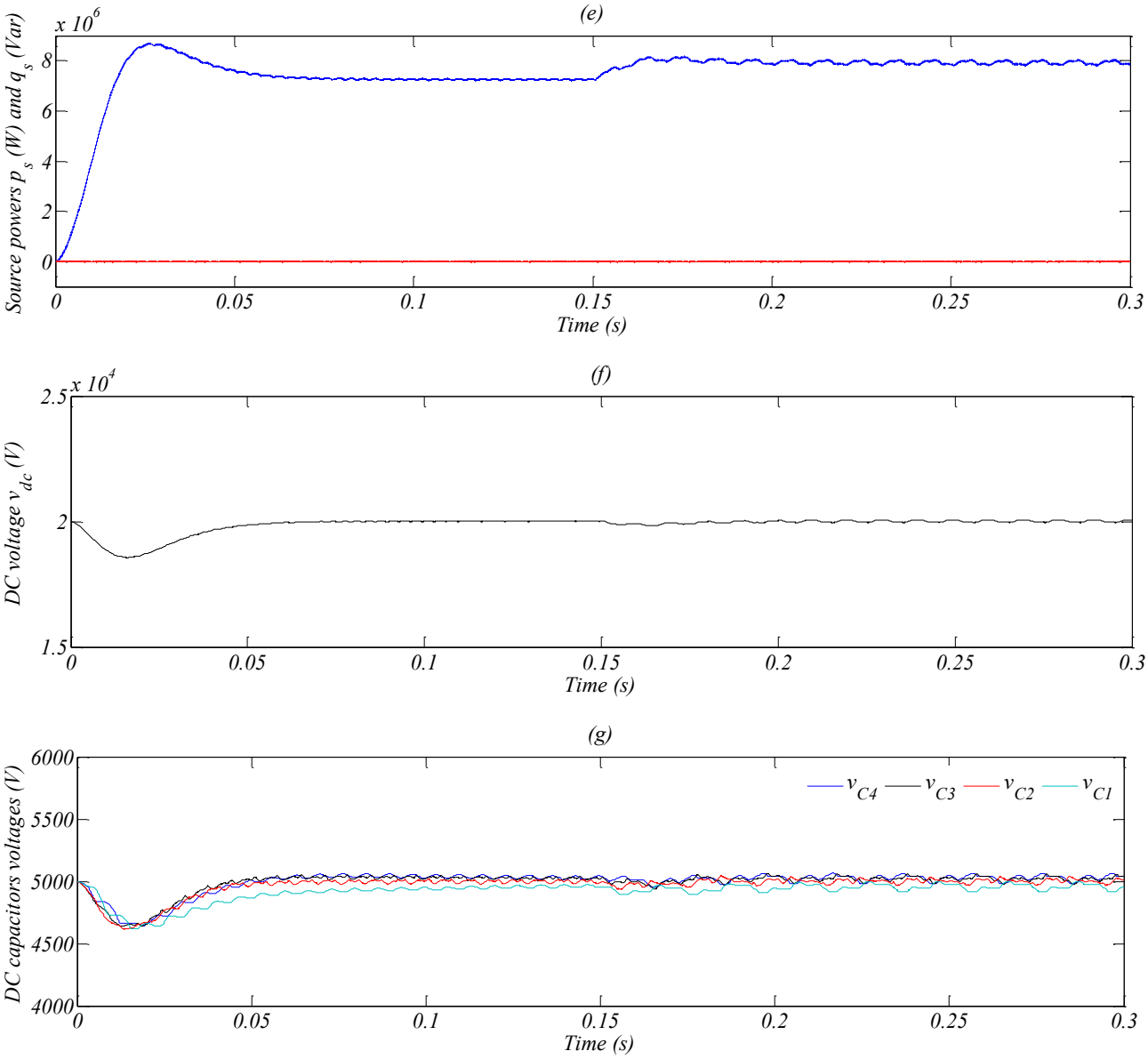

Figure (III.9): Simulation results of the feedback linearization-DPC-3DSVM for the five-level four-leg SAPF under balanced and unbalanced load condition

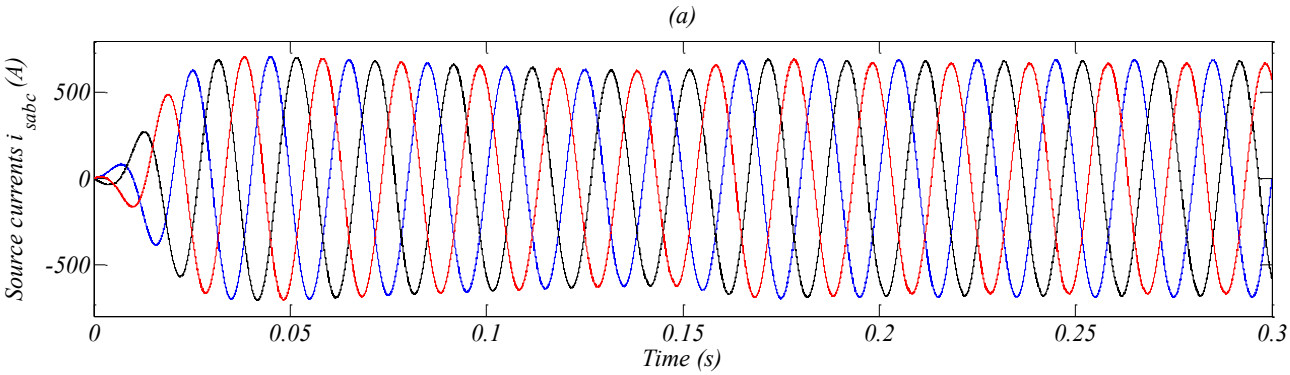

(b)

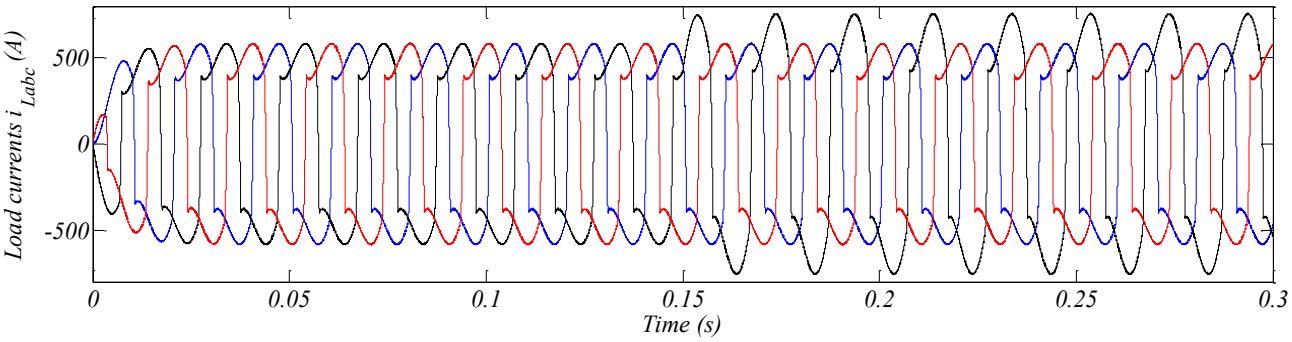
Load currents i_{Labc} (A)
500
0
-500
0
0.05
0.1
0.15
0.2
0.25
0.3
Time (s)

(c)

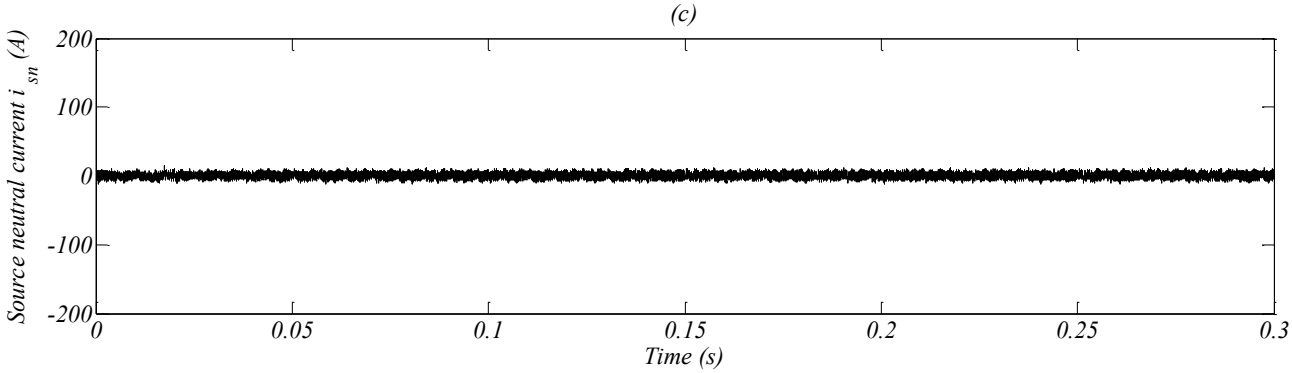
Source neutral current i_{sn} (A)
200
100
0
-100
-200
0
0.05
0.1
0.15
0.2
0.25
0.3
Time (s)

(d)

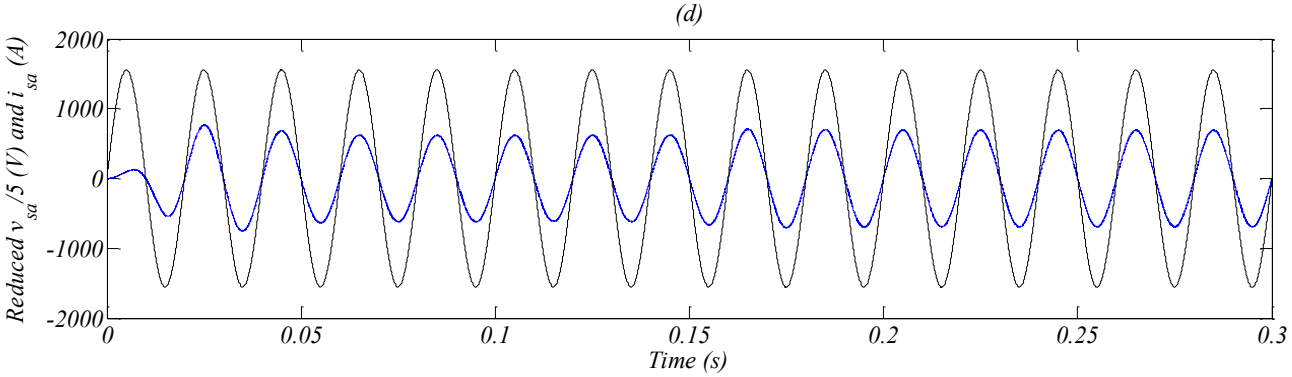
Reduced v_{sa} /5 (V) and i_{sa} (A)
2000
1000
0
-1000
-2000
0
0.05
0.1
0.15
0.2
0.25
0.3
Time (s)

(e)

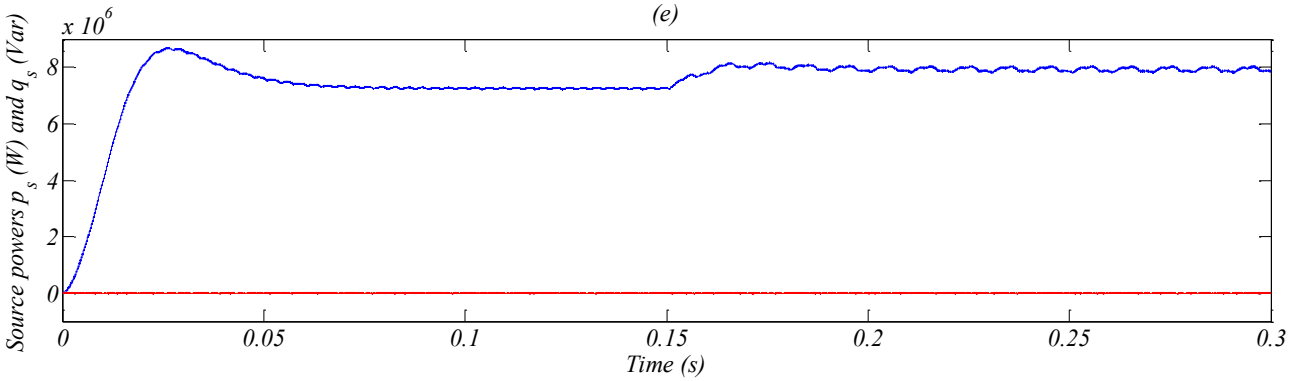
x 10^6
Source powers p_s (W) and q_s (Var)
8
6
4
2
0
0
0.05
0.1
0.15
0.2
0.25
0.3
Time (s)

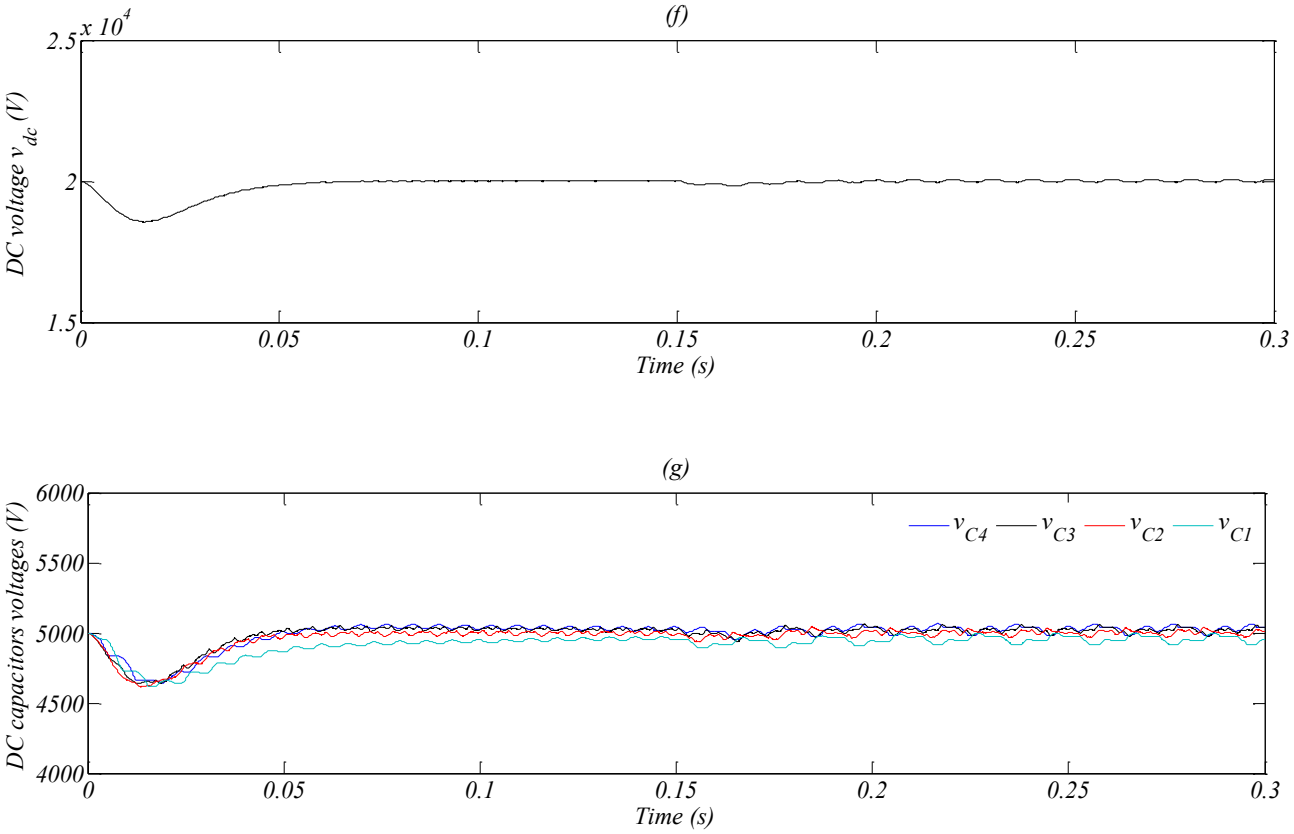

Figure (III.10): Simulation results of the feedback linearization-PDPC-3DSVM for the five-level four-leg SAPF under balanced and unbalanced load condition

III.3.3. Distorted source voltage condition

Figures (III.11) and (III.12) show the waveforms in which a fifth harmonic voltage component of 5% is intentionally superimposed on the fundamental source voltage for DPC-3DSVM and PDPC-3DSVM using nonlinear controllers respectively.

The nonlinear DPC-3DSVM and PDPC-3DSVM have the same sensitivity to this disturbance.

It is clear that the source currents are balanced, the unity power factor operation is successfully achieved, and the neutral current is eliminated under distorted source voltage condition.

The DC voltage drop is lower than 1.4 *kV*, and its recovery time is about 0.08s. Also, it is possible to see how the voltage across each capacitor remains constant.

As shown in figure (III.13) the total harmonic distortion of source current is 5.22% with DPC-3DSVM and 5% with PDPC-3DSVM.

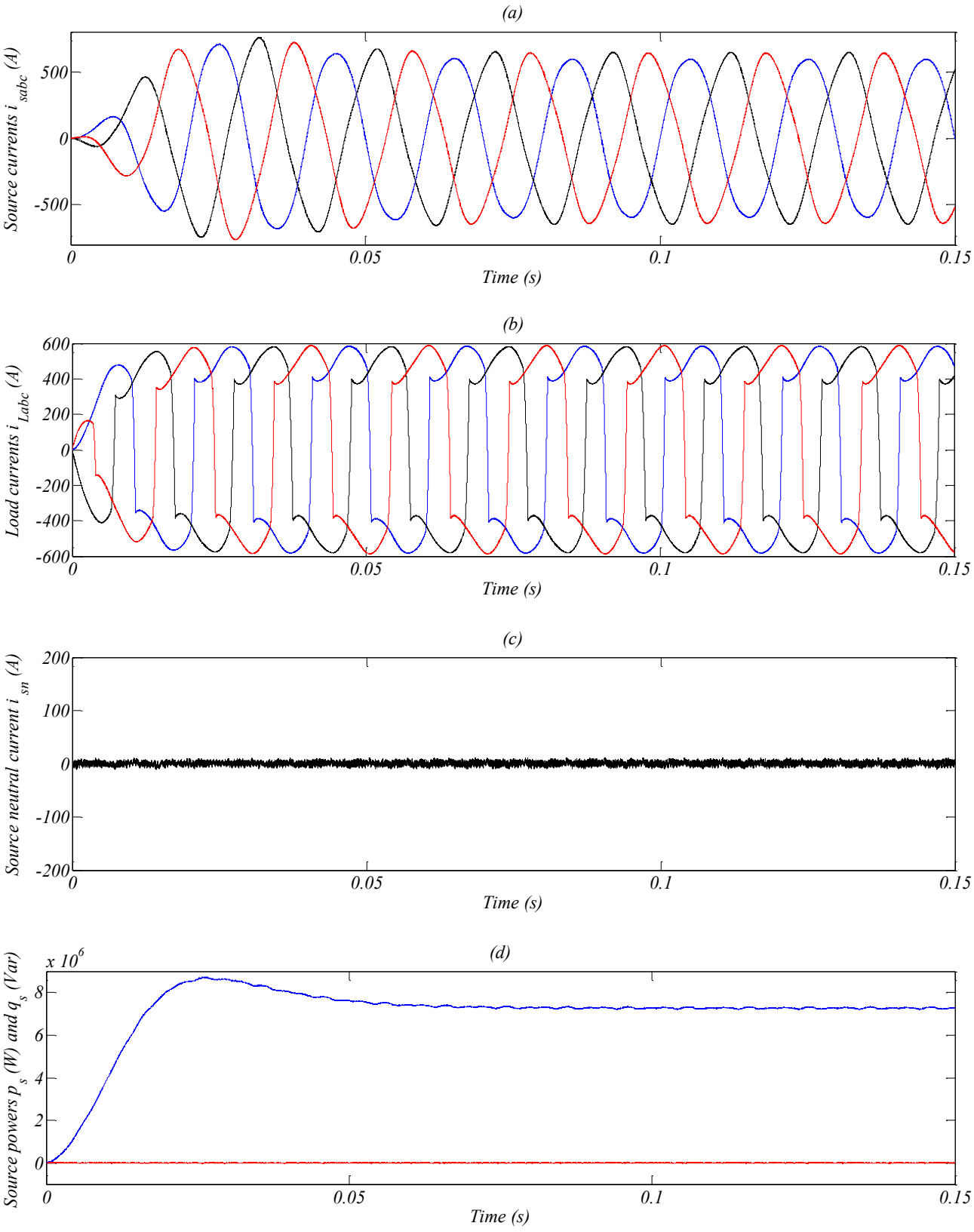
(a)
Source currents i_{sabc} (A)
500
0
-500
0
0.05
0.1
0.15
Time (s)
(b)
Load currents i_{Labc} (A)
600
400
200
0
-200
-400
-600
0
0.05
0.1
0.15
Time (s)
(c)
Source neutral current i_{sn} (A)
200
100
0
-100
-200
0
0.05
0.1
0.15
Time (s)
(d)
x 10^6
Source powers p_s (W) and q_s (Var)
8
6
4
2
0
0
0.05
0.1
0.15
Time (s)

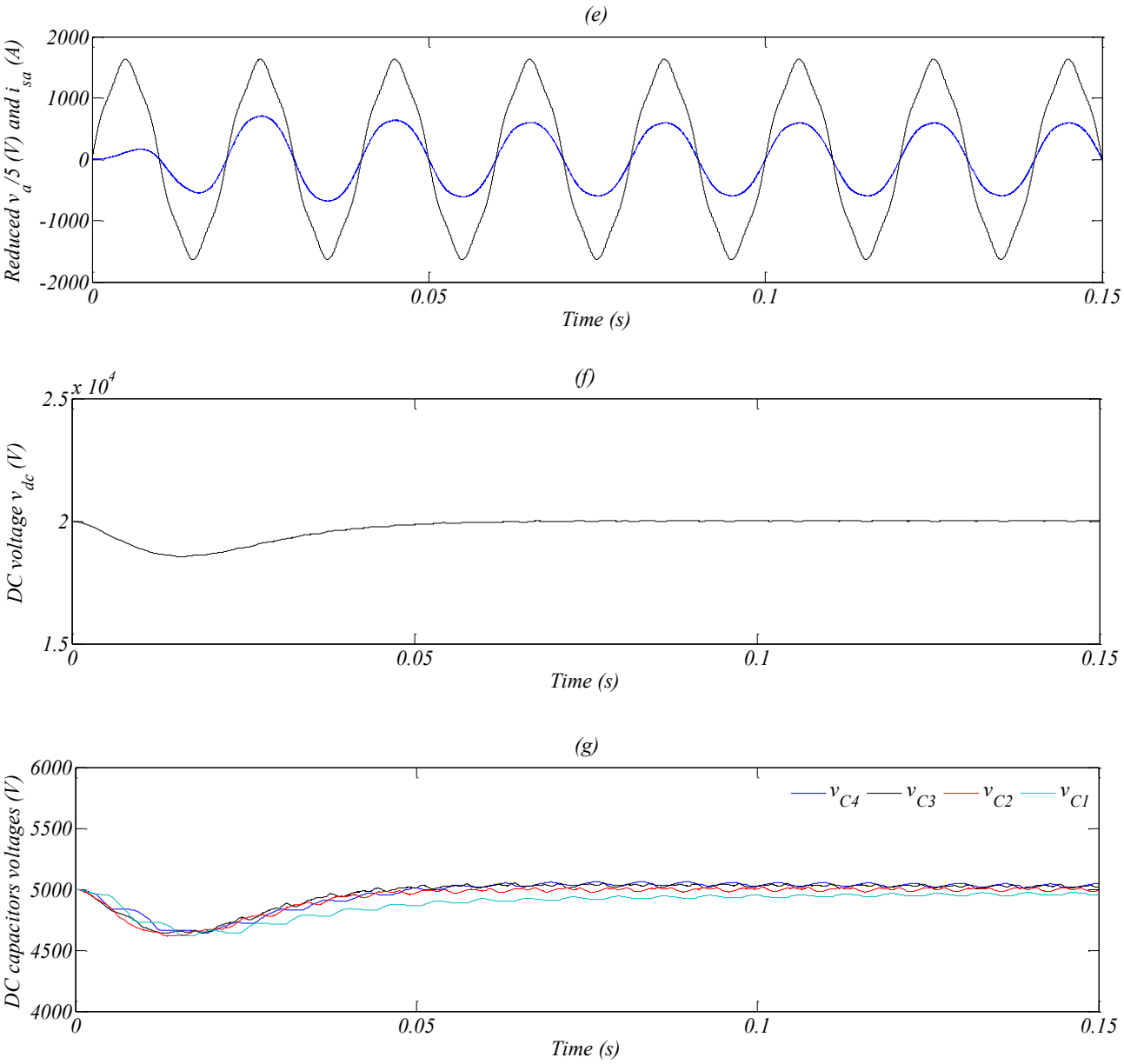

Figure (III.11): Simulation results of the five-level four-leg SAPF controlled by DPC under distorted source voltage

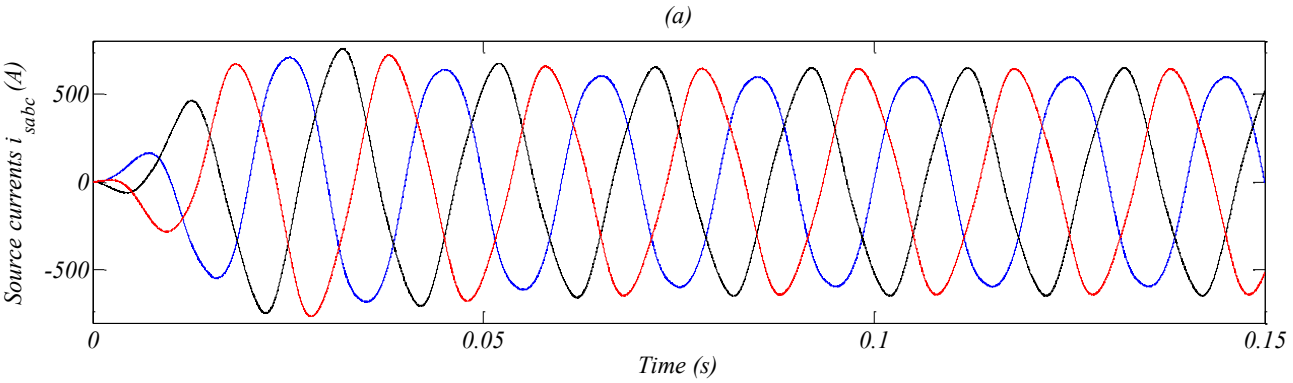

(b)

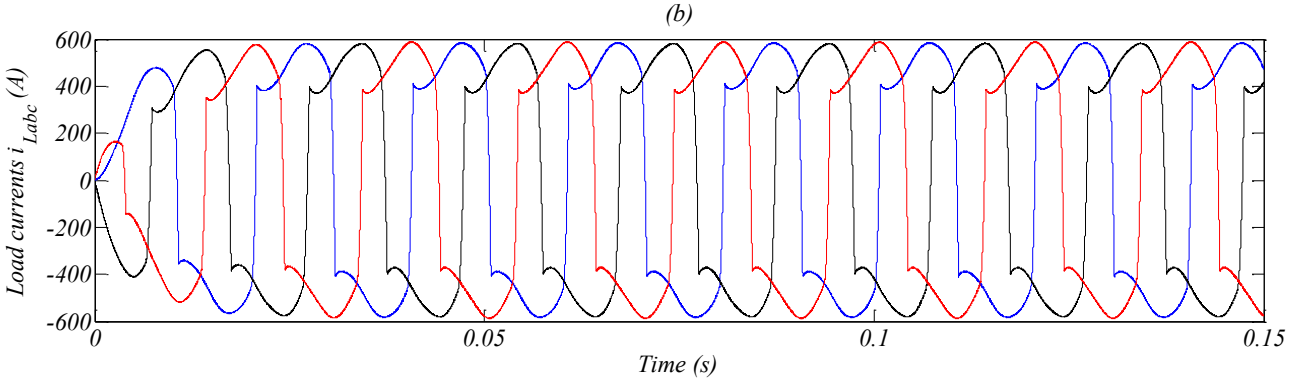
600
400
200
0
-200
-400
-600
Load currents i_{Labc} (A)
0
0.05
0.1
0.15
Time (s)

(c)

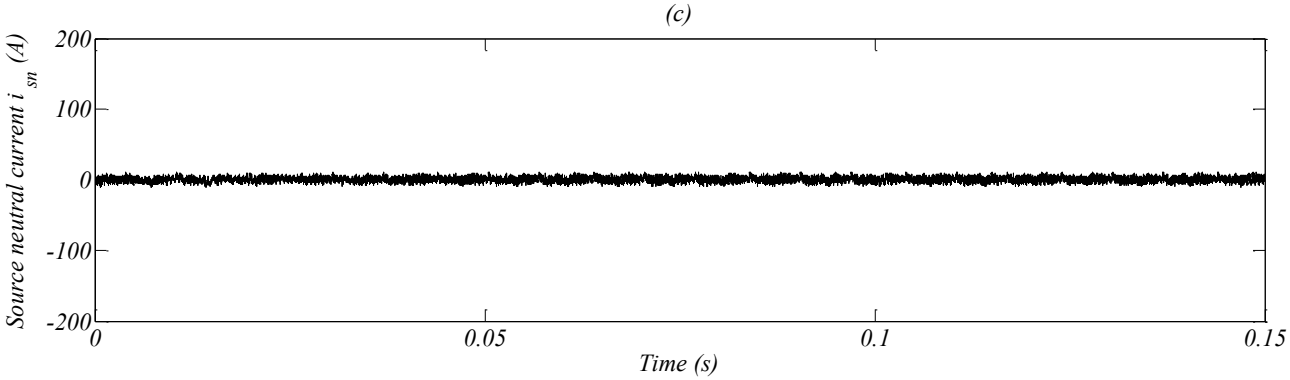
200
100
0
-100
-200
Source neutral current i_{sn} (A)
0
0.05
0.1
0.15
Time (s)

(d)

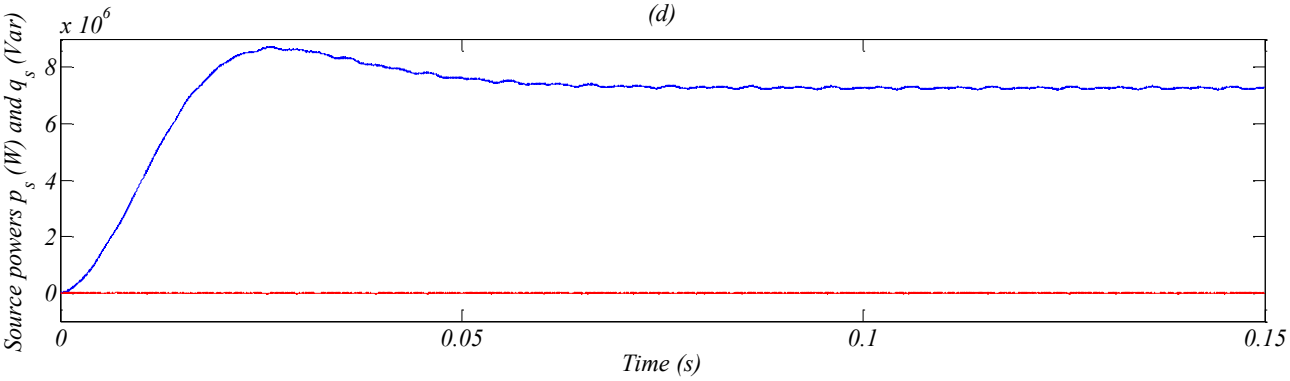
x 10^6
8
6
4
2
0
Source powers p_s (W) and q_s (Var)
0
0.05
0.1
0.15
Time (s)

(e)

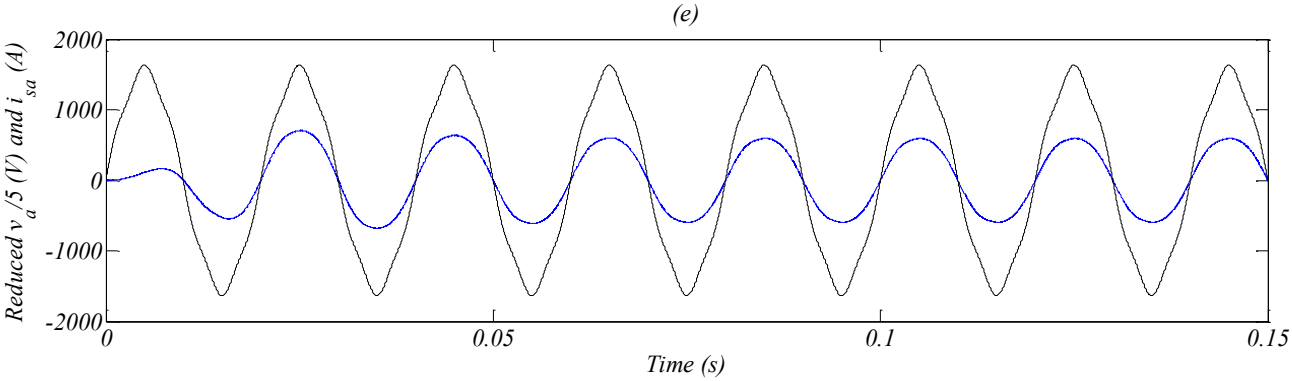
2000
1000
0
-1000
-2000
Reduced v_a /5 (V) and i_{sa} (A)
0
0.05
0.1
0.15
Time (s)

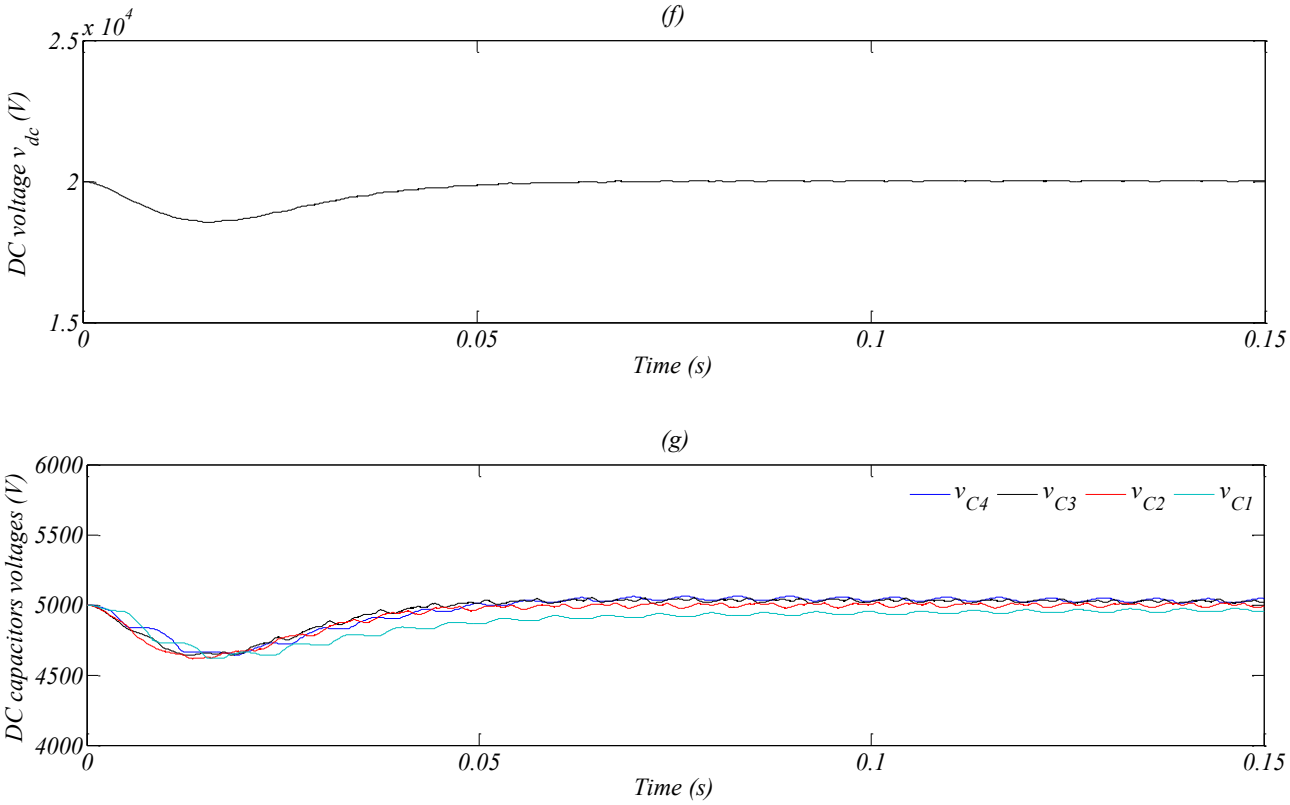

Figure (III.12): Simulation results of the five-level four-leg SAPF controlled by DPC under distorted source voltage

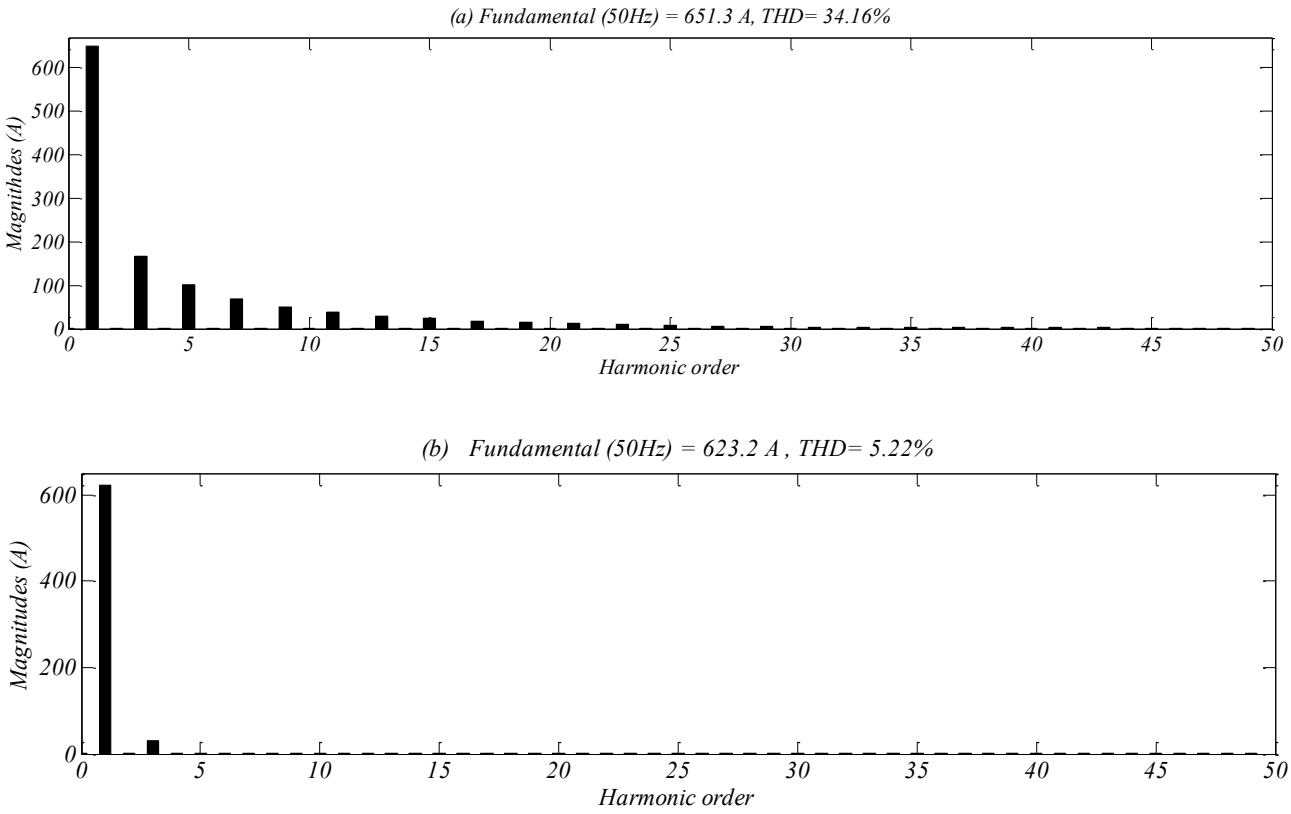

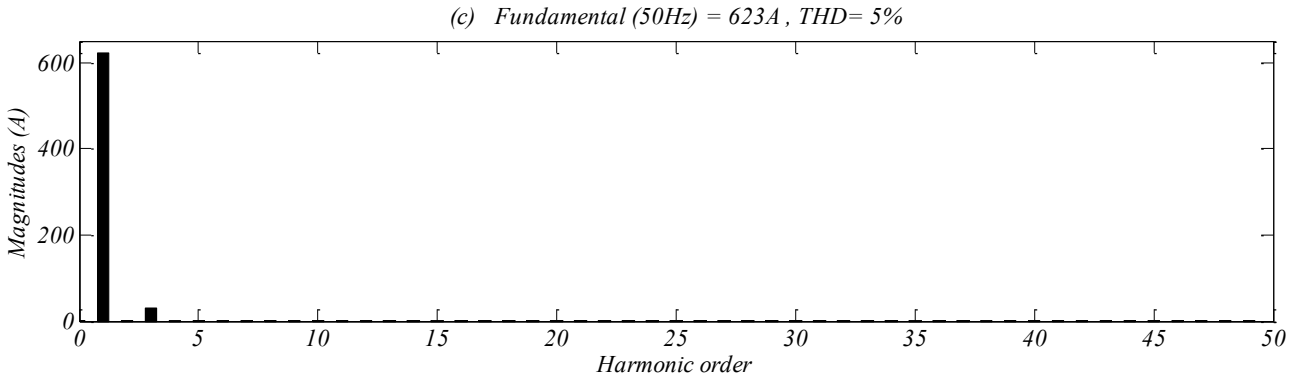

Figure (III.13): Harmonic spectrum of source current under distorted source voltage: (a) Before compensation, (b) After compensation using DPC-3DSVM, (c) After compensation using PDPC-3DSVM

III.4. Conclusion

In this chapter, direct power control and predictive direct power control combined with feedback linearization control for five-level four-leg shunt active power filter have been presented. The performances of the active power filtering system based on nonlinear controller are analyzed and tested for different disturbed conditions. The both control strategies associated with nonlinear controllers illustrate high performance under steady state, unbalanced load, and distorted source voltage operations in terms of the current harmonics filtering, reactive power compensation, source current balancing and neutral current cancellation.

Chapter IV

Direct power control using second order sliding mode for five-level four-leg shunt active power filter

IV.1. Introduction

Sliding mode control is considered to be one of the most effective control techniques that can handle heavy uncertainty conditions [107-109]. The control objectives are attained by constraining the system dynamics on a properly chosen surface by means of discontinuous control laws. This methodology provides for high accuracy and robustness with respect to a wide range of disturbances and uncertainties. However, due to the presence of imperfections in actuators and sensors, such as hysteresis, delays, etc., and to the presence of noise and/or exogenous disturbances, this control approach may produce the undesirable chattering effect [63, 110].

To avoid chattering different approaches have been proposed [63, 107-111]. The main idea of such approaches was to change the dynamics in small vicinity of the discontinuity surface in order to avoid real discontinuity and, at the same time, to preserve the main properties of the whole system. However, the ultimate accuracy and robustness of the sliding mode are partially lost [63].

On the contrary, higher order sliding modes, which generalizes the basic sliding mode idea, acts directly on the higher order time derivatives of the sliding variable instead of influencing its first time derivative like it happens in standard sliding modes. Higher order sliding modes method does not only able to keep the main advantages of the original approach, but also can remove the chattering effect and provide for even higher accuracy in realization [65].

A number of higher order sliding mode controllers are described in the literature [112-114]. However, the main problem in implementation of higher order sliding modes is the increasing information demand. Generally speaking, any r^{th} order sliding controller requires the knowledge of the time derivatives of the sliding variable up to the $(r\text{-}1)^{th}$ order. The only exceptions are given by the twisting controller [65], the super-twisting controller [65] and the sub-optimal algorithm [115] which are second order sliding mode control algorithms.
For this reason these second order sliding mode controllers are the most widely used in practice among higher order sliding mode controllers because of their simplicity and of their low information demand. In the following section, a brief description of second order sliding mode control methodology will be given.

IV.2. Second order sliding mode

Second order sliding mode controllers are the most widely used in practice among higher order sliding mode controllers because of their simplicity and of their low information demand. In particular the super-twisting controllers are considered because of their advantage of not requiring the knowledge of $\dot{\sigma}$.

IV.2.1. Problem statement

Consider a dynamic single-input system of the form:

$$\dot{x} = f(t,x) + g(t,x)u \tag{IV.1}$$

Where $x \in \Re^n$ is the state vector, $u \in \Re$ is the control input vector, f and g are smooth vector fields.
Let $\sigma(t,x) = 0$ be the chosen sliding manifold, then the control objective is to enforce a second order sliding mode on the sliding manifold $\sigma(t,x) = \dot{\sigma}(t,x) = 0$, in finite time.

Depending on the relative degree [90] of the system, two different cases must be considered:

A: relative degree $r = 1$, i.e $\dfrac{\partial \dot{\sigma}}{\partial u} \neq 0.$

B: relative degree $r = 2$, i.e $\dfrac{\partial \dot{\sigma}}{\partial u} = 0,\ \dfrac{\partial \ddot{\sigma}}{\partial u} \neq 0$.

Case A: In this case, the control problem can be solved relying on first order sliding mode control, nevertheless second order sliding mode control can also be used in order to avoid chattering. For this purpose $u(t)$ is considered as an output of some first order dynamic system and the time derivative of the plant control $\dot{u}(t)$ is regarded as an auxiliary control variable [65].

A discontinuous control $\dot{u}$ steers the sliding variable σ to zero, keeping $\sigma = 0$ in second order sliding mode, so that the plant control u is continuous and the chattering is avoided [65, 113].

The first and second time derivatives of the sliding variable are given by:

$$\begin{aligned} \dot{\sigma} &= \frac{\partial}{\partial x}\sigma(t,x)\left[f(t,x) + g(t,x)u(t) \right] \\ \ddot{\sigma} &= \varphi_A(t,x,u) + \gamma_A(t,x)\dot{u} \end{aligned} \tag{IV.2}$$

Where:

$$\varphi_A(t,x,u) = \frac{\partial}{\partial x}\dot{\sigma}(t,x,u)\left[f(t,x) + g(t,x)u(t) \right]$$
$$\gamma_A(t,x) = \frac{\partial}{\partial x}\sigma(t,x)g(t,x)$$

The control input u is understood as an unknown disturbance affecting the drift term $\varphi_A(t,x,u)$. The control derivative $\dot{u}$, used as an auxiliary control variable, is designed in order to satisfy the control objective of steering σ and $\dot{\sigma}$ to zero. Note that the control time derivative $\dot{u}$ affects the $\ddot{\sigma}$ dynamics.

Case B: The control does not affect directly the dynamics of $\dot{\sigma}$, but it affects directly $\ddot{\sigma}$, i.e.,

$$\begin{aligned} \dot{\sigma} &= \frac{\partial}{\partial x}\sigma(t,x)f(t,x) \\ \ddot{\sigma} &= \varphi_B(t,x,u) + \gamma_B(t,x)u(t) \end{aligned} \tag{IV.3}$$

Where:

$$\varphi_B(t,x) = \frac{\partial}{\partial x}\dot{\sigma}(t,x,u)f(t,x)$$
$$\gamma_B(t,x) = \frac{\partial}{\partial x}\dot{\sigma}(t,x,u)g(t,x)$$

It must be assumed that:

$$\gamma_B(t,x) \neq 0 \tag{IV.4}$$

Both cases A and B can be dealt within an unified treatment, as the structure of the system to be stabilized is exactly the same, i.e., a second order uncertain system with affine dependence on the relevant control signal (the control derivative $\dot{u}$ in case A, the actual control u in case B).
For this reason, it will be addressed and solved the stabilization problem for the system:

$$\begin{cases} \zeta_1(t) = \sigma(t,x) \\ \dot{\zeta}_1(t) = \zeta_2(t) \\ \dot{\zeta}_2(t) = \varphi(\cdot) + \gamma(t,x)v(t) \end{cases} \tag{IV.5}$$

Where ζ_1 and ζ_2 represent the actual sliding variable and its derivative, respectively.
As for the terms $\varphi(\cdot)$ and $v(t)$ they have different meaning and structure in cases A and B. More precisely:
Case A:

$$\begin{aligned} \varphi(\cdot) &= \varphi_A(t,x,u) \\ v(t) &= \dot{u}(t) \end{aligned} \tag{IV.6}$$

Case B:

$$\begin{aligned} \varphi(\cdot) &= \varphi_B(t,x) \\ v(t) &= u(t) \end{aligned} \tag{IV.7}$$

Remark
As previously discussed, in case A, called the anti-chattering case, the second order sliding mode approach attains the control objective by means of a continuous control input. In fact, the actual discontinuous control signal $v(t)$ is the derivative of the plant input $u(t)$, which, obtained by integrating the discontinuous derivative, turns out to be continuous. The first order sliding mode control leads to the discontinuous control laws in this case.
In case B, that is the relative degree two case, the actual control $u(t)$ is discontinuous. Note that the traditional first order sliding mode control methodology, if not properly coupled to state observers, fails to solve this problem.

The stabilization problem is solved under the assumption that $\dot{\sigma}$ is not available for measurements. This fact, together with the presence of model uncertainties, makes the problem not easily solvable. The existence of a solution is obviously critically related to the relevant assumptions on the uncertain dynamics.
The historical development of second order sliding mode control algorithms [65, 115] starts considering the global boundedness assumption for the uncertainties, i.e., that in some neighbor of the sliding manifold (not necessarily small) the uncertain terms are bounded by known positive constants according to:

$$\begin{aligned} &\left|\varphi(\cdot)\right| \le \Phi \\ &0 < G_1 \le \gamma(t,x) \le G_2 \end{aligned} \tag{IV.8}$$

To summarize, the second order sliding mode control problem for n^{th} order systems of the type (IV.1), it can be reduced to the stabilization problem of a second order system:

$$\begin{cases} \dot{\zeta}_1(t) = \zeta_2(t) \\ \dot{\zeta}_2(t) = \varphi(\cdot) + \gamma(t,x)v(t) \end{cases} \tag{IV.9}$$

Where: ζ_2 is not available for measurement, and the uncertain terms φ and γ are bounded by known positive constants according to (IV.8).

As previously discussed, depending on the relative degree r between the sliding variable and the actual control input, $v(t)$ may represent either the actual control or its derivative, and, correspondingly, also the uncertain drift term φ may depend on two different sets of variables.

IV.2.2. Super-twisting controller

This control algorithm has been developed to control systems with relative degree one in order to avoid chattering [65]. The trajectory on the phase plane $\sigma O\dot{\sigma}$ is characterized by twisting around the origin as in figure (IV.1). The continuous control law u(t) is constituted by two terms. The first is defined by means of its discontinuous time derivative, while the other is a continuous function of the available sliding variable.

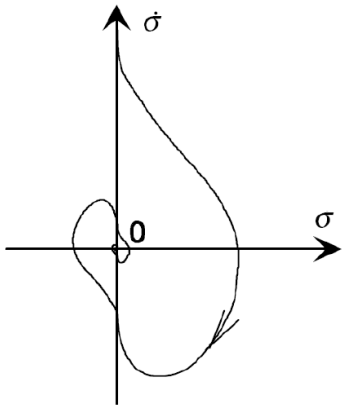

Figure (IV.1): Super-twisting controller trajectory in the phase plane

According to [65, 111] the following theorem can be proved:

Theorem *Consider system (IV.9) with its uncertain dynamics satisfying (IV.8), ζ_2 is not available for measurement, and assume that the relative degree of the system is one. Then, the control algorithm is defined by*:

$$\begin{aligned} u(t) &= -\lambda \left|\zeta_1\right|^{\rho} \operatorname{sign}(\zeta_1) + u_1 \\ \dot{u}_1 &= -\alpha \operatorname{sign}(\zeta_1) \end{aligned} \tag{IV.10}$$

With the constraints:

$$\begin{aligned} &\alpha > \frac{\Phi}{G_1} \\ &\lambda^2 \le \frac{4\Phi G_2(\alpha + \Phi)}{G_1^3(\alpha - \Phi)} \\ &0 < \rho \le 0.5 \end{aligned} \tag{IV.11}$$

The super-twisting controller is capable of enforcing a second order sliding mode on the sliding manifold $\sigma(t,x) = \dot{\sigma}(t,x) = 0$ *in finite time [65].*

Note that the super-twisting algorithm does not need any information on the time derivative of the sliding variable and it is very suitable to control nonlinear systems with a relative degree of one to eliminate chattering. Therefore, this control algorithm will be used to design the controllers of DC voltage and active and reactive powers of DPC-3DSVM and PDPC-3DSVM strategies for the five-level four-leg SAPF.

IV.3. Super-twisting sliding mode control of DPC-3DSVM for SAPF

The block diagram of the DPC-3DSVM combined with super-twisting sliding mode control for five-level four-leg SAPF is represented in figure (IV.2).

Remember that the SAPF model was subdivided in two subsystems as follow:

***Subsystem* 1:**

The first subsystem is defined by the following equation:

$$\begin{aligned} \frac{dp_F}{dt} &= \frac{1}{L_F}(-R_F p_F + V_{F\alpha}) \\ \frac{dq_F}{dt} &= \frac{1}{L_F}(-R_F q_F + V_{F\beta}) \\ \frac{dq_{F\alpha\beta}}{dt} &= \frac{1}{L_F}(-R_F q_{F\alpha\beta} + V_{Fo}) \end{aligned} \tag{IV.12}$$

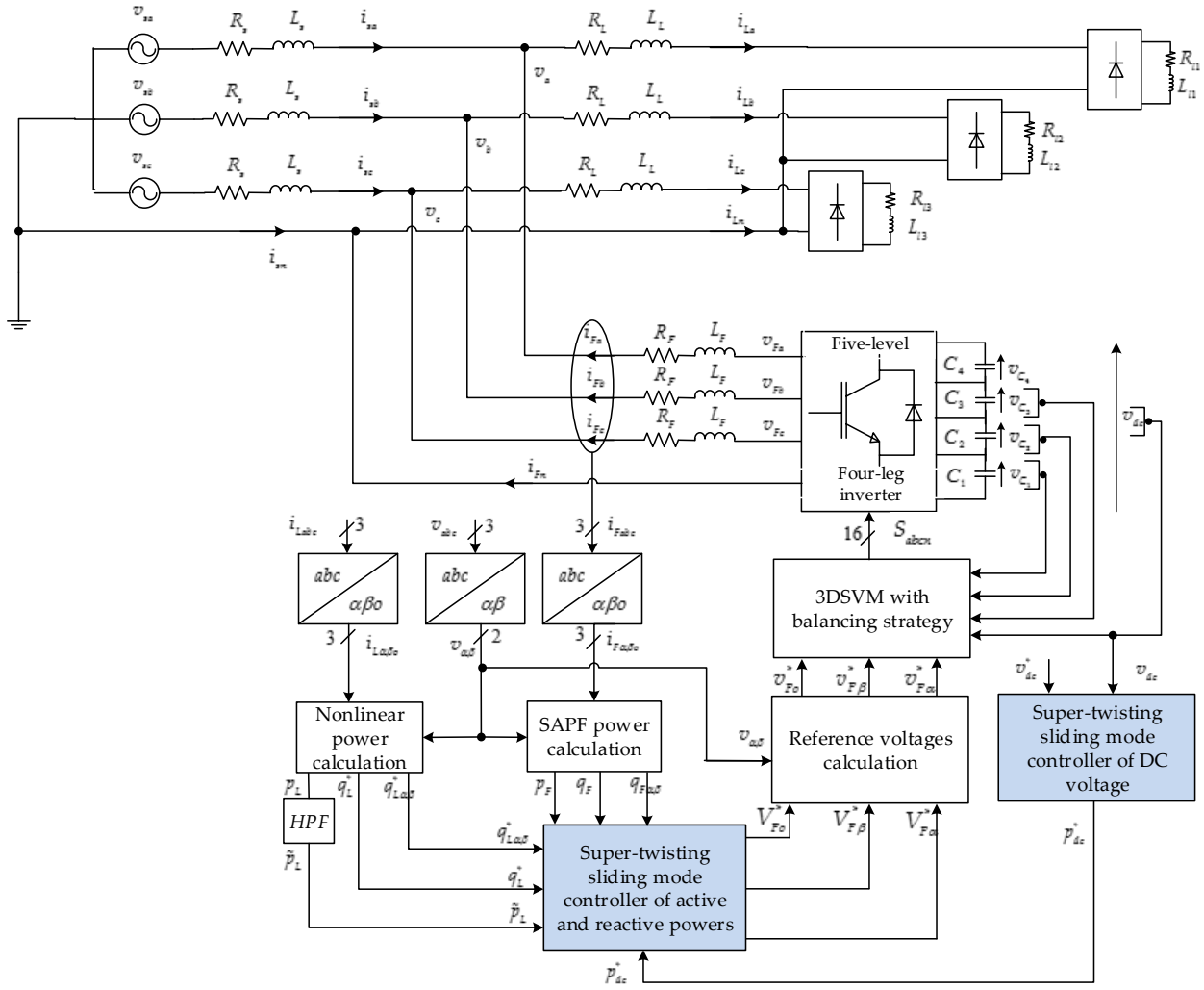

Figure (IV.2): Super-twisting sliding mode control of DPC-3DSVM for five-level four-leg SAPF

It has three states $x=\begin{bmatrix} x_1 & x_2 & x_3 \end{bmatrix}^T=\begin{bmatrix} p_F & q_F & q_{F\alpha\beta} \end{bmatrix}^T$, and three control inputs $u=\begin{bmatrix} u_1 & u_2 & u_3 \end{bmatrix}^T=\begin{bmatrix} V_{F\alpha} & V_{F\beta} & V_{Fo} \end{bmatrix}^T$.

***Subsystem* 2:**

The second subsystem is defined by the following equation:

$$\frac{dv_{dc}^2}{dt}=\frac{2p_{dc}}{C_{eq}} \tag{IV.13}$$

This subsystem has only one state $x=v_{dc}^2$ and only one control input $u=p_{dc}$.

IV.3.1. DC voltage controller synthesis

The synthesis of the DC voltage controller is based on the subsystem 2.

The sliding surface is chosen as:

$$\sigma = v_{dc}^2 - v_{dc}^{*2} \tag{IV.14}$$

The second time derivative of the sliding surface is given by:

$$\ddot{\sigma} = \frac{2}{C_{eq}}\dot{u} \tag{IV.15}$$

Introducing the auxiliary variables $\zeta_1 = \sigma$ and $\zeta_2 = \dot{\sigma}$, the subsystem 2 can be rewritten as:

$$\begin{cases} \dot{\zeta}_1(t) = \zeta_2(t) \\ \dot{\zeta}_2 = \varphi(t,x,u) + \gamma(t,x)\dot{u}(t) \end{cases} \tag{IV.16}$$

Where:

$$\varphi(t,x,u) = 0$$
$$\gamma(t,x) = \frac{2}{C_{eq}}$$

The subsystem (IV.16) is bounded by known positive constants G_1, G_2, and Φ according to:

$$\begin{aligned} &\left|\varphi(t,x,u)\right| \le \Phi \\ &0 < G_1 \le \gamma(t,x) \le G_2 \end{aligned} \tag{IV.17}$$

From the super-twisting algorithm, the control law is given by:

$$u(t) = p_{dc}^* = -\lambda\left|\zeta_1\right|^{\rho} \operatorname{sign}(\zeta_1) - \alpha\int \operatorname{sign}(\zeta_1) \tag{IV.18}$$

Where: α, λ, and ρ are positive constants, and can be chosen as the following condition:

$$\begin{aligned} &\alpha > \frac{\Phi}{G_1} \\ &\lambda^2 \le \frac{4\Phi G_2(\alpha+\Phi)}{G_1^3(\alpha-\Phi)} \\ &0 < \rho \le 0.5 \end{aligned} \tag{IV.19}$$

IV.3.2. Powers controllers synthesis

The sliding surfaces are chosen as:

$$\begin{aligned} \sigma_1 &= p_F - p_F^* \\ \sigma_2 &= q_F - q_F^* \\ \sigma_3 &= q_{F\alpha\beta} - q_{F\alpha\beta}^* \end{aligned} \tag{IV.20}$$

And consequently, their second derivatives are given by:

$$\begin{aligned}\ddot{\sigma}_1 &= \varphi_1(t,x_1,u_1)+\gamma_1(t,x_1)\dot{u}_1\\ \ddot{\sigma}_2 &= \varphi_2(t,x_2,u_2)+\gamma_2(t,x_2)\dot{u}_2\\ \ddot{\sigma}_3 &= \varphi_3(t,x_3,u_3)+\gamma_3(t,x_3)\dot{u}_3\end{aligned} \tag{IV.21}$$

Introducing the auxiliary variables $\zeta_{1i}=\sigma_i$ and $\zeta_{2i}=\dot{\sigma}_i$ $(i=1,2,3)$, the subsystem 1 can be rewritten as:

$$\begin{cases}\dot{\zeta}_{1i}(t)=\zeta_{2i}(t)\\ \dot{\zeta}_{2i}=\varphi_i(t,x_i,u_i)+\gamma_i(t,x_i)\dot{u}_i(t)\end{cases}\quad (i=1,2,3) \tag{IV.22}$$

Where:

$$\begin{aligned}\varphi_1(t,x_1,u_1)&=\frac{R_F^2}{L_F^2}x_1+\frac{R_F}{L_F}\dot{x}_1^*-\frac{R_F}{L_F^2}u_1, \quad \gamma_1(t,x)=\frac{1}{L_F}\\ \varphi_2(t,x_2,u_2)&=\frac{R_F^2}{L_F^2}x_2+\frac{R_F}{L_F}\dot{x}_2^*-\frac{R_F}{L_F^2}u_2, \quad \gamma_2(t,x)=\frac{1}{L_F}\\ \varphi_3(t,x_3,u_3)&=\frac{R_F^2}{L_F^2}x_3+\frac{R_F}{L_F}\dot{x}_3^*-\frac{R_F}{L_F^2}u_3, \quad \gamma_3(t,x)=\frac{1}{L_F}\end{aligned} \tag{IV.23}$$

Where: $\begin{bmatrix}\dot{x}_1^* & \dot{x}_2^* & \dot{x}_3^*\end{bmatrix}^T=\begin{bmatrix}\dot{p}_F^* & \dot{q}_F^* & \dot{q}_{F\alpha\beta}^*\end{bmatrix}^T$ is the derivative of the output reference vector.

The positive constants (G_{1i}, G_{2i}, and Φ_i $(i=1,2,3)$) are selected according to:

$$\begin{aligned}&\left|\varphi_1(t,x,u)\right|\le\Phi_1, \quad 0<G_{11}\le\gamma_1(t,x)\le G_{21}\\ &\left|\varphi_2(t,x,u)\right|\le\Phi_2, \quad 0<G_{12}\le\gamma_2(t,x)\le G_{22}\\ &\left|\varphi_3(t,x,u)\right|\le\Phi_3, \quad 0<G_{13}\le\gamma_3(t,x)\le G_{23}\end{aligned} \tag{IV.24}$$

The control law is given as:

$$\begin{aligned}u_1=V_{F\alpha}^*&=-\lambda_1\left|\zeta_1\right|^{\rho_1}\operatorname{sign}(\zeta_1)-\alpha_1\int\operatorname{sign}(\zeta_1)\\ u_2=V_{F\beta}^*&=-\lambda_2\left|\zeta_2\right|^{\rho_2}\operatorname{sign}(\zeta_2)-\alpha_2\int\operatorname{sign}(\zeta_2)\\ u_3=V_{Fo}^*&=-\lambda_3\left|\zeta_3\right|^{\rho_3}\operatorname{sign}(\zeta_3)-\alpha_3\int\operatorname{sign}(\zeta_3)\end{aligned} \tag{IV.25}$$

Where: α_i, λ_i, and ρ_i $(i=1,2,3)$ are positive constants, and they are chosen such that:

$$\begin{aligned} &\alpha_i > \frac{\Phi_i}{G_{1i}} \\ &\lambda_i^2 \le \frac{4\Phi_i G_{2i}(\alpha_i + \Phi_i)}{G_{1i}^3(\alpha_i - \Phi_i)} \\ &0 < \rho_i \le 0.5 \end{aligned} \tag{IV.26}$$

IV.4. Super-twisting sliding mode of PDPC-3DSVM for SAPF

The schematic diagram of the super-twisting sliding mode control based PDPC-3DSVM for five-level four-leg SAPF is presented by the figure (IV.3). This control method uses the same super-twisting sliding mode controller of the DC voltage developed in the previous section.

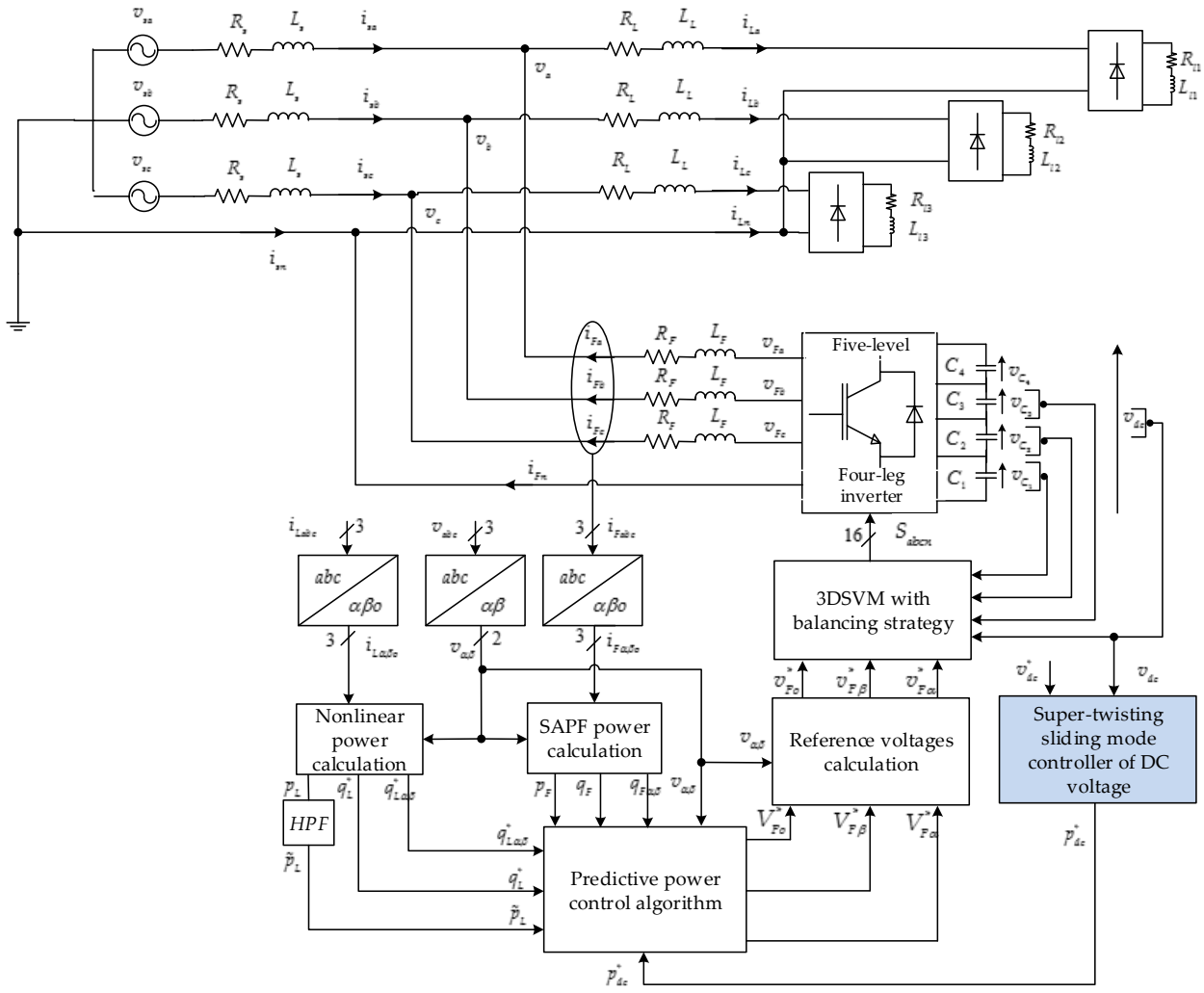

Figure (IV.3): Super-twisting sliding mode control of PDPC-3DSVM for five-level four-leg SAPF

IV.5. Simulation results

The simulation parameters used in this section are the same used in previous chapter. With:

$$\alpha = 10, \lambda = 130, \rho = 0.5;$$
$$\alpha_1 = \alpha_2 = 7.10^4, \lambda_1 = \lambda_2 = 10^5, \rho_1 = \rho_2 = \rho_3 = 0.5;$$
$$\alpha_3 = 10^4, \lambda_3 = 5.10^5.$$

IV.5.1. Steady state operation

Figures (IV.4), (IV.5) and (IV.6) present the source current of the first phase and its harmonic spectrum before and after compensation of five-level four-leg SAPF using super-twisting-DPC-3DSVM, and super-twisting-PDPC-3DSVM, respectively.

The source current is almost sinusoidal with both control strategies. Indeed, the THD value are 0.66% for DPC-3DSVM and 0.66% for PDPC-3DSVM.

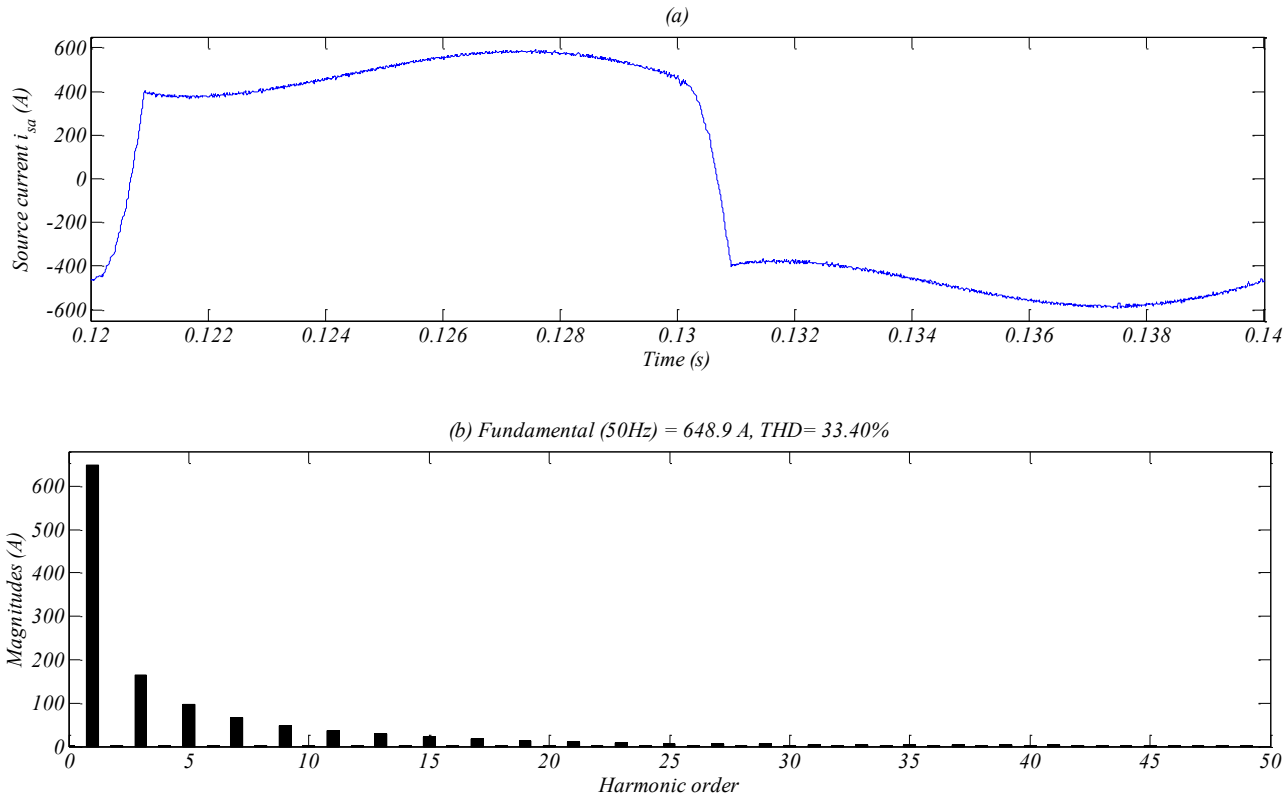

Figure (IV.4): (a): Source current before harmonics compensation, (b): Its harmonic spectrum

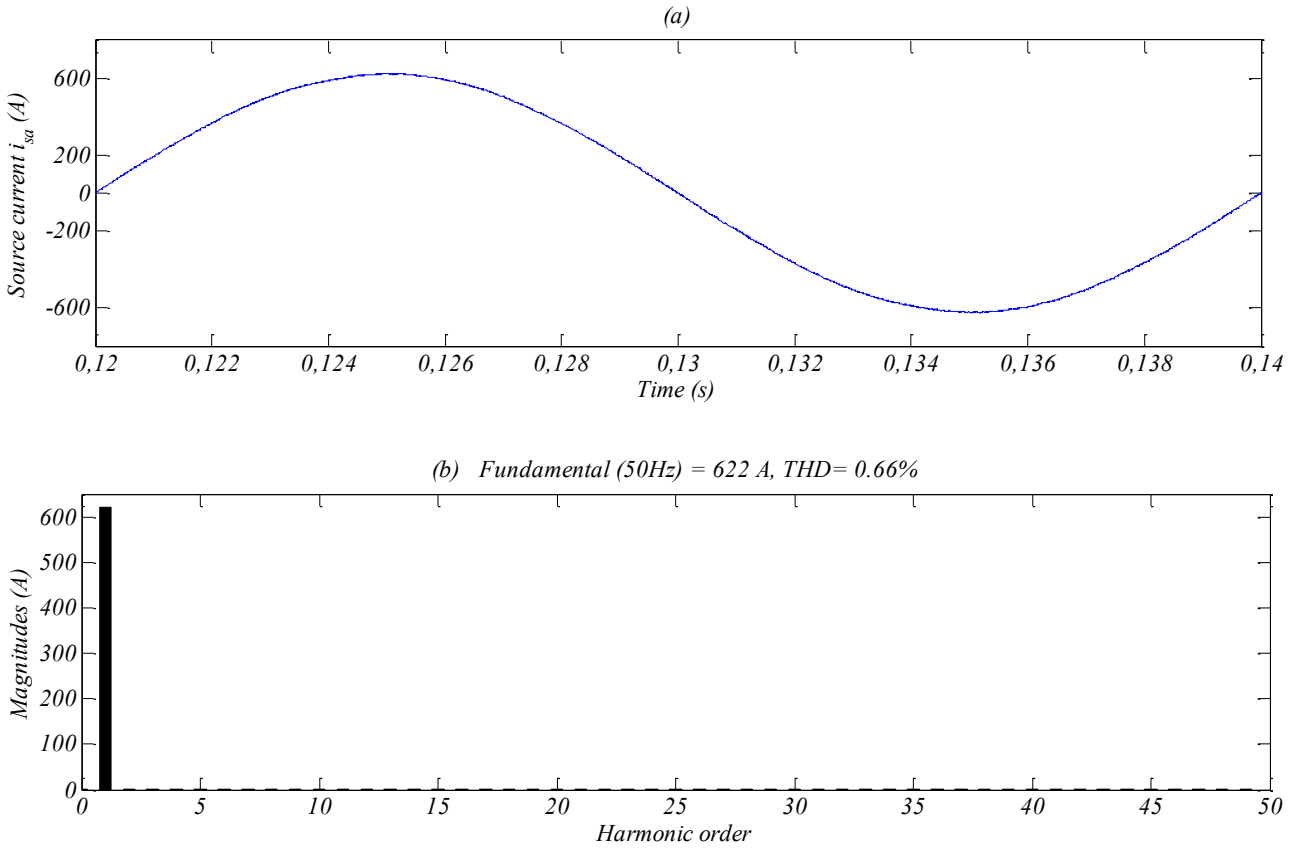

Figure (IV.5): (a): Source current after harmonics compensation using super-twisting-DPC-3DSVM, (b) Its harmonic spectrum

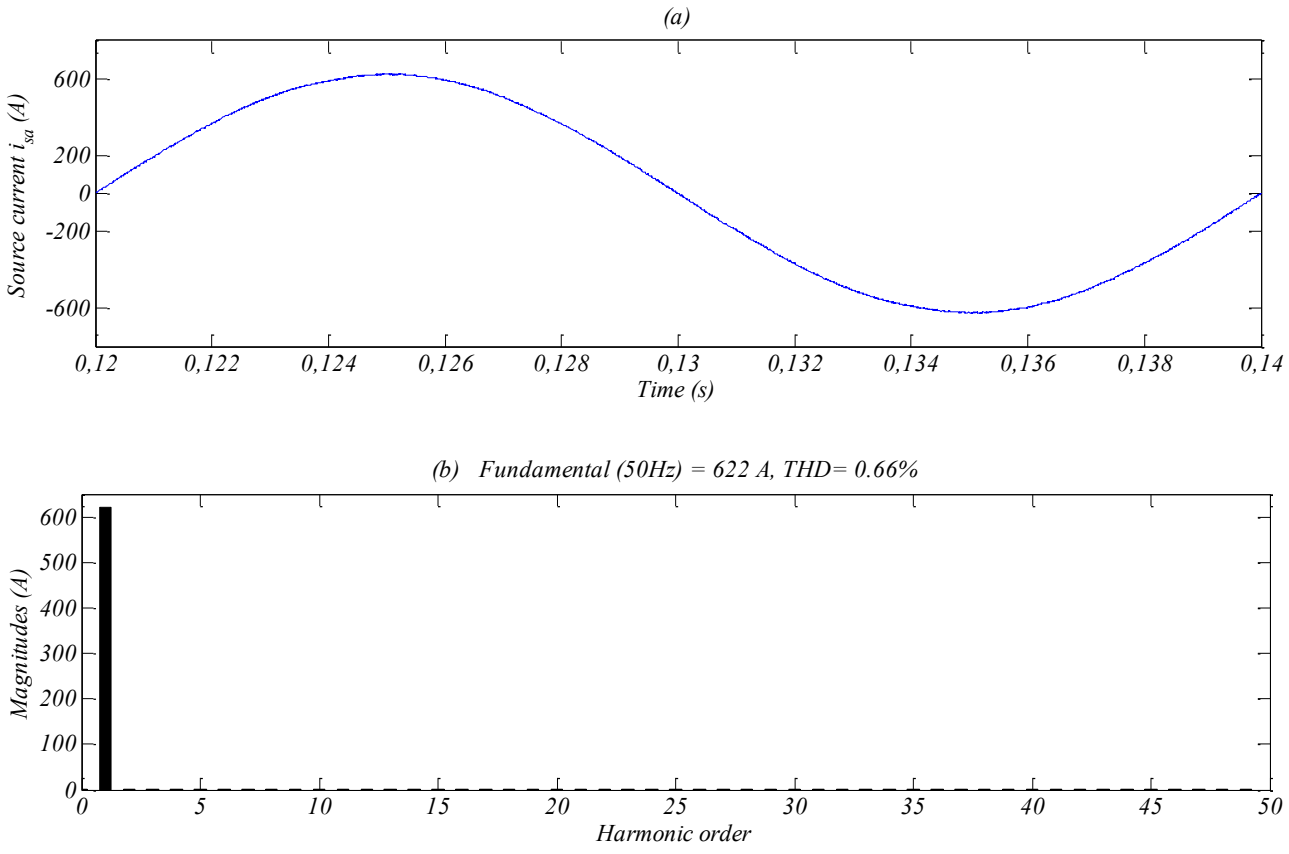

Figure (IV.6): (a): Source current after harmonics compensation using super-twisting -PDPC-3DSVM, (b) Its harmonic spectrum

IV.5.2. Balanced and unbalanced load condition

The dynamic behavior under a step change of the nonlinear load in phase *b* at t = 0.15s of DPC-3DSVM and PDPC-3DSVM with super-twisting controllers are presented respectively in figures (IV.7) and (IV.8).

The unbalanced non-linear load condition does not affect the five-level four-leg SAPF performance with both control strategies.
The application of super-twisting on DPC-3DSVM and PDPC-3DSVM allows simultaneously to full compensation of harmonic currents, reactive power, and neutral current. The source current is in phase with corresponding phase voltage, which means that the unity power factor operation is successfully achieved. The DC voltage is maintained close to its reference value without overshot.

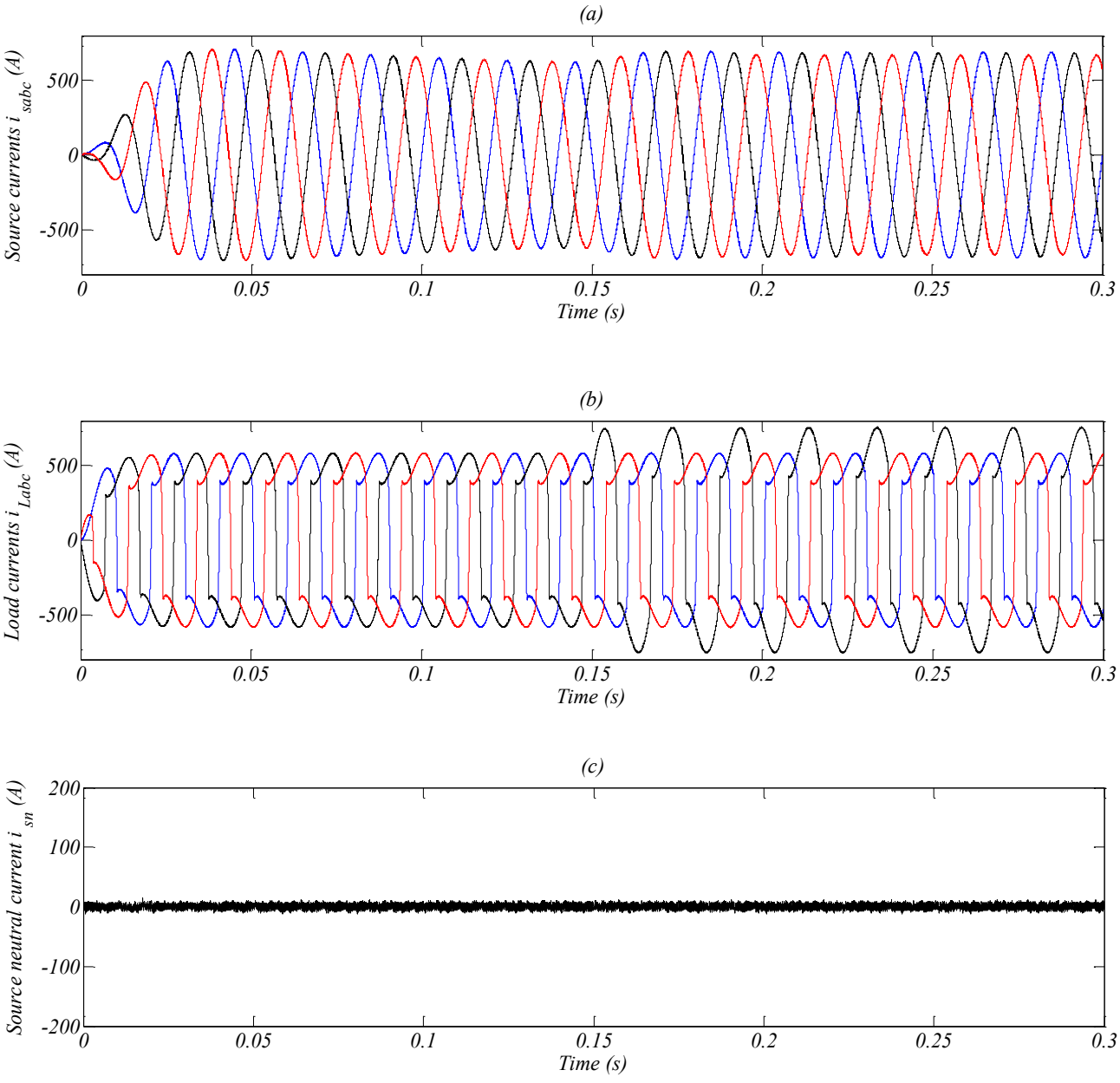

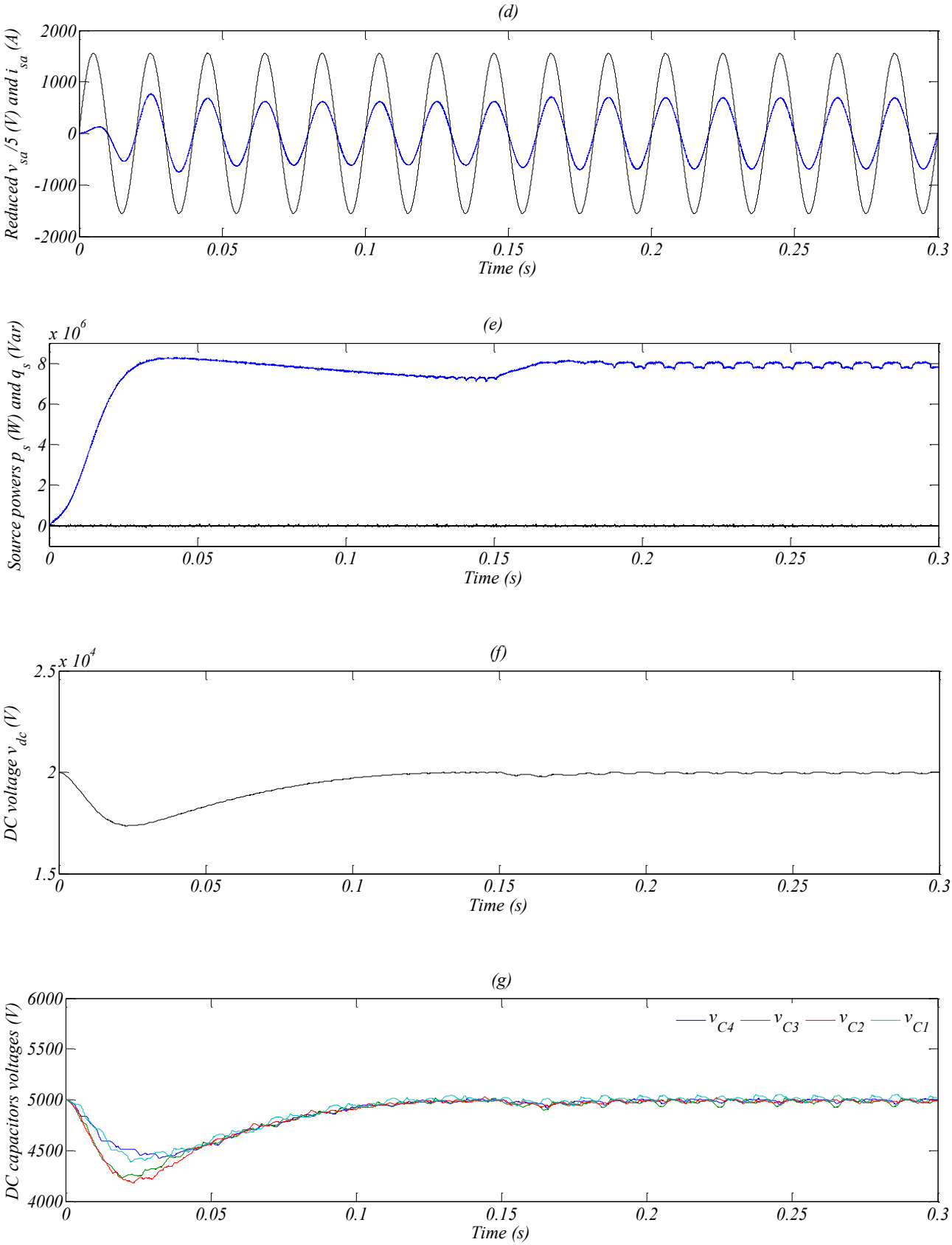

Figure (IV.7): Simulation results of the Super-twisting-DPC-3DSVM for the five-level four-leg SAPF under balanced and unbalanced load condition

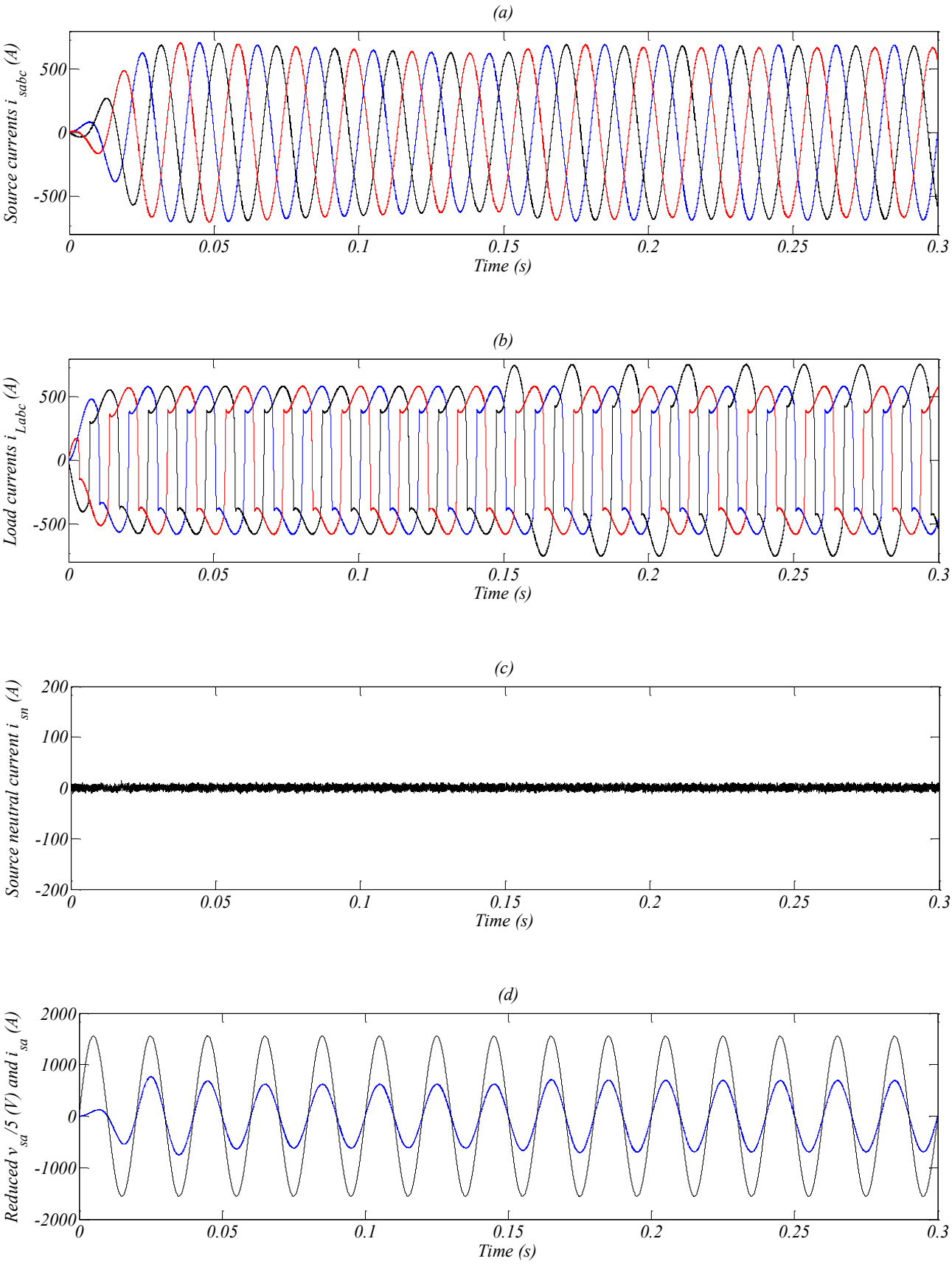
(a)
Source currents i_{sabc} (A)
500
0
-500
0
0.05
0.1
0.15
0.2
0.25
0.3
Time (s)
(b)
Load currents i_{Labc} (A)
500
0
-500
0
0.05
0.1
0.15
0.2
0.25
0.3
Time (s)
(c)
Source neutral current i_{sn} (A)
200
100
0
-100
-200
0
0.05
0.1
0.15
0.2
0.25
0.3
Time (s)
(d)
Reduced v_{sa} /5 (V) and i_{sa} (A)
2000
1000
0
-1000
-2000
0
0.05
0.1
0.15
0.2
0.25
0.3
Time (s)

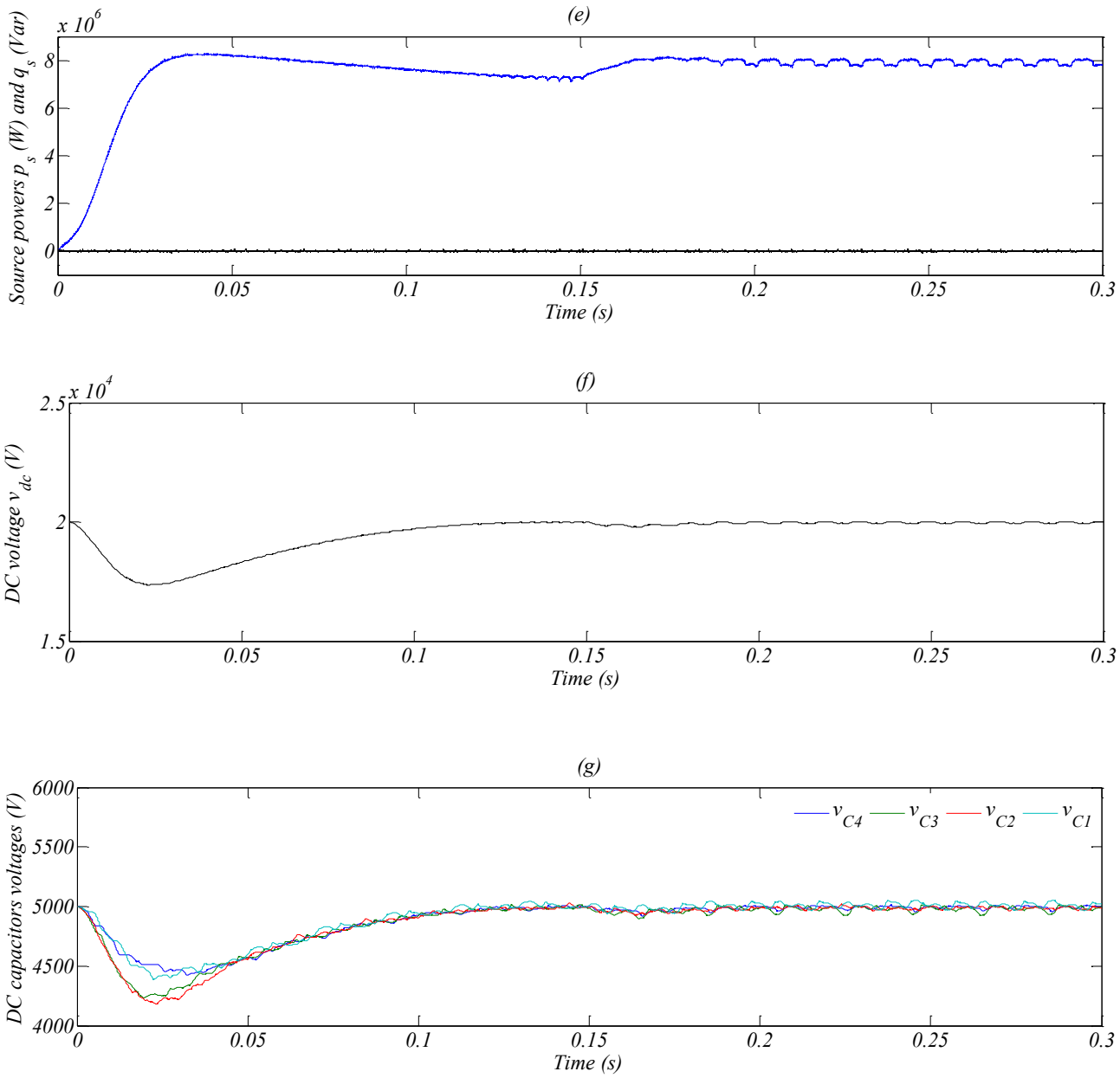

Figure (IV.8): Simulation results of the Super-twisting-PDPC-3DSVM for the five-level four-leg SAPF under balanced and unbalanced load condition

IV.5.3. Distorted source voltage condition

Based on super-twisting controllers, the five-level four-leg SAPF dynamic performances under distorted source voltage condition (5% of fifth harmonic voltage component) are illustrated by the figures (IV.9) and (IV.10) for DPC-3DSVM and PDPC-3DSVM, respectively.

Source currents are balanced and sinusoidal after compensation of harmonic currents. The source neutral current is null. It is also observed that the DC voltage is maintained at its reference value without overshot.
In figure (IV.11), the DPC-3DSVM and PDPC-3DSVM with super-twisting controllers reduce the THD of the compensated source current to 4% and 5% respectively.

(a)

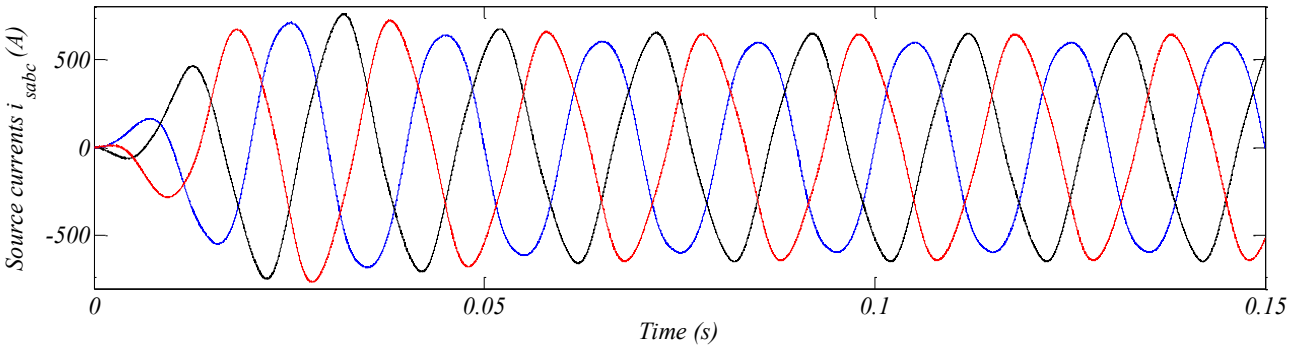
Source currents i_{sabc} (A)
500
0
-500
0
0.05
0.1
0.15
Time (s)

(b)

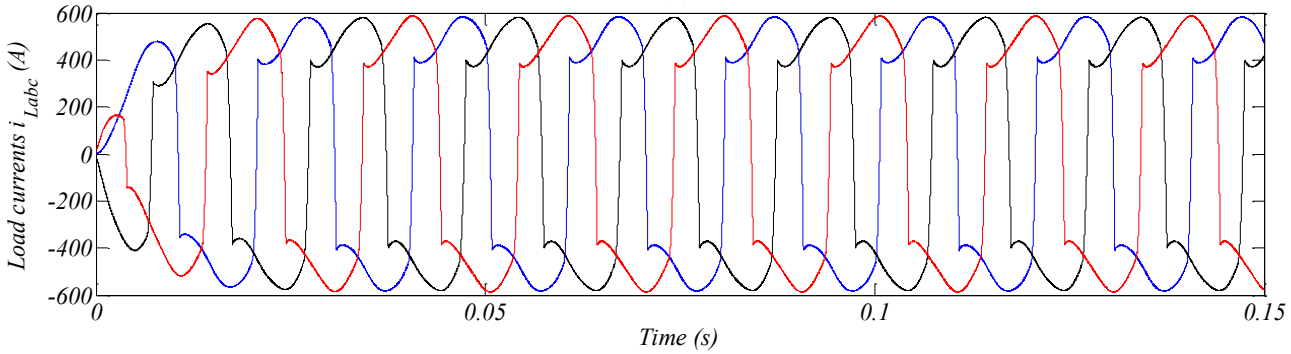
Load currents i_{Labc} (A)
600
400
200
0
-200
-400
-600
0
0.05
0.1
0.15
Time (s)

(c)

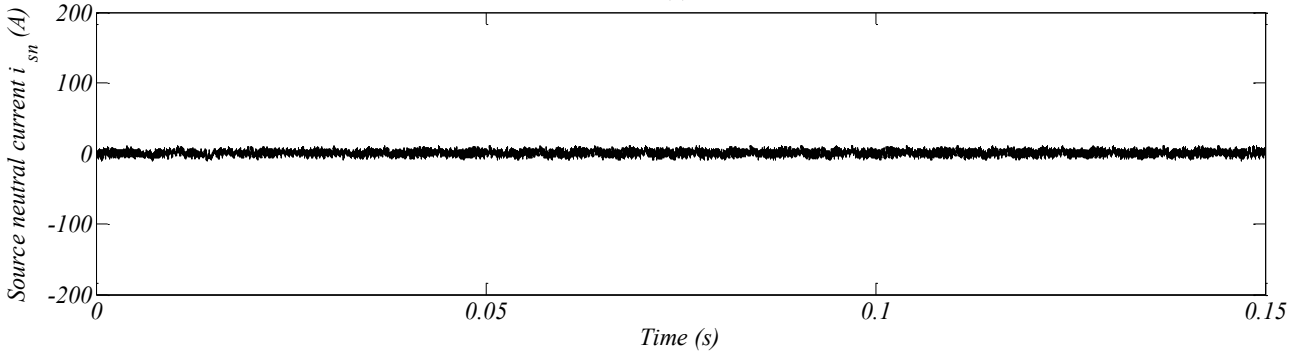
Source neutral current i_{sn} (A)
200
100
0
-100
-200
0
0.05
0.1
0.15
Time (s)

(d)

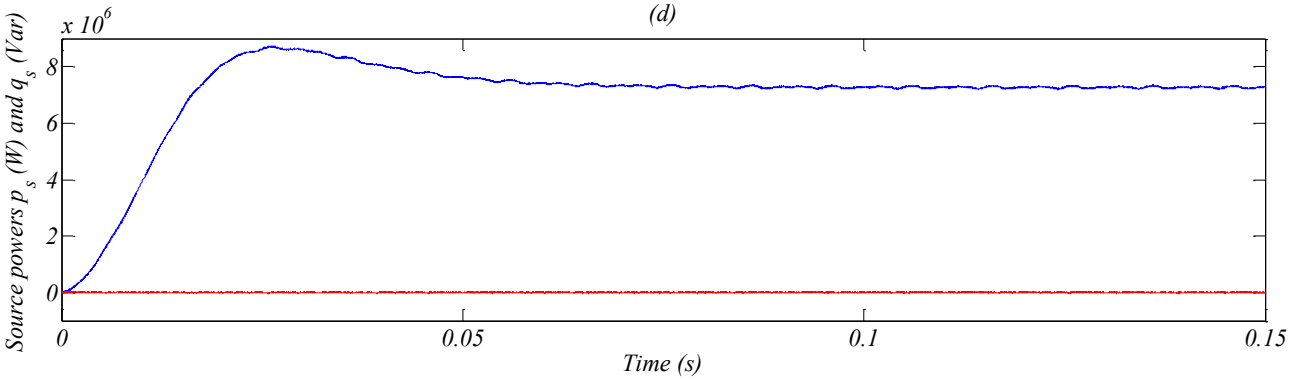
x 10^6
Source powers p_s (W) and q_s (Var)
8
6
4
2
0
0
0.05
0.1
0.15
Time (s)

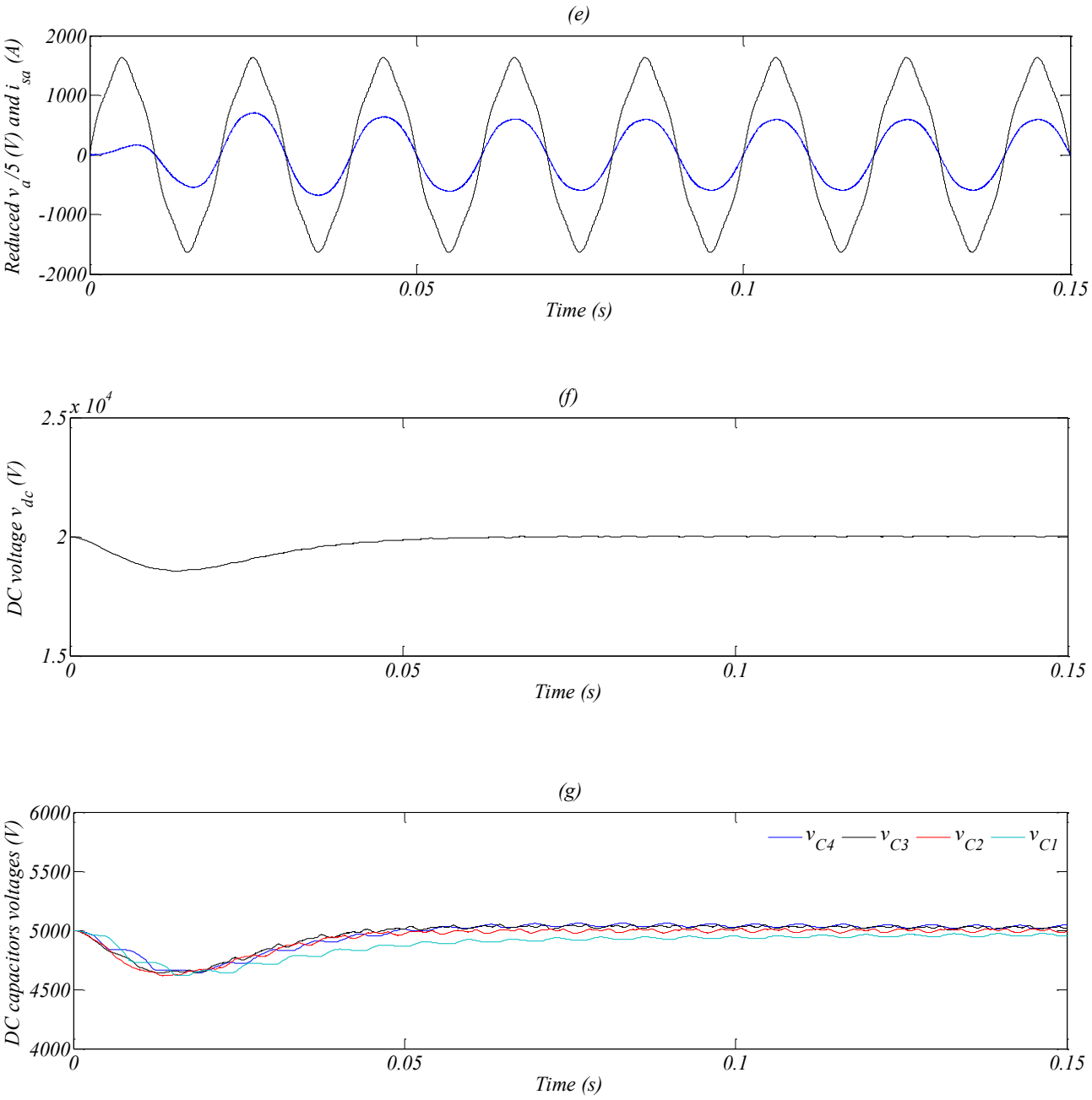

Figure (IV.9): Simulation results of the Super-twisting-DPC-3DSVM for the five-level four-leg SAPF under distorted source voltage

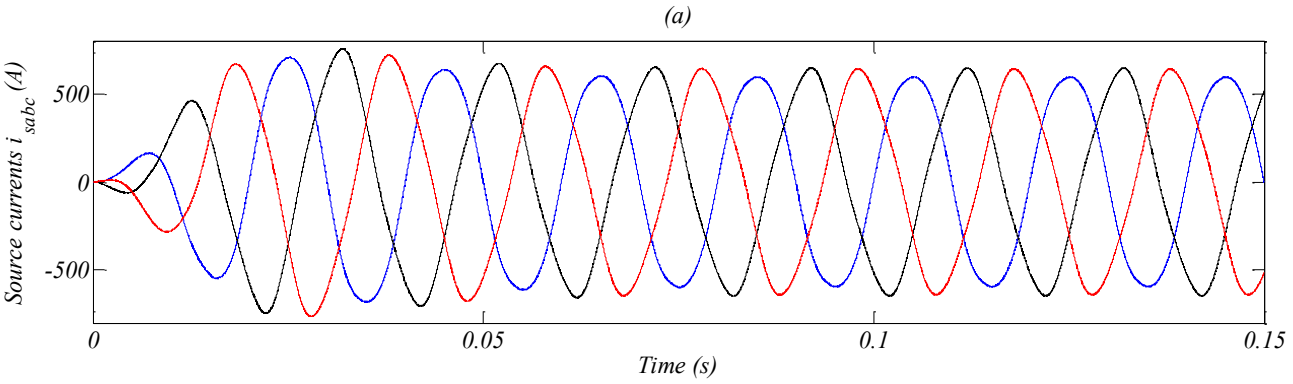

(b)

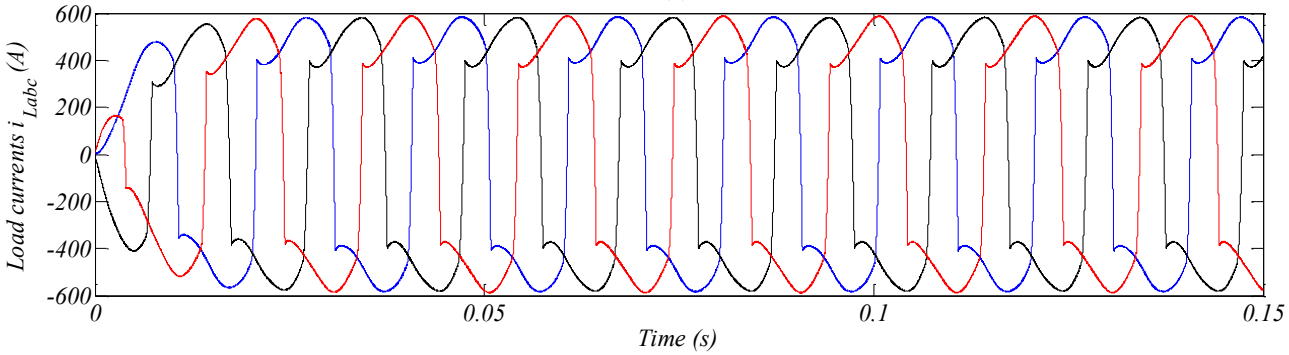
Load currents i_{Labc} (A)
600
400
200
0
-200
-400
-600
0
0.05
0.1
0.15
Time (s)

(c)

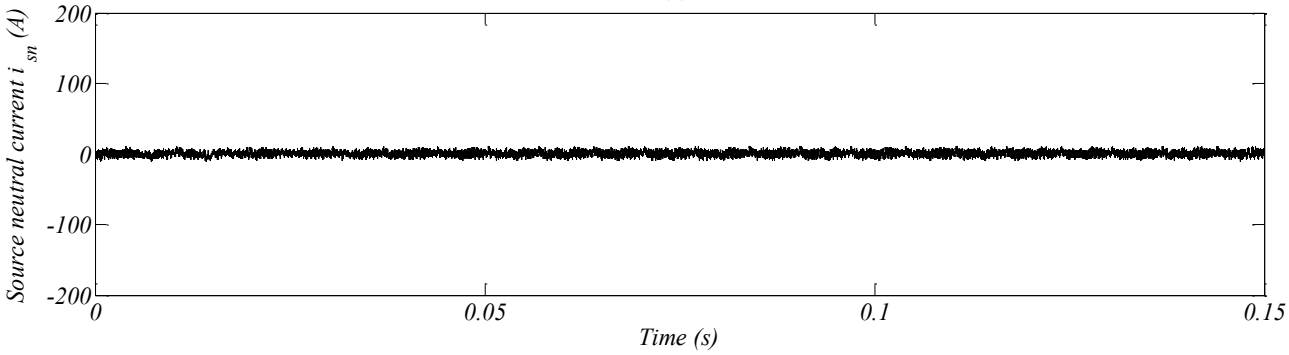
Source neutral current i_{sn} (A)
200
100
0
-100
-200
0
0.05
0.1
0.15
Time (s)

(d)

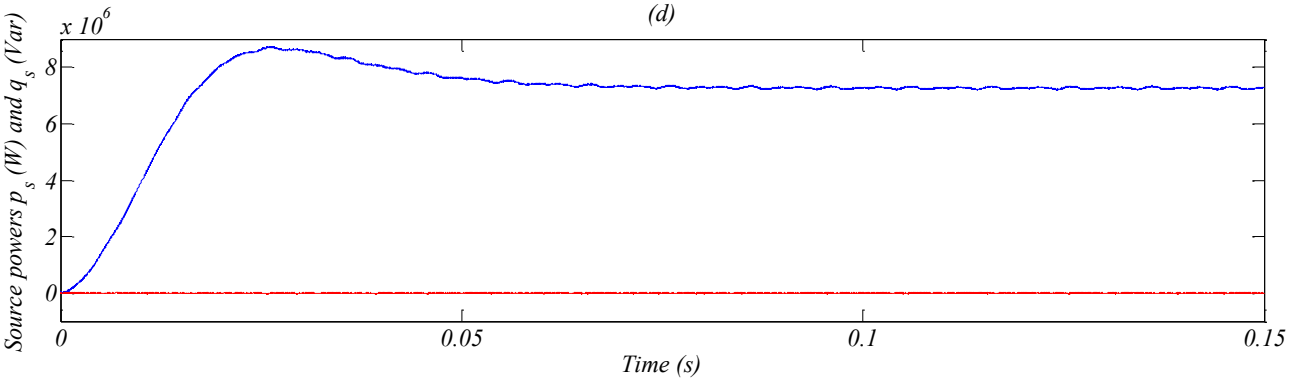
x 10^6
Source powers p_s (W) and q_s (Var)
8
6
4
2
0
0
0.05
0.1
0.15
Time (s)

(e)

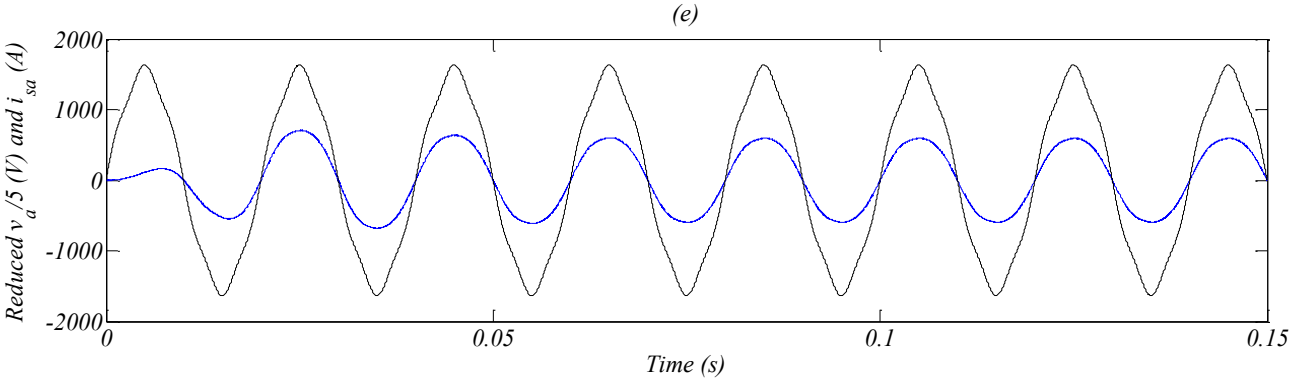
Reduced v_a /5 (V) and i_{sa} (A)
2000
1000
0
-1000
-2000
0
0.05
0.1
0.15
Time (s)

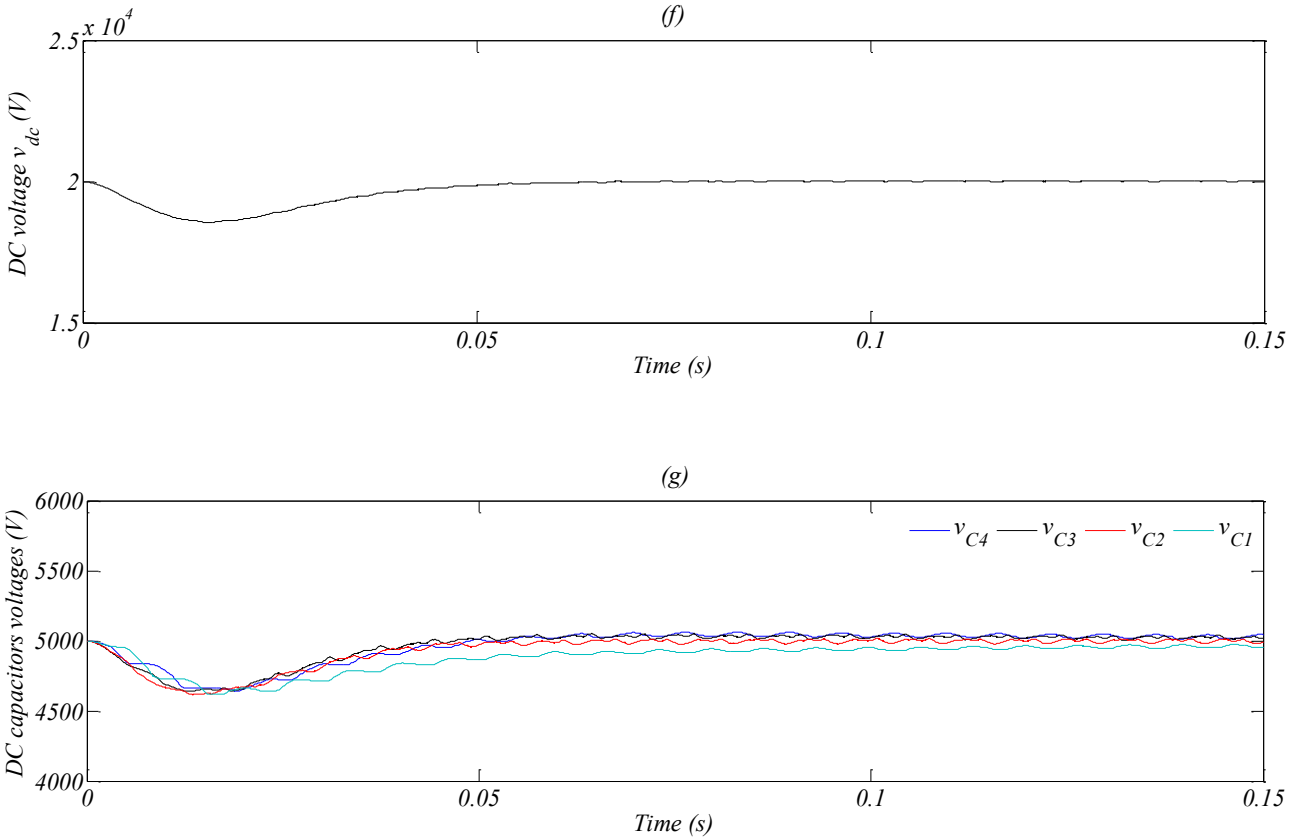

Figure (IV.10): Simulation results of the Super-twisting-PDPC-3DSVM for the five-level four-leg SAPF under distorted source voltage

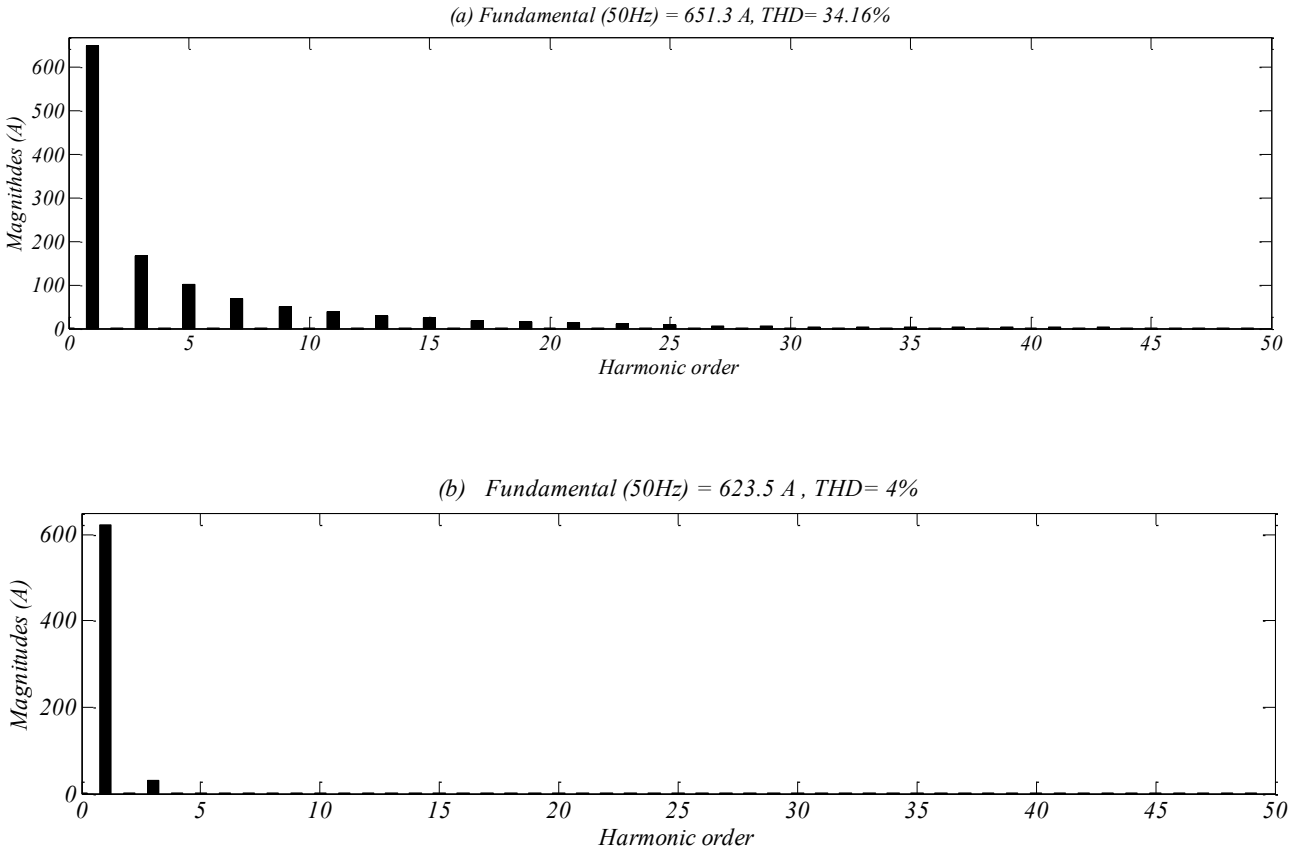

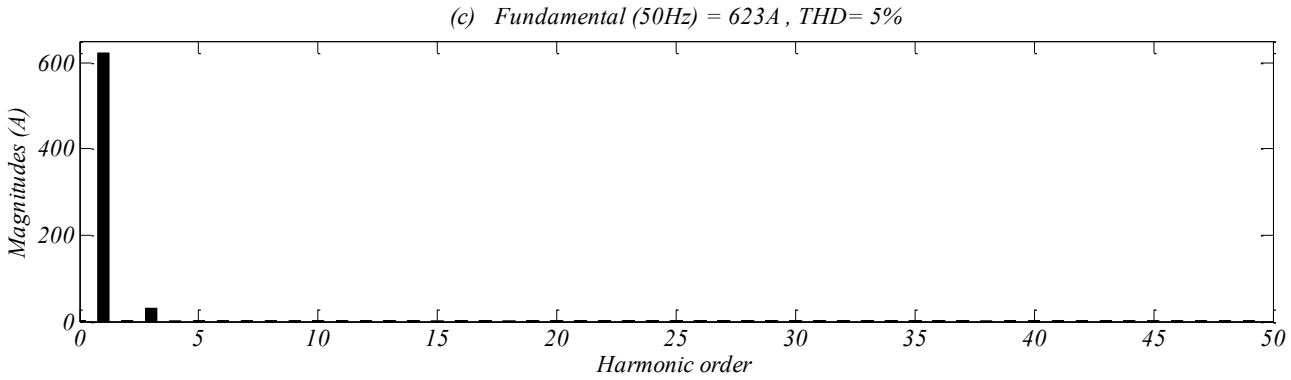

Figure (IV.11): Harmonic spectrum of source current under distorted source voltage: (a) Before compensation, (b) After compensation using super-twisting-DPC-3DSVM, (c) After compensation using super-twisting-PDPC-3DSVM

IV.6. Conclusion

In this chapter, the super-twisting sliding mode control is associated to DPC-3DSVM and PDPC-3DSVM for five level four-leg SAPF in the aim to enhance power quality in four-wire system. Both direct power control strategies with proposed nonlinear control show roughly the similar results.
The simulation results prove that the following objectives have been successfully achieved even under serious conditions like unbalanced load and distorted voltage.

- Current harmonics filtering;
- Reactive power compensation;
- Load current balancing;
- Elimination of excessive neutral current;
- High performance under both dynamic and steady state operation.

The next chapter will be devoted to the fuzzy logic control of the five-level four-leg SAPF.

Chapter V

Direct power control using fuzzy logic of five-level four-leg shunt active power filter

V.1. Introduction

Since the introduction of fuzzy logic, which was first presented by Zadeh [116], many researchers have focused on modeling and control of complex systems. Particularly, fuzzy logic controllers have been broadly used to control imprecise nonlinear systems [118-119].
The advantages of fuzzy logic controllers over conventional controllers (PI) are that they do not require an accurate mathematical model, can work with imprecise inputs, can handle non-linearity, and are more robust than conventional PI controllers [61-62]. Recently, fuzzy logic controllers [61-62] have received a great deal of attention in regards to their application to APFs.

In this chapter, we will provide a summary of those necessary parts of the fuzzy logic literature to understand how a fuzzy logic system works, and develop fuzzy controllers to control DC voltage and active/reactive power of the five-level four-leg SAPF.

V.2. Fuzzy logic theory

V.2.1. Fuzzy sets versus crisp sets

In classical logic an element *x* is either a member or non-member of a crisp set *A*, subset of a set *X*. It is typically defined with zero-one membership functions denoted $\mu_A(x)$ such as [116]:

$$\mu_A(x) = \begin{cases} 1 \text{ if } x \in A \\ 0 \text{ if } x \notin A \end{cases} \tag{V.1}$$

In fuzzy logic theory, an element belongs to a fuzzy subset *A* of the set *X* (The set *X* is called the universe of discourse) with a degree of membership $\mu_A(x) \in [0, 1]$ whose value is proportional to the relevance of the element into the subset *A* [116]. The relations between the values of the universe of discourse and the degrees of membership are characterized with membership functions, which are represented as a set of ordered pairs of each element *x* and its degree of membership $\mu_A(x)$ such as:

$$A = \left[x, \mu_A(x) \right], x \in A, \text{ et } A \subset X \tag{V.2}$$

We recall in this part some essential properties that are associated with fuzzy sets as shown in figure (V.1).

- The *height* of a fuzzy set is defined by:

$$height(A) = \sup(\mu_A(x))_{x \in X} \tag{V.3}$$

- The fuzzy set with a *height* equal to one is called *normal* set.

- The *core* of a fuzzy set is a subset of *X* defined by:

$$core(A) = \left\{ x \in X / \mu_A(x) = 1 \right\} \tag{V.4}$$

- The *support* of a fuzzy set is a subset of *A* defined by:

$$support(A) = \left\{ x \in X / \mu_A(x) > 0 \right\} \tag{V.5}$$

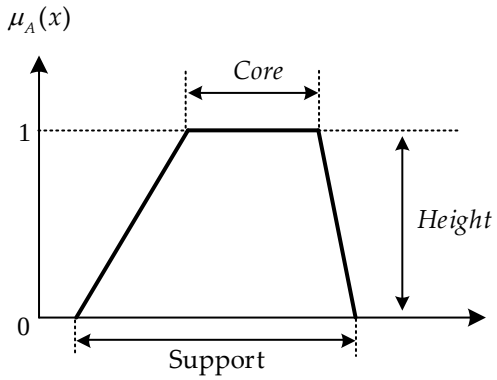

Figure (V.1): Core, support and height of a fuzzy set

- Convex fuzzy subset: a fuzzy subset will be convex if it satisfies:

$$\forall x_1,\ x_2,\ x_3 \in X \text{ if } x_1 \le x_2 \le x_3 \text{ Then } \mu_A(x_2) \ge \min(\mu_A(x_1), \mu_A(x_3)) \tag{V.6}$$

V.2.2. Different shapes of the membership functions

Triangles and trapezoids, which are convex functions, are often used in applications [118]. Graphical representations and operations with these fuzzy sets are very simple. In addition, they can be constructed easily, because of their little information (see figure (V.2)) [118].

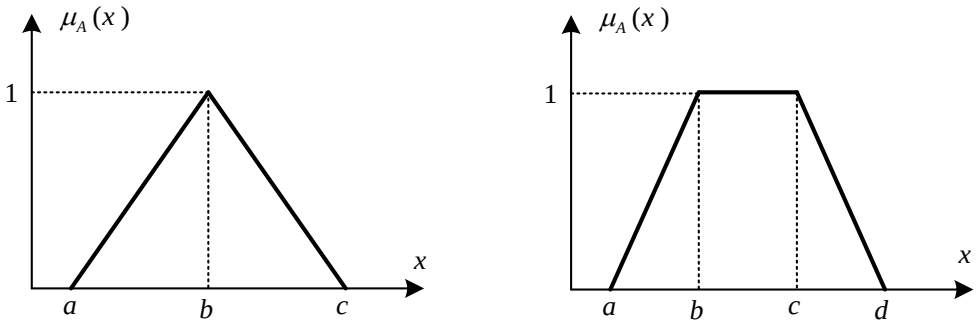

Figure (V.2): Usual forms of membership functions

The degree of membership associated with the triangular shape is defined by one of the following expressions:

$$\mu_A = \begin{cases} \dfrac{x-a}{b-a} & if\ x \in [a,b] \\ \dfrac{c-x}{c-b} & if\ x \in [b,c] \\ 0 & otherwise \end{cases} \tag{V.7}$$

Or:

$$\mu_A(x) = \max\left(\min\left(\frac{x-a}{b-a}, \frac{c-x}{c-b}\right), 0\right) \tag{V.8}$$

For the trapezoidal shape, the membership function is given as:

$$\mu_A = \begin{cases} \frac{x-a}{b-a} & if\ x \in [a,b] \\ 1 & if\ x \in [b,c] \\ \frac{d-x}{d-c} & if\ x \in [c,d] \\ 0 & otherwise \end{cases} \tag{V.9}$$

Or:

$$\mu(x) = \max\left(\min\left(\frac{x-a}{b-a}, 1, \frac{d-x}{d-c}\right), 0\right) \tag{V.10}$$

The universe of discourse of a variable x can be divided into several subsets by means of triangular membership functions (A_i) as shown in figure (V.3).

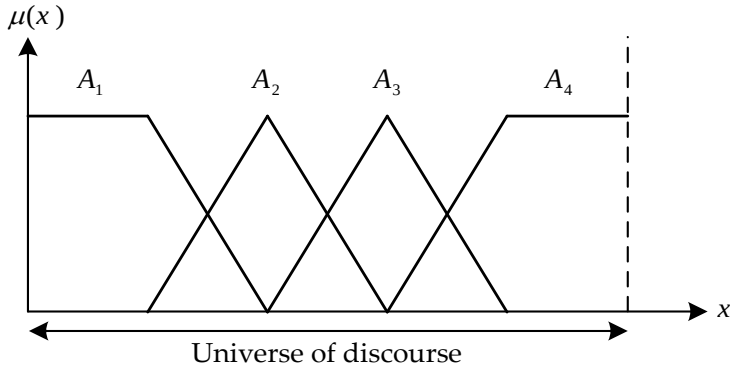

Figure (V.3): Distribution of membership functions

V.2.3. Basic operations with fuzzy sets

Theoretic operations from classical logic such as the intersection (AND), the union (OR) and the complement (NOT) are extended to fuzzy logic to do analogous things with fuzzy sets. Anyway, these extensions are not uniquely defined as in classical logic [116-117].

- The union of two fuzzy sets A and B is written as follows:

$$\forall x \in X, \mu_{A \cup B}(x) = \max(\mu_A(x), \mu_B(x)) \tag{V.11}$$

- The intersection of A and B is defined by:

$$\forall x \in X, \mu_{A \cap B}(x) = \min(\mu_A(x), \mu_B(x)) \tag{V.12}$$

- The complement of a fuzzy set is defined by the membership functions as follow:

$$\forall x \in X, \mu_{\bar{A}}(x) = 1 - \mu_A(x) \tag{V.13}$$

V.3. Fuzzy logic controller

The bock diagram of a fuzzy logic controller is shown in figure (V.4) [119]. It consists of the following main parts:

- Fuzzification
- Fuzzy Inference system
- Knowledge base
- Defuzzification

V.3.1. Fuzzification

The process of converting a numerical variable (real number) to a linguistic variable (fuzzy number) is called fuzzification [120-121].

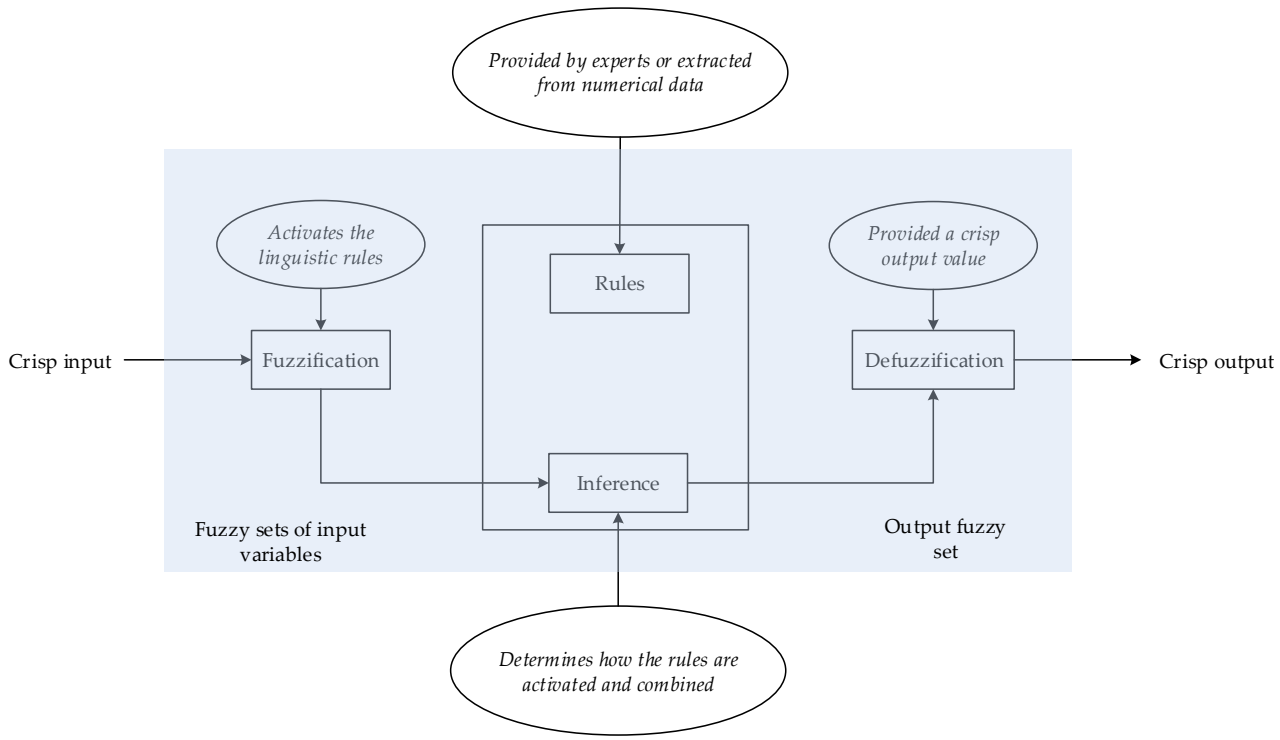

Figure (V.4): Block diagram of fuzzy logic controller

V.3.2. Fuzzy inference system

The basic structure of a fuzzy inference system consists of three components: a rule base, which contains a selection of rules, a database, which defines the membership functions used in the fuzzy rules and a reasoning mechanism, which performs the inference procedure upon the rules and given facts to derive a reasonable output [121-122].

V.3.3. Defuzzification

The rules of fuzzy logic controller generate required output in a linguistic variable [121-122] (Fuzzy number), but according to real world requirements, output linguistic variable has to be transformed to crisp output (Real number).

The most used defuzzification method is the well-known center of gravity. In order to find a crisp value of control output from a fuzzy set B having the universe of discourse Y, the following equation can be used, [121-122]:

$$u = \frac{\int_Y \mu_B(y)\, y\, dy}{\int_Y \mu_B(y)\, dy} \tag{V.14}$$

With a discretized universe of discourse, the expression (V.14) can be rewritten as follows:

$$u = \frac{\sum_{j=1}^{q} \mu_B(y_j)\, y_j}{\sum_{j=1}^{q} \mu_B(y_j)} \tag{V.15}$$

Where: N_q is the number of quantification intervals of the $\mu_B(y)$ function, and y_q correspond center of membership function (b point in figure (V.2)).

V.3.4. Main characteristic of the adopted fuzzy controller

The intern structure of the fuzzy controller proposed by Mamdani of the SISO-system is presented in figure (V.5) [122].

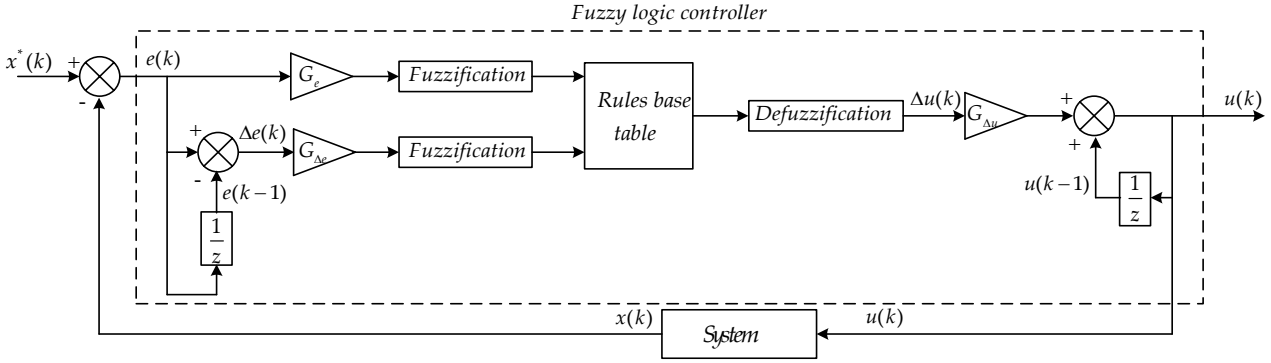

Figure (V.5): Intern structure of the fuzzy logic controller proposed by Mamdani

The controlled variable is compared with its reference value. The obtained error $e(k)=x^*(k)-x\ (k)$ and its variation $\Delta e(k)=e\ (k)-e\ (k-1)$ are normalized through a normalization gains (G_e for error and $G_{\Delta e}$ for change of error).

The output of the fuzzy logic controller is the variation of control law. The final control law is obtained as:

$$u(k)=u(k-1)+G_u\Delta u(k) \tag{V.16}$$

Where: G_u is a denormalization gain.

The adopted fuzzy controller is characterized by:

1- Fuzzification using continuous universe of discourse [-1, 1].
2- Implication using Manidani's "min-max" operator.
3- For each variable, seven fuzzy sets are opted: *NB* (negative big), *NM* (negative medium), *NS* (negative small), *ZE* (zero), *PS* (positive small), *PM* (positive medium), and *PB* (positive big).
4- Each fuzzy set is defined by a triangular membership function as follows (See figure (V.6) :

$$\begin{aligned}
NB &= \max\left(\min\left(1,-(x+b)/(c-b)\right),0\right);\\
NM &= \max\left(\min\left((x+c)/(c-b),-(x+a)/(b-a)\right),0\right);\\
NS &= \max\left(\min\left((x+b)/(b-a),-x/a\right),0\right);\\
ZE &= \max\left(\min\left(1+(x/a),1-(x/a)\right),0\right);\\
PS &= \max\left(\min\left(x/a,(b-x)/(b-a)\right),0\right);\\
PM &= \max\left(\min\left((x-a)/(b-a),(c-x)/(c-b)\right),0\right);\\
PB &= \max\left(\min\left((x-b)/(c-b),1\right),0\right);
\end{aligned}$$

Where: $a=0.25,\ b=0.5$ and $c=0.75$.

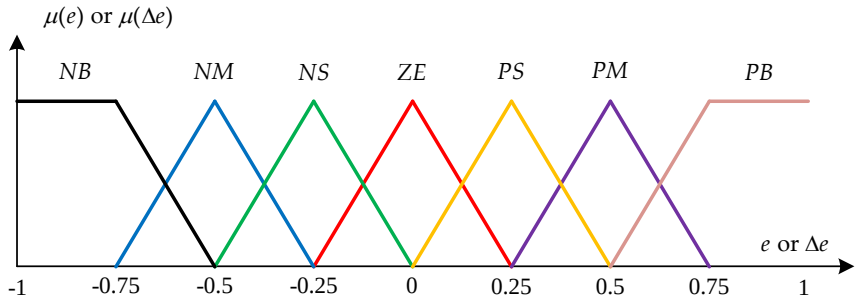

Figure (V.6): Distribution of chosen membership functions

5- The elements of the rule base table are determined based on the theory that in the transient state, large errors need coarse control, which requires coarse input/output variables [62]. In the steady state, small errors need fine control, which requires fine input/output variables [62]. Based on this, the elements of the rule table are obtained as shown in table (V.1) with the error '*e*' and the change of error '*Δe*' are used as inputs [62].

Table (V.1): Fuzzy rules table

		E						
		NB	*NM*	*NS*	*ZE*	*PS*	*PM*	*PB*
Δe	*NB*	*NB*	*NB*	*NB*	*NB*	*NM*	*NS*	*ZE*
	NM	*NB*	*NM*	*NM*	*NM*	*NS*	*ZE*	*PS*
	NS	*NB*	*NM*	*NS*	*NS*	*ZE*	*PS*	*PS*
	ZE	*NM*	*NM*	*NS*	*ZE*	*PS*	*PM*	*PM*
	PS	*NP*	*NS*	*ZE*	*PS*	*PS*	*PM*	*PB*
	PM	*NS*	*ZE*	*PS*	*PM*	*PM*	*PM*	*PB*
	PB	*ZE*	*PS*	*PM*	*PB*	*PB*	*PB*	*PB*

According to the input fuzzy variables, the fuzzy logic controller determines the appropriate control law based on fuzzy rules table like (if *e* is *NM* and *Δe* is *PS* Then the control law *u* is *NS*).

6- Defuzzification is based on the center of gravity method.

V.4. Fuzzy logic control of DPC-3DSVM for five-level four-leg SAPF

Figure (V.6) shows the block diagram of the fuzzy logic controller for PDPC-3DSVM of five-level four-leg SAPF.

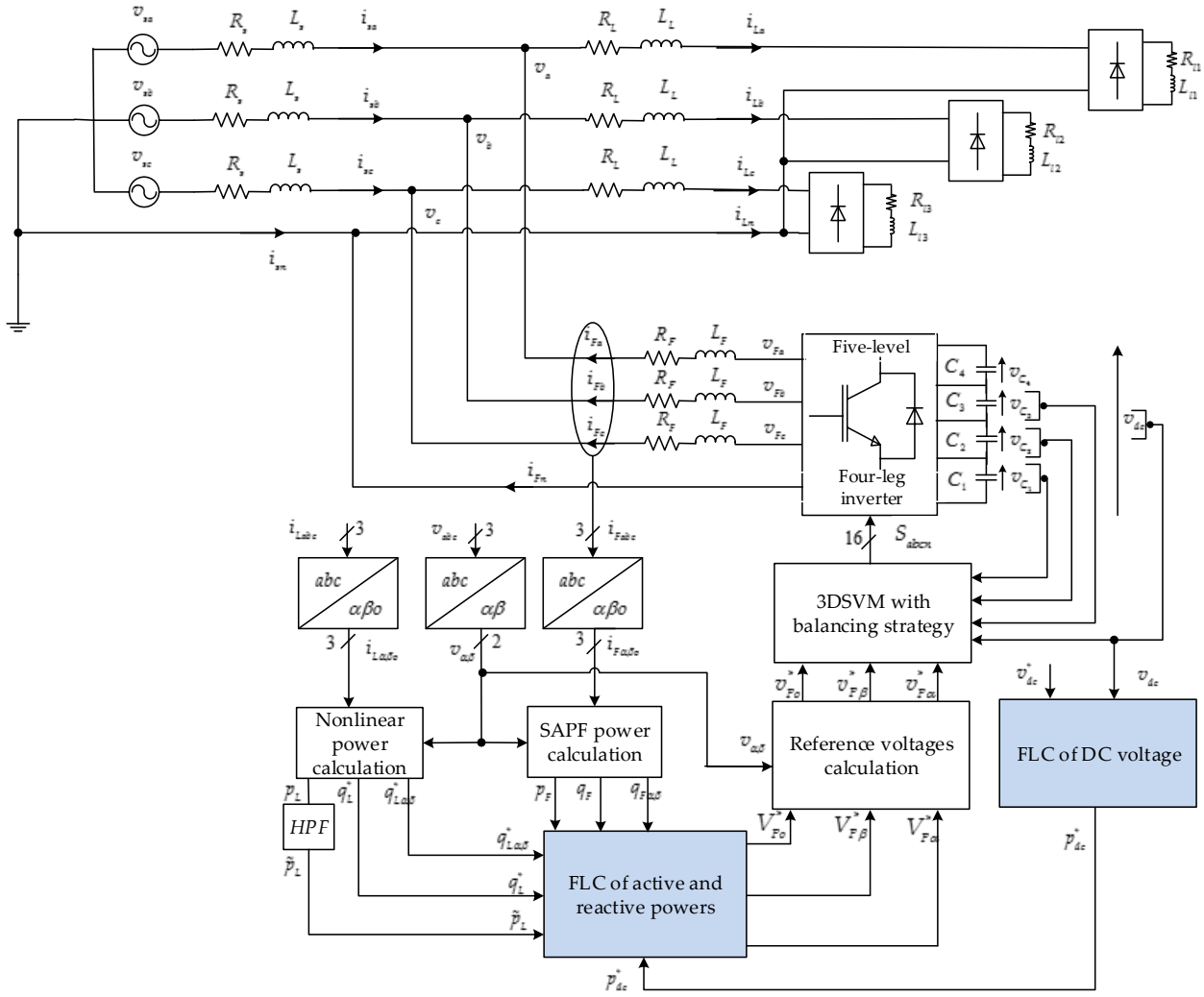

Figure (V.7): Fuzzy logic control of DPC-3DSVM for five-level four-leg SAPF

There are four outputs to be controlled. It is about DC capacitor voltage v_{dc}, active and reactive powers p_F, q_F and $q_{F\alpha\beta}$; these outputs must follow their references v_{dc}^*, p_F^*, q_F^* and $q_{F\alpha\beta}^*$ respectively. To carry out this objective, it is necessary to use four fuzzy logic controllers one for each output.

The normalized errors are defined as:

$$\begin{aligned} e_{v_{dc}}(k) &= G_{e_{v_{dc}}}\left(v_{dc}^{*2}(k) - v_{dc}^{2}(k)\right) \\ e_{p_F}(k) &= G_{e_{p_F}}\left(p_F^{*}(k) - p_F(k)\right) \\ e_{q_F}(k) &= G_{e_{q_F}}\left(q_F^{*}(k) - q_F(k)\right) \\ e_{q_{F\alpha\beta}}(k) &= G_{e_{q_{F\alpha\beta}}}\left(q_{F_{\alpha\beta}}^{*}(k) - q_{F_{\alpha\beta}}(k)\right) \end{aligned} \tag{V.17}$$

Where:

$G_{e_{v_{dc}}}, G_{e_{p_F}}, G_{e_{q_F}}$ and $G_{e_{q_{F\alpha\beta}}}$ are the normalization gains of errors.

The changes of these errors are given as:

$$\begin{aligned} \Delta e_{v_{dc}} &= G_{\Delta e_{v_{dc}}}\left(e_{v_{dc}}(k) - e_{v_{dc}}(k-1)\right) \\ \Delta e_{p_F} &= G_{\Delta e_{p_F}}\left(e_{p_F}(k) - e_{p_F}(k-1)\right) \\ \Delta e_{q_F} &= G_{\Delta e_{q_F}}\left(e_{q_F}(k) - e_{q_F}(k-1)\right) \\ \Delta e_{q_{F\alpha\beta}} &= G_{\Delta e_{q_{F\alpha\beta}}}\left(e_{q_{F\alpha\beta}}(k) - e_{q_{F\alpha\beta}}(k-1)\right) \end{aligned} \tag{V.18}$$

Where:

$G_{\Delta e_{v_{dc}}}, G_{\Delta e_{p_F}}, G_{\Delta e_{q_F}}$ and $G_{\Delta e_{q_{F\alpha\beta}}}$ are the normalization gains of the changes of errors.

The fuzzy control law of each output is given by (V.19).

$$\begin{aligned} p_{dc}^{*}(k) &= p_{dc}^{*}(k-1) + G_{u_{v_{dc}}}\Delta p_{dc}^{*}(k) \\ V_{F\alpha}^{*}(k) &= V_{F\alpha}^{*}(k-1) + G_{u_{p_F}}\Delta V_{F\alpha}^{*}(k) \\ V_{F\beta}^{*}(k) &= V_{F\beta}^{*}(k-1) + G_{u_{q_F}}\Delta V_{F\beta}^{*}(k) \\ V_{Fo}^{*}(k) &= V_{Fo}^{*}(k-1) + G_{u_{q_{F\alpha\beta}}}\Delta V_{Fo}^{*}(k) \end{aligned} \tag{V.19}$$

Where :

$G_{u_{v_{dc}}}, G_{u_{p_F}}, G_{u_{q_F}}$ and $G_{u_{q_{F\alpha\beta}}}$ are the denormalization gains.

To convert these errors and their changes into linguistic variables, seven fuzzy sets are used. Table (V.1) provides the details of 49 rules to carry out the adequate control action, and each rule expresses an operating condition in the inference system.

V.5. Fuzzy logic control of PDPC-3DSVM for SAPF

The schematic diagram of the fuzzy logic control of PDPC-3DSVM for five-level four-leg SAPF is presented by the figure (V.8). This control method uses the same fuzzy logic controller of the DC voltage developed in the previous section.

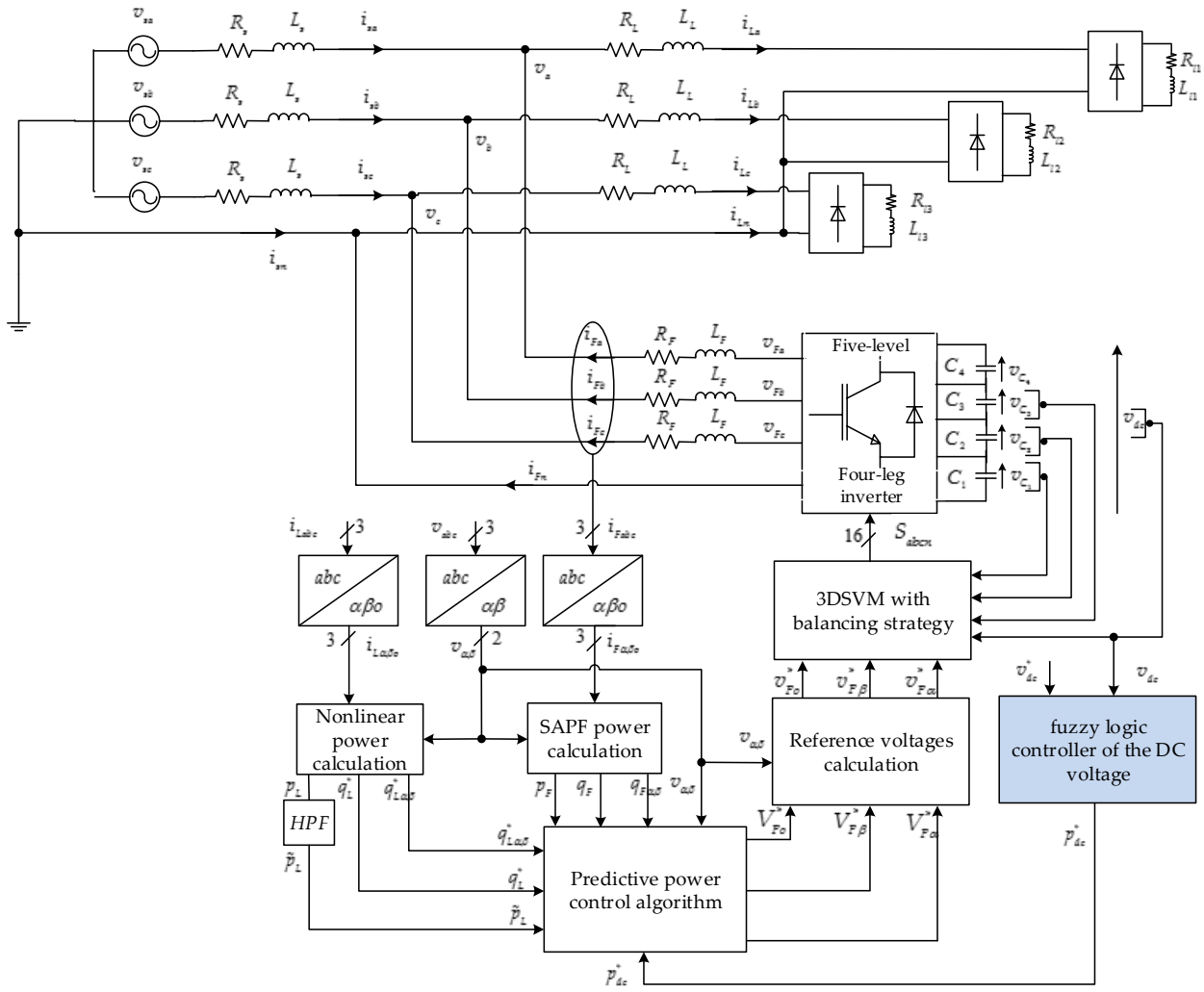

Figure (V.8): Fuzzy logic control of PDPC-3DSVM for five-level four-leg SAPF

V.6. Simulation results

The simulation parameters used in this section are the following:

$$G_{e_{v_{dc}}} = 10^{-6}, G_{\Delta e_{v_{dc}}} = 1, G_{u_{v_{dc}}} 5.10^{-2}.$$

$$G_{e_{p_F}} = G_{e_{q_F}} = G_{e_{q_{F\alpha\beta}}} = 5.10^{-5}, G_{\Delta e_{p_F}} = G_{\Delta e_{q_F}} = G_{\Delta e_{q_{F\alpha\beta}}} = 10^{-4}, G_{u_{p_F}} = G_{u_{q_F}} = G_{u_{q_{F\alpha\beta}}} = 5.10^{6}.$$

V.6.1. Steady state operation

Figures (V.9), (V.10) and (V.11) present the source current of the first phase and its harmonic spectrum before and after compensation of five-level four-leg SAPF using fuzzy logic-DPC-3DSVM and fuzzy logic-PDPC-3DSVM, respectively.
The source current is almost sinusoidal with both control strategies with THD = 0.42% for FLC-DPC-3DSVM and 0.72% for FLC-PDPC-3DSVM.

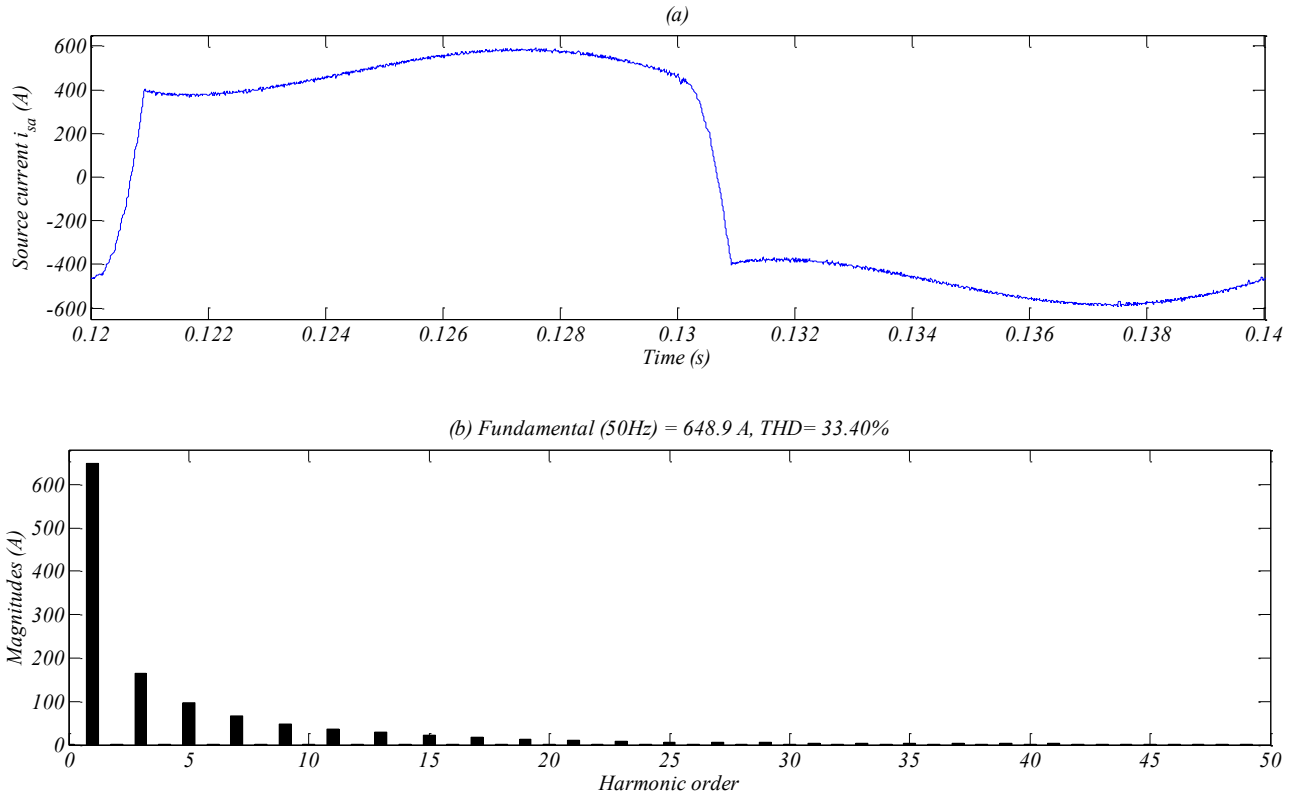

Figure (V.9): (a): Source current before harmonics compensation, (b): Its harmonic spectrum

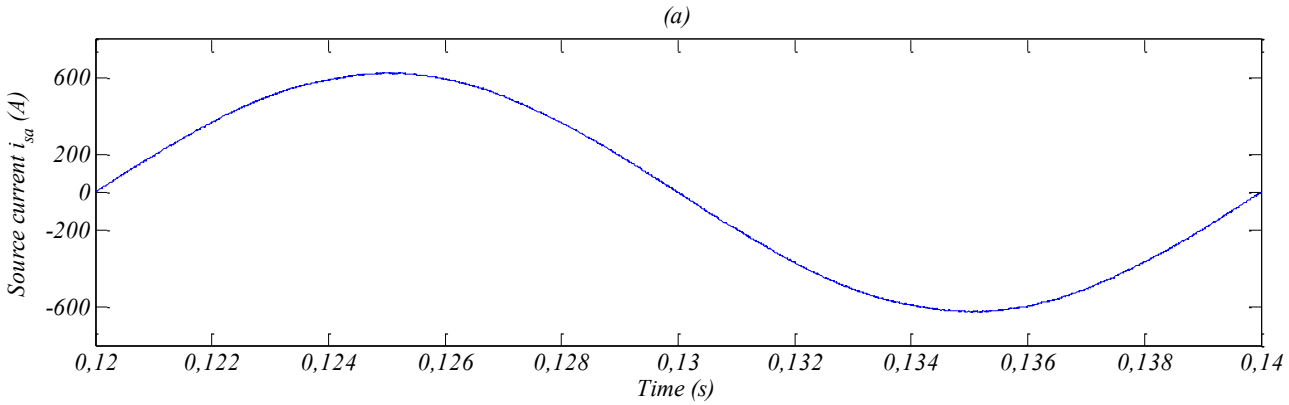

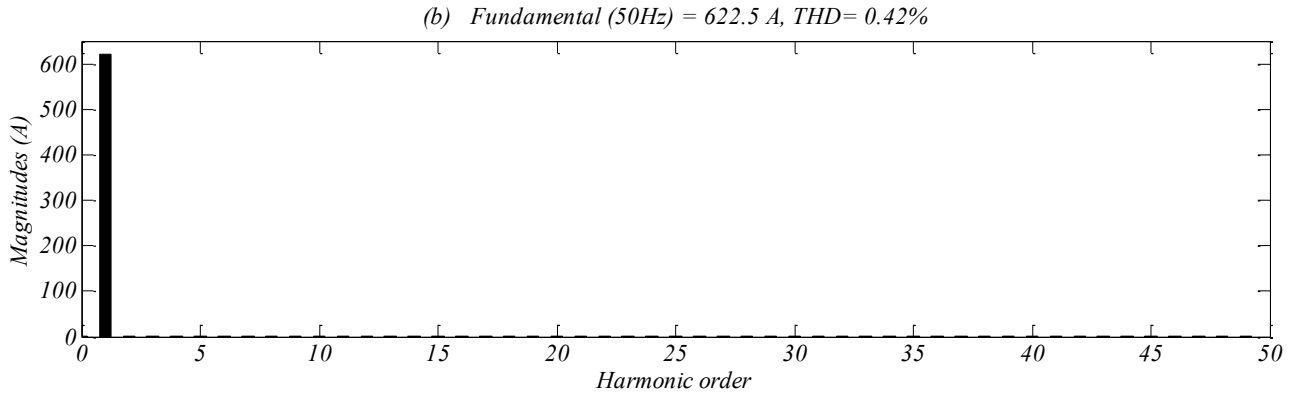

Figure (V.10): (a): Source current after harmonics compensation using fuzzy logic -DPC-3DSVM, (b) Its harmonic spectrum

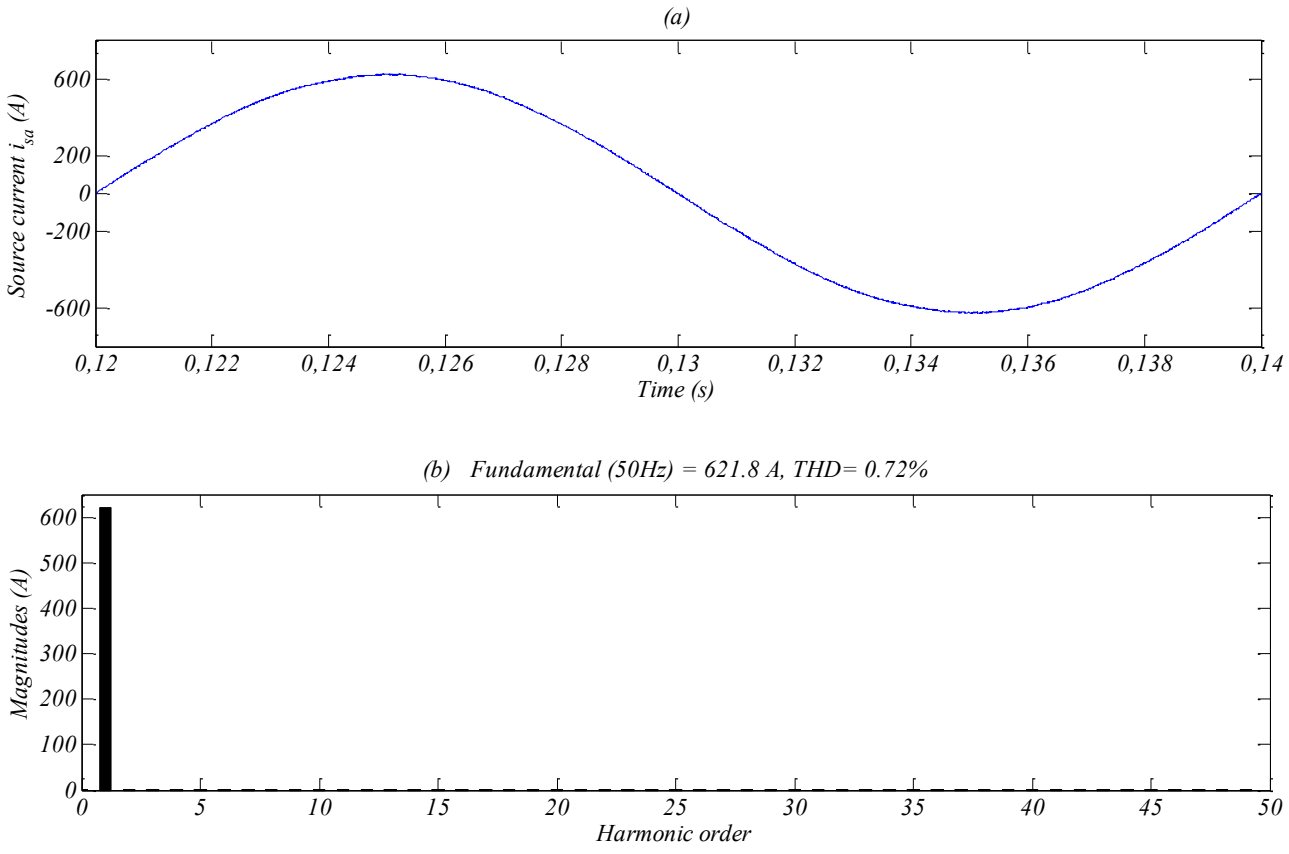

Figure (V.11): (a): Source current after harmonics compensation using fuzzy logic -PDPC-3DSVM, (b) Its harmonic spectrum

V.6.2. Balanced and unbalanced load condition

The dynamic behavior under a step change of the nonlinear load in phase *b* at *t* = 0.15s of DPC-3DSVM and PDPC-3DSVM with fuzzy logic controllers are presented in figures (V.12) and (V.13), respectively.

It can be observed that the three-phase source currents are balanced and sinusoidal after compensation with both control methods. As shown in figures (V.12.c) and (V.13.c), the

neutral current is almost canceled with a low ripple in FLC-PDPC-3DSVM and FLC-PDPC-3DSVM.
In figures (V.12.e) and (V.13.e), one can see that the source active power joins its nominal value while the source reactive power is remaining to its null value. For clarity, the phase-a of source current and its corresponding phase voltage are shown for illustration in figures (V.12.d) and (V.13.d). It can be observed that the unity power factor operation is successfully achieved.

The DC bus voltage variation due to the load change is about 1.5 kV, and the recovery time of DC voltage is about 0.05s. We can see also that the DC capacitors voltages are balanced at their reference values with small ripple around the balance point (1.6%); which confirms the effectiveness of the 3DSVM equipped with balancing strategy.

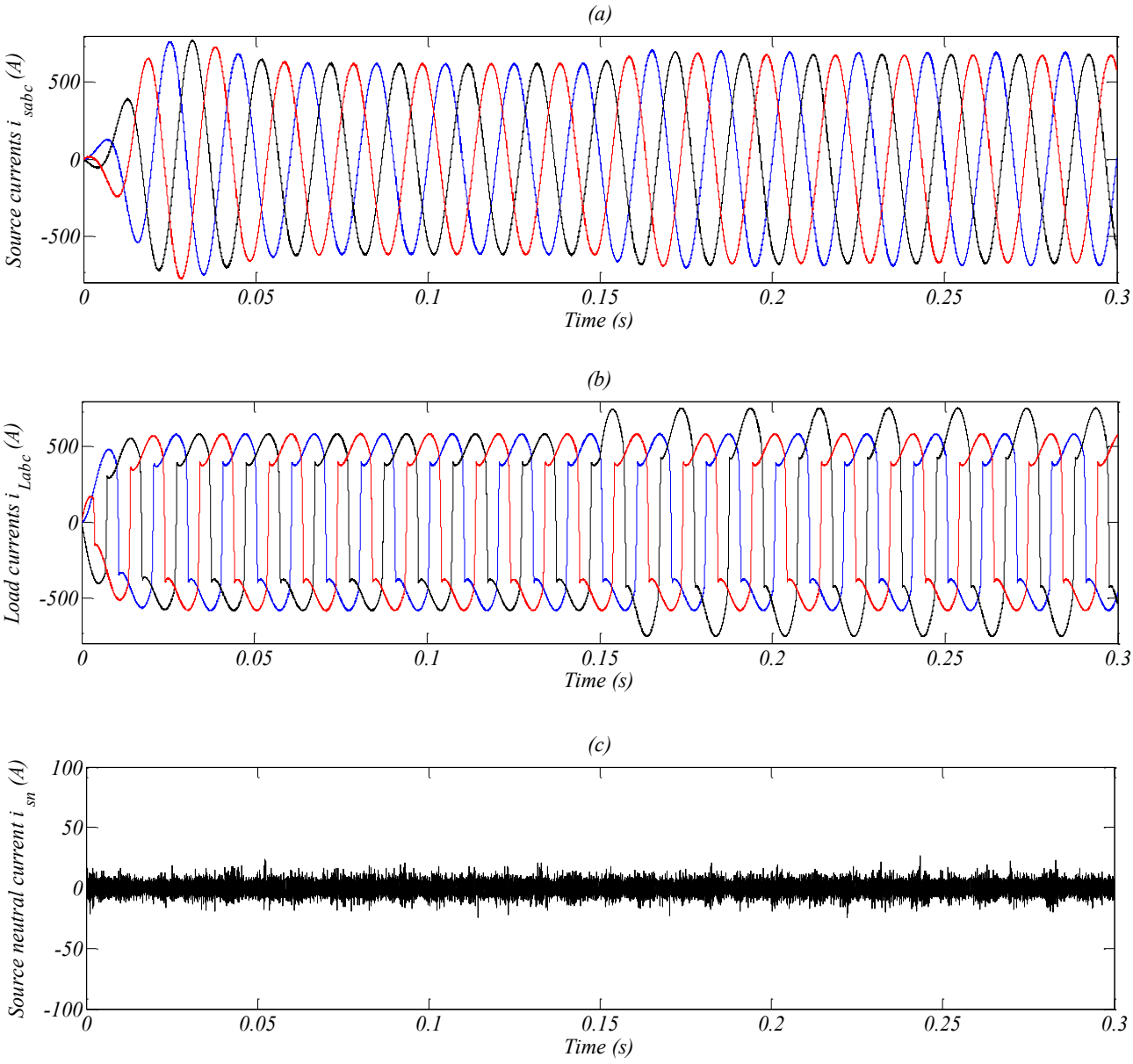

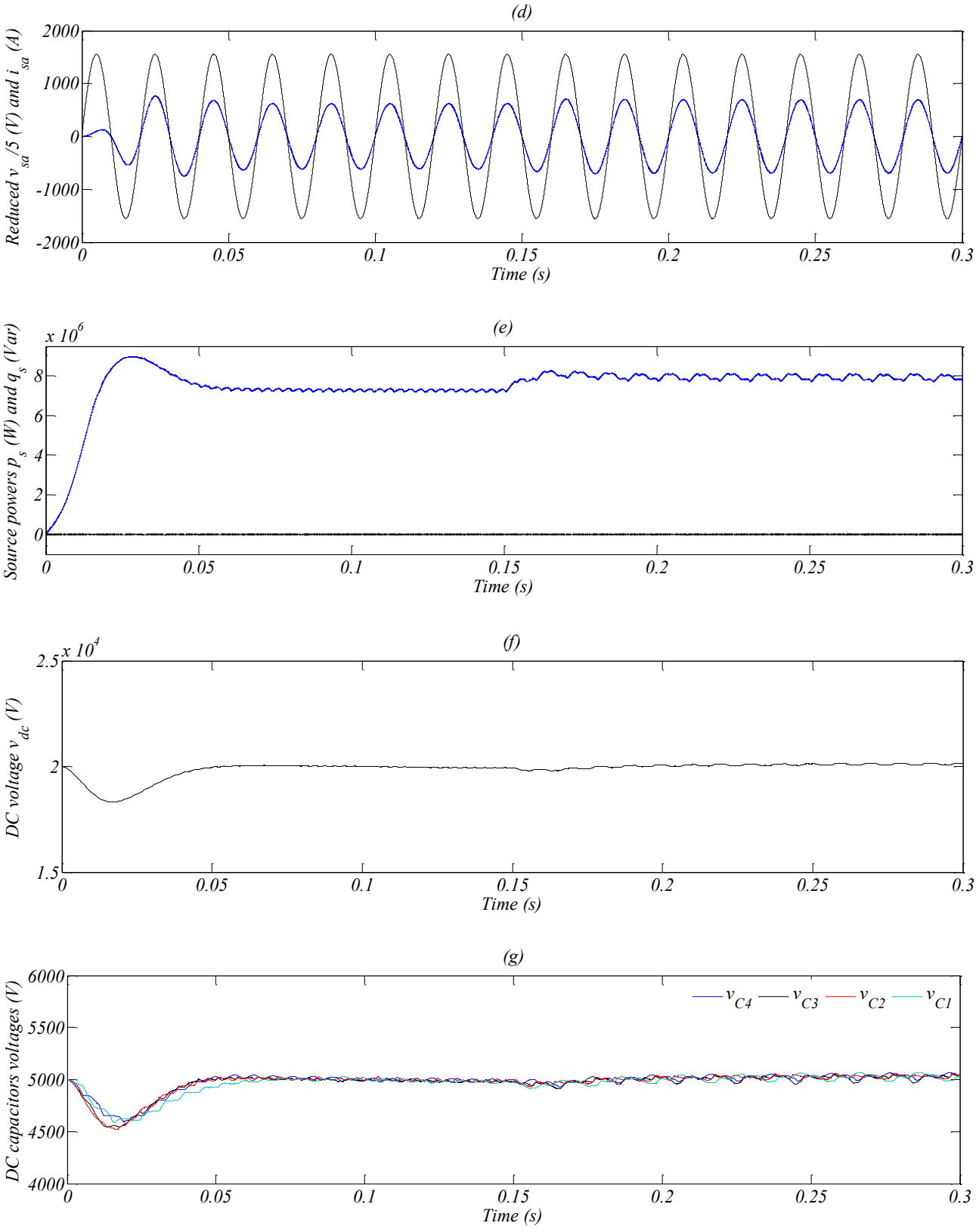

Figure (V.12): Simulation results of the Fuzzy logic-DPC-3DSVM for the five-level four-leg SAPF during balanced and unbalanced load condition

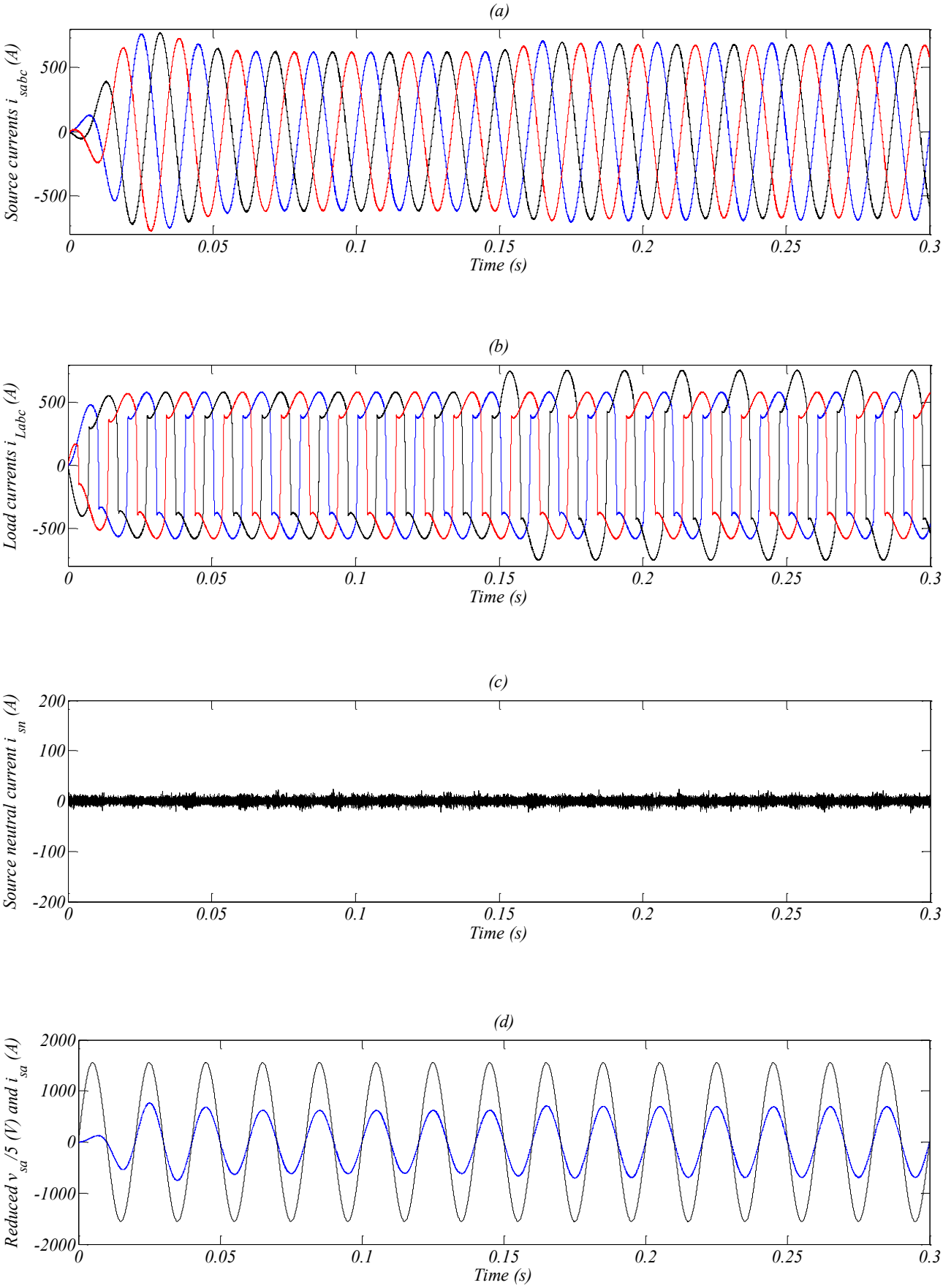
(a)
Source currents i_{sabc} (A)
500
0
-500
0
0.05
0.1
0.15
0.2
0.25
0.3
Time (s)
(b)
Load currents i_{Labc} (A)
500
0
-500
0
0.05
0.1
0.15
0.2
0.25
0.3
Time (s)
(c)
Source neutral current i_{sn} (A)
200
100
0
-100
-200
0
0.05
0.1
0.15
0.2
0.25
0.3
Time (s)
(d)
Reduced v_{sa} /5 (V) and i_{sa} (A)
2000
1000
0
-1000
-2000
0
0.05
0.1
0.15
0.2
0.25
0.3
Time (s)

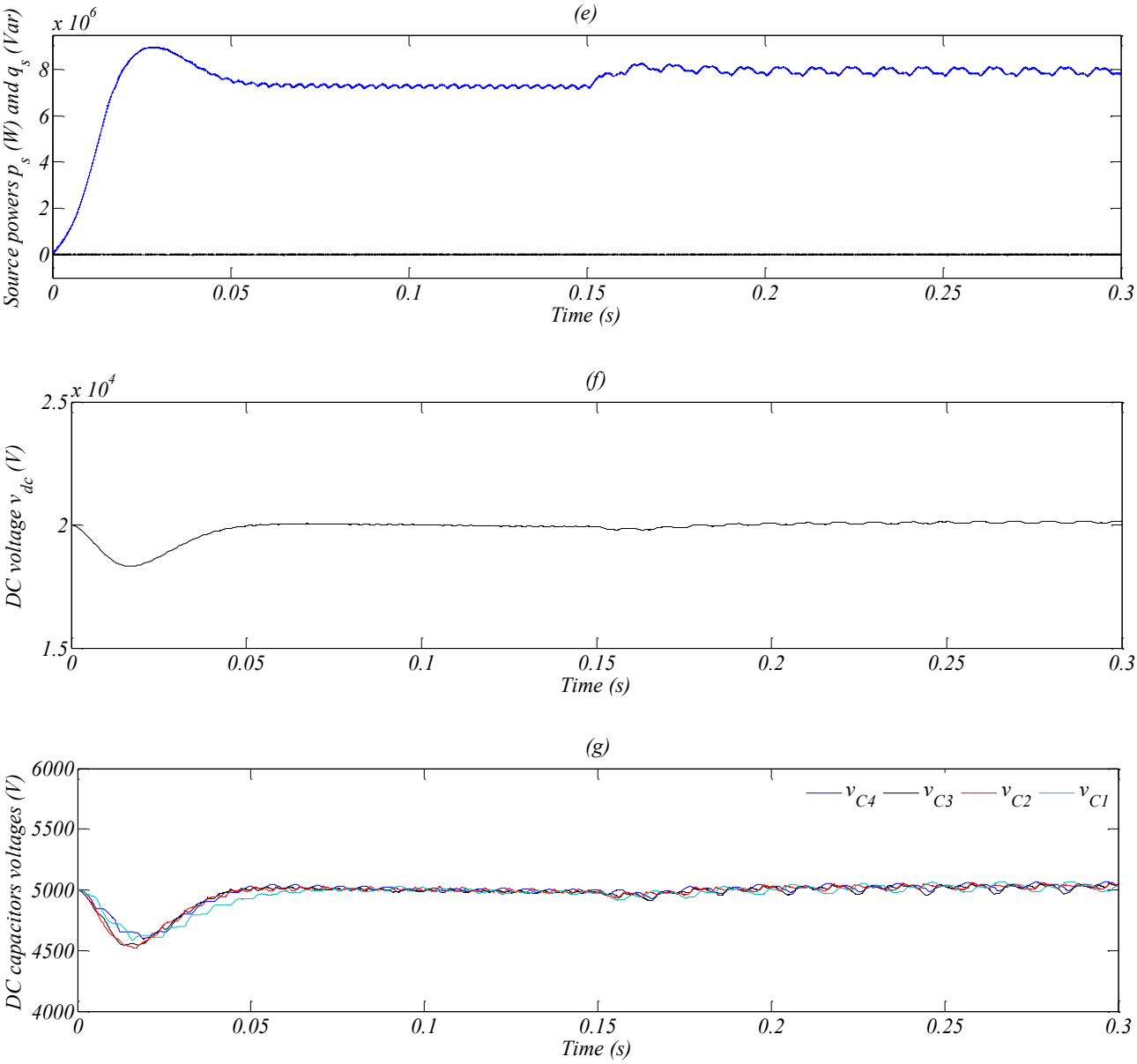

Figure (V.13): Simulation results of the Fuzzy logic-PDPC-3DSVM for the five-level four-leg SAPF during balanced and unbalanced load condition

V.6.3. Distorted source voltage condition

Figures (V.14) and (V.15) show the waveforms in which a fifth harmonic voltage component of 5% is intentionally superimposed on the fundamental source voltage for FLC-DPC-3DSVM and FLC-PDPC-3DSVM, respectively.

It can be observed that the source currents are balanced, the unity power factor operation is successfully achieved, and the neutral current is eliminated under this operating condition. Moreover, the reactive power compensation is successfully achieved with both control strategies. As shown in figure (V.16) the total harmonic distortion of source current is 3% with FLC-DPC-3DSVM and 5% with FLC-PDPC-3DSVM.

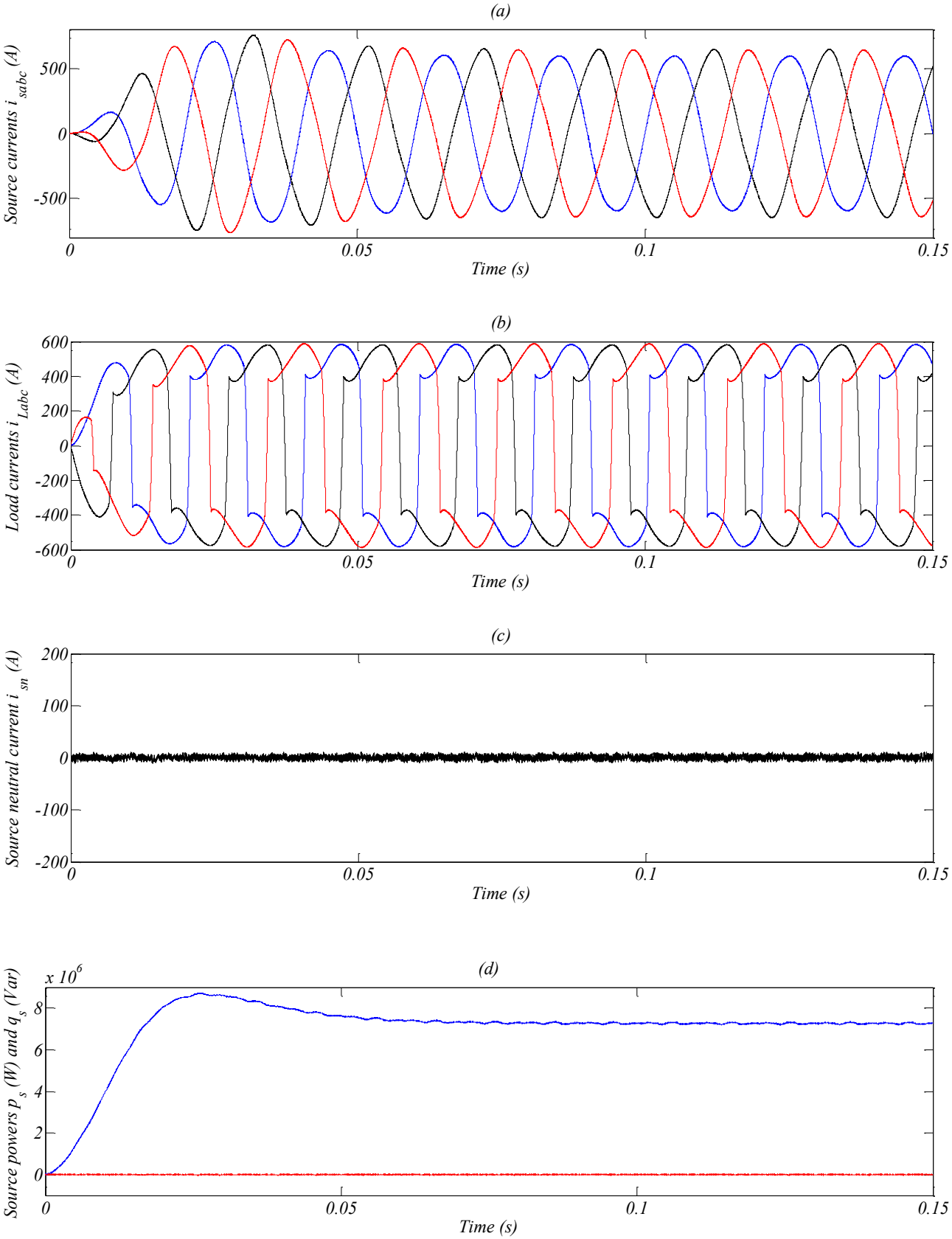
(a)
Source currents i_{sabc} (A)
500
0
-500
0
0.05
0.1
0.15
Time (s)
(b)
Load currents i_{Labc} (A)
600
400
200
0
-200
-400
-600
0
0.05
0.1
0.15
Time (s)
(c)
Source neutral current i_{sn} (A)
200
100
0
-100
-200
0
0.05
0.1
0.15
Time (s)
(d)
x 10^6
Source powers p_s (W) and q_s (Var)
8
6
4
2
0
0
0.05
0.1
0.15
Time (s)

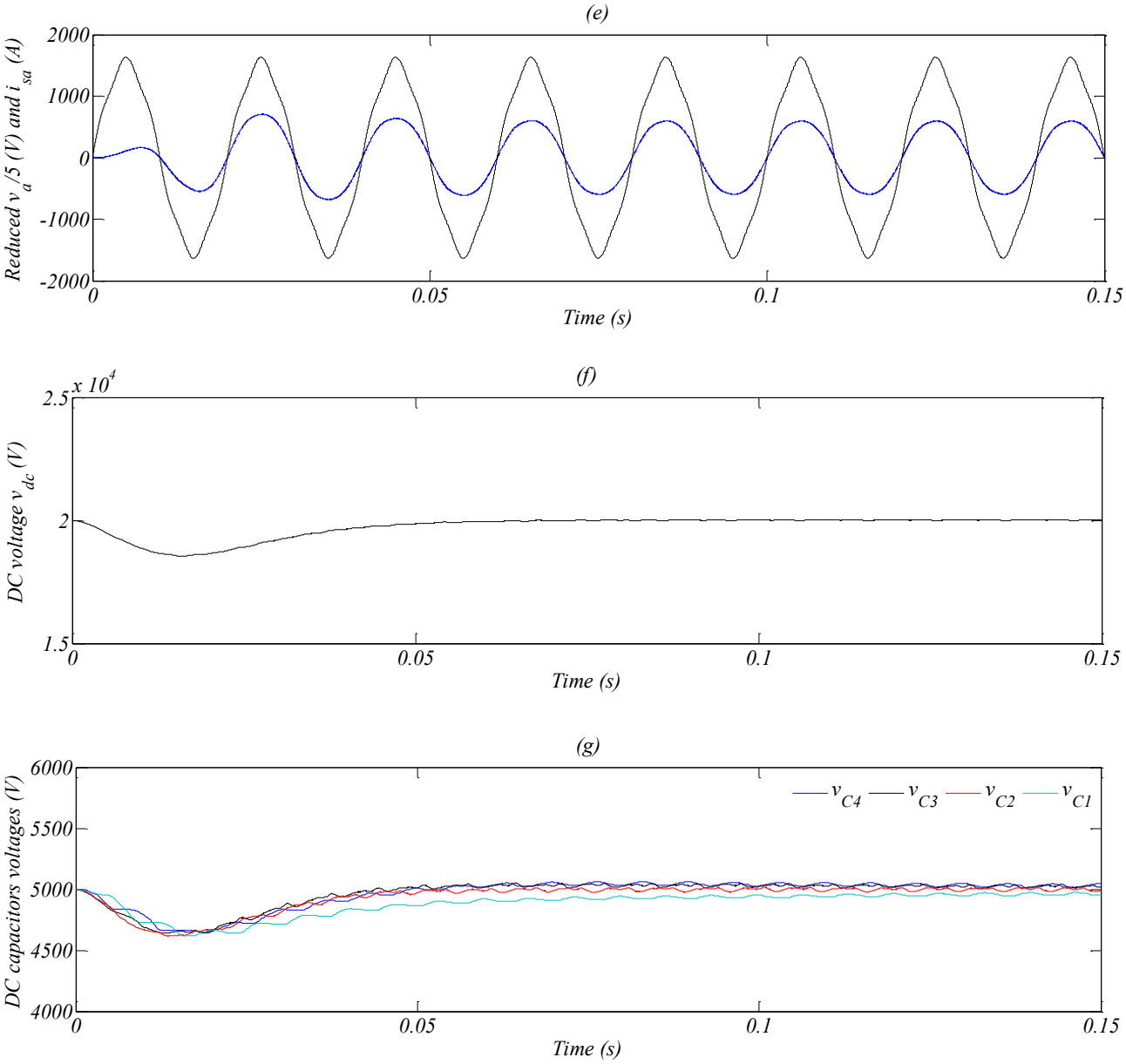

Figure (V.14): Simulation results of the fuzzy logic-DPC-3DSVM for the five-level four-leg SAPF under distorted source voltage

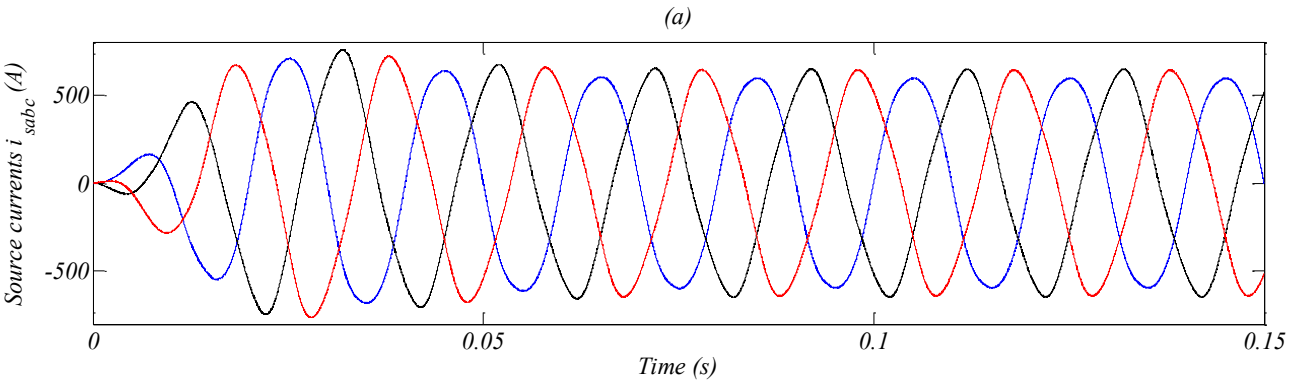

(b)

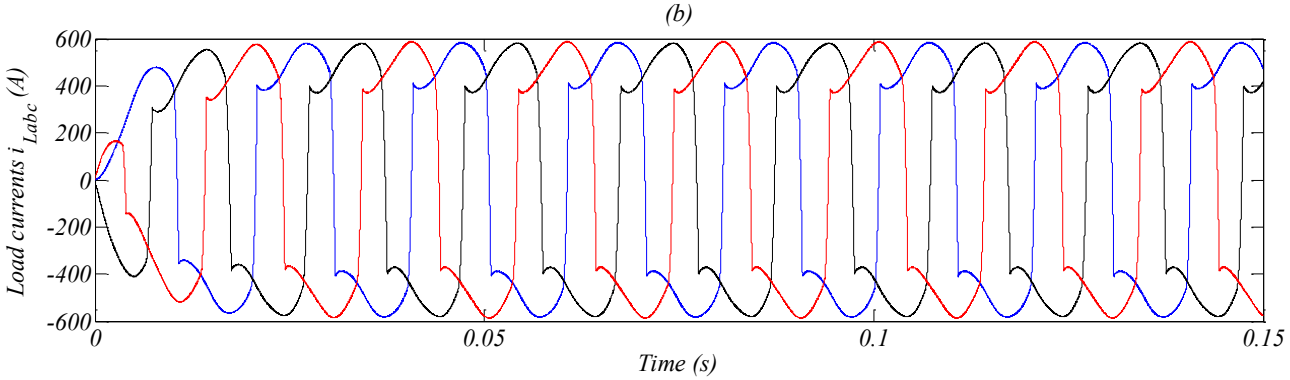
Load currents i_{Labc} (A)
600
400
200
0
-200
-400
-600
0
0.05
0.1
0.15
Time (s)

(c)

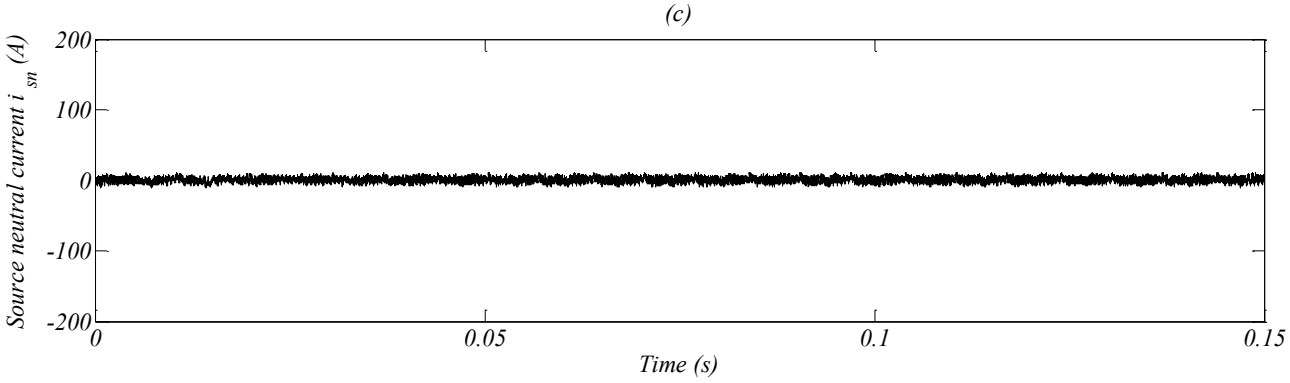
Source neutral current i_{sn} (A)
200
100
0
-100
-200
0
0.05
0.1
0.15
Time (s)

(d)

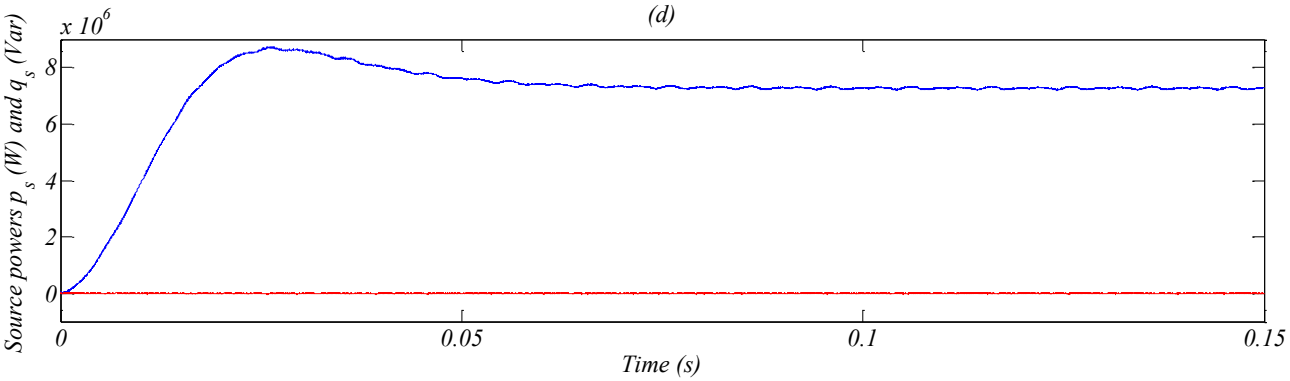
x 10^6
Source powers p_s (W) and q_s (Var)
8
6
4
2
0
0
0.05
0.1
0.15
Time (s)

(e)

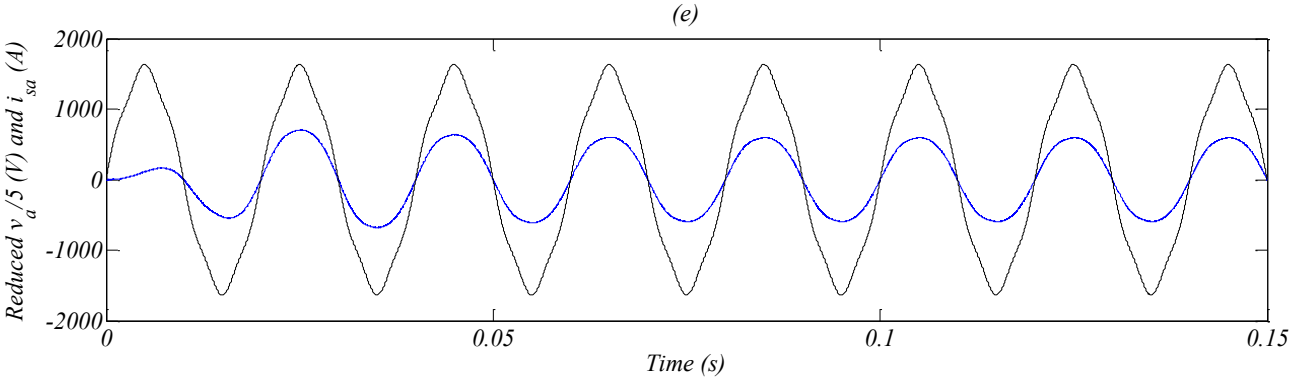
Reduced v_a/5 (V) and i_{sa} (A)
2000
1000
0
-1000
-2000
0
0.05
0.1
0.15
Time (s)

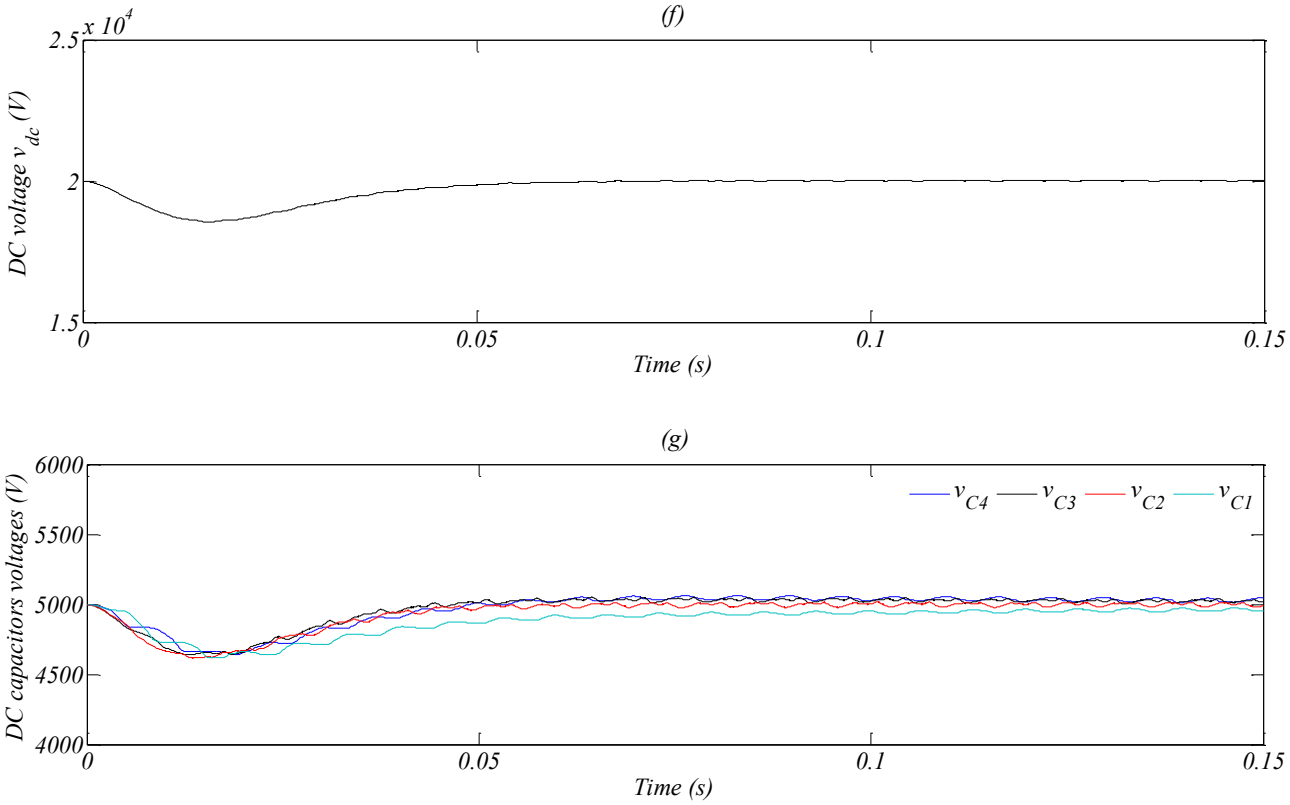

Figure (V.15): Simulation results of the fuzzy logic-PDPC-3DSVM for the five-level four-leg SAPF under distorted source voltage

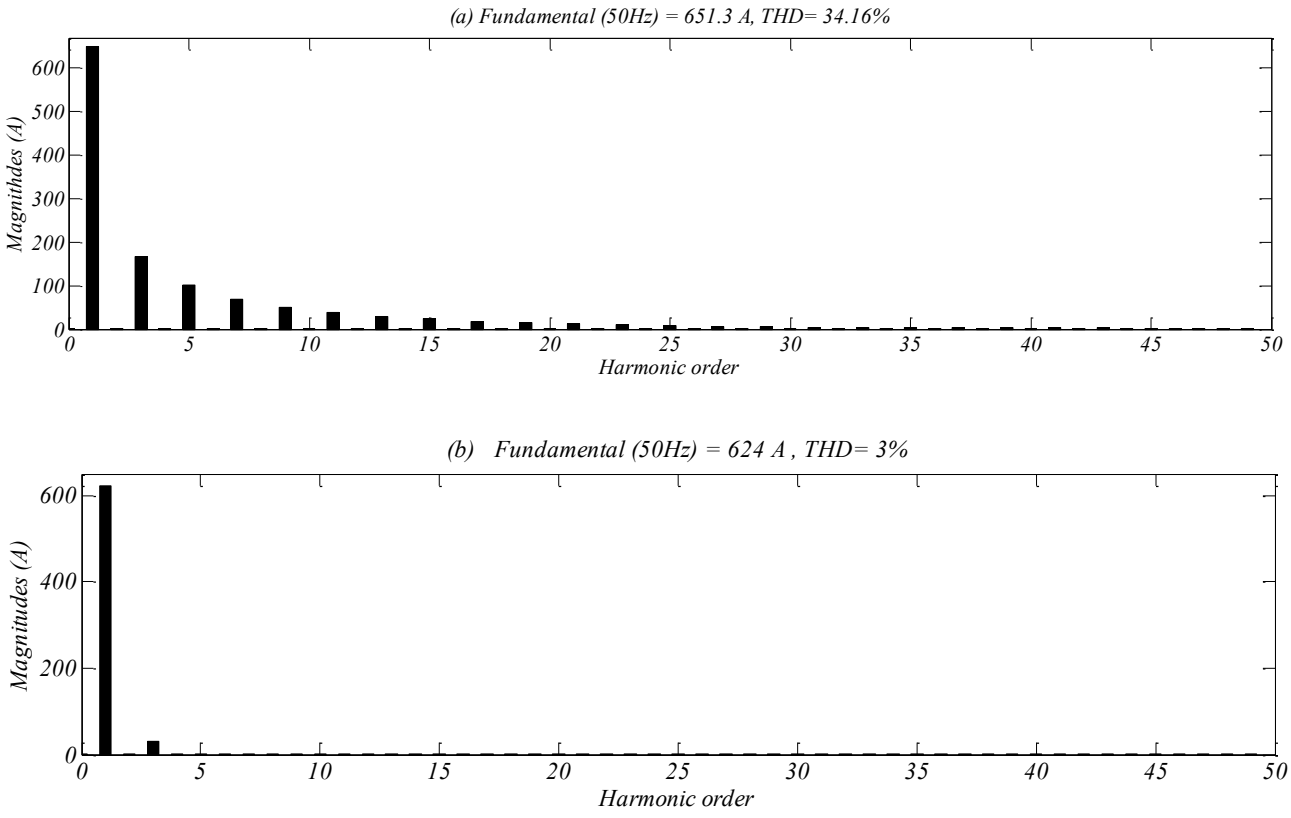

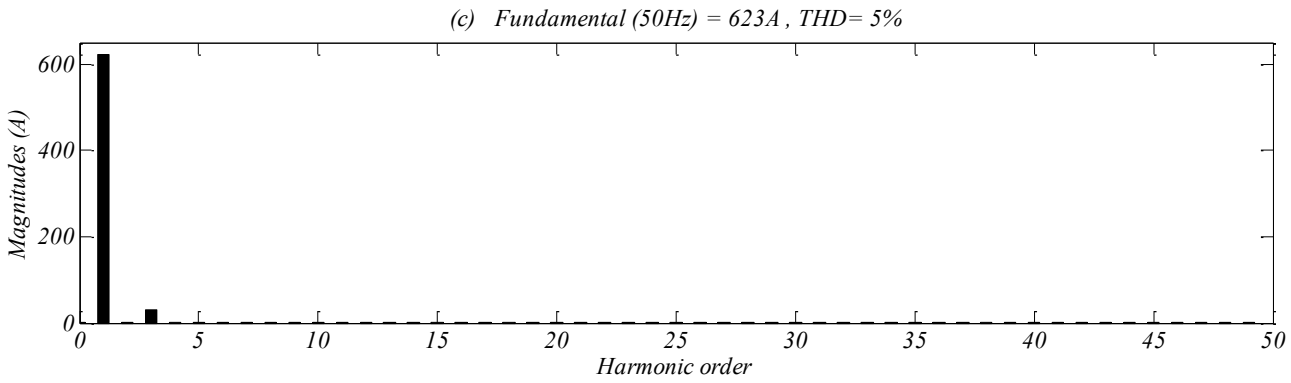

Figure (V.16): Harmonic spectrum of source current under distorted source voltage, (a) Before compensation, (b) After compensation using fuzzy logic-DPC-3DSVM, (c) After compensation using fuzzy logic -PDPC-3DSVM

V.7. Comparative study

In this section, a comparative investigation of both direct power control strategies DPC-3DSVM and PDPC-3DSVM using feedback-linearization, second order-sliding mode and fuzzy logic controllers has been carried out.
The main criteria adopted to conduct this study are source current THD, neutral current ripples, and powers ripples. These criteria are evaluated during many operating conditions such as the balanced/unbalanced nonlinear load, distorted source voltages, source voltages sags, and parameter sensitivity.

V.7.1. Balanced/unbalanced nonlinear load and distorted source voltage

The source current THD for the different control schemes under balanced/unbalanced load and distorted source voltage are illustrated in figure (V.17).
As shown in this figure, under balanced and unbalanced nonlinear load condition, all nonlinear techniques associated with DPC-3DSVM and PDPC-DSVM give acceptable THD values less than 1.3%. However, under distorted source voltage condition, only the DPC-3DSVM with fuzzy logic control can keep the THD less than 5%. The other control techniques are unable to mitigate harmonics completely and fortunately their THD values are nearer to 5%. Consequently, the obtained results have shown a better performance of four-leg SAPF controlled with DPC-3DSVM-fuzzy logic.

Figures (V.18) and (V.19) present the neutral current and power ripples for different control techniques. It found out that all control strategies are good enough to mitigate the neutral current and powers ripples. From these figures, it can be see also that the DPC-3DSVM using fuzzy logic has smaller ripples compared to other control methods, this results confirms once again the superior performance of the fuzzy controller when it applied on the DPC-3DSVM.

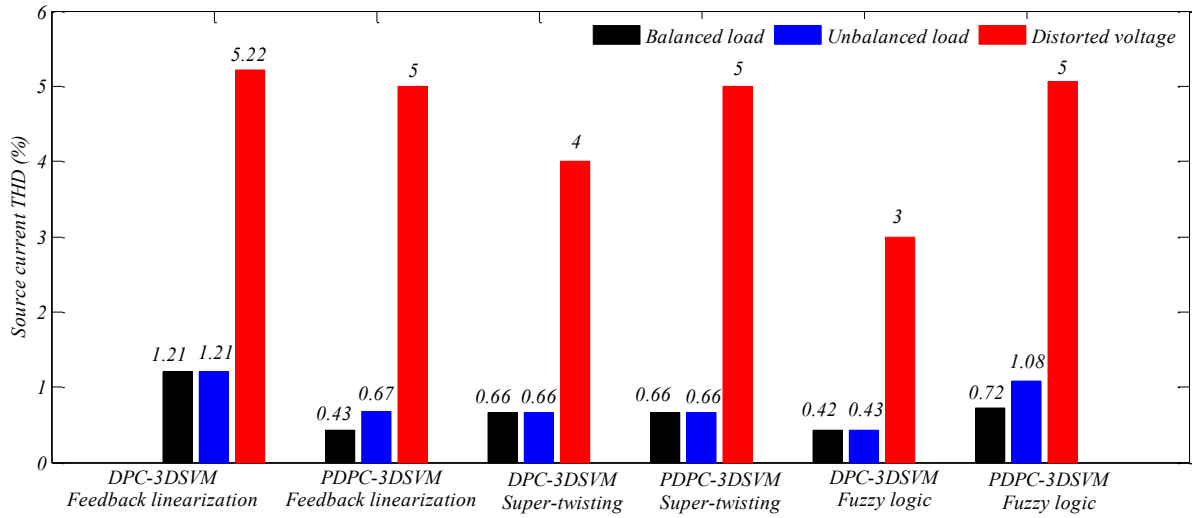

Figure (V.17): Source current THD under balanced/unbalanced nonlinear load and distorted source voltage

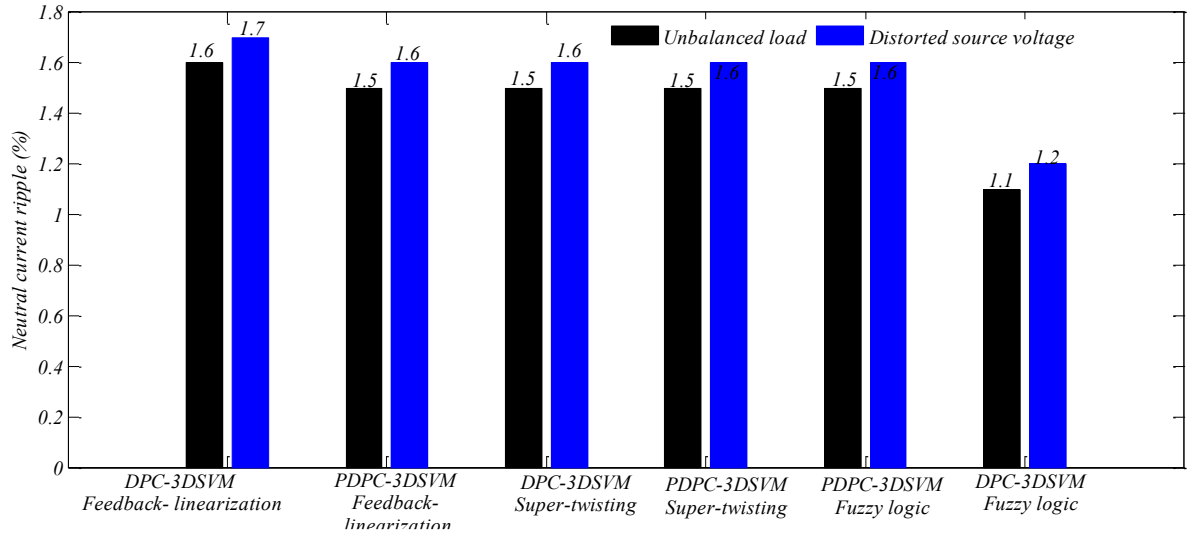

Figure (V.18): Neutral current ripple under unbalanced nonlinear load and distorted source voltage

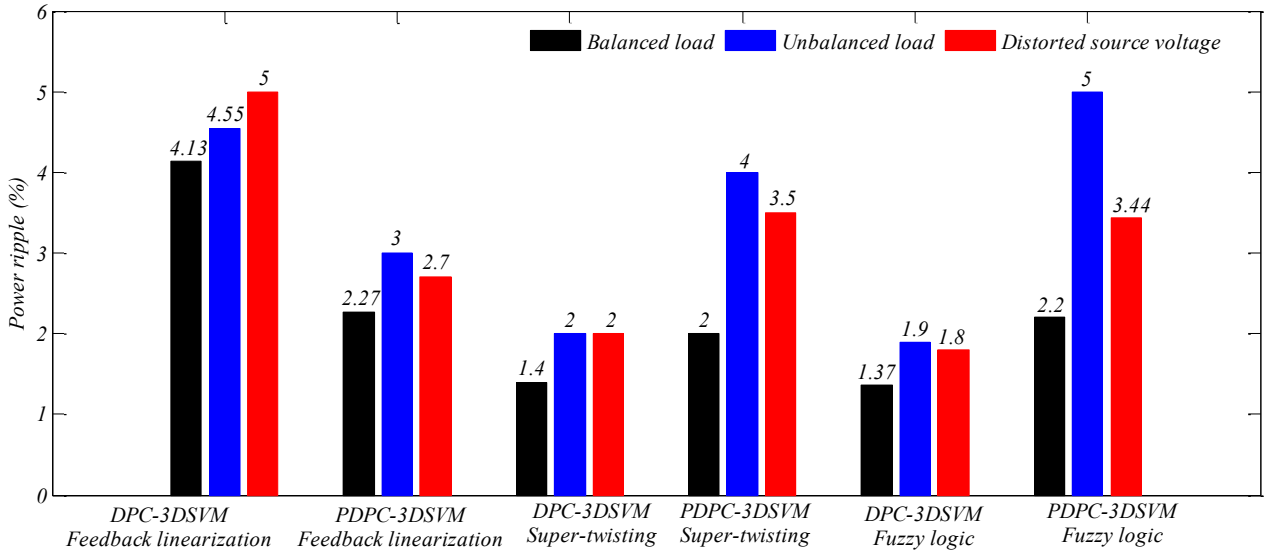

Figure (V.19): Source active and reactive powers ripples under balanced/unbalanced nonlinear load and distorted source voltage

V.7.2. Coupling filter variations

Figure (V.20) shows the dependence of the source current THD on variations of the coupling inductance. As expected, the DPC-3DSVM associated with super-twisting and fuzzy logic techniques is insensitive to these variations, because the control laws in these nonlinear controllers are independent to the system parameters. To the contrary, in the DPC-3DSVM-feedback linearization method, the control law of active and reactive powers is strongly dependent on coupling inductance; therefore, a small deviation of this parameter affects directly the source current quality.

In the other hand, a small sensitivity can be observed in case of PDPC-3DSVM combined with the three nonlinear techniques. In the PDPC strategy the DC voltage is the only variable nonlinearly controlled whereas the active and reactive powers are regulated using a predictive control algorithm. This last is not dependent strongly on the coupling inductance (see equation (II.29)).

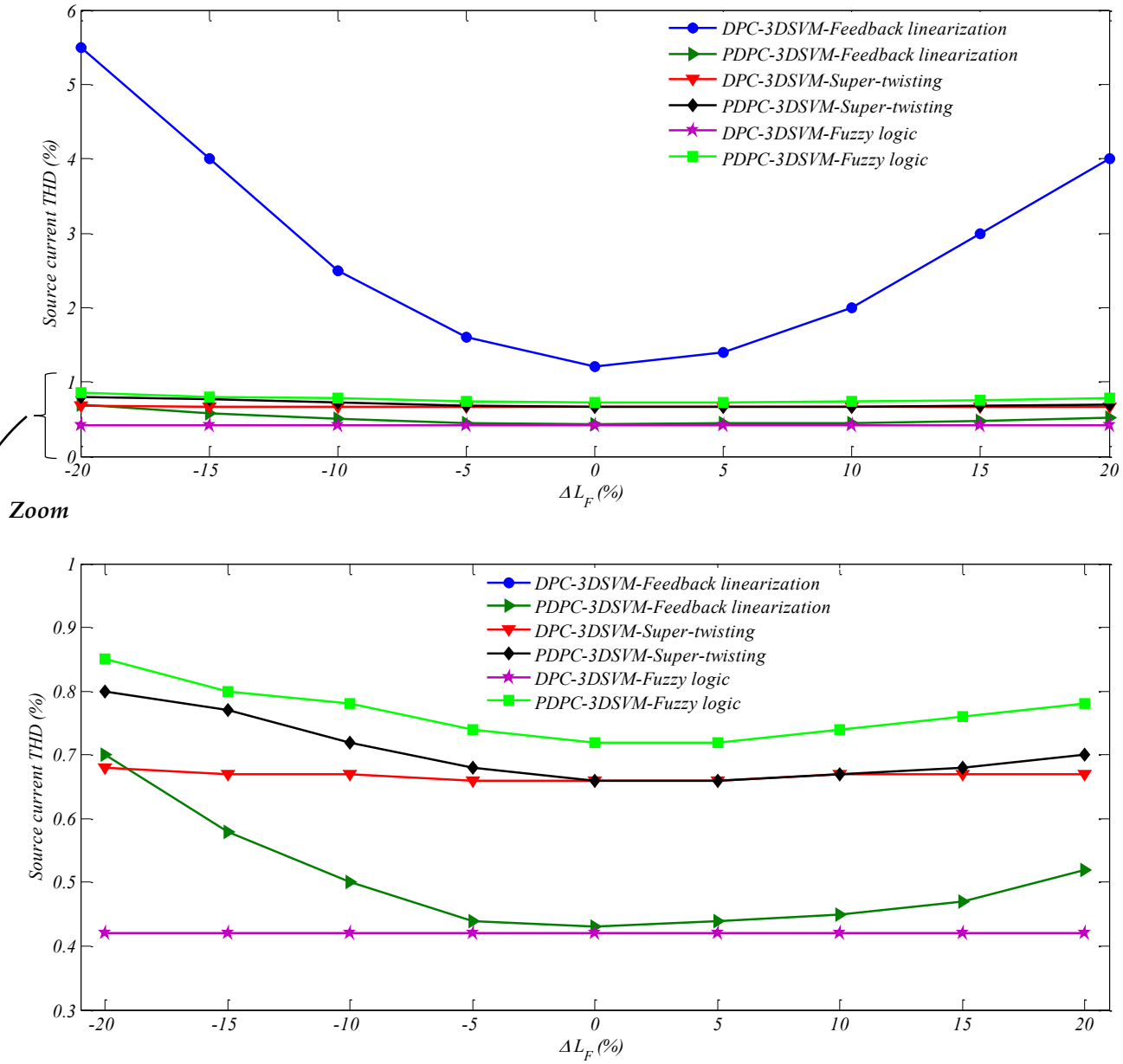

Figure (V.20): Source current THD versus coupling inductance variations ΔL_F (%)

It can be seen in figure (V.21) that the R_F variation does not have influence on control performance in all control techniques. The voltage drop on coupling resistance is much less than voltage drop on coupling inductance. Therefore, for further investigations R_F changes will not be performed.

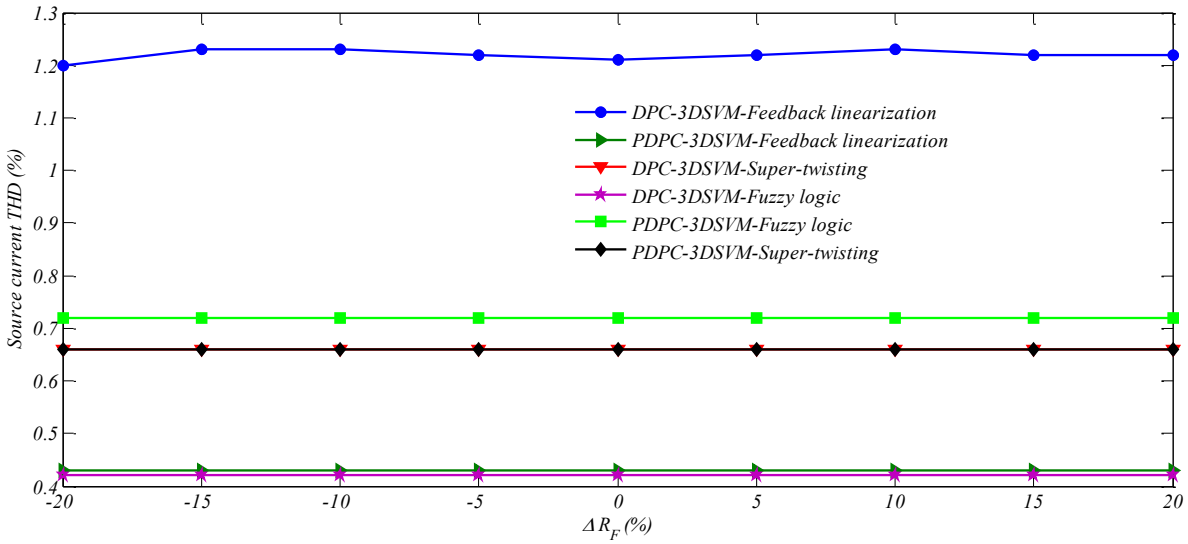

Figure (V.21): Source current THD versus coupling resistance variations ΔR_F (%)

V.6.3. Influence of source voltage sags

The voltage sag can be defined as a strong drop in source voltage (between 10% and 90% of nominal value) during a short period of time, which is usually established between 10ms, and 1min. These kind of disturbances are typically originated by short-circuits and grid connection/disconnection of large loads (transformers, motors and others) within the distribution power system [123].

Figure (V.22) shows several current THD measurements in presence of different magnitudes of three-phase source voltage sags for each control strategies. As a result, a decrease in the magnitude of source voltage sag involves decreasing in the source currents, which increases the source current ripples and, as a result, the current THD. From this figure, it can be observed that the DPC-3DSVM-Fuzzy logic can keep the current THD at reduced values.

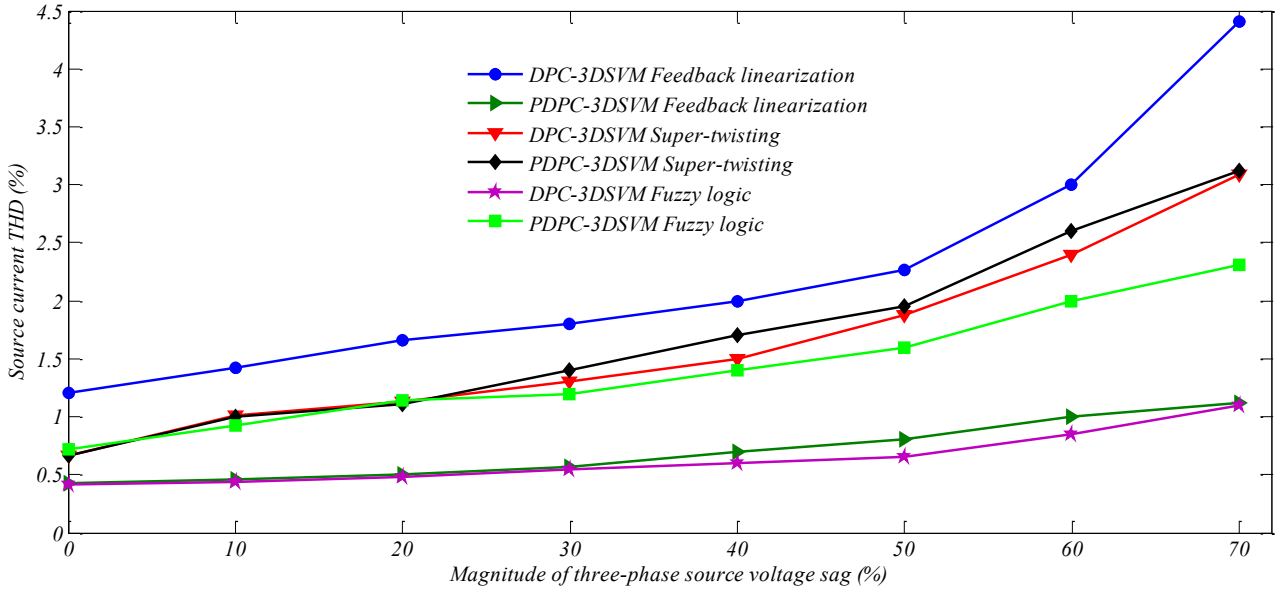

Figure (V.22): Source current THD versus three-phase source voltage sag (%)

Finally, the comparative study between all nonlinear techniques associated with DPC-3DSVM and PDPC-3DSVM for five-level four-leg SAPF is summarized in table (V.2).

Table (V.2): Comparative study between all nonlinear techniques associated with DPC-3DSVM and PDPC-3DSVM for five-level four-leg SAPF

		Balanced nonlinear load		***Unbalanced nonlinear load***			***Distorted source voltage with 5% of the 5th harmonic***			***Source voltage sag of 50%***	***Robustness against L_F variation***
		Source current THD (%)	*Power ripple (%)*	*Source current THD (%)*	*Power ripple (%)*	*Neutral current ripple (%)*	*Source current THD (%)*	*Power ripple (%)*	*Neutral current ripple (%)*	*Source current THD (%)*	
Feedback linearization control	*DPC-3DSVM*	1.21	4.13	1.21	4.55	1.60	5.22	5.00	1.70	2.27	-
	PDPC-3DSVM	0.43	2.27	0.67%	3.00	1.50	5.00	2.70	1.60	0.81	+
Super-twisting	*DPC-3DSVM*	0.66	1.40	0.66	2.00	1.50	4.00	2.00	1.60	1.81	+++
	PDPC-3DSVM	0.66	2.00	0.66	4.00	1.50	5.00	3.50	1.60	1.95	+
Fuzzy logic control	*DPC-3DSVM*	0.42	1.37	0.43	1.90	1.50	3.00	1.80	1.60	0.65	+++
	PDPC-3DSVM	0.72	2.20	1.08	5.00	1.10	5.00	3.44	1.20	1.6	+

V.8. Conclusion

In this chapter, a special attention is paid on the application of the fuzzy logic controller to regulate the DC voltage and active/reactive powers in both DPC-3DSVM and PDPC-3DSVM for five-level four-leg SAPF.

The obtained results show that, the proposed five-level four-leg SAPF controlled by direct power control strategies based on fuzzy controllers suppresses successfully harmonic current and compensates reactive power as well as neutral source current under balanced/ unbalanced nonlinear load and distorted voltage conditions.

A comparative evaluation of the three different nonlinear control techniques for DPC-3DSVM and PDPC-3DSVM applied on the five-level four-leg SAPF has been presented also in this chapter. The performance of these control techniques has been evaluated under various source voltage and nonlinear load conditions. The simulation results indicate that if one seeks compliance with harmonic standards, imbalance mitigation, source neutral current and reactive power compensation, DPC-3DSVM based on fuzzy logic controllers is the most effective control method, which is capable of taking corrective action under severe operating conditions.

General conclusion and future work

In order to improve the power quality in a four-wire electric distribution system, this thesis has been devoted to the research of direct power control strategies with three-dimensional space vector modulation for multilevel four-leg shunt active power filter.

In the first part of this dissertation, a new simplified algorithm of multilevel 3DSVM in $\alpha\beta o$ coordinate is proposed to control *m*-level four-leg diode clamped inverter. The idea is to perform the different steps of 3DSVM such as: determination of the space vector location, duration time calculation, and pulses generation, in only one sector. The proposed algorithm is much simpler and easier for digital implementation since it reduces the hardware and software complexity and decreases the required computational time.
Simulation results have shown that increasing the number of inverter's levels greatly improves the harmonic quality of the output voltage and current. However, with a high number of levels, the power structure is more expensive and its control is more complicated.
The voltage-balancing issue in multilevel inverters with more than three levels requires special attention. Therefore, the voltage balancing control of DC capacitors of the five-level four-leg inverter is achieved using 3DSVM with balancing strategy, which is based on the effective use of the redundant switching states of the inverter voltage vectors. The study results show that the voltage balancing of the DC capacitors have three-dimensional limits depends on modulation index, load power factor, and unbalancing output voltages.

In order to control and improve the performance of the five-level four-leg shunt active power filter, direct power control and predictive direct power control strategies are synthesized by a new model of four-leg SAPF which based on active and reactive powers derivatives in $\alpha\beta o$ coordinates.
In DPC, the traditional switching table has been replaced by a 3DSVM, and three PI controllers in the stationary reference frame were added instead of the hysteresis comparators to cancel the errors between active/reactive powers and their reference values.

The PDPC is based on the computation of the SAPF average voltage vector using a predictive control algorithm, which makes instantaneous active and reactive powers equal to their reference values at each sampling period.
One can see that the control algorithm of both control methods is simple, coordinate transformation and decoupling between active and reactive current are not required. In this control method, the switching frequency is constant and there is no need to current regulation. According to simulation results, the PDPC-3DSVM control method outperform its counterpart DPC-3DSVM under both dynamic and steady state operations in terms of the current harmonics filtering, reactive power compensation, source current balancing, and neutral current elimination.

In order to enhance the performances of both direct power control strategies on the four-leg SAPF, nonlinear controllers based on the feedback linearization, super-twisting sliding mode, and fuzzy logic are associated to DPC-3DSVM and PDPC-3DSVM. A comparative study between these nonlinear control methods under various source voltage and nonlinear load conditions reveals that the DPC-3DSVM based on fuzzy logic controllers is the most effective control method. Chiefly, it is capable to track corrective action under severe operating conditions.

The control schemes proposed in this thesis can be expanded and improved along several lines. The following topics can be suggested for the future researches:

- Association of DPC with other nonlinear and intelligent control methods,
- Extension of DPC and their variants to other types of active filters,
- Exploitation of the multilevel four-leg inverter in the flexible AC transmission systems controllers,
- Practical implementation of the proposed control algorithms.

References

[1] **X. Zhichao, L. Xiaoming**, "The construction of interconnected communication system among smart grid and a variety of networks", Power and energy engineering conference, Chengdu, China, pp. 1-5, 2010.

[2] **A. Ghosh, G. Ledwich**, "Power quality enhancement using custom power devices", Kluver academic publishers, USA, 2002.

[3] **H.L. Jou, K.D. Wu, J.C. Wu, W.J. Chiang**, "A three-phase four-wire power filter comprising a three-phase three-wire active power filter and a zig-zag transformer", IEEE Transaction on power electronics, Vol. 23, No. 1, pp. 252–259, 2008.

[4] **S. Choi, M. Jang**, "Analysis and control of a single-phase-inverter–zig-zag transformer hybrid neutral-current suppressor in three-phase four-wire systems", IEEE Transaction on industrial electronics, Vol. 54, No. 4, pp. 2201-2208, 2007.

[5] **B. Singh, P. Jayaprakash, T.R. Somayajulu, D.P. Kothari**, "Reduced rating VSC with a zig-zag transformer for current compensation in a three-phase four-wire distribution system, IEEE Transaction on power delivery, Vol. 24, No. 1, pp. 249-259, 2009.

[6] **P. Rodriguez, J. Ignacio Candela, A. Luna, L. Asiminoaei, R. Teodorescu, F. Blaabjerg**, "Current harmonics cancellation in three-phase, four-wire systems by using a four-branch star filtering topology", IEEE Transaction on power electronics, Vol. 24, No. 8, pp. 1939–1950, 2009.

[7] **J.C. Das**, "Passive filters – potentialities and limitations", IEEE Transaction on industry applications, Vol. 40, No. 1, pp. 232–241, 2004.

[8] **C.J. Wu, J.C. Chiang, S.S. Yen, C.J. Liao, J.S. Yang, T.Y. Guo**, "Investigation and mitigation of harmonic amplification problems caused by single-tuned filters", IEEE Transaction on power delivery, Vol. 13, No.3, pp. 800–806, 1998.

[9] **T. Fukami, T. Onchi, N. Naoe, R. Hanaoka**, "Compensation for neutral current harmonics in a three-phase, four-wire system by a synchronous machine", IEEE Transaction on industry applications", Vol. 38, No. 5, pp. 1232–1236, 2002.

[10] **H.L. Jou, J.C. Wu, K.D. Wu, W.J. Chiang, Y.H. Chen**, "Analysis of zig-zag transformer applying in the three-phase, four-wire distribution power system", IEEE Transaction on power delivery, Vol. 20, No. 2, pp. 168–1173, 2005.

[11] **B. Singh, P. Jayaprakash, D.P. Kothari**, "A T-connected transformer and three-leg VSC based DSTATCOM for power quality improvement", IEEE Transaction on power electronics, Vol. 23, No. 6, pp. 2710–2718, 2008.

[12] **G. Olivier, R. Cojocaru, A. Lefèvre**, "Analytical model of a T-connected three-phase transformer", Mathematics and computers in simulation, Vol. 63, No. 3-5, pp. 407–419, 2003.

[13] **P. Jayaprakash, B. Singh, D.P. Kothari**, "Three-phase 4-wire DSTATCOM based on H-bridge VSC with a star/hexagon transformer for power quality improvement", IEEE 3rd international conference on industrial and information systems, Kharagpur, India, pp. 1–6, 2008.

[14] **B. Singh, P. Jayaprakash, D.P. Kothari**, "Three leg VSC with a star-hexagon transformer based DSTATCOM for power quality improvement in three-phase four-wire distribution system", International journal of electrical power & energy systems, Vol. 9, No. 8, pp. 964-970, 2008.

[15] **P. Verdelho, G. Marques**, "Four-wire current-regulated PWM voltage converter", IEEE Transaction on industrial electronics, Vol. 45, No. 5, pp. 761-770, 1998.

[16] **R. Grino, R. Cardoner, R. Costa-Castello, E. Fossas**, "Digital repetitive control of a three-phase four-wire shunt active filter", IEEE Transaction on industrial electronics, Vol. 54, No. 3, pp. 1495-1503, 2007.

[17] **G. Escobar, A. Valdez, R. Torres-Olguin, M. Martinez-Montejano**, "A model-based controller for a three-phase four-wire shunt active filter with compensation of the neutral line current", IEEE Transaction on power electronics, Vol. 22, No. 6, pp. 2261-2270, 2007.

[18] **V. Khadkikar, A. Chandra, B. Singh**, "Digital signal processor implementation and performance evaluation of split capacitor, four-leg and three H-bridge-based three-phase four-wire shunt active filters", IET Power electronics, Vol. 4, No. 4, pp. 463-470, 2011.

[19] **D. Sreenivasarao, Pramod Agarwal, Biswarup Das**, "Neutral current compensation in three-phase, four-wire systems: A review", Electric power systems research, Vol. 86, pp. 170-180, 2012.

[20] **V. Khadkikar, A. Chandra**, "An independent control approach for three-phase, four-wire shunt active filter based on three H-bridge topology under unbalanced load conditions", IEEE Power electronics specialists conference, Rhodes, Greece, 2008, pp. 4643-4649.

[21] **A. Chaghi, A. Guetta, A. Benoudjit**, "Four legged active power filter compensation for a utility distribution system", Journal of electrical engineering, Vol. 55, No. 1-2, pp. 31-35, 2004.

[22] **M. Bouzidi, A. Benaissa, S. Barkat**, "Sliding mode control using 3D-SVM for three-phase four-leg shunt active filter", International journal of power electronics and drive system, Vol. 3, No. 2, pp. 147-154, 2013.

[23] **M. Ucar, E. Ozdemir**, "Control of a 3-phase 4-leg active power filter under non-ideal mains voltage condition", Electric power systems research, Vol. 78, pp. 58-73, 2008.

[24] **I. Colak, E. Kabalci, R. Bay**, "Review of multilevel voltage source inverter topologies and control schemes", Energy conversion and management, Vol. 52, No. 2, pp. 1114-1128, 2010.

[25] **E. Babaei, S.H. Hosseini, G.B. Gharehpetian, M. Tarafdar Haque, M. Sabahi**, "Reduction of dc voltage sources and switches in asymmetrical multilevel converters using a novel topology", Electric power systems research, Vol. 77, No. 8, pp. 1073-1085, 2007.

[26] **N.F. Mailah, S.M. Bashi, I. Aris, N. Mariun**, "Neutral-Point-Clamped multilevel inverter using space vector modulation", European journal of scientific research, Vol.28, No. 1, pp. 82-91, 2009.

[27] **S. Barkati, L. Baghli, E. Berkouk, M. Boucherit**, "Harmonic elimination in diode-clamped multilevel inverter using evolutionary algorithms", Electric power systems research, Vol. 78, Vol. 8, pp. 1736-1746, 2008.

[28] **M.E. Ortúzar, R.E. Carmi, J.W. Dixon, L. Morán**, "Voltage-Source active power filter based on multilevel converter and ultra-capacitor dc link", IEEE Transaction on industrial power electronics, Vol. 53, No. 3, pp. 477-485, 2006.

[29] **S. Saad, L. Zellouma**, "Fuzzy logic controller for three-level shunt active filter compensating harmonics and reactive power", Electric power systems research, Vol. 79, No. 10, pp. 1337-1341, 2009.

[30] **A. Munduate, E. Figueres, G. Garcera**, "Robust Model-Following control of a three-level neutral point clamped shunt active filter in the medium voltage range", International journal of electrical power & energy systems, Vol. 31, No. 10, pp. 577-588, 2009.

[31] **G. Zhou, B. Wu, D. Xu**, "Direct power control of a multilevel inverter based active power filter", Electric power systems research, Vol. 77, No. 4, pp. 284-294, 2007.

[32] **H.F. Farahani, and F. Rashidi**, "A novel method for selective harmonic elimination and current control in multilevel current source inverters", International review of electrical engineering, Vol. 5, No. 2, pp. 356-363, 2010.

[33] **A. Chaoui, J.P. Gaubert, F. Krim**, "Experimental evaluation of a simple robust control for active power filtering under unfavorable conditions", 13th Enropean conference on power electronics and applications, Barcelona, Spain, 2009, pp. 1-11.

[34] **M. liserre, A.D. Aquila, F. Blaabjerg**, "Design and control of a three-phase active rectifier under non-ideal operation conditions", IEEE Conference record of the industry applications, Pittsburgh, USA, 2002, pp. 1181-1188.

[35] **A. Chaoui, J.P. Gaubert, F. Krim**, "Power quality improvement using DPC controlled three-phase shunt active filter", Electric power systems research, Vol. 80, No.6 , pp. 657-666, 2010.

[36] **Z. Minglian, L. Ruiqiang, H. Enyong, X. Chunhua, Y. Xuefeng**, "Research on direct power control strategy", IEEE 2nd International conference on artificial

intelligence, management science and electronic commerce, Zhengzhou, China, 2011, pp. 7195-7197.

[37] **D. Wojciechowski**, "Predictive control of high power active filter system with LCL circuit", IEEE International symposium on industrial electronics, Bari, Italy, 2010, pp. 2575-2580.

[38] **I. Takahashi, T. Noguchi**, "A New quick-response and High-Efficiency control strategy of an induction motor", IEEE Transaction on industry applications, Vol. 22, No. 5, pp. 820-827, 1986.

[39] **V. Manninen**, "Application of torque control modulation technology to a line converter", EPE'95-Europeen power electronics conference, Sevilla, Spain 1995, pp.1292-1296.

[40] **T. Noguchi, H. Tomiki, S. Kondo**, "Direct power control of PWM converter without power source voltage sensors", IEEE Transaction on industry applications, Vol. 34, No. 3, pp. 473- 479, 1998.

[41] **M. Malinowski, M. P. Kaźmierkowski, S. Hansen S., F. Blaabjerg, G. D. Marques**, "Virtual flux based direct power control of three-phase PWM rectifiers", IEEE Transaction on industry applications, Vol. 37, No. 4, pp. 1019-1027, 2001.

[42] **M. Cichowlas, M. Malinowski, M.P. Kazmierkowski, D.L. Sobczuk, P. Rodríguez, J. Pou**, "Active filtering function of three-phase PWM boost rectifier under different line voltage conditions", IEEE Transaction on industrial power electronics, Vol. 52, No. 2, pp. 410-419, 2005.

[43] **S. Aurtenechea, M. A. Rodriguez, E. Oyarbide, J. R. Torrealday**, "Predictive direct power control - a new control strategy for dc/ac converters," IEEE 32nd Annual conference on industrial electronics, Paris, 2006, pp. 1661-1666.

[44] **P. Antoniewicz, M. P. Kazmierkowski, S. Aurtenechea, M. A. Rodriguez**, "Comparative study of two predictive direct power control algorithms for three-phase ac/dc converters," European conference on power electronics and applications, Aalborg, Denmark, 2007, pp. 1-10.

[45] **S. Aurtenechea, M. A. Rodriguez, E. Oyarbide, J. R. Torrealday**, "Predictive control strategy for dc/ac converters based on direct power control," IEEE Transaction on industrial electronics, Vol. 54, No. 3, pp. 1261–1271, 2007.

[46] **P. Antoniewicz, M. P. Kazmierkowski**, "Virtual-Flux-Based predictive direct power control of ac/dc converters with online inductance estimation", IEEE Transactions on industrial electronics, Vol. 55, No. 12, pp. 4381- 4390, 2008.

[47] **A. Bouafia, J. P. Gaubert, F. Krim**, "Predictive direct power control of three-phase pulse-width modulation (PWM) rectifier using space-vector modulation (SVM)", IEEE Transactions on power electronics, Vol. 25, No. 1, pp. 228-236, 2010.

[48] **R. Zhang, V.H. Prasad, D. Boroyevich, F.C. Lee**, "Three-Dimensional space vector modulation for four-leg voltage source converters", IEEE Transaction on industrial power electronics, Vol. 17, No. 3, pp. 314-326, 2002.

[49] **R. Zhang, D. Boroyevich, V.H. Prasad**, "A Three-Phase inverter with a neutral leg with space vector modulation", IEEE applied power electronics conference and exposition, Atlanta, USA, 1997, pp. 857-863.

[50] **M. Saeedifard, R. Iravani, J. Pou**, "Analysis and control of dc-capacitor-voltage-drift phenomenon of a passive front-end five-level converter," IEEE Transaction on industrial electronics, Vol. 54, No. 6, pp. 3255-3266, 2007.

[51] **H.A. Hotait, A.M. Massoud, S.J. Finney, B.W. Williams**, "Capacitor voltage balancing using redundant states of space vector modulation for five-level diode clamped inverters", IET Power electronics, Vol. 3, No. 2, pp. 292-313, 2010.

[52] **K. Hasegawa, H. Akagi**, "A new dc-voltage-balancing circuit including a single coupled inductor for a five-level diode clamped pwm inverter", IEEE Transaction on industry applications, Vol. 47, No. 2, pp. 841-852, 2011.

[53] **Z. Pan, F.Z. Peng, K.A. Corzine, Stefanovic, R. Victor, J.M. Leuthen, S. Gataric,** "Voltage balancing control of diode-clamped multilevel rectifier/inverter systems", IEEE Transaction on industry applications, Vol. 41, No. 6, pp. 1698-1706, 2005.

[54] **T. Ishida, T. Miyamoto, T. Oota, K. Matsuse, K. Sasagawa, H. Lipei**, "A control strategy for a five-level double converter with adjustable dc link voltage" Conference record of the industry applications, Pittsburgh, USA, 2002, pp. 530-536.

[55] **A. Saha, Y. Sozer,** " Capacitor voltage balancing using minimum loss SVPWM for a five-level dio de-clamped converter", 29th Annual IEEE applied power electronics conference and exposition (APEC), 2014 , Fort Worth, USA, 2014, pp. 225-230.

[56] **J. Dannehl, C. Wessels, F.W. Fuchs**, "Limitations of voltage-oriented PI current control of grid-connected PWM rectifiers with LCL filters", IEEE Transaction on industry Electronics, Vol. 56, No. 2, pp. 380-8, 2009.

[57] **L. Tzann-Shin**, "Input-output linearization and zero-dynamics control of three-phase AC/DC voltage-source converters", IEEE Transaction on power electronics, Vol. 18, No. 1, pp. 11-22, 2003.

[58] **X. Bao; F. Zhuo; Y. Tian; P. Tan**, "Simplified feedback linearization control of three-phase photovoltaic inverter with an LCL filter", IEEE Transaction on power electronics, Vol. 28, No. 6, pp. 2739–2752, 2013.

[59] **M. Bouzidi, A. Benaissa, S. Barkat**, "Application of feedback linearization to the virtual flux direct power control of three-level three-phase shunt active power filter", International review of electrical engineering, Vol. 5, No. 3, pp. 1128-1140, 2012.

[60] **M. Bouzidi, A. Benaissa, S. Barkat**, "Hybrid direct power/current control using feedback linearization of three-level four-leg voltage source shunt active power filter", International journal of electrical power & energy systems, Vol. 61, pp. 629-646, 2014.

[61] **S. Mikkili, A.K. Panda**, "Real-time implementation of PI and fuzzy logic controllers based Shunt active filter control strategies for power quality improvement", International journal of electrical power & energy systems, Vol. 43, No. 1, pp. 1114-1126, 2012.

[62] **S. Mikkili, A.K. Panda**, "PI and fuzzy logic controller based 3-phase 4-wire shunt active filter for mitigation of current harmonics with I_d–I_q control strategy", Journal of power electronics, Vol. 11, No. 6, pp. 914-921, 2011.

[63] **L. Fridman**, "An averaging approach to chattering", IEEE Transactions on automatic control, Vol. 46, No. 8, pp. 1260-1265, 2001.

[64] **Y. Shtessel, M. Taleb, F. Plestan**, "A novel adaptive-gain supertwisting sliding mode controller: methodology and application", Automatica, Vol. 48, No. 5, pp. 759-769, 2012.

[65] **A. Levant**, "Sliding order and sliding accuracy in sliding mode control", International journal of control", Vol. 58, No. 6, pp. 1247-1263, 1993.

[66] **J. Rodríguez, J. Lai, F. Peng**, "Multilevel inverters: A survey of topologies, controls and applications," IEEE Transaction on industrial electronics, Vol. 49, No. 4, pp. 724-738, 2002.

[67] **L. Demas, T.A, Meynard, H. Foch, G. Gateau**, "Comparative study of multilevel topologies: NPC, multicellular inverter and SMC with IGBT," 28th IEEE Annual conference of the industrial electronics society, Sevilla, Spain, 2002, vol. 1, pp. 828-833.

[68] **B.A. Welchko, M.B.de.R. Correa, T.A. Lipo**, "A three-level MOSFET inverter for low-power drives," IEEE Transaction on industrial electronics, Vol. 51, No. 3, pp. 669-674, 2004.

[69] **R. Teichmann S. Bernet**, "A comparison of three-level converters versus two-level converters for low-voltage drives, traction, and utility applications," IEEE Transaction on industry applications, Vol. 41, No. 3, pp. 855-865, 2005.

[70] **K.S. Gayathri Devi, S. Arun, C. Sreeja**, "Comparative study on different five level inverter topologies", International journal of electrical power & energy systems, Vol. 63, pp. 363-372, 2014.

[71] **A. Benaissa, B. Rabhi, A. Moussi**, "Fuzzy logic controller for three-phase four-leg five-level shunt active power filter under unbalanced non-linear load and distorted voltage conditions", International journal of systems assurance engineering and management, Vol. 5, No. 3, pp. 361-370, 2014.

[72] **N.Y Dai, M.C. Wong, Y.H Chen, Y.D. Han**, "A 3-D generalized direct PWM algorithm for multilevel converters, "IEEE Power electronics letters, Vol. 3, No. 3, pp. 85-88, 2005.

[73] **L.G. Franquelo, M.M. Prats, R. Portillo, J.I. Leon, M. Perales, J.M. Carrasco, E. Galvan, J.L. Mora**, "Simple and advanced three dimensional space vector modulation algorithm for four-leg multilevel converters topology", 30th IEEE Annual conference of industrial electronics society, Arizona, USA, 2004, Vol.3, pp. 2285 – 2289.

[74] **F. Botteron, R.F. Camargo, H.L. Hey, J.R. Pinheiro, H.A. Grundling, H. Pinheiro**, "New limiting algorithms for space vector modulated three-phase

four-leg voltage source inverters", IEE Proceedings electric power applications, Vol. 150, No. 6-7, pp. 733-742, 2003.

[75] **M.A. Perales, M.M. Prats, R. Portillo, J.L. Mora, J.I. Leon, L.G. Franquelo**, "Three-dimensional space vector modulation in abc coordinates for four-leg voltage source converters", IEEE Power electronics letters, Vol. 1, No. 4, pp. 104-109, 2003.

[76] **H. Ertl, T. Wiesinger, J.W. Kolar**, "Active voltage balancing of DC-link electrolytic capacitors", IET Power Electronics, Vol. 1, No. 4, pp. 488-496, 2008.

[77] **S. Hive, K. Chatterjee, B.G. Fernandes**, "Var compensation and elimination of harmonics in three-phase four-wire system based on unified constant-frequency integration control," IEEE 11th International conference on harmonics and quality of power, Lake Placid, NY, USA, 2004, pp. 647-651.

[78] **M. George, K.P. Basu**, "Modeling and control of three-phase shunt active power filter," American journal of applied sciences, Vol. 5, No. 5, pp. 1064-1070, 2008.

[79] **B. Singh, A. Chandra, K. Al-Haddad**, "Reactive power compensation and load balancing in electric power distribution systems," International Journal of Electrical Power & Energy Systems, Vol. 20, pp. 375-381, 1998.

[80] **I. Zamora, A.J. Mazon, P. Eguia, I. Albizu, K.J. Sagastabeitia, E. Fernhdez**, "Simulation by MATLAB / Simulink of active filters for reducing THD created by industrial systems," IEEE Power Tech Conference Proceedings, Bologna, Italy, 2003.

[81] **I.I. Abdalla, K.S.R. Rao, N. Perumal**, "Harmonics mitigation and power factor correction with a modern three-phase four-leg shunt active power filter," IEEE International Conference on Power and Energy, Kuala Lumpur, Malaysia, 2010, pp. 156-161.

[82] **H. Akagi**, "Active harmonic filters," Proceedings of the IEEE, Vol. 93, pp. 2128-2141, 2005.

[83] **P. Lohia, M.K. Mishra, K. Karthikeyan, K. Vasudevan**, "A minimally switched control algorithm for three-phase four-leg VSI topology to compensate unbalanced and nonlinear load," IEEE Transactions on power electronics, Vol. 23, No. 4, pp. 1935-1944, 2008.

[84] **M.K. Mishra, and K. Karthikeyan**, "A study on design and dynamics of voltage source inverter in current control mode to compensate unbalanced and non-linear loads", IEEE International Conference on Power Electronic, Drives and Energy Systems, New Delhi, India, 2006, pp. 1-8.

[85] **N.Y. Dai, M.C. Wong, F. Ng, Y.D. Han**, "A FPGA-based generalized pulse width modulator for three-leg center-split and four-leg voltage source inverters", IEEE Transaction on power electronics, Vol. 23, No. 3, pp. 1472-1484, 2008.

[86] **S. Srikanthan, M.K. Mishra**, "DC capacitor voltage equalization in neutral clamped inverters for DSTATCOM application", IEEE Transaction industrial electronics, Vol. 57, No. 8, pp. 2768-2775, 2010.

[87] **M. Kale, E. Ozdemir**, "An adaptive hysteresis band current controller for shunt active power filter" Electric power system research, Vol. 73, pp.113-119, 2005.

[88] **J.V. Wijayakulasooriya, G.A. Putrus, C.H. Ng,** "Fast noncursive extraction of individual harmonics using artificial neural networks", IEE Proceedings, Vol. 152, No. 4, pp. 539-543, 2005.

[89] **H. Akagi, E. H. Watanabe, M. Aredes,** "Instantaneous power theory and application to power conditioning ", John Wiley & Sons, 2007.

[90] **A. Isidori, Nonlinear control systems, Springer. Berlin, 1995.**

[91] **S. Ponnaluri, A. Brickwedde**, "System design of three phase active filters using time domain techniques", 9th European conference on power electronics and applications, Graz, Austria, 2001.

[92] **S. Ponnaluri, A. Brickwedde**, "Generalized system design of three phases active filters", IEEE Annual power electronics specialists conference, Vancouver, Canada, 2001, pp. 1414-1419.

[93] **S.K. Jain, P.H.O. Agarwal**, "Design simulation and experimental investigations, on a shunt active power filter for harmonics, and reactive power compensation", Electric power components and systems, Vol. 31, No. 7, pp. 671-692, 2003.

[94] **F. Ronchi, A. Tilli**, "Design methodology for active filters", Proceedings international test conference, Washington, 1990, pp. 183-192.

[95] **B.N. Singh, P. Rastgoufard, B. Singh, A. Chandra K. Al-haddad**, "Design, simulation and implementation of three-pole/four-pole topologies for active filter ", IEEE Proceedings-Electric power applications, Vol. 151, No. 4, pp. 467-476, 2004.

[96] **S. Zhang, V.H. Prasad, D. Boroyevivh, F.C. Lee**, "Analyze and design of three-phase inverter with a neutral leg", 7th European conference on power electronics and applications, Trondheim, Norway, 1997.

[97] **S. Aurtenechea Larrinaga**, "Predictive control of the 2L-VSI and 3L-NPC VSI based on direct power control for MV grid connected power applications", Ph.D Thesis, Faculty of engineering, Arrasate-Mondragon, Spain, 2007.

[98] **S. Saetieo, R. Devaraj, D.A. Torrey**, "The design and implementation of a three phase active power filter based on sliding mode control". IEEE Transaction on industry applications, Vol. 31, No. 5, pp. 993-1000, 1995.

[99] **Q. Zhong, K.W. Eric Cheng, N.C. Cheung, J. Pan, J. Wu**, "Passivity based control of the shunt active power filters", IEEE International conference on control and automation, Christchurch, New Zealand, 2009, pp. 2106-2110.

[100] **C.N. Bhende, S. Mishra, S.K. Jain**, "TS-Fuzzy controlled active power filter for load compensation". IEEE Transaction on power delivery, Vol. 21, No. 3, pp. 1459-1465, 2006.

[101] **K. Cagatay Bayındır, M. Ugras Cuma, M. Tumay**, "Hierarchical neuro fuzzy current control for a shunt active power filter". Neural computing & applications, Vol. No. 3, pp. 223-238, 2006.

[102] **H. Kömürcügil, O. Kükrer**, "Globally stable control of three phase three wire shunt active power filters", Electrical engineering, Vol. 89, No. 5, pp. 411-418, 2006.

[103] **A. Munduate, E. Figueres, G. Garcera**, "Robust model-following control of a three level neutral point clamped shunt active filter in the medium voltage range". International journal of electrical power & energy systems, Vol. 31, pp. 577-588, 2009.

[104] **H.K. Khalil**, "Nonlinear Systems", Pearson Education, USA, 2000.

[105] **D.C. Lee, G.M. Lee, K.D. Lee**, "DC bus voltage control of three phase AC-DC PWM converters using feedback linearization", IEEE Transactions on industry application, Vol. 36, pp. 826-833, 2000.

[106] **T.S. Lee**, "Input-Output linearizing and zero dynamics control of three-phase AC-DC voltage source converters", IEEE Transactions on power electronics, Vol. 18, pp. 11-22, 2003.

[107] **V.I. Utkin**, "Sliding modes in control optimization", Springer-Verlag, Berlin, 1992.

[108] **A.S.I. Zinober**, "Variable structure and lyapunov control", Springer-Verlag, USA, 1994.

[109] **C. Edwards, K.S. Spurgeon**, "Sliding mode control: theory and applications", Taylor & Francis. London, 1998.

[110] **I. Boiko, L. Fridman M.I. Castellanos**, "Analysis of second order sliding mode algorithms in the frequency domain". IEEE Transactions on automatic control, Vol. 49, No. 6, pp. 946-950, 2004.

[111] **J.J.E. Slotine, W. Li**, "Applied nonlinear control", Prentice Hall, USA, 1991.

[112] **L. Fridman, A. Levant**, "Higher order sliding modes as a natural phenomenon in control theory", Robust control via variable structure and lyapunov techniques, Springer, Vol. 217, pp. 107-133, 1993.

[113] **G. Bartolini, A. Ferrara, E. Usai**, "Chattering avoidance by second-order sliding mode control". IEEE Transactions on automatic control, Vol. 43, No. 2, pp. 241-246, 1998.

[114] **A. Levant**, "Higher-order sliding modes, differentiation and output feedback control", International journal of control, Vol. 76, No. 9, pp. 924-941, 2003.

[115] **G. Bartolini, A. Ferrara E. Usai**, "Applications of a sub-optimal discontinuous control algorithm for uncertain second order systems", International journal of robust and nonlinear control, Vol. 7, pp. 299-319, 1997.

[116] **L.A. Zadeh**, "Fuzzy sets", Information and control, Vol. 8, pp. 338-353, 1965.

[117] **L.A. Zadeh**, "Outline of a new approach to the analysis of complex systems and decision processes", IEEE Transaction on systems, Vol. 3, No. 1, pp. 28-44, 1973.

[118] **C. Lee**, "Fuzzy logic in control systems, fuzzy logic controller, parts I and II," IEEE transactions on systems, Vol. 3, No. 1, 1973.

[119] **S. Mikkili A.K. Panda**, "Simulation and real-time implementation of shunt active filter I_d–I_q control strategy for mitigation of harmonics with different Fuzzy membership functions", IET Power electronics, Vol. 5, No. 9, pp. 1856-1872, 2012.

[120] **J. Zhao, B.K. Bose**, "Evaluation of membership functions for Fuzzy logic controlled induction motor drive", IEEE 28th Annual conference of the industrial electronics society, Sevilla, 2002, Vol. 1, pp. 229-234.

[121] **C.C. Lee**, "Fuzzy logic in control systems: Fuzzy logic controller - Part I, II", IEEE Transactions on systems, Vol. 20, No. 2, pp. 404-418, 1990.

[122] **W.J.M. Kickert, E.H. Mamdani**, "Analysis of a fuzzy logic controller", Fuzzy sets and systems, Vol. 1, No. 1, pp. 29–114, 1978.

[123] **S.A. Larrinaga**, "Predictive Control of the 2l-VSI and 3l-NPC VSI based on direct power control for MV grid connected power applications", Ph.D, Faculty of engineering, Arrasate-Mondragon, Spain, 2007.

Appendix

A.1. Tetrahedron identification

The localization condition of all tetrahedrons located in the first sector are summarized in table (A.1).

Table (A.1): Localization condition of all tetrahedrons of the first sector

PR_1					
TeT_1^1	$U_o^* < -\sqrt{2}U_\alpha^* + \sqrt{3}v_{dc}$ $U_o^* \geq \frac{1}{\sqrt{2}}U_\alpha^* + \sqrt{\frac{3}{2}}U_\beta^*$	TeT_2^1	$U_o^* < \frac{1}{\sqrt{2}}U_\alpha^* + \sqrt{\frac{3}{2}}U_\beta^*$ $U_o^* \geq \frac{1}{\sqrt{2}}U_\alpha^* - \sqrt{\frac{3}{2}}U_\beta^*$	TeT_3^1	$U_o^* < \frac{1}{\sqrt{2}}U_\alpha^* - \sqrt{\frac{3}{2}}U_\beta^*$ $U_o^* \geq -\sqrt{2}U_\alpha^* + \frac{3\sqrt{3}v_{dc}}{4}$
TeT_4^1	$U_o^* < -\sqrt{2}U_\alpha^* + \frac{3\sqrt{3}v_{dc}}{4}$ $U_o^* \geq \frac{1}{\sqrt{2}}U_\alpha^* + \sqrt{\frac{3}{2}}U_\beta^* - \frac{\sqrt{3}v_{dc}}{4}$	TeT_5^1	$U_o^* < \frac{1}{\sqrt{2}}U_\alpha^* + \sqrt{\frac{3}{2}}U_\beta^* - \frac{\sqrt{3}v_{dc}}{4}$ $U_o^* \geq \frac{1}{\sqrt{2}}U_\alpha^* - \sqrt{\frac{3}{2}}U_\beta^* - \frac{\sqrt{3}v_{dc}}{4}$	TeT_6^1	$U_o^* < \frac{1}{\sqrt{2}}U_\alpha^* - \sqrt{\frac{3}{2}}U_\beta^* - \frac{\sqrt{3}v_{dc}}{4}$ $U_o^* \geq -\sqrt{2}U_\alpha^* + \frac{\sqrt{3}v_{dc}}{2}$
TeT_7^1	$U_o^* < -\sqrt{2}U_\alpha^* + \frac{\sqrt{3}v_{dc}}{2}$ $U_o^* \geq \frac{1}{\sqrt{2}}U_\alpha^* + \sqrt{\frac{3}{2}}U_\beta^* - \frac{\sqrt{3}v_{dc}}{2}$	TeT_8^1	$U_o^* < \frac{1}{\sqrt{2}}U_\alpha^* + \sqrt{\frac{3}{2}}U_\beta^* - \frac{\sqrt{3}v_{dc}}{2}$ $U_o^* \geq \frac{1}{\sqrt{2}}U_\alpha^* - \sqrt{\frac{3}{2}}U_\beta^* - \frac{\sqrt{3}v_{dc}}{2}$	TeT_9^1	$U_o^* < \frac{1}{\sqrt{2}}U_\alpha^* - \sqrt{\frac{3}{2}}U_\beta^* - \frac{\sqrt{3}v_{dc}}{2}$ $U_o^* \geq -\sqrt{2}U_\alpha^* + \frac{\sqrt{3}v_{dc}}{4}$
TeT_{10}^1	$U_o^* < -\sqrt{2}U_\alpha^* + \frac{\sqrt{3}v_{dc}}{4}$ $U_o^* \geq \frac{1}{\sqrt{2}}U_\alpha^* + \sqrt{\frac{3}{2}}U_\beta^* - \frac{3\sqrt{3}v_{dc}}{4}$	TeT_{11}^1	$U_o^* < \frac{1}{\sqrt{2}}U_\alpha^* + \sqrt{\frac{3}{2}}U_\beta^* - \frac{3\sqrt{3}v_{dc}}{4}$ $U_o^* \geq \frac{1}{\sqrt{2}}U_\alpha^* - \sqrt{\frac{3}{2}}U_\beta^* - \frac{3\sqrt{3}v_{dc}}{4}$	TeT_{12}^1	$U_o^* < \frac{1}{\sqrt{2}}U_\alpha^* - \sqrt{\frac{3}{2}}U_\beta^* - \frac{3\sqrt{3}v_{dc}}{4}$ $U_o^* \geq -\sqrt{2}U_\alpha^*$
TeT_{13}^1	$U_o^* < -\sqrt{2}U_\alpha^*$ $U_o^* \geq \frac{1}{\sqrt{2}}U_\alpha^* + \sqrt{\frac{3}{2}}U_\beta^* - \sqrt{3}v_{dc}$				

PR_2					
TeT_1^2	$U_o^* < -\sqrt{2}U_\alpha^* + \sqrt{3}v_{dc}$ $U_o^* \geq \frac{1}{\sqrt{2}}U_\alpha^* - \sqrt{\frac{3}{2}}U_\beta^* + \frac{\sqrt{3}v_{dc}}{4}$	TeT_2^2	$U_o^* < \frac{1}{\sqrt{2}}U_\alpha^* - \sqrt{\frac{3}{2}}U_\beta^* + \frac{\sqrt{3}v_{dc}}{4}$ $U_o^* \geq \frac{1}{\sqrt{2}}U_\alpha^* + \sqrt{\frac{3}{2}}U_\beta^*$	TeT_3^2	$U_o^* < \frac{1}{\sqrt{2}}U_\alpha^* + \sqrt{\frac{3}{2}}U_\beta^*$ $U_o^* \geq -\sqrt{2}U_\alpha^* + \frac{3\sqrt{3}v_{dc}}{4}$
TeT_4^2	$U_o^* < -\sqrt{2}U_\alpha^* + \frac{3\sqrt{3}v_{dc}}{4}$ $U_o^* \geq \frac{1}{\sqrt{2}}U_\alpha^* - \sqrt{\frac{3}{2}}U_\beta^*$	TeT_5^2	$U_o^* < \frac{1}{\sqrt{2}}U_\alpha^* - \sqrt{\frac{3}{2}}U_\beta^*$ $U_o^* \geq \frac{1}{\sqrt{2}}U_\alpha^* + \sqrt{\frac{3}{2}}U_\beta^* - \frac{\sqrt{3}v_{dc}}{4}$	TeT_6^2	$U_o^* < \frac{1}{\sqrt{2}}U_\alpha^* + \sqrt{\frac{3}{2}}U_\beta^* - \frac{\sqrt{3}v_{dc}}{4}$ $U_o^* \geq -\sqrt{2}U_\alpha^* + \frac{\sqrt{3}v_{dc}}{2}$
TeT_7^2	$U_o^* < -\sqrt{2}U_\alpha^* + \frac{\sqrt{3}v_{dc}}{2}$ $U_o^* \geq \frac{1}{\sqrt{2}}U_\alpha^* - \sqrt{\frac{3}{2}}U_\beta^* - \frac{\sqrt{3}v_{dc}}{4}$	TeT_8^2	$U_o^* < \frac{1}{\sqrt{2}}U_\alpha^* - \sqrt{\frac{3}{2}}U_\beta^* - \frac{\sqrt{3}v_{dc}}{4}$ $U_o^* \geq \frac{1}{\sqrt{2}}U_\alpha^* + \sqrt{\frac{3}{2}}U_\beta^* - \frac{\sqrt{3}v_{dc}}{2}$	TeT_9^2	$U_o^* < \frac{1}{\sqrt{2}}U_\alpha^* + \sqrt{\frac{3}{2}}U_\beta^* - \frac{\sqrt{3}v_{dc}}{2}$ $U_o^* \geq -\sqrt{2}U_\alpha^* + \frac{\sqrt{3}v_{dc}}{4}$
TeT_{10}^2	$U_o^* < -\sqrt{2}U_\alpha^* + \frac{\sqrt{3}v_{dc}}{4}$ $U_o^* \geq \frac{1}{\sqrt{2}}U_\alpha^* - \sqrt{\frac{3}{2}}U_\beta^* - \frac{\sqrt{3}v_{dc}}{2}$	TeT_{11}^2	$U_o^* < \frac{1}{\sqrt{2}}U_\alpha^* - \sqrt{\frac{3}{2}}U_\beta^* - \frac{\sqrt{3}v_{dc}}{2}$ $U_o^* \geq \frac{1}{\sqrt{2}}U_\alpha^* + \sqrt{\frac{3}{2}}U_\beta^* - \frac{3\sqrt{3}v_{dc}}{4}$	TeT_{12}^2	$U_o^* < \frac{1}{\sqrt{2}}U_\alpha^* + \sqrt{\frac{3}{2}}U_\beta^* - \frac{3\sqrt{3}v_{dc}}{4}$ $U_o^* \geq -\sqrt{2}U_\alpha^*$
TeT_{13}^2	$U_o^* < -\sqrt{2}U_\alpha^*$ $U_o^* \geq \frac{1}{\sqrt{2}}U_\alpha^* - \sqrt{\frac{3}{2}}U_\beta^* - \frac{3\sqrt{3}v_{dc}}{4}$	TeT_{14}^2	$U_o^* < \frac{1}{\sqrt{2}}U_\alpha^* - \sqrt{\frac{3}{2}}U_\beta^* - \frac{3\sqrt{3}v_{dc}}{4}$ $U_o^* \geq \frac{1}{\sqrt{2}}U_\alpha^* + \sqrt{\frac{3}{2}}U_\beta^* - \sqrt{3}v_{dc}$		

PR_3					
TeT_1^3	$U_o^* < -\sqrt{2}U_\alpha^* + \sqrt{3}v_{dc}$ $U_o^* \geq \frac{1}{\sqrt{2}}U_\alpha^* + \sqrt{\frac{3}{2}}U_\beta^*$	TeT_2^3	$U_o^* < \frac{1}{\sqrt{2}}U_\alpha^* + \sqrt{\frac{3}{2}}U_\beta^*$ $U_o^* \geq \frac{1}{\sqrt{2}}U_\alpha^* - \sqrt{\frac{3}{2}}U_\beta^* + \frac{\sqrt{3}v_{dc}}{4}$	TeT_3^3	$U_o^* < \frac{1}{\sqrt{2}}U_\alpha^* - \sqrt{\frac{3}{2}}U_\beta^* + \frac{\sqrt{3}v_{dc}}{4}$ $U_o^* \geq -\sqrt{2}U_\alpha^* + \frac{3\sqrt{3}v_{dc}}{4}$
TeT_4^3	$U_o^* < -\sqrt{2}U_\alpha^* + \frac{3\sqrt{3}v_{dc}}{4}$ $U_o^* \geq \frac{1}{\sqrt{2}}U_\alpha^* + \sqrt{\frac{3}{2}}U_\beta^* - \frac{\sqrt{3}v_{dc}}{4}$	TeT_5^3	$U_o^* < \frac{1}{\sqrt{2}}U_\alpha^* + \sqrt{\frac{3}{2}}U_\beta^* - \frac{\sqrt{3}v_{dc}}{4}$ $U_o^* \geq \frac{1}{\sqrt{2}}U_\alpha^* - \sqrt{\frac{3}{2}}U_\beta^*$	TeT_6^3	$U_o^* < \frac{1}{\sqrt{2}}U_\alpha^* - \sqrt{\frac{3}{2}}U_\beta^*$ $U_o^* \geq -\sqrt{2}U_\alpha^* + \frac{\sqrt{3}v_{dc}}{2}$
TeT_7^3	$U_o^* < -\sqrt{2}U_\alpha^* + \frac{\sqrt{3}v_{dc}}{2}$ $U_o^* \geq \frac{1}{\sqrt{2}}U_\alpha^* + \sqrt{\frac{3}{2}}U_\beta^* - \frac{\sqrt{3}v_{dc}}{2}$	TeT_8^3	$U_o^* < \frac{1}{\sqrt{2}}U_\alpha^* + \sqrt{\frac{3}{2}}U_\beta^* - \frac{\sqrt{3}v_{dc}}{2}$ $U_o^* \geq \frac{1}{\sqrt{2}}U_\alpha^* - \sqrt{\frac{3}{2}}U_\beta^* - \frac{\sqrt{3}v_{dc}}{4}$	TeT_9^3	$U_o^* < \frac{1}{\sqrt{2}}U_\alpha^* - \sqrt{\frac{3}{2}}U_\beta^* - \frac{\sqrt{3}v_{dc}}{4}$ $U_o^* \geq -\sqrt{2}U_\alpha^* + \frac{\sqrt{3}v_{dc}}{4}$
TeT_{10}^3	$U_o^* < -\sqrt{2}U_\alpha^* + \frac{\sqrt{3}v_{dc}}{4}$ $U_o^* \geq \frac{1}{\sqrt{2}}U_\alpha^* + \sqrt{\frac{3}{2}}U_\beta^* - \frac{3\sqrt{3}v_{dc}}{4}$	TeT_{11}^3	$U_o^* < \frac{1}{\sqrt{2}}U_\alpha^* + \sqrt{\frac{3}{2}}U_\beta^* - \frac{3\sqrt{3}v_{dc}}{4}$ $U_o^* \geq \frac{1}{\sqrt{2}}U_\alpha^* - \sqrt{\frac{3}{2}}U_\beta^* - \frac{\sqrt{3}v_{dc}}{2}$	TeT_{12}^3	$U_o^* < \frac{1}{\sqrt{2}}U_\alpha^* - \sqrt{\frac{3}{2}}U_\beta^* - \frac{\sqrt{3}v_{dc}}{2}$ $U_o^* \geq -\sqrt{2}U_\alpha^*$
TeT_{13}^3	$U_o^* < -\sqrt{2}U_\alpha^*$ $U_o^* \geq \frac{1}{\sqrt{2}}U_\alpha^* + \sqrt{\frac{3}{2}}U_\beta^* - \sqrt{3}v_{dc}$				

PR_4					
TeT_1^4	$U_o^* < -\sqrt{2}U_\alpha^* + \sqrt{3}v_{dc}$ $U_o^* \geq \frac{1}{\sqrt{2}}U_\alpha^* - \sqrt{\frac{3}{2}}U_\beta^* + \frac{\sqrt{3}v_{dc}}{2}$	TeT_2^4	$U_o^* < \frac{1}{\sqrt{2}}U_\alpha^* - \sqrt{\frac{3}{2}}U_\beta^* + \frac{\sqrt{3}v_{dc}}{2}$ $U_o^* \geq \frac{1}{\sqrt{2}}U_\alpha^* + \sqrt{\frac{3}{2}}U_\beta^*$	TeT_3^4	$U_o^* < \frac{1}{\sqrt{2}}U_\alpha^* + \sqrt{\frac{3}{2}}U_\beta^*$ $U_o^* \geq -\sqrt{2}U_\alpha^* + \frac{3\sqrt{3}v_{dc}}{4}$
TeT_4^4	$U_o^* < -\sqrt{2}U_\alpha^* + \frac{3\sqrt{3}v_{dc}}{4}$ $U_o^* \geq \frac{1}{\sqrt{2}}U_\alpha^* - \sqrt{\frac{3}{2}}U_\beta^* + \frac{\sqrt{3}v_{dc}}{4}$	TeT_5^4	$U_o^* < \frac{1}{\sqrt{2}}U_\alpha^* - \sqrt{\frac{3}{2}}U_\beta^* + \frac{\sqrt{3}v_{dc}}{4}$ $U_o^* \geq \frac{1}{\sqrt{2}}U_\alpha^* + \sqrt{\frac{3}{2}}U_\beta^* - \frac{\sqrt{3}v_{dc}}{4}$	TeT_6^4	$U_o^* < \frac{1}{\sqrt{2}}U_\alpha^* + \sqrt{\frac{3}{2}}U_\beta^* - \frac{\sqrt{3}v_{dc}}{4}$ $U_o^* \geq -\sqrt{2}U_\alpha^* + \frac{\sqrt{3}v_{dc}}{2}$
TeT_7^4	$U_o^* < -\sqrt{2}U_\alpha^* + \frac{\sqrt{3}v_{dc}}{2}$ $U_o^* \geq \frac{1}{\sqrt{2}}U_\alpha^* - \sqrt{\frac{3}{2}}U_\beta^*$	TeT_8^4	$U_o^* < \frac{1}{\sqrt{2}}U_\alpha^* - \sqrt{\frac{3}{2}}U_\beta^*$ $U_o^* \geq \frac{1}{\sqrt{2}}U_\alpha^* + \sqrt{\frac{3}{2}}U_\beta^* - \frac{\sqrt{3}v_{dc}}{2}$	TeT_9^4	$U_o^* < \frac{1}{\sqrt{2}}U_\alpha^* + \sqrt{\frac{3}{2}}U_\beta^* - \frac{\sqrt{3}v_{dc}}{2}$ $U_o^* \geq -\sqrt{2}U_\alpha^* + \frac{\sqrt{3}v_{dc}}{4}$
TeT_{10}^4	$U_o^* < -\sqrt{2}U_\alpha^* + \frac{\sqrt{3}v_{dc}}{4}$ $U_o^* \geq \frac{1}{\sqrt{2}}U_\alpha^* - \sqrt{\frac{3}{2}}U_\beta^* - \frac{\sqrt{3}v_{dc}}{4}$	TeT_{11}^4	$U_o^* < \frac{1}{\sqrt{2}}U_\alpha^* - \sqrt{\frac{3}{2}}U_\beta^* - \frac{\sqrt{3}v_{dc}}{4}$ $U_o^* \geq \frac{1}{\sqrt{2}}U_\alpha^* + \sqrt{\frac{3}{2}}U_\beta^* - \frac{3\sqrt{3}v_{dc}}{4}$	TeT_{12}^4	$U_o^* < \frac{1}{\sqrt{2}}U_\alpha^* + \sqrt{\frac{3}{2}}U_\beta^* - \frac{3\sqrt{3}v_{dc}}{4}$ $U_o^* \geq -\sqrt{2}U_\alpha^*$
TeT_{13}^4	$U_o^* < -\sqrt{2}U_\alpha^*$ $U_o^* \geq \frac{1}{\sqrt{2}}U_\alpha^* - \sqrt{\frac{3}{2}}U_\beta^* - \frac{\sqrt{3}v_{dc}}{2}$	TeT_{14}^4	$U_o^* < \frac{1}{\sqrt{2}}U_\alpha^* - \sqrt{\frac{3}{2}}U_\beta^* - \frac{\sqrt{3}v_{dc}}{2}$ $U_o^* \geq \frac{1}{\sqrt{2}}U_\alpha^* + \sqrt{\frac{3}{2}}U_\beta^* - \sqrt{3}v_{dc}$		

PR_5					
TeT_1^5	$U_o^* < -\sqrt{2}U_\alpha^* + \sqrt{3}v_{dc}$ $U_o^* \geq \frac{1}{\sqrt{2}}U_\alpha^* + \sqrt{\frac{3}{2}}U_\beta^*$	TeT_2^5	$U_o^* < \frac{1}{\sqrt{2}}U_\alpha^* + \sqrt{\frac{3}{2}}U_\beta^*$ $U_o^* \geq \frac{1}{\sqrt{2}}U_\alpha^* - \sqrt{\frac{3}{2}}U_\beta^* + \frac{\sqrt{3}v_{dc}}{2}$	TeT_3^5	$U_o^* < \frac{1}{\sqrt{2}}U_\alpha^* - \sqrt{\frac{3}{2}}U_\beta^* + \frac{\sqrt{3}v_{dc}}{2}$ $U_o^* \geq -\sqrt{2}U_\alpha^* + \frac{3\sqrt{3}v_{dc}}{4}$
TeT_4^5	$U_o^* < -\sqrt{2}U_\alpha^* + \frac{3\sqrt{3}v_{dc}}{4}$ $U_o^* \geq \frac{1}{\sqrt{2}}U_\alpha^* + \sqrt{\frac{3}{2}}U_\beta^* - \frac{\sqrt{3}v_{dc}}{4}$	TeT_5^5	$U_o^* < \frac{1}{\sqrt{2}}U_\alpha^* + \sqrt{\frac{3}{2}}U_\beta^* - \frac{\sqrt{3}v_{dc}}{4}$ $U_o^* \geq \frac{1}{\sqrt{2}}U_\alpha^* - \sqrt{\frac{3}{2}}U_\beta^* + \frac{\sqrt{3}v_{dc}}{4}$	TeT_6^5	$U_o^* < \frac{1}{\sqrt{2}}U_\alpha^* - \sqrt{\frac{3}{2}}U_\beta^* + \frac{\sqrt{3}v_{dc}}{4}$ $U_o^* \geq -\sqrt{2}U_\alpha^* + \frac{\sqrt{3}v_{dc}}{2}$
TeT_7^5	$U_o^* < -\sqrt{2}U_\alpha^* + \frac{\sqrt{3}v_{dc}}{2}$ $U_o^* \geq \frac{1}{\sqrt{2}}U_\alpha^* + \sqrt{\frac{3}{2}}U_\beta^* - \frac{\sqrt{3}v_{dc}}{2}$	TeT_8^5	$U_o^* < \frac{1}{\sqrt{2}}U_\alpha^* + \sqrt{\frac{3}{2}}U_\beta^* - \frac{\sqrt{3}v_{dc}}{2}$ $U_o^* \geq \frac{1}{\sqrt{2}}U_\alpha^* - \sqrt{\frac{3}{2}}U_\beta^*$	TeT_9^5	$U_o^* < \frac{1}{\sqrt{2}}U_\alpha^* - \sqrt{\frac{3}{2}}U_\beta^*$ $U_o^* \geq -\sqrt{2}U_\alpha^* + \frac{\sqrt{3}v_{dc}}{4}$
TeT_{10}^5	$U_o^* < -\sqrt{2}U_\alpha^* + \frac{\sqrt{3}v_{dc}}{4}$ $U_o^* \geq \frac{1}{\sqrt{2}}U_\alpha^* + \sqrt{\frac{3}{2}}U_\beta^* - \frac{3\sqrt{3}v_{dc}}{4}$	TeT_{11}^5	$U_o^* < \frac{1}{\sqrt{2}}U_\alpha^* + \sqrt{\frac{3}{2}}U_\beta^* - \frac{3\sqrt{3}v_{dc}}{4}$ $U_o^* \geq \frac{1}{\sqrt{2}}U_\alpha^* - \sqrt{\frac{3}{2}}U_\beta^* - \frac{\sqrt{3}v_{dc}}{4}$	TeT_{12}^5	$U_o^* < \frac{1}{\sqrt{2}}U_\alpha^* - \sqrt{\frac{3}{2}}U_\beta^* - \frac{\sqrt{3}v_{dc}}{4}$ $U_o^* \geq -\sqrt{2}U_\alpha^*$
TeT_{13}^5	$U_o^* < -\sqrt{2}U_\alpha^*$ $U_o^* \geq \frac{1}{\sqrt{2}}U_\alpha^* + \sqrt{\frac{3}{2}}U_\beta^* - \sqrt{3}v_{dc}$				

PR_6					
TeT_1^6	$U_o^* < -\sqrt{2}U_\alpha^* + \sqrt{3}v_{dc}$ $U_o^* \geq \frac{1}{\sqrt{2}}U_\alpha^* - \sqrt{\frac{3}{2}}U_\beta^* + \frac{3\sqrt{3}v_{dc}}{4}$	TeT_2^6	$U_o^* < \frac{1}{\sqrt{2}}U_\alpha^* - \sqrt{\frac{3}{2}}U_\beta^* + \frac{3\sqrt{3}v_{dc}}{4}$ $U_o^* \geq \frac{1}{\sqrt{2}}U_\alpha^* + \sqrt{\frac{3}{2}}U_\beta^*$	TeT_3^6	$U_o^* < \frac{1}{\sqrt{2}}U_\alpha^* + \sqrt{\frac{3}{2}}U_\beta^*$ $U_o^* \geq -\sqrt{2}U_\alpha^* + \frac{3\sqrt{3}v_{dc}}{4}$
TeT_4^6	$U_o^* < -\sqrt{2}U_\alpha^* + \frac{3\sqrt{3}v_{dc}}{4}$ $U_o^* \geq \frac{1}{\sqrt{2}}U_\alpha^* - \sqrt{\frac{3}{2}}U_\beta^* + \frac{\sqrt{3}v_{dc}}{2}$	TeT_5^6	$U_o^* < \frac{1}{\sqrt{2}}U_\alpha^* - \sqrt{\frac{3}{2}}U_\beta^* + \frac{\sqrt{3}v_{dc}}{2}$ $U_o^* \geq \frac{1}{\sqrt{2}}U_\alpha^* + \sqrt{\frac{3}{2}}U_\beta^* - \frac{\sqrt{3}v_{dc}}{4}$	TeT_6^6	$U_o^* < \frac{1}{\sqrt{2}}U_\alpha^* + \sqrt{\frac{3}{2}}U_\beta^* - \frac{\sqrt{3}v_{dc}}{4}$ $U_o^* \geq -\sqrt{2}U_\alpha^* + \frac{\sqrt{3}v_{dc}}{2}$
TeT_7^6	$U_o^* < -\sqrt{2}U_\alpha^* + \frac{\sqrt{3}v_{dc}}{2}$ $U_o^* \geq \frac{1}{\sqrt{2}}U_\alpha^* - \sqrt{\frac{3}{2}}U_\beta^* + \frac{\sqrt{3}v_{dc}}{4}$	TeT_8^6	$U_o^* < \frac{1}{\sqrt{2}}U_\alpha^* - \sqrt{\frac{3}{2}}U_\beta^* + \frac{\sqrt{3}v_{dc}}{4}$ $U_o^* \geq \frac{1}{\sqrt{2}}U_\alpha^* + \sqrt{\frac{3}{2}}U_\beta^* - \frac{\sqrt{3}v_{dc}}{2}$	TeT_9^6	$U_o^* < \frac{1}{\sqrt{2}}U_\alpha^* + \sqrt{\frac{3}{2}}U_\beta^* - \frac{\sqrt{3}v_{dc}}{2}$ $U_o^* \geq -\sqrt{2}U_\alpha^* + \frac{\sqrt{3}v_{dc}}{4}$
TeT_{10}^6	$U_o^* < -\sqrt{2}U_\alpha^* + \frac{\sqrt{3}v_{dc}}{4}$ $U_o^* \geq \frac{1}{\sqrt{2}}U_\alpha^* - \sqrt{\frac{3}{2}}U_\beta^*$	TeT_{11}^6	$U_o^* < \frac{1}{\sqrt{2}}U_\alpha^* - \sqrt{\frac{3}{2}}U_\beta^*$ $U_o^* \geq \frac{1}{\sqrt{2}}U_\alpha^* + \sqrt{\frac{3}{2}}U_\beta^* - \frac{3\sqrt{3}v_{dc}}{4}$	TeT_{12}^6	$U_o^* < \frac{1}{\sqrt{2}}U_\alpha^* + \sqrt{\frac{3}{2}}U_\beta^* - \frac{3\sqrt{3}v_{dc}}{4}$ $U_o^* \geq -\sqrt{2}U_\alpha^*$
TeT_{13}^6	$U_o^* < -\sqrt{2}U_\alpha^*$ $U_o^* \geq \frac{1}{\sqrt{2}}U_\alpha^* - \sqrt{\frac{3}{2}}U_\beta^* - \frac{\sqrt{3}v_{dc}}{4}$	TeT_{14}^6	$U_o^* < \frac{1}{\sqrt{2}}U_\alpha^* - \sqrt{\frac{3}{2}}U_\beta^* - \frac{\sqrt{3}v_{dc}}{4}$ $U_o^* \geq \frac{1}{\sqrt{2}}U_\alpha^* + \sqrt{\frac{3}{2}}U_\beta^* - \sqrt{3}v_{dc}$		

PR_7					
TeT_1^7	$U_o^* < -\sqrt{2}U_\alpha^* + \sqrt{3}v_{dc}$ $U_o^* \geq \frac{1}{\sqrt{2}}U_\alpha^* + \sqrt{\frac{3}{2}}U_\beta^*$	TeT_2^7	$U_o^* < \frac{1}{\sqrt{2}}U_\alpha^* + \sqrt{\frac{3}{2}}U_\beta^*$ $U_o^* \geq \frac{1}{\sqrt{2}}U_\alpha^* - \sqrt{\frac{3}{2}}U_\beta^* + \frac{3\sqrt{3}v_{dc}}{4}$	TeT_3^7	$U_o^* < \frac{1}{\sqrt{2}}U_\alpha^* - \sqrt{\frac{3}{2}}U_\beta^* + \frac{3\sqrt{3}v_{dc}}{4}$ $U_o^* \geq -\sqrt{2}U_\alpha^* + \frac{3\sqrt{3}v_{dc}}{4}$
TeT_4^7	$U_o^* < -\sqrt{2}U_\alpha^* + \frac{3\sqrt{3}v_{dc}}{4}$ $U_o^* \geq \frac{1}{\sqrt{2}}U_\alpha^* + \sqrt{\frac{3}{2}}U_\beta^* - \frac{\sqrt{3}v_{dc}}{4}$	TeT_5^7	$U_o^* < \frac{1}{\sqrt{2}}U_\alpha^* + \sqrt{\frac{3}{2}}U_\beta^* - \frac{\sqrt{3}v_{dc}}{4}$ $U_o^* \geq \frac{1}{\sqrt{2}}U_\alpha^* - \sqrt{\frac{3}{2}}U_\beta^* + \frac{\sqrt{3}v_{dc}}{2}$	TeT_6^7	$U_o^* < \frac{1}{\sqrt{2}}U_\alpha^* - \sqrt{\frac{3}{2}}U_\beta^* + \frac{\sqrt{3}v_{dc}}{2}$ $U_o^* \geq -\sqrt{2}U_\alpha^* + \frac{\sqrt{3}v_{dc}}{2}$
TeT_7^7	$U_o^* < -\sqrt{2}U_\alpha^* + \frac{\sqrt{3}v_{dc}}{2}$ $U_o^* \geq \frac{1}{\sqrt{2}}U_\alpha^* + \sqrt{\frac{3}{2}}U_\beta^* - \frac{\sqrt{3}v_{dc}}{2}$	TeT_8^7	$U_o^* < \frac{1}{\sqrt{2}}U_\alpha^* + \sqrt{\frac{3}{2}}U_\beta^* - \frac{\sqrt{3}v_{dc}}{2}$ $U_o^* \geq \frac{1}{\sqrt{2}}U_\alpha^* - \sqrt{\frac{3}{2}}U_\beta^* + \frac{\sqrt{3}v_{dc}}{4}$	TeT_9^7	$U_o^* < \frac{1}{\sqrt{2}}U_\alpha^* - \sqrt{\frac{3}{2}}U_\beta^* + \frac{\sqrt{3}v_{dc}}{4}$ $U_o^* \geq -\sqrt{2}U_\alpha^* + \frac{\sqrt{3}v_{dc}}{4}$
TeT_{10}^7	$U_o^* < -\sqrt{2}U_\alpha^* + \frac{\sqrt{3}v_{dc}}{4}$ $U_o^* \geq \frac{1}{\sqrt{2}}U_\alpha^* + \sqrt{\frac{3}{2}}U_\beta^* - \frac{3\sqrt{3}v_{dc}}{4}$	TeT_{11}^7	$U_o^* < \frac{1}{\sqrt{2}}U_\alpha^* + \sqrt{\frac{3}{2}}U_\beta^* - \frac{3\sqrt{3}v_{dc}}{4}$ $U_o^* \geq \frac{1}{\sqrt{2}}U_\alpha^* - \sqrt{\frac{3}{2}}U_\beta^*$	TeT_{12}^7	$U_o^* < \frac{1}{\sqrt{2}}U_\alpha^* - \sqrt{\frac{3}{2}}U_\beta^*$ $U_o^* \geq -\sqrt{2}U_\alpha^*$
TeT_{13}^7	$U_o^* < -\sqrt{2}U_\alpha^*$ $U_o^* \geq \frac{1}{\sqrt{2}}U_\alpha^* + \sqrt{\frac{3}{2}}U_\beta^* - \sqrt{3}v_{dc}$				

PR_8					
TeT_1^8	$U_o^* < -\sqrt{2}U_\alpha^* + \sqrt{3}v_{dc}$ $U_o^* \geq \frac{1}{\sqrt{2}}U_\alpha^* + \sqrt{\frac{3}{2}}U_\beta^* + \frac{\sqrt{3}v_{dc}}{4}$	TeT_2^8	$U_o^* < \frac{1}{\sqrt{2}}U_\alpha^* + \sqrt{\frac{3}{2}}U_\beta^* + \frac{\sqrt{3}v_{dc}}{4}$ $U_o^* \geq \frac{1}{\sqrt{2}}U_\alpha^* - \sqrt{\frac{3}{2}}U_\beta^* + \frac{\sqrt{3}v_{dc}}{4}$	TeT_3^8	$U_o^* < \frac{1}{\sqrt{2}}U_\alpha^* - \sqrt{\frac{3}{2}}U_\beta^* + \frac{\sqrt{3}v_{dc}}{4}$ $U_o^* \geq -\sqrt{2}U_\alpha^* + \frac{3\sqrt{3}v_{dc}}{4}$
TeT_4^8	$U_o^* < -\sqrt{2}U_\alpha^* + \frac{3\sqrt{3}v_{dc}}{4}$ $U_o^* \geq \frac{1}{\sqrt{2}}U_\alpha^* + \sqrt{\frac{3}{2}}U_\beta^*$	TeT_5^8	$U_o^* < \frac{1}{\sqrt{2}}U_\alpha^* + \sqrt{\frac{3}{2}}U_\beta^*$ $U_o^* \geq \frac{1}{\sqrt{2}}U_\alpha^* - \sqrt{\frac{3}{2}}U_\beta^*$	TeT_6^8	$U_o^* < \frac{1}{\sqrt{2}}U_\alpha^* - \sqrt{\frac{3}{2}}U_\beta^*$ $U_o^* \geq -\sqrt{2}U_\alpha^* + \frac{\sqrt{3}v_{dc}}{2}$
TeT_7^8	$U_o^* < -\sqrt{2}U_\alpha^* + \frac{\sqrt{3}v_{dc}}{2}$ $U_o^* \geq \frac{1}{\sqrt{2}}U_\alpha^* + \sqrt{\frac{3}{2}}U_\beta^* - \frac{\sqrt{3}v_{dc}}{4}$	TeT_8^8	$U_o^* < \frac{1}{\sqrt{2}}U_\alpha^* + \sqrt{\frac{3}{2}}U_\beta^* - \frac{\sqrt{3}v_{dc}}{4}$ $U_o^* \geq \frac{1}{\sqrt{2}}U_\alpha^* - \sqrt{\frac{3}{2}}U_\beta^* - \frac{\sqrt{3}v_{dc}}{4}$	TeT_9^8	$U_o^* < \frac{1}{\sqrt{2}}U_\alpha^* - \sqrt{\frac{3}{2}}U_\beta^* - \frac{\sqrt{3}v_{dc}}{4}$ $U_o^* \geq -\sqrt{2}U_\alpha^* + \frac{\sqrt{3}v_{dc}}{4}$
TeT_{10}^8	$U_o^* < -\sqrt{2}U_\alpha^* + \frac{\sqrt{3}v_{dc}}{4}$ $U_o^* \geq \frac{1}{\sqrt{2}}U_\alpha^* + \sqrt{\frac{3}{2}}U_\beta^* - \frac{\sqrt{3}v_{dc}}{2}$	TeT_{11}^8	$U_o^* < \frac{1}{\sqrt{2}}U_\alpha^* + \sqrt{\frac{3}{2}}U_\beta^* - \frac{\sqrt{3}v_{dc}}{2}$ $U_o^* \geq \frac{1}{\sqrt{2}}U_\alpha^* - \sqrt{\frac{3}{2}}U_\beta^* - \frac{\sqrt{3}v_{dc}}{2}$	TeT_{12}^8	$U_o^* < \frac{1}{\sqrt{2}}U_\alpha^* - \sqrt{\frac{3}{2}}U_\beta^* - \frac{\sqrt{3}v_{dc}}{2}$ $U_o^* \geq -\sqrt{2}U_\alpha^*$
TeT_{13}^8	$U_o^* < -\sqrt{2}U_\alpha^*$ $U_o^* \geq \frac{1}{\sqrt{2}}U_\alpha^* + \sqrt{\frac{3}{2}}U_\beta^* - \frac{3\sqrt{3}v_{dc}}{4}$	TeT_{14}^8	$U_o^* < \frac{1}{\sqrt{2}}U_\alpha^* + \sqrt{\frac{3}{2}}U_\beta^* - \frac{3\sqrt{3}v_{dc}}{4}$ $U_o^* \geq \frac{1}{\sqrt{2}}U_\alpha^* - \sqrt{\frac{3}{2}}U_\beta^* - \frac{3\sqrt{3}v_{dc}}{4}$	TeT_{15}^8	$U_o^* < \frac{1}{\sqrt{2}}U_\alpha^* - \sqrt{\frac{3}{2}}U_\beta^* - \frac{3\sqrt{3}v_{dc}}{4}$ $U_o^* \geq -\sqrt{2}U_\alpha^* - \frac{\sqrt{3}v_{dc}}{4}$
TeT_{16}^8	$U_o^* < -\sqrt{2}U_\alpha^* - \frac{\sqrt{3}v_{dc}}{4}$ $U_o^* \geq \frac{1}{\sqrt{2}}U_\alpha^* + \sqrt{\frac{3}{2}}U_\beta^* - \sqrt{3}v_{dc}$				

PR_9					
TeT_1^9	$U_o^* < -\sqrt{2}U_\alpha^* + \sqrt{3}v_{dc}$ $U_o^* \geq \frac{1}{\sqrt{2}}U_\alpha^* - \sqrt{\frac{3}{2}}U_\beta^* + \frac{\sqrt{3}v_{dc}}{2}$	TeT_2^9	$U_o^* < \frac{1}{\sqrt{2}}U_\alpha^* - \sqrt{\frac{3}{2}}U_\beta^* + \frac{\sqrt{3}v_{dc}}{2}$ $U_o^* \geq \frac{1}{\sqrt{2}}U_\alpha^* + \sqrt{\frac{3}{2}}U_\beta^* + \frac{\sqrt{3}v_{dc}}{4}$	TeT_3^9	$U_o^* < \frac{1}{\sqrt{2}}U_\alpha^* + \sqrt{\frac{3}{2}}U_\beta^* + \frac{\sqrt{3}v_{dc}}{4}$ $U_o^* \geq -\sqrt{2}U_\alpha^* + \frac{3\sqrt{3}v_{dc}}{4}$
TeT_4^9	$U_o^* < -\sqrt{2}U_\alpha^* + \frac{3\sqrt{3}v_{dc}}{4}$ $U_o^* \geq \frac{1}{\sqrt{2}}U_\alpha^* - \sqrt{\frac{3}{2}}U_\beta^* + \frac{\sqrt{3}v_{dc}}{4}$	TeT_5^9	$U_o^* < \frac{1}{\sqrt{2}}U_\alpha^* - \sqrt{\frac{3}{2}}U_\beta^* + \frac{\sqrt{3}v_{dc}}{4}$ $U_o^* \geq \frac{1}{\sqrt{2}}U_\alpha^* + \sqrt{\frac{3}{2}}U_\beta^*$	TeT_6^9	$U_o^* < \frac{1}{\sqrt{2}}U_\alpha^* + \sqrt{\frac{3}{2}}U_\beta^*$ $U_o^* \geq -\sqrt{2}U_\alpha^* + \frac{\sqrt{3}v_{dc}}{2}$
TeT_7^9	$U_o^* < -\sqrt{2}U_\alpha^* + \frac{\sqrt{3}v_{dc}}{2}$ $U_o^* \geq \frac{1}{\sqrt{2}}U_\alpha^* - \sqrt{\frac{3}{2}}U_\beta^*$	TeT_8^9	$U_o^* < \frac{1}{\sqrt{2}}U_\alpha^* - \sqrt{\frac{3}{2}}U_\beta^*$ $U_o^* \geq \frac{1}{\sqrt{2}}U_\alpha^* + \sqrt{\frac{3}{2}}U_\beta^* - \frac{\sqrt{3}v_{dc}}{4}$	TeT_9^9	$U_o^* < \frac{1}{\sqrt{2}}U_\alpha^* + \sqrt{\frac{3}{2}}U_\beta^* - \frac{\sqrt{3}v_{dc}}{4}$ $U_o^* \geq -\sqrt{2}U_\alpha^* + \frac{\sqrt{3}v_{dc}}{4}$
TeT_{10}^9	$U_o^* < -\sqrt{2}U_\alpha^* + \frac{\sqrt{3}v_{dc}}{4}$ $U_o^* \geq \frac{1}{\sqrt{2}}U_\alpha^* - \sqrt{\frac{3}{2}}U_\beta^* - \frac{\sqrt{3}v_{dc}}{4}$	TeT_{11}^9	$U_o^* < \frac{1}{\sqrt{2}}U_\alpha^* - \sqrt{\frac{3}{2}}U_\beta^* - \frac{\sqrt{3}v_{dc}}{4}$ $U_o^* \geq \frac{1}{\sqrt{2}}U_\alpha^* + \sqrt{\frac{3}{2}}U_\beta^* - \frac{\sqrt{3}v_{dc}}{2}$	TeT_{12}^9	$U_o^* < \frac{1}{\sqrt{2}}U_\alpha^* + \sqrt{\frac{3}{2}}U_\beta^* - \frac{\sqrt{3}v_{dc}}{2}$ $U_o^* \geq -\sqrt{2}U_\alpha^*$
TeT_{13}^9	$U_o^* < -\sqrt{2}U_\alpha^*$ $U_o^* \geq \frac{1}{\sqrt{2}}U_\alpha^* - \sqrt{\frac{3}{2}}U_\beta^* - \frac{\sqrt{3}v_{dc}}{2}$	TeT_{14}^9	$U_o^* < \frac{1}{\sqrt{2}}U_\alpha^* - \sqrt{\frac{3}{2}}U_\beta^* - \frac{\sqrt{3}v_{dc}}{2}$ $U_o^* \geq \frac{1}{\sqrt{2}}U_\alpha^* + \sqrt{\frac{3}{2}}U_\beta^* - \frac{3\sqrt{3}v_{dc}}{4}$	TeT_{15}^9	$U_o^* < \frac{1}{\sqrt{2}}U_\alpha^* + \sqrt{\frac{3}{2}}U_\beta^* - \frac{3\sqrt{3}v_{dc}}{4}$ $U_o^* \geq -\sqrt{2}U_\alpha^* - \frac{\sqrt{3}v_{dc}}{4}$
TeT_{16}^9	$U_o^* < -\sqrt{2}U_\alpha^* - \frac{\sqrt{3}v_{dc}}{4}$ $U_o^* \geq \frac{1}{\sqrt{2}}U_\alpha^* - \sqrt{\frac{3}{2}}U_\beta^* - \frac{3\sqrt{3}v_{dc}}{4}$	TeT_{17}^9	$U_o^* < \frac{1}{\sqrt{2}}U_\alpha^* - \sqrt{\frac{3}{2}}U_\beta^* - \frac{3\sqrt{3}v_{dc}}{4}$ $U_o^* \geq \frac{1}{\sqrt{2}}U_\alpha^* + \sqrt{\frac{3}{2}}U_\beta^* - \sqrt{3}v_{dc}$		

PR_{10}					
TeT_1^{10}	$U_o^* < -\sqrt{2}U_\alpha^* + \sqrt{3}v_{dc}$ $U_o^* \geq \frac{1}{\sqrt{2}}U_\alpha^* + \sqrt{\frac{3}{2}}U_\beta^* + \frac{\sqrt{3}v_{dc}}{4}$	TeT_2^{10}	$U_o^* < \frac{1}{\sqrt{2}}U_\alpha^* + \sqrt{\frac{3}{2}}U_\beta^* + \frac{\sqrt{3}v_{dc}}{4}$ $U_o^* \geq \frac{1}{\sqrt{2}}U_\alpha^* - \sqrt{\frac{3}{2}}U_\beta^* + \frac{\sqrt{3}v_{dc}}{2}$	TeT_3^{10}	$U_o^* < \frac{1}{\sqrt{2}}U_\alpha^* - \sqrt{\frac{3}{2}}U_\beta^* + \frac{\sqrt{3}v_{dc}}{2}$ $U_o^* \geq -\sqrt{2}U_\alpha^* + \frac{3\sqrt{3}v_{dc}}{4}$
TeT_4^{10}	$U_o^* < -\sqrt{2}U_\alpha^* + \frac{3\sqrt{3}v_{dc}}{4}$ $U_o^* \geq \frac{1}{\sqrt{2}}U_\alpha^* + \sqrt{\frac{3}{2}}U_\beta^*$	TeT_5^{10}	$U_o^* < \frac{1}{\sqrt{2}}U_\alpha^* + \sqrt{\frac{3}{2}}U_\beta^*$ $U_o^* \geq \frac{1}{\sqrt{2}}U_\alpha^* - \sqrt{\frac{3}{2}}U_\beta^* + \frac{\sqrt{3}v_{dc}}{4}$	TeT_6^{10}	$U_o^* < \frac{1}{\sqrt{2}}U_\alpha^* - \sqrt{\frac{3}{2}}U_\beta^* + \frac{\sqrt{3}v_{dc}}{4}$ $U_o^* \geq -\sqrt{2}U_\alpha^* + \frac{\sqrt{3}v_{dc}}{2}$
TeT_7^{10}	$U_o^* < -\sqrt{2}U_\alpha^* + \frac{\sqrt{3}v_{dc}}{2}$ $U_o^* \geq \frac{1}{\sqrt{2}}U_\alpha^* + \sqrt{\frac{3}{2}}U_\beta^* - \frac{\sqrt{3}v_{dc}}{4}$	TeT_8^{10}	$U_o^* < \frac{1}{\sqrt{2}}U_\alpha^* + \sqrt{\frac{3}{2}}U_\beta^* - \frac{\sqrt{3}v_{dc}}{4}$ $U_o^* \geq \frac{1}{\sqrt{2}}U_\alpha^* - \sqrt{\frac{3}{2}}U_\beta^*$	TeT_9^{10}	$U_o^* < \frac{1}{\sqrt{2}}U_\alpha^* - \sqrt{\frac{3}{2}}U_\beta^*$ $U_o^* \geq -\sqrt{2}U_\alpha^* + \frac{\sqrt{3}v_{dc}}{4}$
TeT_{10}^{10}	$U_o^* < -\sqrt{2}U_\alpha^* + \frac{\sqrt{3}v_{dc}}{4}$ $U_o^* \geq \frac{1}{\sqrt{2}}U_\alpha^* + \sqrt{\frac{3}{2}}U_\beta^* - \frac{\sqrt{3}v_{dc}}{2}$	TeT_{11}^{10}	$U_o^* < \frac{1}{\sqrt{2}}U_\alpha^* + \sqrt{\frac{3}{2}}U_\beta^* - \frac{\sqrt{3}v_{dc}}{2}$ $U_o^* \geq \frac{1}{\sqrt{2}}U_\alpha^* - \sqrt{\frac{3}{2}}U_\beta^* - \frac{\sqrt{3}v_{dc}}{4}$	TeT_{12}^{10}	$U_o^* < \frac{1}{\sqrt{2}}U_\alpha^* - \sqrt{\frac{3}{2}}U_\beta^* - \frac{\sqrt{3}v_{dc}}{4}$ $U_o^* \geq -\sqrt{2}U_\alpha^*$
TeT_{13}^{10}	$U_o^* < -\sqrt{2}U_\alpha^*$ $U_o^* \geq \frac{1}{\sqrt{2}}U_\alpha^* + \sqrt{\frac{3}{2}}U_\beta^* - \frac{3\sqrt{3}v_{dc}}{4}$	TeT_{14}^{10}	$U_o^* < \frac{1}{\sqrt{2}}U_\alpha^* + \sqrt{\frac{3}{2}}U_\beta^* - \frac{3\sqrt{3}v_{dc}}{4}$ $U_o^* \geq \frac{1}{\sqrt{2}}U_\alpha^* - \sqrt{\frac{3}{2}}U_\beta^* - \frac{\sqrt{3}v_{dc}}{2}$	TeT_{15}^{10}	$U_o^* < \frac{1}{\sqrt{2}}U_\alpha^* - \sqrt{\frac{3}{2}}U_\beta^* - \frac{\sqrt{3}v_{dc}}{2}$ $U_o^* \geq -\sqrt{2}U_\alpha^* - \frac{\sqrt{3}v_{dc}}{4}$
TeT_{16}^{10}	$U_o^* < -\sqrt{2}U_\alpha^* - \frac{\sqrt{3}v_{dc}}{4}$ $U_o^* \geq \frac{1}{\sqrt{2}}U_\alpha^* + \sqrt{\frac{3}{2}}U_\beta^* - \sqrt{3}v_{dc}$				

PR_{11}					
TeT_1^{11}	$U_o^* < -\sqrt{2}U_\alpha^* + \sqrt{3}v_{dc}$ $U_o^* \geq \frac{1}{\sqrt{2}}U_\alpha^* - \sqrt{\frac{3}{2}}U_\beta^* + \frac{3\sqrt{3}v_{dc}}{4}$	TeT_2^{11}	$U_o^* < \frac{1}{\sqrt{2}}U_\alpha^* - \sqrt{\frac{3}{2}}U_\beta^* + \frac{3\sqrt{3}v_{dc}}{4}$ $U_o^* \geq \frac{1}{\sqrt{2}}U_\alpha^* + \sqrt{\frac{3}{2}}U_\beta^* + \frac{\sqrt{3}v_{dc}}{4}$	TeT_3^{11}	$U_o^* < \frac{1}{\sqrt{2}}U_\alpha^* + \sqrt{\frac{3}{2}}U_\beta^* + \frac{\sqrt{3}v_{dc}}{4}$ $U_o^* \geq -\sqrt{2}U_\alpha^* + \frac{3\sqrt{3}v_{dc}}{4}$
TeT_4^{11}	$U_o^* < -\sqrt{2}U_\alpha^* + \frac{3\sqrt{3}v_{dc}}{4}$ $U_o^* \geq \frac{1}{\sqrt{2}}U_\alpha^* - \sqrt{\frac{3}{2}}U_\beta^* + \frac{\sqrt{3}v_{dc}}{2}$	TeT_5^{11}	$U_o^* < \frac{1}{\sqrt{2}}U_\alpha^* - \sqrt{\frac{3}{2}}U_\beta^* + \frac{\sqrt{3}v_{dc}}{2}$ $U_o^* \geq \frac{1}{\sqrt{2}}U_\alpha^* + \sqrt{\frac{3}{2}}U_\beta^*$	TeT_6^{11}	$U_o^* < \frac{1}{\sqrt{2}}U_\alpha^* + \sqrt{\frac{3}{2}}U_\beta^*$ $U_o^* \geq -\sqrt{2}U_\alpha^* + \frac{\sqrt{3}v_{dc}}{2}$
TeT_7^{11}	$U_o^* < -\sqrt{2}U_\alpha^* + \frac{\sqrt{3}v_{dc}}{2}$ $U_o^* \geq \frac{1}{\sqrt{2}}U_\alpha^* - \sqrt{\frac{3}{2}}U_\beta^* + \frac{\sqrt{3}v_{dc}}{4}$	TeT_8^{11}	$U_o^* < \frac{1}{\sqrt{2}}U_\alpha^* - \sqrt{\frac{3}{2}}U_\beta^* + \frac{\sqrt{3}v_{dc}}{4}$ $U_o^* \geq \frac{1}{\sqrt{2}}U_\alpha^* + \sqrt{\frac{3}{2}}U_\beta^* - \frac{\sqrt{3}v_{dc}}{4}$	TeT_9^{11}	$U_o^* < \frac{1}{\sqrt{2}}U_\alpha^* + \sqrt{\frac{3}{2}}U_\beta^* - \frac{\sqrt{3}v_{dc}}{4}$ $U_o^* \geq -\sqrt{2}U_\alpha^* + \frac{\sqrt{3}v_{dc}}{4}$
TeT_{10}^{11}	$U_o^* < -\sqrt{2}U_\alpha^* + \frac{\sqrt{3}v_{dc}}{4}$ $U_o^* \geq \frac{1}{\sqrt{2}}U_\alpha^* - \sqrt{\frac{3}{2}}U_\beta^*$	TeT_{11}^{11}	$U_o^* < \frac{1}{\sqrt{2}}U_\alpha^* - \sqrt{\frac{3}{2}}U_\beta^*$ $U_o^* \geq \frac{1}{\sqrt{2}}U_\alpha^* + \sqrt{\frac{3}{2}}U_\beta^* - \frac{\sqrt{3}v_{dc}}{2}$	TeT_{12}^{11}	$U_o^* < \frac{1}{\sqrt{2}}U_\alpha^* + \sqrt{\frac{3}{2}}U_\beta^* - \frac{\sqrt{3}v_{dc}}{2}$ $U_o^* \geq -\sqrt{2}U_\alpha^*$
TeT_{13}^{11}	$U_o^* < -\sqrt{2}U_\alpha^*$ $U_o^* \geq \frac{1}{\sqrt{2}}U_\alpha^* - \sqrt{\frac{3}{2}}U_\beta^* - \frac{\sqrt{3}v_{dc}}{4}$	TeT_{14}^{11}	$U_o^* < \frac{1}{\sqrt{2}}U_\alpha^* - \sqrt{\frac{3}{2}}U_\beta^* - \frac{\sqrt{3}v_{dc}}{4}$ $U_o^* \geq \frac{1}{\sqrt{2}}U_\alpha^* + \sqrt{\frac{3}{2}}U_\beta^* - \frac{3\sqrt{3}v_{dc}}{4}$	TeT_{15}^{11}	$U_o^* < \frac{1}{\sqrt{2}}U_\alpha^* + \sqrt{\frac{3}{2}}U_\beta^* - \frac{3\sqrt{3}v_{dc}}{4}$ $U_o^* \geq -\sqrt{2}U_\alpha^* - \frac{\sqrt{3}v_{dc}}{4}$
TeT_{16}^{11}	$U_o^* < -\sqrt{2}U_\alpha^* - \frac{\sqrt{3}v_{dc}}{4}$ $U_o^* \geq \frac{1}{\sqrt{2}}U_\alpha^* - \sqrt{\frac{3}{2}}U_\beta^* - \frac{\sqrt{3}v_{dc}}{2}$	TeT_{17}^{11}	$U_o^* < \frac{1}{\sqrt{2}}U_\alpha^* - \sqrt{\frac{3}{2}}U_\beta^* - \frac{\sqrt{3}v_{dc}}{2}$ $U_o^* \geq \frac{1}{\sqrt{2}}U_\alpha^* + \sqrt{\frac{3}{2}}U_\beta^* - \sqrt{3}v_{dc}$		

PR_{12}					
TeT_1^{12}	$u_o^* < -\sqrt{2}u_\alpha^* + \sqrt{3}v_{dc}$ $u_o^* \geq \frac{1}{\sqrt{2}}u_\alpha^* + \sqrt{\frac{3}{2}}u_\beta^* + \frac{\sqrt{3}v_{dc}}{4}$	TeT_2^{12}	$u_o^* < \frac{1}{\sqrt{2}}u_\alpha^* + \sqrt{\frac{3}{2}}u_\beta^* + \frac{\sqrt{3}v_{dc}}{4}$ $u_o^* \geq \frac{1}{\sqrt{2}}u_\alpha^* - \sqrt{\frac{3}{2}}u_\beta^* + \frac{3\sqrt{3}v_{dc}}{4}$	TeT_3^{12}	$u_o^* < \frac{1}{\sqrt{2}}u_\alpha^* - \sqrt{\frac{3}{2}}u_\beta^* + \frac{3\sqrt{3}v_{dc}}{4}$ $u_o^* \geq -\sqrt{2}u_\alpha^* + \frac{3\sqrt{3}v_{dc}}{4}$
TeT_4^{12}	$u_o^* < -\sqrt{2}u_\alpha^* + \frac{3\sqrt{3}v_{dc}}{4}$ $u_o^* \geq \frac{1}{\sqrt{2}}u_\alpha^* + \sqrt{\frac{3}{2}}u_\beta^*$	TeT_5^{12}	$u_o^* < \frac{1}{\sqrt{2}}u_\alpha^* + \sqrt{\frac{3}{2}}u_\beta^*$ $u_o^* \geq \frac{1}{\sqrt{2}}u_\alpha^* - \sqrt{\frac{3}{2}}u_\beta^* + \frac{\sqrt{3}v_{dc}}{2}$	TeT_6^{12}	$u_o^* < \frac{1}{\sqrt{2}}u_\alpha^* - \sqrt{\frac{3}{2}}u_\beta^* + \frac{\sqrt{3}v_{dc}}{2}$ $u_o^* \geq -\sqrt{2}u_\alpha^* + \frac{\sqrt{3}v_{dc}}{2}$
TeT_7^{12}	$u_o^* < -\sqrt{2}u_\alpha^* + \frac{\sqrt{3}v_{dc}}{2}$ $u_o^* \geq \frac{1}{\sqrt{2}}u_\alpha^* + \sqrt{\frac{3}{2}}u_\beta^* - \frac{\sqrt{3}v_{dc}}{4}$	TeT_8^{12}	$u_o^* < \frac{1}{\sqrt{2}}u_\alpha^* + \sqrt{\frac{3}{2}}u_\beta^* - \frac{\sqrt{3}v_{dc}}{4}$ $u_o^* \geq \frac{1}{\sqrt{2}}u_\alpha^* - \sqrt{\frac{3}{2}}u_\beta^* + \frac{\sqrt{3}v_{dc}}{4}$	TeT_9^{12}	$u_o^* < \frac{1}{\sqrt{2}}u_\alpha^* - \sqrt{\frac{3}{2}}u_\beta^* + \frac{\sqrt{3}v_{dc}}{4}$ $u_o^* \geq -\sqrt{2}u_\alpha^* + \frac{\sqrt{3}v_{dc}}{4}$
TeT_{10}^{12}	$u_o^* < -\sqrt{2}u_\alpha^* + \frac{\sqrt{3}v_{dc}}{4}$ $u_o^* \geq \frac{1}{\sqrt{2}}u_\alpha^* + \sqrt{\frac{3}{2}}u_\beta^* - \frac{\sqrt{3}v_{dc}}{2}$	TeT_{11}^{12}	$u_o^* < \frac{1}{\sqrt{2}}u_\alpha^* + \sqrt{\frac{3}{2}}u_\beta^* - \frac{\sqrt{3}v_{dc}}{2}$ $u_o^* \geq \frac{1}{\sqrt{2}}u_\alpha^* - \sqrt{\frac{3}{2}}u_\beta^*$	TeT_{12}^{12}	$u_o^* < \frac{1}{\sqrt{2}}u_\alpha^* - \sqrt{\frac{3}{2}}u_\beta^*$ $u_o^* \geq -\sqrt{2}u_\alpha^*$
TeT_{13}^{12}	$u_o^* < -\sqrt{2}u_\alpha^*$ $u_o^* \geq \frac{1}{\sqrt{2}}u_\alpha^* + \sqrt{\frac{3}{2}}u_\beta^* - \frac{3\sqrt{3}v_{dc}}{4}$	TeT_{14}^{12}	$u_o^* < \frac{1}{\sqrt{2}}u_\alpha^* + \sqrt{\frac{3}{2}}u_\beta^* - \frac{3\sqrt{3}v_{dc}}{4}$ $u_o^* \geq \frac{1}{\sqrt{2}}u_\alpha^* - \sqrt{\frac{3}{2}}u_\beta^* - \frac{\sqrt{3}v_{dc}}{4}$	TeT_{15}^{12}	$u_o^* < \frac{1}{\sqrt{2}}u_\alpha^* - \sqrt{\frac{3}{2}}u_\beta^* - \frac{\sqrt{3}v_{dc}}{4}$ $u_o^* \geq -\sqrt{2}u_\alpha^* - \frac{\sqrt{3}v_{dc}}{4}$
TeT_{16}^{12}	$u_o^* < -\sqrt{2}u_\alpha^* - \frac{\sqrt{3}v_{dc}}{4}$ $u_o^* \geq \frac{1}{\sqrt{2}}u_\alpha^* + \sqrt{\frac{3}{2}}u_\beta^* - \sqrt{3}v_{dc}$				

PR_{13}					
TeT_1^{13}	$U_o^* < -\sqrt{2}U_\alpha^* + \sqrt{3}v_{dc}$ $U_o^* \geq \frac{1}{\sqrt{2}}U_\alpha^* + \sqrt{\frac{3}{2}}U_\beta^* + \frac{\sqrt{3}v_{dc}}{2}$	TeT_2^{13}	$U_o^* < \frac{1}{\sqrt{2}}U_\alpha^* + \sqrt{\frac{3}{2}}U_\beta^* + \frac{\sqrt{3}v_{dc}}{2}$ $U_o^* \geq \frac{1}{\sqrt{2}}U_\alpha^* - \sqrt{\frac{3}{2}}U_\beta^* + \frac{\sqrt{3}v_{dc}}{2}$	TeT_3^{13}	$U_o^* < \frac{1}{\sqrt{2}}U_\alpha^* - \sqrt{\frac{3}{2}}U_\beta^* + \frac{\sqrt{3}v_{dc}}{2}$ $U_o^* \geq -\sqrt{2}U_\alpha^* + \frac{3\sqrt{3}v_{dc}}{4}$
TeT_4^{13}	$U_o^* < -\sqrt{2}U_\alpha^* + \frac{3\sqrt{3}v_{dc}}{4}$ $U_o^* \geq \frac{1}{\sqrt{2}}U_\alpha^* + \sqrt{\frac{3}{2}}U_\beta^* + \frac{\sqrt{3}v_{dc}}{4}$	TeT_5^{13}	$U_o^* < \frac{1}{\sqrt{2}}U_\alpha^* + \sqrt{\frac{3}{2}}U_\beta^* + \frac{\sqrt{3}v_{dc}}{4}$ $U_o^* \geq \frac{1}{\sqrt{2}}U_\alpha^* - \sqrt{\frac{3}{2}}U_\beta^* + \frac{\sqrt{3}v_{dc}}{4}$	TeT_6^{13}	$U_o^* < \frac{1}{\sqrt{2}}U_\alpha^* - \sqrt{\frac{3}{2}}U_\beta^* + \frac{\sqrt{3}v_{dc}}{4}$ $U_o^* \geq -\sqrt{2}U_\alpha^* + \frac{\sqrt{3}v_{dc}}{2}$
TeT_7^{13}	$U_o^* < -\sqrt{2}U_\alpha^* + \frac{\sqrt{3}v_{dc}}{2}$ $U_o^* \geq \frac{1}{\sqrt{2}}U_\alpha^* + \sqrt{\frac{3}{2}}U_\beta^*$	TeT_8^{13}	$U_o^* < \frac{1}{\sqrt{2}}U_\alpha^* + \sqrt{\frac{3}{2}}U_\beta^*$ $U_o^* \geq \frac{1}{\sqrt{2}}U_\alpha^* - \sqrt{\frac{3}{2}}U_\beta^*$	TeT_9^{13}	$U_o^* < \frac{1}{\sqrt{2}}U_\alpha^* - \sqrt{\frac{3}{2}}U_\beta^*$ $U_o^* \geq -\sqrt{2}U_\alpha^* + \frac{\sqrt{3}v_{dc}}{4}$
TeT_{10}^{13}	$U_o^* < -\sqrt{2}U_\alpha^* + \frac{\sqrt{3}v_{dc}}{4}$ $U_o^* \geq \frac{1}{\sqrt{2}}U_\alpha^* + \sqrt{\frac{3}{2}}U_\beta^* - \frac{\sqrt{3}v_{dc}}{4}$	TeT_{11}^{13}	$U_o^* < \frac{1}{\sqrt{2}}U_\alpha^* + \sqrt{\frac{3}{2}}U_\beta^* - \frac{\sqrt{3}v_{dc}}{4}$ $U_o^* \geq \frac{1}{\sqrt{2}}U_\alpha^* - \sqrt{\frac{3}{2}}U_\beta^* - \frac{\sqrt{3}v_{dc}}{4}$	TeT_{12}^{13}	$U_o^* < \frac{1}{\sqrt{2}}U_\alpha^* - \sqrt{\frac{3}{2}}U_\beta^* - \frac{\sqrt{3}v_{dc}}{4}$ $U_o^* \geq -\sqrt{2}U_\alpha^*$
TeT_{13}^{13}	$U_o^* < -\sqrt{2}U_\alpha^*$ $U_o^* \geq \frac{1}{\sqrt{2}}U_\alpha^* + \sqrt{\frac{3}{2}}U_\beta^* - \frac{\sqrt{3}v_{dc}}{2}$	TeT_{14}^{13}	$U_o^* < \frac{1}{\sqrt{2}}U_\alpha^* + \sqrt{\frac{3}{2}}U_\beta^* - \frac{\sqrt{3}v_{dc}}{2}$ $U_o^* \geq \frac{1}{\sqrt{2}}U_\alpha^* - \sqrt{\frac{3}{2}}U_\beta^* - \frac{\sqrt{3}v_{dc}}{2}$	TeT_{15}^{13}	$U_o^* < \frac{1}{\sqrt{2}}U_\alpha^* - \sqrt{\frac{3}{2}}U_\beta^* - \frac{\sqrt{3}v_{dc}}{2}$ $U_o^* \geq -\sqrt{2}U_\alpha^* - \frac{\sqrt{3}v_{dc}}{4}$
TeT_{16}^{13}	$U_o^* < -\sqrt{2}U_\alpha^* - \frac{\sqrt{3}v_{dc}}{4}$ $U_o^* \geq \frac{1}{\sqrt{2}}U_\alpha^* + \sqrt{\frac{3}{2}}U_\beta^* - \frac{3\sqrt{3}v_{dc}}{4}$	TeT_{17}^{13}	$U_o^* < \frac{1}{\sqrt{2}}U_\alpha^* + \sqrt{\frac{3}{2}}U_\beta^* - \frac{3\sqrt{3}v_{dc}}{4}$ $U_o^* \geq \frac{1}{\sqrt{2}}U_\alpha^* + \sqrt{\frac{3}{2}}U_\beta^* - \frac{3\sqrt{3}v_{dc}}{4}$	TeT_{18}^{13}	$U_o^* < \frac{1}{\sqrt{2}}U_\alpha^* + \sqrt{\frac{3}{2}}U_\beta^* - \frac{3\sqrt{3}v_{dc}}{4}$ $U_o^* \geq -\sqrt{2}U_\alpha^* - \frac{\sqrt{3}v_{dc}}{2}$
TeT_{19}^{13}	$U_o^* < -\sqrt{2}U_\alpha^* - \frac{\sqrt{3}v_{dc}}{2}$ $U_o^* \geq \frac{1}{\sqrt{2}}U_\alpha^* + \sqrt{\frac{3}{2}}U_\beta^* - \sqrt{3}v_{dc}$				

PR_{14}					
TeT_1^{14}	$U_o^* < -\sqrt{2}U_\alpha^* + \sqrt{3}v_{dc}$ $U_o^* \geq \frac{1}{\sqrt{2}}U_\alpha^* - \sqrt{\frac{3}{2}}U_\beta^* + \frac{3\sqrt{3}v_{dc}}{4}$	TeT_2^{14}	$U_o^* < \frac{1}{\sqrt{2}}U_\alpha^* - \sqrt{\frac{3}{2}}U_\beta^* + \frac{3\sqrt{3}v_{dc}}{4}$ $U_o^* \geq \frac{1}{\sqrt{2}}U_\alpha^* + \sqrt{\frac{3}{2}}U_\beta^* + \frac{\sqrt{3}v_{dc}}{2}$	TeT_3^{14}	$U_o^* < \frac{1}{\sqrt{2}}U_\alpha^* + \sqrt{\frac{3}{2}}U_\beta^* + \frac{\sqrt{3}v_{dc}}{2}$ $U_o^* \geq -\sqrt{2}U_\alpha^* + \frac{3\sqrt{3}v_{dc}}{4}$
TeT_4^{14}	$U_o^* < -\sqrt{2}U_\alpha^* + \frac{3\sqrt{3}v_{dc}}{4}$ $U_o^* \geq \frac{1}{\sqrt{2}}U_\alpha^* - \sqrt{\frac{3}{2}}U_\beta^* + \frac{\sqrt{3}v_{dc}}{2}$	TeT_5^{14}	$U_o^* < \frac{1}{\sqrt{2}}U_\alpha^* - \sqrt{\frac{3}{2}}U_\beta^* + \frac{\sqrt{3}v_{dc}}{2}$ $U_o^* \geq \frac{1}{\sqrt{2}}U_\alpha^* + \sqrt{\frac{3}{2}}U_\beta^* + \frac{\sqrt{3}v_{dc}}{4}$	TeT_6^{14}	$U_o^* < \frac{1}{\sqrt{2}}U_\alpha^* + \sqrt{\frac{3}{2}}U_\beta^* + \frac{\sqrt{3}v_{dc}}{4}$ $U_o^* \geq -\sqrt{2}U_\alpha^* + \frac{\sqrt{3}v_{dc}}{2}$
TeT_7^{14}	$U_o^* < -\sqrt{2}U_\alpha^* + \frac{\sqrt{3}v_{dc}}{2}$ $U_o^* \geq \frac{1}{\sqrt{2}}U_\alpha^* - \sqrt{\frac{3}{2}}U_\beta^* + \frac{\sqrt{3}v_{dc}}{4}$	TeT_8^{14}	$U_o^* < \frac{1}{\sqrt{2}}U_\alpha^* - \sqrt{\frac{3}{2}}U_\beta^* + \frac{\sqrt{3}v_{dc}}{4}$ $U_o^* \geq \frac{1}{\sqrt{2}}U_\alpha^* + \sqrt{\frac{3}{2}}U_\beta^*$	TeT_9^{14}	$U_o^* < \frac{1}{\sqrt{2}}U_\alpha^* + \sqrt{\frac{3}{2}}U_\beta^*$ $U_o^* \geq -\sqrt{2}U_\alpha^* + \frac{\sqrt{3}v_{dc}}{4}$
TeT_{10}^{14}	$U_o^* < -\sqrt{2}U_\alpha^* + \frac{\sqrt{3}v_{dc}}{4}$ $U_o^* \geq \frac{1}{\sqrt{2}}U_\alpha^* - \sqrt{\frac{3}{2}}U_\beta^*$	TeT_{11}^{14}	$U_o^* < \frac{1}{\sqrt{2}}U_\alpha^* - \sqrt{\frac{3}{2}}U_\beta^*$ $U_o^* \geq \frac{1}{\sqrt{2}}U_\alpha^* + \sqrt{\frac{3}{2}}U_\beta^* - \frac{\sqrt{3}v_{dc}}{4}$	TeT_{12}^{14}	$U_o^* < \frac{1}{\sqrt{2}}U_\alpha^* + \sqrt{\frac{3}{2}}U_\beta^* - \frac{\sqrt{3}v_{dc}}{4}$ $U_o^* \geq -\sqrt{2}U_\alpha^*$
TeT_{13}^{14}	$U_o^* < -\sqrt{2}U_\alpha^*$ $U_o^* \geq \frac{1}{\sqrt{2}}U_\alpha^* - \sqrt{\frac{3}{2}}U_\beta^* - \frac{\sqrt{3}v_{dc}}{4}$	TeT_{14}^{14}	$U_o^* < \frac{1}{\sqrt{2}}U_\alpha^* - \sqrt{\frac{3}{2}}U_\beta^* - \frac{\sqrt{3}v_{dc}}{4}$ $U_o^* \geq \frac{1}{\sqrt{2}}U_\alpha^* + \sqrt{\frac{3}{2}}U_\beta^* - \frac{\sqrt{3}v_{dc}}{2}$	TeT_{15}^{14}	$U_o^* < \frac{1}{\sqrt{2}}U_\alpha^* + \sqrt{\frac{3}{2}}U_\beta^* - \frac{\sqrt{3}v_{dc}}{2}$ $U_o^* \geq -\sqrt{2}U_\alpha^* - \frac{\sqrt{3}v_{dc}}{4}$
TeT_{16}^{14}	$U_o^* < -\sqrt{2}U_\alpha^* - \frac{\sqrt{3}v_{dc}}{4}$ $U_o^* \geq \frac{1}{\sqrt{2}}U_\alpha^* - \sqrt{\frac{3}{2}}U_\beta^* - \frac{\sqrt{3}v_{dc}}{2}$	TeT_{17}^{14}	$U_o^* < \frac{1}{\sqrt{2}}U_\alpha^* - \sqrt{\frac{3}{2}}U_\beta^* - \frac{\sqrt{3}v_{dc}}{2}$ $U_o^* \geq \frac{1}{\sqrt{2}}U_\alpha^* + \sqrt{\frac{3}{2}}U_\beta^* - \frac{3\sqrt{3}v_{dc}}{4}$	TeT_{18}^{14}	$U_o^* < \frac{1}{\sqrt{2}}U_\alpha^* + \sqrt{\frac{3}{2}}U_\beta^* - \frac{3\sqrt{3}v_{dc}}{4}$ $U_o^* \geq -\sqrt{2}U_\alpha^* - \frac{\sqrt{3}v_{dc}}{2}$
TeT_{19}^{14}	$U_o^* < -\sqrt{2}U_\alpha^* - \frac{\sqrt{3}v_{dc}}{2}$ $U_o^* \geq \frac{1}{\sqrt{2}}U_\alpha^* - \sqrt{\frac{3}{2}}U_\beta^* - \frac{3\sqrt{3}v_{dc}}{4}$	TeT_{20}^{14}	$U_o^* < \frac{1}{\sqrt{2}}U_\alpha^* - \sqrt{\frac{3}{2}}U_\beta^* - \frac{3\sqrt{3}v_{dc}}{4}$ $U_o^* \geq \frac{1}{\sqrt{2}}U_\alpha^* + \sqrt{\frac{3}{2}}U_\beta^* - \sqrt{3}v_{dc}$		

PR_{15}					
TeT_1^{15}	$U_o^* < -\sqrt{2}U_\alpha^* + \sqrt{3}v_{dc}$ $U_o^* \geq \frac{1}{\sqrt{2}}U_\alpha^* + \sqrt{\frac{3}{2}}U_\beta^* + \frac{\sqrt{3}v_{dc}}{2}$	TeT_2^{15}	$U_o^* < \frac{1}{\sqrt{2}}U_\alpha^* + \sqrt{\frac{3}{2}}U_\beta^* + \frac{\sqrt{3}v_{dc}}{2}$ $U_o^* \geq \frac{1}{\sqrt{2}}U_\alpha^* - \sqrt{\frac{3}{2}}U_\beta^* + \frac{3\sqrt{3}v_{dc}}{4}$	TeT_3^{15}	$U_o^* < \frac{1}{\sqrt{2}}U_\alpha^* - \sqrt{\frac{3}{2}}U_\beta^* + \frac{3\sqrt{3}v_{dc}}{4}$ $U_o^* \geq -\sqrt{2}U_\alpha^* + \frac{3\sqrt{3}v_{dc}}{4}$
TeT_4^{15}	$U_o^* < -\sqrt{2}U_\alpha^* + \frac{3\sqrt{3}v_{dc}}{4}$ $U_o^* \geq \frac{1}{\sqrt{2}}U_\alpha^* + \sqrt{\frac{3}{2}}U_\beta^* + \frac{\sqrt{3}v_{dc}}{4}$	TeT_5^{15}	$U_o^* < \frac{1}{\sqrt{2}}U_\alpha^* + \sqrt{\frac{3}{2}}U_\beta^* + \frac{\sqrt{3}v_{dc}}{4}$ $U_o^* \geq \frac{1}{\sqrt{2}}U_\alpha^* - \sqrt{\frac{3}{2}}U_\beta^* + \frac{\sqrt{3}v_{dc}}{2}$	TeT_6^{15}	$U_o^* < \frac{1}{\sqrt{2}}U_\alpha^* - \sqrt{\frac{3}{2}}U_\beta^* + \frac{\sqrt{3}v_{dc}}{2}$ $U_o^* \geq -\sqrt{2}U_\alpha^* + \frac{\sqrt{3}v_{dc}}{2}$
TeT_7^{15}	$U_o^* < -\sqrt{2}U_\alpha^* + \frac{\sqrt{3}v_{dc}}{2}$ $U_o^* \geq \frac{1}{\sqrt{2}}U_\alpha^* + \sqrt{\frac{3}{2}}U_\beta^*$	TeT_8^{15}	$U_o^* < \frac{1}{\sqrt{2}}U_\alpha^* + \sqrt{\frac{3}{2}}U_\beta^*$ $U_o^* \geq \frac{1}{\sqrt{2}}U_\alpha^* - \sqrt{\frac{3}{2}}U_\beta^* + \frac{\sqrt{3}v_{dc}}{4}$	TeT_9^{15}	$U_o^* < \frac{1}{\sqrt{2}}U_\alpha^* - \sqrt{\frac{3}{2}}U_\beta^* + \frac{\sqrt{3}v_{dc}}{4}$ $U_o^* \geq -\sqrt{2}U_\alpha^* + \frac{\sqrt{3}v_{dc}}{4}$
TeT_{10}^{15}	$U_o^* < -\sqrt{2}U_\alpha^* + \frac{\sqrt{3}v_{dc}}{4}$ $U_o^* \geq \frac{1}{\sqrt{2}}U_\alpha^* + \sqrt{\frac{3}{2}}U_\beta^* - \frac{\sqrt{3}v_{dc}}{4}$	TeT_{11}^{15}	$U_o^* < \frac{1}{\sqrt{2}}U_\alpha^* + \sqrt{\frac{3}{2}}U_\beta^* - \frac{\sqrt{3}v_{dc}}{4}$ $U_o^* \geq \frac{1}{\sqrt{2}}U_\alpha^* - \sqrt{\frac{3}{2}}U_\beta^*$	TeT_{12}^{15}	$U_o^* < \frac{1}{\sqrt{2}}U_\alpha^* - \sqrt{\frac{3}{2}}U_\beta^*$ $U_o^* \geq -\sqrt{2}U_\alpha^*$
TeT_{13}^{15}	$U_o^* < -\sqrt{2}U_\alpha^*$ $U_o^* \geq \frac{1}{\sqrt{2}}U_\alpha^* + \sqrt{\frac{3}{2}}U_\beta^* - \frac{\sqrt{3}v_{dc}}{2}$	TeT_{14}^{15}	$U_o^* < \frac{1}{\sqrt{2}}U_\alpha^* + \sqrt{\frac{3}{2}}U_\beta^* - \frac{\sqrt{3}v_{dc}}{2}$ $U_o^* \geq \frac{1}{\sqrt{2}}U_\alpha^* - \sqrt{\frac{3}{2}}U_\beta^* - \frac{\sqrt{3}v_{dc}}{4}$	TeT_{15}^{15}	$U_o^* < \frac{1}{\sqrt{2}}U_\alpha^* - \sqrt{\frac{3}{2}}U_\beta^* - \frac{\sqrt{3}v_{dc}}{4}$ $U_o^* \geq -\sqrt{2}U_\alpha^* - \frac{\sqrt{3}v_{dc}}{4}$
TeT_{16}^{15}	$U_o^* < -\sqrt{2}U_\alpha^* - \frac{\sqrt{3}v_{dc}}{4}$ $U_o^* \geq \frac{1}{\sqrt{2}}U_\alpha^* + \sqrt{\frac{3}{2}}U_\beta^* - \frac{3\sqrt{3}v_{dc}}{4}$	TeT_{17}^{15}	$U_o^* < \frac{1}{\sqrt{2}}U_\alpha^* + \sqrt{\frac{3}{2}}U_\beta^* - \frac{3\sqrt{3}v_{dc}}{4}$ $U_o^* \geq \frac{1}{\sqrt{2}}U_\alpha^* + \sqrt{\frac{3}{2}}U_\beta^* - \frac{\sqrt{3}v_{dc}}{2}$	TeT_{18}^{15}	$U_o^* < \frac{1}{\sqrt{2}}U_\alpha^* + \sqrt{\frac{3}{2}}U_\beta^* - \frac{\sqrt{3}v_{dc}}{2}$ $U_o^* \geq -\sqrt{2}U_\alpha^* - \frac{\sqrt{3}v_{dc}}{2}$
TeT_{19}^{15}	$U_o^* < -\sqrt{2}U_\alpha^* - \frac{\sqrt{3}v_{dc}}{2}$ $U_o^* \geq \frac{1}{\sqrt{2}}U_\alpha^* + \sqrt{\frac{3}{2}}U_\beta^* - \sqrt{3}v_{dc}$				

PR_{16}					
TeT_1^{16}	$U_o^* < -\sqrt{2}U_\alpha^* + \sqrt{3}v_{dc}$ $U_o^* \geq \frac{1}{\sqrt{2}}U_\alpha^* + \sqrt{\frac{3}{2}}U_\beta^* + \frac{3\sqrt{3}v_{dc}}{4}$	TeT_2^{16}	$U_o^* < \frac{1}{\sqrt{2}}U_\alpha^* + \sqrt{\frac{3}{2}}U_\beta^* + \frac{3\sqrt{3}v_{dc}}{4}$ $U_o^* \geq \frac{1}{\sqrt{2}}U_\alpha^* - \sqrt{\frac{3}{2}}U_\beta^* + \frac{3\sqrt{3}v_{dc}}{4}$	TeT_3^{16}	$U_o^* < \frac{1}{\sqrt{2}}U_\alpha^* - \sqrt{\frac{3}{2}}U_\beta^* + \frac{3\sqrt{3}v_{dc}}{4}$ $U_o^* \geq -\sqrt{2}U_\alpha^* + \frac{3\sqrt{3}v_{dc}}{4}$
TeT_4^{16}	$U_o^* < -\sqrt{2}U_\alpha^* + \frac{3\sqrt{3}v_{dc}}{4}$ $U_o^* \geq \frac{1}{\sqrt{2}}U_\alpha^* + \sqrt{\frac{3}{2}}U_\beta^* + \frac{\sqrt{3}v_{dc}}{2}$	TeT_5^{16}	$U_o^* < \frac{1}{\sqrt{2}}U_\alpha^* + \sqrt{\frac{3}{2}}U_\beta^* + \frac{\sqrt{3}v_{dc}}{2}$ $U_o^* \geq \frac{1}{\sqrt{2}}U_\alpha^* - \sqrt{\frac{3}{2}}U_\beta^* + \frac{\sqrt{3}v_{dc}}{2}$	TeT_6^{16}	$U_o^* < \frac{1}{\sqrt{2}}U_\alpha^* - \sqrt{\frac{3}{2}}U_\beta^* + \frac{\sqrt{3}v_{dc}}{2}$ $U_o^* \geq -\sqrt{2}U_\alpha^* + \frac{\sqrt{3}v_{dc}}{2}$
TeT_7^{16}	$U_o^* < -\sqrt{2}U_\alpha^* + \frac{\sqrt{3}v_{dc}}{2}$ $U_o^* \geq \frac{1}{\sqrt{2}}U_\alpha^* + \sqrt{\frac{3}{2}}U_\beta^* + \frac{\sqrt{3}v_{dc}}{4}$	TeT_8^{16}	$U_o^* < \frac{1}{\sqrt{2}}U_\alpha^* + \sqrt{\frac{3}{2}}U_\beta^* + \frac{\sqrt{3}v_{dc}}{4}$ $U_o^* \geq \frac{1}{\sqrt{2}}U_\alpha^* - \sqrt{\frac{3}{2}}U_\beta^* + \frac{\sqrt{3}v_{dc}}{4}$	TeT_9^{16}	$U_o^* < \frac{1}{\sqrt{2}}U_\alpha^* - \sqrt{\frac{3}{2}}U_\beta^* + \frac{\sqrt{3}v_{dc}}{4}$ $U_o^* \geq -\sqrt{2}U_\alpha^* + \frac{\sqrt{3}v_{dc}}{4}$
TeT_{10}^{16}	$U_o^* < -\sqrt{2}U_\alpha^* + \frac{\sqrt{3}v_{dc}}{4}$ $U_o^* \geq \frac{1}{\sqrt{2}}U_\alpha^* + \sqrt{\frac{3}{2}}U_\beta^*$	TeT_{11}^{16}	$U_o^* < \frac{1}{\sqrt{2}}U_\alpha^* + \sqrt{\frac{3}{2}}U_\beta^*$ $U_o^* \geq \frac{1}{\sqrt{2}}U_\alpha^* - \sqrt{\frac{3}{2}}U_\beta^*$	TeT_{12}^{16}	$U_o^* < \frac{1}{\sqrt{2}}U_\alpha^* - \sqrt{\frac{3}{2}}U_\beta^*$ $U_o^* \geq -\sqrt{2}U_\alpha^*$
TeT_{13}^{16}	$U_o^* < -\sqrt{2}U_\alpha^*$ $U_o^* \geq \frac{1}{\sqrt{2}}U_\alpha^* + \sqrt{\frac{3}{2}}U_\beta^* - \frac{\sqrt{3}v_{dc}}{4}$	TeT_{14}^{16}	$U_o^* < \frac{1}{\sqrt{2}}U_\alpha^* + \sqrt{\frac{3}{2}}U_\beta^* - \frac{\sqrt{3}v_{dc}}{4}$ $U_o^* \geq \frac{1}{\sqrt{2}}U_\alpha^* - \sqrt{\frac{3}{2}}U_\beta^* - \frac{\sqrt{3}v_{dc}}{4}$	TeT_{15}^{16}	$U_o^* < \frac{1}{\sqrt{2}}U_\alpha^* - \sqrt{\frac{3}{2}}U_\beta^* - \frac{\sqrt{3}v_{dc}}{4}$ $U_o^* \geq -\sqrt{2}U_\alpha^* - \frac{\sqrt{3}v_{dc}}{4}$
TeT_{16}^{16}	$U_o^* < -\sqrt{2}U_\alpha^* - \frac{\sqrt{3}v_{dc}}{4}$ $U_o^* \geq \frac{1}{\sqrt{2}}U_\alpha^* + \sqrt{\frac{3}{2}}U_\beta^* - \frac{\sqrt{3}v_{dc}}{2}$	TeT_{17}^{16}	$U_o^* < \frac{1}{\sqrt{2}}U_\alpha^* + \sqrt{\frac{3}{2}}U_\beta^* - \frac{\sqrt{3}v_{dc}}{2}$ $U_o^* \geq \frac{1}{\sqrt{2}}U_\alpha^* - \sqrt{\frac{3}{2}}U_\beta^* - \frac{\sqrt{3}v_{dc}}{2}$	TeT_{18}^{16}	$U_o^* < \frac{1}{\sqrt{2}}U_\alpha^* - \sqrt{\frac{3}{2}}U_\beta^* - \frac{\sqrt{3}v_{dc}}{2}$ $U_o^* \geq -\sqrt{2}U_\alpha^* - \frac{\sqrt{3}v_{dc}}{2}$
TeT_{19}^{16}	$U_o^* < -\sqrt{2}U_\alpha^* - \frac{\sqrt{3}v_{dc}}{2}$ $U_o^* \geq \frac{1}{\sqrt{2}}U_\alpha^* + \sqrt{\frac{3}{2}}U_\beta^* - \frac{3\sqrt{3}v_{dc}}{4}$	TeT_{20}^{16}	$U_o^* < \frac{1}{\sqrt{2}}U_\alpha^* + \sqrt{\frac{3}{2}}U_\beta^* - \frac{3\sqrt{3}v_{dc}}{4}$ $U_o^* \geq \frac{1}{\sqrt{2}}U_\alpha^* - \sqrt{\frac{3}{2}}U_\beta^* - \frac{3\sqrt{3}v_{dc}}{4}$	TeT_{21}^{16}	$U_o^* < \frac{1}{\sqrt{2}}U_\alpha^* - \sqrt{\frac{3}{2}}U_\beta^* - \frac{3\sqrt{3}v_{dc}}{4}$ $U_o^* \geq -\sqrt{2}U_\alpha^* - \frac{3\sqrt{3}v_{dc}}{4}$
TeT_{22}^{16}	$U_o^* < -\sqrt{2}U_\alpha^* - \frac{3\sqrt{3}v_{dc}}{4}$ $U_o^* \geq \frac{1}{\sqrt{2}}U_\alpha^* + \sqrt{\frac{3}{2}}U_\beta^* - \sqrt{3}v_{dc}$				

A.2. Duration time calculation

In each tetrahedron of the first sector, we have an equation like (A.1), which must be solved.

$$\begin{bmatrix} v_{1\alpha} & v_{2\alpha} & v_{3\alpha} & v_{4\alpha} \\ v_{1\beta} & v_{2\beta} & v_{3\beta} & v_{4\beta} \\ v_{1o} & v_{2o} & v_{3o} & v_{4o} \\ 1 & 1 & 1 & 1 \end{bmatrix} \begin{bmatrix} t_1 \\ t_2 \\ t_3 \\ t_4 \end{bmatrix} = \begin{bmatrix} U_\alpha^* T_s \\ U_\beta^* T_s \\ U_o^* T_s \\ T_s \end{bmatrix} \tag{A.1}$$

Where : ($v_{i\alpha}, v_{i\beta}$ and v_{io}), $i \in \{1,2,3,4\}$ are the $\alpha\beta$o components of the adjacent switching vectors v_1, v_2, v_3 and v_4 .

With the proposed algorithm, the on duration time intervals are calculated only in the first sector.

All matrixes of all tetrahedrons of the first sector are given in table (A.2).

Table (A.2): Matrixes of all tetrahedrons of the first sector

PR_1		
TeT_1^1	TeT_2^1	TeT_3^1
$\begin{bmatrix} \frac{\sqrt{3}v_{dc}}{2\sqrt{2}} & \frac{7v_{dc}}{4\sqrt{6}} & \sqrt{\frac{2}{3}}v_{dc} & \frac{\sqrt{3}v_{dc}}{2\sqrt{2}} \\ 0 & \frac{v_{dc}}{4\sqrt{2}} & 0 & 0 \\ \frac{\sqrt{3}v_{dc}}{2} & \frac{5v_{dc}}{4\sqrt{3}} & \frac{v_{dc}}{\sqrt{3}} & \frac{\sqrt{3}v_{dc}}{4} \\ 1 & 1 & 1 & 1 \end{bmatrix}$	$\begin{bmatrix} \frac{7v_{dc}}{4\sqrt{6}} & \frac{7v_{dc}}{4\sqrt{6}} & \sqrt{\frac{2}{3}}v_{dc} & \frac{\sqrt{3}v_{dc}}{2\sqrt{2}} \\ \frac{v_{dc}}{4\sqrt{2}} & \frac{v_{dc}}{4\sqrt{2}} & 0 & 0 \\ \frac{v_{dc}}{2\sqrt{3}} & \frac{5v_{dc}}{4\sqrt{3}} & \frac{v_{dc}}{\sqrt{3}} & \frac{\sqrt{3}v_{dc}}{4} \\ 1 & 1 & 1 & 1 \end{bmatrix}$	$\begin{bmatrix} \frac{7v_{dc}}{4\sqrt{6}} & \sqrt{\frac{2}{3}}v_{dc} & \sqrt{\frac{2}{3}}v_{dc} & \frac{\sqrt{3}v_{dc}}{2\sqrt{2}} \\ \frac{v_{dc}}{4\sqrt{2}} & 0 & 0 & 0 \\ \frac{v_{dc}}{2\sqrt{3}} & \frac{v_{dc}}{4\sqrt{3}} & \frac{v_{dc}}{\sqrt{3}} & \frac{\sqrt{3}v_{dc}}{4} \\ 1 & 1 & 1 & 1 \end{bmatrix}$
TeT_4^1	TeT_5^1	TeT_6^1
$\begin{bmatrix} \frac{7v_{dc}}{4\sqrt{6}} & \sqrt{\frac{2}{3}}v_{dc} & \frac{\sqrt{3}v_{dc}}{2\sqrt{2}} & \frac{\sqrt{3}v_{dc}}{2\sqrt{2}} \\ \frac{v_{dc}}{4\sqrt{2}} & 0 & 0 & 0 \\ \frac{v_{dc}}{2\sqrt{3}} & \frac{v_{dc}}{4\sqrt{3}} & 0 & \frac{\sqrt{3}v_{dc}}{4} \\ 1 & 1 & 1 & 1 \end{bmatrix}$	$\begin{bmatrix} \frac{7v_{dc}}{4\sqrt{6}} & \sqrt{\frac{2}{3}}v_{dc} & \frac{\sqrt{3}v_{dc}}{2\sqrt{2}} & \frac{7v_{dc}}{4\sqrt{6}} \\ \frac{v_{dc}}{4\sqrt{2}} & 0 & 0 & \frac{v_{dc}}{4\sqrt{2}} \\ \frac{v_{dc}}{2\sqrt{3}} & \frac{v_{dc}}{4\sqrt{3}} & 0 & \frac{-v_{dc}}{4\sqrt{3}} \\ 1 & 1 & 1 & 1 \end{bmatrix}$	$\begin{bmatrix} \sqrt{\frac{2}{3}}v_{dc} & \sqrt{\frac{2}{3}}v_{dc} & \frac{\sqrt{3}v_{dc}}{2\sqrt{2}} & \frac{7v_{dc}}{4\sqrt{6}} \\ 0 & 0 & 0 & \frac{v_{dc}}{4\sqrt{2}} \\ \frac{-v_{dc}}{2\sqrt{3}} & \frac{v_{dc}}{4\sqrt{3}} & 0 & \frac{-v_{dc}}{4\sqrt{3}} \\ 1 & 1 & 1 & 1 \end{bmatrix}$

TeT_7^1	TeT_8^1	TeT_9^1
$\begin{bmatrix} \sqrt{\frac{2}{3}}v_{dc} & \frac{\sqrt{3}v_{dc}}{2\sqrt{2}} & \frac{\sqrt{3}v_{dc}}{2\sqrt{2}} & \frac{7v_{dc}}{4\sqrt{6}} \\ 0 & 0 & 0 & \frac{v_{dc}}{4\sqrt{2}} \\ \frac{-v_{dc}}{2\sqrt{3}} & \frac{-\sqrt{3}v_{dc}}{4} & 0 & \frac{-v_{dc}}{4\sqrt{3}} \\ 1 & 1 & 1 & 1 \end{bmatrix}$	$\begin{bmatrix} \sqrt{\frac{2}{3}}v_{dc} & \frac{\sqrt{3}v_{dc}}{2\sqrt{2}} & \frac{7v_{dc}}{4\sqrt{6}} & \frac{7v_{dc}}{4\sqrt{6}} \\ 0 & 0 & \frac{v_{dc}}{4\sqrt{2}} & \frac{v_{dc}}{4\sqrt{2}} \\ \frac{-v_{dc}}{2\sqrt{3}} & \frac{-\sqrt{3}v_{dc}}{4} & \frac{-v_{dc}}{\sqrt{3}} & \frac{-v_{dc}}{4\sqrt{3}} \\ 1 & 1 & 1 & 1 \end{bmatrix}$	$\begin{bmatrix} \sqrt{\frac{2}{3}}v_{dc} & \frac{\sqrt{3}v_{dc}}{2\sqrt{2}} & \frac{7v_{dc}}{4\sqrt{6}} & \sqrt{\frac{2}{3}}v_{dc} \\ 0 & 0 & \frac{v_{dc}}{4\sqrt{2}} & 0 \\ \frac{-v_{dc}}{2\sqrt{3}} & \frac{-\sqrt{3}v_{dc}}{4} & \frac{-v_{dc}}{\sqrt{3}} & \frac{-5v_{dc}}{4\sqrt{3}} \\ 1 & 1 & 1 & 1 \end{bmatrix}$
TeT_{10}^1	TeT_{11}^1	TeT_{12}^1
$\begin{bmatrix} \frac{\sqrt{3}v_{dc}}{2\sqrt{2}} & \frac{\sqrt{3}v_{dc}}{2\sqrt{2}} & \frac{7v_{dc}}{4\sqrt{6}} & \sqrt{\frac{2}{3}}v_{dc} \\ 0 & 0 & \frac{v_{dc}}{4\sqrt{2}} & 0 \\ \frac{-\sqrt{3}v_{dc}}{2} & \frac{-\sqrt{3}v_{dc}}{4} & \frac{-v_{dc}}{\sqrt{3}} & \frac{-5v_{dc}}{4\sqrt{3}} \\ 1 & 1 & 1 & 1 \end{bmatrix}$	$\begin{bmatrix} \frac{\sqrt{3}v_{dc}}{2\sqrt{2}} & \frac{7v_{dc}}{4\sqrt{6}} & \frac{7v_{dc}}{4\sqrt{6}} & \sqrt{\frac{2}{3}}v_{dc} \\ 0 & \frac{v_{dc}}{4\sqrt{2}} & \frac{v_{dc}}{4\sqrt{2}} & 0 \\ \frac{-\sqrt{3}v_{dc}}{2} & \frac{-7v_{dc}}{4\sqrt{3}} & \frac{-v_{dc}}{\sqrt{3}} & \frac{-5v_{dc}}{4\sqrt{3}} \\ 1 & 1 & 1 & 1 \end{bmatrix}$	$\begin{bmatrix} \frac{\sqrt{3}v_{dc}}{2\sqrt{2}} & \frac{7v_{dc}}{4\sqrt{6}} & \sqrt{\frac{2}{3}}v_{dc} & \sqrt{\frac{2}{3}}v_{dc} \\ 0 & \frac{v_{dc}}{4\sqrt{2}} & 0 & 0 \\ \frac{-\sqrt{3}v_{dc}}{2} & \frac{-7v_{dc}}{4\sqrt{3}} & \frac{-2v_{dc}}{\sqrt{3}} & \frac{-5v_{dc}}{4\sqrt{3}} \\ 1 & 1 & 1 & 1 \end{bmatrix}$
TeT_{13}^1		
$\begin{bmatrix} \frac{\sqrt{3}v_{dc}}{2\sqrt{2}} & \frac{7v_{dc}}{4\sqrt{6}} & \sqrt{\frac{2}{3}}v_{dc} & \frac{\sqrt{3}v_{dc}}{2\sqrt{2}} \\ 0 & \frac{v_{dc}}{4\sqrt{2}} & 0 & 0 \\ \frac{-\sqrt{3}v_{dc}}{2} & \frac{-7v_{dc}}{4\sqrt{3}} & \frac{-2v_{dc}}{\sqrt{3}} & \frac{-3\sqrt{3}v_{dc}}{4} \\ 1 & 1 & 1 & 1 \end{bmatrix}$		

PR_2		
TeT_1^2	TeT_2^2	TeT_3^2
$\begin{bmatrix} \frac{5v_{dc}}{4\sqrt{6}} & \frac{\sqrt{3}v_{dc}}{2\sqrt{2}} & \frac{7v_{dc}}{4\sqrt{6}} & \frac{5v_{dc}}{4\sqrt{6}} \\ \frac{v_{dc}}{4\sqrt{2}} & 0 & \frac{v_{dc}}{4\sqrt{2}} & \frac{v_{dc}}{4\sqrt{2}} \\ \frac{7v_{dc}}{4\sqrt{3}} & \frac{\sqrt{3}v_{dc}}{2} & \frac{5v_{dc}}{4\sqrt{3}} & \frac{v_{dc}}{\sqrt{3}} \\ 1 & 1 & 1 & 1 \end{bmatrix}$	$\begin{bmatrix} \frac{\sqrt{3}v_{dc}}{2\sqrt{2}} & \frac{\sqrt{3}v_{dc}}{2\sqrt{2}} & \frac{7v_{dc}}{4\sqrt{6}} & \frac{5v_{dc}}{4\sqrt{6}} \\ 0 & 0 & \frac{v_{dc}}{4\sqrt{2}} & \frac{v_{dc}}{4\sqrt{2}} \\ \frac{\sqrt{3}v_{dc}}{4} & \frac{\sqrt{3}v_{dc}}{2} & \frac{5v_{dc}}{4\sqrt{3}} & \frac{v_{dc}}{\sqrt{3}} \\ 1 & 1 & 1 & 1 \end{bmatrix}$	$\begin{bmatrix} \frac{\sqrt{3}v_{dc}}{2\sqrt{2}} & \frac{7v_{dc}}{4\sqrt{6}} & \frac{7v_{dc}}{4\sqrt{6}} & \frac{5v_{dc}}{4\sqrt{6}} \\ 0 & \frac{v_{dc}}{4\sqrt{2}} & \frac{v_{dc}}{4\sqrt{2}} & \frac{v_{dc}}{4\sqrt{2}} \\ \frac{\sqrt{3}v_{dc}}{4} & \frac{v_{dc}}{2\sqrt{3}} & \frac{5v_{dc}}{4\sqrt{3}} & \frac{v_{dc}}{\sqrt{3}} \\ 1 & 1 & 1 & 1 \end{bmatrix}$
TeT_4^2	TeT_5^2	TeT_6^2

$\begin{bmatrix} \frac{\sqrt{3}v_{dc}}{2\sqrt{2}} & \frac{7v_{dc}}{4\sqrt{6}} & \frac{5v_{dc}}{4\sqrt{6}} & \frac{5v_{dc}}{4\sqrt{6}} \\ 0 & \frac{v_{dc}}{4\sqrt{2}} & \frac{v_{dc}}{4\sqrt{2}} & \frac{v_{dc}}{4\sqrt{2}} \\ \frac{\sqrt{3}v_{dc}}{4} & \frac{v_{dc}}{2\sqrt{3}} & \frac{v_{dc}}{4\sqrt{3}} & \frac{v_{dc}}{\sqrt{3}} \\ 1 & 1 & 1 & 1 \end{bmatrix}$	$\begin{bmatrix} \frac{\sqrt{3}v_{dc}}{2\sqrt{2}} & \frac{7v_{dc}}{4\sqrt{6}} & \frac{5v_{dc}}{4\sqrt{6}} & \frac{\sqrt{3}v_{dc}}{2\sqrt{2}} \\ 0 & \frac{v_{dc}}{4\sqrt{2}} & \frac{v_{dc}}{4\sqrt{2}} & 0 \\ \frac{\sqrt{3}v_{dc}}{4} & \frac{v_{dc}}{2\sqrt{3}} & \frac{v_{dc}}{4\sqrt{3}} & 0 \\ 1 & 1 & 1 & 1 \end{bmatrix}$	$\begin{bmatrix} \frac{7v_{dc}}{4\sqrt{6}} & \frac{7v_{dc}}{4\sqrt{6}} & \frac{5v_{dc}}{4\sqrt{6}} & \frac{\sqrt{3}v_{dc}}{2\sqrt{2}} \\ \frac{v_{dc}}{4\sqrt{2}} & \frac{v_{dc}}{4\sqrt{2}} & \frac{v_{dc}}{4\sqrt{2}} & 0 \\ \frac{-v_{dc}}{4\sqrt{3}} & \frac{v_{dc}}{2\sqrt{3}} & \frac{v_{dc}}{4\sqrt{3}} & 0 \\ 1 & 1 & 1 & 1 \end{bmatrix}$
TeT_7^2	TeT_8^2	TeT_9^2
$\begin{bmatrix} \frac{7v_{dc}}{4\sqrt{6}} & \frac{5v_{dc}}{4\sqrt{6}} & \frac{5v_{dc}}{4\sqrt{6}} & \frac{\sqrt{3}v_{dc}}{2\sqrt{2}} \\ \frac{v_{dc}}{4\sqrt{2}} & \frac{v_{dc}}{4\sqrt{2}} & \frac{v_{dc}}{4\sqrt{2}} & 0 \\ \frac{-v_{dc}}{4\sqrt{3}} & \frac{-v_{dc}}{2\sqrt{3}} & \frac{v_{dc}}{4\sqrt{3}} & 0 \\ 1 & 1 & 1 & 1 \end{bmatrix}$	$\begin{bmatrix} \frac{7v_{dc}}{4\sqrt{6}} & \frac{5v_{dc}}{4\sqrt{6}} & \frac{\sqrt{3}v_{dc}}{2\sqrt{2}} & \frac{\sqrt{3}v_{dc}}{2\sqrt{2}} \\ \frac{v_{dc}}{4\sqrt{2}} & \frac{v_{dc}}{4\sqrt{2}} & 0 & 0 \\ \frac{-v_{dc}}{4\sqrt{3}} & \frac{-v_{dc}}{2\sqrt{3}} & \frac{-\sqrt{3}v_{dc}}{4} & 0 \\ 1 & 1 & 1 & 1 \end{bmatrix}$	$\begin{bmatrix} \frac{7v_{dc}}{4\sqrt{6}} & \frac{5v_{dc}}{4\sqrt{6}} & \frac{\sqrt{3}v_{dc}}{2\sqrt{2}} & \frac{7v_{dc}}{4\sqrt{6}} \\ \frac{v_{dc}}{4\sqrt{2}} & \frac{v_{dc}}{4\sqrt{2}} & 0 & \frac{v_{dc}}{4\sqrt{2}} \\ \frac{-v_{dc}}{4\sqrt{3}} & \frac{-v_{dc}}{2\sqrt{3}} & \frac{-\sqrt{3}v_{dc}}{4} & \frac{-v_{dc}}{\sqrt{3}} \\ 1 & 1 & 1 & 1 \end{bmatrix}$
TeT_{10}^2	TeT_{11}^2	TeT_{12}^2
$\begin{bmatrix} \frac{5v_{dc}}{4\sqrt{6}} & \frac{5v_{dc}}{4\sqrt{6}} & \frac{\sqrt{3}v_{dc}}{2\sqrt{2}} & \frac{7v_{dc}}{4\sqrt{6}} \\ \frac{v_{dc}}{4\sqrt{2}} & \frac{v_{dc}}{4\sqrt{2}} & 0 & \frac{v_{dc}}{4\sqrt{2}} \\ \frac{-5v_{dc}}{4\sqrt{3}} & \frac{-v_{dc}}{2\sqrt{3}} & \frac{-\sqrt{3}v_{dc}}{4} & \frac{-v_{dc}}{\sqrt{3}} \\ 1 & 1 & 1 & 1 \end{bmatrix}$	$\begin{bmatrix} \frac{5v_{dc}}{4\sqrt{6}} & \frac{\sqrt{3}v_{dc}}{2\sqrt{2}} & \frac{\sqrt{3}v_{dc}}{2\sqrt{2}} & \frac{7v_{dc}}{4\sqrt{6}} \\ \frac{v_{dc}}{4\sqrt{2}} & 0 & 0 & \frac{v_{dc}}{4\sqrt{2}} \\ \frac{-5v_{dc}}{4\sqrt{3}} & \frac{-\sqrt{3}v_{dc}}{2} & \frac{-\sqrt{3}v_{dc}}{4} & \frac{-v_{dc}}{\sqrt{3}} \\ 1 & 1 & 1 & 1 \end{bmatrix}$	$\begin{bmatrix} \frac{5v_{dc}}{4\sqrt{6}} & \frac{\sqrt{3}v_{dc}}{2\sqrt{2}} & \frac{7v_{dc}}{4\sqrt{6}} & \frac{7v_{dc}}{4\sqrt{6}} \\ \frac{v_{dc}}{4\sqrt{2}} & 0 & \frac{v_{dc}}{4\sqrt{2}} & \frac{v_{dc}}{4\sqrt{2}} \\ \frac{-5v_{dc}}{4\sqrt{3}} & \frac{-\sqrt{3}v_{dc}}{2} & \frac{-7v_{dc}}{4\sqrt{3}} & \frac{-v_{dc}}{\sqrt{3}} \\ 1 & 1 & 1 & 1 \end{bmatrix}$
TeT_{13}^2	TeT_{14}^2	
$\begin{bmatrix} \frac{5v_{dc}}{4\sqrt{6}} & \frac{\sqrt{3}v_{dc}}{2\sqrt{2}} & \frac{7v_{dc}}{4\sqrt{6}} & \frac{5v_{dc}}{4\sqrt{6}} \\ \frac{v_{dc}}{4\sqrt{2}} & 0 & \frac{v_{dc}}{4\sqrt{2}} & \frac{v_{dc}}{4\sqrt{2}} \\ \frac{-5v_{dc}}{4\sqrt{3}} & \frac{-\sqrt{3}v_{dc}}{2} & \frac{-7v_{dc}}{4\sqrt{3}} & \frac{-2v_{dc}}{\sqrt{3}} \\ 1 & 1 & 1 & 1 \end{bmatrix}$	$\begin{bmatrix} \frac{\sqrt{3}v_{dc}}{2\sqrt{2}} & \frac{\sqrt{3}v_{dc}}{2\sqrt{2}} & \frac{7v_{dc}}{4\sqrt{6}} & \frac{5v_{dc}}{4\sqrt{6}} \\ 0 & 0 & \frac{v_{dc}}{4\sqrt{2}} & \frac{v_{dc}}{4\sqrt{2}} \\ \frac{-3\sqrt{3}v_{dc}}{4} & \frac{-\sqrt{3}v_{dc}}{2} & \frac{-7v_{dc}}{4\sqrt{3}} & \frac{-2v_{dc}}{\sqrt{3}} \\ 1 & 1 & 1 & 1 \end{bmatrix}$	

PR_3		
TeT_1^3	TeT_2^3	TeT_3^3
$\begin{bmatrix} \frac{5v_{dc}}{4\sqrt{6}} & \frac{\sqrt{3}v_{dc}}{2\sqrt{2}} & \frac{7v_{dc}}{4\sqrt{6}} & \frac{5v_{dc}}{4\sqrt{6}} \\ \frac{v_{dc}}{4\sqrt{2}} & \frac{v_{dc}}{2\sqrt{2}} & \frac{v_{dc}}{4\sqrt{2}} & \frac{v_{dc}}{4\sqrt{2}} \\ \frac{7v_{dc}}{4\sqrt{3}} & \frac{\sqrt{3}v_{dc}}{2} & \frac{5v_{dc}}{4\sqrt{3}} & \frac{v_{dc}}{\sqrt{3}} \\ 1 & 1 & 1 & 1 \end{bmatrix}$	$\begin{bmatrix} \frac{\sqrt{3}v_{dc}}{2\sqrt{2}} & \frac{\sqrt{3}v_{dc}}{2\sqrt{2}} & \frac{7v_{dc}}{4\sqrt{6}} & \frac{5v_{dc}}{4\sqrt{6}} \\ \frac{v_{dc}}{2\sqrt{2}} & \frac{v_{dc}}{2\sqrt{2}} & \frac{v_{dc}}{4\sqrt{2}} & \frac{v_{dc}}{4\sqrt{2}} \\ \frac{\sqrt{3}v_{dc}}{4} & \frac{\sqrt{3}v_{dc}}{2} & \frac{5v_{dc}}{4\sqrt{3}} & \frac{v_{dc}}{\sqrt{3}} \\ 1 & 1 & 1 & 1 \end{bmatrix}$	$\begin{bmatrix} \frac{\sqrt{3}v_{dc}}{2\sqrt{2}} & \frac{7v_{dc}}{4\sqrt{6}} & \frac{7v_{dc}}{4\sqrt{6}} & \frac{5v_{dc}}{4\sqrt{6}} \\ \frac{v_{dc}}{2\sqrt{2}} & \frac{v_{dc}}{4\sqrt{2}} & \frac{v_{dc}}{4\sqrt{2}} & \frac{v_{dc}}{4\sqrt{2}} \\ \frac{\sqrt{3}v_{dc}}{4} & \frac{v_{dc}}{2\sqrt{3}} & \frac{5v_{dc}}{4\sqrt{3}} & \frac{v_{dc}}{\sqrt{3}} \\ 1 & 1 & 1 & 1 \end{bmatrix}$
TeT_4^3	TeT_5^3	TeT_6^3
$\begin{bmatrix} \frac{\sqrt{3}v_{dc}}{2\sqrt{2}} & \frac{7v_{dc}}{4\sqrt{6}} & \frac{5v_{dc}}{4\sqrt{6}} & \frac{5v_{dc}}{4\sqrt{6}} \\ \frac{v_{dc}}{2\sqrt{2}} & \frac{v_{dc}}{4\sqrt{2}} & \frac{v_{dc}}{4\sqrt{2}} & \frac{v_{dc}}{4\sqrt{2}} \\ \frac{\sqrt{3}v_{dc}}{4} & \frac{v_{dc}}{2\sqrt{3}} & \frac{v_{dc}}{4\sqrt{3}} & \frac{v_{dc}}{\sqrt{3}} \\ 1 & 1 & 1 & 1 \end{bmatrix}$	$\begin{bmatrix} \frac{\sqrt{3}v_{dc}}{2\sqrt{2}} & \frac{7v_{dc}}{4\sqrt{6}} & \frac{5v_{dc}}{4\sqrt{6}} & \frac{\sqrt{3}v_{dc}}{2\sqrt{2}} \\ \frac{v_{dc}}{2\sqrt{2}} & \frac{v_{dc}}{4\sqrt{2}} & \frac{v_{dc}}{4\sqrt{2}} & \frac{v_{dc}}{2\sqrt{2}} \\ \frac{\sqrt{3}v_{dc}}{4} & \frac{v_{dc}}{2\sqrt{3}} & \frac{v_{dc}}{4\sqrt{3}} & 0 \\ 1 & 1 & 1 & 1 \end{bmatrix}$	$\begin{bmatrix} \frac{7v_{dc}}{4\sqrt{6}} & \frac{7v_{dc}}{4\sqrt{6}} & \frac{5v_{dc}}{4\sqrt{6}} & \frac{\sqrt{3}v_{dc}}{2\sqrt{2}} \\ \frac{v_{dc}}{4\sqrt{2}} & \frac{v_{dc}}{4\sqrt{2}} & \frac{v_{dc}}{4\sqrt{2}} & \frac{v_{dc}}{2\sqrt{2}} \\ \frac{-v_{dc}}{4\sqrt{3}} & \frac{v_{dc}}{2\sqrt{3}} & \frac{v_{dc}}{4\sqrt{3}} & 0 \\ 1 & 1 & 1 & 1 \end{bmatrix}$
TeT_7^3	TeT_8^3	TeT_9^3
$\begin{bmatrix} \frac{7v_{dc}}{4\sqrt{6}} & \frac{5v_{dc}}{4\sqrt{6}} & \frac{5v_{dc}}{4\sqrt{6}} & \frac{\sqrt{3}v_{dc}}{2\sqrt{2}} \\ \frac{v_{dc}}{4\sqrt{2}} & \frac{v_{dc}}{4\sqrt{2}} & \frac{v_{dc}}{4\sqrt{2}} & \frac{v_{dc}}{2\sqrt{2}} \\ \frac{-v_{dc}}{4\sqrt{3}} & \frac{-v_{dc}}{2\sqrt{3}} & \frac{v_{dc}}{4\sqrt{3}} & 0 \\ 1 & 1 & 1 & 1 \end{bmatrix}$	$\begin{bmatrix} \frac{7v_{dc}}{4\sqrt{6}} & \frac{5v_{dc}}{4\sqrt{6}} & \frac{\sqrt{3}v_{dc}}{2\sqrt{2}} & \frac{\sqrt{3}v_{dc}}{2\sqrt{2}} \\ \frac{v_{dc}}{4\sqrt{2}} & \frac{v_{dc}}{4\sqrt{2}} & \frac{v_{dc}}{2\sqrt{2}} & \frac{v_{dc}}{2\sqrt{2}} \\ \frac{-v_{dc}}{4\sqrt{3}} & \frac{-v_{dc}}{2\sqrt{3}} & \frac{-\sqrt{3}v_{dc}}{4} & 0 \\ 1 & 1 & 1 & 1 \end{bmatrix}$	$\begin{bmatrix} \frac{7v_{dc}}{4\sqrt{6}} & \frac{5v_{dc}}{4\sqrt{6}} & \frac{\sqrt{3}v_{dc}}{2\sqrt{2}} & \frac{7v_{dc}}{4\sqrt{6}} \\ \frac{v_{dc}}{4\sqrt{2}} & \frac{v_{dc}}{4\sqrt{2}} & \frac{v_{dc}}{2\sqrt{2}} & \frac{v_{dc}}{4\sqrt{2}} \\ \frac{-v_{dc}}{4\sqrt{3}} & \frac{-v_{dc}}{2\sqrt{3}} & \frac{-\sqrt{3}v_{dc}}{4} & \frac{-v_{dc}}{\sqrt{3}} \\ 1 & 1 & 1 & 1 \end{bmatrix}$
TeT_{10}^3	TeT_{11}^3	TeT_{12}^3
$\begin{bmatrix} \frac{5v_{dc}}{4\sqrt{6}} & \frac{5v_{dc}}{4\sqrt{6}} & \frac{\sqrt{3}v_{dc}}{2\sqrt{2}} & \frac{7v_{dc}}{4\sqrt{6}} \\ \frac{v_{dc}}{4\sqrt{2}} & \frac{v_{dc}}{4\sqrt{2}} & \frac{v_{dc}}{2\sqrt{2}} & \frac{v_{dc}}{4\sqrt{2}} \\ \frac{-5v_{dc}}{4\sqrt{3}} & \frac{-v_{dc}}{2\sqrt{3}} & \frac{-\sqrt{3}v_{dc}}{4} & \frac{-v_{dc}}{\sqrt{3}} \\ 1 & 1 & 1 & 1 \end{bmatrix}$	$\begin{bmatrix} \frac{5v_{dc}}{4\sqrt{6}} & \frac{\sqrt{3}v_{dc}}{2\sqrt{2}} & \frac{\sqrt{3}v_{dc}}{2\sqrt{2}} & \frac{7v_{dc}}{4\sqrt{6}} \\ \frac{v_{dc}}{4\sqrt{2}} & \frac{v_{dc}}{2\sqrt{2}} & \frac{v_{dc}}{2\sqrt{2}} & \frac{v_{dc}}{4\sqrt{2}} \\ \frac{-5v_{dc}}{4\sqrt{3}} & \frac{-\sqrt{3}v_{dc}}{2} & \frac{-\sqrt{3}v_{dc}}{4} & \frac{-v_{dc}}{\sqrt{3}} \\ 1 & 1 & 1 & 1 \end{bmatrix}$	$\begin{bmatrix} \frac{5v_{dc}}{4\sqrt{6}} & \frac{\sqrt{3}v_{dc}}{2\sqrt{2}} & \frac{7v_{dc}}{4\sqrt{6}} & \frac{7v_{dc}}{4\sqrt{6}} \\ \frac{v_{dc}}{4\sqrt{2}} & \frac{v_{dc}}{2\sqrt{2}} & \frac{v_{dc}}{4\sqrt{2}} & \frac{v_{dc}}{4\sqrt{2}} \\ \frac{-5v_{dc}}{4\sqrt{3}} & \frac{-\sqrt{3}v_{dc}}{2} & \frac{-7v_{dc}}{4\sqrt{3}} & \frac{-v_{dc}}{\sqrt{3}} \\ 1 & 1 & 1 & 1 \end{bmatrix}$
TeT_{13}^3		

$$\begin{bmatrix} \frac{5v_{dc}}{4\sqrt{6}} & \frac{\sqrt{3}v_{dc}}{2\sqrt{2}} & \frac{7v_{dc}}{4\sqrt{6}} & \frac{5v_{dc}}{4\sqrt{6}} \\ \frac{v_{dc}}{4\sqrt{2}} & \frac{v_{dc}}{2\sqrt{2}} & \frac{v_{dc}}{4\sqrt{2}} & \frac{v_{dc}}{4\sqrt{2}} \\ \frac{-5v_{dc}}{4\sqrt{3}} & \frac{-\sqrt{3}v_{dc}}{2} & \frac{-7v_{dc}}{4\sqrt{3}} & \frac{-2v_{dc}}{\sqrt{3}} \\ 1 & 1 & 1 & 1 \end{bmatrix}$$

PR_4		
TeT_1^4	TeT_2^4	TeT_3^4
$\begin{bmatrix} \frac{v_{dc}}{\sqrt{6}} & \frac{5v_{dc}}{4\sqrt{6}} & \frac{\sqrt{3}v_{dc}}{2\sqrt{2}} & \frac{v_{dc}}{\sqrt{6}} \\ \frac{v_{dc}}{2\sqrt{2}} & \frac{v_{dc}}{4\sqrt{2}} & \frac{v_{dc}}{2\sqrt{2}} & \frac{v_{dc}}{2\sqrt{2}} \\ \frac{2v_{dc}}{\sqrt{3}} & \frac{7v_{dc}}{4\sqrt{3}} & \frac{\sqrt{3}v_{dc}}{2} & \frac{5v_{dc}}{4\sqrt{3}} \\ 1 & 1 & 1 & 1 \end{bmatrix}$	$\begin{bmatrix} \frac{5v_{dc}}{4\sqrt{6}} & \frac{5v_{dc}}{4\sqrt{6}} & \frac{\sqrt{3}v_{dc}}{2\sqrt{2}} & \frac{v_{dc}}{\sqrt{6}} \\ \frac{v_{dc}}{4\sqrt{2}} & \frac{v_{dc}}{4\sqrt{2}} & \frac{v_{dc}}{2\sqrt{2}} & \frac{v_{dc}}{2\sqrt{2}} \\ \frac{v_{dc}}{\sqrt{3}} & \frac{7v_{dc}}{4\sqrt{3}} & \frac{\sqrt{3}v_{dc}}{2} & \frac{5v_{dc}}{4\sqrt{3}} \\ 1 & 1 & 1 & 1 \end{bmatrix}$	$\begin{bmatrix} \frac{5v_{dc}}{4\sqrt{6}} & \frac{\sqrt{3}v_{dc}}{2\sqrt{2}} & \frac{\sqrt{3}v_{dc}}{2\sqrt{2}} & \frac{v_{dc}}{\sqrt{6}} \\ \frac{v_{dc}}{4\sqrt{2}} & \frac{v_{dc}}{2\sqrt{2}} & \frac{v_{dc}}{2\sqrt{2}} & \frac{v_{dc}}{2\sqrt{2}} \\ \frac{v_{dc}}{\sqrt{3}} & \frac{\sqrt{3}v_{dc}}{4} & \frac{\sqrt{3}v_{dc}}{2} & \frac{5v_{dc}}{4\sqrt{3}} \\ 1 & 1 & 1 & 1 \end{bmatrix}$
TeT_4^4	TeT_5^4	TeT_6^4
$\begin{bmatrix} \frac{5v_{dc}}{4\sqrt{6}} & \frac{\sqrt{3}v_{dc}}{2\sqrt{2}} & \frac{v_{dc}}{\sqrt{6}} & \frac{v_{dc}}{\sqrt{6}} \\ \frac{v_{dc}}{4\sqrt{2}} & \frac{v_{dc}}{2\sqrt{2}} & \frac{v_{dc}}{2\sqrt{2}} & \frac{v_{dc}}{2\sqrt{2}} \\ \frac{v_{dc}}{\sqrt{3}} & \frac{\sqrt{3}v_{dc}}{4} & \frac{v_{dc}}{2\sqrt{3}} & \frac{5v_{dc}}{4\sqrt{3}} \\ 1 & 1 & 1 & 1 \end{bmatrix}$	$\begin{bmatrix} \frac{5v_{dc}}{4\sqrt{6}} & \frac{\sqrt{3}v_{dc}}{2\sqrt{2}} & \frac{v_{dc}}{\sqrt{6}} & \frac{5v_{dc}}{4\sqrt{6}} \\ \frac{v_{dc}}{4\sqrt{2}} & \frac{v_{dc}}{2\sqrt{2}} & \frac{v_{dc}}{2\sqrt{2}} & \frac{v_{dc}}{4\sqrt{2}} \\ \frac{v_{dc}}{\sqrt{3}} & \frac{\sqrt{3}v_{dc}}{4} & \frac{v_{dc}}{2\sqrt{3}} & \frac{v_{dc}}{4\sqrt{3}} \\ 1 & 1 & 1 & 1 \end{bmatrix}$	$\begin{bmatrix} \frac{\sqrt{3}v_{dc}}{2\sqrt{2}} & \frac{\sqrt{3}v_{dc}}{2\sqrt{2}} & \frac{v_{dc}}{\sqrt{6}} & \frac{5v_{dc}}{4\sqrt{6}} \\ \frac{v_{dc}}{2\sqrt{2}} & \frac{v_{dc}}{2\sqrt{2}} & \frac{v_{dc}}{2\sqrt{2}} & \frac{v_{dc}}{4\sqrt{2}} \\ 0 & \frac{\sqrt{3}v_{dc}}{4} & \frac{v_{dc}}{2\sqrt{3}} & \frac{v_{dc}}{4\sqrt{3}} \\ 1 & 1 & 1 & 1 \end{bmatrix}$
TeT_7^4	TeT_8^4	TeT_9^4
$\begin{bmatrix} \frac{\sqrt{3}v_{dc}}{2\sqrt{2}} & \frac{v_{dc}}{\sqrt{6}} & \frac{v_{dc}}{\sqrt{6}} & \frac{5v_{dc}}{4\sqrt{6}} \\ \frac{v_{dc}}{2\sqrt{2}} & \frac{v_{dc}}{2\sqrt{2}} & \frac{v_{dc}}{2\sqrt{2}} & \frac{v_{dc}}{4\sqrt{2}} \\ 0 & \frac{-v_{dc}}{4\sqrt{3}} & \frac{v_{dc}}{2\sqrt{3}} & \frac{v_{dc}}{4\sqrt{3}} \\ 1 & 1 & 1 & 1 \end{bmatrix}$	$\begin{bmatrix} \frac{\sqrt{3}v_{dc}}{2\sqrt{2}} & \frac{v_{dc}}{\sqrt{6}} & \frac{5v_{dc}}{4\sqrt{6}} & \frac{5v_{dc}}{4\sqrt{6}} \\ \frac{v_{dc}}{2\sqrt{2}} & \frac{v_{dc}}{2\sqrt{2}} & \frac{v_{dc}}{4\sqrt{2}} & \frac{v_{dc}}{4\sqrt{2}} \\ 0 & \frac{-v_{dc}}{4\sqrt{3}} & \frac{-v_{dc}}{2\sqrt{3}} & \frac{v_{dc}}{4\sqrt{3}} \\ 1 & 1 & 1 & 1 \end{bmatrix}$	$\begin{bmatrix} \frac{\sqrt{3}v_{dc}}{2\sqrt{2}} & \frac{v_{dc}}{\sqrt{6}} & \frac{5v_{dc}}{4\sqrt{6}} & \frac{\sqrt{3}v_{dc}}{2\sqrt{2}} \\ \frac{v_{dc}}{2\sqrt{2}} & \frac{v_{dc}}{2\sqrt{2}} & \frac{v_{dc}}{4\sqrt{2}} & \frac{v_{dc}}{2\sqrt{2}} \\ 0 & \frac{-v_{dc}}{4\sqrt{3}} & \frac{-v_{dc}}{2\sqrt{3}} & \frac{-\sqrt{3}v_{dc}}{4} \\ 1 & 1 & 1 & 1 \end{bmatrix}$
TeT_{10}^4	TeT_{11}^4	TeT_{12}^4

$\begin{bmatrix} \frac{v_{dc}}{\sqrt{6}} & \frac{v_{dc}}{\sqrt{6}} & \frac{5v_{dc}}{4\sqrt{6}} & \frac{\sqrt{3}v_{dc}}{2\sqrt{2}} \\ \frac{v_{dc}}{2\sqrt{2}} & \frac{v_{dc}}{2\sqrt{2}} & \frac{v_{dc}}{4\sqrt{2}} & \frac{v_{dc}}{2\sqrt{2}} \\ \frac{-v_{dc}}{\sqrt{3}} & \frac{-v_{dc}}{4\sqrt{3}} & \frac{-v_{dc}}{2\sqrt{3}} & \frac{-\sqrt{3}v_{dc}}{4} \\ 1 & 1 & 1 & 1 \end{bmatrix}$	$\begin{bmatrix} \frac{v_{dc}}{\sqrt{6}} & \frac{5v_{dc}}{4\sqrt{6}} & \frac{5v_{dc}}{4\sqrt{6}} & \frac{\sqrt{3}v_{dc}}{2\sqrt{2}} \\ \frac{v_{dc}}{2\sqrt{2}} & \frac{v_{dc}}{4\sqrt{2}} & \frac{v_{dc}}{4\sqrt{2}} & \frac{v_{dc}}{2\sqrt{2}} \\ \frac{-v_{dc}}{\sqrt{3}} & \frac{-5v_{dc}}{4\sqrt{3}} & \frac{-v_{dc}}{2\sqrt{3}} & \frac{-\sqrt{3}v_{dc}}{4} \\ 1 & 1 & 1 & 1 \end{bmatrix}$	$\begin{bmatrix} \frac{v_{dc}}{\sqrt{6}} & \frac{5v_{dc}}{4\sqrt{6}} & \frac{\sqrt{3}v_{dc}}{2\sqrt{2}} & \frac{\sqrt{3}v_{dc}}{2\sqrt{2}} \\ \frac{v_{dc}}{2\sqrt{2}} & \frac{v_{dc}}{4\sqrt{2}} & \frac{v_{dc}}{2\sqrt{2}} & \frac{v_{dc}}{2\sqrt{2}} \\ \frac{-v_{dc}}{\sqrt{3}} & \frac{-5v_{dc}}{4\sqrt{3}} & \frac{-\sqrt{3}v_{dc}}{2} & \frac{-\sqrt{3}v_{dc}}{4} \\ 1 & 1 & 1 & 1 \end{bmatrix}$
TeT_{13}^4	TeT_{14}^4	
$\begin{bmatrix} \frac{v_{dc}}{\sqrt{6}} & \frac{5v_{dc}}{4\sqrt{6}} & \frac{\sqrt{3}v_{dc}}{2\sqrt{2}} & \frac{v_{dc}}{\sqrt{6}} \\ \frac{v_{dc}}{2\sqrt{2}} & \frac{v_{dc}}{4\sqrt{2}} & \frac{v_{dc}}{2\sqrt{2}} & \frac{v_{dc}}{2\sqrt{2}} \\ \frac{-v_{dc}}{\sqrt{3}} & \frac{-5v_{dc}}{4\sqrt{3}} & \frac{-\sqrt{3}v_{dc}}{2} & \frac{-7v_{dc}}{4\sqrt{3}} \\ 1 & 1 & 1 & 1 \end{bmatrix}$	$\begin{bmatrix} \frac{5v_{dc}}{4\sqrt{6}} & \frac{5v_{dc}}{4\sqrt{6}} & \frac{\sqrt{3}v_{dc}}{2\sqrt{2}} & \frac{v_{dc}}{\sqrt{6}} \\ \frac{v_{dc}}{4\sqrt{2}} & \frac{v_{dc}}{4\sqrt{2}} & \frac{v_{dc}}{2\sqrt{2}} & \frac{v_{dc}}{2\sqrt{2}} \\ \frac{-2v_{dc}}{\sqrt{3}} & \frac{-5v_{dc}}{4\sqrt{3}} & \frac{-\sqrt{3}v_{dc}}{2} & \frac{-7v_{dc}}{4\sqrt{3}} \\ 1 & 1 & 1 & 1 \end{bmatrix}$	

PR_5		
TeT_1^5	TeT_2^5	TeT_3^5
$\begin{bmatrix} \frac{v_{dc}}{\sqrt{6}} & \frac{5v_{dc}}{4\sqrt{6}} & \frac{\sqrt{3}v_{dc}}{2\sqrt{2}} & \frac{v_{dc}}{\sqrt{6}} \\ \frac{v_{dc}}{2\sqrt{2}} & \frac{3v_{dc}}{4\sqrt{2}} & \frac{v_{dc}}{2\sqrt{2}} & \frac{v_{dc}}{2\sqrt{2}} \\ \frac{2v_{dc}}{\sqrt{3}} & \frac{7v_{dc}}{4\sqrt{3}} & \frac{\sqrt{3}v_{dc}}{2} & \frac{5v_{dc}}{4\sqrt{3}} \\ 1 & 1 & 1 & 1 \end{bmatrix}$	$\begin{bmatrix} \frac{5v_{dc}}{4\sqrt{6}} & \frac{5v_{dc}}{4\sqrt{6}} & \frac{\sqrt{3}v_{dc}}{2\sqrt{2}} & \frac{v_{dc}}{\sqrt{6}} \\ \frac{3v_{dc}}{4\sqrt{2}} & \frac{3v_{dc}}{4\sqrt{2}} & \frac{v_{dc}}{2\sqrt{2}} & \frac{v_{dc}}{2\sqrt{2}} \\ \frac{v_{dc}}{\sqrt{3}} & \frac{7v_{dc}}{4\sqrt{3}} & \frac{\sqrt{3}v_{dc}}{2} & \frac{5v_{dc}}{4\sqrt{3}} \\ 1 & 1 & 1 & 1 \end{bmatrix}$	$\begin{bmatrix} \frac{5v_{dc}}{4\sqrt{6}} & \frac{\sqrt{3}v_{dc}}{2\sqrt{2}} & \frac{\sqrt{3}v_{dc}}{2\sqrt{2}} & \frac{v_{dc}}{\sqrt{6}} \\ \frac{3v_{dc}}{4\sqrt{2}} & \frac{v_{dc}}{2\sqrt{2}} & \frac{v_{dc}}{2\sqrt{2}} & \frac{v_{dc}}{2\sqrt{2}} \\ \frac{v_{dc}}{\sqrt{3}} & \frac{\sqrt{3}v_{dc}}{4} & \frac{\sqrt{3}v_{dc}}{2} & \frac{5v_{dc}}{4\sqrt{3}} \\ 1 & 1 & 1 & 1 \end{bmatrix}$
TeT_4^5	TeT_5^5	TeT_6^5
$\begin{bmatrix} \frac{5v_{dc}}{4\sqrt{6}} & \frac{\sqrt{3}v_{dc}}{2\sqrt{2}} & \frac{v_{dc}}{\sqrt{6}} & \frac{v_{dc}}{\sqrt{6}} \\ \frac{3v_{dc}}{4\sqrt{2}} & \frac{v_{dc}}{2\sqrt{2}} & \frac{v_{dc}}{2\sqrt{2}} & \frac{v_{dc}}{2\sqrt{2}} \\ \frac{v_{dc}}{\sqrt{3}} & \frac{\sqrt{3}v_{dc}}{4} & \frac{v_{dc}}{2\sqrt{3}} & \frac{5v_{dc}}{4\sqrt{3}} \\ 1 & 1 & 1 & 1 \end{bmatrix}$	$\begin{bmatrix} \frac{5v_{dc}}{4\sqrt{6}} & \frac{\sqrt{3}v_{dc}}{2\sqrt{2}} & \frac{v_{dc}}{\sqrt{6}} & \frac{5v_{dc}}{4\sqrt{6}} \\ \frac{3v_{dc}}{4\sqrt{2}} & \frac{v_{dc}}{2\sqrt{2}} & \frac{v_{dc}}{2\sqrt{2}} & \frac{3v_{dc}}{4\sqrt{2}} \\ \frac{v_{dc}}{\sqrt{3}} & \frac{\sqrt{3}v_{dc}}{4} & \frac{v_{dc}}{2\sqrt{3}} & \frac{v_{dc}}{4\sqrt{3}} \\ 1 & 1 & 1 & 1 \end{bmatrix}$	$\begin{bmatrix} \frac{\sqrt{3}v_{dc}}{2\sqrt{2}} & \frac{\sqrt{3}v_{dc}}{2\sqrt{2}} & \frac{v_{dc}}{\sqrt{6}} & \frac{5v_{dc}}{4\sqrt{6}} \\ \frac{v_{dc}}{2\sqrt{2}} & \frac{v_{dc}}{2\sqrt{2}} & \frac{v_{dc}}{2\sqrt{2}} & \frac{3v_{dc}}{4\sqrt{2}} \\ 0 & \frac{\sqrt{3}v_{dc}}{4} & \frac{v_{dc}}{2\sqrt{3}} & \frac{v_{dc}}{4\sqrt{3}} \\ 1 & 1 & 1 & 1 \end{bmatrix}$
TeT_7^5	TeT_8^5	TeT_9^5

$\begin{bmatrix} \frac{\sqrt{3}v_{dc}}{2\sqrt{2}} & \frac{v_{dc}}{\sqrt{6}} & \frac{v_{dc}}{\sqrt{6}} & \frac{5v_{dc}}{4\sqrt{6}} \\ \frac{v_{dc}}{2\sqrt{2}} & \frac{v_{dc}}{2\sqrt{2}} & \frac{v_{dc}}{2\sqrt{2}} & \frac{3v_{dc}}{4\sqrt{2}} \\ 0 & \frac{-v_{dc}}{4\sqrt{3}} & \frac{v_{dc}}{2\sqrt{3}} & \frac{v_{dc}}{4\sqrt{3}} \\ 1 & 1 & 1 & 1 \end{bmatrix}$	$\begin{bmatrix} \frac{\sqrt{3}v_{dc}}{2\sqrt{2}} & \frac{v_{dc}}{\sqrt{6}} & \frac{5v_{dc}}{4\sqrt{6}} & \frac{5v_{dc}}{4\sqrt{6}} \\ \frac{v_{dc}}{2\sqrt{2}} & \frac{v_{dc}}{2\sqrt{2}} & \frac{3v_{dc}}{4\sqrt{2}} & \frac{3v_{dc}}{4\sqrt{2}} \\ 0 & \frac{-v_{dc}}{4\sqrt{3}} & \frac{-v_{dc}}{2\sqrt{3}} & \frac{v_{dc}}{4\sqrt{3}} \\ 1 & 1 & 1 & 1 \end{bmatrix}$	$\begin{bmatrix} \frac{\sqrt{3}v_{dc}}{2\sqrt{2}} & \frac{v_{dc}}{\sqrt{6}} & \frac{5v_{dc}}{4\sqrt{6}} & \frac{\sqrt{3}v_{dc}}{2\sqrt{2}} \\ \frac{v_{dc}}{2\sqrt{2}} & \frac{v_{dc}}{2\sqrt{2}} & \frac{3v_{dc}}{4\sqrt{2}} & \frac{v_{dc}}{2\sqrt{2}} \\ 0 & \frac{-v_{dc}}{4\sqrt{3}} & \frac{-v_{dc}}{2\sqrt{3}} & \frac{-\sqrt{3}v_{dc}}{4} \\ 1 & 1 & 1 & 1 \end{bmatrix}$
TeT_{10}^{5}	TeT_{11}^{5}	TeT_{12}^{5}
$\begin{bmatrix} \frac{v_{dc}}{\sqrt{6}} & \frac{v_{dc}}{\sqrt{6}} & \frac{5v_{dc}}{4\sqrt{6}} & \frac{\sqrt{3}v_{dc}}{2\sqrt{2}} \\ \frac{v_{dc}}{2\sqrt{2}} & \frac{v_{dc}}{2\sqrt{2}} & \frac{3v_{dc}}{4\sqrt{2}} & \frac{v_{dc}}{2\sqrt{2}} \\ \frac{-v_{dc}}{\sqrt{3}} & \frac{-v_{dc}}{4\sqrt{3}} & \frac{-v_{dc}}{2\sqrt{3}} & \frac{-\sqrt{3}v_{dc}}{4} \\ 1 & 1 & 1 & 1 \end{bmatrix}$	$\begin{bmatrix} \frac{v_{dc}}{\sqrt{6}} & \frac{5v_{dc}}{4\sqrt{6}} & \frac{5v_{dc}}{4\sqrt{6}} & \frac{\sqrt{3}v_{dc}}{2\sqrt{2}} \\ \frac{v_{dc}}{2\sqrt{2}} & \frac{3v_{dc}}{4\sqrt{2}} & \frac{3v_{dc}}{4\sqrt{2}} & \frac{v_{dc}}{2\sqrt{2}} \\ \frac{-v_{dc}}{\sqrt{3}} & \frac{-5v_{dc}}{4\sqrt{3}} & \frac{-v_{dc}}{2\sqrt{3}} & \frac{-\sqrt{3}v_{dc}}{4} \\ 1 & 1 & 1 & 1 \end{bmatrix}$	$\begin{bmatrix} \frac{v_{dc}}{\sqrt{6}} & \frac{5v_{dc}}{4\sqrt{6}} & \frac{\sqrt{3}v_{dc}}{2\sqrt{2}} & \frac{\sqrt{3}v_{dc}}{2\sqrt{2}} \\ \frac{v_{dc}}{2\sqrt{2}} & \frac{3v_{dc}}{4\sqrt{2}} & \frac{v_{dc}}{2\sqrt{2}} & \frac{v_{dc}}{2\sqrt{2}} \\ \frac{-v_{dc}}{\sqrt{3}} & \frac{-5v_{dc}}{4\sqrt{3}} & \frac{-\sqrt{3}v_{dc}}{2} & \frac{-\sqrt{3}v_{dc}}{4} \\ 1 & 1 & 1 & 1 \end{bmatrix}$
TeT_{13}^{5}		
$\begin{bmatrix} \frac{v_{dc}}{\sqrt{6}} & \frac{5v_{dc}}{4\sqrt{6}} & \frac{\sqrt{3}v_{dc}}{2\sqrt{2}} & \frac{v_{dc}}{\sqrt{6}} \\ \frac{v_{dc}}{2\sqrt{2}} & \frac{3v_{dc}}{4\sqrt{2}} & \frac{v_{dc}}{2\sqrt{2}} & \frac{v_{dc}}{2\sqrt{2}} \\ \frac{-v_{dc}}{\sqrt{3}} & \frac{-5v_{dc}}{4\sqrt{3}} & \frac{-\sqrt{3}v_{dc}}{2} & \frac{-7v_{dc}}{4\sqrt{3}} \\ 1 & 1 & 1 & 1 \end{bmatrix}$		

PR_6		
TeT_{1}^{6}	TeT_{2}^{6}	TeT_{3}^{6}
$\begin{bmatrix} \frac{\sqrt{3}v_{dc}}{4\sqrt{2}} & \frac{v_{dc}}{\sqrt{6}} & \frac{5v_{dc}}{4\sqrt{6}} & \frac{\sqrt{3}v_{dc}}{4\sqrt{2}} \\ \frac{3v_{dc}}{4\sqrt{2}} & \frac{v_{dc}}{2\sqrt{2}} & \frac{3v_{dc}}{4\sqrt{2}} & \frac{3v_{dc}}{4\sqrt{2}} \\ \frac{3\sqrt{3}v_{dc}}{4} & \frac{2v_{dc}}{\sqrt{3}} & \frac{7v_{dc}}{4\sqrt{3}} & \frac{\sqrt{3}v_{dc}}{2} \\ 1 & 1 & 1 & 1 \end{bmatrix}$	$\begin{bmatrix} \frac{v_{dc}}{\sqrt{6}} & \frac{v_{dc}}{\sqrt{6}} & \frac{5v_{dc}}{4\sqrt{6}} & \frac{\sqrt{3}v_{dc}}{4\sqrt{2}} \\ \frac{v_{dc}}{2\sqrt{2}} & \frac{v_{dc}}{2\sqrt{2}} & \frac{3v_{dc}}{4\sqrt{2}} & \frac{3v_{dc}}{4\sqrt{2}} \\ \frac{5v_{dc}}{4\sqrt{3}} & \frac{2v_{dc}}{\sqrt{3}} & \frac{7v_{dc}}{4\sqrt{3}} & \frac{\sqrt{3}v_{dc}}{2} \\ 1 & 1 & 1 & 1 \end{bmatrix}$	$\begin{bmatrix} \frac{v_{dc}}{\sqrt{6}} & \frac{5v_{dc}}{4\sqrt{6}} & \frac{5v_{dc}}{4\sqrt{6}} & \frac{\sqrt{3}v_{dc}}{4\sqrt{2}} \\ \frac{v_{dc}}{2\sqrt{2}} & \frac{3v_{dc}}{4\sqrt{2}} & \frac{3v_{dc}}{4\sqrt{2}} & \frac{3v_{dc}}{4\sqrt{2}} \\ \frac{5v_{dc}}{4\sqrt{3}} & \frac{v_{dc}}{\sqrt{3}} & \frac{7v_{dc}}{4\sqrt{3}} & \frac{\sqrt{3}v_{dc}}{2} \\ 1 & 1 & 1 & 1 \end{bmatrix}$
TeT_{4}^{6}	TeT_{5}^{6}	TeT_{6}^{6}

$\begin{bmatrix} \frac{v_{dc}}{\sqrt{6}} & \frac{5v_{dc}}{4\sqrt{6}} & \frac{\sqrt{3}v_{dc}}{4\sqrt{2}} & \frac{\sqrt{3}v_{dc}}{4\sqrt{2}} \\ \frac{v_{dc}}{2\sqrt{2}} & \frac{3v_{dc}}{4\sqrt{2}} & \frac{3v_{dc}}{4\sqrt{2}} & \frac{3v_{dc}}{4\sqrt{2}} \\ \frac{5v_{dc}}{4\sqrt{3}} & \frac{v_{dc}}{\sqrt{3}} & \frac{\sqrt{3}v_{dc}}{4} & \frac{\sqrt{3}v_{dc}}{2} \\ 1 & 1 & 1 & 1 \end{bmatrix}$	$\begin{bmatrix} \frac{v_{dc}}{\sqrt{6}} & \frac{5v_{dc}}{4\sqrt{6}} & \frac{\sqrt{3}v_{dc}}{4\sqrt{2}} & \frac{v_{dc}}{\sqrt{6}} \\ \frac{v_{dc}}{2\sqrt{2}} & \frac{3v_{dc}}{4\sqrt{2}} & \frac{3v_{dc}}{4\sqrt{2}} & \frac{v_{dc}}{2\sqrt{2}} \\ \frac{5v_{dc}}{4\sqrt{3}} & \frac{v_{dc}}{\sqrt{3}} & \frac{\sqrt{3}v_{dc}}{4} & \frac{v_{dc}}{2\sqrt{3}} \\ 1 & 1 & 1 & 1 \end{bmatrix}$	$\begin{bmatrix} \frac{5v_{dc}}{4\sqrt{6}} & \frac{5v_{dc}}{4\sqrt{6}} & \frac{\sqrt{3}v_{dc}}{4\sqrt{2}} & \frac{v_{dc}}{\sqrt{6}} \\ \frac{3v_{dc}}{4\sqrt{2}} & \frac{3v_{dc}}{4\sqrt{2}} & \frac{3v_{dc}}{4\sqrt{2}} & \frac{v_{dc}}{2\sqrt{2}} \\ \frac{v_{dc}}{4\sqrt{3}} & \frac{v_{dc}}{\sqrt{3}} & \frac{\sqrt{3}v_{dc}}{4} & \frac{v_{dc}}{2\sqrt{3}} \\ 1 & 1 & 1 & 1 \end{bmatrix}$
TeT_7^6	TeT_8^6	TeT_9^6
$\begin{bmatrix} \frac{5v_{dc}}{4\sqrt{6}} & \frac{\sqrt{3}v_{dc}}{4\sqrt{2}} & \frac{\sqrt{3}v_{dc}}{4\sqrt{2}} & \frac{v_{dc}}{\sqrt{6}} \\ \frac{3v_{dc}}{4\sqrt{2}} & \frac{3v_{dc}}{4\sqrt{2}} & \frac{3v_{dc}}{4\sqrt{2}} & \frac{v_{dc}}{2\sqrt{2}} \\ \frac{v_{dc}}{4\sqrt{3}} & 0 & \frac{\sqrt{3}v_{dc}}{4} & \frac{v_{dc}}{2\sqrt{3}} \\ 1 & 1 & 1 & 1 \end{bmatrix}$	$\begin{bmatrix} \frac{5v_{dc}}{4\sqrt{6}} & \frac{\sqrt{3}v_{dc}}{4\sqrt{2}} & \frac{v_{dc}}{\sqrt{6}} & \frac{v_{dc}}{\sqrt{6}} \\ \frac{3v_{dc}}{4\sqrt{2}} & \frac{3v_{dc}}{4\sqrt{2}} & \frac{v_{dc}}{2\sqrt{2}} & \frac{v_{dc}}{2\sqrt{2}} \\ \frac{v_{dc}}{4\sqrt{3}} & 0 & \frac{-v_{dc}}{4\sqrt{3}} & \frac{v_{dc}}{2\sqrt{3}} \\ 1 & 1 & 1 & 1 \end{bmatrix}$	$\begin{bmatrix} \frac{5v_{dc}}{4\sqrt{6}} & \frac{\sqrt{3}v_{dc}}{4\sqrt{2}} & \frac{v_{dc}}{\sqrt{6}} & \frac{5v_{dc}}{4\sqrt{6}} \\ \frac{3v_{dc}}{4\sqrt{2}} & \frac{3v_{dc}}{4\sqrt{2}} & \frac{v_{dc}}{2\sqrt{2}} & \frac{3v_{dc}}{4\sqrt{2}} \\ \frac{v_{dc}}{4\sqrt{3}} & 0 & \frac{-v_{dc}}{4\sqrt{3}} & \frac{-v_{dc}}{2\sqrt{3}} \\ 1 & 1 & 1 & 1 \end{bmatrix}$
TeT_{10}^6	TeT_{11}^6	TeT_{12}^6
$\begin{bmatrix} \frac{\sqrt{3}v_{dc}}{4\sqrt{2}} & \frac{\sqrt{3}v_{dc}}{4\sqrt{2}} & \frac{v_{dc}}{\sqrt{6}} & \frac{5v_{dc}}{4\sqrt{6}} \\ \frac{3v_{dc}}{4\sqrt{2}} & \frac{3v_{dc}}{4\sqrt{2}} & \frac{v_{dc}}{2\sqrt{2}} & \frac{3v_{dc}}{4\sqrt{2}} \\ \frac{-\sqrt{3}v_{dc}}{4} & 0 & \frac{-v_{dc}}{4\sqrt{3}} & \frac{-v_{dc}}{2\sqrt{3}} \\ 1 & 1 & 1 & 1 \end{bmatrix}$	$\begin{bmatrix} \frac{\sqrt{3}v_{dc}}{4\sqrt{2}} & \frac{v_{dc}}{\sqrt{6}} & \frac{v_{dc}}{\sqrt{6}} & \frac{5v_{dc}}{4\sqrt{6}} \\ \frac{3v_{dc}}{4\sqrt{2}} & \frac{v_{dc}}{2\sqrt{2}} & \frac{v_{dc}}{2\sqrt{2}} & \frac{3v_{dc}}{4\sqrt{2}} \\ \frac{-\sqrt{3}v_{dc}}{4} & \frac{-v_{dc}}{\sqrt{3}} & \frac{-v_{dc}}{4\sqrt{3}} & \frac{-v_{dc}}{2\sqrt{3}} \\ 1 & 1 & 1 & 1 \end{bmatrix}$	$\begin{bmatrix} \frac{\sqrt{3}v_{dc}}{4\sqrt{2}} & \frac{v_{dc}}{\sqrt{6}} & \frac{5v_{dc}}{4\sqrt{6}} & \frac{5v_{dc}}{4\sqrt{6}} \\ \frac{3v_{dc}}{4\sqrt{2}} & \frac{v_{dc}}{2\sqrt{2}} & \frac{3v_{dc}}{4\sqrt{2}} & \frac{3v_{dc}}{4\sqrt{2}} \\ \frac{-\sqrt{3}v_{dc}}{4} & \frac{-v_{dc}}{\sqrt{3}} & \frac{-5v_{dc}}{4\sqrt{3}} & \frac{-v_{dc}}{2\sqrt{3}} \\ 1 & 1 & 1 & 1 \end{bmatrix}$
TeT_{13}^6	TeT_{14}^6	
$\begin{bmatrix} \frac{\sqrt{3}v_{dc}}{4\sqrt{2}} & \frac{v_{dc}}{\sqrt{6}} & \frac{5v_{dc}}{4\sqrt{6}} & \frac{\sqrt{3}v_{dc}}{4\sqrt{2}} \\ \frac{3v_{dc}}{4\sqrt{2}} & \frac{v_{dc}}{2\sqrt{2}} & \frac{3v_{dc}}{4\sqrt{2}} & \frac{3v_{dc}}{4\sqrt{2}} \\ \frac{-\sqrt{3}v_{dc}}{4} & \frac{-v_{dc}}{\sqrt{3}} & \frac{-5v_{dc}}{4\sqrt{3}} & \frac{-\sqrt{3}v_{dc}}{2} \\ 1 & 1 & 1 & 1 \end{bmatrix}$	$\begin{bmatrix} \frac{v_{dc}}{\sqrt{6}} & \frac{v_{dc}}{\sqrt{6}} & \frac{5v_{dc}}{4\sqrt{6}} & \frac{\sqrt{3}v_{dc}}{4\sqrt{2}} \\ \frac{v_{dc}}{2\sqrt{2}} & \frac{v_{dc}}{2\sqrt{2}} & \frac{3v_{dc}}{4\sqrt{2}} & \frac{3v_{dc}}{4\sqrt{2}} \\ \frac{-7v_{dc}}{4\sqrt{3}} & \frac{-v_{dc}}{\sqrt{3}} & \frac{-5v_{dc}}{4\sqrt{3}} & \frac{-\sqrt{3}v_{dc}}{2} \\ 1 & 1 & 1 & 1 \end{bmatrix}$	

PR_7		
TeT_1^7	TeT_2^7	TeT_3^7
$\begin{bmatrix} \frac{\sqrt{3}v_{dc}}{4\sqrt{2}} & \frac{v_{dc}}{\sqrt{6}} & \frac{5v_{dc}}{4\sqrt{6}} & \frac{\sqrt{3}v_{dc}}{4\sqrt{2}} \\ \frac{3v_{dc}}{4\sqrt{2}} & \frac{v_{dc}}{\sqrt{2}} & \frac{3v_{dc}}{4\sqrt{2}} & \frac{3v_{dc}}{4\sqrt{2}} \\ \frac{3\sqrt{3}v_{dc}}{4} & \frac{2v_{dc}}{\sqrt{3}} & \frac{7v_{dc}}{4\sqrt{3}} & \frac{\sqrt{3}v_{dc}}{2} \\ 1 & 1 & 1 & 1 \end{bmatrix}$	$\begin{bmatrix} \frac{v_{dc}}{\sqrt{6}} & \frac{v_{dc}}{\sqrt{6}} & \frac{5v_{dc}}{4\sqrt{6}} & \frac{\sqrt{3}v_{dc}}{4\sqrt{2}} \\ \frac{v_{dc}}{\sqrt{2}} & \frac{v_{dc}}{\sqrt{2}} & \frac{3v_{dc}}{4\sqrt{2}} & \frac{3v_{dc}}{4\sqrt{2}} \\ \frac{5v_{dc}}{4\sqrt{3}} & \frac{2v_{dc}}{\sqrt{3}} & \frac{7v_{dc}}{4\sqrt{3}} & \frac{\sqrt{3}v_{dc}}{2} \\ 1 & 1 & 1 & 1 \end{bmatrix}$	$\begin{bmatrix} \frac{v_{dc}}{\sqrt{6}} & \frac{5v_{dc}}{4\sqrt{6}} & \frac{5v_{dc}}{4\sqrt{6}} & \frac{\sqrt{3}v_{dc}}{4\sqrt{2}} \\ \frac{v_{dc}}{\sqrt{2}} & \frac{3v_{dc}}{4\sqrt{2}} & \frac{3v_{dc}}{4\sqrt{2}} & \frac{3v_{dc}}{4\sqrt{2}} \\ \frac{5v_{dc}}{4\sqrt{3}} & \frac{v_{dc}}{\sqrt{3}} & \frac{7v_{dc}}{4\sqrt{3}} & \frac{\sqrt{3}v_{dc}}{2} \\ 1 & 1 & 1 & 1 \end{bmatrix}$
TeT_4^7	TeT_5^7	TeT_6^7
$\begin{bmatrix} \frac{v_{dc}}{\sqrt{6}} & \frac{5v_{dc}}{4\sqrt{6}} & \frac{\sqrt{3}v_{dc}}{4\sqrt{2}} & \frac{\sqrt{3}v_{dc}}{4\sqrt{2}} \\ \frac{v_{dc}}{\sqrt{2}} & \frac{3v_{dc}}{4\sqrt{2}} & \frac{3v_{dc}}{4\sqrt{2}} & \frac{3v_{dc}}{4\sqrt{2}} \\ \frac{5v_{dc}}{4\sqrt{3}} & \frac{v_{dc}}{\sqrt{3}} & \frac{\sqrt{3}v_{dc}}{4} & \frac{\sqrt{3}v_{dc}}{2} \\ 1 & 1 & 1 & 1 \end{bmatrix}$	$\begin{bmatrix} \frac{v_{dc}}{\sqrt{6}} & \frac{5v_{dc}}{4\sqrt{6}} & \frac{\sqrt{3}v_{dc}}{4\sqrt{2}} & \frac{v_{dc}}{\sqrt{6}} \\ \frac{v_{dc}}{\sqrt{2}} & \frac{3v_{dc}}{4\sqrt{2}} & \frac{3v_{dc}}{4\sqrt{2}} & \frac{v_{dc}}{\sqrt{2}} \\ \frac{5v_{dc}}{4\sqrt{3}} & \frac{v_{dc}}{\sqrt{3}} & \frac{\sqrt{3}v_{dc}}{4} & \frac{v_{dc}}{2\sqrt{3}} \\ 1 & 1 & 1 & 1 \end{bmatrix}$	$\begin{bmatrix} \frac{5v_{dc}}{4\sqrt{6}} & \frac{5v_{dc}}{4\sqrt{6}} & \frac{\sqrt{3}v_{dc}}{4\sqrt{2}} & \frac{v_{dc}}{\sqrt{6}} \\ \frac{3v_{dc}}{4\sqrt{2}} & \frac{3v_{dc}}{4\sqrt{2}} & \frac{3v_{dc}}{4\sqrt{2}} & \frac{v_{dc}}{\sqrt{2}} \\ \frac{v_{dc}}{4\sqrt{3}} & \frac{v_{dc}}{\sqrt{3}} & \frac{\sqrt{3}v_{dc}}{4} & \frac{v_{dc}}{2\sqrt{3}} \\ 1 & 1 & 1 & 1 \end{bmatrix}$
TeT_7^7	TeT_8^7	TeT_9^7
$\begin{bmatrix} \frac{5v_{dc}}{4\sqrt{6}} & \frac{\sqrt{3}v_{dc}}{4\sqrt{2}} & \frac{\sqrt{3}v_{dc}}{4\sqrt{2}} & \frac{v_{dc}}{\sqrt{6}} \\ \frac{3v_{dc}}{4\sqrt{2}} & \frac{3v_{dc}}{4\sqrt{2}} & \frac{3v_{dc}}{4\sqrt{2}} & \frac{v_{dc}}{\sqrt{2}} \\ \frac{v_{dc}}{4\sqrt{3}} & 0 & \frac{\sqrt{3}v_{dc}}{4} & \frac{v_{dc}}{2\sqrt{3}} \\ 1 & 1 & 1 & 1 \end{bmatrix}$	$\begin{bmatrix} \frac{5v_{dc}}{4\sqrt{6}} & \frac{\sqrt{3}v_{dc}}{4\sqrt{2}} & \frac{v_{dc}}{\sqrt{6}} & \frac{v_{dc}}{\sqrt{6}} \\ \frac{3v_{dc}}{4\sqrt{2}} & \frac{3v_{dc}}{4\sqrt{2}} & \frac{v_{dc}}{\sqrt{2}} & \frac{v_{dc}}{\sqrt{2}} \\ \frac{v_{dc}}{4\sqrt{3}} & 0 & \frac{-v_{dc}}{4\sqrt{3}} & \frac{v_{dc}}{2\sqrt{3}} \\ 1 & 1 & 1 & 1 \end{bmatrix}$	$\begin{bmatrix} \frac{5v_{dc}}{4\sqrt{6}} & \frac{\sqrt{3}v_{dc}}{4\sqrt{2}} & \frac{v_{dc}}{\sqrt{6}} & \frac{5v_{dc}}{4\sqrt{6}} \\ \frac{3v_{dc}}{4\sqrt{2}} & \frac{3v_{dc}}{4\sqrt{2}} & \frac{v_{dc}}{\sqrt{2}} & \frac{3v_{dc}}{4\sqrt{2}} \\ \frac{v_{dc}}{4\sqrt{3}} & 0 & \frac{-v_{dc}}{4\sqrt{3}} & \frac{-v_{dc}}{2\sqrt{3}} \\ 1 & 1 & 1 & 1 \end{bmatrix}$
TeT_{10}^7	TeT_{11}^7	TeT_{12}^7
$\begin{bmatrix} \frac{\sqrt{3}v_{dc}}{4\sqrt{2}} & \frac{\sqrt{3}v_{dc}}{4\sqrt{2}} & \frac{v_{dc}}{\sqrt{6}} & \frac{5v_{dc}}{4\sqrt{6}} \\ \frac{3v_{dc}}{4\sqrt{2}} & \frac{3v_{dc}}{4\sqrt{2}} & \frac{v_{dc}}{\sqrt{2}} & \frac{3v_{dc}}{4\sqrt{2}} \\ \frac{-\sqrt{3}v_{dc}}{4} & 0 & \frac{-v_{dc}}{4\sqrt{3}} & \frac{-v_{dc}}{2\sqrt{3}} \\ 1 & 1 & 1 & 1 \end{bmatrix}$	$\begin{bmatrix} \frac{\sqrt{3}v_{dc}}{4\sqrt{2}} & \frac{v_{dc}}{\sqrt{6}} & \frac{v_{dc}}{\sqrt{6}} & \frac{5v_{dc}}{4\sqrt{6}} \\ \frac{3v_{dc}}{4\sqrt{2}} & \frac{v_{dc}}{\sqrt{2}} & \frac{v_{dc}}{\sqrt{2}} & \frac{3v_{dc}}{4\sqrt{2}} \\ \frac{-\sqrt{3}v_{dc}}{4} & \frac{-v_{dc}}{\sqrt{3}} & \frac{-v_{dc}}{4\sqrt{3}} & \frac{-v_{dc}}{2\sqrt{3}} \\ 1 & 1 & 1 & 1 \end{bmatrix}$	$\begin{bmatrix} \frac{\sqrt{3}v_{dc}}{4\sqrt{2}} & \frac{v_{dc}}{\sqrt{6}} & \frac{5v_{dc}}{4\sqrt{6}} & \frac{5v_{dc}}{4\sqrt{6}} \\ \frac{3v_{dc}}{4\sqrt{2}} & \frac{v_{dc}}{\sqrt{2}} & \frac{3v_{dc}}{4\sqrt{2}} & \frac{3v_{dc}}{4\sqrt{2}} \\ \frac{-\sqrt{3}v_{dc}}{4} & \frac{-v_{dc}}{\sqrt{3}} & \frac{-5v_{dc}}{4\sqrt{3}} & \frac{-v_{dc}}{2\sqrt{3}} \\ 1 & 1 & 1 & 1 \end{bmatrix}$
TeT_{13}^7		

$$\begin{bmatrix} \frac{\sqrt{3}v_{dc}}{4\sqrt{2}} & \frac{v_{dc}}{\sqrt{6}} & \frac{5v_{dc}}{4\sqrt{6}} & \frac{\sqrt{3}v_{dc}}{4\sqrt{2}} \\ \frac{3v_{dc}}{4\sqrt{2}} & \frac{v_{dc}}{\sqrt{2}} & \frac{3v_{dc}}{4\sqrt{2}} & \frac{3v_{dc}}{4\sqrt{2}} \\ \frac{-\sqrt{3}v_{dc}}{4} & \frac{-v_{dc}}{\sqrt{3}} & \frac{-5v_{dc}}{4\sqrt{3}} & \frac{-\sqrt{3}v_{dc}}{2} \\ 1 & 1 & 1 & 1 \end{bmatrix}$$

PR_8		
TeT_1^8	TeT_2^8	TeT_3^8
$\begin{bmatrix} \frac{v_{dc}}{\sqrt{6}} & \frac{5v_{dc}}{4\sqrt{6}} & \frac{\sqrt{3}v_{dc}}{2\sqrt{2}} & \frac{v_{dc}}{\sqrt{6}} \\ 0 & \frac{v_{dc}}{4\sqrt{2}} & 0 & 0 \\ \frac{2v_{dc}}{\sqrt{3}} & \frac{7v_{dc}}{4\sqrt{3}} & \frac{\sqrt{3}v_{dc}}{2} & \frac{5v_{dc}}{4\sqrt{3}} \\ 1 & 1 & 1 & 1 \end{bmatrix}$	$\begin{bmatrix} \frac{5v_{dc}}{4\sqrt{6}} & \frac{5v_{dc}}{4\sqrt{6}} & \frac{\sqrt{3}v_{dc}}{2\sqrt{2}} & \frac{v_{dc}}{\sqrt{6}} \\ \frac{v_{dc}}{4\sqrt{2}} & \frac{v_{dc}}{4\sqrt{2}} & 0 & 0 \\ \frac{v_{dc}}{\sqrt{3}} & \frac{7v_{dc}}{4\sqrt{3}} & \frac{\sqrt{3}v_{dc}}{2} & \frac{5v_{dc}}{4\sqrt{3}} \\ 1 & 1 & 1 & 1 \end{bmatrix}$	$\begin{bmatrix} \frac{5v_{dc}}{4\sqrt{6}} & \frac{\sqrt{3}v_{dc}}{2\sqrt{2}} & \frac{\sqrt{3}v_{dc}}{2\sqrt{2}} & \frac{v_{dc}}{\sqrt{6}} \\ \frac{v_{dc}}{4\sqrt{2}} & 0 & 0 & 0 \\ \frac{v_{dc}}{\sqrt{3}} & \frac{\sqrt{3}v_{dc}}{4} & \frac{\sqrt{3}v_{dc}}{2} & \frac{5v_{dc}}{4\sqrt{3}} \\ 1 & 1 & 1 & 1 \end{bmatrix}$
TeT_4^8	TeT_5^8	TeT_6^8
$\begin{bmatrix} \frac{5v_{dc}}{4\sqrt{6}} & \frac{\sqrt{3}v_{dc}}{2\sqrt{2}} & \frac{v_{dc}}{\sqrt{6}} & \frac{v_{dc}}{\sqrt{6}} \\ \frac{v_{dc}}{4\sqrt{2}} & 0 & 0 & 0 \\ \frac{v_{dc}}{\sqrt{3}} & \frac{\sqrt{3}v_{dc}}{4} & \frac{v_{dc}}{2\sqrt{3}} & \frac{5v_{dc}}{4\sqrt{3}} \\ 1 & 1 & 1 & 1 \end{bmatrix}$	$\begin{bmatrix} \frac{5v_{dc}}{4\sqrt{6}} & \frac{\sqrt{3}v_{dc}}{2\sqrt{2}} & \frac{v_{dc}}{\sqrt{6}} & \frac{5v_{dc}}{4\sqrt{6}} \\ \frac{v_{dc}}{4\sqrt{2}} & 0 & 0 & \frac{v_{dc}}{4\sqrt{2}} \\ \frac{v_{dc}}{\sqrt{3}} & \frac{\sqrt{3}v_{dc}}{4} & \frac{v_{dc}}{2\sqrt{3}} & \frac{v_{dc}}{4\sqrt{3}} \\ 1 & 1 & 1 & 1 \end{bmatrix}$	$\begin{bmatrix} \frac{\sqrt{3}v_{dc}}{2\sqrt{2}} & \frac{\sqrt{3}v_{dc}}{2\sqrt{2}} & \frac{v_{dc}}{\sqrt{6}} & \frac{5v_{dc}}{4\sqrt{6}} \\ 0 & 0 & 0 & \frac{v_{dc}}{4\sqrt{2}} \\ 0 & \frac{\sqrt{3}v_{dc}}{4} & \frac{v_{dc}}{2\sqrt{3}} & \frac{v_{dc}}{4\sqrt{3}} \\ 1 & 1 & 1 & 1 \end{bmatrix}$
TeT_7^8	TeT_8^8	TeT_9^8
$\begin{bmatrix} \frac{\sqrt{3}v_{dc}}{2\sqrt{2}} & \frac{v_{dc}}{\sqrt{6}} & \frac{v_{dc}}{\sqrt{6}} & \frac{5v_{dc}}{4\sqrt{6}} \\ 0 & 0 & 0 & \frac{v_{dc}}{4\sqrt{2}} \\ 0 & \frac{-v_{dc}}{4\sqrt{3}} & \frac{v_{dc}}{2\sqrt{3}} & \frac{v_{dc}}{4\sqrt{3}} \\ 1 & 1 & 1 & 1 \end{bmatrix}$	$\begin{bmatrix} \frac{\sqrt{3}v_{dc}}{2\sqrt{2}} & \frac{v_{dc}}{\sqrt{6}} & \frac{5v_{dc}}{4\sqrt{6}} & \frac{5v_{dc}}{4\sqrt{6}} \\ 0 & 0 & \frac{v_{dc}}{4\sqrt{2}} & \frac{v_{dc}}{4\sqrt{2}} \\ 0 & \frac{-v_{dc}}{4\sqrt{3}} & \frac{-v_{dc}}{2\sqrt{3}} & \frac{v_{dc}}{4\sqrt{3}} \\ 1 & 1 & 1 & 1 \end{bmatrix}$	$\begin{bmatrix} \frac{\sqrt{3}v_{dc}}{2\sqrt{2}} & \frac{v_{dc}}{\sqrt{6}} & \frac{5v_{dc}}{4\sqrt{6}} & \frac{\sqrt{3}v_{dc}}{2\sqrt{2}} \\ 0 & 0 & \frac{v_{dc}}{4\sqrt{2}} & 0 \\ 0 & \frac{-v_{dc}}{4\sqrt{3}} & \frac{-v_{dc}}{2\sqrt{3}} & \frac{-\sqrt{3}v_{dc}}{4} \\ 1 & 1 & 1 & 1 \end{bmatrix}$
TeT_{10}^7	TeT_{11}^7	TeT_{12}^7

$\begin{bmatrix} \frac{v_{dc}}{\sqrt{6}} & \frac{v_{dc}}{\sqrt{6}} & \frac{5v_{dc}}{4\sqrt{6}} & \frac{\sqrt{3}v_{dc}}{2\sqrt{2}} \\ 0 & 0 & \frac{v_{dc}}{4\sqrt{2}} & 0 \\ \frac{-v_{dc}}{\sqrt{3}} & \frac{-v_{dc}}{4\sqrt{3}} & \frac{-v_{dc}}{2\sqrt{3}} & \frac{-\sqrt{3}v_{dc}}{4} \\ 1 & 1 & 1 & 1 \end{bmatrix}$	$\begin{bmatrix} \frac{v_{dc}}{\sqrt{6}} & \frac{5v_{dc}}{4\sqrt{6}} & \frac{5v_{dc}}{4\sqrt{6}} & \frac{\sqrt{3}v_{dc}}{2\sqrt{2}} \\ 0 & \frac{v_{dc}}{4\sqrt{2}} & \frac{v_{dc}}{4\sqrt{2}} & 0 \\ \frac{-v_{dc}}{\sqrt{3}} & \frac{-5v_{dc}}{4\sqrt{3}} & \frac{-v_{dc}}{2\sqrt{3}} & \frac{-\sqrt{3}v_{dc}}{4} \\ 1 & 1 & 1 & 1 \end{bmatrix}$	$\begin{bmatrix} \frac{v_{dc}}{\sqrt{6}} & \frac{5v_{dc}}{4\sqrt{6}} & \frac{\sqrt{3}v_{dc}}{2\sqrt{2}} & \frac{\sqrt{3}v_{dc}}{2\sqrt{2}} \\ 0 & \frac{v_{dc}}{4\sqrt{2}} & 0 & 0 \\ \frac{-v_{dc}}{\sqrt{3}} & \frac{-5v_{dc}}{4\sqrt{3}} & \frac{-\sqrt{3}v_{dc}}{2} & \frac{-\sqrt{3}v_{dc}}{4} \\ 1 & 1 & 1 & 1 \end{bmatrix}$
TeT_{13}^{8}	TeT_{14}^{8}	TeT_{15}^{8}
$\begin{bmatrix} \frac{v_{dc}}{\sqrt{6}} & \frac{5v_{dc}}{4\sqrt{6}} & \frac{\sqrt{3}v_{dc}}{2\sqrt{2}} & \frac{v_{dc}}{\sqrt{6}} \\ 0 & \frac{v_{dc}}{4\sqrt{2}} & 0 & 0 \\ \frac{-v_{dc}}{\sqrt{3}} & \frac{-5v_{dc}}{4\sqrt{3}} & \frac{-\sqrt{3}v_{dc}}{2} & \frac{-7v_{dc}}{4\sqrt{3}} \\ 1 & 1 & 1 & 1 \end{bmatrix}$	$\begin{bmatrix} \frac{5v_{dc}}{4\sqrt{6}} & \frac{5v_{dc}}{4\sqrt{6}} & \frac{\sqrt{3}v_{dc}}{2\sqrt{2}} & \frac{v_{dc}}{\sqrt{6}} \\ \frac{v_{dc}}{4\sqrt{2}} & \frac{v_{dc}}{4\sqrt{2}} & 0 & 0 \\ \frac{-2v_{dc}}{\sqrt{3}} & \frac{-5v_{dc}}{4\sqrt{3}} & \frac{-\sqrt{3}v_{dc}}{2} & \frac{-7v_{dc}}{4\sqrt{3}} \\ 1 & 1 & 1 & 1 \end{bmatrix}$	$\begin{bmatrix} \frac{5v_{dc}}{4\sqrt{6}} & \frac{\sqrt{3}v_{dc}}{2\sqrt{2}} & \frac{\sqrt{3}v_{dc}}{2\sqrt{2}} & \frac{v_{dc}}{\sqrt{6}} \\ \frac{v_{dc}}{4\sqrt{2}} & 0 & 0 & 0 \\ \frac{-2v_{dc}}{\sqrt{3}} & \frac{-3\sqrt{3}v_{dc}}{4} & \frac{-\sqrt{3}v_{dc}}{2} & \frac{-7v_{dc}}{4\sqrt{3}} \\ 1 & 1 & 1 & 1 \end{bmatrix}$
TeT_{16}^{8}		
$\begin{bmatrix} \frac{5v_{dc}}{4\sqrt{6}} & \frac{\sqrt{3}v_{dc}}{2\sqrt{2}} & \frac{v_{dc}}{\sqrt{6}} & \frac{v_{dc}}{\sqrt{6}} \\ \frac{v_{dc}}{4\sqrt{2}} & 0 & 0 & 0 \\ \frac{-2v_{dc}}{\sqrt{3}} & \frac{-3\sqrt{3}v_{dc}}{4} & \frac{-5v_{dc}}{2\sqrt{3}} & \frac{-7v_{dc}}{4\sqrt{3}} \\ 1 & 1 & 1 & 1 \end{bmatrix}$		

PR_9		
TeT_{1}^{9}	TeT_{2}^{9}	TeT_{3}^{9}
$\begin{bmatrix} \frac{\sqrt{3}v_{dc}}{4\sqrt{2}} & \frac{v_{dc}}{\sqrt{6}} & \frac{5v_{dc}}{4\sqrt{6}} & \frac{\sqrt{3}v_{dc}}{4\sqrt{2}} \\ \frac{v_{dc}}{4\sqrt{2}} & 0 & \frac{v_{dc}}{4\sqrt{2}} & \frac{v_{dc}}{4\sqrt{2}} \\ \frac{3\sqrt{3}v_{dc}}{4} & \frac{2v_{dc}}{\sqrt{3}} & \frac{7v_{dc}}{4\sqrt{3}} & \frac{\sqrt{3}v_{dc}}{2} \\ 1 & 1 & 1 & 1 \end{bmatrix}$	$\begin{bmatrix} \frac{v_{dc}}{\sqrt{6}} & \frac{v_{dc}}{\sqrt{6}} & \frac{5v_{dc}}{4\sqrt{6}} & \frac{\sqrt{3}v_{dc}}{4\sqrt{2}} \\ 0 & 0 & \frac{v_{dc}}{4\sqrt{2}} & \frac{v_{dc}}{4\sqrt{2}} \\ \frac{5v_{dc}}{4\sqrt{3}} & \frac{2v_{dc}}{\sqrt{3}} & \frac{7v_{dc}}{4\sqrt{3}} & \frac{\sqrt{3}v_{dc}}{2} \\ 1 & 1 & 1 & 1 \end{bmatrix}$	$\begin{bmatrix} \frac{v_{dc}}{\sqrt{6}} & \frac{5v_{dc}}{4\sqrt{6}} & \frac{5v_{dc}}{4\sqrt{6}} & \frac{\sqrt{3}v_{dc}}{4\sqrt{2}} \\ 0 & \frac{v_{dc}}{4\sqrt{2}} & \frac{v_{dc}}{4\sqrt{2}} & \frac{v_{dc}}{4\sqrt{2}} \\ \frac{5v_{dc}}{4\sqrt{3}} & \frac{v_{dc}}{\sqrt{3}} & \frac{7v_{dc}}{4\sqrt{3}} & \frac{\sqrt{3}v_{dc}}{2} \\ 1 & 1 & 1 & 1 \end{bmatrix}$
TeT_{4}^{9}	TeT_{5}^{9}	TeT_{6}^{9}

$\begin{bmatrix} \frac{v_{dc}}{\sqrt{6}} & \frac{5v_{dc}}{4\sqrt{6}} & \frac{\sqrt{3}v_{dc}}{4\sqrt{2}} & \frac{\sqrt{3}v_{dc}}{4\sqrt{2}} \\ 0 & \frac{v_{dc}}{4\sqrt{2}} & \frac{v_{dc}}{4\sqrt{2}} & \frac{v_{dc}}{4\sqrt{2}} \\ \frac{5v_{dc}}{4\sqrt{3}} & \frac{v_{dc}}{\sqrt{3}} & \frac{\sqrt{3}v_{dc}}{4} & \frac{\sqrt{3}v_{dc}}{2} \\ 1 & 1 & 1 & 1 \end{bmatrix}$	$\begin{bmatrix} \frac{v_{dc}}{\sqrt{6}} & \frac{5v_{dc}}{4\sqrt{6}} & \frac{\sqrt{3}v_{dc}}{4\sqrt{2}} & \frac{v_{dc}}{\sqrt{6}} \\ 0 & \frac{v_{dc}}{4\sqrt{2}} & \frac{v_{dc}}{4\sqrt{2}} & 0 \\ \frac{5v_{dc}}{4\sqrt{3}} & \frac{v_{dc}}{\sqrt{3}} & \frac{\sqrt{3}v_{dc}}{4} & \frac{v_{dc}}{2\sqrt{3}} \\ 1 & 1 & 1 & 1 \end{bmatrix}$	$\begin{bmatrix} \frac{5v_{dc}}{4\sqrt{6}} & \frac{5v_{dc}}{4\sqrt{6}} & \frac{\sqrt{3}v_{dc}}{4\sqrt{2}} & \frac{v_{dc}}{\sqrt{6}} \\ \frac{v_{dc}}{4\sqrt{2}} & \frac{v_{dc}}{4\sqrt{2}} & \frac{v_{dc}}{4\sqrt{2}} & 0 \\ \frac{v_{dc}}{4\sqrt{3}} & \frac{v_{dc}}{\sqrt{3}} & \frac{\sqrt{3}v_{dc}}{4} & \frac{v_{dc}}{2\sqrt{3}} \\ 1 & 1 & 1 & 1 \end{bmatrix}$
TeT_7^9	TeT_8^9	TeT_9^9
$\begin{bmatrix} \frac{5v_{dc}}{4\sqrt{6}} & \frac{\sqrt{3}v_{dc}}{4\sqrt{2}} & \frac{\sqrt{3}v_{dc}}{4\sqrt{2}} & \frac{v_{dc}}{\sqrt{6}} \\ \frac{v_{dc}}{4\sqrt{2}} & \frac{v_{dc}}{4\sqrt{2}} & \frac{v_{dc}}{4\sqrt{2}} & 0 \\ \frac{v_{dc}}{4\sqrt{3}} & 0 & \frac{\sqrt{3}v_{dc}}{4} & \frac{v_{dc}}{2\sqrt{3}} \\ 1 & 1 & 1 & 1 \end{bmatrix}$	$\begin{bmatrix} \frac{5v_{dc}}{4\sqrt{6}} & \frac{\sqrt{3}v_{dc}}{4\sqrt{2}} & \frac{v_{dc}}{\sqrt{6}} & \frac{v_{dc}}{\sqrt{6}} \\ \frac{v_{dc}}{4\sqrt{2}} & \frac{v_{dc}}{4\sqrt{2}} & 0 & 0 \\ \frac{v_{dc}}{4\sqrt{3}} & 0 & \frac{v_{dc}}{4\sqrt{3}} & \frac{v_{dc}}{2\sqrt{3}} \\ 1 & 1 & 1 & 1 \end{bmatrix}$	$\begin{bmatrix} \frac{5v_{dc}}{4\sqrt{6}} & \frac{\sqrt{3}v_{dc}}{4\sqrt{2}} & \frac{v_{dc}}{\sqrt{6}} & \frac{5v_{dc}}{4\sqrt{6}} \\ \frac{v_{dc}}{4\sqrt{2}} & \frac{v_{dc}}{4\sqrt{2}} & 0 & \frac{v_{dc}}{4\sqrt{2}} \\ \frac{v_{dc}}{4\sqrt{3}} & 0 & \frac{v_{dc}}{4\sqrt{3}} & \frac{-v_{dc}}{2\sqrt{3}} \\ 1 & 1 & 1 & 1 \end{bmatrix}$
TeT_{10}^9	TeT_{11}^9	TeT_{12}^9
$\begin{bmatrix} \frac{\sqrt{3}v_{dc}}{4\sqrt{2}} & \frac{\sqrt{3}v_{dc}}{4\sqrt{2}} & \frac{v_{dc}}{\sqrt{6}} & \frac{5v_{dc}}{4\sqrt{6}} \\ \frac{v_{dc}}{4\sqrt{2}} & \frac{v_{dc}}{4\sqrt{2}} & 0 & \frac{v_{dc}}{4\sqrt{2}} \\ \frac{-\sqrt{3}v_{dc}}{4} & 0 & \frac{v_{dc}}{4\sqrt{3}} & \frac{-v_{dc}}{2\sqrt{3}} \\ 1 & 1 & 1 & 1 \end{bmatrix}$	$\begin{bmatrix} \frac{\sqrt{3}v_{dc}}{4\sqrt{2}} & \frac{v_{dc}}{\sqrt{6}} & \frac{v_{dc}}{\sqrt{6}} & \frac{5v_{dc}}{4\sqrt{6}} \\ \frac{v_{dc}}{4\sqrt{2}} & 0 & 0 & \frac{v_{dc}}{4\sqrt{2}} \\ \frac{-\sqrt{3}v_{dc}}{4} & \frac{-v_{dc}}{\sqrt{3}} & \frac{v_{dc}}{4\sqrt{3}} & \frac{-v_{dc}}{2\sqrt{3}} \\ 1 & 1 & 1 & 1 \end{bmatrix}$	$\begin{bmatrix} \frac{\sqrt{3}v_{dc}}{4\sqrt{2}} & \frac{v_{dc}}{\sqrt{6}} & \frac{5v_{dc}}{4\sqrt{6}} & \frac{5v_{dc}}{4\sqrt{6}} \\ \frac{v_{dc}}{4\sqrt{2}} & 0 & \frac{v_{dc}}{4\sqrt{2}} & \frac{v_{dc}}{4\sqrt{2}} \\ \frac{-\sqrt{3}v_{dc}}{4} & \frac{-v_{dc}}{\sqrt{3}} & \frac{-5v_{dc}}{4\sqrt{3}} & \frac{-v_{dc}}{2\sqrt{3}} \\ 1 & 1 & 1 & 1 \end{bmatrix}$
TeT_{13}^9	TeT_{14}^9	TeT_{15}^9
$\begin{bmatrix} \frac{\sqrt{3}v_{dc}}{4\sqrt{2}} & \frac{v_{dc}}{\sqrt{6}} & \frac{5v_{dc}}{4\sqrt{6}} & \frac{\sqrt{3}v_{dc}}{4\sqrt{2}} \\ \frac{v_{dc}}{4\sqrt{2}} & 0 & \frac{v_{dc}}{4\sqrt{2}} & \frac{v_{dc}}{4\sqrt{2}} \\ \frac{-\sqrt{3}v_{dc}}{4} & \frac{-v_{dc}}{\sqrt{3}} & \frac{-5v_{dc}}{4\sqrt{3}} & \frac{-\sqrt{3}v_{dc}}{2} \\ 1 & 1 & 1 & 1 \end{bmatrix}$	$\begin{bmatrix} \frac{v_{dc}}{\sqrt{6}} & \frac{v_{dc}}{\sqrt{6}} & \frac{5v_{dc}}{4\sqrt{6}} & \frac{\sqrt{3}v_{dc}}{4\sqrt{2}} \\ 0 & 0 & \frac{v_{dc}}{4\sqrt{2}} & \frac{v_{dc}}{4\sqrt{2}} \\ \frac{-7v_{dc}}{4\sqrt{3}} & \frac{-v_{dc}}{\sqrt{3}} & \frac{-5v_{dc}}{4\sqrt{3}} & \frac{-\sqrt{3}v_{dc}}{2} \\ 1 & 1 & 1 & 1 \end{bmatrix}$	$\begin{bmatrix} \frac{v_{dc}}{\sqrt{6}} & \frac{5v_{dc}}{4\sqrt{6}} & \frac{5v_{dc}}{4\sqrt{6}} & \frac{\sqrt{3}v_{dc}}{4\sqrt{2}} \\ 0 & \frac{v_{dc}}{4\sqrt{2}} & \frac{v_{dc}}{4\sqrt{2}} & \frac{v_{dc}}{4\sqrt{2}} \\ \frac{-7v_{dc}}{4\sqrt{3}} & \frac{-2v_{dc}}{\sqrt{3}} & \frac{-5v_{dc}}{4\sqrt{3}} & \frac{-\sqrt{3}v_{dc}}{2} \\ 1 & 1 & 1 & 1 \end{bmatrix}$
TeT_{16}^9	TeT_{17}^9	

$\begin{bmatrix} \frac{v_{dc}}{\sqrt{6}} & \frac{5v_{dc}}{4\sqrt{6}} & \frac{\sqrt{3}v_{dc}}{4\sqrt{2}} & \frac{\sqrt{3}v_{dc}}{4\sqrt{2}} \\ 0 & \frac{v_{dc}}{4\sqrt{2}} & \frac{v_{dc}}{4\sqrt{2}} & \frac{v_{dc}}{4\sqrt{2}} \\ \frac{-7v_{dc}}{4\sqrt{3}} & \frac{-2v_{dc}}{\sqrt{3}} & \frac{-3\sqrt{3}v_{dc}}{4} & \frac{-\sqrt{3}v_{dc}}{2} \\ 1 & 1 & 1 & 1 \end{bmatrix}$	$\begin{bmatrix} \frac{v_{dc}}{\sqrt{6}} & \frac{5v_{dc}}{4\sqrt{6}} & \frac{\sqrt{3}v_{dc}}{4\sqrt{2}} & \frac{v_{dc}}{\sqrt{6}} \\ 0 & \frac{v_{dc}}{4\sqrt{2}} & \frac{v_{dc}}{4\sqrt{2}} & 0 \\ \frac{-7v_{dc}}{4\sqrt{3}} & \frac{-2v_{dc}}{\sqrt{3}} & \frac{-3\sqrt{3}v_{dc}}{4} & \frac{-5v_{dc}}{2\sqrt{3}} \\ 1 & 1 & 1 & 1 \end{bmatrix}$

PR_{10}		
TeT_1^{10}	TeT_2^{10}	TeT_3^{10}
$\begin{bmatrix} \frac{\sqrt{3}v_{dc}}{4\sqrt{2}} & \frac{v_{dc}}{\sqrt{6}} & \frac{5v_{dc}}{4\sqrt{6}} & \frac{\sqrt{3}v_{dc}}{4\sqrt{2}} \\ \frac{v_{dc}}{4\sqrt{2}} & \frac{v_{dc}}{2\sqrt{2}} & \frac{v_{dc}}{4\sqrt{2}} & \frac{v_{dc}}{4\sqrt{2}} \\ \frac{3\sqrt{3}v_{dc}}{4} & \frac{2v_{dc}}{\sqrt{3}} & \frac{7v_{dc}}{4\sqrt{3}} & \frac{\sqrt{3}v_{dc}}{2} \\ 1 & 1 & 1 & 1 \end{bmatrix}$	$\begin{bmatrix} \frac{v_{dc}}{\sqrt{6}} & \frac{v_{dc}}{\sqrt{6}} & \frac{5v_{dc}}{4\sqrt{6}} & \frac{\sqrt{3}v_{dc}}{4\sqrt{2}} \\ \frac{v_{dc}}{2\sqrt{2}} & \frac{v_{dc}}{2\sqrt{2}} & \frac{v_{dc}}{4\sqrt{2}} & \frac{v_{dc}}{4\sqrt{2}} \\ \frac{5v_{dc}}{4\sqrt{3}} & \frac{2v_{dc}}{\sqrt{3}} & \frac{7v_{dc}}{4\sqrt{3}} & \frac{\sqrt{3}v_{dc}}{2} \\ 1 & 1 & 1 & 1 \end{bmatrix}$	$\begin{bmatrix} \frac{v_{dc}}{\sqrt{6}} & \frac{5v_{dc}}{4\sqrt{6}} & \frac{5v_{dc}}{4\sqrt{6}} & \frac{\sqrt{3}v_{dc}}{4\sqrt{2}} \\ \frac{v_{dc}}{2\sqrt{2}} & \frac{v_{dc}}{4\sqrt{2}} & \frac{v_{dc}}{4\sqrt{2}} & \frac{v_{dc}}{4\sqrt{2}} \\ \frac{5v_{dc}}{4\sqrt{3}} & \frac{v_{dc}}{\sqrt{3}} & \frac{7v_{dc}}{4\sqrt{3}} & \frac{\sqrt{3}v_{dc}}{2} \\ 1 & 1 & 1 & 1 \end{bmatrix}$
TeT_4^{10}	TeT_5^{10}	TeT_6^{10}
$\begin{bmatrix} \frac{v_{dc}}{\sqrt{6}} & \frac{5v_{dc}}{4\sqrt{6}} & \frac{\sqrt{3}v_{dc}}{4\sqrt{2}} & \frac{\sqrt{3}v_{dc}}{4\sqrt{2}} \\ \frac{v_{dc}}{2\sqrt{2}} & \frac{v_{dc}}{4\sqrt{2}} & \frac{v_{dc}}{4\sqrt{2}} & \frac{v_{dc}}{4\sqrt{2}} \\ \frac{5v_{dc}}{4\sqrt{3}} & \frac{v_{dc}}{\sqrt{3}} & \frac{\sqrt{3}v_{dc}}{4} & \frac{\sqrt{3}v_{dc}}{2} \\ 1 & 1 & 1 & 1 \end{bmatrix}$	$\begin{bmatrix} \frac{v_{dc}}{\sqrt{6}} & \frac{5v_{dc}}{4\sqrt{6}} & \frac{\sqrt{3}v_{dc}}{4\sqrt{2}} & \frac{v_{dc}}{\sqrt{6}} \\ \frac{v_{dc}}{2\sqrt{2}} & \frac{v_{dc}}{4\sqrt{2}} & \frac{v_{dc}}{4\sqrt{2}} & \frac{v_{dc}}{2\sqrt{2}} \\ \frac{5v_{dc}}{4\sqrt{3}} & \frac{v_{dc}}{\sqrt{3}} & \frac{\sqrt{3}v_{dc}}{4} & \frac{v_{dc}}{2\sqrt{3}} \\ 1 & 1 & 1 & 1 \end{bmatrix}$	$\begin{bmatrix} \frac{5v_{dc}}{4\sqrt{6}} & \frac{5v_{dc}}{4\sqrt{6}} & \frac{\sqrt{3}v_{dc}}{4\sqrt{2}} & \frac{v_{dc}}{\sqrt{6}} \\ \frac{v_{dc}}{4\sqrt{2}} & \frac{v_{dc}}{4\sqrt{2}} & \frac{v_{dc}}{4\sqrt{2}} & \frac{v_{dc}}{2\sqrt{2}} \\ \frac{v_{dc}}{4\sqrt{3}} & \frac{v_{dc}}{\sqrt{3}} & \frac{\sqrt{3}v_{dc}}{4} & \frac{v_{dc}}{2\sqrt{3}} \\ 1 & 1 & 1 & 1 \end{bmatrix}$
TeT_7^{10}	TeT_8^{10}	TeT_9^{10}
$\begin{bmatrix} \frac{5v_{dc}}{4\sqrt{6}} & \frac{\sqrt{3}v_{dc}}{4\sqrt{2}} & \frac{\sqrt{3}v_{dc}}{4\sqrt{2}} & \frac{v_{dc}}{\sqrt{6}} \\ \frac{v_{dc}}{4\sqrt{2}} & \frac{v_{dc}}{4\sqrt{2}} & \frac{v_{dc}}{4\sqrt{2}} & \frac{v_{dc}}{2\sqrt{2}} \\ \frac{v_{dc}}{4\sqrt{3}} & 0 & \frac{\sqrt{3}v_{dc}}{4} & \frac{v_{dc}}{2\sqrt{3}} \\ 1 & 1 & 1 & 1 \end{bmatrix}$	$\begin{bmatrix} \frac{5v_{dc}}{4\sqrt{6}} & \frac{\sqrt{3}v_{dc}}{4\sqrt{2}} & \frac{v_{dc}}{\sqrt{6}} & \frac{v_{dc}}{\sqrt{6}} \\ \frac{v_{dc}}{4\sqrt{2}} & \frac{v_{dc}}{4\sqrt{2}} & \frac{v_{dc}}{2\sqrt{2}} & \frac{v_{dc}}{2\sqrt{2}} \\ \frac{v_{dc}}{4\sqrt{3}} & 0 & \frac{-v_{dc}}{4\sqrt{3}} & \frac{v_{dc}}{2\sqrt{3}} \\ 1 & 1 & 1 & 1 \end{bmatrix}$	$\begin{bmatrix} \frac{5v_{dc}}{4\sqrt{6}} & \frac{\sqrt{3}v_{dc}}{4\sqrt{2}} & \frac{v_{dc}}{\sqrt{6}} & \frac{5v_{dc}}{4\sqrt{6}} \\ \frac{v_{dc}}{4\sqrt{2}} & \frac{v_{dc}}{4\sqrt{2}} & \frac{v_{dc}}{2\sqrt{2}} & \frac{v_{dc}}{4\sqrt{2}} \\ \frac{v_{dc}}{4\sqrt{3}} & 0 & \frac{-v_{dc}}{4\sqrt{3}} & \frac{-v_{dc}}{2\sqrt{3}} \\ 1 & 1 & 1 & 1 \end{bmatrix}$
TeT_{10}^{10}	TeT_{11}^{10}	TeT_{12}^{10}

$\begin{bmatrix} \frac{\sqrt{3}v_{dc}}{4\sqrt{2}} & \frac{\sqrt{3}v_{dc}}{4\sqrt{2}} & \frac{v_{dc}}{\sqrt{6}} & \frac{5v_{dc}}{4\sqrt{6}} \\ \frac{v_{dc}}{4\sqrt{2}} & \frac{v_{dc}}{4\sqrt{2}} & \frac{v_{dc}}{2\sqrt{2}} & \frac{v_{dc}}{4\sqrt{2}} \\ \frac{-\sqrt{3}v_{dc}}{4} & 0 & \frac{-v_{dc}}{4\sqrt{3}} & \frac{-v_{dc}}{2\sqrt{3}} \\ 1 & 1 & 1 & 1 \end{bmatrix}$	$\begin{bmatrix} \frac{\sqrt{3}v_{dc}}{4\sqrt{2}} & \frac{v_{dc}}{\sqrt{6}} & \frac{v_{dc}}{\sqrt{6}} & \frac{5v_{dc}}{4\sqrt{6}} \\ \frac{v_{dc}}{4\sqrt{2}} & \frac{v_{dc}}{2\sqrt{2}} & \frac{v_{dc}}{2\sqrt{2}} & \frac{v_{dc}}{4\sqrt{2}} \\ \frac{-\sqrt{3}v_{dc}}{4} & \frac{-v_{dc}}{\sqrt{3}} & \frac{-v_{dc}}{4\sqrt{3}} & \frac{-v_{dc}}{2\sqrt{3}} \\ 1 & 1 & 1 & 1 \end{bmatrix}$	$\begin{bmatrix} \frac{\sqrt{3}v_{dc}}{4\sqrt{2}} & \frac{v_{dc}}{\sqrt{6}} & \frac{5v_{dc}}{4\sqrt{6}} & \frac{5v_{dc}}{4\sqrt{6}} \\ \frac{v_{dc}}{4\sqrt{2}} & \frac{v_{dc}}{2\sqrt{2}} & \frac{v_{dc}}{4\sqrt{2}} & \frac{v_{dc}}{4\sqrt{2}} \\ \frac{-\sqrt{3}v_{dc}}{4} & \frac{-v_{dc}}{\sqrt{3}} & \frac{-5v_{dc}}{4\sqrt{3}} & \frac{-v_{dc}}{2\sqrt{3}} \\ 1 & 1 & 1 & 1 \end{bmatrix}$
TeT_{13}^{10}	TeT_{14}^{10}	TeT_{15}^{10}
$\begin{bmatrix} \frac{\sqrt{3}v_{dc}}{4\sqrt{2}} & \frac{v_{dc}}{\sqrt{6}} & \frac{5v_{dc}}{4\sqrt{6}} & \frac{\sqrt{3}v_{dc}}{4\sqrt{2}} \\ \frac{v_{dc}}{4\sqrt{2}} & \frac{v_{dc}}{2\sqrt{2}} & \frac{v_{dc}}{4\sqrt{2}} & \frac{v_{dc}}{4\sqrt{2}} \\ \frac{-\sqrt{3}v_{dc}}{4} & \frac{-v_{dc}}{\sqrt{3}} & \frac{-5v_{dc}}{4\sqrt{3}} & \frac{-\sqrt{3}v_{dc}}{2} \\ 1 & 1 & 1 & 1 \end{bmatrix}$	$\begin{bmatrix} \frac{v_{dc}}{\sqrt{6}} & \frac{v_{dc}}{\sqrt{6}} & \frac{5v_{dc}}{4\sqrt{6}} & \frac{\sqrt{3}v_{dc}}{4\sqrt{2}} \\ \frac{v_{dc}}{2\sqrt{2}} & \frac{v_{dc}}{2\sqrt{2}} & \frac{v_{dc}}{4\sqrt{2}} & \frac{v_{dc}}{4\sqrt{2}} \\ \frac{-7v_{dc}}{4\sqrt{3}} & \frac{-v_{dc}}{\sqrt{3}} & \frac{-5v_{dc}}{4\sqrt{3}} & \frac{-\sqrt{3}v_{dc}}{2} \\ 1 & 1 & 1 & 1 \end{bmatrix}$	$\begin{bmatrix} \frac{\sqrt{3}v_{dc}}{4\sqrt{2}} & \frac{5v_{dc}}{4\sqrt{6}} & \frac{5v_{dc}}{4\sqrt{6}} & \frac{\sqrt{3}v_{dc}}{4\sqrt{2}} \\ \frac{v_{dc}}{4\sqrt{2}} & \frac{v_{dc}}{4\sqrt{2}} & \frac{v_{dc}}{4\sqrt{2}} & \frac{v_{dc}}{4\sqrt{2}} \\ \frac{-\sqrt{3}v_{dc}}{4} & \frac{-2v_{dc}}{\sqrt{3}} & \frac{-5v_{dc}}{4\sqrt{3}} & \frac{-\sqrt{3}v_{dc}}{2} \\ 1 & 1 & 1 & 1 \end{bmatrix}$
TeT_{16}^{10}		
$\begin{bmatrix} \frac{\sqrt{3}v_{dc}}{4\sqrt{2}} & \frac{5v_{dc}}{4\sqrt{6}} & \frac{\sqrt{3}v_{dc}}{4\sqrt{2}} & \frac{\sqrt{3}v_{dc}}{4\sqrt{2}} \\ \frac{v_{dc}}{4\sqrt{2}} & \frac{v_{dc}}{4\sqrt{2}} & \frac{v_{dc}}{4\sqrt{2}} & \frac{v_{dc}}{4\sqrt{2}} \\ \frac{-\sqrt{3}v_{dc}}{4} & \frac{-2v_{dc}}{\sqrt{3}} & \frac{-3\sqrt{3}v_{dc}}{4} & \frac{-\sqrt{3}v_{dc}}{2} \\ 1 & 1 & 1 & 1 \end{bmatrix}$		

PR_{11}		
TeT_{1}^{11}	TeT_{2}^{11}	TeT_{3}^{11}
$\begin{bmatrix} \frac{v_{dc}}{2\sqrt{6}} & \frac{\sqrt{3}v_{dc}}{4\sqrt{2}} & \frac{v_{dc}}{\sqrt{6}} & \frac{v_{dc}}{2\sqrt{6}} \\ \frac{v_{dc}}{2\sqrt{2}} & \frac{v_{dc}}{4\sqrt{2}} & \frac{v_{dc}}{2\sqrt{2}} & \frac{v_{dc}}{2\sqrt{2}} \\ \frac{5v_{dc}}{4\sqrt{3}} & \frac{3\sqrt{3}v_{dc}}{4} & \frac{2v_{dc}}{\sqrt{3}} & \frac{7v_{dc}}{4\sqrt{3}} \\ 1 & 1 & 1 & 1 \end{bmatrix}$	$\begin{bmatrix} \frac{\sqrt{3}v_{dc}}{4\sqrt{2}} & \frac{\sqrt{3}v_{dc}}{4\sqrt{2}} & \frac{v_{dc}}{\sqrt{6}} & \frac{v_{dc}}{2\sqrt{6}} \\ \frac{v_{dc}}{4\sqrt{2}} & \frac{v_{dc}}{4\sqrt{2}} & \frac{v_{dc}}{2\sqrt{2}} & \frac{v_{dc}}{2\sqrt{2}} \\ \frac{\sqrt{3}v_{dc}}{2} & \frac{3\sqrt{3}v_{dc}}{4} & \frac{2v_{dc}}{\sqrt{3}} & \frac{7v_{dc}}{4\sqrt{3}} \\ 1 & 1 & 1 & 1 \end{bmatrix}$	$\begin{bmatrix} \frac{\sqrt{3}v_{dc}}{4\sqrt{2}} & \frac{v_{dc}}{\sqrt{6}} & \frac{v_{dc}}{\sqrt{6}} & \frac{v_{dc}}{2\sqrt{6}} \\ \frac{v_{dc}}{4\sqrt{2}} & \frac{v_{dc}}{2\sqrt{2}} & \frac{v_{dc}}{2\sqrt{2}} & \frac{v_{dc}}{2\sqrt{2}} \\ \frac{\sqrt{3}v_{dc}}{2} & \frac{5v_{dc}}{4\sqrt{3}} & \frac{2v_{dc}}{\sqrt{3}} & \frac{7v_{dc}}{4\sqrt{3}} \\ 1 & 1 & 1 & 1 \end{bmatrix}$
TeT_{4}^{11}	TeT_{5}^{11}	TeT_{6}^{11}

$\begin{bmatrix} \frac{\sqrt{3}v_{dc}}{4\sqrt{2}} & \frac{v_{dc}}{\sqrt{6}} & \frac{v_{dc}}{2\sqrt{6}} & \frac{v_{dc}}{2\sqrt{6}} \\ \frac{v_{dc}}{4\sqrt{2}} & \frac{v_{dc}}{2\sqrt{2}} & \frac{v_{dc}}{2\sqrt{2}} & \frac{v_{dc}}{2\sqrt{2}} \\ \frac{\sqrt{3}v_{dc}}{2} & \frac{5v_{dc}}{4\sqrt{3}} & \frac{v_{dc}}{\sqrt{3}} & \frac{7v_{dc}}{4\sqrt{3}} \\ 1 & 1 & 1 & 1 \end{bmatrix}$	$\begin{bmatrix} \frac{\sqrt{3}v_{dc}}{4\sqrt{2}} & \frac{v_{dc}}{\sqrt{6}} & \frac{v_{dc}}{2\sqrt{6}} & \frac{\sqrt{3}v_{dc}}{4\sqrt{2}} \\ \frac{v_{dc}}{4\sqrt{2}} & \frac{v_{dc}}{2\sqrt{2}} & \frac{v_{dc}}{2\sqrt{2}} & \frac{v_{dc}}{4\sqrt{2}} \\ \frac{\sqrt{3}v_{dc}}{2} & \frac{5v_{dc}}{4\sqrt{3}} & \frac{v_{dc}}{\sqrt{3}} & \frac{\sqrt{3}v_{dc}}{4} \\ 1 & 1 & 1 & 1 \end{bmatrix}$	$\begin{bmatrix} \frac{v_{dc}}{\sqrt{6}} & \frac{v_{dc}}{\sqrt{6}} & \frac{v_{dc}}{2\sqrt{6}} & \frac{\sqrt{3}v_{dc}}{4\sqrt{2}} \\ \frac{v_{dc}}{2\sqrt{2}} & \frac{v_{dc}}{2\sqrt{2}} & \frac{v_{dc}}{2\sqrt{2}} & \frac{v_{dc}}{4\sqrt{2}} \\ \frac{v_{dc}}{2\sqrt{3}} & \frac{5v_{dc}}{4\sqrt{3}} & \frac{v_{dc}}{\sqrt{3}} & \frac{\sqrt{3}v_{dc}}{4} \\ 1 & 1 & 1 & 1 \end{bmatrix}$
TeT_7^{11}	TeT_8^{11}	TeT_9^{11}
$\begin{bmatrix} \frac{v_{dc}}{\sqrt{6}} & \frac{v_{dc}}{2\sqrt{6}} & \frac{v_{dc}}{2\sqrt{6}} & \frac{\sqrt{3}v_{dc}}{4\sqrt{2}} \\ \frac{v_{dc}}{2\sqrt{2}} & \frac{v_{dc}}{2\sqrt{2}} & \frac{v_{dc}}{2\sqrt{2}} & \frac{v_{dc}}{4\sqrt{2}} \\ \frac{v_{dc}}{2\sqrt{3}} & \frac{v_{dc}}{4\sqrt{3}} & \frac{v_{dc}}{\sqrt{3}} & \frac{\sqrt{3}v_{dc}}{4} \\ 1 & 1 & 1 & 1 \end{bmatrix}$	$\begin{bmatrix} \frac{v_{dc}}{\sqrt{6}} & \frac{v_{dc}}{2\sqrt{6}} & \frac{\sqrt{3}v_{dc}}{4\sqrt{2}} & \frac{\sqrt{3}v_{dc}}{4\sqrt{2}} \\ \frac{v_{dc}}{2\sqrt{2}} & \frac{v_{dc}}{2\sqrt{2}} & \frac{v_{dc}}{1\sqrt{2}} & \frac{v_{dc}}{4\sqrt{2}} \\ \frac{v_{dc}}{2\sqrt{3}} & \frac{v_{dc}}{4\sqrt{3}} & 0 & \frac{\sqrt{3}v_{dc}}{4} \\ 1 & 1 & 1 & 1 \end{bmatrix}$	$\begin{bmatrix} \frac{v_{dc}}{\sqrt{6}} & \frac{v_{dc}}{2\sqrt{6}} & \frac{\sqrt{3}v_{dc}}{4\sqrt{2}} & \frac{v_{dc}}{\sqrt{6}} \\ \frac{v_{dc}}{2\sqrt{2}} & \frac{v_{dc}}{2\sqrt{2}} & \frac{v_{dc}}{1\sqrt{2}} & \frac{v_{dc}}{2\sqrt{2}} \\ \frac{v_{dc}}{2\sqrt{3}} & \frac{v_{dc}}{4\sqrt{3}} & 0 & \frac{-v_{dc}}{4\sqrt{3}} \\ 1 & 1 & 1 & 1 \end{bmatrix}$
TeT_{10}^{11}	TeT_{11}^{11}	TeT_{12}^{11}
$\begin{bmatrix} \frac{v_{dc}}{2\sqrt{6}} & \frac{v_{dc}}{2\sqrt{6}} & \frac{\sqrt{3}v_{dc}}{4\sqrt{2}} & \frac{v_{dc}}{\sqrt{6}} \\ \frac{v_{dc}}{2\sqrt{2}} & \frac{v_{dc}}{2\sqrt{2}} & \frac{v_{dc}}{4\sqrt{2}} & \frac{v_{dc}}{2\sqrt{2}} \\ \frac{-v_{dc}}{2\sqrt{3}} & \frac{v_{dc}}{4\sqrt{3}} & 0 & \frac{-v_{dc}}{4\sqrt{3}} \\ 1 & 1 & 1 & 1 \end{bmatrix}$	$\begin{bmatrix} \frac{v_{dc}}{2\sqrt{6}} & \frac{\sqrt{3}v_{dc}}{4\sqrt{2}} & \frac{\sqrt{3}v_{dc}}{4\sqrt{2}} & \frac{v_{dc}}{\sqrt{6}} \\ \frac{v_{dc}}{2\sqrt{2}} & \frac{v_{dc}}{4\sqrt{2}} & \frac{v_{dc}}{4\sqrt{2}} & \frac{v_{dc}}{2\sqrt{2}} \\ \frac{-v_{dc}}{2\sqrt{3}} & \frac{-\sqrt{3}v_{dc}}{4} & 0 & \frac{-v_{dc}}{4\sqrt{3}} \\ 1 & 1 & 1 & 1 \end{bmatrix}$	$\begin{bmatrix} \frac{v_{dc}}{2\sqrt{6}} & \frac{\sqrt{3}v_{dc}}{4\sqrt{2}} & \frac{v_{dc}}{\sqrt{6}} & \frac{v_{dc}}{\sqrt{6}} \\ \frac{v_{dc}}{2\sqrt{2}} & \frac{v_{dc}}{4\sqrt{2}} & \frac{v_{dc}}{2\sqrt{2}} & \frac{v_{dc}}{2\sqrt{2}} \\ \frac{-v_{dc}}{2\sqrt{3}} & \frac{-\sqrt{3}v_{dc}}{4} & \frac{-v_{dc}}{\sqrt{3}} & \frac{-v_{dc}}{4\sqrt{3}} \\ 1 & 1 & 1 & 1 \end{bmatrix}$
TeT_{13}^{11}	TeT_{14}^{11}	TeT_{15}^{11}
$\begin{bmatrix} \frac{v_{dc}}{2\sqrt{6}} & \frac{\sqrt{3}v_{dc}}{4\sqrt{2}} & \frac{v_{dc}}{\sqrt{6}} & \frac{v_{dc}}{2\sqrt{6}} \\ \frac{v_{dc}}{2\sqrt{2}} & \frac{v_{dc}}{4\sqrt{2}} & \frac{v_{dc}}{2\sqrt{2}} & \frac{v_{dc}}{2\sqrt{2}} \\ \frac{-v_{dc}}{2\sqrt{3}} & \frac{-\sqrt{3}v_{dc}}{4} & \frac{-v_{dc}}{\sqrt{3}} & \frac{-5v_{dc}}{4\sqrt{3}} \\ 1 & 1 & 1 & 1 \end{bmatrix}$	$\begin{bmatrix} \frac{\sqrt{3}v_{dc}}{4\sqrt{2}} & \frac{\sqrt{3}v_{dc}}{4\sqrt{2}} & \frac{v_{dc}}{\sqrt{6}} & \frac{v_{dc}}{2\sqrt{6}} \\ \frac{v_{dc}}{4\sqrt{2}} & \frac{v_{dc}}{4\sqrt{2}} & \frac{v_{dc}}{2\sqrt{2}} & \frac{v_{dc}}{2\sqrt{2}} \\ \frac{-\sqrt{3}v_{dc}}{2} & \frac{-\sqrt{3}v_{dc}}{4} & \frac{-v_{dc}}{\sqrt{3}} & \frac{-5v_{dc}}{4\sqrt{3}} \\ 1 & 1 & 1 & 1 \end{bmatrix}$	$\begin{bmatrix} \frac{\sqrt{3}v_{dc}}{4\sqrt{2}} & \frac{v_{dc}}{\sqrt{6}} & \frac{v_{dc}}{\sqrt{6}} & \frac{v_{dc}}{2\sqrt{6}} \\ \frac{v_{dc}}{4\sqrt{2}} & \frac{v_{dc}}{2\sqrt{2}} & \frac{v_{dc}}{2\sqrt{2}} & \frac{v_{dc}}{2\sqrt{2}} \\ \frac{-\sqrt{3}v_{dc}}{2} & \frac{-7v_{dc}}{4\sqrt{3}} & \frac{-v_{dc}}{\sqrt{3}} & \frac{-5v_{dc}}{4\sqrt{3}} \\ 1 & 1 & 1 & 1 \end{bmatrix}$
TeT_{16}^{11}	TeT_{17}^{11}	

$\begin{bmatrix} \frac{\sqrt{3}v_{dc}}{4\sqrt{2}} & \frac{v_{dc}}{\sqrt{6}} & \frac{v_{dc}}{2\sqrt{6}} & \frac{v_{dc}}{2\sqrt{6}} \\ \frac{v_{dc}}{4\sqrt{2}} & \frac{v_{dc}}{2\sqrt{2}} & \frac{v_{dc}}{2\sqrt{2}} & \frac{v_{dc}}{2\sqrt{2}} \\ \frac{-\sqrt{3}v_{dc}}{2} & \frac{-7v_{dc}}{4\sqrt{3}} & \frac{-2v_{dc}}{\sqrt{3}} & \frac{-5v_{dc}}{4\sqrt{3}} \\ 1 & 1 & 1 & 1 \end{bmatrix}$	$\begin{bmatrix} \frac{\sqrt{3}v_{dc}}{4\sqrt{2}} & \frac{v_{dc}}{\sqrt{6}} & \frac{v_{dc}}{2\sqrt{6}} & \frac{\sqrt{3}v_{dc}}{4\sqrt{2}} \\ \frac{v_{dc}}{4\sqrt{2}} & \frac{v_{dc}}{2\sqrt{2}} & \frac{v_{dc}}{2\sqrt{2}} & \frac{v_{dc}}{4\sqrt{2}} \\ \frac{-\sqrt{3}v_{dc}}{2} & \frac{-7v_{dc}}{4\sqrt{3}} & \frac{-2v_{dc}}{\sqrt{3}} & \frac{-3\sqrt{3}v_{dc}}{4} \\ 1 & 1 & 1 & 1 \end{bmatrix}$

PR_{12}		
TeT_1^{12}	TeT_2^{12}	TeT_3^{12}
$\begin{bmatrix} \frac{v_{dc}}{2\sqrt{6}} & \frac{\sqrt{3}v_{dc}}{4\sqrt{2}} & \frac{v_{dc}}{\sqrt{6}} & \frac{v_{dc}}{2\sqrt{6}} \\ \frac{3v_{dc}}{4\sqrt{2}} & \frac{3v_{dc}}{4\sqrt{2}} & \frac{v_{dc}}{2\sqrt{2}} & \frac{v_{dc}}{2\sqrt{2}} \\ \frac{5v_{dc}}{4\sqrt{3}} & \frac{3\sqrt{3}v_{dc}}{4} & \frac{2v_{dc}}{\sqrt{3}} & \frac{7v_{dc}}{4\sqrt{3}} \\ 1 & 1 & 1 & 1 \end{bmatrix}$	$\begin{bmatrix} \frac{\sqrt{3}v_{dc}}{4\sqrt{2}} & \frac{\sqrt{3}v_{dc}}{4\sqrt{2}} & \frac{v_{dc}}{\sqrt{6}} & \frac{v_{dc}}{2\sqrt{6}} \\ \frac{3v_{dc}}{4\sqrt{2}} & \frac{3v_{dc}}{4\sqrt{2}} & \frac{v_{dc}}{2\sqrt{2}} & \frac{v_{dc}}{2\sqrt{2}} \\ \frac{\sqrt{3}v_{dc}}{2} & \frac{3\sqrt{3}v_{dc}}{4} & \frac{2v_{dc}}{\sqrt{3}} & \frac{7v_{dc}}{4\sqrt{3}} \\ 1 & 1 & 1 & 1 \end{bmatrix}$	$\begin{bmatrix} \frac{\sqrt{3}v_{dc}}{4\sqrt{2}} & \frac{v_{dc}}{\sqrt{6}} & \frac{v_{dc}}{\sqrt{6}} & \frac{v_{dc}}{2\sqrt{6}} \\ \frac{3v_{dc}}{4\sqrt{2}} & \frac{v_{dc}}{2\sqrt{2}} & \frac{v_{dc}}{2\sqrt{2}} & \frac{v_{dc}}{2\sqrt{2}} \\ \frac{\sqrt{3}v_{dc}}{2} & \frac{5v_{dc}}{4\sqrt{3}} & \frac{2v_{dc}}{\sqrt{3}} & \frac{7v_{dc}}{4\sqrt{3}} \\ 1 & 1 & 1 & 1 \end{bmatrix}$
TeT_4^{12}	TeT_5^{12}	TeT_6^{12}
$\begin{bmatrix} \frac{\sqrt{3}v_{dc}}{4\sqrt{2}} & \frac{v_{dc}}{\sqrt{6}} & \frac{v_{dc}}{2\sqrt{6}} & \frac{v_{dc}}{2\sqrt{6}} \\ \frac{3v_{dc}}{4\sqrt{2}} & \frac{v_{dc}}{2\sqrt{2}} & \frac{v_{dc}}{2\sqrt{2}} & \frac{v_{dc}}{2\sqrt{2}} \\ \frac{\sqrt{3}v_{dc}}{2} & \frac{5v_{dc}}{4\sqrt{3}} & \frac{v_{dc}}{\sqrt{3}} & \frac{7v_{dc}}{4\sqrt{3}} \\ 1 & 1 & 1 & 1 \end{bmatrix}$	$\begin{bmatrix} \frac{\sqrt{3}v_{dc}}{4\sqrt{2}} & \frac{v_{dc}}{\sqrt{6}} & \frac{v_{dc}}{2\sqrt{6}} & \frac{\sqrt{3}v_{dc}}{4\sqrt{2}} \\ \frac{3v_{dc}}{4\sqrt{2}} & \frac{v_{dc}}{2\sqrt{2}} & \frac{v_{dc}}{2\sqrt{2}} & \frac{3v_{dc}}{4\sqrt{2}} \\ \frac{\sqrt{3}v_{dc}}{2} & \frac{5v_{dc}}{4\sqrt{3}} & \frac{v_{dc}}{\sqrt{3}} & \frac{\sqrt{3}v_{dc}}{4} \\ 1 & 1 & 1 & 1 \end{bmatrix}$	$\begin{bmatrix} \frac{v_{dc}}{\sqrt{6}} & \frac{v_{dc}}{\sqrt{6}} & \frac{v_{dc}}{2\sqrt{6}} & \frac{\sqrt{3}v_{dc}}{4\sqrt{2}} \\ \frac{v_{dc}}{2\sqrt{2}} & \frac{v_{dc}}{2\sqrt{2}} & \frac{v_{dc}}{2\sqrt{2}} & \frac{3v_{dc}}{4\sqrt{2}} \\ \frac{v_{dc}}{2\sqrt{3}} & \frac{5v_{dc}}{4\sqrt{3}} & \frac{v_{dc}}{\sqrt{3}} & \frac{\sqrt{3}v_{dc}}{4} \\ 1 & 1 & 1 & 1 \end{bmatrix}$
TeT_7^{12}	TeT_8^{12}	TeT_9^{12}
$\begin{bmatrix} \frac{v_{dc}}{\sqrt{6}} & \frac{v_{dc}}{2\sqrt{6}} & \frac{v_{dc}}{2\sqrt{6}} & \frac{\sqrt{3}v_{dc}}{4\sqrt{2}} \\ \frac{v_{dc}}{2\sqrt{2}} & \frac{v_{dc}}{2\sqrt{2}} & \frac{v_{dc}}{2\sqrt{2}} & \frac{3v_{dc}}{4\sqrt{2}} \\ \frac{v_{dc}}{2\sqrt{3}} & \frac{v_{dc}}{4\sqrt{3}} & \frac{v_{dc}}{\sqrt{3}} & \frac{\sqrt{3}v_{dc}}{4} \\ 1 & 1 & 1 & 1 \end{bmatrix}$	$\begin{bmatrix} \frac{v_{dc}}{\sqrt{6}} & \frac{v_{dc}}{2\sqrt{6}} & \frac{\sqrt{3}v_{dc}}{4\sqrt{2}} & \frac{\sqrt{3}v_{dc}}{4\sqrt{2}} \\ \frac{v_{dc}}{2\sqrt{2}} & \frac{v_{dc}}{2\sqrt{2}} & \frac{3v_{dc}}{4\sqrt{2}} & \frac{3v_{dc}}{4\sqrt{2}} \\ \frac{v_{dc}}{2\sqrt{3}} & \frac{v_{dc}}{4\sqrt{3}} & 0 & \frac{\sqrt{3}v_{dc}}{4} \\ 1 & 1 & 1 & 1 \end{bmatrix}$	$\begin{bmatrix} \frac{v_{dc}}{\sqrt{6}} & \frac{v_{dc}}{2\sqrt{6}} & \frac{\sqrt{3}v_{dc}}{4\sqrt{2}} & \frac{v_{dc}}{\sqrt{6}} \\ \frac{v_{dc}}{2\sqrt{2}} & \frac{v_{dc}}{2\sqrt{2}} & \frac{3v_{dc}}{4\sqrt{2}} & \frac{v_{dc}}{2\sqrt{2}} \\ \frac{v_{dc}}{2\sqrt{3}} & \frac{v_{dc}}{4\sqrt{3}} & 0 & \frac{-v_{dc}}{4\sqrt{3}} \\ 1 & 1 & 1 & 1 \end{bmatrix}$
TeT_{10}^{12}	TeT_{11}^{12}	TeT_{12}^{12}

$\begin{bmatrix} \frac{v_{dc}}{2\sqrt{6}} & \frac{v_{dc}}{2\sqrt{6}} & \frac{\sqrt{3}v_{dc}}{4\sqrt{2}} & \frac{v_{dc}}{\sqrt{6}} \\ \frac{v_{dc}}{2\sqrt{2}} & \frac{v_{dc}}{2\sqrt{2}} & \frac{3v_{dc}}{4\sqrt{2}} & \frac{v_{dc}}{2\sqrt{2}} \\ \frac{-v_{dc}}{2\sqrt{3}} & \frac{v_{dc}}{4\sqrt{3}} & 0 & \frac{-v_{dc}}{4\sqrt{3}} \\ 1 & 1 & 1 & 1 \end{bmatrix}$	$\begin{bmatrix} \frac{v_{dc}}{2\sqrt{6}} & \frac{\sqrt{3}v_{dc}}{4\sqrt{2}} & \frac{\sqrt{3}v_{dc}}{4\sqrt{2}} & \frac{v_{dc}}{\sqrt{6}} \\ \frac{v_{dc}}{2\sqrt{2}} & \frac{3v_{dc}}{4\sqrt{2}} & \frac{3v_{dc}}{4\sqrt{2}} & \frac{v_{dc}}{2\sqrt{2}} \\ \frac{-v_{dc}}{2\sqrt{3}} & \frac{-\sqrt{3}v_{dc}}{4} & 0 & \frac{-v_{dc}}{4\sqrt{3}} \\ 1 & 1 & 1 & 1 \end{bmatrix}$	$\begin{bmatrix} \frac{v_{dc}}{2\sqrt{6}} & \frac{\sqrt{3}v_{dc}}{4\sqrt{2}} & \frac{v_{dc}}{\sqrt{6}} & \frac{v_{dc}}{\sqrt{6}} \\ \frac{v_{dc}}{2\sqrt{2}} & \frac{3v_{dc}}{4\sqrt{2}} & \frac{v_{dc}}{2\sqrt{2}} & \frac{v_{dc}}{2\sqrt{2}} \\ \frac{-v_{dc}}{2\sqrt{3}} & \frac{-\sqrt{3}v_{dc}}{4} & \frac{-v_{dc}}{\sqrt{3}} & \frac{-v_{dc}}{4\sqrt{3}} \\ 1 & 1 & 1 & 1 \end{bmatrix}$
TeT_{13}^{12}	TeT_{14}^{12}	TeT_{15}^{12}
$\begin{bmatrix} \frac{v_{dc}}{2\sqrt{6}} & \frac{\sqrt{3}v_{dc}}{4\sqrt{2}} & \frac{v_{dc}}{\sqrt{6}} & \frac{v_{dc}}{2\sqrt{6}} \\ \frac{v_{dc}}{2\sqrt{2}} & \frac{3v_{dc}}{4\sqrt{2}} & \frac{v_{dc}}{2\sqrt{2}} & \frac{v_{dc}}{2\sqrt{2}} \\ \frac{-v_{dc}}{2\sqrt{3}} & \frac{-\sqrt{3}v_{dc}}{4} & \frac{-v_{dc}}{\sqrt{3}} & \frac{-5v_{dc}}{4\sqrt{3}} \\ 1 & 1 & 1 & 1 \end{bmatrix}$	$\begin{bmatrix} \frac{\sqrt{3}v_{dc}}{4\sqrt{2}} & \frac{\sqrt{3}v_{dc}}{4\sqrt{2}} & \frac{v_{dc}}{\sqrt{6}} & \frac{v_{dc}}{2\sqrt{6}} \\ \frac{3v_{dc}}{4\sqrt{2}} & \frac{3v_{dc}}{4\sqrt{2}} & \frac{v_{dc}}{2\sqrt{2}} & \frac{v_{dc}}{2\sqrt{2}} \\ \frac{-\sqrt{3}v_{dc}}{2} & \frac{-\sqrt{3}v_{dc}}{4} & \frac{-v_{dc}}{\sqrt{3}} & \frac{-5v_{dc}}{4\sqrt{3}} \\ 1 & 1 & 1 & 1 \end{bmatrix}$	$\begin{bmatrix} \frac{\sqrt{3}v_{dc}}{4\sqrt{2}} & \frac{v_{dc}}{\sqrt{6}} & \frac{v_{dc}}{\sqrt{6}} & \frac{v_{dc}}{2\sqrt{6}} \\ \frac{3v_{dc}}{4\sqrt{2}} & \frac{v_{dc}}{2\sqrt{2}} & \frac{v_{dc}}{2\sqrt{2}} & \frac{v_{dc}}{2\sqrt{2}} \\ \frac{-\sqrt{3}v_{dc}}{2} & \frac{-7v_{dc}}{4\sqrt{3}} & \frac{-v_{dc}}{\sqrt{3}} & \frac{-5v_{dc}}{4\sqrt{3}} \\ 1 & 1 & 1 & 1 \end{bmatrix}$
TeT_{16}^{12}		
$\begin{bmatrix} \frac{\sqrt{3}v_{dc}}{4\sqrt{2}} & \frac{v_{dc}}{\sqrt{6}} & \frac{v_{dc}}{2\sqrt{6}} & \frac{v_{dc}}{2\sqrt{6}} \\ \frac{3v_{dc}}{4\sqrt{2}} & \frac{v_{dc}}{2\sqrt{2}} & \frac{v_{dc}}{2\sqrt{2}} & \frac{v_{dc}}{2\sqrt{2}} \\ \frac{-\sqrt{3}v_{dc}}{2} & \frac{-7v_{dc}}{4\sqrt{3}} & \frac{-2v_{dc}}{\sqrt{3}} & \frac{-5v_{dc}}{4\sqrt{3}} \\ 1 & 1 & 1 & 1 \end{bmatrix}$		

PR_{13}		
TeT_1^{13}	TeT_2^{13}	TeT_3^{13}
$\begin{bmatrix} \frac{v_{dc}}{2\sqrt{6}} & \frac{\sqrt{3}v_{dc}}{4\sqrt{2}} & \frac{v_{dc}}{\sqrt{6}} & \frac{v_{dc}}{2\sqrt{6}} \\ 0 & \frac{v_{dc}}{4\sqrt{2}} & 0 & 0 \\ \frac{5v_{dc}}{4\sqrt{3}} & \frac{3\sqrt{3}v_{dc}}{4} & \frac{2v_{dc}}{\sqrt{3}} & \frac{7v_{dc}}{4\sqrt{3}} \\ 1 & 1 & 1 & 1 \end{bmatrix}$	$\begin{bmatrix} \frac{\sqrt{3}v_{dc}}{4\sqrt{2}} & \frac{\sqrt{3}v_{dc}}{4\sqrt{2}} & \frac{v_{dc}}{\sqrt{6}} & \frac{v_{dc}}{2\sqrt{6}} \\ \frac{v_{dc}}{4\sqrt{2}} & \frac{v_{dc}}{4\sqrt{2}} & 0 & 0 \\ \frac{\sqrt{3}v_{dc}}{2} & \frac{3\sqrt{3}v_{dc}}{4} & \frac{2v_{dc}}{\sqrt{3}} & \frac{7v_{dc}}{4\sqrt{3}} \\ 1 & 1 & 1 & 1 \end{bmatrix}$	$\begin{bmatrix} \frac{\sqrt{3}v_{dc}}{4\sqrt{2}} & \frac{v_{dc}}{\sqrt{6}} & \frac{v_{dc}}{\sqrt{6}} & \frac{v_{dc}}{2\sqrt{6}} \\ \frac{v_{dc}}{4\sqrt{2}} & 0 & 0 & 0 \\ \frac{\sqrt{3}v_{dc}}{2} & \frac{5v_{dc}}{4\sqrt{3}} & \frac{2v_{dc}}{\sqrt{3}} & \frac{7v_{dc}}{4\sqrt{3}} \\ 1 & 1 & 1 & 1 \end{bmatrix}$
TeT_4^{13}	TeT_5^{13}	TeT_6^{13}

$\begin{bmatrix} \frac{\sqrt{3}v_{dc}}{4\sqrt{2}} & \frac{v_{dc}}{\sqrt{6}} & \frac{v_{dc}}{2\sqrt{6}} & \frac{v_{dc}}{2\sqrt{6}} \\ \frac{v_{dc}}{4\sqrt{2}} & 0 & 0 & 0 \\ \frac{\sqrt{3}v_{dc}}{2} & \frac{5v_{dc}}{4\sqrt{3}} & \frac{v_{dc}}{\sqrt{3}} & \frac{7v_{dc}}{4\sqrt{3}} \\ 1 & 1 & 1 & 1 \end{bmatrix}$	$\begin{bmatrix} \frac{\sqrt{3}v_{dc}}{4\sqrt{2}} & \frac{v_{dc}}{\sqrt{6}} & \frac{v_{dc}}{2\sqrt{6}} & \frac{\sqrt{3}v_{dc}}{4\sqrt{2}} \\ \frac{v_{dc}}{4\sqrt{2}} & 0 & 0 & \frac{v_{dc}}{4\sqrt{2}} \\ \frac{\sqrt{3}v_{dc}}{2} & \frac{5v_{dc}}{4\sqrt{3}} & \frac{v_{dc}}{\sqrt{3}} & \frac{\sqrt{3}v_{dc}}{4} \\ 1 & 1 & 1 & 1 \end{bmatrix}$	$\begin{bmatrix} \frac{v_{dc}}{\sqrt{6}} & \frac{v_{dc}}{\sqrt{6}} & \frac{v_{dc}}{2\sqrt{6}} & \frac{\sqrt{3}v_{dc}}{4\sqrt{2}} \\ 0 & 0 & 0 & \frac{v_{dc}}{4\sqrt{2}} \\ \frac{v_{dc}}{2\sqrt{3}} & \frac{5v_{dc}}{4\sqrt{3}} & \frac{v_{dc}}{\sqrt{3}} & \frac{\sqrt{3}v_{dc}}{4} \\ 1 & 1 & 1 & 1 \end{bmatrix}$
TeT_7^{13}	TeT_8^{13}	TeT_9^{13}
$\begin{bmatrix} \frac{v_{dc}}{\sqrt{6}} & \frac{v_{dc}}{2\sqrt{6}} & \frac{v_{dc}}{2\sqrt{6}} & \frac{\sqrt{3}v_{dc}}{4\sqrt{2}} \\ 0 & 0 & 0 & \frac{v_{dc}}{4\sqrt{2}} \\ \frac{v_{dc}}{2\sqrt{3}} & \frac{v_{dc}}{4\sqrt{3}} & \frac{v_{dc}}{\sqrt{3}} & \frac{\sqrt{3}v_{dc}}{4} \\ 1 & 1 & 1 & 1 \end{bmatrix}$	$\begin{bmatrix} \frac{v_{dc}}{\sqrt{6}} & \frac{v_{dc}}{2\sqrt{6}} & \frac{\sqrt{3}v_{dc}}{4\sqrt{2}} & \frac{\sqrt{3}v_{dc}}{4\sqrt{2}} \\ 0 & 0 & \frac{v_{dc}}{4\sqrt{2}} & \frac{v_{dc}}{4\sqrt{2}} \\ \frac{v_{dc}}{2\sqrt{3}} & \frac{v_{dc}}{4\sqrt{3}} & 0 & \frac{\sqrt{3}v_{dc}}{4} \\ 1 & 1 & 1 & 1 \end{bmatrix}$	$\begin{bmatrix} \frac{v_{dc}}{\sqrt{6}} & \frac{v_{dc}}{2\sqrt{6}} & \frac{\sqrt{3}v_{dc}}{4\sqrt{2}} & \frac{v_{dc}}{\sqrt{6}} \\ 0 & 0 & \frac{v_{dc}}{4\sqrt{2}} & 0 \\ \frac{v_{dc}}{2\sqrt{3}} & \frac{v_{dc}}{4\sqrt{3}} & 0 & \frac{-v_{dc}}{4\sqrt{3}} \\ 1 & 1 & 1 & 1 \end{bmatrix}$
TeT_{10}^{13}	TeT_{11}^{13}	TeT_{12}^{13}
$\begin{bmatrix} \frac{v_{dc}}{2\sqrt{6}} & \frac{v_{dc}}{2\sqrt{6}} & \frac{\sqrt{3}v_{dc}}{4\sqrt{2}} & \frac{v_{dc}}{\sqrt{6}} \\ 0 & 0 & \frac{v_{dc}}{4\sqrt{2}} & 0 \\ \frac{-v_{dc}}{2\sqrt{3}} & \frac{v_{dc}}{4\sqrt{3}} & 0 & \frac{-v_{dc}}{4\sqrt{3}} \\ 1 & 1 & 1 & 1 \end{bmatrix}$	$\begin{bmatrix} \frac{v_{dc}}{2\sqrt{6}} & \frac{\sqrt{3}v_{dc}}{4\sqrt{2}} & \frac{\sqrt{3}v_{dc}}{4\sqrt{2}} & \frac{v_{dc}}{\sqrt{6}} \\ 0 & \frac{v_{dc}}{4\sqrt{2}} & \frac{v_{dc}}{4\sqrt{2}} & 0 \\ \frac{-v_{dc}}{2\sqrt{3}} & \frac{-\sqrt{3}v_{dc}}{4} & 0 & \frac{-v_{dc}}{4\sqrt{3}} \\ 1 & 1 & 1 & 1 \end{bmatrix}$	$\begin{bmatrix} \frac{v_{dc}}{2\sqrt{6}} & \frac{\sqrt{3}v_{dc}}{4\sqrt{2}} & \frac{v_{dc}}{\sqrt{6}} & \frac{v_{dc}}{\sqrt{6}} \\ 0 & \frac{v_{dc}}{4\sqrt{2}} & 0 & 0 \\ \frac{-v_{dc}}{2\sqrt{3}} & \frac{-\sqrt{3}v_{dc}}{4} & \frac{-v_{dc}}{\sqrt{3}} & \frac{-v_{dc}}{4\sqrt{3}} \\ 1 & 1 & 1 & 1 \end{bmatrix}$
TeT_{13}^{13}	TeT_{14}^{13}	TeT_{15}^{13}
$\begin{bmatrix} \frac{v_{dc}}{2\sqrt{6}} & \frac{\sqrt{3}v_{dc}}{4\sqrt{2}} & \frac{v_{dc}}{\sqrt{6}} & \frac{v_{dc}}{2\sqrt{6}} \\ 0 & \frac{v_{dc}}{4\sqrt{2}} & 0 & 0 \\ \frac{-v_{dc}}{2\sqrt{3}} & \frac{-\sqrt{3}v_{dc}}{4} & \frac{-v_{dc}}{\sqrt{3}} & \frac{-5v_{dc}}{4\sqrt{3}} \\ 1 & 1 & 1 & 1 \end{bmatrix}$	$\begin{bmatrix} \frac{\sqrt{3}v_{dc}}{4\sqrt{2}} & \frac{\sqrt{3}v_{dc}}{4\sqrt{2}} & \frac{v_{dc}}{\sqrt{6}} & \frac{v_{dc}}{2\sqrt{6}} \\ \frac{v_{dc}}{4\sqrt{2}} & \frac{v_{dc}}{4\sqrt{2}} & 0 & 0 \\ \frac{-\sqrt{3}v_{dc}}{2} & \frac{-\sqrt{3}v_{dc}}{4} & \frac{-v_{dc}}{\sqrt{3}} & \frac{-5v_{dc}}{4\sqrt{3}} \\ 1 & 1 & 1 & 1 \end{bmatrix}$	$\begin{bmatrix} \frac{\sqrt{3}v_{dc}}{4\sqrt{2}} & \frac{v_{dc}}{\sqrt{6}} & \frac{v_{dc}}{\sqrt{6}} & \frac{v_{dc}}{2\sqrt{6}} \\ \frac{v_{dc}}{4\sqrt{2}} & 0 & 0 & 0 \\ \frac{-\sqrt{3}v_{dc}}{2} & \frac{-7v_{dc}}{4\sqrt{3}} & \frac{-v_{dc}}{\sqrt{3}} & \frac{-5v_{dc}}{4\sqrt{3}} \\ 1 & 1 & 1 & 1 \end{bmatrix}$
TeT_{16}^{13}	TeT_{17}^{13}	TeT_{18}^{13}

$\begin{bmatrix} \frac{\sqrt{3}v_{dc}}{4\sqrt{2}} & \frac{v_{dc}}{\sqrt{6}} & \frac{v_{dc}}{2\sqrt{6}} & \frac{v_{dc}}{2\sqrt{6}} \\ \frac{v_{dc}}{4\sqrt{2}} & 0 & 0 & 0 \\ \frac{-\sqrt{3}v_{dc}}{2} & \frac{-7v_{dc}}{4\sqrt{3}} & \frac{-2v_{dc}}{\sqrt{3}} & \frac{-5v_{dc}}{4\sqrt{3}} \\ 1 & 1 & 1 & 1 \end{bmatrix}$	$\begin{bmatrix} \frac{\sqrt{3}v_{dc}}{4\sqrt{2}} & \frac{v_{dc}}{\sqrt{6}} & \frac{v_{dc}}{2\sqrt{6}} & \frac{\sqrt{3}v_{dc}}{4\sqrt{2}} \\ \frac{v_{dc}}{4\sqrt{2}} & 0 & 0 & \frac{v_{dc}}{4\sqrt{2}} \\ \frac{-\sqrt{3}v_{dc}}{2} & \frac{-7v_{dc}}{4\sqrt{3}} & \frac{-2v_{dc}}{\sqrt{3}} & \frac{-3\sqrt{3}v_{dc}}{4} \\ 1 & 1 & 1 & 1 \end{bmatrix}$	$\begin{bmatrix} \frac{v_{dc}}{\sqrt{6}} & \frac{v_{dc}}{\sqrt{6}} & \frac{v_{dc}}{2\sqrt{6}} & \frac{\sqrt{3}v_{dc}}{4\sqrt{2}} \\ 0 & 0 & 0 & \frac{v_{dc}}{4\sqrt{2}} \\ \frac{-5v_{dc}}{2\sqrt{3}} & \frac{-7v_{dc}}{4\sqrt{3}} & \frac{-2v_{dc}}{\sqrt{3}} & \frac{-3\sqrt{3}v_{dc}}{4} \\ 1 & 1 & 1 & 1 \end{bmatrix}$
TeT_{19}^{13}		
$\begin{bmatrix} \frac{v_{dc}}{\sqrt{6}} & \frac{v_{dc}}{\sqrt{6}} & \frac{v_{dc}}{2\sqrt{6}} & \frac{\sqrt{3}v_{dc}}{4\sqrt{2}} \\ 0 & 0 & 0 & \frac{v_{dc}}{4\sqrt{2}} \\ \frac{-5v_{dc}}{2\sqrt{3}} & \frac{-7v_{dc}}{4\sqrt{3}} & \frac{-2v_{dc}}{\sqrt{3}} & \frac{-3\sqrt{3}v_{dc}}{4} \\ 1 & 1 & 1 & 1 \end{bmatrix}$		

PR_{14}		
TeT_{1}^{14}	TeT_{2}^{14}	TeT_{3}^{14}
$\begin{bmatrix} \frac{v_{dc}}{4\sqrt{6}} & \frac{v_{dc}}{2\sqrt{6}} & \frac{\sqrt{3}v_{dc}}{4\sqrt{2}} & \frac{v_{dc}}{4\sqrt{6}} \\ \frac{v_{dc}}{4\sqrt{2}} & 0 & \frac{v_{dc}}{4\sqrt{2}} & \frac{v_{dc}}{4\sqrt{2}} \\ \frac{11v_{dc}}{4\sqrt{3}} & \frac{5v_{dc}}{2\sqrt{3}} & \frac{3\sqrt{3}v_{dc}}{4} & \frac{2v_{dc}}{\sqrt{3}} \\ 1 & 1 & 1 & 1 \end{bmatrix}$	$\begin{bmatrix} \frac{v_{dc}}{2\sqrt{6}} & \frac{v_{dc}}{2\sqrt{6}} & \frac{\sqrt{3}v_{dc}}{4\sqrt{2}} & \frac{v_{dc}}{4\sqrt{6}} \\ 0 & 0 & \frac{v_{dc}}{4\sqrt{2}} & \frac{v_{dc}}{4\sqrt{2}} \\ \frac{7v_{dc}}{4\sqrt{3}} & \frac{5v_{dc}}{2\sqrt{3}} & \frac{3\sqrt{3}v_{dc}}{4} & \frac{2v_{dc}}{\sqrt{3}} \\ 1 & 1 & 1 & 1 \end{bmatrix}$	$\begin{bmatrix} \frac{v_{dc}}{2\sqrt{6}} & \frac{\sqrt{3}v_{dc}}{4\sqrt{2}} & \frac{\sqrt{3}v_{dc}}{4\sqrt{2}} & \frac{v_{dc}}{4\sqrt{6}} \\ 0 & \frac{v_{dc}}{4\sqrt{2}} & \frac{v_{dc}}{4\sqrt{2}} & \frac{v_{dc}}{4\sqrt{2}} \\ \frac{7v_{dc}}{4\sqrt{3}} & \frac{\sqrt{3}v_{dc}}{2} & \frac{3\sqrt{3}v_{dc}}{4} & \frac{2v_{dc}}{\sqrt{3}} \\ 1 & 1 & 1 & 1 \end{bmatrix}$
TeT_{4}^{14}	TeT_{5}^{14}	TeT_{6}^{14}
$\begin{bmatrix} \frac{v_{dc}}{2\sqrt{6}} & \frac{\sqrt{3}v_{dc}}{4\sqrt{2}} & \frac{v_{dc}}{4\sqrt{6}} & \frac{v_{dc}}{4\sqrt{6}} \\ 0 & \frac{v_{dc}}{4\sqrt{2}} & \frac{v_{dc}}{4\sqrt{2}} & \frac{v_{dc}}{4\sqrt{2}} \\ \frac{7v_{dc}}{4\sqrt{3}} & \frac{\sqrt{3}v_{dc}}{2} & \frac{5v_{dc}}{4\sqrt{3}} & \frac{2v_{dc}}{\sqrt{3}} \\ 1 & 1 & 1 & 1 \end{bmatrix}$	$\begin{bmatrix} \frac{v_{dc}}{2\sqrt{6}} & \frac{\sqrt{3}v_{dc}}{4\sqrt{2}} & \frac{v_{dc}}{4\sqrt{6}} & \frac{v_{dc}}{2\sqrt{6}} \\ 0 & \frac{v_{dc}}{4\sqrt{2}} & \frac{v_{dc}}{4\sqrt{2}} & 0 \\ \frac{7v_{dc}}{4\sqrt{3}} & \frac{\sqrt{3}v_{dc}}{2} & \frac{5v_{dc}}{4\sqrt{3}} & \frac{v_{dc}}{\sqrt{3}} \\ 1 & 1 & 1 & 1 \end{bmatrix}$	$\begin{bmatrix} \frac{\sqrt{3}v_{dc}}{4\sqrt{2}} & \frac{\sqrt{3}v_{dc}}{4\sqrt{2}} & \frac{v_{dc}}{4\sqrt{6}} & \frac{v_{dc}}{2\sqrt{6}} \\ \frac{v_{dc}}{4\sqrt{2}} & \frac{v_{dc}}{4\sqrt{2}} & \frac{v_{dc}}{4\sqrt{2}} & 0 \\ \frac{\sqrt{3}v_{dc}}{4} & \frac{\sqrt{3}v_{dc}}{2} & \frac{5v_{dc}}{4\sqrt{3}} & \frac{v_{dc}}{\sqrt{3}} \\ 1 & 1 & 1 & 1 \end{bmatrix}$
TeT_{7}^{14}	TeT_{8}^{14}	TeT_{9}^{14}

$\begin{bmatrix} \frac{\sqrt{3}v_{dc}}{4\sqrt{2}} & \frac{v_{dc}}{4\sqrt{6}} & \frac{v_{dc}}{4\sqrt{6}} & \frac{v_{dc}}{2\sqrt{6}} \\ \frac{v_{dc}}{4\sqrt{2}} & \frac{v_{dc}}{4\sqrt{2}} & \frac{v_{dc}}{4\sqrt{2}} & 0 \\ \frac{\sqrt{3}v_{dc}}{4} & \frac{v_{dc}}{2\sqrt{3}} & \frac{5v_{dc}}{4\sqrt{3}} & \frac{v_{dc}}{\sqrt{3}} \\ 1 & 1 & 1 & 1 \end{bmatrix}$	$\begin{bmatrix} \frac{\sqrt{3}v_{dc}}{4\sqrt{2}} & \frac{v_{dc}}{4\sqrt{6}} & \frac{v_{dc}}{2\sqrt{6}} & \frac{v_{dc}}{2\sqrt{6}} \\ \frac{v_{dc}}{4\sqrt{2}} & \frac{v_{dc}}{4\sqrt{2}} & 0 & 0 \\ \frac{\sqrt{3}v_{dc}}{4} & \frac{v_{dc}}{2\sqrt{3}} & \frac{v_{dc}}{4\sqrt{3}} & \frac{v_{dc}}{\sqrt{3}} \\ 1 & 1 & 1 & 1 \end{bmatrix}$	$\begin{bmatrix} \frac{\sqrt{3}v_{dc}}{4\sqrt{2}} & \frac{v_{dc}}{4\sqrt{6}} & \frac{v_{dc}}{2\sqrt{6}} & \frac{\sqrt{3}v_{dc}}{4\sqrt{2}} \\ \frac{v_{dc}}{4\sqrt{2}} & \frac{v_{dc}}{4\sqrt{2}} & 0 & \frac{v_{dc}}{4\sqrt{2}} \\ \frac{\sqrt{3}v_{dc}}{4} & \frac{v_{dc}}{2\sqrt{3}} & \frac{v_{dc}}{4\sqrt{3}} & 0 \\ 1 & 1 & 1 & 1 \end{bmatrix}$
TeT_{10}^{14}	TeT_{11}^{14}	TeT_{12}^{14}
$\begin{bmatrix} \frac{v_{dc}}{4\sqrt{6}} & \frac{v_{dc}}{4\sqrt{6}} & \frac{v_{dc}}{2\sqrt{6}} & \frac{\sqrt{3}v_{dc}}{4\sqrt{2}} \\ \frac{v_{dc}}{4\sqrt{2}} & \frac{v_{dc}}{4\sqrt{2}} & 0 & \frac{v_{dc}}{4\sqrt{2}} \\ \frac{-v_{dc}}{4\sqrt{3}} & \frac{v_{dc}}{2\sqrt{3}} & \frac{v_{dc}}{4\sqrt{3}} & 0 \\ 1 & 1 & 1 & 1 \end{bmatrix}$	$\begin{bmatrix} \frac{v_{dc}}{4\sqrt{6}} & \frac{v_{dc}}{2\sqrt{6}} & \frac{v_{dc}}{2\sqrt{6}} & \frac{\sqrt{3}v_{dc}}{4\sqrt{2}} \\ \frac{v_{dc}}{4\sqrt{2}} & 0 & 0 & \frac{v_{dc}}{4\sqrt{2}} \\ \frac{-v_{dc}}{4\sqrt{3}} & \frac{-v_{dc}}{2\sqrt{3}} & \frac{v_{dc}}{4\sqrt{3}} & 0 \\ 1 & 1 & 1 & 1 \end{bmatrix}$	$\begin{bmatrix} \frac{v_{dc}}{4\sqrt{6}} & \frac{v_{dc}}{2\sqrt{6}} & \frac{\sqrt{3}v_{dc}}{4\sqrt{2}} & \frac{\sqrt{3}v_{dc}}{4\sqrt{2}} \\ \frac{v_{dc}}{4\sqrt{2}} & 0 & \frac{v_{dc}}{4\sqrt{2}} & \frac{v_{dc}}{4\sqrt{2}} \\ \frac{-v_{dc}}{4\sqrt{3}} & \frac{-v_{dc}}{2\sqrt{3}} & \frac{-\sqrt{3}v_{dc}}{4} & 0 \\ 1 & 1 & 1 & 1 \end{bmatrix}$
TeT_{13}^{14}	TeT_{14}^{14}	TeT_{15}^{14}
$\begin{bmatrix} \frac{v_{dc}}{4\sqrt{6}} & \frac{v_{dc}}{2\sqrt{6}} & \frac{\sqrt{3}v_{dc}}{4\sqrt{2}} & \frac{v_{dc}}{4\sqrt{6}} \\ \frac{v_{dc}}{4\sqrt{2}} & 0 & \frac{v_{dc}}{4\sqrt{2}} & \frac{v_{dc}}{4\sqrt{2}} \\ \frac{-v_{dc}}{4\sqrt{3}} & \frac{-v_{dc}}{2\sqrt{3}} & \frac{-\sqrt{3}v_{dc}}{4} & \frac{-v_{dc}}{\sqrt{3}} \\ 1 & 1 & 1 & 1 \end{bmatrix}$	$\begin{bmatrix} \frac{v_{dc}}{2\sqrt{6}} & \frac{v_{dc}}{2\sqrt{6}} & \frac{\sqrt{3}v_{dc}}{4\sqrt{2}} & \frac{v_{dc}}{4\sqrt{6}} \\ 0 & 0 & \frac{v_{dc}}{4\sqrt{2}} & \frac{v_{dc}}{4\sqrt{2}} \\ \frac{-5v_{dc}}{4\sqrt{3}} & \frac{-v_{dc}}{2\sqrt{3}} & \frac{-\sqrt{3}v_{dc}}{4} & \frac{-v_{dc}}{\sqrt{3}} \\ 1 & 1 & 1 & 1 \end{bmatrix}$	$\begin{bmatrix} \frac{v_{dc}}{2\sqrt{6}} & \frac{\sqrt{3}v_{dc}}{4\sqrt{2}} & \frac{\sqrt{3}v_{dc}}{4\sqrt{2}} & \frac{v_{dc}}{4\sqrt{6}} \\ 0 & \frac{v_{dc}}{4\sqrt{2}} & \frac{v_{dc}}{4\sqrt{2}} & \frac{v_{dc}}{4\sqrt{2}} \\ \frac{-5v_{dc}}{4\sqrt{3}} & \frac{-\sqrt{3}v_{dc}}{2} & \frac{-\sqrt{3}v_{dc}}{4} & \frac{-v_{dc}}{\sqrt{3}} \\ 1 & 1 & 1 & 1 \end{bmatrix}$
TeT_{16}^{14}	TeT_{17}^{14}	TeT_{18}^{14}
$\begin{bmatrix} \frac{v_{dc}}{2\sqrt{6}} & \frac{\sqrt{3}v_{dc}}{4\sqrt{2}} & \frac{v_{dc}}{4\sqrt{6}} & \frac{v_{dc}}{4\sqrt{6}} \\ 0 & \frac{v_{dc}}{4\sqrt{2}} & \frac{v_{dc}}{4\sqrt{2}} & \frac{v_{dc}}{4\sqrt{2}} \\ \frac{-5v_{dc}}{4\sqrt{3}} & \frac{-\sqrt{3}v_{dc}}{2} & \frac{-7v_{dc}}{4\sqrt{3}} & \frac{-v_{dc}}{\sqrt{3}} \\ 1 & 1 & 1 & 1 \end{bmatrix}$	$\begin{bmatrix} \frac{v_{dc}}{2\sqrt{6}} & \frac{\sqrt{3}v_{dc}}{4\sqrt{2}} & \frac{v_{dc}}{4\sqrt{6}} & \frac{v_{dc}}{2\sqrt{6}} \\ 0 & \frac{v_{dc}}{4\sqrt{2}} & \frac{v_{dc}}{4\sqrt{2}} & 0 \\ \frac{-5v_{dc}}{4\sqrt{3}} & \frac{-\sqrt{3}v_{dc}}{2} & \frac{-7v_{dc}}{4\sqrt{3}} & \frac{-2v_{dc}}{\sqrt{3}} \\ 1 & 1 & 1 & 1 \end{bmatrix}$	$\begin{bmatrix} \frac{\sqrt{3}v_{dc}}{4\sqrt{2}} & \frac{\sqrt{3}v_{dc}}{4\sqrt{2}} & \frac{v_{dc}}{4\sqrt{6}} & \frac{v_{dc}}{2\sqrt{6}} \\ \frac{v_{dc}}{4\sqrt{2}} & \frac{v_{dc}}{4\sqrt{2}} & \frac{v_{dc}}{4\sqrt{2}} & 0 \\ \frac{-3\sqrt{3}v_{dc}}{4} & \frac{-\sqrt{3}v_{dc}}{2} & \frac{-7v_{dc}}{4\sqrt{3}} & \frac{-2v_{dc}}{\sqrt{3}} \\ 1 & 1 & 1 & 1 \end{bmatrix}$
TeT_{19}^{14}	TeT_{20}^{14}	

$\begin{bmatrix} \frac{\sqrt{3}v_{dc}}{4\sqrt{2}} & \frac{v_{dc}}{4\sqrt{6}} & \frac{v_{dc}}{4\sqrt{6}} & \frac{v_{dc}}{2\sqrt{6}} \\ \frac{v_{dc}}{4\sqrt{2}} & \frac{v_{dc}}{4\sqrt{2}} & \frac{v_{dc}}{4\sqrt{2}} & 0 \\ \frac{-3\sqrt{3}v_{dc}}{4} & \frac{-5v_{dc}}{2\sqrt{3}} & \frac{-7v_{dc}}{4\sqrt{3}} & \frac{-2v_{dc}}{\sqrt{3}} \\ 1 & 1 & 1 & 1 \end{bmatrix}$	$\begin{bmatrix} \frac{\sqrt{3}v_{dc}}{4\sqrt{2}} & \frac{v_{dc}}{4\sqrt{6}} & \frac{v_{dc}}{2\sqrt{6}} & \frac{v_{dc}}{2\sqrt{6}} \\ \frac{v_{dc}}{4\sqrt{2}} & \frac{v_{dc}}{4\sqrt{2}} & 0 & 0 \\ \frac{-3\sqrt{3}v_{dc}}{4} & \frac{-5v_{dc}}{2\sqrt{3}} & \frac{-11v_{dc}}{4\sqrt{3}} & \frac{-2v_{dc}}{\sqrt{3}} \\ 1 & 1 & 1 & 1 \end{bmatrix}$

PR_{15}		
TeT_1^{15}	TeT_2^{15}	TeT_3^{15}
$\begin{bmatrix} \frac{v_{dc}}{4\sqrt{6}} & \frac{v_{dc}}{2\sqrt{6}} & \frac{\sqrt{3}v_{dc}}{4\sqrt{2}} & \frac{v_{dc}}{4\sqrt{6}} \\ \frac{v_{dc}}{4\sqrt{2}} & \frac{v_{dc}}{2\sqrt{2}} & \frac{v_{dc}}{4\sqrt{2}} & \frac{v_{dc}}{4\sqrt{2}} \\ \frac{11v_{dc}}{4\sqrt{3}} & \frac{5v_{dc}}{2\sqrt{3}} & \frac{3\sqrt{3}v_{dc}}{4} & \frac{2v_{dc}}{\sqrt{3}} \\ 1 & 1 & 1 & 1 \end{bmatrix}$	$\begin{bmatrix} \frac{v_{dc}}{2\sqrt{6}} & \frac{v_{dc}}{2\sqrt{6}} & \frac{\sqrt{3}v_{dc}}{4\sqrt{2}} & \frac{v_{dc}}{4\sqrt{6}} \\ \frac{v_{dc}}{2\sqrt{2}} & \frac{v_{dc}}{2\sqrt{2}} & \frac{v_{dc}}{4\sqrt{2}} & \frac{v_{dc}}{4\sqrt{2}} \\ \frac{7v_{dc}}{4\sqrt{3}} & \frac{5v_{dc}}{2\sqrt{3}} & \frac{3\sqrt{3}v_{dc}}{4} & \frac{2v_{dc}}{\sqrt{3}} \\ 1 & 1 & 1 & 1 \end{bmatrix}$	$\begin{bmatrix} \frac{v_{dc}}{2\sqrt{6}} & \frac{\sqrt{3}v_{dc}}{4\sqrt{2}} & \frac{\sqrt{3}v_{dc}}{4\sqrt{2}} & \frac{v_{dc}}{4\sqrt{6}} \\ \frac{v_{dc}}{2\sqrt{2}} & \frac{v_{dc}}{4\sqrt{2}} & \frac{v_{dc}}{4\sqrt{2}} & \frac{v_{dc}}{4\sqrt{2}} \\ \frac{7v_{dc}}{4\sqrt{3}} & \frac{\sqrt{3}v_{dc}}{2} & \frac{3\sqrt{3}v_{dc}}{4} & \frac{2v_{dc}}{\sqrt{3}} \\ 1 & 1 & 1 & 1 \end{bmatrix}$
TeT_4^{15}	TeT_5^{15}	TeT_6^{15}
$\begin{bmatrix} \frac{v_{dc}}{2\sqrt{6}} & \frac{\sqrt{3}v_{dc}}{4\sqrt{2}} & \frac{v_{dc}}{4\sqrt{6}} & \frac{v_{dc}}{4\sqrt{6}} \\ \frac{v_{dc}}{2\sqrt{2}} & \frac{v_{dc}}{4\sqrt{2}} & \frac{v_{dc}}{4\sqrt{2}} & \frac{v_{dc}}{4\sqrt{2}} \\ \frac{7v_{dc}}{4\sqrt{3}} & \frac{\sqrt{3}v_{dc}}{2} & \frac{5v_{dc}}{4\sqrt{3}} & \frac{2v_{dc}}{\sqrt{3}} \\ 1 & 1 & 1 & 1 \end{bmatrix}$	$\begin{bmatrix} \frac{v_{dc}}{2\sqrt{6}} & \frac{\sqrt{3}v_{dc}}{4\sqrt{2}} & \frac{v_{dc}}{4\sqrt{6}} & \frac{v_{dc}}{2\sqrt{6}} \\ \frac{v_{dc}}{2\sqrt{2}} & \frac{v_{dc}}{4\sqrt{2}} & \frac{v_{dc}}{4\sqrt{2}} & \frac{v_{dc}}{2\sqrt{2}} \\ \frac{7v_{dc}}{4\sqrt{3}} & \frac{\sqrt{3}v_{dc}}{2} & \frac{5v_{dc}}{4\sqrt{3}} & \frac{v_{dc}}{\sqrt{3}} \\ 1 & 1 & 1 & 1 \end{bmatrix}$	$\begin{bmatrix} \frac{\sqrt{3}v_{dc}}{4\sqrt{2}} & \frac{\sqrt{3}v_{dc}}{4\sqrt{2}} & \frac{v_{dc}}{4\sqrt{6}} & \frac{v_{dc}}{2\sqrt{6}} \\ \frac{v_{dc}}{4\sqrt{2}} & \frac{v_{dc}}{4\sqrt{2}} & \frac{v_{dc}}{4\sqrt{2}} & \frac{v_{dc}}{2\sqrt{2}} \\ \frac{\sqrt{3}v_{dc}}{4} & \frac{\sqrt{3}v_{dc}}{2} & \frac{5v_{dc}}{4\sqrt{3}} & \frac{v_{dc}}{\sqrt{3}} \\ 1 & 1 & 1 & 1 \end{bmatrix}$
TeT_7^{15}	TeT_8^{15}	TeT_9^{15}
$\begin{bmatrix} \frac{\sqrt{3}v_{dc}}{4\sqrt{2}} & \frac{v_{dc}}{4\sqrt{6}} & \frac{v_{dc}}{4\sqrt{6}} & \frac{v_{dc}}{2\sqrt{6}} \\ \frac{v_{dc}}{4\sqrt{2}} & \frac{v_{dc}}{4\sqrt{2}} & \frac{v_{dc}}{4\sqrt{2}} & \frac{v_{dc}}{2\sqrt{2}} \\ \frac{\sqrt{3}v_{dc}}{4} & \frac{v_{dc}}{2\sqrt{3}} & \frac{5v_{dc}}{4\sqrt{3}} & \frac{v_{dc}}{\sqrt{3}} \\ 1 & 1 & 1 & 1 \end{bmatrix}$	$\begin{bmatrix} \frac{\sqrt{3}v_{dc}}{4\sqrt{2}} & \frac{v_{dc}}{4\sqrt{6}} & \frac{v_{dc}}{2\sqrt{6}} & \frac{v_{dc}}{2\sqrt{6}} \\ \frac{v_{dc}}{4\sqrt{2}} & \frac{v_{dc}}{4\sqrt{2}} & \frac{v_{dc}}{2\sqrt{2}} & \frac{v_{dc}}{2\sqrt{2}} \\ \frac{\sqrt{3}v_{dc}}{4} & \frac{v_{dc}}{2\sqrt{3}} & \frac{v_{dc}}{4\sqrt{3}} & \frac{v_{dc}}{\sqrt{3}} \\ 1 & 1 & 1 & 1 \end{bmatrix}$	$\begin{bmatrix} \frac{\sqrt{3}v_{dc}}{4\sqrt{2}} & \frac{v_{dc}}{4\sqrt{6}} & \frac{v_{dc}}{2\sqrt{6}} & \frac{\sqrt{3}v_{dc}}{4\sqrt{2}} \\ \frac{v_{dc}}{4\sqrt{2}} & \frac{v_{dc}}{4\sqrt{2}} & \frac{v_{dc}}{2\sqrt{2}} & \frac{v_{dc}}{4\sqrt{2}} \\ \frac{\sqrt{3}v_{dc}}{4} & \frac{v_{dc}}{2\sqrt{3}} & \frac{v_{dc}}{4\sqrt{3}} & 0 \\ 1 & 1 & 1 & 1 \end{bmatrix}$
TeT_{10}^{15}	TeT_{11}^{15}	TeT_{12}^{15}

$$\begin{bmatrix} \frac{v_{dc}}{4\sqrt{6}} & \frac{v_{dc}}{4\sqrt{6}} & \frac{v_{dc}}{2\sqrt{6}} & \frac{\sqrt{3}v_{dc}}{4\sqrt{2}} \\ \frac{v_{dc}}{4\sqrt{2}} & \frac{v_{dc}}{4\sqrt{2}} & \frac{v_{dc}}{2\sqrt{2}} & \frac{v_{dc}}{4\sqrt{2}} \\ \frac{-v_{dc}}{4\sqrt{3}} & \frac{v_{dc}}{2\sqrt{3}} & \frac{v_{dc}}{4\sqrt{3}} & 0 \\ 1 & 1 & 1 & 1 \end{bmatrix}$$

TeT_{13}^{15}

$$\begin{bmatrix} \frac{v_{dc}}{4\sqrt{6}} & \frac{v_{dc}}{2\sqrt{6}} & \frac{v_{dc}}{2\sqrt{6}} & \frac{\sqrt{3}v_{dc}}{4\sqrt{2}} \\ \frac{v_{dc}}{4\sqrt{2}} & \frac{v_{dc}}{2\sqrt{2}} & \frac{v_{dc}}{2\sqrt{2}} & \frac{v_{dc}}{4\sqrt{2}} \\ \frac{-v_{dc}}{4\sqrt{3}} & \frac{-v_{dc}}{2\sqrt{3}} & \frac{v_{dc}}{4\sqrt{3}} & 0 \\ 1 & 1 & 1 & 1 \end{bmatrix}$$

TeT_{14}^{15}

$$\begin{bmatrix} \frac{v_{dc}}{4\sqrt{6}} & \frac{v_{dc}}{2\sqrt{6}} & \frac{\sqrt{3}v_{dc}}{4\sqrt{2}} & \frac{\sqrt{3}v_{dc}}{4\sqrt{2}} \\ \frac{v_{dc}}{4\sqrt{2}} & \frac{v_{dc}}{2\sqrt{2}} & \frac{v_{dc}}{4\sqrt{2}} & \frac{v_{dc}}{4\sqrt{2}} \\ \frac{-v_{dc}}{4\sqrt{3}} & \frac{-v_{dc}}{2\sqrt{3}} & \frac{-\sqrt{3}v_{dc}}{4} & 0 \\ 1 & 1 & 1 & 1 \end{bmatrix}$$

TeT_{15}^{15}

$$\begin{bmatrix} \frac{v_{dc}}{4\sqrt{6}} & \frac{v_{dc}}{2\sqrt{6}} & \frac{\sqrt{3}v_{dc}}{4\sqrt{2}} & \frac{v_{dc}}{4\sqrt{6}} \\ \frac{v_{dc}}{4\sqrt{2}} & \frac{v_{dc}}{2\sqrt{2}} & \frac{v_{dc}}{4\sqrt{2}} & \frac{v_{dc}}{4\sqrt{2}} \\ \frac{-v_{dc}}{4\sqrt{3}} & \frac{-v_{dc}}{2\sqrt{3}} & \frac{-\sqrt{3}v_{dc}}{4} & \frac{-v_{dc}}{\sqrt{3}} \\ 1 & 1 & 1 & 1 \end{bmatrix}$$

TeT_{16}^{15}

$$\begin{bmatrix} \frac{v_{dc}}{2\sqrt{6}} & \frac{v_{dc}}{2\sqrt{6}} & \frac{\sqrt{3}v_{dc}}{4\sqrt{2}} & \frac{v_{dc}}{4\sqrt{6}} \\ \frac{v_{dc}}{2\sqrt{2}} & \frac{v_{dc}}{2\sqrt{2}} & \frac{v_{dc}}{4\sqrt{2}} & \frac{v_{dc}}{4\sqrt{2}} \\ \frac{-5v_{dc}}{4\sqrt{3}} & \frac{-v_{dc}}{2\sqrt{3}} & \frac{-\sqrt{3}v_{dc}}{4} & \frac{-v_{dc}}{\sqrt{3}} \\ 1 & 1 & 1 & 1 \end{bmatrix}$$

TeT_{17}^{15}

$$\begin{bmatrix} \frac{v_{dc}}{2\sqrt{6}} & \frac{\sqrt{3}v_{dc}}{4\sqrt{2}} & \frac{\sqrt{3}v_{dc}}{4\sqrt{2}} & \frac{v_{dc}}{4\sqrt{6}} \\ \frac{v_{dc}}{2\sqrt{2}} & \frac{v_{dc}}{4\sqrt{2}} & \frac{v_{dc}}{4\sqrt{2}} & \frac{v_{dc}}{4\sqrt{2}} \\ \frac{-5v_{dc}}{4\sqrt{3}} & \frac{-\sqrt{3}v_{dc}}{2} & \frac{-\sqrt{3}v_{dc}}{4} & \frac{-v_{dc}}{\sqrt{3}} \\ 1 & 1 & 1 & 1 \end{bmatrix}$$

TeT_{18}^{15}

$$\begin{bmatrix} \frac{v_{dc}}{2\sqrt{6}} & \frac{\sqrt{3}v_{dc}}{4\sqrt{2}} & \frac{v_{dc}}{4\sqrt{6}} & \frac{v_{dc}}{4\sqrt{6}} \\ \frac{v_{dc}}{2\sqrt{2}} & \frac{v_{dc}}{4\sqrt{2}} & \frac{v_{dc}}{4\sqrt{2}} & \frac{v_{dc}}{4\sqrt{2}} \\ \frac{-5v_{dc}}{4\sqrt{3}} & \frac{-\sqrt{3}v_{dc}}{2} & \frac{-7v_{dc}}{4\sqrt{3}} & \frac{-v_{dc}}{\sqrt{3}} \\ 1 & 1 & 1 & 1 \end{bmatrix}$$

TeT_{19}^{15}

$$\begin{bmatrix} \frac{\sqrt{3}v_{dc}}{4\sqrt{2}} & \frac{\sqrt{3}v_{dc}}{4\sqrt{2}} & \frac{v_{dc}}{4\sqrt{6}} & \frac{v_{dc}}{2\sqrt{6}} \\ \frac{v_{dc}}{4\sqrt{2}} & \frac{v_{dc}}{4\sqrt{2}} & \frac{v_{dc}}{4\sqrt{2}} & \frac{v_{dc}}{2\sqrt{2}} \\ \frac{-3\sqrt{3}v_{dc}}{4} & \frac{-\sqrt{3}v_{dc}}{2} & \frac{-7v_{dc}}{4\sqrt{3}} & \frac{-2v_{dc}}{\sqrt{3}} \\ 1 & 1 & 1 & 1 \end{bmatrix}$$

$$\begin{bmatrix} \frac{\sqrt{3}v_{dc}}{4\sqrt{2}} & \frac{v_{dc}}{4\sqrt{6}} & \frac{v_{dc}}{4\sqrt{6}} & \frac{v_{dc}}{2\sqrt{6}} \\ \frac{v_{dc}}{4\sqrt{2}} & \frac{v_{dc}}{4\sqrt{2}} & \frac{v_{dc}}{4\sqrt{2}} & \frac{v_{dc}}{2\sqrt{2}} \\ \frac{-3\sqrt{3}v_{dc}}{4} & \frac{-10v_{dc}}{4\sqrt{3}} & \frac{-7v_{dc}}{4\sqrt{3}} & \frac{-2v_{dc}}{\sqrt{3}} \\ 1 & 1 & 1 & 1 \end{bmatrix}$$

PR_{16}		
TeT_1^{16}	TeT_2^{16}	TeT_3^{16}
$\begin{bmatrix} 0 & \frac{v_{dc}}{4\sqrt{6}} & \frac{v_{dc}}{2\sqrt{6}} & 0 \\ 0 & \frac{v_{dc}}{4\sqrt{2}} & 0 & 0 \\ \sqrt{3}v_{dc} & \frac{11v_{dc}}{2\sqrt{3}} & \frac{5v_{dc}}{2\sqrt{3}} & \frac{3\sqrt{3}v_{dc}}{4} \\ 1 & 1 & 1 & 1 \end{bmatrix}$	$\begin{bmatrix} \frac{v_{dc}}{4\sqrt{6}} & \frac{v_{dc}}{4\sqrt{6}} & \frac{v_{dc}}{2\sqrt{6}} & 0 \\ \frac{v_{dc}}{4\sqrt{2}} & \frac{v_{dc}}{4\sqrt{2}} & 0 & 0 \\ \frac{2v_{dc}}{\sqrt{3}} & \frac{11v_{dc}}{2\sqrt{3}} & \frac{5v_{dc}}{2\sqrt{3}} & \frac{3\sqrt{3}v_{dc}}{4} \\ 1 & 1 & 1 & 1 \end{bmatrix}$	$\begin{bmatrix} \frac{v_{dc}}{4\sqrt{6}} & \frac{v_{dc}}{2\sqrt{6}} & \frac{v_{dc}}{2\sqrt{6}} & 0 \\ \frac{v_{dc}}{4\sqrt{2}} & 0 & 0 & 0 \\ \frac{2v_{dc}}{\sqrt{3}} & \frac{7v_{dc}}{2\sqrt{3}} & \frac{5v_{dc}}{2\sqrt{3}} & \frac{3\sqrt{3}v_{dc}}{4} \\ 1 & 1 & 1 & 1 \end{bmatrix}$
TeT_4^{16}	TeT_5^{16}	TeT_6^{16}
$\begin{bmatrix} \frac{v_{dc}}{4\sqrt{6}} & \frac{v_{dc}}{2\sqrt{6}} & 0 & 0 \\ \frac{v_{dc}}{4\sqrt{2}} & 0 & 0 & 0 \\ \frac{2v_{dc}}{\sqrt{3}} & \frac{7v_{dc}}{2\sqrt{3}} & \frac{\sqrt{3}v_{dc}}{2} & \frac{3\sqrt{3}v_{dc}}{4} \\ 1 & 1 & 1 & 1 \end{bmatrix}$	$\begin{bmatrix} \frac{v_{dc}}{4\sqrt{6}} & \frac{v_{dc}}{2\sqrt{6}} & 0 & \frac{v_{dc}}{4\sqrt{6}} \\ \frac{v_{dc}}{4\sqrt{2}} & 0 & 0 & \frac{v_{dc}}{4\sqrt{2}} \\ \frac{2v_{dc}}{\sqrt{3}} & \frac{7v_{dc}}{2\sqrt{3}} & \frac{\sqrt{3}v_{dc}}{2} & \frac{5v_{dc}}{4\sqrt{3}} \\ 1 & 1 & 1 & 1 \end{bmatrix}$	$\begin{bmatrix} \frac{v_{dc}}{2\sqrt{6}} & \frac{v_{dc}}{2\sqrt{6}} & 0 & \frac{v_{dc}}{4\sqrt{6}} \\ 0 & 0 & 0 & \frac{v_{dc}}{4\sqrt{2}} \\ \frac{v_{dc}}{\sqrt{3}} & \frac{7v_{dc}}{2\sqrt{3}} & \frac{\sqrt{3}v_{dc}}{2} & \frac{5v_{dc}}{4\sqrt{3}} \\ 1 & 1 & 1 & 1 \end{bmatrix}$
TeT_7^{16}	TeT_8^{16}	TeT_9^{16}
$\begin{bmatrix} \frac{v_{dc}}{2\sqrt{6}} & 0 & 0 & \frac{v_{dc}}{4\sqrt{6}} \\ 0 & 0 & 0 & \frac{v_{dc}}{4\sqrt{2}} \\ \frac{v_{dc}}{\sqrt{3}} & \frac{\sqrt{3}v_{dc}}{4} & \frac{\sqrt{3}v_{dc}}{2} & \frac{5v_{dc}}{4\sqrt{3}} \\ 1 & 1 & 1 & 1 \end{bmatrix}$	$\begin{bmatrix} \frac{v_{dc}}{2\sqrt{6}} & 0 & \frac{v_{dc}}{4\sqrt{6}} & \frac{v_{dc}}{4\sqrt{6}} \\ 0 & 0 & \frac{v_{dc}}{4\sqrt{2}} & \frac{v_{dc}}{4\sqrt{2}} \\ \frac{v_{dc}}{\sqrt{3}} & \frac{\sqrt{3}v_{dc}}{4} & \frac{v_{dc}}{2\sqrt{3}} & \frac{5v_{dc}}{4\sqrt{3}} \\ 1 & 1 & 1 & 1 \end{bmatrix}$	$\begin{bmatrix} \frac{v_{dc}}{2\sqrt{6}} & 0 & \frac{v_{dc}}{4\sqrt{6}} & \frac{v_{dc}}{2\sqrt{6}} \\ 0 & 0 & \frac{v_{dc}}{4\sqrt{2}} & 0 \\ \frac{v_{dc}}{\sqrt{3}} & \frac{\sqrt{3}v_{dc}}{4} & \frac{v_{dc}}{2\sqrt{3}} & \frac{v_{dc}}{4\sqrt{3}} \\ 1 & 1 & 1 & 1 \end{bmatrix}$
TeT_{10}^{16}	TeT_{11}^{16}	TeT_{12}^{16}
$\begin{bmatrix} 0 & 0 & \frac{v_{dc}}{4\sqrt{6}} & \frac{v_{dc}}{2\sqrt{6}} \\ 0 & 0 & \frac{v_{dc}}{4\sqrt{2}} & 0 \\ 0 & \frac{\sqrt{3}v_{dc}}{4} & \frac{v_{dc}}{2\sqrt{3}} & \frac{v_{dc}}{4\sqrt{3}} \\ 1 & 1 & 1 & 1 \end{bmatrix}$	$\begin{bmatrix} 0 & \frac{v_{dc}}{4\sqrt{6}} & \frac{v_{dc}}{4\sqrt{6}} & \frac{v_{dc}}{2\sqrt{6}} \\ 0 & \frac{v_{dc}}{4\sqrt{2}} & \frac{v_{dc}}{4\sqrt{2}} & 0 \\ 0 & \frac{-v_{dc}}{4\sqrt{3}} & \frac{v_{dc}}{2\sqrt{3}} & \frac{v_{dc}}{4\sqrt{3}} \\ 1 & 1 & 1 & 1 \end{bmatrix}$	$\begin{bmatrix} 0 & \frac{v_{dc}}{4\sqrt{6}} & \frac{v_{dc}}{2\sqrt{6}} & \frac{v_{dc}}{2\sqrt{6}} \\ 0 & \frac{v_{dc}}{4\sqrt{2}} & 0 & 0 \\ 0 & \frac{-v_{dc}}{4\sqrt{3}} & \frac{-v_{dc}}{2\sqrt{3}} & \frac{v_{dc}}{4\sqrt{3}} \\ 1 & 1 & 1 & 1 \end{bmatrix}$
TeT_{13}^{16}	TeT_{14}^{16}	TeT_{15}^{16}

$\begin{bmatrix} 0 & \frac{v_{dc}}{4\sqrt{6}} & \frac{v_{dc}}{2\sqrt{6}} & 0 \\ 0 & \frac{v_{dc}}{4\sqrt{2}} & 0 & 0 \\ 0 & \frac{-v_{dc}}{4\sqrt{3}} & \frac{-v_{dc}}{2\sqrt{3}} & \frac{-\sqrt{3}v_{dc}}{4} \\ 1 & 1 & 1 & 1 \end{bmatrix}$	$\begin{bmatrix} \frac{v_{dc}}{4\sqrt{6}} & \frac{v_{dc}}{4\sqrt{6}} & \frac{v_{dc}}{2\sqrt{6}} & 0 \\ \frac{v_{dc}}{4\sqrt{2}} & \frac{v_{dc}}{4\sqrt{2}} & 0 & 0 \\ \frac{-v_{dc}}{\sqrt{3}} & \frac{-v_{dc}}{4\sqrt{3}} & \frac{-v_{dc}}{2\sqrt{3}} & \frac{-\sqrt{3}v_{dc}}{4} \\ 1 & 1 & 1 & 1 \end{bmatrix}$	$\begin{bmatrix} \frac{v_{dc}}{4\sqrt{6}} & \frac{v_{dc}}{2\sqrt{6}} & \frac{v_{dc}}{2\sqrt{6}} & 0 \\ \frac{v_{dc}}{4\sqrt{2}} & 0 & 0 & 0 \\ \frac{-v_{dc}}{\sqrt{3}} & \frac{-5v_{dc}}{4\sqrt{3}} & \frac{-v_{dc}}{2\sqrt{3}} & \frac{-\sqrt{3}v_{dc}}{4} \\ 1 & 1 & 1 & 1 \end{bmatrix}$
TeT_{16}^{16}	TeT_{17}^{16}	TeT_{18}^{16}
$\begin{bmatrix} \frac{v_{dc}}{4\sqrt{6}} & \frac{v_{dc}}{2\sqrt{6}} & 0 & 0 \\ \frac{v_{dc}}{4\sqrt{2}} & 0 & 0 & 0 \\ \frac{-v_{dc}}{\sqrt{3}} & \frac{-5v_{dc}}{4\sqrt{3}} & \frac{-\sqrt{3}v_{dc}}{2} & \frac{-\sqrt{3}v_{dc}}{4} \\ 1 & 1 & 1 & 1 \end{bmatrix}$	$\begin{bmatrix} \frac{v_{dc}}{4\sqrt{6}} & \frac{v_{dc}}{2\sqrt{6}} & 0 & \frac{v_{dc}}{4\sqrt{6}} \\ \frac{v_{dc}}{4\sqrt{2}} & 0 & 0 & \frac{v_{dc}}{4\sqrt{2}} \\ \frac{-v_{dc}}{\sqrt{3}} & \frac{-5v_{dc}}{4\sqrt{3}} & \frac{-\sqrt{3}v_{dc}}{2} & \frac{-7v_{dc}}{4\sqrt{3}} \\ 1 & 1 & 1 & 1 \end{bmatrix}$	$\begin{bmatrix} \frac{v_{dc}}{2\sqrt{6}} & \frac{v_{dc}}{2\sqrt{6}} & 0 & \frac{v_{dc}}{4\sqrt{6}} \\ 0 & 0 & 0 & \frac{v_{dc}}{4\sqrt{2}} \\ \frac{-2v_{dc}}{\sqrt{3}} & \frac{-5v_{dc}}{4\sqrt{3}} & \frac{-\sqrt{3}v_{dc}}{2} & \frac{-7v_{dc}}{4\sqrt{3}} \\ 1 & 1 & 1 & 1 \end{bmatrix}$
TeT_{19}^{16}	TeT_{20}^{16}	TeT_{21}^{16}
$\begin{bmatrix} \frac{v_{dc}}{2\sqrt{6}} & 0 & 0 & \frac{v_{dc}}{4\sqrt{6}} \\ 0 & 0 & 0 & \frac{v_{dc}}{4\sqrt{2}} \\ \frac{-2v_{dc}}{\sqrt{3}} & \frac{-3\sqrt{3}v_{dc}}{4} & \frac{-\sqrt{3}v_{dc}}{2} & \frac{-7v_{dc}}{4\sqrt{3}} \\ 1 & 1 & 1 & 1 \end{bmatrix}$	$\begin{bmatrix} \frac{v_{dc}}{2\sqrt{6}} & 0 & \frac{v_{dc}}{4\sqrt{6}} & \frac{v_{dc}}{4\sqrt{6}} \\ 0 & 0 & \frac{v_{dc}}{4\sqrt{2}} & \frac{v_{dc}}{4\sqrt{2}} \\ \frac{-2v_{dc}}{\sqrt{3}} & \frac{-3\sqrt{3}v_{dc}}{4} & \frac{-5v_{dc}}{2\sqrt{3}} & \frac{-7v_{dc}}{4\sqrt{3}} \\ 1 & 1 & 1 & 1 \end{bmatrix}$	$\begin{bmatrix} \frac{v_{dc}}{2\sqrt{6}} & 0 & \frac{v_{dc}}{4\sqrt{6}} & \frac{v_{dc}}{2\sqrt{6}} \\ 0 & 0 & \frac{v_{dc}}{4\sqrt{2}} & 0 \\ \frac{-2v_{dc}}{\sqrt{3}} & \frac{-3\sqrt{3}v_{dc}}{4} & \frac{-5v_{dc}}{2\sqrt{3}} & \frac{-11v_{dc}}{4\sqrt{3}} \\ 1 & 1 & 1 & 1 \end{bmatrix}$
TeT_{22}^{16}		
$\begin{bmatrix} 0 & 0 & \frac{v_{dc}}{4\sqrt{6}} & \frac{v_{dc}}{2\sqrt{6}} \\ 0 & 0 & \frac{v_{dc}}{4\sqrt{2}} & 0 \\ -\sqrt{3}v_{dc} & \frac{-3\sqrt{3}v_{dc}}{4} & \frac{-5v_{dc}}{2\sqrt{3}} & \frac{-11v_{dc}}{4\sqrt{3}} \\ 1 & 1 & 1 & 1 \end{bmatrix}$		

Nonlinear direct power control of a multilevel diode-clamped four-leg shunt active power filter

Abstract

In this thesis, the direct power control and predictive direct power control using three-dimensional space vector modulation for three-phase five-level four-leg shunt active power filter (SAPF) have been proposed. Thanks to the four-leg SAPF, it is possible to ensure full compensation of harmonic currents, harmonic neutral current, reactive power, and unbalanced nonlinear load currents. Furthermore, it can regulate its self-sustaining DC bus voltage efficiently. The voltage-balancing control of DC capacitors of the five-level four-leg SAPF is achieved using a new algorithm of five-level three-dimensional space vector modulation equipped by a balancing strategy. Mainly, this strategy is based on the effective use of the redundant switching states of the inverter voltage vectors.

In order to improve the performances of the four-leg SAPF, nonlinear controllers based on the feedback linearization, second order sliding mode, and fuzzy logic are associated to direct power control and predictive direct power control. Finally, a comparative study between both direct power controls strategies combined with the three aforementioned nonlinear control techniques is provided.

Keywords

Direct power control, Predictive control, Four-leg shunt active power filter, Multilevel-level four-leg inverter, Three-dimensional space vector modulation, Feedback linearization, Sliding mode, Fuzzy logic.

Commande directe de puissance non linéaire d'un filtre active parallèle multiniveaux à quatre-bras

Résumé

Dans cette thèse, la commande directe de puissance et la commande directe de puissance prédictive utilisant une modulation vectorielle tridimensionnelle dédiées au contrôle d'un filtre actif parallèle cinq-niveaux à quatre bras (FAP) ont été proposées. A ce dernier, il est possible d'assurer la pleine compensation des courants harmoniques, le courant du neutre, la puissance réactive et le déséquilibre des courants de la charge non linéaire. En outre, il est capable de contrôler la tension du bus continu d'une manière efficace. L'équilibrage des tensions des condensateurs du FAP à cinq-niveaux à quatre bras est réalisé à l'aide d'un nouvel algorithme de la modulation vectorielle à cinq-niveaux tridimensionnelle doté d'une stratégie d'équilibrage. Cette dernière est basée sur l'utilisation efficace des états de commutation redondants des vecteurs de tension de l'onduleur.

Afin d'améliorer les performances du FAP à quatre bras, des contrôleurs non linéaires basés sur le retour d'état linéarisant, le mode glissant d'ordre deux, et la logique floue sont associés au contrôle direct de puissance et le contrôle direct de puissance prédictive. Enfin, une étude comparative entre les deux stratégies du contrôle directe de puissances combinées avec les trois techniques non linéaires susmentionnées est fournie.

Mots de clés

Commande directe de puissance, Commande prédictive, Filtre actif parallèle à quatre bras, Onduleur multiniveaux à quatre-bras, MLI vectorielle tridimensionnelle, Retour d'état linéarisant, Mode glissant, Logique floue.

التحكم المباشر للاستطاعة اللاخطي لمرشح متوازي متعدد المستويات ذو أربع سيقان

ملخص

في هذه الرسالة تم اقتراح التحكم المباشر للاستطاعة والتحكم التنبئي المباشر للاستطاعة باستخدام التعديل الشعاعي لعرض النبضة ثلاثي الأبعاد للمرشح المتوازي ذو خمس مستويات وأربع سيقان. اللجوء الى المرشح الفعال المتوازي ذو أربع سيقان من شأنه ان يضمن التعويض الكامل للتيارات التوافقية، التيار المحايد، الاستطاعة الخاملة، وكذا عدم توازن التيارات الناتجة عن الحمولة الغير خطية. كما يمكنه التحكم بالجهد المستمر لمكثفته بصورة فعالة. تم تحقيق السيطرة على موازنة الجهد لمكثفات المرشح الفعال المتوازي ذو الخمس مستويات وأربع سيقان باستخدام خوارزمية جديدة للتعديل الشعاعي لعرض النبضة ثلاثي الأبعاد ذو الخمس مستويات مزودة باستراتيجية للتوازن. هذه الأخيرة تعتمد على الاستعمال الفعال للحالات الزائدة لأشعة الجهد للعاكس الكهربائي.

من أجل تحسين أداء المرشح الفعال المتوازي ذو الأربع سيقان، عدة تقنيات في التحكم الغير خطي كالتي تعتمد على الرجوع الى الحالة الخطية، النمط الانزلاقي من الدرجة الثانية، والمنطق الغامض أدمجت في التحكم المباشر في الاستطاعة وكذا التحكم المباشر التنبئي في الاستطاعة. و في الأخير، تم اجراء دراسة مقارنة بين استراتيجيات التحكم المباشر في الاستطاعة مقترنة بتقنيات التحكم الغير خطي الثلاث السالفة الذكر.

كلمات مفتاحية

التحكم المباشر في الاستطاعة، التحكم التنبئي، المرشح الفعال المتوازي ذو أربع سيقان، العاكس الكهربائي ذو عدة مستويات وأربع سيقان، التحكم بالرجوع الى الحالة الخطي، التحكم بالنمط الانزلاقي، التحكم عن طريق المنطق الغامض.